GAIT STUDY

OF DYSVASCULAR

LOWER LIMB AMPUTEES

IN EARLY STAGE OF REHABILITATION

Michel J. PILLU **DEA**

This thesis is submitted in fulfilment of the requirements
for the degree of Doctor in Philosophy in the
Bioengineering Unit
University of Strathclyde
Scotland

2000

The copyright of this thesis belongs to the author under the terms of the United Kingdom Copyright Acts as qualified by University of Strathclyde Regulation 3.49. Due acknowledgement must always be made of the use of any material contained in, or derived from, this thesis.

ABSTRACT

The study has investigated some load aspects of the gait of elderly, vascular, lower limb amputees in early stage of rehabilitation, in day to day realistic conditions.

The aims were: 1) to understand the gait of recent vascular amputees better, 2) to quantify mechanical loads with two different assistive walking devices.

To reach these targets: a removable novel pylon transducer was designed; a fully portable data acquisition system and instrumented canes were used.

The new pylon transducer comprised two main parts so that the prosthesis did not need to be altered: 1) an « aluminium bell » placed within the prosthetic shank tube, having a flange at its base on which the tube of the prosthesis comes to bear; 2) the body of the transducer located inside the bell with an upper contact flange and having clearance to allow the bonding of strain gauges in four levels. A full calibration of the six channels followed by static and dynamic validation tests has been undertaken. They showed a mean accuracy of 7 % with a sufficient linearity to be confident in the provided results.

Data were recorded through an eight channels 12-bit data acquisition system. At a sampling frequency of 64Hz, the recording duration was 1 hour.

Two series of patients have been included in the sample: 30 transtibial and 10 transfemoral amputees.

A new pattern for the vertical ground reaction force is described: the second peak was absent, evidently transmitted by the load on the walking devices. The mean load on the walking devices was 35 percent of the body weight. It was also shown that the walking devices not only transmitted axial load but also assisted in the forward acceleration of the body.

Three typical gait patterns have been found in the temporal parameters of the gait but none could be discerned for the load distribution.

To Fatima, Nadia and Benoît

To my Parents

To Estelle, *in memoriam*

TABLE OF CONTENTS

1 INTRODUCTION 1-1

1.1 INITIAL CONSIDERATIONS 1-1
1.2 AMPUTEE POPULATION UNDER CONSIDERATION 1-4
1.3 MAIN RESEARCH PURPOSES 1-5
1.3.1 Formulation of the thesis objectives 1-9
1.4 NECESSARY DEVICES FOR THIS INVESTIGATION 1-9

2 PRELIMINARY STUDY 2-11

2.1 DESCRIPTION OF THE HOPITAL DE VILLIERS-SAINT-DENIS, FRENCH REHABILITATION CENTRE 2-11
2.1.1 Historical Background 2-11
2.1.2 The vascular department 2-12
2.1.3 Descriptive Statistics of Patients staying in Villiers-Saint-Denis Rehabilitation Centre 2-12
2.2 LITERATURE REVIEW ON ELDERLY AND VASCULAR AMPUTEES 2-14
2.2.1 Introduction 2-14
2.2.2 Elderly and peripheral vascular disease patients 2-15
2.2.3 Cane-Assisted Gait 2-16
2.3 REQUIREMENTS FOR GAIT ASSESSMENT 2-20
2.3.1 Definition 2-20
2.3.2 Techniques used for gait analysis 2-21
2.3.3 Unfinished Conclusions 2-32
2.3.4 Recording Systems 2-33
2.4 LITERATURE REVIEW OF GAIT ASSESSMENT OR GAIT ANALYSIS 2-35
2.4.1 Temporal and Distance Characteristics 2-36
2.4.2 Temporal and distance parameters: Response to Training 2-37
2.4.3 Kinetics 2-38
2.4.4 Gait Analysis in Clinical Applications 2-39
2.5 PRELIMINARY CONCLUSION 2-40
2.6 DEFINITIONS AND CONVENTIONS USED 2-43
2.6.1 Introduction 2-43
2.6.2 Terminology 2-43
2.6.3 Frames of reference 2-45
2.6.4 Units of measurement 2-49
2.6.5 Alignment parameters 2-49
2.6.6 Forces and moments 2-49
2.6.7 Gait description and vocabulary 2-53
2.6.8 Summary 2-57

3 DESCRIPTION AND USE OF THE FIRST NEW REMOVABLE TRANSDUCER (MODEL I) 3-59

3.1 INTRODUCTION 3-59
3.2 DESCRIPTION OF THE PROSTHETIC ANKLE 3-59
3.3 THEORETICAL ANALYSIS OF THE ARTIFICIAL ANKLE / FOOT DEVICE 3-60
3.3.1 Theoretical static equilibrium with foot flat 3-60
3.3.2 Theoretical static equilibrium at heel - strike 3-61
3.3.3 Theoretical static equilibrium at toe - off 3-62
3.3.4 Numerical Application 3-63
3.4 FINITE ELEMENT ANALYSIS OF THE ANKLE 3-64
3.4.1 Design of the prosthetic ankle device 3-65
3.4.2 Results 3-65
3.4.3 Design of the ankle axle 3-66
3.4.4 Final description of the ankle transducer 3-67
3.4.5 Gauge location 3-68

3.5 CALIBRATION 3-70
3.5.1 Introduction *3-70*
3.5.2 Amplifiers and recording system used *3-70*
3.5.3 Following method *3-71*
3.5.4 Results *3-72*
3.5.5 Comments *3-73*
3.6 STRENGTH MEASUREMENT 3-74
3.7 CONCLUSION 3-75

4 OPTIMISATION OF TRANSDUCER SHAPE BY STRESS / STRAIN ANALYSIS.... 4-76

4.1 INTRODUCTION 4-76
4.2 CHOICE OF THE MATERIAL 4-76
4.2.1 Description of the new transducer *4-76*
4.3 DESCRIPTION OF THE TWO PROTOTYPES OF THE NEW TRANSDUCER (MODEL II AND MODEL III)4-78
4.4 STUDY OF THE MECHANICAL BEHAVIOUR OF THE TWO PROTOTYPES 4-79
4.4.1 Linearity in deflection of the two models II and III *4-81*
4.4.2 Static proof test of the connection saddles *4-82*
4.4.3 Partial conclusion *4-83*
4.5 STUDY OF THE ELECTRICAL BEHAVIOUR OF THE CHOSEN TRANSDUCER (MODEL III) 4-83
4.6 TESTS DESCRIPTIONS 4-84
4.6.1 Set-up descriptions *4-84*
4.6.2 Loading descriptions *4-86*
4.6.3 Test procedures *4-87*
4.7 PARTIAL CONCLUSION 4-93
4.8 FINAL DESCRIPTION OF THE NEW VILLIERS PYLON TRANSDUCER 4-94
4.8.1 Introduction *4-94*
4.8.2 Description of the new pylon transducer *4-94*
4.9 THE DESCRIPTION OF THE GAUGING 4-97
4.9.1 The choice of the gauges *4-97*
4.9.2 The gauging *4-98*
4.9.3 Description of the bridges *4-100*
4.9.4 The wiring of the full Wheatstone bridges *4-100*
4.10 CONCLUSION 4-102

5 DESCRIPTION OF THE EQUIPMENT USED 5-104

5.1 INTRODUCTION 5-104
5.2 THE FIRST DATA ACQUISITION SYSTEM 5-105
5.2.1 General description *5-105*
5.2.2 Adjustments of the new transducer *5-107*
5.2.3 Using Acquire *5-110*
5.2.4 Partial conclusion on the design of the first data acquisition system *5-110*
5.3 THE DEFINITIVE PORTABLE DATA ACQUISITION SYSTEM 5-110
5.3.1 Introduction *5-110*
5.3.2 The portable recording and data acquisition unit: Myodata *5-111*
5.3.3 Partial conclusion about the definitive portable data acquisition system *5-119*
5.4 THE INSTRUMENTED ASSISTIVE WALKING DEVICES 5-120
5.4.1 Introduction *5-120*
5.4.2 Description *5-120*
5.4.3 Calibration of the two assistive walking devices *5-121*
5.4.4 Calibration results *5-122*
5.4.5 Validation tests and results of the two assistive walking devices *5-124*
5.5 SUMMARY 5-125

6 THE NEW VILLIERS PYLON TRANSDUCER CALIBRATION 6-127

6.1 INTRODUCTION 6-127
6.2 LINEAR APPROACH 6-128
6.3 DESCRIPTION OF TESTS 6-132

6.3.1 Shear Force Fx and Fz *6-133*
6.3.2 Axial Load Calibration Fy *6-134*
6.3.3 Transverse Torque Calibration My *6-135*
6.3.4 Bending Moments Calibration Mx and Mz *6-136*
6.4 RAW DATA STUDIES IN EACH LOADING CASE 6-137
6.4.1 Shear force Fx *6-138*
6.4.2 Axial Load Fy *6-140*
6.4.3 Shear Force Fz *6-140*
6.4.4 Bending Moment Mx *6-141*
6.4.5 Torque My *6-145*
6.4.6 Bending Moment Mz *6-146*
6.4.7 Summary and Discussion *6-150*
6.5 STATISTICAL ANALYSIS OF CALIBRATION RAW DATA 6-150
6.6 DATA PROCESSING 6-152
6.6.1 Signs of the mean values *6-153*
6.6.2 P-value statistical analysis *6-153*
6.6.3 Calibration matrices [M] and [M]$^{-1}$ = [C] *6-154*
6.6.4 Comparison with the Strathclyde Pylon Transducer *6-155*
6.6.5 Using calibration matrix [C] *6-156*
6.7 CALIBRATION RESULTS USING THE PORTABLE DATA ACQUISITION SYSTEM 6-156
6.8 DISCUSSION 6-157

7 VALIDATION TESTS OF THE CALIBRATION MATRIX APPLIED ON THE NEW VILLIERS PYLON TRANSDUCER 7-159

7.1 INTRODUCTION 7-159
7.2 STATIC TESTS WITH SPECIAL DEVICE 7-159
7.2.1 Description of the device used *7-160*
7.2.2 Mathematical considerations *7-162*
7.2.3 Description of the tests *7-163*
7.2.4 Results *7-165*
7.3 STATIC TESTS WITH BENCH TABLE 7-168
7.3.1 Description of the bench heavy table and tests made *7-168*
7.3.2 Mathematical considerations *7-168*
7.3.3 Loading cases and results *7-169*
7.3.4 Torque study *7-170*
7.4 STATIC VALIDATION TESTS USING SIMULTANEOUSLY TWO TRANSDUCERS 7-173
7.4.1 Description of the set-up with data acquisition systems used *7-173*
7.4.2 Mathematical considerations *7-174*
7.4.3 Description of the tests *7-174*
7.4.4 Results *7-174*
7.4.5 Torque study *7-176*
7.5 PARTIAL CONCLUSION FROM STATIC VALIDATION TESTS 7-177
7.6 DYNAMIC TESTS 7-178
7.6.1 Description of the set-up, the subject and the different tests *7-178*
7.6.2 Results *7-179*
7.7 DYNAMIC VALIDATION TEST USING SIMULTANEOUSLY THE VILLIERS PYLON TRANSDUCER AND A FORCE PLATFORM 7-183
7.8 DISCUSSION 7-185
7.8.1 Followed method to calculate the amending factors *7-185*
7.8.2 Verification of the correcting factors *7-186*
7.9 CONCLUSION 7-187

8 TESTS, RESULTS AND DISCUSSION 8-192

8.1 INTRODUCTION 8-192
8.2 THE PROGRESS OF THE TESTS PERFORMED 8-192
8.2.1 Patient's consent *8-193*
8.2.2 Successive stages of a gait evaluation test *8-195*

8.2.3 Data treatment.....8-200
8.3 SUBJECTS' SELECTION AND DESCRIPTION 8-204
8.3.1 The 40 patients: kinetic study (30 transtibial, 10 transfemoral amputees: series 1a and 1b) 8-205
8.3.2 Comparison between different gait assistive devices (10 transtibial subjects: series 2)8-207
8.3.3 Follow-up Rehabilitation (9 transtibial subjects: series 3).....8-207
8.3.4 Main gait parameters and time events of recent vascular transtibial amputees (14 transtibial amputees: series 4).....8-208
8.3.5 Ramp ascent and descent (4 transtibial patients: series 5) and presentation of the results 8-208
8.3.6 Comparison between different gait assistive devices (4 transfemoral subjects: series 6)8-209
8.4 HAND OR COMPUTER DATA TREATMENT AND PRESENTATION OF THE RESULTS 8-209
8.4.1 Hand data treatment.....8-209
8.4.2 Computer screen data treatment and presentation of the results 8-212
8.4.3 Description of the common statistical analysis of the results.....8-212
8.5 RESULTS FOR TRANSTIBIAL PATIENTS.....8-214
8.5.1 Gait Phase Duration.....8-214
8.5.2 The ground reaction forces 8-216
8.5.3 The fore-aft shear force 8-222
8.5.4 The flexion - extension bending moments at the artificial ankle joint.....8-225
8.5.5 Temporal parameters: Chronology of gait events and loads during transtibial amputees ambulation.....8-227
8.6 RAMP ASCENT AND DESCENT (TRANSTIBIAL AMPUTEES).....8-236
8.7 RESULTS FOR TRANSFEMORAL AMPUTEES (10 PATIENTS) 8-239
8.7.1 Gait Phase Duration.....8-239
8.7.2 The ground reaction forces for transfemoral patients 8-241
8.7.3 The fore-aft shear force 8-244
8.7.4 The flexion - extension bending moments at the artificial ankle joint.....8-245
8.8 RESULTS FOR TRANSFEMORAL AMPUTEES: 2 STICKS VS. 2 CANES (4 PATIENTS).....8-247
8.8.1 Gait Phase Duration.....8-247
8.8.2 The ground reaction forces 8-247
8.8.3 The fore-aft shear force 8-251
8.8.4 The anterio-posterior bending moments at the artificial ankle joint.....8-253
8.8.5 Temporal parameters: Chronology of gait events and loads during transfemoral amputees ambulation.....8-254
8.9 SUMMARY AND CONCLUSIONS 8-261
8.9.1 Axial Loads 8-262
8.9.2 Anterio-posterior shear forces and bending moments 8-263
8.9.3 Temporal parameters.....8-264
8.9.4 Strategy of using the walking aids.....8-265

9 CONCLUSION.....9-266

10 REFERENCES.....10-271

11 APPENDICES (VOLUME 2).....11-294

ACKNOWLEDGEMENTS

I acknowledge the feedback and guidance of Professor John P. Paul and my supervisor Mr. Stephan E. Solomonidis from the Bioengineering Unit (Professor J.C. Barbenel, Past Head of Unit and Professor J.M. Courtney, Head of Unit) of the University of Strathclyde, Scotland.

I would like to say many thanks to all the staff members of the Bioengineering Unit; this includes a special acknowledge to M. A.J. Tullis (Electronic Laboratory), W.D. Spence (Prosthetic Laboratory) and D.A Robb (Mechanical Workshop).

I would like to acknowledge the feedback and guidance of Monsieur le Professeur J.J. Laboisse from l'Ecole Nationale Supérieure des Arts et Métiers de Châlons en Champagne, France.

I would like to make a special mention of Messieurs les Professeurs F. Lavaste and B. Landjerit with the following students: F. Dacquait, P.H. Ferry, C Martin et E. Garrate, from l'Ecole Nationale Supérieure des Arts et Métiers de Paris, France.

I would like to acknowledge the strong support I have had from my colleagues of the Rehabilitation Centre of the Hôpital de Villiers-Saint-Denis: M. E Dechamps (Chef du Service d'Appareillage) and all the prosthetists and physiotherapists with whose I am proud to work.

Funding for this project was from a special grant awarded by the Fondation Hospitalière « La Renaissance Sanitaire » represented by Monsieur Daniel Manach (past president), Monsieur F. Gobet (past general manager), Monsieur M. Ladegaillerie (present president of the board of governors) and Monsieur J.L. Yonnet (present director of the Hôpital de Villiers-Saint-Denis).

1 INTRODUCTION

1.1 INITIAL CONSIDERATIONS

In countries such as Great Britain and France, with the "baby boom" generation entering middle age, health care systems will soon be expected to service a large senior citizen population. This may lead to an increase in the number of elderly amputees since non-traumatic loss of a limb is most prevalent in the aged. Therefore, peripheral vascular disease, which is the most common way to lose a lower limb for elderly people, is increasing. This illness follows the ageing of the population and its prevalence is increased by the better long-term survival of diabetes mellitus patients and some bad habits such as tobacco smocking (especially in the female population) or a fatty diet.

In some cases, the final step of the peripheral vascular disease (PVD) is an amputation in which three levels can be recognised: transfemoral, transtibial, and partial foot. According to statistical studies conducted in the Western World by various National Health Services and quoted by De Frang *et al.* (1991) for USA, Condie *et al.* (1996) for Scotland and Germanaud (1996) in France, the new PVD amputee/population ratio is about 0.144 ‰, per year, in Northern Europe and America.

Due to the high level of this population of recent vascular amputees, a plan to study the biomechanics of the gait of these subjects was made, having the main target to improve the rehabilitation process of the patients attending the author's centre. There is a lack of gait studies concerning PVD patients, which is due to patient variability and the complexity in obtaining a standardised population with common characteristics. This is particularly true for new vascular amputees experiencing problems with their residual limb, general health and stump pain. Rehabilitation to satisfactory patterns of movement takes a long time after surgery, most of the patients are thus discharged from the rehabilitation centre before stabilisation of the gait pattern. It is therefore difficult to have a large enough controlled population of

new PVD amputees (Ottenbacher, 1995). Clinical case reports are common but offer few objective data. Most research on peripheral vascular disease amputees is conducted at least six months after the end of their rehabilitation training (Anderson, 1995; Czerniecki *et al.*, 1990; Powers *et al.*, 1996; Subbarao, 1995). Furthermore, in scientific research on amputees gait, most of the papers published are on reasonably fit young traumatic amputees. One of the strongest beliefs of the author of this thesis is that vascular amputees are totally different from traumatic ones, since the main characteristics of these patients are the following:

1. probable short survival;
2. elderly people;
3. concurrent medical problems.

The two first points highlight the fragility of the population while the third one exhibits the large diversity of the patients. Moreover, this difference, between vascular and traumatic amputees, is not only survival, age or polypathology but also the choice of the prosthesis, the immediate goal, and the daily job. It is relevant that these elderly subjects have not the same target as the young who have their whole future before them. For example, the elderly dysvascular diabetic amputee who comprises greater than 60 % of the amputee population may only have the functional goals of independence in self care, with minimal household and community ambulation. In contrast, the young traumatic amputees, at the conclusion of rehabilitation, are very hopeful of taking part of sports and have the vocational goal of working. Can the results of investigations in young traumatic amputees be generalised and applied to the elderly? The answer of this question, in the opinion of the author, who has worked for more than 25 years with PVD amputees, must be negative. Therefore, it is a not reasonable to compare traumatic amputees data with those obtained from vascular patients' biomechanical studies. In other words, it is necessary to obtain specific elderly vascular amputees' benchmark data, especially from those who have recently lost a lower limb.

Another important consideration must be highlighted: the type of surgery and the amputation level in vascular disease is important in comparing the final outcomes of

patients coming from different countries or surgical teams. In other words, it seems to the author of this work that the test patients of this project were usually amputated at a lower level than patients reported in the literature, following the method introduced in France by a vascular surgeon (Cormier, 1982; see section 2.1.3) and since widely adopted in France. The importance of a low level of amputation is well known since a long time (Murdoch, 1967) but all the consequences of such a low level were not enough emphasised. Due to both post-surgical and revascularisation oedema, the stump must be left with a large open wound and the healing is delayed. However, the prognosis of tissue viability in relation with the amputation level selection is affected by a by-pass surgery, an early limb fitting with adapted physiotherapy and influenced by the general status of the patient (see chapter 11, volume 2). For example, a transtibial amputee could be a transfemoral in another surgical, social or economical background. If it is so, the patient, amputated at a lower level, suffers more pain with a residual limb in a bad condition and a general status more precarious than a patient being amputated at a higher level. This important remark could explain the lower level of outcomes, at discharge time, between most of the patients having their rehabilitation process in the Villiers-Saint-Denis (VSD) Centre and other patients described in the literature. Most of our patients use at least one walking aid while, in other rehabilitation centres, it appears that patients do not use any walking aid. By the end of six months of rehabilitation, the percentage of patients from the VSD Centre who were able to walk without aids was apparently significantly lower than that achieved in some other centres (Durance *et al.*, 1989; Collin *et al.*, 1992; Pinzur *et al.*, 1993; Hubbard & McElroy, 1994; Leung *et al.*, 1996). Despite this surgical difference and thus, the difficulty of comparing the patients' results from different rehabilitation teams, the launching of a biomechanical study of the gait pattern of VSD patients was necessary to provide an assessment tool to the physiotherapist staff of the VSD Rehabilitation Centre.

Due to the lack of clinical evaluation tools, it was difficult to assert why VSD patients had such a functional outcome. Some hypotheses could be suggested: low gait rate, insufficient practice in the use of both the prosthesis and the walking aids,

hospital stay too short, residual stump wound at hospital discharge, ... This list is not limited.

To check the validity of the two first assumptions (low gait rate and inefficient practice concerning the assisted prosthetic gait), a clinical evaluation tool to study the gait of new vascular amputees was found necessary.

Studying the literature (see section 2.2.3), it was unexpected to detect another important lack of research concerning the biomechanic of the assisted-gait of amputees. The main problems, such as: axial forces, moments and torque, strain balance between the forearm counter load and the stick handle, were not studied. Consequently, one of the main purposes of the work presented below is to remedy this deficiency in research on recent vascular amputees assisted-gait.

Two further considerations may be stated. If the relevant literature is surveyed, it is surprising to see how little attention is given to the quantitative assessment of the errors, which affect the results of gait analyses (Cappozzo, 1991; Boonstra *et al.*, 1993). Therefore, particular attention is paid in this work to validation tests of all the devices used. Without full awareness of the inaccuracy, any attempt to clinically validate these methods is doomed to failure. The second consideration refers to what may be termed "inter-disciplinary disagreement": that is, the ever lasting communication problem between engineers and clinicians, a communication problem which goes well beyond the difficulty in transferring information and involves the will to collaborate.

This is why the work presented in this thesis has the intent to be a "communication interface" between the biomechanical scientific and the basic physiotherapy world (Cappozzo, 1991). On the other hand, this work might offer the possibility of bridging the conceptual gap between every day clinical practice and scientific gait analysis techniques. It might also serve as a starting point in providing knowledge of biomechanics to physiotherapists, working in the amputation field.

1.2 AMPUTEE POPULATION UNDER CONSIDERATION

The hospital in which the author of this thesis has worked for more than 25

years includes a Vascular Rehabilitation Unit linked with a limb-fitting centre. It is possible to say that the vascular rehabilitation unit of Villiers-Saint-Denis is one of the largest in France in respect of the number of amputees and prostheses fitted. The patients appear to be identical to those found in other places in the Western World (except the surgical dissimilarity mentioned above). They are discharged from the Rehabilitation Centre within six months of the amputation surgery. This comment requires the following remarks:

- Most of the subjects use walking aids such as canes, sticks, or frames, even 6 months after surgery.

- Most of the patients are elderly and fragile. This is why most of them cannot usually walk outside and use a staircase without a banister. Following the methods described by Day (1981) and O'Toole *et al.* (1985), their daily activity score is low. Their Russek's score was usually between 2 and 3 instead of 3 and 4 in Scotland at in-patient discharge (Condie *et al.*, 1996).

- Most of the subjects have pain and an unhealed stump wound. Therefore, they have a fluctuating gait pattern.

This is why, in the following chapters, all the subjects have been tested within six months after amputation and were using two walking aids.

1.3 MAIN RESEARCH PURPOSES

During a conference in Chicago, in 1992, reported by Michael & Bowker (1994), on prosthetics and orthotics research for the twenty-first century, one important goal was to highlight areas where research results were expected to be clinically relevant, thereby directly benefiting lower limb amputees.

There are two major steps in research: fundamental studies and clinical evaluation. That is for maximum patient benefit, research should strive for developments that can ultimately culminate in clinical, practical, integrated and affordable techniques.

Consequently, the aims of this project are in decreasing order of importance:

- To develop a temporal and kinetic gait study of vascular amputees in realistic conditions and daily rehabilitation, at an early stage of this activity, to assess and improve the rehabilitation of patients, and to provide objective indications and contraindications during the physiotherapy process, to verify some hypotheses concerning the final level of the functional outcomes of patients.

This target is given despite the misgiving of Paul (1994) who reported: "Although equipment is available which would allow easy acquisition of kinematic and kinetic data, its capital and running costs and the time required for test subject preparation and data analysis, generally militate against extensive utilisation in the clinical scene.".

For clinical gait analysis, the objective must be clearly specified at the outset. Over - optimistic purchases of sophisticated equipment have frequently led to disappointment, disillusion, and rejection of gait analysis in routine tasks. Consequently, the feasibility of employing such a system in a clinical setting must be evaluated in terms of cost, simplicity of use, encumbrance for the patient, time taken to obtain the results, the manner of results presentation, and finally, accuracy. As in everything, there are no easy solutions, but there is no doubt that wisely chosen equipment, used with care and thought, allows better assessment of the patients.

Therefore, particular attention is paid to these points, especially the convenience of routine use of all the designed devices. Because it is a plain kinetic study without any measurement of joint range of motions and gait velocity, the research could be named **"gait monitoring"** rather than **"gait assessment"** or **"gait analysis"** (see the following chapter 2). Besides its direct use in treatment planning, gait monitoring is also a powerful research tool, particularly in assessing the outcome of different forms of physiotherapist treatment.

- To understand the gait patterns of amputees using different walking aids with the major objective of improving the advice physiotherapists give to patients.

Therefore, from these two points, it is possible to indicate one purpose of this work. The intent was to develop a "physiotherapy tool" that therapists could use to

study day-to-day tasks. Furthermore, present treatment guidelines are typically subjective and lacking in scientific assessment to prove their efficiency (Durance, 1989; Biefang & Potthof, 1995).

- To compare walking behaviour and gait patterns when the same patient uses successively the provisional Plaster of Paris socket then the definitive acrylic resin socket.

- To increase benchmark data for elderly vascular amputees in correlation with those found in the literature (ISO, the Philadelphia Report 1978), (Lovely 1981), (Pashalides 1989), (Hubbard & McElroy 1994). Especially, when patients are using their prosthesis in daily use: outside the gait laboratory, to compare the performance of individual patients with averages from an established database and to accelerate the introduction of research findings into clinical practice application.

- To introduce the use of strain gauged transducers and rigorous calibration in the rehabilitation field of amputees in France.

Because the author of this thesis is a physiotherapist, the main goal was not to improve prostheses nor to evaluate the best prosthetic alignment but, to determine which factors of rehabilitation affect both the quality and the quantity of patients' ambulation. The opposite reasoning might be to exhibit the relationship between gait patterns, specially the way of using the walking devices in assisted ambulation and the rehabilitation process performed by the physiotherapist on the patient.

As previously stated, the study was conducted without any measurement of joint range of motions. Furthermore, no measurements were performed concerning the length of the prostheses, residual limb and thigh segment (for transtibial amputees). Consequently, no calculations of hip or knee intersegmental moments were conducted.

Thus, the common target shared with physiotherapy teams who work in this field, that is data for elderly vascular amputees could be used to compare outcomes with that of rehabilitated amputees in different programmes with different philosophies, to ensure that they were chosen on merit, rather than on fashion. A

spin-off was also to refute the common assertion (especially in France) that "what is conspicuously missing is the collaboration between clinical practitioners and quality researchers which will result in the most rapid advantages" (Becquet *et al.*, 1996).

To reach this objective, some patients, both transtibial and transfemoral may be followed all along their Rehabilitation Centre stay-in, at different stages of the rehabilitation programme.

For many reasons in elderly PVD patients, such as age, stump length, pain, health background (the list is not limited), it seems very difficult to compare patients among themselves. It is easier with traumatic patients to have a "control population" with a high enough activity score and established prosthesis users. It is also easier to consider traumatic stumps when mature and suitable for any fitting.

Usually, as already stated above, the stay of vascular amputees at Villiers-Saint-Denis Rehabilitation Centre is a few months, commencing two or three weeks after amputation. The wound of the stump is never totally closed, even on discharge. The stump volume is more or less still unstable.

This is why it seems significant to insist the criteria for patients inclusion:

1. peripheral Vascular Disease patient, including Buerger's disease;
2. period since amputation less than six months but if it is longer the patient should not be discharged from the Rehabilitation Centre;
3. presence of a stump wound which was never totally healed; this is why some patients stay for a long time in the Centre;
4. stump pain or residual ache;
5. use of two canes but most often two sticks (see definition and difference in section 2.6.7.3).

The last consequence of the weakness of the subjects was that it has not been possible to perform all planned tests with all patients (i.e., stair, outside gait). This is why the whole population was divided in several parts, each of them having its own protocol (see section 8.3).

1.3.1 Formulation of the thesis objectives

From these initial considerations, it is possible to state the main objectives of the presented work:

1. to develop a system for monitoring the gait of vascular amputees during the daily rehabilitation programme, at an early stage of this activity,
2. to improve the rehabilitation process and the advice given by physiotherapists to patients;
3. to attempt to acquire a knowledge of why VSD patients have commonly a less efficient outcome — walking aids are widely used — than those trained in other Rehabilitation Centres (Joublin & Joublin, 1986; Collin, *et al.*, 1992; Nagashima, *et al.*, 1993; Cutson, *et al.*, 1994; Ng, *et al.*, 1996).

To attain these targets, two intermediate steps were essential:

→ to understand the gait patterns of amputees using different walking aids;

→ to compare the walking behaviour and gait patterns when the same patient uses successively a provisional Plaster of Paris socket then a definitive acrylic resin socket.

Taking into account the above targets and the population studied, a fully portable data acquisition system, totally carried by the patient, was necessary. The author of this thesis did not wish to repeat the usual research process found in literature: a patient walking artificially, straight between video cameras, trying to hit a forceplate on the perfectly flat floor of a gait laboratory. It seems obvious that the weak, old and impressionable amputees must change their gait pattern in such surroundings (Grabiner *et al.*, 1995; Paul, 1996). Therefore, it was obvious that the patients might be studied in an environment similar to their usual gait-training atmosphere.

1.4 NECESSARY DEVICES FOR THIS INVESTIGATION

A simple catalogue of essential devices is presented.

1. **an easily removable pylon load transducer** (see chapters 3 & 4)

being able to measure at least the six signals corresponding to the components of ground force forwards, upwards and laterally, together with the moments of the resultant force about the vertical, forward and lateral axes. Thus, there are: 1)anterio-posterior and 2)lateral shear forces; 3)axial load; 4)anterio-posterior and 5)lateral moments plus 6)torque about the longitudinal axis of the prosthesis. However, torque is usually very small and it could eventually be neglected without any substantial decreasing the validity of the results. To reach this target, a new transducer had to be designed. The rational choice of such a novel device and its particular design is explained in the following section 2.3. A full calibration was conducted. Paul (1994) strongly asserted the importance of such a calibration taking regard of cross sensitivities (see chapter 6). Considering the removability of the new transducer, its dimensions are small and thus, a thorough discussion must be made about both the reliability and accuracy of it by means of some full validation tests, having both static and dynamic aspects (see chapter 7).

2. **two instrumented walking sticks or canes** able to measure accurately axial load. These devices must be calibrated and some validation tests have to be done (see section 5.3.3).

3. **a portable data recording unit,** accurate and reliable, capable of recording data from the transducer and walking sticks during sufficient time to test patients in realistic day to day life situations (more than ten minutes). This device must be carefully chosen to be fully compatible with the requirements for the gait assessment. Running costs and time required for test and data analyses have to be taken into account about the best choice (see section 5.2).

4. **a computer program** doing automatically the following tasks: reading raw data, applying the calibration matrix, providing processed data in an intelligible format such as graphs having standardised scales. Thus, it must be easy to run from raw to processed data and friendly enough to be used by a non-computer specialist such as a physiotherapist (see section 8.2).

The work presented in this thesis will show the efforts made to reach these goals.

2 PRELIMINARY STUDY

2.1 DESCRIPTION OF THE HOPITAL DE VILLIERS-SAINT-DENIS, FRENCH REHABILITATION CENTRE

2.1.1 Historical Background

Villiers-Saint-Denis is a small village of 798 inhabitants situated 80 kilometres East of Paris, midway between the French Capital and Rheims. Ten per cent of the village area is Champagne vineyards. Since the Middle Age, there has been a castle nearby the village. The present day "château" was built in early 18th century. In 1927, the property owner gave it to a Private Hospital Foundation « La Renaissance Sanitaire ».

This semi-public organisation had been founded a few years before to fight tuberculosis. In the early thirties, three pavilions were built in a woody park of 45 hectares. The hospital started its activity with 750 beds as a sanatorium. The buildings were abandoned during the Second World War and were re-opened from 1943 as a rest-hospital used for French Prisoners of War, coming back from Germany. In 1948, the hospital was modernised and tuberculosis patients started again to have treatment.

From the end of the sixties, the Centre Médico-Chirurgical had to address new pathologies considering the changes and improvement in tuberculosis treatment. The sanatorium started to be a Rehabilitation Centre.

Its administrative status is a non-profit private hospital, linked with the French National Health Service. It works under state administrative supervision. Each year, there is a discussion and a negotiation about the next budget between the hospital board of governors and the government administration.

The new pathologies admitted since the late sixties were orthopaedic and traumatic rehabilitation; cardiac health care; pneumology and peripheral vascular disease rehabilitation linked with a limb-fitting centre.

In 1968, the first dysvascular amputee was admitted to a new unit that

	Number	SPECIALITIES
Doctors of Medicine	4	2 PVD specialists 1 Physiotherapy specialist 1 PVD functional exploration specialist
Assistant Doctors	3	
Nurses	39	including 4 chief-nurses
Junior Nurses	15	for day and night duty
Physiotherapists	9	2 chief-physiotherapists included
Prosthetists	9	1 chief-prosthetist included
Occupational Therapist	1	
Cleaning Staff	21	

Table 2.1: The staff members of the Villiers-Saint-Denis Rehabilitation Centre

	Number of Patients admitted in VSD Rehabilitation Centre		
AMPUTATION LEVELS	**1984** Dupré *et al.*, 1985	**1996** Internal Report (unpublished)	**1997** Internal Report (unpublished)
Bilateral transfemoral	4	3	4
Transfemoral	105	82	77
Bilateral transfemoral / transtibial	10	7	8
Through - Knee	2	5	6
Bilateral transtibial	19	13	12
Transtibial	201	215	207
Partial Foot	48	86	91
TOTAL	**389**	**411**	**405**
Ratio transfemoral / transtibial	0.52	0.38	0.37
Ratio transfemoral / partial foot	2.18	0.95	0.84
Ratio transtibial / partial foot	4.18	2.50	2.27

Table 2.2: Patient distribution by amputation levels in the Villiers-Saint-Denis Rehabilitation Centre

expanded rapidly to an average of 120 amputees (the maximum at one time was 175 in the early eighties) permanently in-patient.

All patients are amputated in Vascular Surgery Units, mostly in Paris. Patients are transferred to the Villiers-Saint-Denis Unit within two or three weeks of amputation for wound healing, prosthetic management and rehabilitation training. All patients are full board. The duration of the in-hospital's stay-in time will be discussed later.

Since this date, more than 15 000 amputees have gone through the Vascular Unit. Most of them (about 90 %) were peripheral vascular disease patients.

2.1.2 The vascular department

The Peripheral Vascular Unit of Hôpital de Villiers-Saint-Denis is situated in a pavilion of 153 beds. The staff members are shown in table 2.1 and the patient distribution by amputation level in table 2.2.

In addition, they are many people common to all departments of the hospital: Kitchen's Staff, Maintenance Team, Administration ...etc... For the whole hospital, there are 520 staff members for 489 beds.

2.1.3 Descriptive Statistics of Patients staying in Villiers-Saint-Denis Rehabilitation Centre

In the following section, some descriptive data about patients of Villiers-Saint-Denis are given. Listing the categories of patients in our wards is important in order to give an appreciation of the population of subjects on which the tests presented later in this work have been made. Some characteristics of the amputees of Villiers-Saint-Denis justify some requirements, difficulties, and limits but introduce novelty to the research, presented in the following sections.

Dupré *et al.* (1985) carried out a complete statistical analysis of the year 1984 and it is useful to compare this with the VSD Hospital statistics (not published) for 1996 and 1997 to examine changes in the trend of amputation level. The number of patients and their amputation level are shown in table 2.2 while table 2.3 shows the distribution between the genders and the age of the population. There are still more

	1984		1996 Internal report (unpublished)	
MALE	70 %	≤ 70 years = 57 % ≥ 71 years = 43 %	68 %	≤ 70 years = 62 % ≥ 71 years = 38 %
FEMALE	30 %	≤ 70 years = 20 % ≥ 71 years = 80 %	32 %	≤ 70 years = 18 % ≥ 71 years = 82 %

Table 2.3: The distribution between the genders and the age of the amputee population of the Villiers-Saint-Denis Rehabilitation Centre, in 1984 and 1996.

DIABETES MELLITUS	1984 among all patients Dupré *et al.*, 1985	1996 among all patients Internal report (unpublished)
MALE	14 %	28 %
FEMALE	30 %	55 %

Table 2.4: Table showing the increasing trend of diabetes mellitus as related pathology in peripheral vascular disease.

male than female amputees because of the influence of tobacco abuse, which is greater in male subjects. All patients were amputated for peripheral vascular disease due to gangrene or acute ischaemia. Table 2.4 shows the diabetes mellitus ratio which is the most important related pathology. All of these statistics were in accordance with those found in the literature:

- most of them were amputated according to the method introduced in France by Cormier (1982) in the late sixties. The amputation was done at the limit of dead and live tissues. The surgical wound of the stump was not closed and second intention healing was awaited. An early ambulation programme speeds up the healing process, decreasing oedema and venous stasis. It was therefore easy to appreciate the extent of pain, denutrition and insomnia which the patients suffered.

- the mean age of patients and their probable survival (not shown). Stewart & Jain (1992) reported that the median survival of lower limb amputees was 4 years over a 25-year period. In other countries, previous reports by Harris in the USA (1988, quoted by Stewart *et al.*, 1992) and Eneroth & Persson in Sweden (1992) indicated that the mortality at 6 months was 38 %, at 3 years 52 % and at 4 years 72 %. Regarding the age of amputation, Eneroth & Persson (1992), reported a mean age at amputation of 77 (43 - 95) years, 75 years were men and 80 years were women; 49 % of amputees were aged 80 years or older. Joublin & Joublin (1986), in France, found that 75 % of women and 41 % of men were more than 70 years of age among a population of 252 PVD amputees.

- the higher rate of transtibial level versus transfemoral in 1996 and 1997 than that in 1984. The increase of below the knee amputations was highlighted by Stewart & Jain (1993). The general by decreasing trend of transfemoral versus transtibial and transfemoral versus partial foot amputees due to new vascular surgery techniques has been reported in countries such as Denmark (Ellitsgaard *et al.*,1997). Ebskov (1992) however pointed out that if a separation between non-diabetic and diabetic PVD amputees was made, the ratio between transfemoral and transtibial was inverted (60 % transfemoral / 40 % transtibial with vascular insufficiency aetiology versus 40 % transfemoral / 60 % transtibial with diabetes mellitus). This long term incidence of diabetes mellitus in lower extremity amputations was emphasised by

Moss *et al.* (1996).

- the importance of smoking habits in male elderly population was noted by Kulkarni & Kearsley (1993) which explains the majority of men found in the tested population shown in section 8.3.

- the high incidence of diabetes mellitus in female dysvascular amputation for whom this defect was the most important aetiology has been brought to the fore by De Frang *et al.* (1991) among a population of 2532 patients as shown in table 2.4.

- many amputees also have other concurrent medical problems. Troup (1976, quoted by Stewart & Jain 1992) reported that 75 % of primary amputees had at least one other significant pathology. In decreasing order, the most usual were: high blood pressure, coronary disease, breathing problems, arthrosis, etc.

In conclusion, it is possible to say that the vascular rehabilitation unit of Villiers-Saint-Denis is one of the most important in France: 411 patients in 1996 over a total of 8000 amputees in France (see table 2.2 and Germanaud, 1996) and the patients were similar to those shown in the literature review.

2.2 LITERATURE REVIEW ON ELDERLY AND VASCULAR AMPUTEES

2.2.1 Introduction

Due to the high level of the population of recent vascular amputees (about 8 000 new vascular lower limb amputees each year in France according to the French National Health Service and 35 000 in USA, average 0.14 ‰, as previously stated), a plan to study the biomechanical gait pattern of the amputees was made. Furthermore, in most scientific gait studies, most of the papers published are on traumatic amputees (reasonably fit young amputees). A primordial comment to insist on must be made: when research is about peripheral vascular disease amputees, for all subjects their movement only becomes standardised long after, (at least six months) the end of rehabilitation (Hubbard & McElroy, 1994). When recent amputees are

studied, the aetiology of the amputation is unknown (Cheung *et al.*, 1983). One of the strongest beliefs of the author of this thesis is that vascular amputees (mostly elderly) are so different to traumatic that a mixing of data would be a source of mistakes and erroneous conclusions (Dechamps & Pillu, 1994).

2.2.2 Elderly and peripheral vascular disease patients

Concerning elderly subjects only, Lemaire *et al.* (1993) wrote that a satisfactory level of clinical experience with the elderly exists in the prosthetic field but scientific research involving the gait of this group is lacking. The population for the Lemaire's study included eight men with transtibial amputations who were over 65 years of age but they had lost their leg due to trauma and had worn a prosthesis for at least 25 years. All of them were Canadian veterans of the Second World War. In addition, none of the subjects in the study had stump problems such as: pain, swelling, or pressure sores. This population was far from ours.

Concerning recent amputees, Cheung *et al.* (1983) do not indicate the pathology the selected subjects. However, studying the patient statistics such as age (49 - 71) and concurrent disabilities (among eight patients: one subject had the big toe of the anatomic leg amputated, one was blind and the one, being 70 years old, was bilateral transtibial with a time interval of three years between the two amputations), it could probably be concluded that most of them were PVD patients. The study focused on temporal asymmetry of gait at various stages of their training programme (see the discussion of results in chapter 8).

Concerning elderly patients with vascular disease, Hubbard & McElroy (1994) reported that benchmark data for lower limb amputees is often limited to young subjects who have had their amputations as the result of trauma. To fulfil this lack, these researchers tested a population of twenty elderly vascular transtibial amputees about seven months post - amputation and six months after the completion of the rehabilitation programme with gait training regimen. This is why all subjects walked without any walking aids during the test, although three (15 %) required a cane for outdoor ambulation. These subjects were therefore different from VSD amputees. The study was conducted in respect of kinetic (studies of forces and moments) and

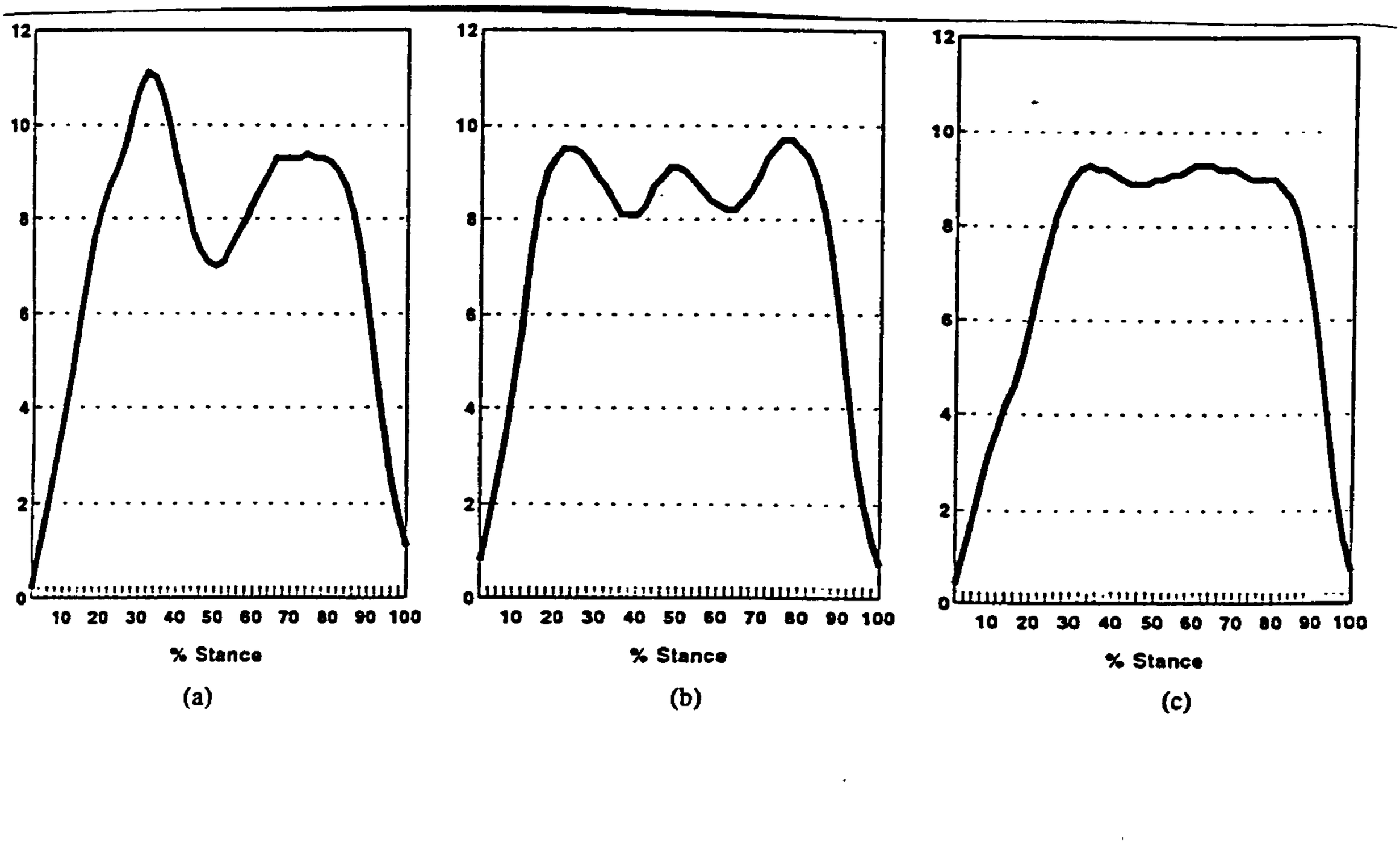

Figure 2.1: Three sample patterns of vertical ground reaction force in $N.kg^{-1}$ versus prosthetic stance phase: a) two peak pattern, b) three peak pattern and c) flattened pattern (extracted from Hubbard & McElroy, 1994).

kinematic (studies of position of the body segments) parameters (see the complete definitions in section 2.4). The level of variability in knee power was found to be significantly related to the preferred walking speed ($r = 0.68$, $p = 0.01$), indicating that consistency in power patterns at this joint is related to a better gait performance. One of the main results that it is possible to extract from this paper is the following: the mean stride time was 1.3 s with a statistically significant association between prosthetic stride time and gait speed. Three basic patterns in the vertical ground reaction forces were identified: two peak pattern, typically recorded in normal gait pattern (Seliktar & Mizrahi, 1986); three peak pattern (the second peak corresponds to the vertical position of the prosthetic shank tube) and flattened pattern as shown in figure 2.1. The authors revealed a relationship between the pattern type and the preferred walking speed: those walking at fast speed (but they did not specify from which value a walking speed is fast) wave most likely have a three peak pattern while those walking slowly have a flattened pattern. Because the test subjects (elderly PVD amputees) are close to those studied in this work, a comparison with the results expressed by these two researchers would be essential and a thorough discussion will be opened in sections 8.5 and 8.7.

Another important remark must be made about the way in which these research projects were conducted: in all of them, the subjects were asked to walk indoors, in a gait laboratory, most often in a straight line between a set of cameras and putting one foot on a force plate. When a transducer is used, an umbilical electric wire hampers the ambulation of the subject, even if the cable is long enough. This way of ambulation seems artificial and not able to reflect daily walking reality of weak and vulnerable elderly amputees. Therefore, as Paul (1994) reported: the major disadvantage of most prosthetic gait analysis is that it is undertaken in a gait analysis laboratory. The performance of the amputee in this situation does not correspond to his normal gait outside the laboratory, as shown by Grabiner *et al* (1995) and Paul (1996).

2.2.3 Cane-Assisted Gait

Murray *et al.* (1969) have conducted an investigation on 53 disabled men having unilateral disabilities of the lower limb. Among the tested subjects, there were

5 transfemoral, 2 transtibial amputees and 1 patient with a Syme amputation. Apart from this 30-year-old paper, the author of this thesis could not find any other papers concerning amputee assisted gait. Some papers have however been published in related topics, such as assisted gait with total hip replacement, bone fractures and paraplegia (Seireg *et al*, 1968; Ely & Smidt, 1977; Opila *et al*, 1987; Winter *et al*, 1993). Thus, very few research teams had the opportunity to use assistive walking devices fitted with load transducers despite the fact that most elderly amputees use at least one assistive walking device. This is why a lack of research on these patients can be noted.

Concerning the major results, it is possible to extract from these various papers the following considerations. Murray *et al.* (1969) noted the use of the canes in the sagittal and coronal planes. These researchers studied the percentage of the cane-floor contact time during the total cane cycle. They investigated the position of the canes when peak cane forces were applied by means of photographic records. The conclusion was that many of the test subjects applied peak force late in the stance phase on the disabled limb when both the cane and the disabled limb were directed obliquely backward. Therefore, since an assistive walking device is frequently used to compensate for deficiencies of functions normally performed by the neuro-musculo-skeletal system, the use of such a device may provide more than the obvious function of providing a prop for support. It may be used to provide forces to push or to pull the body forward, or provide forces to restrain the forward motion of the walking subject. However, all these data have shown wide variation in both the amplitude and duration of applied forces on the ground from one patient to another. Unfortunately, the main lack in such research is the lack of information: the test subjects were mixed.

Ely & Smidt (1977) investigated the effect of a cane, used in the hand contralateral to the involved hip, on patients' floor reaction forces and on selected time and distance measurements of gait. The average peak axial cane force was 15 percent of the body weight. Therefore, the patients exerted a significant amount of force on the cane, which was reflected primarily in lowering the axial loading and an anterior bending moment on the limb.

Opila *et al.* (1987) analysed twelve subjects who required two walking aids principally for one of three functions as follows: stability (temporal factors such as duration of double stance and velocity), support (ground and aids forces) and restraint/propulsion (impulse and transfer of mechanical energy). They included total hip replacement, tibial fracture, and paraplegic subjects. The authors affirmed that for such a study, there were three items to be measured: magnitude of the forces, symmetry of the restraining, propelling phases and timing of the stance phases of the aids and limbs. The results have shown a large variation in inter subject gait patterns and to protect both affected and unaffected limbs and joints from excessive loading, proper training and evaluation are essential.

Winter *et al.* (1993) described a technique and showed a standardised methodology to analyse the kinetics of cane - assisted gait. All profiles from recorded forces may be plotted on a normalised time base where one stride = 100 %, with heel strike (HS) at 0 % and the following HS at 100 %. The cadence of the gait has steps/min as unit while the gait rate is in $s.stride^{-1}$. All forces can be shown on two normalised forms: percentage of body-weight or force per unit mass of the subject. In other words, the results were normalised in force versus time. The results from Winter's study showed that the maximum vertical ground reaction force under the foot was reduced to about 75 % of that reported for unassisted gait. Hence, the single cane used made up about 25 % of the total reaction force. The anterio - posterior shear force peaks are drastically reduced, especially during the negative ground reaction force, i.e., during early stance phase (0 to 30 % of stride). However, two limitations were noted in their paper: 1) only maximum values were compared; 2) kinematics were not studied, therefore, limping which allows prosthetic force less than body weight even without cane was not recorded. These authors however noted the importance of the longer duration of the positive anterio - posterior force on the walking devices which indicated that the cane may be assisting in the forward propulsion of the body.

An important comment must be made concerning the equipment used by all these teams: the walking aids used were instrumented for more than one channel, at least three forces: axial and two shear forces in the case of Opila *et al.* (1987) and

Winter *et al.*(1993) or one compression force acting axially on the cane shaft; sagittal and frontal bending moments and torque in the case of Siereg *et al.*(1968), Murray *et al.* (1969) and Ely & Smidt (1977). This important point will be considered when the description (see section 5.4) and the results (see sections 8.5 and 8.8) from the instrumented walking aids used in this thesis will be presented

Despite the lack of research about amputees and aided gait, it is possible to indicate in which direction the work presented in this thesis has been conducted:

1. to describe the partitioning of the axial forces between the two assistive walking aids (ratio ipsilateral versus contralateral), then separating the left and right sticks or canes data from those of the artificial foot for right or left amputees. Two descriptive pictorial sketches, derived from Opila (1985), will only be used as a visualisation of various gait patterns, in order to improve the understanding at a glance rather than the use of sentences:

- a gait patient line (GPL) in which the chronology of gait events such as heel strike, toe off, sticks or canes strike and off will be shown;

- a vertical impulse histogram (VIH) in which the magnitude of axial forces on both sticks and limbs as a fraction of body weight are proportionally shown (see figures 8.8 and 8.9 in section 8.4);

2. to investigate the temporal parameters of the maximum peak forces on both the prosthesis and the walking aids (ratio of prosthetic stance phase force vs. stick or cane stance phase force; ratio stick or cane stance phase vs. gait rate). All the results will be discussed in chapter 8.

3. to analyse the gait patterns of recent transtibial and transfemoral amputees in the anterio - posterior plane, that is, in particular, the axial force, the A/P shear force and the A/P bending moment on the artificial limb in comparison to the forces acting on the walking aids.

However, to conduct such a study a carefully controlled gait procedure is mandatory, following the recommendations given by Winter (1994c, 1994d), then a thorough comparison with the papers mentioned above could be undertaken.

Consequently, a literature review, representative of the actual research in this field, is presented in the following section, showing which gait procedure was followed. Most of the papers, reviewed below, have two or more main topics, such as kinetics, kinematics, or metabolic energy consumption. They are, therefore, shown and commented upon at least twice (in each relevant section) before any conclusion relative to the validity of the present research and the asserted conclusions.

2.3 REQUIREMENTS FOR GAIT ASSESSMENT

2.3.1 Definition

In usual rehabilitation vocabulary, the term gait assessment should be applied to the whole process of examining a patient's gait and making suggestions for treatment. Therefore, gait assessment usually consists of six main elements: clinical analysis, videotape examination, measurement of general gait parameters including temporal ones, kinematic analysis, kinetic measurement, and electromyography (EMG). In contrast, Rose (1983) suggested that the term gait analysis should be reserved for the technical side of the gait assessment, i.e., kinematic, kinetic and EMG. This could be defined as the analysis of a subject's gait, based on the recording of one or several quantities derived from human movement science, primarily described in units used in the natural sciences (Harlaar, 1991). Although this terminology is not universally accepted, it makes a useful distinction between the overall assessment process and the procedure, which would normally take place in the gait laboratory. In the work presented below, only kinetics and temporal parameters will be studied, consequently, the terms gait assessment or gait analysis are not appropriate.

Therefore, the term gait monitoring (or ambulatory monitoring) could be chosen. Its definition should be the following:

gait monitoring: to carefully and thoroughly observe and check the patient's gait in order to see how it changes or progresses over a period of time (modified from Longman, Dictionary of Contemporary English, 1995).

2.3.2 Techniques used for gait analysis

2.3.2.1 VIDEO CAMERAS FOR KINEMATIC STUDIES

As stated above, gait analysis is mainly referred to kinematics and kinetics. For kinematics, the principal technique is to use video cameras linked with a computer. For kinetics, the use of force platforms is the most common.

If an overview of the studies conducted during the last 15 years is done, it is possible to bring out some of the main ideas. James & Öberg (1973) performed an investigation concerning prosthetic gait patterns in unilateral above-knee amputees, using two test shoes fitted with switches and goniometers to monitor knee motion. The thirty-four subjects were amputated due to trauma, all of them were active, with no complicating diseases or injuries. The mean period from amputation was 18 years. The mean stump length was 30 cm (range 16 - 41). By means of a long cable leading from the patient, electrical signals could be recorded. It allowed the subject to walk five strides (20-metre long level area). The main results, i.e., those important for the study presented in this thesis, were as follows: mean prosthetic stride time: 1.37 $s.stride^{-1}$, prosthetic stance phase: 0.77 s and swing phase: 0.60 s.

Cheung *et al.* (1983) used a walkway, 4.88 m in length, and two sets of photoelectric beam relays. The walkway was designed to measure the temporal parameters of the gait. Neither forces nor moments were recorded. As a group, the transtibial amputees displayed a higher walking speed and a shorter stride time than the transfemoral amputees. The authors emphasised that the results from the study were obtained from the subjects walking with the use of the parallel bars for support. This may be an important consideration when one wishes to compare these results with those from other studies. In Winter & Sienko (1988), each of eight transtibial amputees was asked to walk along a 10 m walkway. The biomechanical analyses used synchronised cine and force plate data along with a six channels EMG telemetry system. The aim of such a study was to conduct a range of biomechanical analyses (forces, moments and kinematics of the gait) and EMG profiles. The results showed several trends that indicated a somewhat modified, relative to normals, motor patterns from the residual muscles. Various artificial feet were studied which showed similar inverting moments of force patterns at the ankle: the dorsiflexor moment commencing at heel strike continued much longer into stance and the plantarflexor

moment reached about 2/3 of that seen in normals. Nissan (1991), working on the initiation of gait utilised two Kistler force platforms[1] and a Vicon system[2] using four TV cameras to test ten transtibial and eight transfemoral amputees. Among the thirty-one parameters, ground-foot forces, movements of the lower limb joints, and timing of the gait cycle at the ankle joint were measured. The amputees were divided into two sub-groups: those who start walking with their prosthesis and those starting with their normal leg. To facilitate comparison, all the results were normalised as recommended by most of the researcher teams, namely % of BW versus % of stride. According to the author (Nissan, 1991), the major inaccuracy of such a study was due to the small sizes of the various groups and the large numbers of variables involved. Therefore, a discussion about sample size will be conducted in chapter 8. Nissan (1991) also asked a number of gait laboratories to cooperate on this subject. Wirta *et al.* (1991) asked his subjects to walk on a level, vinyl tiled floor 7.5 m long and 2 m wide walkway. Furthermore, the subjects carried a flat multiconductor cable. However, the main lack of such a study is that the pathology was never mentioned. The main interest of the paper was the thorough description of the protocol (i.e., self-selected pace) and data treatment to compare results among subjects:

1) the beginning of the prosthetic limb support period (heel strike HS) has been defined as the beginning of the cycle starting with the prosthetic stance phase (PSP);

2) gait cycles not included were those clearly accelerative at initiation of gait and decelerative at cessation of gait;

3) normalised residual limb length was determined as a percentage of body height.

In section 8.2.3, the data treatment used in the presented work will be discussed and the method described by Wirta *et al.* (1991) will be partially taken into account. These authors made two important comments:

1) the large degree of bilateral asymmetry. This will not be recorded in the present research because no device has been fitted on the sound limb;

2) the value of the plantarflexion bending moment which is a reflection of the

---

[1]Kistler Instrumente AG, Switzerland.
[2]Oxford Metrics Ltd. Great Britain

anterio-posterior rotational angle of the artificial ankle axis at heel strike. This plantarflexion bending moment increased with the length of the stump, partly attributable to the longer limb developing a longer lever arm and thereby increasing the "stiffness of the system, socket-stump". In chapter 8, a discussion will be opened concerning this phenomenon.

Begg *et al.* (1991) described a low-cost (- 25 % of others available devices) microcomputer-based gait recording system which can be used to analyse gait routinely in the clinical environment. Foot-ground reaction forces are acquired and processed and the resultant force vector is superimposed on the television image of the subject in real time. Yang *et al.* (1991) reported important studies made in the Bioengineering Unit of the University of Strathclyde on the influence of limb alignment on the gait of transfemoral amputees. These researchers also used video markers and force plates. The main procedure quoted by Yang *et al.* (1991) about results is the following: most results were shown in the form of mean values of several test runs for each alignment setting rather than for any one particular run. The authors emphasised the considerable step-to-step variation for any gait variable, as already shown by Zahedi *et al.*, (1985). Therefore, averaging data of several test runs will reveal the trend along which a gait variable changes. In the Yang *et al.* (1991) paper also, the body build of the subject was taken into account, the kinetic gait variables were normalised to be a dimensionless form, that is, the ground reaction forces were normalised by the body weight (BW). Only A/P moments are shown in this paper. However, the main topic of this paper concerned the influence of the alignment of artificial limbs on the gait patterns. As previously stated, prosthetic alignment is not a preoccupation of the research described in this thesis, thus the investigation performed by Yang *et al.* (1991) has only been consulted in order to study their data processing techniques (see section 8.4).

Pinzur (1993) working on PVD through-knee amputees reported that he performed gait analysis with two AMTI Biomechanics Force Platforms[3] and a WATSMART Motion Monitoring System[4]. This review paper presented a compilation of data and

---

[3]Advanced Medical Technologies, Inc. MA. USA
[4]Northern Digital, Waterloo, Ontario, Canada.

the results were shown in a form, which was not very clear because the scale of the graph of the figure showing ground reaction forces was not indicated. In Boonstra *et al.* (1993) paper, the gait analysis was performed on a 10 m conductive level floor area and on a treadmill and by means of a questionnaire and measurement of energy expenditure. Presenting the subjects, the authors stated that 4 patients out of 29 walked with a stick, even for short distances but the importance of this fact was not mentioned in their method. The results focused on prosthetic stride time (PST = 1.38 $s.stride^{-1}$), showing a negative correlation with age; prosthetic swing phase (PSwP = 0.63 s, hence a prosthetic stance phase PSP of 1.38-0.63 = 0.75 s) and the range of motion at the hip and knee joints. These reported results, shown only in the form of tables rather than figures, will be discussed when the tests of this project are presented (see chapter 8).

Both Lemaire *et al.* (1993) and Hubbard & McElroy (1994) used video cameras and force platforms with subjects walking short distances. In the paper presented by Lemaire *et al.* (1993), the individual results were normalised to 100 % of the stride time and to body mass before overall averages were calculated for each subject and then for all subjects. The average curves were used for all analyses and comparisons between the test results and other data. This method of presenting the results will be discussed later in chapter 8.

Hermodsson *et al.* (1994b) used a Vifor[5] system for data collection of the gait performance. The main components of the Vifor system are a single force platform (Kistler) and two video cameras. The force platform was incorporated into the floor in the middle of an eight metres walkway and on a level with it. Only one step was studied. Both Hermodsson *et al.* (1994a) and Stefanyshin *et al.* (1994) had the aim to compare the gait performance of two groups with unilateral transtibial amputations for either vascular disease or trauma, and to compare the results with those from a group of healthy subjects. One of the criteria for inclusion of the study was to allow walking without using a walking aid. The vascular patients had a range of years since the amputation of 0 - 18, with a mean of 7; far from the criteria of the study

---

[5]Vifor, Uppsala: Uppsala University Departement of Technology, UPTEC 92011 R, Sweden;

	vascular group	trauma group	healthy group
prosthetic stance phase (PSP) s.stride^{-1}	0.83	0.80	0.67
maximum PGRF % BW	106	107	123

Table 2.5: The gait performance of three different groups of subjects (from Hermodsson *et al.*, 1994b).

presented in this thesis. Concerning gait performance, the main results could be summarised as shown in table 2.5.

The gait behaviour of amputees, having significantly reduced gait rate compared to healthy subjects, is confirmed. However, since the subjects had been amputated a long time ago, the PSP and PGRF of the vascular group did not differ from that of the trauma group. These results will be discussed again in chapter 8.

In France, Michaut *et al.* (1975) were the first researchers to study the gait of amputees on a long force platform. Pelisse (1981) developed the computer program for use with a single and double long force plate (see the next section 2.3.3.2 for a complete description).

2.3.2.2 FORCE PLATFORMS

A complete review of force measurement in human locomotion by the means of force platforms and pylon transducers was presented by Cunningham & Brown (1952). These authors reported the earliest contributions in this field.

The first approaches mainly concentrated on the vertical component of the force applied on the body by the ground. The first use of a force platform was reported by Amar in 1916. The design used by Amar was based on a plate supported by springs in three directions: vertical, medio-lateral, and anterio-posterior. The variations on the springs length were meant to reflect the loads applied on the platform.

The same principle was also used by Elftman in 1938. Displacements in vertical springs reflected the vertical load while displacements in the horizontal springs reflected the lateral and fore-and-aft shears. Measurement of the individual displacements of the vertical springs allowed the determination of the magnitude and position of the resultant reaction force. The three components and the position were then used to derive and calculate the torque about a vertical axis. This apparatus was a very important contribution to the study of kinetics of human locomotion but due to

- the large amount of deflection on the springs;
- the inertia effect on the platform;

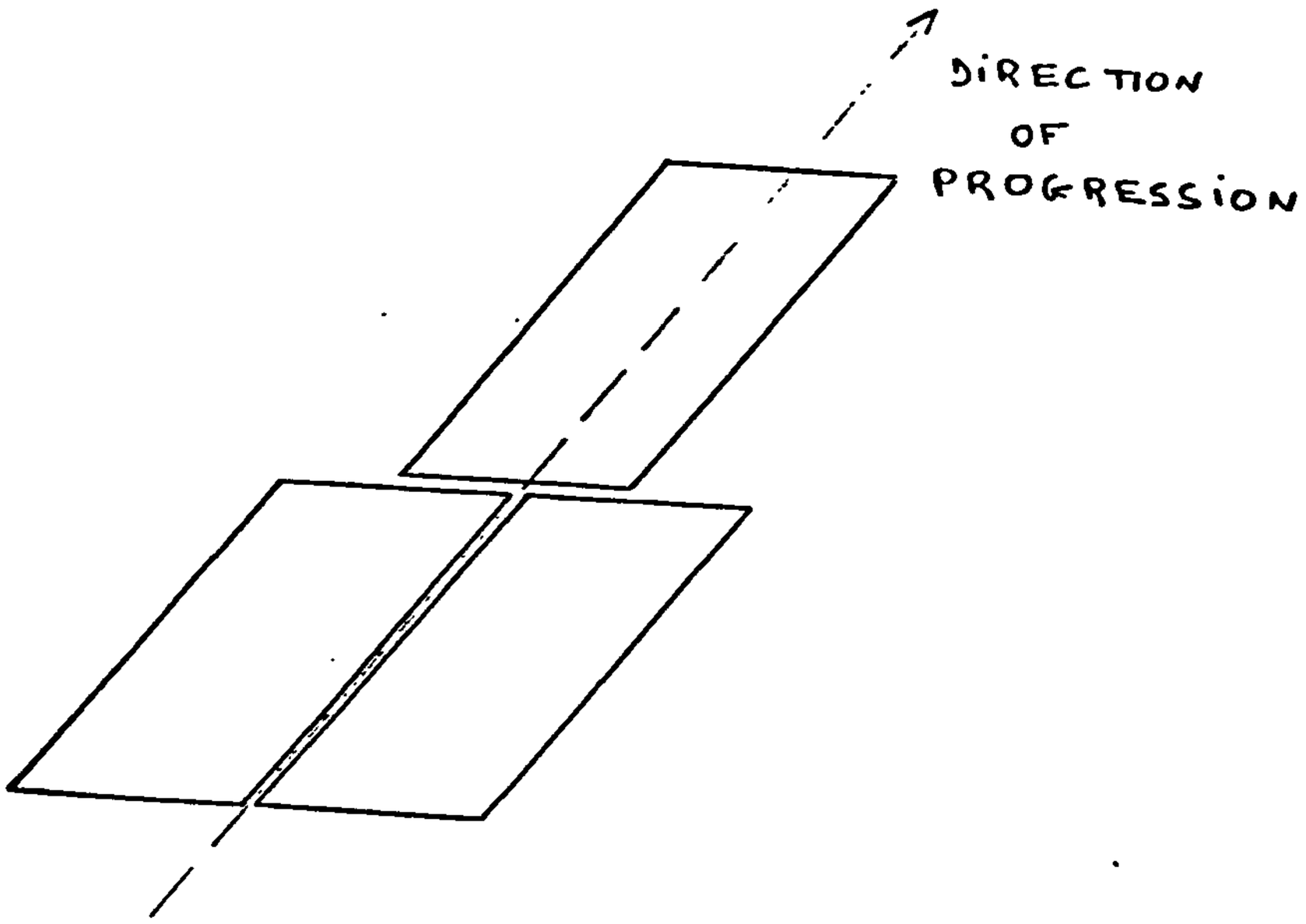

Figure 2.2: The set up of the three force platforms used in the Bioengineering Unit, University of Strathclyde

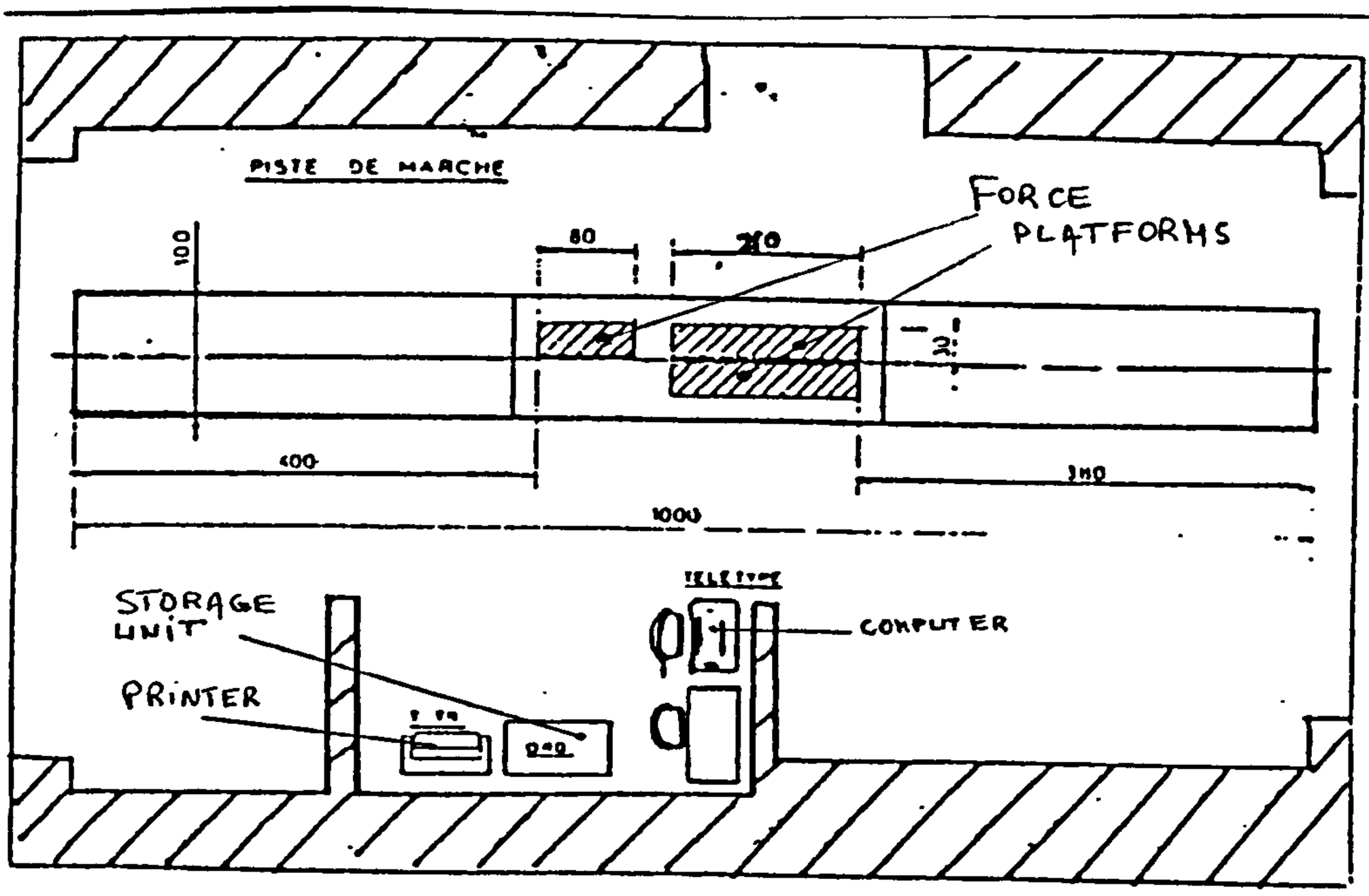

Figure 2.3: The walkway of the Rehabilitation Centre of Valenton (France) with three force platforms (all dimensions in centimetres)

- the high level of friction on the recording system;

it was not considered sufficiently accurate.

A second generation of force platforms was reported by Cunningham & Brown (1952). They described a device designed and used for the study of human gait carried by the University of California, Berkeley and reported by Eberhart *et al.* (1947). The principle was to use four electrical resistance strain gauged tubular columns bolted between a top plate and a steel base. Any load applied onto the top plate resulted in the generation of corresponding electrical signals from the gauges. These signals were monitored and recorded. A full calibration of the device was carried out and the new force platform provided the possibility of measuring the three components of the reaction force as well as the torque about a vertical axis applied by the ground on the foot. The location of the centre of pressure could also be calculated.

Cunningham & Brown (1952) raised the problem of oscillatory characteristics of both the electrical network and the mechanical system. They highlighted the fact that the natural frequency of a force measuring device should be far over 100 Hz. Their own force platform, due to viscous damping, had a frequency of 105 Hz for shear and 140 Hz for torque.

The next generation of force platform used piezoelectric crystals instead of the strain gauged pillars. This technology allowed a higher rigidity, natural frequency and sensitivity. In 1975, the Kistler Company marketed a force platform using the piezoelectric principle. Two cast aluminium plates were separated by four 3-force component quartz transducers. Loads in all directions could be measured, as well as the position of the centre of pressure. The natural frequency was higher than 200 Hz. This device is now commonly used in many countries for kinetic studies. Three of these plates are used in the Bioengineering Unit, arranged as shown in figure 2.2. This set up allows the recording of only one step defined as two successive identical events of the two feet (see section 2.6.7.1).

To monitor more than one step, Michaut *et al.* (1975) designed and developed two long force platforms installed side-by-side. The device was described by Levy

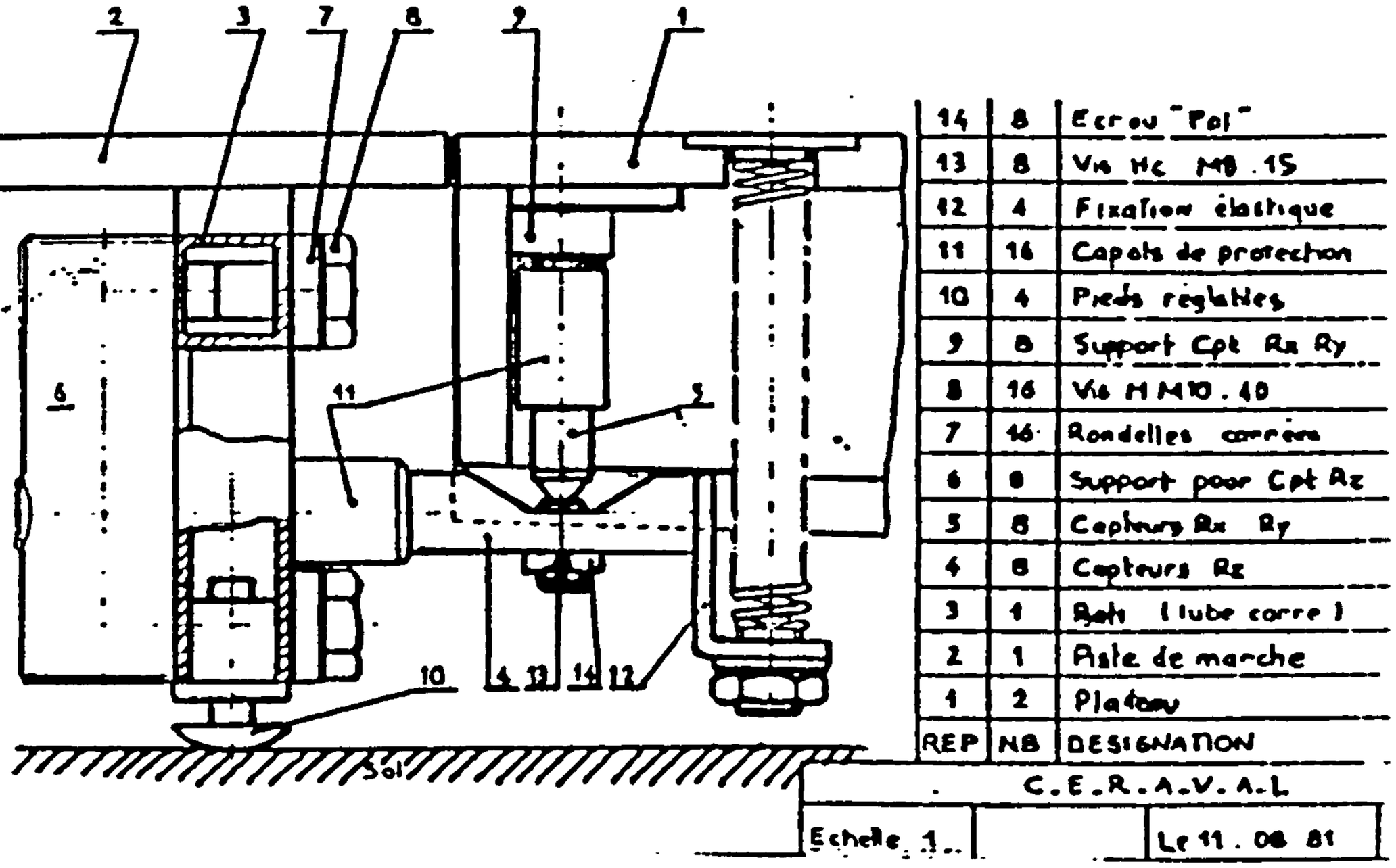

Figure 2.4: The set up of strain gauged transducers installed in the walkway of the Rehabilitation Centre of Valenton (France), from Levy, 1984-1985.-

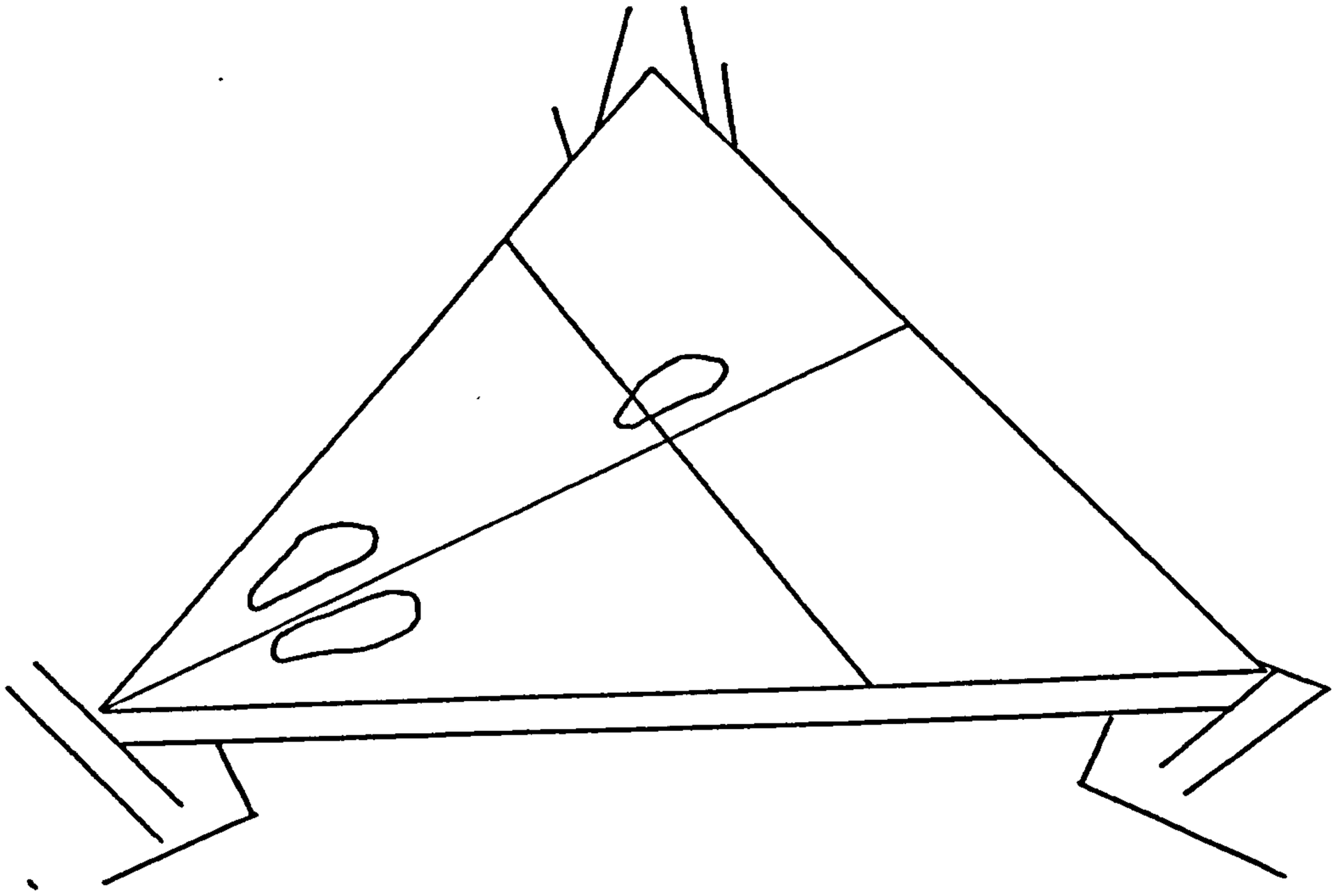

Figure 2.5: The triangular force platform of the Movement Laboratory in the Science University of Orsay (France), from Breniere *et al.*, 1981.

(1985): the walkway is 10 metres long and 1 metre wide in which three force platforms were included under a continuous vinyl floor cover and thus out of the view of the subject to minimise bias in the gait pattern as shown in figure 2.3. Two adjacent force platforms were 2.1 metres long and 0.3 metre wide. The third force plate was 0.8 x 0.3 metre, i.e., similar in size to the Kistler device. The axis of the latter was offset relative to the walkway axis to record the stride parameters from one foot, i.e., two successive events of the same foot. The transducers used were strain gauged (figure 2.4) as it was in Cunningham & Brown's (1952) with the same disadvantage about the frequency response. However, because of the physical properties of the set-up, it was easier for the subject to hit the three force platforms and therefore, the authors claimed that results would be better.

Another effort to improve force platform was made later by Brenière *et al.* (1981). These researchers designed a new shape (figure 2.5). The force platform consisted of an equilateral triangle, each side measuring two metres and suspended by means of cables with strain gauge systems that were sensitive to vertical force variations. This cable suspension left six degrees of freedom to the mechanical system and thus permitted measurements of the resultant and the moment of exterior forces exerted on the platform at any given point. Although, the frequency of the platform when loaded was only approximately 50 Hz, that was considered enough for their study. The initiation of the gait, which they were studying, did not produce frequencies as high as those of normal walking.

Besser *et al.* (1993) tried to expand the piezoelectric force platform technology to stair climbing but the authors said that large errors would result from small offsets in the centre of pressure, particularly due to abduction / adduction moments. Peak errors of 35 % were noted.

However, whatever the shape of the force platform, recording more than one or two steps proved impossible. This is unacceptable for the purpose of the study presented in this thesis. Granat *et al.* (1995) stated that all these systems such as video cameras and force platforms have several disadvantages these being: lack of portability, requirement of a dedicated laboratory and evaluated on the surface defined by the system. This lack was noticed in the past by several researchers who

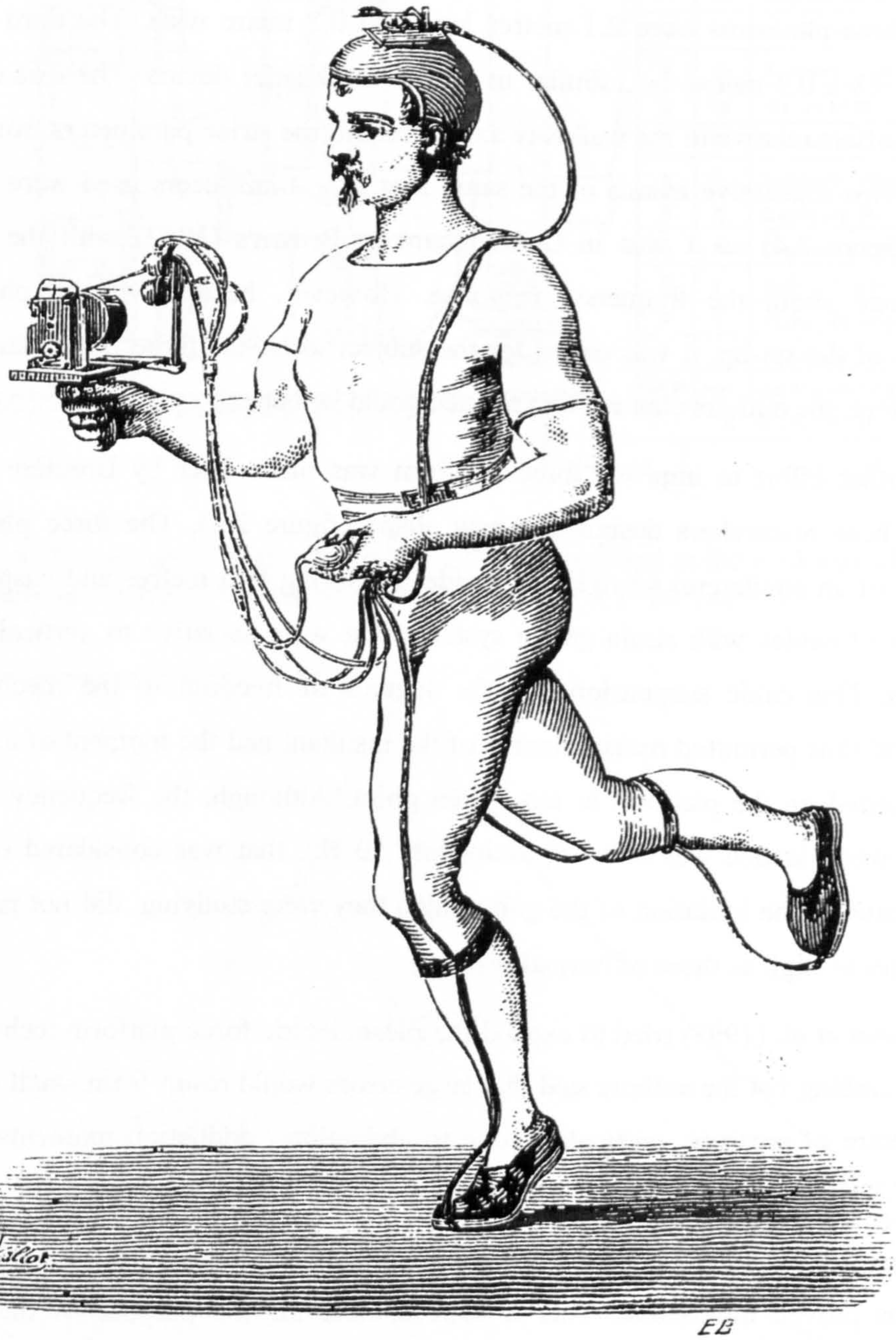

Figure 2.6: The « first transducer » used by E.J. Marey (France), from Marey, 1873.

recommended the use of pylon transducers. In 1973 and 1974 reports of ISPO Dundee Conference and DHSS Heathrow Conference respectively pointed out several advantages of pylon transducers over other methods of gait analysis. These reports highlighted three advantages:

1. Subject walkpath is not restricted;
2. Data from more than one step are obtainable;
3. Prosthesis loading data can be obtained without the need of any kinematic data.

These reports included an important recommendation: the pylon transducer should be manufactured from a material that will introduce little extra weight when inserted into the prosthesis.

However, to offset these advantages, two major drawbacks were stated and reported by Lovely (1982):

1. the umbilical cables interfere with the amputee's gait pattern
2. the length of the pylon transducer limited its use for transfemoral or transtibial amputees to those with rather short stumps.

Later in this dissertation (see section 2.3.5), methods are discussed for bypassing the trailing cables problem. The next section will discuss the size of pylon transducers.

2.3.2.3 PYLON TRANSDUCERS

A transducer is a device that converts a measurement of one physical quantity into another, in this case mechanical force into electrical voltage.

The first description of a "gait transducer" for gait studies was made by two French persons Carlet (1872) then Marey (1873). It was a pneumatic cell in the sole of the shoe and only the vertical component of the force applied on the body by the ground during a particular step was studied. Carlet's pneumatic apparatus consisted of a circular walkway twenty metres in circumference with a central recording instrument attached to the subject's shoes by long rubber hose. Marey (1873) modified the device to make the recording instrument portable and in doing so used

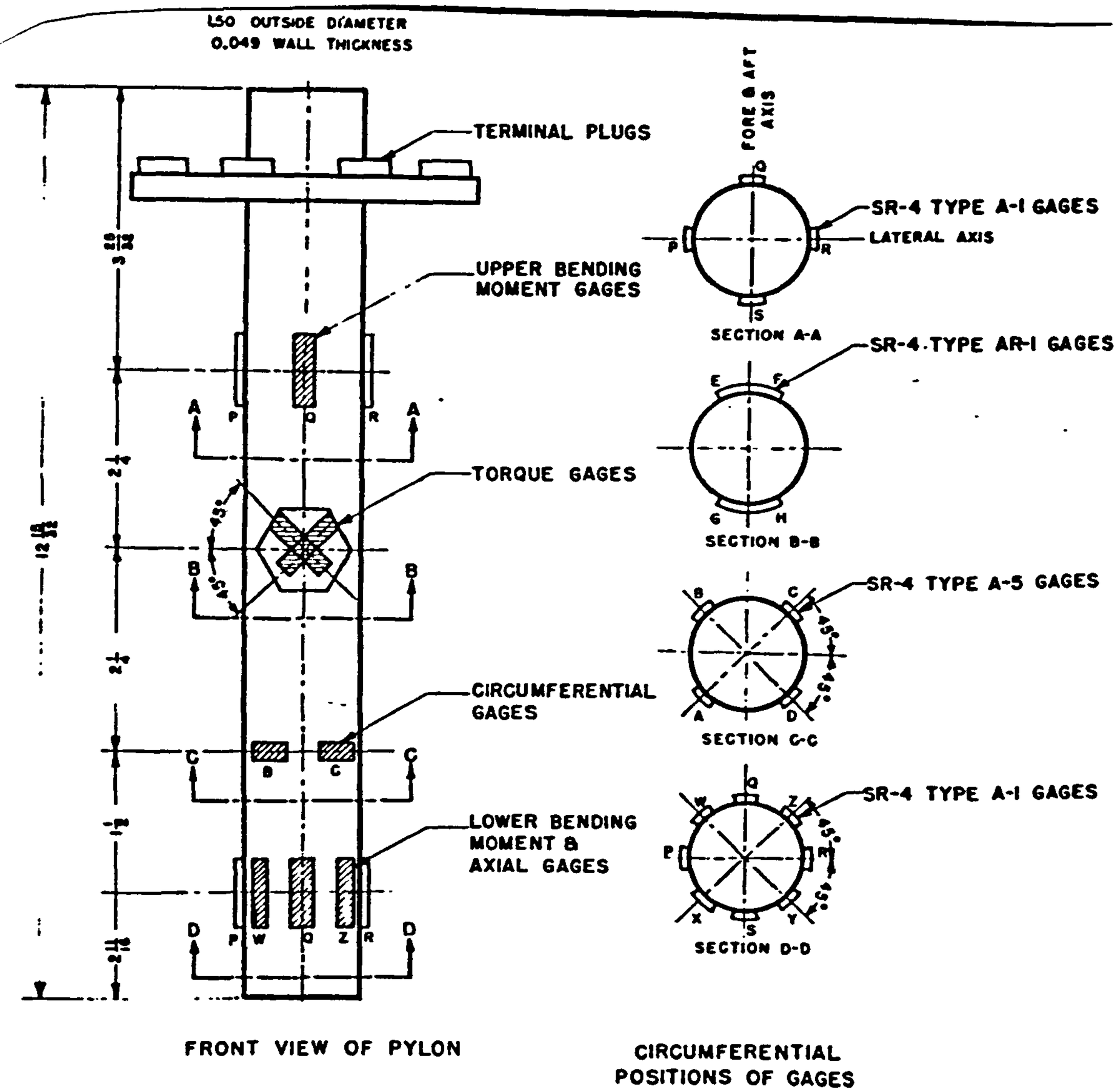

Figure 2.7: The pylon transducer designed in the late forties by Cunningham & Brown at Berkeley, University of California (from Cunningham & Brown, 1952) All dimensions are in inches.

one pneumatic cell instead of two in the sole designed by Carlet, as shown in figure 2.6. This was done with a non-amputated individual but the first thought of recording a subject walking freely was launched.

Recently, Alexander *et al.* (1990) reported a full description of foot to ground contact forces and plantar pressure distribution with a review of the evolution of current techniques and clinical applications. There is a place in the research setting for both floor-mounted and in-shoe devices. The same idea was adopted by those who designed, developed, and used a portable insole plantar pressure system (Wertsch *et al.* 1992) or a footswitch system to record temporal parameters of gait (Hausdorff *et al.* 1995).

With the arrival of modular prosthetic legs, gait analysis with pylon transducer also got underway. The first team who started such researches was in the University of California, Berkeley, in the late forties (Eberhart, 1947). One of the main tasks of the studies carried out was the understanding and measurement of the differences in walking patterns adopted by amputees when carrying loads, using different sockets or walking on different ground surfaces and slopes.

For that goal, a pylon transducer was developed and it was reported by Cunningham & Brown (1952). Their design consisted of a 304.8 mm long strain gauged aluminium alloy column with an external diameter of 38.1 mm and a wall thickness of 1.2 mm. This pylon transducer was meant to replace the shank tube of the artificial limb and record loads applied on it. It is shown in figure 2.7. The gauges were placed at four levels along the tubular surface and monitored the axial load, the torque and the bending moments in the anterio-posterior and medio-lateral directions at two levels. This particular configuration allowed indirectly the calculation of the shear forces in both directions, relative to the prosthetic leg.

Cunningham & Brown (1952) reported that the frequency response of the new device in dynamic loads was acceptable. The only limitation they noticed was the time required for a shock wave to travel along the pylon. It was obvious from the start that the pylon length should be decreased if a large population of amputees was to be tested. The shortest possible length in any transducer is necessary so that the

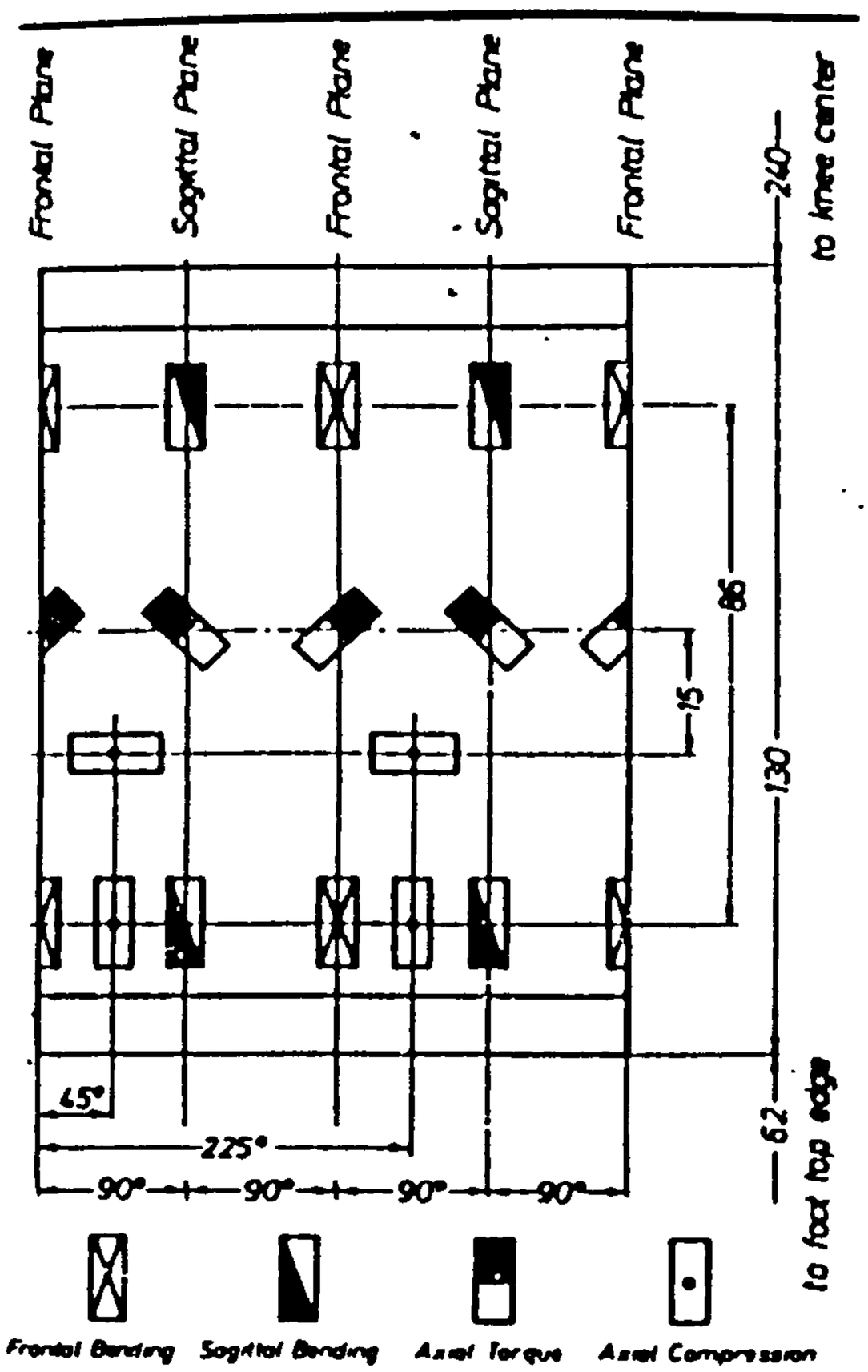

Figure 2.8: Arrangement of the strain gauged "Berlin" transducer on shin tube pylon (all dimensions in millimetres), (extracted from Boenick *et al.*, 1979)

device could be fitted to a large number of amputees.

Lowe (1969) reported the development of a pylon transducer with a length shorter than Cunningham & Brown's design: 127 mm. However, the external diameter remained exactly the same at 38.1 mm. Lowe used the same principle as Cunningham & Brown: the shear force signals were derived by measuring the bending moments at two different levels on the pylon. This method of determining the shear forces induced a conflict on the pylon design. Since shear force was calculated from the difference in bending moments at two levels: the larger the separation distance of the levels the more accurately the shear forces would thus be measured. The maximum distance between the levels is determined by the overall pylon length. Moreover, the strain gauges must not be too close to the end flanges, for fear of introducing undesired end-effects. Lowe (1969) made an engineering compromise which he claimed was successful.

Solomonidis (1989) reported that the design adopted by Lowe (1969) was not well constructed and as a result not very reliable. The method used for mounting the two glued flanges to the main test piece as well as the rather inaccurate bonding of the gauges introduced many unwanted cross-effects among the various channels.

Other research institutes developed other pylon transducers based on the Cunningham & Brown principle. Dewar & Judge (1980) at the Biomechanical Research and Development Unit (BRADU in Roehampton) and Boenick *et al.* (1979) at the Technical University of Berlin used a pylon with respectively 100 mm and 130 mm as length. The Berlin transducer was circular in cross section with external and internal diameters of 30 mm and 28 mm, respectively. The strain gauges were arranged as shown in figure 2.8. There were two independent strain gauge bridges for the bending stresses at different levels. This arrangement was necessary to calculate the moments acting at both the knee and the ankle which, due to the limited length of the pylon, could not be measured directly. Consequently, this applies to every pylon transducer.

However, in order to develop a shorter pylon, it was evident that a new design was required.

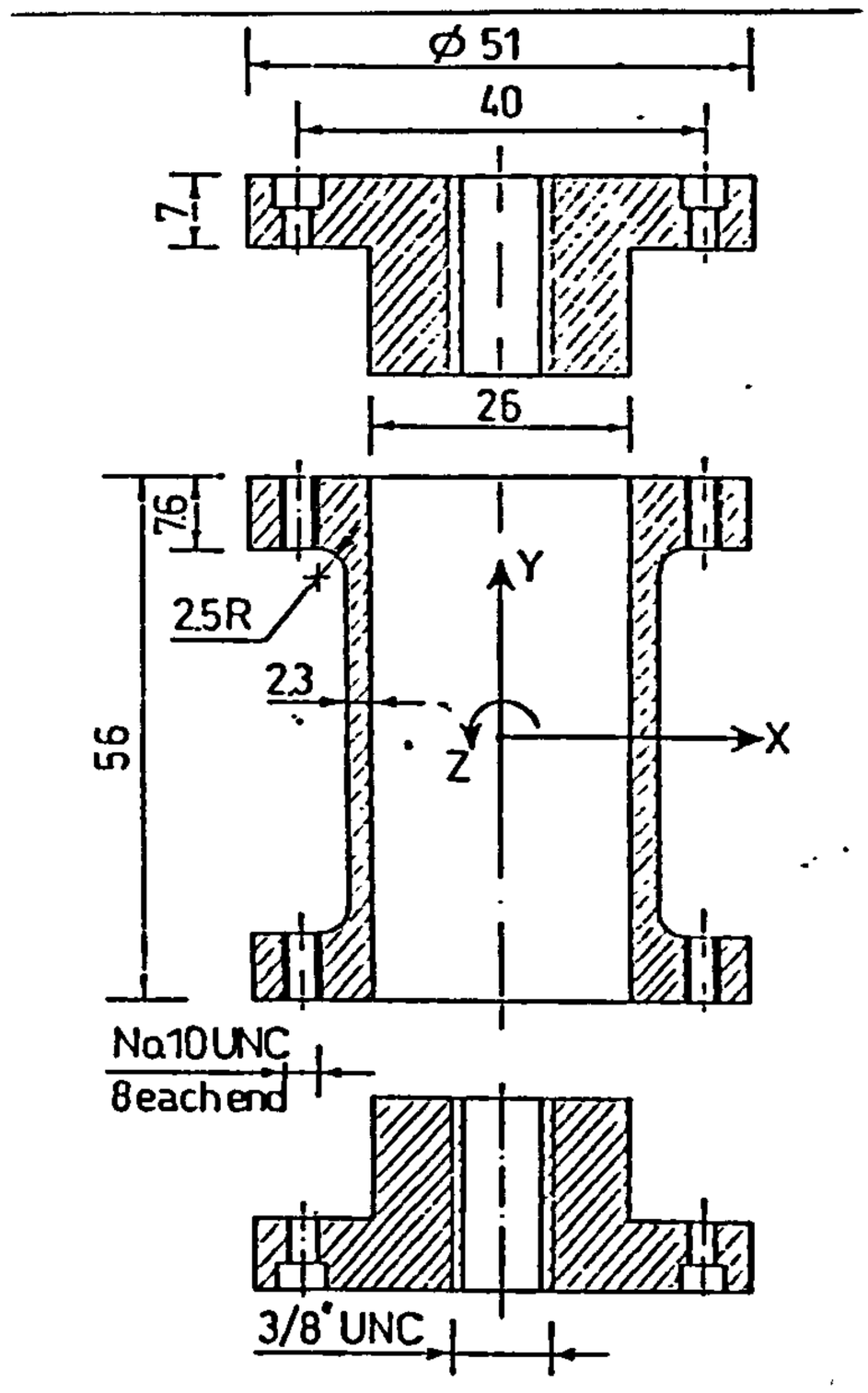

Figure 2.9: The transducer designed by Berme *et al.*, in 1975 in the Bioengineering Unit of the University of Strathclyde (Glasgow, Scotland), named Strathclyde Pylon Transducer (SPT) (extracted from Berme *et al.*, 1975)

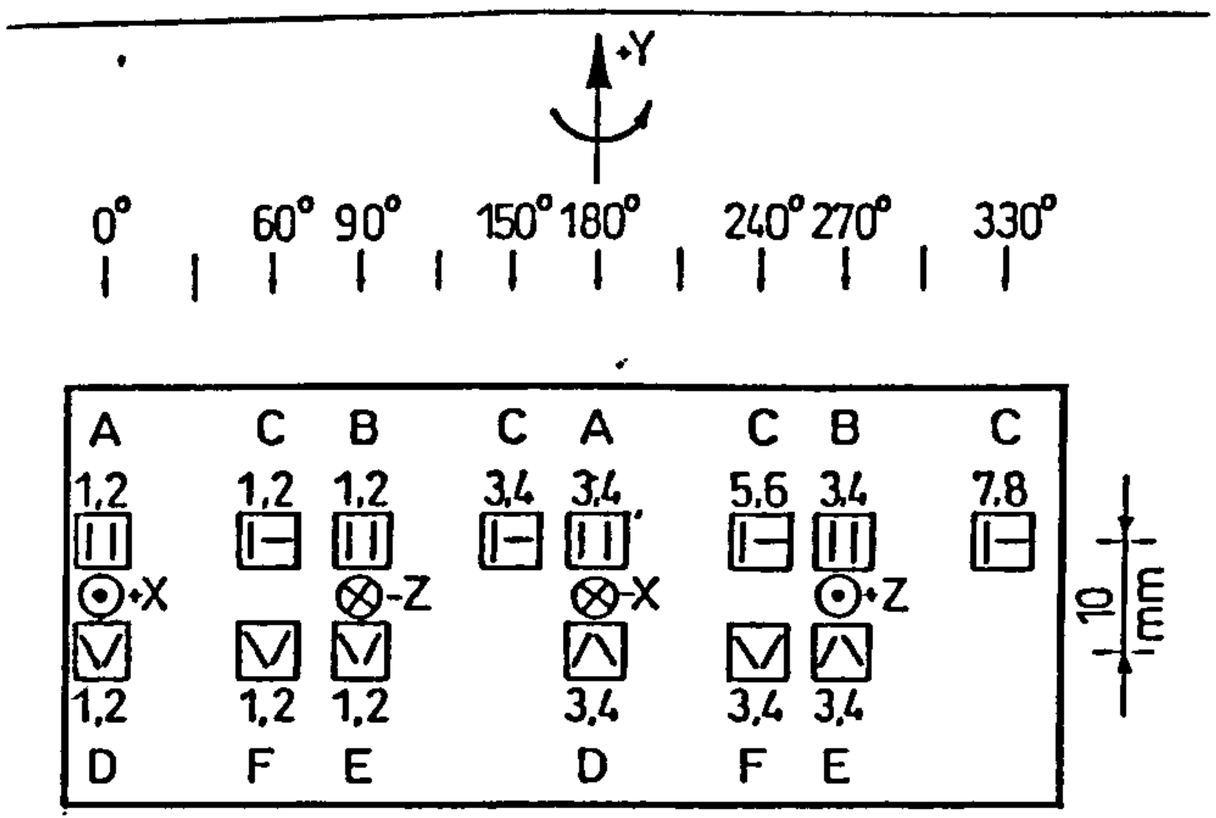

Figure 2.10: Lay out of the strain gauges fitted on the Strathclyde Pylon Transducer (SPT) (extracted from Magnissalis, 1992)

Berme *et al.* (1975) overcame the problem of pylon length by describing a new short pylon transducer for the measurement of prosthetic forces and moments. Their design deviated from that of Cunningham & Brown (1952) in that the shear forces in both anterio-posterior and medio-lateral planes were measured directly at a single level (fig 2.9 and 2.10). This change in design enabled the pylon transducer length to be reduced to 71 mm.

Calibration of this "new" pylon transducer was carried out by Berme *et al.* (1975), Grant-Thomson (1977), Lovely (1981), Pashalides (1989) and a full PhD thesis on the calibration, the behaviour and application of this device was written by Magnissalis (1992).

This short pylon has now become a standard in the Bioengineering Unit of the University of Strathclyde for a number of biomechanics research programmes. It will be used later in this work and referred to as "standard pylon" and reference device. In all the following chapters, this pylon, designed by Berme *et al.* (1975) will be named: the Strathclyde Pylon Transducer (SPT).

Morimoto & Tsuchiya (1984) and Nishiara *et al.* (1989) designed a pylon transducer described as a 30 mm long pylon cell, although, to date no full description of its design features nor experimental results have been published.

Sanders *et al* (1997) described a new generation of transducer as shown in figure 2.11. The sensing unit design is an improvement over previous transducers in that it is very thin (19 mm) and lightweight (527.5 g, including signal-conditioning unit). This new device has the drawback in that the outer ring dimension is 10 cm, which could be cumbersome during amputee ambulation by possible contact with the contralateral limb.

This non - exhaustive catalogue of transducers highlights three important observations:

1. Most kinetic studies used a force platform, in other words, only one gait event concerning one foot may be tested if one force platform is used. The usual set up is to use three force platforms (see section 2.3.2.2). Even when a long force platform is used, the subject must only walk straight ahead. Subjects always walk

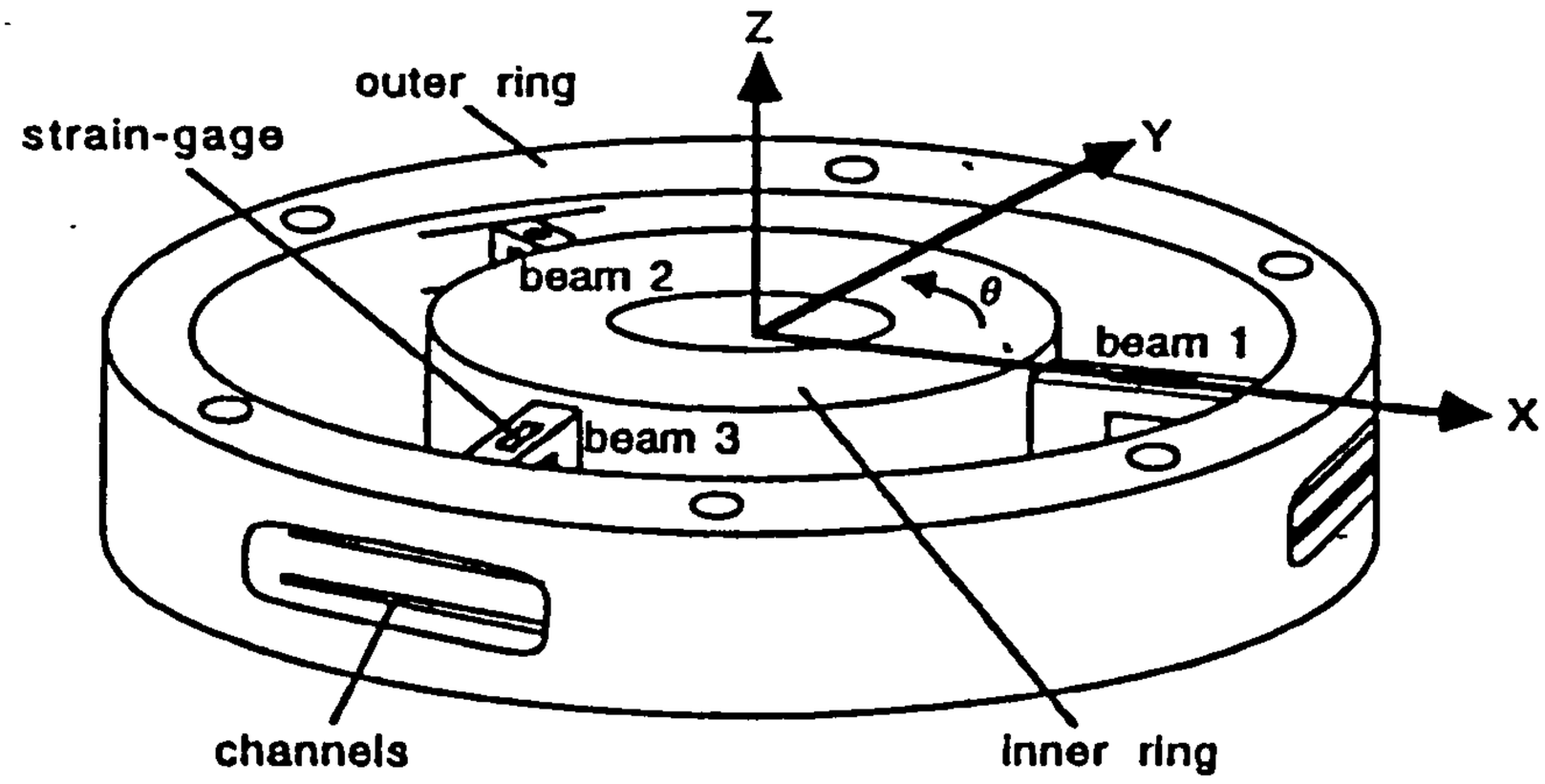

Figure 2.11: Schematic view of a modular six-directional force sensor for prosthetic assessment (extracted from Sanders *et al.*, 1997)

short distances, inside a Gait Laboratory on a flat floor, often between video cameras for kinematic data capture;

2. The use of portable pylon transducers is not common;

3. There is a complete lack of amputee gait studies, which uses both load measuring prostheses and assistive walking devices.

2.3.3 Unfinished Conclusions

For the acquisition of kinetic data, concerning the loads applied during locomotion, two types of force measuring systems have been mainly used since the last century: force platforms and transducers. As the years advanced, component forces were increasingly recorded while accuracy and sensitivity were progressively improved. Force platforms have the main disadvantage of recording only a particular step but some researchers have developed long force platforms avoiding this limitation. In addition, because the subject must hit the plate, it is difficult for psychological reasons to avoid unbiased data (Paul, 1994). Pylon transducers were introduced simultaneously with force platform (Cunnningham & Brown, 1952), which expanded the measurements to a larger number of steps without the necessity to walk on a straight line. The miniaturisation of all successive pylon transducers was another important field of research during the last fifty years.

As already mentioned, although its use is restricted, a force platform has been widely employed instead of pylon transducers; mainly, because pylon transducers cannot be readily incorporated into a prosthesis. The prosthetic shank tube has to be replaced by another one including the transducer while maintaining the height of the prosthesis.

As pylon transducers, the use of a force platform has also two main advantages: accuracy and repeatability. The time and the distance, between consecutive events of the feet, can be measured. An additional device, such as foot/floor contact switches, allows a count of the number of steps. It is therefore easy to calculate walking speed, step length, and almost all the gait parameters a researcher needs.

However, the lack of autonomy in gait ambulation is a difficulty for rehabilitation assessment: a force plate imposes to test patients on a flat ground floor in a gait laboratory. The solution has been known since a long time: what is required is an easily removable pylon transducer included into the prosthesis coupled up with a portable system for data acquisition (Boenick *et al.*, 1979, Lovely, 1981, Pashalides, 1989).

2.3.4 Recording Systems

Basically, there are two possibilities to allow free data acquisition (i.e., eliminated the umbilical cord) during the walking tests of patients:

1. data are immediately transferred from the patient to a storage unit by radio waves. This involves telemetric technology in real time.

2. data are stored in analogue or digital form and then transferred into a computer for analysis when the test is finished. This is a delayed time technology.

Rainaut (1974, quoted by Martinet *et al.* 1996) started to record electrogoniometry of the knee by the use of single channel telemetry.

Boenick *et al.* (1979) reported data collected from a freely walking amputee using telemetry to collect data from a resistance strain gauged pylon. The instrument recorded the maximum value of forces and moments by means of a transducer in the prosthesis. Lovely (1981) developed a portable recording system based on a personal dictating machine that allowed the acquisition of the time varying values of force and moment components allowing the comparison of the different values of individual load actions at any instant of time. The device provided the possibility of recording eight channels simultaneously during one hour with a C 120 cassette tape.

Hsu (1983, quoted by Martinet *et al.* 1996) reported an electromyography study with 4 channels and Gronley (1983, quoted by Martinet *et al.* 1996) used a 7 channels telemetric transmission.

The Lovely (1981) system was revised and a completely new design was produced by Pashalides (1989). This was based on a microprocessor system, which converted the data into digital form but stored it in analogue form on a basic audio

tape. Because of that, the reliability of both the devices used by Lovely and Pashalides was not faultless and random failures occurred causing loss of a channel. The solution appeared to re-design to a completely digital system. However, it must be recognised that laboratories and manufacturers cannot justify developing sophisticated devices in small quantities for small populations based on projected sales. This is why, in the disability field, such as amputees, low cost systems have been developed. Wertsch *et al.*, (1992) described a 8 bit digital portable data acquisition system whose main characteristics are: 14 channels, 5 seconds every minute over a 2-hour recording at a sampling frequency of 100 Hz. Sanders *et al.*, (1995) described a 19 channels numerical portable measurement system. A 4 Mbytes PCMCIA card was used for data storage and allowed collection of data for approximately 5 minutes of continuous monitoring. The system designed by Wertsch *et al.*, (1992) has been improved by Abu-Faraj *et al.*, (1997) and allowed real-time recording of both pressure and gait parameters (16 channels) for up to 8 hours (dependent on sampling rate).

Despite the uncertainty of the Pashalides (1989) recording system mentioned above, records of force and moment values have been obtained for test subjects walking on grass, gravel, stairs, slopes and in negotiating obstacles (Pashalides, 1989). Some comments on the results will be given later in this thesis in comparison to those obtained from the system in question in this work except that the subjects tested by Pashalides were not vascular amputees. Moreover, it is noticed that most often in the literature (except in Cheung *et al.*, 1983; see above section 2.2.2, where no specific pathology is stated), the population is under the age of fifty and the amputation is due to trauma.

Another important observation, which illustrates VSD requirements, was that the Berme *et al's* SPT (1975) used by all the researchers mentioned above was not easily removable without dismantling the shank tube. It will be shown, in appendix 11.II, that this task was not easy with the prostheses fitted in Villiers-Saint-Denis Rehabilitation Centre (see section 11.II.3.3.1).

It is therefore possible to draw a conclusion that VSD requirements: an easily removable pylon transducer plus two instrumented walking devices working coupled

to a portable data recording unit totally carried by the patient. The main goals are to study the temporal and kinetic aspects of the gait of recent vascular amputees and to describe the gait patterns of amputees using different assistive walking aids during the early stages of their rehabilitation.

2.4 LITERATURE REVIEW OF GAIT ASSESSMENT OR GAIT ANALYSIS

Porter & Roberts (1989) reported on the need for quantitative measurements of gait. They outlined how a skilled clinician will probably be able to recognise the major improvements of the patient's walk but minor changes will be much more difficult to detect. Among all the parameters reviewed by these two authors, two of them were especially important for the present research: temporal / distance and kinetic parameters.

Esquenazi (1994) showed how kinetic data can also be helpful in monitoring the progress in rehabilitation and the effectiveness of a particular intervention, i.e., changes to socket prosthetic components.

Whittle (1996) asserted the importance of gait analysis which has now advanced to the point where it is used as a routine part of patient management in certain Centres. He insisted that the major components to be measured were kinetic and kinematic factors. By combining kinematic and kinetic data, it is possible to calculate the joint moments and powers. However, according to Winter (1984), varying kinetics behaviour coexist with the same kinematic pattern. Kadaba *et al.* (1989, quoted by Baumann, 1991) asserted that kinematic patterns are typical for a particular person and they can be tested repetitively with a high constancy of results.

In the work presented in chapter 8, there are no kinematic investigations; hence, it will not be possible to evaluate joint moments or powers. As explained before, the tests conducted cannot be considered to constitute gait analysis but gait monitoring.

2.4.1 Temporal and Distance Characteristics

When studying the temporal and distance parameters of gait, three measurements give a general idea of how well a patient walks. They are (Whittle, 1996):

1. the cadence (stride.min^{-1}), gradually being superseded by the gait rate in s.stride^{-1};

2. the stride length;

3. the speed.

The full gait monitoring system described in this work will only be able to measure the gait rate, which is strongly linked with the speed (the mean speed is also named gait velocity in several papers). Since the stride length will always be unknown in the presented work, the gait rate will be used as the informative measure of general walking ability, as shown by Waters *et al.* (1976), Dewar & Judge (1980), and Perry (1992) (see section2.6.7.1).

The findings and conclusions of the various time/distance investigations can be summarised as follows: the single limb support time spent on the prosthetic limb is significantly less than that spent on the contralateral limb. This is 37 % of the gait cycle for the amputated limb and 43 % for the normal limb (Zuniga *et al.* 1972, Breakey, 1976). Single limb support time is the time spent weight bearing on only one extremity and is indicative of the time a patient is willing to tolerate weight bearing on an uncomfortable or weak limb. It is obvious that these considerations could only be determined for unassisted gait. A discussion concerning the single limb support for the tested subjects using two assistive walking devices will be opened when the recorded results are studied (see section 8.5 to 8.8). Studying forward gait velocity of transfemoral amputees, James & Oberg (1973) showed that this is reduced significantly (an average of 38 %), assumed to be caused by a shorter step length and a longer gait cycle than normal. Other researchers, such as Robinson *et al.*, (1977) and Waters *et al.* (1976) have confirmed these observations for both transtibial and transfemoral amputees. These subjects had a significantly lower free walking speed, cadence and stride length in comparison to normal subjects.

Moreover, Waters *et al.*, (1976) found the velocity of all vascular and traumatic transfemoral amputee subjects to be more than two standard deviations below the mean normal velocity. Öberg *et al.*, (1993) have conducted a thorough study (233 healthy subjects) concerning basic gait parameters and they presented reference data for normal subjects 10 - 79 years of age. Step frequency was as follows: from 1.05 stride.s^{-1} (40-49) to 0.91 stride.s^{-1} (70-79) for a normal gait speed (1.18-1.34 m.s^{-1} for men and 1.10-1.29 m.s^{-1} for women for self-selected gait). This gives an equivalent gait rate of respectively 0.95 to 1.09 s.stride^{-1}.

Boonstra *et al.*, (1994) reported important research about the gait of unilateral transfemoral amputees measuring temporal variables. Most patients (29 subjects) were amputated for traumatic reasons with only one because of acute arterial occlusion without signs of chronic vascular disease. Four patients walked with a stick, even for short distances. Unfortunately, these researchers did not mention the method they used to study these particular patients. The authors have corroborated other findings: the gait of transfemoral amputees was asymmetrical as far as temporal variables were concerned. The walking speed of the amputees was lower than that of non-amputees and showed a positive correlation with residual limb length and a negative correlation with age and stride time.

It will be interesting to compare these temporal characteristics to those found and shown in chapter 8. A thorough discussion, comparing normal subjects, traumatic and vascular amputees will be therefore conducted.

2.4.2 Temporal and distance parameters: Response to Training

Responses to training have also been studied. Kegel *et al.*, (1981) reported on the use of gait analysis to study the effects of strengthening the muscles of the residual limb of four traumatic transtibial amputees. All subjects showed an increase in gait speed (average of 13 %) over the training period. The study of Cheung *et al.*, (1983) is particularly interesting because it is believed that the subjects were recent vascular amputees. During training, the transtibial amputees always displayed a higher walking speed than the transfemoral amputees. The stride time of the transtibial amputee group was shorter than that of the transfemoral group. A marked

improvement in the walking speed of both transtibial and transfemoral amputees over the training period was shown, linked with a decreased stride time.

Here also, a comparison with the findings exhibited in the tests in this project will be interesting. This will be shown in chapter 8.

2.4.3 Kinetics

As already stated, most of the current gait research has been performed on young men with transtibial amputations. Seliktar & Mizrahi (1986) have conducted a study (using force plate analysis) involving the kinetics of transtibial amputee gait which provided important information regarding amputee locomotion. These authors suggested that the vertical impulse ratio, (the vertical impulse for the prosthetic leg divided by the vertical impulse for the sound leg), would be adequate for the assessment of amputee relaxed walking at a self-selected pace. Therefore, these researchers have focused on the non-amputated limb during locomotion of young amputees. Trying to corroborate these findings, Lemaire *et al.*, (1993) studied gait patterns from the non-amputated leg of experienced, elderly men with transtibial amputations.

Harris & Wertsch (1994) have made a full review of procedures for gait analysis. Concerning kinetics, these researchers emphasised one aspect of this part of the gait analysis: the ground reaction forces (GRF). They described the vertical component of the GRF trace looking like an "M" shaped curve with peaks typically of about 110 % body weight, in normal individuals walking at a fixed normal cadence (not defined in the paper). However, they found the vertical load curve to be unreliable as a clinical measure. This was largely due to its sensitivity to any action or reaction altering the ground reaction vector, such as arm lifting, trunk rotation or canes, which can diminish the peak component. An identical comment has also been made by Czerniecki & Gitter (1996) who tried to evaluate gait analysis for the development of improved prosthetic components. Shear forces were found to be affected by position and motion of body segments. Alterations in the vertical force pattern were reported as a result of weakness, pain and any unilateral lower limb pathology. Changes in gait rate also affected the magnitude and duration of the

vertical load curve, and the slope of the "M" curve, which reflects the rate of limb loading. Czerniecki & Gitter (1996) reported that amputees exhibit reduced loading rates on the prosthetic limb compared to normal subjects.

All these important comments will be raised in discussion of the tests carried out in this project (see chapter 8). However, it is important to note that the test subjects who are in question in this review paper were neither vascular nor elderly amputees.

Harris & Wertsch (1994) also recommended normalising moments to body weight and segment length. Hence, results might be expressed as a percent of body weight times residual limb length.

2.4.4 Gait Analysis in Clinical Applications

Rozendal (1991) has foreseen the main question: the physiotherapist or rehabilitation specialist seeks for an evaluation of the capacities of a patient, objectified and documented for future reference. Progress or the lack of it, and if possible a prognosis if progress is to be expected in a special case are problems posed by the clinician. Esquenazi (1994) commented that gait analysis should be a powerful tool to assess the gait of amputees. However, Esquenazi noticed that the current state of clinical care of amputees only permits the routine used of visual evaluation of gait.

Harlaar (1991) reported on the clinical use of biomechanics in gait analysis. The main part of his article concerned the conditions for clinical feasibility of biomechanical gait analysis. He focused his reflections on three conditions:

- Only those clinical decisions, where traditional assessment methods at the functional level lack discriminating power, should be subjected to possible improvement by means of gait analysis.

- A second condition for clinical feasibility is that the cost of equipment, time investment, and patient discomfort must be limited.

- A third condition is that « magical » parameters must be avoided, i.e., any new developed parameter resulting from biomechanical gait analysis, must have a

connection to the current ideas of clinicians. On the other hand, the limited knowledge of biomechanics amongst clinicians must not lead to a simplistic description of complex phenomena.

Baumann (1991) added some more particular requirements for clinical gait analysis such as:

- A representative number of step cycles must be evaluated and presented, usually 5. The variability within a series of steps represents a clinically important factor for gait assessment.

- The recording and testing instruments must provide sufficient temporal and spatial resolution, especially at the transitions from swing to stance phase.

- Special attention must be paid to measurements because they could produce results which are not only useless but which can also be misleading. Hence, it is mandatory to check the accuracy of recorded measurements and the calculations, which are performed.

Baumann (1991) also identified the importance of a few areas, which need particular attention:

- Body parameters such as standing height, sitting height and body weight;

- In persons such as amputees, mass distribution among and within the body segments can be greatly modified. This is of clinical relevance.

2.5 PRELIMINARY CONCLUSION

In summary, to reach the targets expressed in section 1.3 and 1.4 and following the recommendations of previous researchers, the research in this project was based on three main topics:

1. **Temporal parameters**: With the equipment designed and presented in this thesis, only temporal parameters will be studied such as gait rate (s.stride^{-1}), stance and swing time of both the residual limb and the assistive device. These parameters should be investigated: at different stages of training, for different types

of socket and different assistive walking devices. Hence, there will be successive studies of different patients (intra - subject investigation). Inter - subjects comparison will be conducted but with care to avoid unreliable conclusions. Due to the equipment used (see chapter 5), there will be no study of the sound leg, of gait velocity study or of stride lengths.

2. **Kinetics:** Despite the assertion of Harris & Wertstch (1994, see section 2.4.3), the longitudinal loading force (relative to the prosthetic shank tube), corresponding to the axial Ground Reaction Force (GRF), has been studied and used as an indicator of amputees locomotion. In the present study, the truthfulness of the axial GRF to accurately depict the gait pattern of the patients shall be linked with the low gait rate, assistive walking aids used, sockets worn and periods of training.

3. **Combined Studies of Temporal Parameters and Kinetics:** As already mentioned, there is a lack of information on assisted gait for amputees. Therefore, one of the original features of the work presented in this dissertation is the exploration of temporal and kinetic parameters of the walking aids used by individual patients compared to the axial load force, anterio-posterior shear forces and bending moments applied on the prosthesis.

The necessity of a transducer was dictated by the need of a portable device able to measure the gait rate. To have enough accuracy concerning the gait rate, the recording of several (an average of 10) gait events such as heel strike or toe off was necessary. The use of a force platform, which records only one step, was thus unacceptable. A sole sensor, such as the portable insole plantar pressure measurement system described by Wertsch *et al.* (1992) could have been considered. However, the mean accuracy of such a device is less than a transducer's as shown by Doutrellot *et al.* (1997). Moreover, a plantar pressure measurement device only expresses the axial load and the measurement of the A/P shear force and bending moments was likewise needed. However, it is obvious that a transducer, recording the six components of the gait (3 forces, 3 moments), provides more information that it was necessary for the presented work. However, due to the unknown and unexpected levels of inter-action effects when the calibration and the validation of the new transducer were performed, the recording and the study of the six

components of the gait cycle was necessary. Moreover, the novel transducer designed in the presented work could be used in the future for other research. The recording, the calibration and the validation of the six components of the gait cycle was thus an "investment" for the future.

Because we wanted the subjects to walk freely, on different terrains, the use of fixed video cameras was impossible. This is why the choice of a recording system, totally carried by the patient, was made. The data acquisition system chosen and described in section 5.3 has only 8 channels. Due to the recording of the 6 components of the gait cycle and the 2 axial loads on the walking aids, the 8 available channels were used. The addition of any other devices such as, electrogoniometers, accelerometers, or switches within the sole of the opposite footwear was thus impossible.

These decisions and the available equipment had two main drawbacks: no kinematics knowledge and a lack of measurements concerning the opposite sound limb. Hence,

- no information will be provided concerning the sound limb of the tested subjects is included in chapter 8, although its influence on the gait pattern has been noted by Hurley *et al.* (1990). These researchers studied 7 transtibial amputees (including one PVD patient having his amputation 2 years before) versus 4 non amputees. The amputees demonstrated a lower degree of symmetry than the non-amputees but forces acting across the joints of the contralateral limb were not significantly higher than of the non amputees. The PVD amputee displayed the lowest degree of lower limb symmetry, except a traumatic amputee recently amputated. In the presented thesis, the absence of such information regarding the sound limb is due to a lack of available channels on the recorder. It was thus impossible to record any information concerning the sound limb, even with a simple on/off switches sole between the foot and the shoe, as shown in section 5.3.

- no information on joint angles and limb segment lengths in included. As already stated, no calculations have been performed to determine the knee and hip moments. All the results are referred to the centre of the artificial ankle axis (see

sections 2.6.3 and 4.9). The lack of such information is due to the fact that no additional channel for an electrogoniometer was available on the recorder and the Rehabilitation Centre in which the tests were performed did not provide any video gait analysis facilities.

Before starting to describe the present study, a presentation of both the definitions used and conventions applied is necessary. These are presented in the following sections.

2.6 DEFINITIONS AND CONVENTIONS USED

2.6.1 Introduction

Biomechanics is a science in which mechanical principles are applied to the analysis of biological systems. Obviously, in the scientific field, all terms have distinct mechanical definitions and discussion of human performance, behaviour and response to environmental factors should adhere to exact definitions. This is why, at the beginning of any scientific investigation, a study of the vocabulary, definitions and terminology is necessary (Seliktar, 1994).

2.6.2 Terminology

In 1989, the International Standards Organisation (ISO) adopted terms intended for descriptive use in prosthetics (Schuch & Pritham, 1994). Since 1993, this terminology has also been supported and endorsed by the International Society for Prosthetics and Orthotics (ISPO Consensus Conference, in Copenhagen, 1992) and the International Society of Biomechanics.

2.6.2.1 APPLIANCES, PERSONNEL AND PROCEDURES

A prosthesis, named also a prosthetic device is an external device used to replace wholly, or in part, an absent limb segment. In classical Greek and Latin, one of the meanings of the prefix « pro » is « to stand for » or « instead of ».

A prosthetist is a person who, having completed an approved course of education and training, is authorised by an appropriate national authority to design, measure and fit prostheses. This person makes a prosthetic assessment, which is a

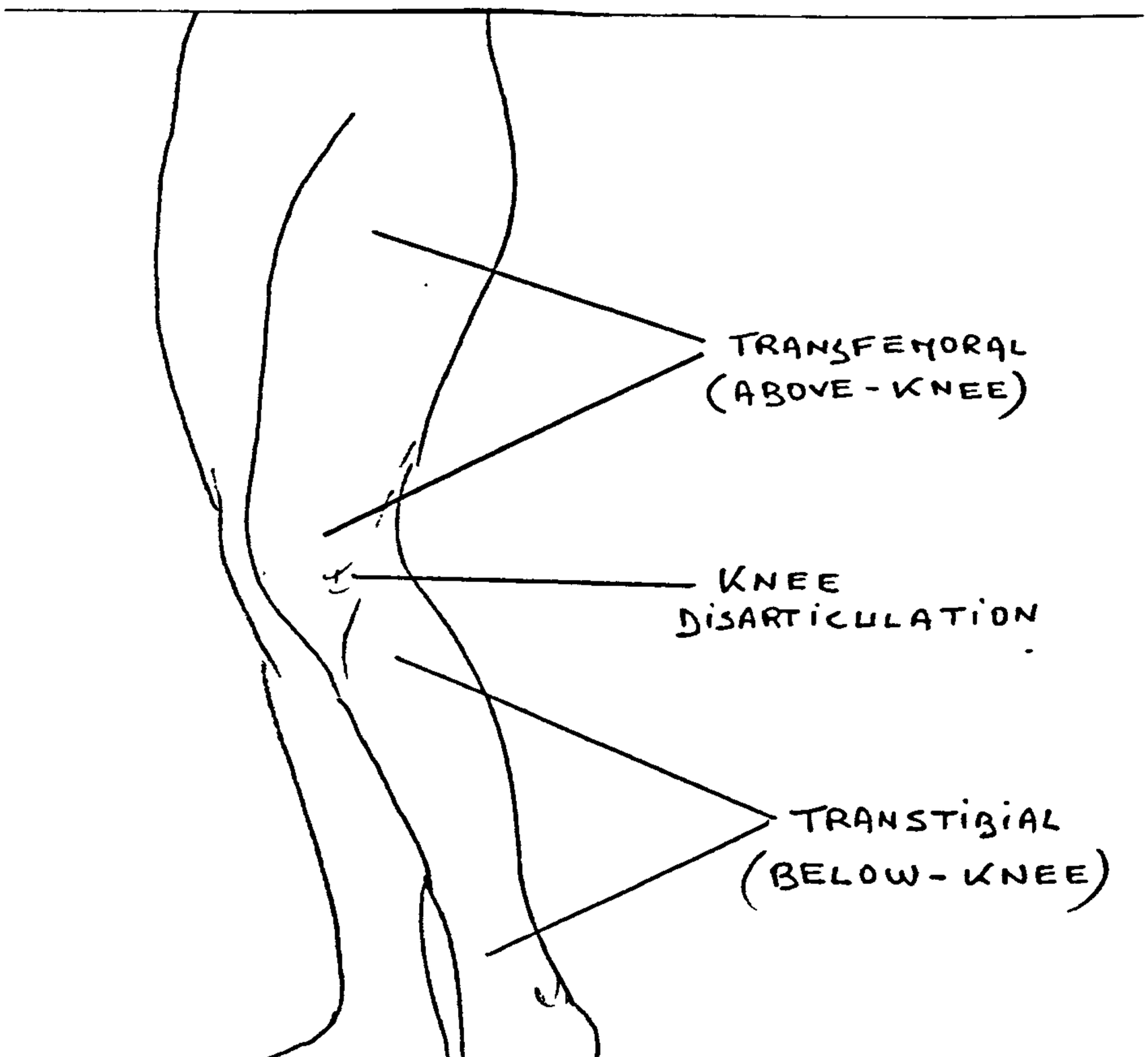

Figure 2.12: A depiction of the acquired amputation levels, the ISO terms and where applicable, the previously accepted terms.

review of the over-all condition of the patient by those involved in the treatment, and recommends the components and clinical fitting procedures best suited to the circumstances of that patient. The final assessment is referred to as the "check-out". The term fitting is used for the shaping and contouring of the inner surfaces of the socket to match the outer surface of the stump. The term alignment refers to the orientation and position in space of the components of the prosthesis relative to each other.

2.6.2.2 ANATOMICAL TERMS

The lower limb is that part of the body comprising the foot, the leg, the thigh, the pelvic girdle and the intermediate joints.

The ISO terminology about level of amputations of limbs with acquired amputations uses the prefix "trans" and the adjective disarticulation.

The prefix "trans" is used when the amputation is across the axis of a long bone, such as transfemoral or transtibial. Therefore, the transfemoral stump begins at any level above the femoral condyles and extends to ten centimetres below the hip joint while the transtibial amputations start above the ankle and extend to just below the tibial condyles. The optimal transtibial stump ranges between one-half and one-third of the length of the shank. In vascular surgery, it is difficult to perform plastic surgery covering the distal part of the bones by means of soft tissues (see appendix 11.II). Hence, this necessity renders the stump fleshy at its posterior aspect and bony at its anterior proximal and distal aspects. In both transfemoral and transtibial cases, a mechanically good stump should be long enough but should also allow sufficient room for the incorporation of prosthetic apparatus and alignment devices. However, the previously accepted practice of using the terms above knee and below knee is so common that these pairs of terms will be used as synonymous as shown in figure 2.12.

When the amputation is between long bones, which anatomically is through the centre of a joint, the adjective disarticulation is used (e.g., knee disarticulation). However, for the same reasons as above, the term through - knee shall also be used. Regarding general location of the section of amputation, the terms upper - third, middle - third and lower - third are strongly recommended by the ISO committee

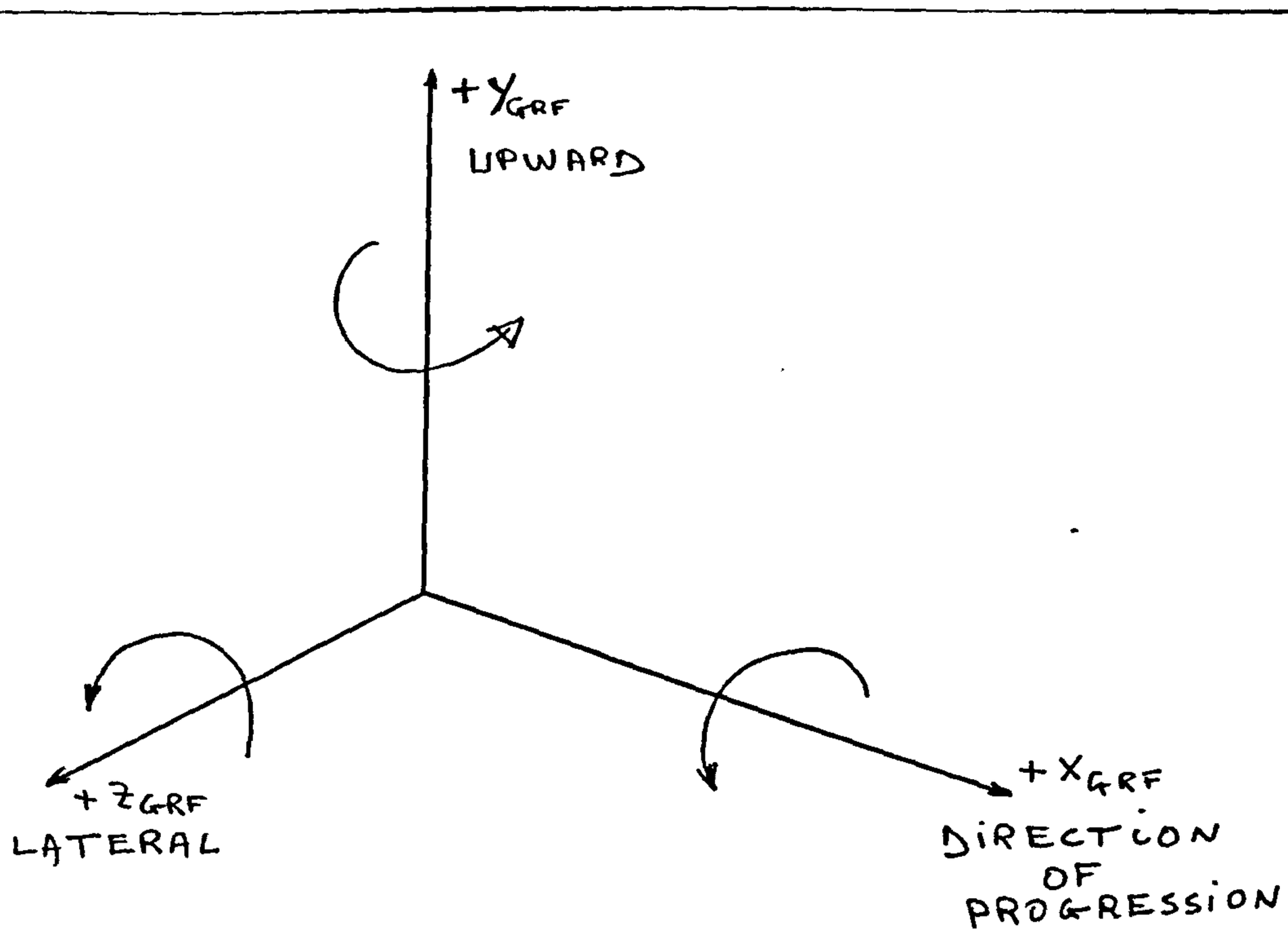

Figure 2.13: Cartesian co-ordinate system, right – hand rule, for the static reference standard. (extracted from Magnissalis, 1992)

(Schuch & Pritham, 1994).

2.6.3 Frames of reference

A frame of reference, that is a co-ordinate system, is required to describe the orientation and position in space of all devices and to characterise locomotion performance. In other words, a frame of reference has been always recognised as necessary for improving the effectiveness of the understanding of a report. The lack of uniformity is often an impediment to the reader who must resort to conversions in interpreting results.

2.6.3.1 GLOBAL REFERENCE FRAME

The frames used are all Cartesian X-Y-Z axes. In this thesis, the International Society of Biomechanics (ISB) recommendations and terminology for standardisation on the reporting of kinematic data (Wu & Cavanagh, 1995) are adopted but adapted to the application.

ISB gives the following definition to the Global Reference Frame (GloRF) with the direction of the global axes being consistent, no matter which activity or subject are being studied. The GloRF is on the form of a right-handed orthogonal triad fixed on the ground with the positive Y_{GloRF} axis upward and parallel with the field of gravity. X_{GloRF} and Z_{GloRF} axes are in a plane that is perpendicular to the Y_{GloRF} axis. Where there is a clear direction of travel (as it is in amputee's and normal gait), the positive X_{GloRF} axis is defined as the direction of travel and the positive Z_{GloRF} axis being defined by a left to right direction.

Thus, for linear measurements:

1. The X_{GloRF} axis is horizontal and positive in the direction of progression
2. The Y_{GloRF} axis is vertical and positive in the upward direction
3. The Z_{GloRF} axis is horizontal and positive in the left - to - right direction

This system offers the advantage that the anterio - posterior plane is marked out by the Y_{GloRF} axis as the ordinate while the X_{GloRF} axis is the abscissa. This system offers the disadvantage that the positive Z_{GloRF} direction is lateralward for the right side of the body and medialward for the left side of the body.

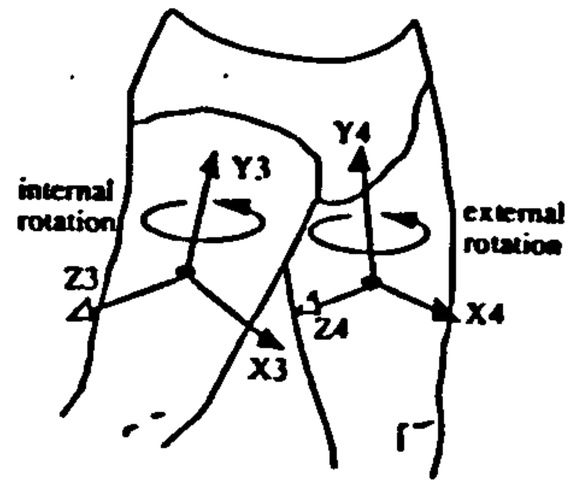

Figure 2.14: The same direction of rotations about segmental local centre of mass reference frames produce different motions on the left and right sides of the body (from Wu & Cavanagh, 1995)

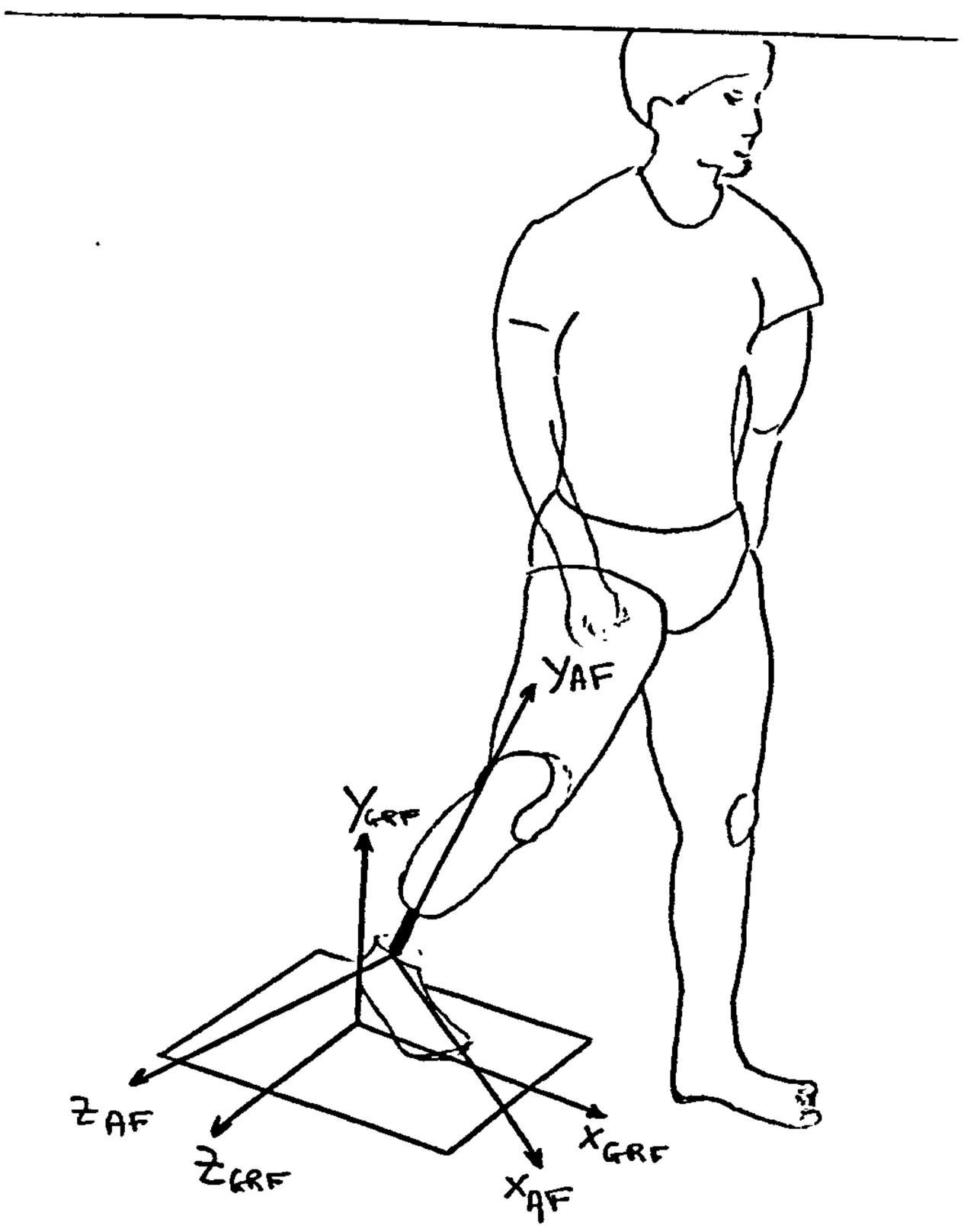

Figure 2.15: The foot and ankle axes (All directions shown are positive)

For angular measurements, the right - hand rule applies, that is, with the right hand grasping the axis and the thumb pointing in the positive direction of the axis, the fingers indicate the direction of positive direction. Accordingly, a clockwise rotation viewed in the positive direction of an axis is termed a positive rotation, as shown in figure 2.13.

ISB also recommends for segmental local centre of mass reference frames the use a right hand reference frame for both left and right body segments. This implies that for a segment on the right side of the body the positive local Z_{GRF} axis is pointing laterally while for a segment on the left side, the positive local Z_{GRF} axis is pointing medially. In other words, some forces or moments, although they are of the same nature, could have a different algebraic sign, as shown in figure 2.14. This could be a source of confusion and this is why a modification of the ISB proposition has been adopted:

- a right hand system for the right side
- a left hand system for the left side

As it was stated, because in gait, there is a clear direction of progression, the positive X_{GloRF} axis is defined as the direction of travel. This is true for both lower limbs of the subject. The Z_{GloRF} axis is perpendicular to the other two axes and positive towards the lateral side of the body. It is obvious that the direction of the Z_{GloRF} axis (if directed and positive) depends on whether the prosthesis is a right or a left side one, for reasons due to symmetry.

Therefore, the left and right side of the body Global References Frame is shown in figure 2.17, modified from Magnissalis (1992).

2.6.3.2 SEGMENTAL LOCAL CENTRE OF MASS REFERENCE FRAMES

Mainly because the prosthesis components are mechanical parts with well-defined dimensions and axes, the segmental local centre of mass reference frames can generally be readily define.

2.6.3.2.1 Foot and Ankle

At the middle point of the ankle axis of the artificial foot used in this work, an

origin for the three axes (see description of the monoaxial foot in appendix 11.II.4.2) could be defined. From this origin point, a frame can be defined for both foot and ankle. The Y_{AF} - axis joins the middle point of the ankle axis to the middle point of the knee joint axes. The X_{AF} - axis is perpendicular to the ankle axis and it has an external angle (relatively to the X_{GloRF} axis), the Z_{AF} - axis being mutually perpendicular to the X_{AF} and the Y_{AF} axes. In other words, the Z - axis of both ankle and foot is the axis of the rotational ankle hinge as shown in figure 2.15, in which the three arrows are in the positive directions. It is obvious that the segmental ankle-foot frame $(X, Y, Z)_{AF}$ is moving relative to the Global Reference Frame $(X, Y, Z)_{GloRF}$ when a subject is walking during a gait test.

2.6.3.2.2 Knee joint

Obviously, this is only used for transfemoral prostheses. Exactly as it is for the ankle, the middle point of the knee hinge axis can be defined as an origin point. This is possible whatever the prosthetic knee device is. From this point, the Y_K - axis joins, positively, the middle of the knee axis to the rotational centre of the hip joint; the X_K - axis is perpendicular to the knee axis and positive forwards while the Z_K - axis is perpendicular to the other two and positive laterally.

2.6.3.3 FRAME OF REFERENCE USED

All frames are thus defined and using them, it is possible to identify the position and orientation of any prosthetic component, just as easily with respect to any local system or to the GRF. For this purpose, three approaches can be adopted:

1. considering the Global Reference Frame as the universal reference and any part of the prosthesis, can be described with respect to it.

2. considering the ankle - foot frame as the universal reference and any part of the prosthesis, can be described with respect to it.

3. considering the socket frame as the universal reference and any part of the prosthesis, can be described with respect to it.

In our daily vocabulary, shared between physiotherapists, prosthetists, medicine doctors and patients, the socket with the patient's stump inside is used as the reference frame. For example, from this point of view, an external rotation of the

ankle - foot axis is called a toe - out angle. It was thought that accurately determining socket axes is not easy and subject to many uncertainties. Therefore, this medical approach, as it was noted by Magnissalis (1992), could not be used in biomechanical studies because it lacks of precision.

Thus, from an engineering point of view, only the two first approaches may be used. The ground or the entire ankle - foot are the contact zone through which the ground forces are transmitted to the amputee's body, via the prosthesis.

Therefore, two choices are possible; each having advantages and disadvantages. An adaptation of the approach number two was chosen because it offers a good compromise between the daily medical vocabulary used in a Rehabilitation Centre and the language of engineers.

In this thesis, the Foot-Ankle Reference Frame $(X, Y, Z)_{AF}$ (see section 2.7.1.1.1), having its origin at the middle point of the rotational artificial ankle axis, will be the universal reference frame (URF) of the prosthesis and the new Villiers Pylon Transducer presented in section 4.8. Consequently, all alignment parameters described later in this work are considered with the centre of the ankle - foot rotational axis being the origin of the unique frame of reference. This unique frame of reference will be merged with the pylon frame of reference defined in chapter 6. In other words, the axis system used in the presented work is moving relative to the Global Reference Frame defined in section 2.7 but it is fixed relative to the prosthesis and the new Villiers Pylon Transducer. This axis system also follows the recommendation of the ISO which axis system is based on the line from ankle centre to knee centre. In the following chapters and for simplification reasons, the Universal Reference Frame chosen will be named X, Y and Z, without any subscript. Any confusion with the axis convention used in previous researches is avoided (Berme *et al.*, 1975; Lawes, 1982; Pashalides, 1989; Magnissalis, 1992).

It is also important to note that no measurement was taken of angles between the shank tube of the prosthesis and the Global Reference Frame. Therefore, no relationship between the Global Reference Frame and the Universal Reference Frame used can be given.

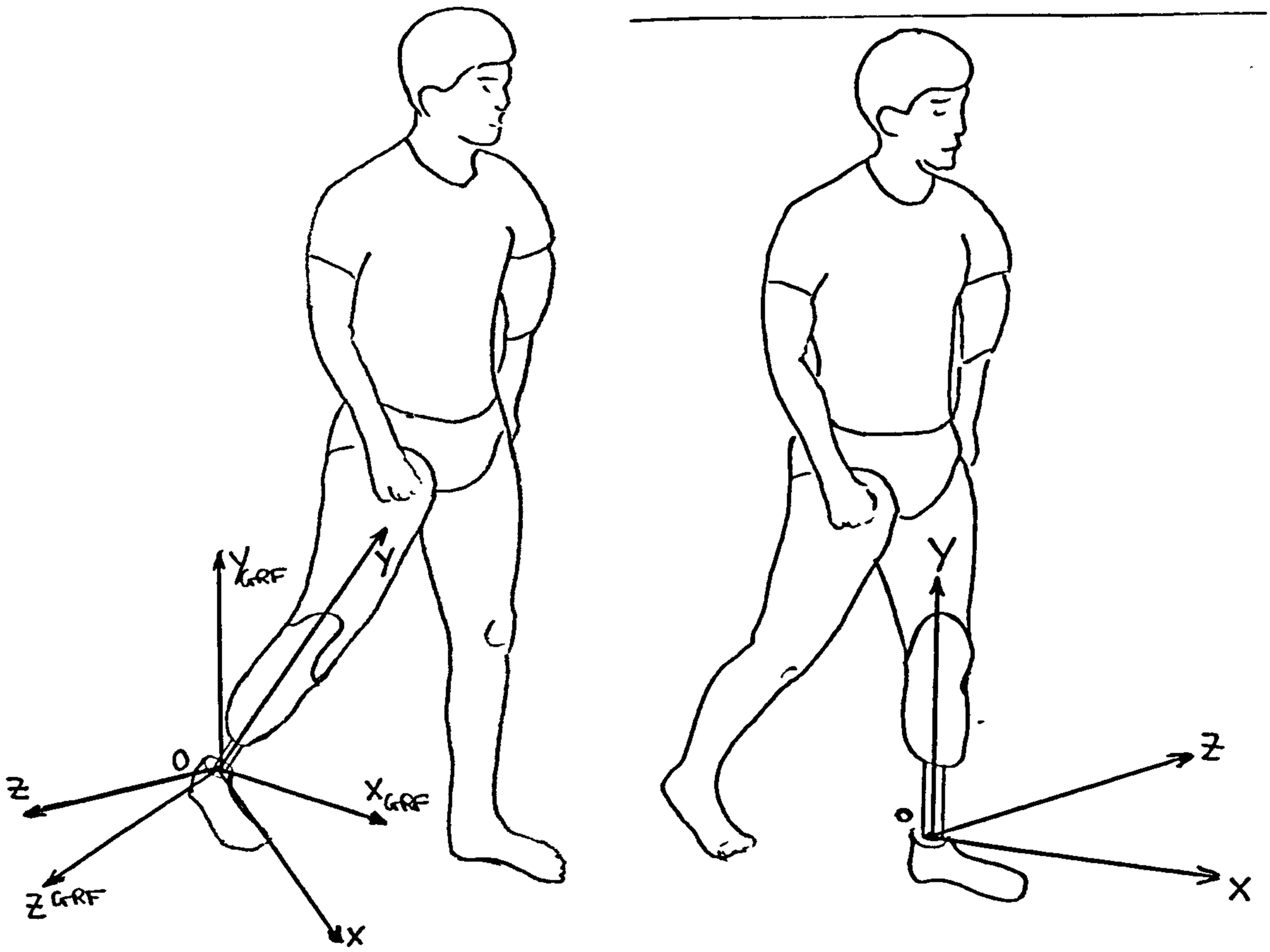

Figure 2.16: The Global and Local Frames of Reference (GloRF and AF) for both sides. The origin point is the middle of the artificial ankle axis. All directions are positive.

BASIC UNITS		
length	metre	m
mass	kilogram	kg
time	second	s
DERIVED UNITS		
force	Newton	N
moment or torque	Newton - metre	N m
pressure and stress	Pascal (N/m^2)	Pa
frequency	Hertz (1/s)	Hz
plane angle	radian degree is also used	rad $0.5\ \Pi = 90°$

Table 2.6: The system of units used

Figure 2.16 exhibits the GloRF for left and right sides of the amputee's body. From this URF, it is easy to describe and to name the three planes of Cartesian space:

- the medio-lateral plane also named frontal or coronal plane
- the anterio-posterior plane also named sagittal plane or fore-aft plane
- the transverse plane

2.6.4 Units of measurement

For many years, researchers have used the "Système International d'Unités" (SI). The basic units of the SI useful in locomotion studies are presented in table 2.6. The presentation order corresponds to the one most frequently used in the prosthetic research field. These units will be used throughout this thesis, except where stated.

2.6.5 Alignment parameters

As already mentioned, the term "alignment" refers to the inclination and position in space of the components of the prosthesis relative to each other or to the Universal Reference Frame, defined in the previous section. The term "alignment parameters" of a prosthesis is defined as the position of the socket relative to the other prosthetic components of the limb. It can be used to refer to the elements necessary for the qualitative description and quantitative assessment of the configuration of the prosthesis (Zahedi *et al.*, 1986).

The author of this thesis is a physiotherapist working in a clinical environment. The purpose of the dissertation therefore is not to study prosthetic alignment itself nor the modification of gait patterns with different prosthetic alignments. Therefore, in the following chapters, prosthetic alignment will not be studied or mentioned.

2.6.6 Forces and moments

Force is a fundamental variable responsible for causing motion while moment is a force multiplied by a lever arm about any axis (Seliktar, 1994).

The study of forces and moments is called kinetics. Its definition is: the study of the forces acting upon the various segments, as a result of gravity and inertia effects (external causes) or muscles and ligaments (internal causes) and their effects

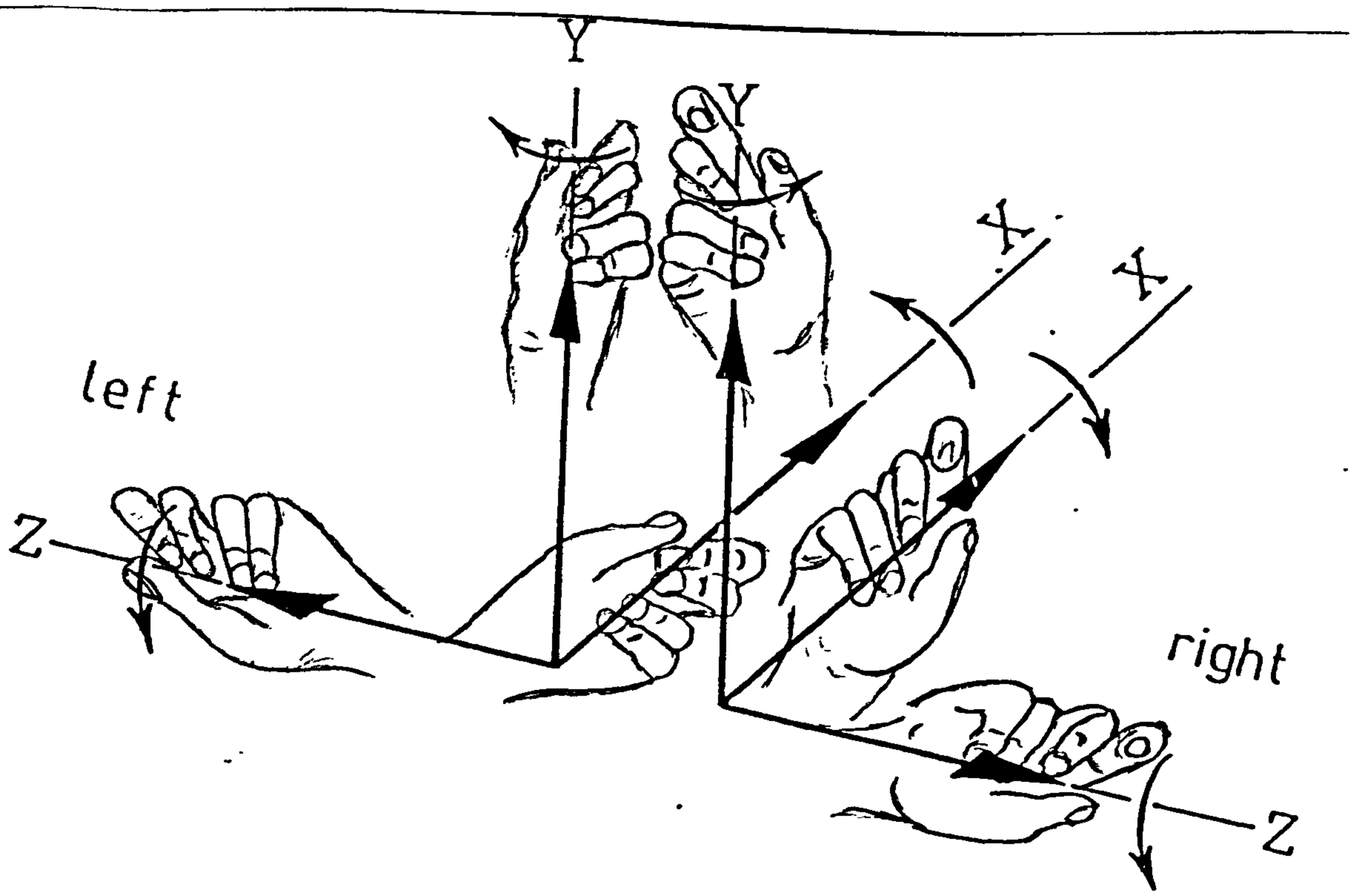

Figure 2.17: All the positive forces and moments for both sides
(extracted from Magnissalis, 1992)

on the motion of the body. At each joint, a state of dynamic equilibrium exists such that the internal joint forces and moments generated by muscle, ligament and bony structure balance the externally applied forces. At each instant of any motion, the existing equilibrium could be described as a static state of all the structure. In other words, kinetics is the investigation of the relationship between factors causing motion such as forces and moments and the motion itself (Harris & Wertsch, 1994).

Both the forces and moments are defined as positive when they act from distal to proximal on the body, in the positive direction of the co-ordinate axes.

A positive force is one that tends to accelerate the body or a body segment in the positive direction.

A positive moment is one that tends to produce a positive angular acceleration of the proximal part according to the right or left hand rules.

Two conventions are essential:

1. For reasons given above (see section 2.6.3.1), the following convention was adopted:

- *a right - hand rule is used for right limb prostheses*
- *a left - hand rule is used for left limb prostheses*

2. When positive loads are applied, the positive directions of forces and moments are considered acting from the distal to the proximal side of a free body. The section which is the free body's boundary could be the ground - to - foot interface or any other transverse section along the limb.

2.6.6.1 FORCES

2.6.6.1.1 Definition

A force F (in N) is the mechanical action or the effect of one body on another, which causes the bodies to accelerate relative to an inertial reference frame (ISB, 1987). Weight is the force of gravitational attraction acting on a body, being equal to the mass of the body (in kg) multiplied by the gravitational acceleration, that is 9.81 $m.s^{-2}$ (value used in all the following chapters).

By convention, all the following load actions are **BY** the distal region **ON** the proximal.

2.6.6.1.2 Anterio-posterior shear force

The fore - aft shear force is denoted Fx and it is positive when it acts on the foot in the direction of progression of gait. The sign convention is the same for both sides of the patient's body.

2.6.6.1.3 Axial force

The axial load is termed Fy and it is positive when it acts proximally on the body. This is true whatever the side is.

2.6.6.1.4 Medio-lateral shear force

The frontal plane shear force is denoted Fz and it is positive when it acts in a lateral direction. For a right amputated subject, Fz positive acts from left - to -right on the foot while for a left amputated subject , Fz positive acts from right to left on the foot (see figure 2.16 or 2.17).

2.6.6.2 MOMENTS

2.6.6.2.1 Definition

A moment is the turning effect of a force about a point, measured by the product of the force and the perpendicular distance of its line of action (equivalent to an axis) from that point (ISB, 1987). The symbol of a moment is M having N m as unit. For a right amputee, the right - hand rule is used: when the thumb of the right hand is placed in the positive axis direction, the fingers indicate the turning effect of a positive moment about that axis exerted by the ground on the proximal part. Symmetrically, the left - hand rule is used for the left side. The numerical value of a moment is the product of the force and the perpendicular offset of its line of action from the axis being considered.

2.6.6.2.2 Medio - lateral moment

The medio - lateral moment Mx acts about the X axis, in association with the medio - lateral shear forces and axial loads Fy in coronal plane. When it is positive, it

		RIGHT SIDE right - hand rule	**LEFT SIDE left - hand rule**	RIGHT SIDE ISB Recommendation	LEFT SIDE ISB Recommendation
Fx	A/P shear force positive	**forward**	**forward**	forward	forward
	A/P shear force negative	**backward**	**backward**	backward	backward
Fy	Axial load	**upward**	**upward**	upward	upward
Fz	M/L shear force positive	**outward**	**outward**	outward	*inward*
	M/L shear force negative	**inward**	**inward**	inward	*outward*
Mx	M/L moment positive	**inversion**	**inversion**	inversion	*eversion*
	M/L moment negative	**eversion**	**eversion**	eversion	*inversion*
My	Horizontal moment positive	**medialward (internal rotation)**	**medialward (internal rotation)**	medialward	*lateralward*
	Horizontal moment negative	**lateralward (external rotation)**	**lateralward (external rotation)**	lateralward	*medialward*
Mz	A/P moment positive	**dorsiflexion**	**dorsiflexion**	dorsiflexion	dorsiflexion
	A/P moment negative	**plantarflexion**	**plantarflexion**	plantarflexion	plantarflexion

Table 2.7: The correspondence between the mechanical definition and clinical names in bold letters. At the right side of the table, the ISB recommendations are given. I*talic letters* (slopped) are used to show changes to the relative to the sign convention (mainly, the left side of the body). All load actions are **BY** the distal region **ON** the proximal region.

tends to adduct ankle, knee and hip joints. Concerning the foot, it is an inversion or a varus moment.

Because the left - hand rule is used on the left side, the same Mx positive adducts the three lower limb joints and inverts the left foot.

2.6.6.2.3 Transverse plane torque

The torque about the Y axis, My, is positive if acting on the distal leg it tends to produce an internal rotation. In practice, the name "torque" is always used.

2.6.6.2.4 Anterio-posterior moment

The flexion-extension moment or sagittal plane moment Mz tends to cause rotation about the Z axis, in association with the anterio-posterior shear force Fx and axial loads Fy in fore-aft plane. Positive Mz produces:

- <u>at the ankle</u> a dorsiflexion, i.e. the dorsal side of the foot is drawing nearer to the shank front face
- <u>at the knee</u> a joint extension, i.e. the anterior part of the shank is moving towards the front face of the thigh
- <u>at the hip</u> a joint flexion, i.e. the thigh or the residual limb with its socket, for above-knee amputees, is moving towards the anterior part of the trunk.

All of these descriptions hold for both sides of the body.

The kinematic variables of locomotion are known as a description of movements in terms of linear and angular displacements, velocities and acceleration, without any reference to the forces causing the motion (Porter & Roberts, 1989). Kinematics can be described as the geometry of motion. In other words, in the strict sense, kinematics is concerned with the study of the motion of particles and rigid bodies with no consideration of what has caused the motion (Harris & Wertsch, 1994).

It is important to note that, with only a load measuring transducer, forces and moments alone are studied.

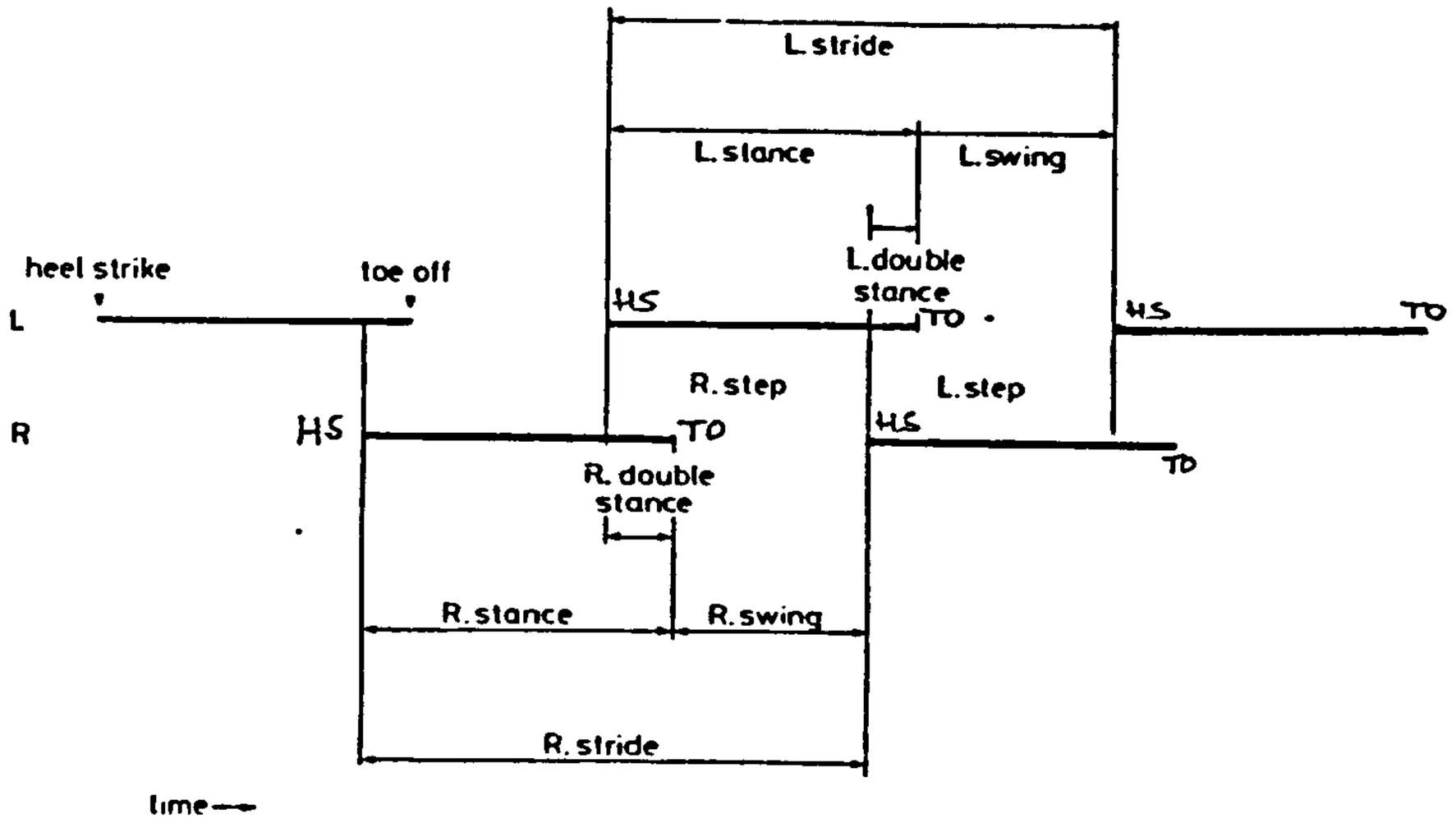

Figure 2.18: Main temporal components of the walking cycle based on a simple foot contact (heel strike to toe off), for a normal subject, from Dewar & Judge, 1980. The double stance can also be named: double support.

heel strike at 0 %	early stance
foot flat when the whole foot is in ground contact at 15 %	mid stance
heel - off at 30 %	
hip and knee flexion (knee bend point) in preparation for acceleration of the swing leg at 45 % of the gait cycle	late stance
double support during two periods of about 10 % eac, making a total 20 % of the gait cycle. Pinzur *et al.* (1984) reported a double support time of 13.04 per cent of the gait cycle. It is an overlap of the ground contact of the two lower limbs: from foot flat to toe - off on the leading side and heel strike to foot flat on the contralateral side (HS_{RIGHT} to TO_{LEFT} and HS_{LEFT} to TO_{RIGHT})	
toe - off when toes leave the ground at 60 % (Heel - strike begins the stance phase of the step (see below the definition) while toe - off ends it and signals the beginning of the swing phase of the ipsilateral foot)	early swing
at 80 % of the gait cycle, the tibia is vertical and the angular speed of the hip and the knee is at its maximum (Whittle, 1996)	mid swing
from 80 to 100 %, muscles are working to decelerate the lower limb	late swing

Table 2.8: The main events of the walking cycle (normal gait).

Figure 2.17 shows all positive forces and moments for both sides. Table 2.7 exhibits all forces and moments with the corresponding clinical names. The right side of table 2.7 shows what could be the sign convention if the ISB recommendation was completely followed. The differences between the two systems (mainly, the left side of the body) are shown in italics and the possible confusion in Fz, Mx and My is outlined.

2.6.7 Gait description and vocabulary

2.6.7.1 DESCRIPTION AND EVENTS OF NORMAL GAIT

Walking involves motion, and the basic variables which describe motion are time and distance. Walking is characterised by its cyclic nature and the basic cycle of human gait is the stride. The stride consists of the interval between any two successive, unilateral occurrences of any recognisable event in the cyclic process. It is measured in seconds or metres.

The gait cycle is the activity that occurs between heel - strike of one leg and the subsequent heel strike of the same leg (Lehmann *et al.*, 1992). In the prosthetic field, most researchers have identified heel contact as the start of the gait cycle and they present data with stance followed by swing phases (Winter, 1984; Winter & Sienko, 1988; Harris & Wertsch, 1994). However, some researchers have identified toe - off as the start of the cycle (DeVita, 1994). Despite this difference, the ISB recommendations will be followed and heel strike will always mark the start of the gait cycle.

The main temporal components of the walking cycle are shown in figure 2.18 (Dewar & Judge, 1980). The timing of the gait cycle is indicated as an approximate percentage of the cycle: 60 % for the stance phase and 40 % for the swing phase. For example, Pinzur *et al.* (1984) reported respectively 61.49 per cent and 38.51 per cent of the gait cycle for normal subjects. Specific points during these phases can be clearly identified by clinical observation.

The main points of the walking cycle are shown in table 2.8.

The intervals between these gait events and phases are presented in table 2.9.

The thigh is accelerated during the end of the stance phase and the whole leg is

early stance phase		0 - 15 %	from heel - strike to foot flat
mid stance phase		16 - 30 %	from foot flat to heel - off
late stance phase	push - off phase	31 - 45 %	from heel - off to knee bend
	limb acceleration (pre-swing)	46 - 60 %	from knee bend to toe - off
early swing phase	limb acceleration	61 - 79 %	from toe - off to the vertical position
mid swing phase	vertical position	80 %	
late swing phase	limb deceleration	81 - 100 %	from the vertical position to the heel - strike of the next stride

Table 2.9: The different events and phases during one stride (extracted from Plas *et al., 1979)*

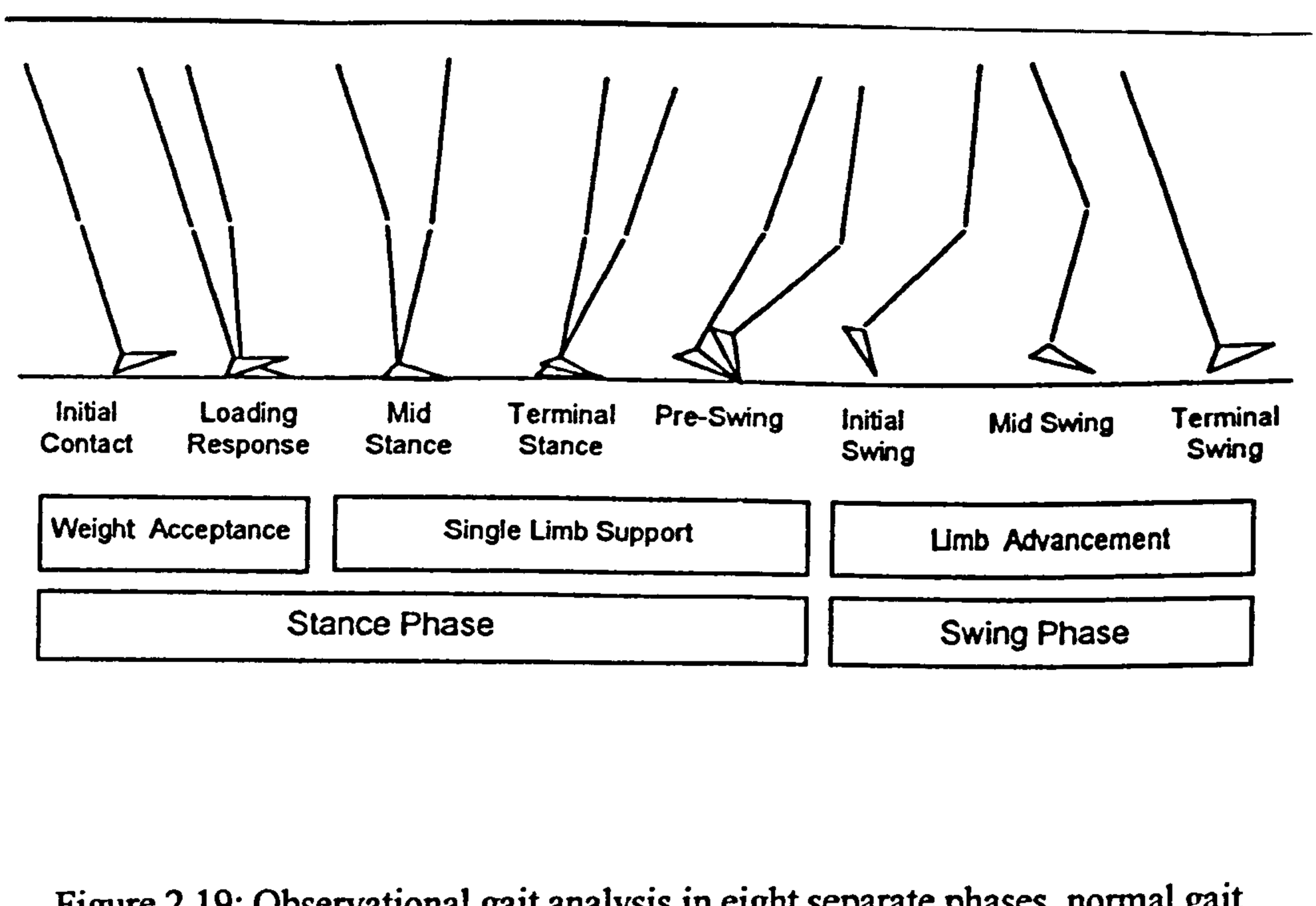

Figure 2.19: Observational gait analysis in eight separate phases, normal gait (extracted from Perry, 1992)

at the beginning of the swing phase (50 - 70 % of the gait cycle): leg acceleration phase. The period from 70 to 100 % represents the rest of the swing phase in which the lower limb is decelerated (i.e., leg deceleration phase).

The stride is defined as the interval between two successive identical events of the same foot.

The stride length is defined as the distance from heel strike of one foot to the next heel strike of the same foot. Stride time is the duration of the complete walking cycle: generally taken as the mean of several strides.

The step is defined as the interval between the heel strike of one foot to the next heel strike of the other foot.

The step length is defined as the distance from the position on the ground of heel strike of one foot to that of heel strike of the other foot. It is obvious that left step + right step equals one stride. It is also possible to evaluate the step in time, but only in absolutely symmetrical gait when left step length is equal to right step length.

Regarding the sides of the body, the step length and the stride length are defined as follows: left step length is the distance from heel contact of the right foot to heel contact of the left foot while the right step length is the distance from heel contact on the left foot to the heel contact of the right foot. The stride length is the sum of these two distances.

The cadence (stride frequency) is the number of complete strides per unit time, e.g., stride.s^{-1} or stride.min^{-1}. The duration of one stride is not much used in the literature, it will be named in the following chapters as the gait rate: s.$stride^{-1}$. Waters *et al.* (1976) have indicated that gait rate is a particularly informative measure of general walking ability. It is thus a reasonable hypothesis that for pathological gait such as for amputees; gait rate, as well the cadence can provide as much information as velocity as a measure of walking ability.

Both cadence and gait rate have the considerable practical advantage that they can be derived solely from the output of the transducer without the need for an additional measure of distance. In all tests presented later in this work, the gait rate or

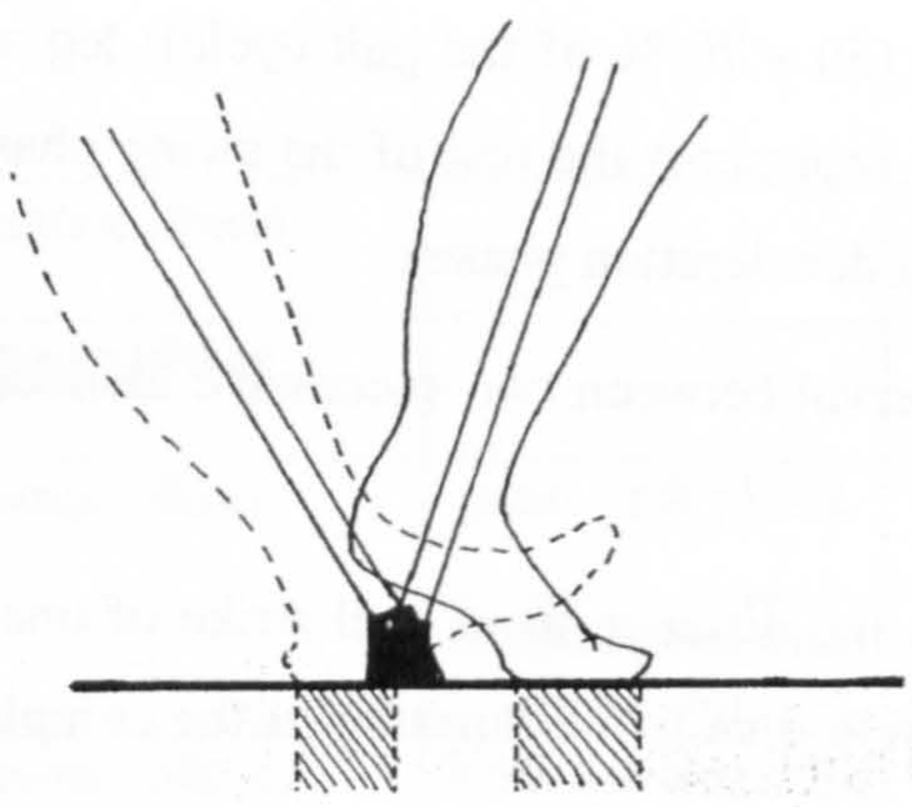

a

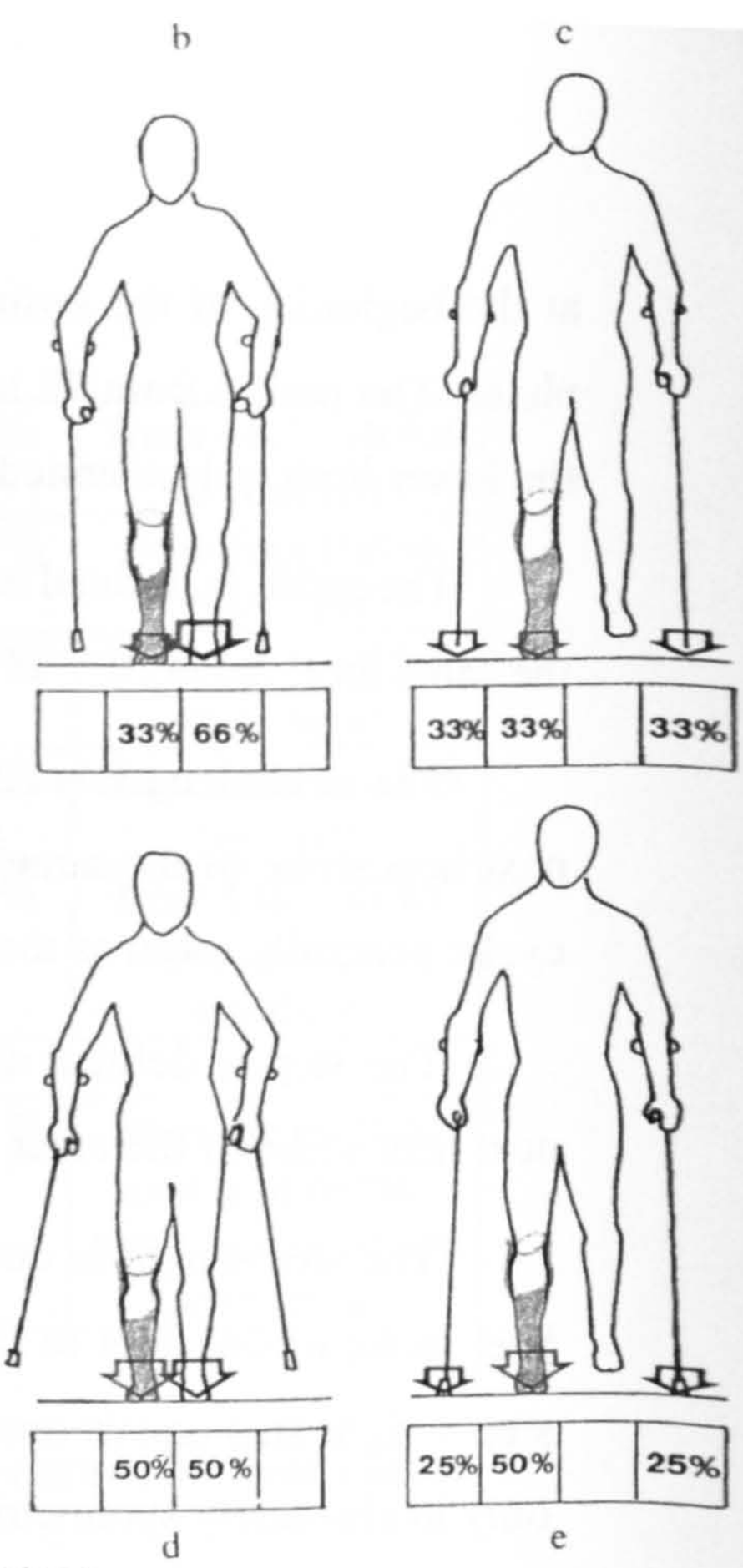

Figure 2.20: The Unilateral Pendular Strolling gait (UPS)
(adapted from Berthe & Dotte, 1987)
a: deformation of the heel of the footwear at heel-contact
b and c: a transtibial amputee at early stage of rehabilitation: 33% load on the stump and 33% load on each walking aids
d and e: the same transtibial patient later during the rehabilitation process: 50% load on the stump and 25% on each walking aids.

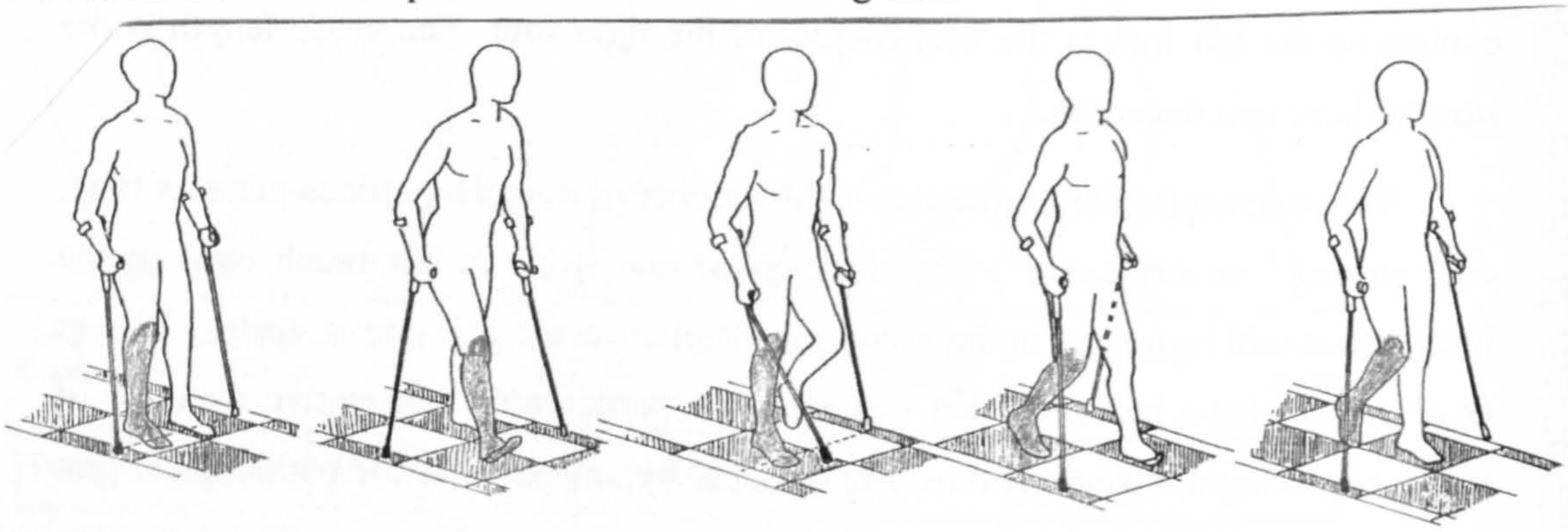

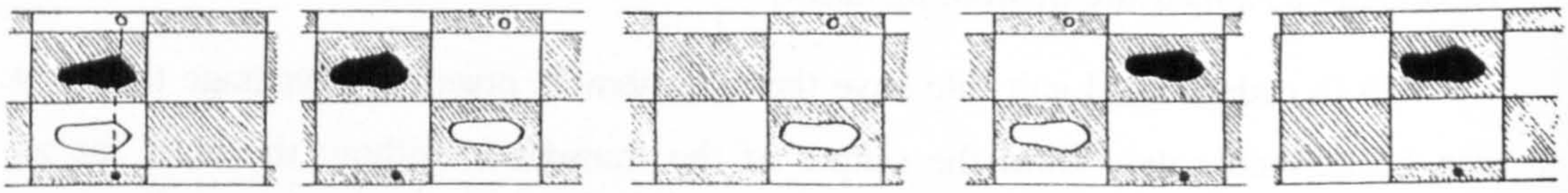

Figure 2.21: The Unilateral Cross Strolling gait (UCS)
(adapted from Berthe & Dotte, 1987)

the cadence (cadence in stride per minute $= \frac{60}{\text{gait rate in second per stride}}$) will be widely used because the equipment presented in chapter 5 will not be able to measure distance (see chapter 8). Although, stride length expresses best the patients strength and skill in walking and is easily obtained by counting the number of strides required to cover a specified distance.

The walking speed (or velocity in $m.s^{-1}$) is the gait rate multiplied by the stride length. Dewar & Judge (1980) established that there is a linear relation between gait rate and walking speed. However, the tests presented in chapter 8 will introduce a discussion on this relationship.

The percentage analysis of the gait cycle is customarily used in the biomechanics field for both normal and pathological gaits. A complete description on which the description and events of lower limb amputee gait (see section 2.7.5.2) is based was reported by Eberhart *et al.* (1947). However, by elimination of some of the gait cycle events, it is possible to describe the amputee gait in a manner which avoids confusion and inaccuracies. This system recognises that there are three basic tasks to be achieved during gait: weight acceptance, single limb support and limb advancement. There are eight separate phases in these three tasks (Perry, 1992) as shown in figure 2.19.

2.6.7.2 DESCRIPTION AND EVENTS OF LOWER LIMB AMPUTEE GAIT

The frail elderly PVD patients who are the subject of this project have a particular pattern of walking, due to the use of two assistive aids such as sticks or canes (see description in section 2.6.7.3).

None of the patients tested, presented in chapter 8, has a swing-through gait of the type described by Stallard *et al.*, 1978. Most of them used a Unilateral Pendular Strolling (UPS) gait, described by Berthe & Dotte, 1987. The two sticks encircle the amputated limb, particularly during its stance phase. The patient does this to minimise the load bearing between the stump and the prosthesis. Figure 2.20a shows how the heel of the footwear deforms under load at heel-contact; figures 2.20b and c show a 33 % of body weight on the stump while figures 2.20d and e show a 50 % body weight on the stump. In the UPS gait, there is no alternate oscillation of the

Figure 2.22: A stick also named a forearm-crutch

Figure 2.23: A transtibial amputee using a stick.

In figure 2.23, 2.25 and 2.26, the stick is on the ipsilateral side relative to the prosthesis. However, the drawing is from a veritable patient through a photograph taken by the author of this thesis in his Rehabilitation Centre. The patient was suffering an arthrosis of the right knee joint. He was well accustomed to the prosthesis; thus, his right side was the "bad" one, which needed to be at the maximum "off load".

arms. Regarding the residual limb, this gait pattern could be described in three parts:

1. loading the two sticks ahead of the coronal plane of the patient

2. swing and stance phases of the residual limb with its prosthesis while both sound limb and sticks are in stance, applying loads on the floor

3. swing phases of the sound limb and the sticks could occur when the amputated side is in stance. With the VSD patients presented in this thesis, these two swing phases do not usually overlap as they do with subjects, having their amputation due to trauma (see description and discussion in sections 8.5.5 and 8.8.5).

The gait rate is low and the patient could have at a minimum of two loading points on the ground during the assistive aids swing phase. The chronological study of such an assisted gait is one of the main features of the work presented in this thesis (see section 8.9.4).

Some patients have a gait pattern named Cross Strolling (CS). In that case, each stick or cane is bearing on the ground when the contralateral limb is in its stance phase as shown in figure 2.21. The CS can thus be described in two stages:

1. one walking device plus the contralateral limb are loaded

2. the second walking device with the other limb are in the swing phase

The CS gait rate is higher, the strides are linked up, the power consumption is lower (Didier & Casillas, 1986) but the stress at the interface between the stump and the socket is increased.

2.6.7.3 DESCRIPTION OF ASSISTIVE WALKING DEVICES

Commonly, the patients use two sorts of assistive walking devices.

1. A stick that has a forearm counter–load is shown in figure 2.22. In the literature, it is also named a forearm crutch (Joyce & Kirby, 1991). The height of the handle is adjusted to have an angle of flexion about thirty degrees at the elbow, which optimises the efficiency of the Triceps Brachii muscle, as shown in figure 2.23. This task is conducted as follows: the wrist of the patient must be placed facing the great trochanter by means of the telescopic lower tube of the walking device. This stick is usually named "canne anglaise or canne canadienne" in French. Patients

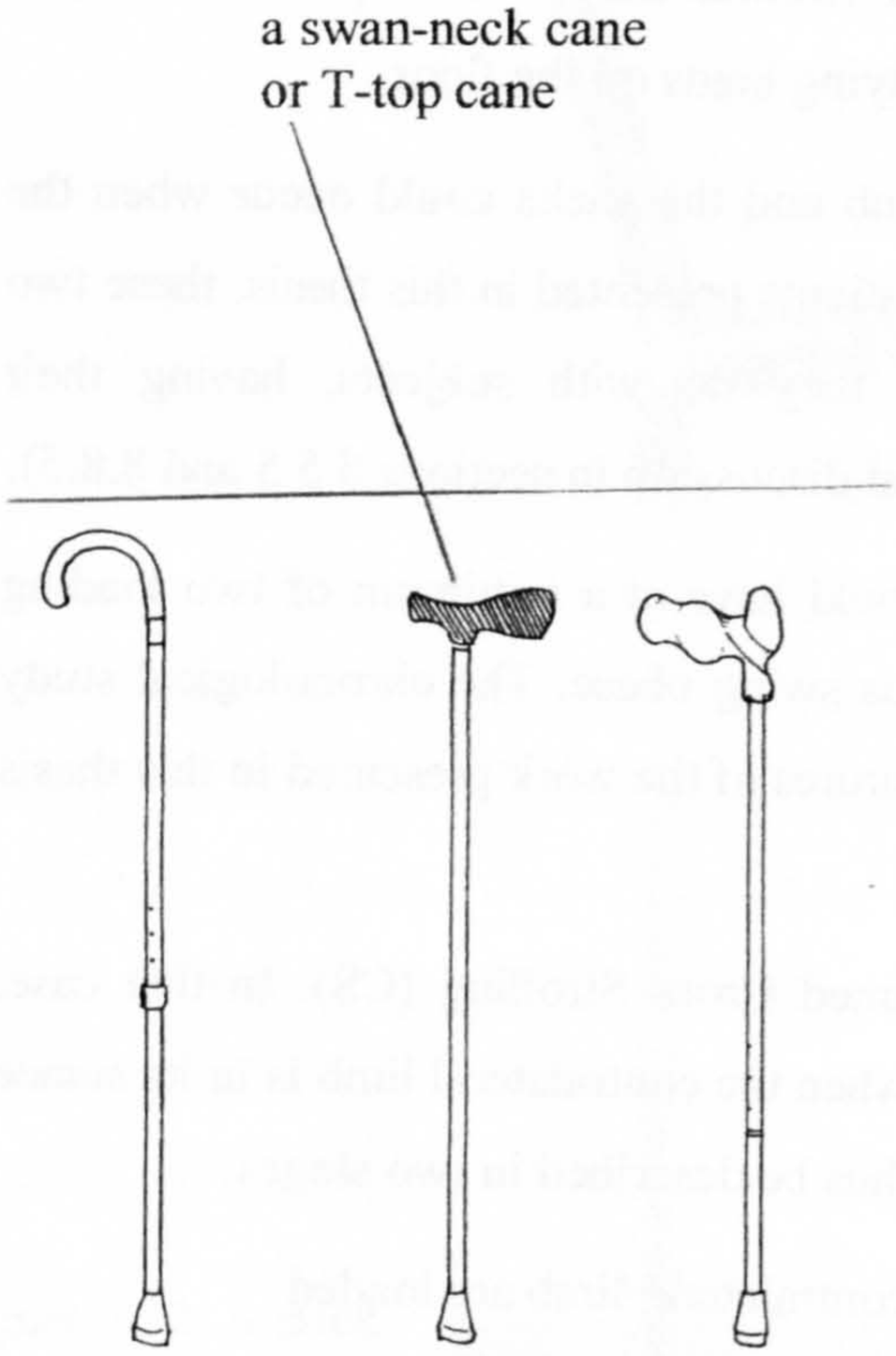

Figure 2.24: Three types of canes

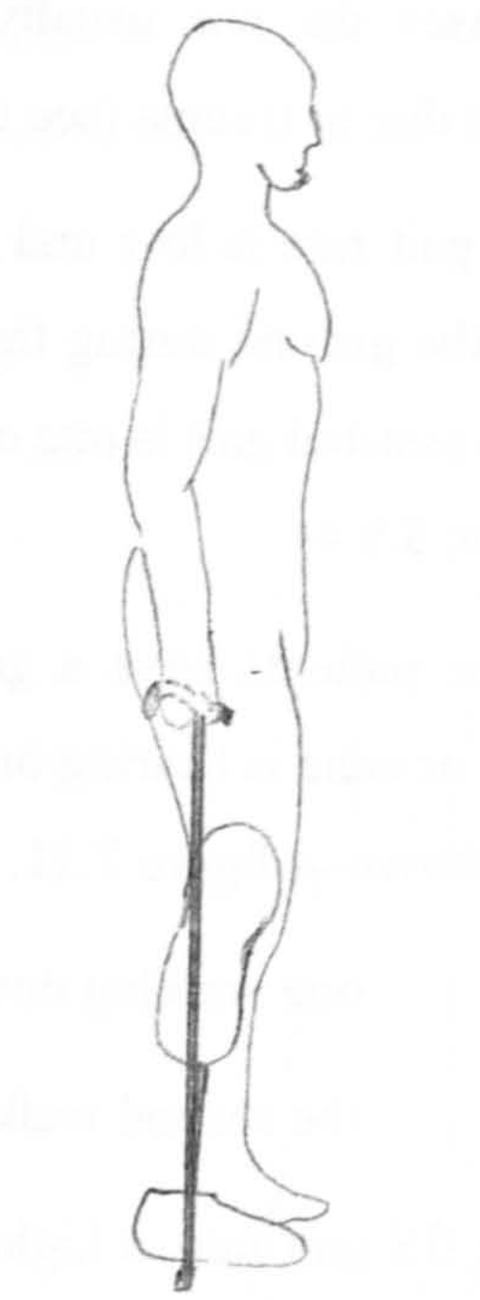

Figure 2.25: The same transtibial patient as in figure 2.23 is using a cane

habitually used two sticks.

2. A cane without any counter-load. The handle has a shape of a swan-neck, as shown in figure 2.24. It is sometimes named T-top or straight top cane (Joyce & Kirby, 1991). The stability and equilibrium are more precarious. The patient must expend more energy to control his movements as demonstrated by McDonough & Razza-Doherty (1988). It is usually used in the final stage of rehabilitation of the peripheral vascular disease amputees. The height of the handle is usually set at the level of the great trochanter of the femur which is the level of the wrist when the upper limb is in extension along the trunk (figure 2.25). The patients can use one or two canes. To walk efficiently with this device, the user must place the rod of the cane between his forefinger and middle finger or between his middle and ring fingers. This depends of the size of the hand. When the position of the hand is correct, the load, coming from the ground or the upper limb, is transmitted efficiently through the swan-neck of the cane and the central area of the palm of the hand.

Since no canes were instrumented, a different type of the stick was used. It is called: the reversed stick, as shown in figure 2.26. Because the stick handle is not built for this purpose, the patient had to put the rod of the stick between his forefinger and his middle finger or middle and ring finger as shown in figure 2.27, to have the same loading set up as the one he had with a swan-neck cane. Because of the larger circumference of the stick rod, this position of the fingers could be slightly uncomfortable. Patients were able to use one or two reversed sticks.

These walking assistive aids are used in two tasks:

1. frontal plane: to transfer the weight from one side of the body to the other;

2. sagittal plane: to accelerate and decelerate forward movement.

A study of the use of these assistive walking devices is developed in chapter 8.

2.6.8 Summary

Some complete definitions and vocabulary descriptions have been presented as the terminology used in this thesis. The terms employed are derived from the International Society of Biomechanics recommendations (Wu & Cavanagh, 1995).

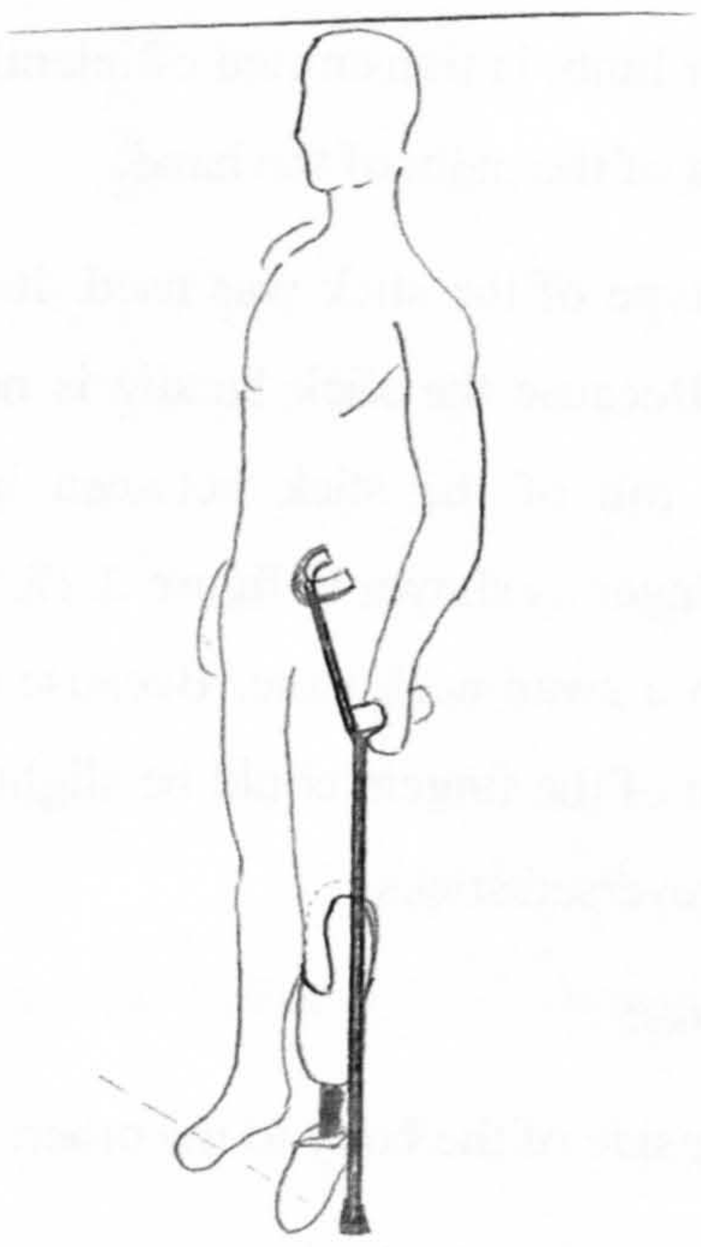

Figure 2.26: The same transtibial patient as in figure 2.23 and 2.25 is using a reversed stick

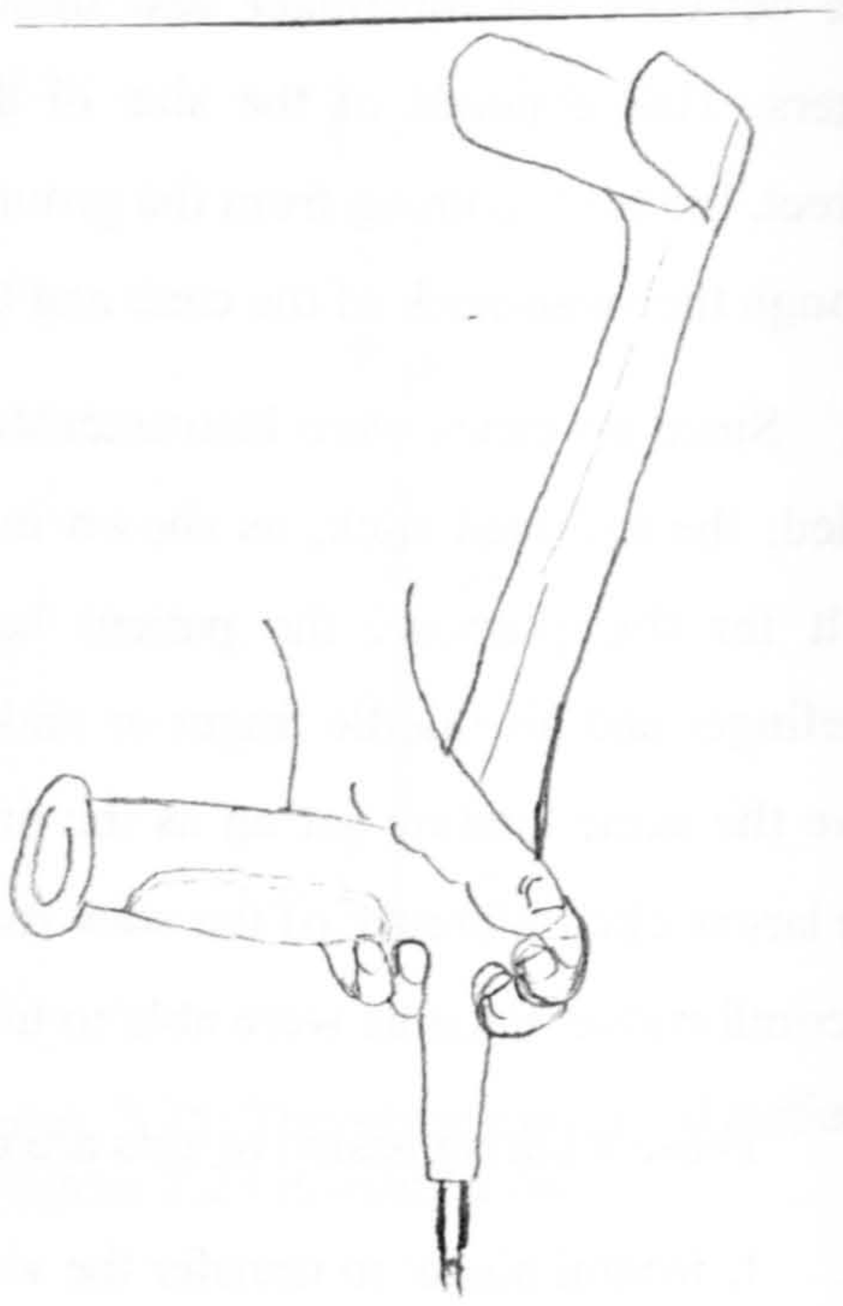

Figure 2.27: The patient's hand around the reversed stick handle (here, it is the ring and the middle fingers)

The most important point is to note that the origin point of the frame of reference is defined as the middle point of the artificial ankle axis. From this point, three planes were set up corresponding to three orthogonal axes. The directions of the forces and moments are described relative to these axis directions. In other words, the Y axis is the axis of the shank tube of the prosthesis.

For rotation and moment positive directions, a left - hand rule is used for the left limb while a right - hand rule is used for the right limb of the patient.

This nomenclature was adopted for both normal and lower limb amputee gaits. Special attention was given to the difference between the step and the stride. In clinical gait assessment, the whole body of the patient is often studied. In kinetic gait analysis, only one leg is studied, namely the one fitted with the prosthesis and the transducer.

A survey of the assistive walking devices used by the patients was carried out. A special highlighted point was that because instrumented sticks were used; it was not possible to carry out the study on patients using one or two canes. It was an obligation to investigate the effect of using reverse sticks. However, this introduced an uncomfortable gesture of the patient's hand around the stick handle and the rod.

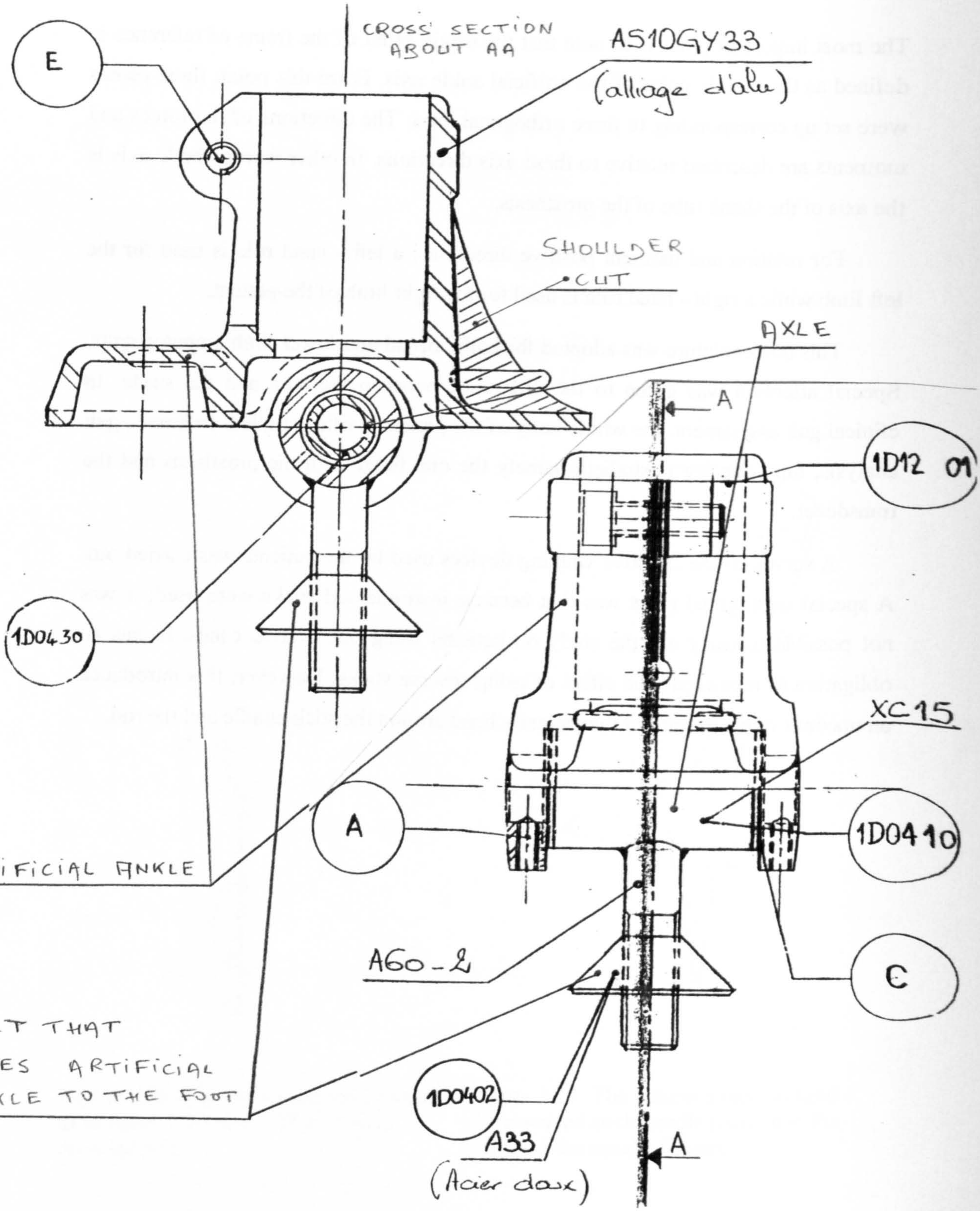

Figure 3.1: The prosthetic ankle used with the Proteor® monoaxial artificial foot (Scale 1: 1).
The shoulder at the top part of the front flat flange was cut when the prosthetic ankle was used as a transducer, as shown in the top sketch.

3 DESCRIPTION AND USE OF THE FIRST NEW REMOVABLE TRANSDUCER (MODEL I)

3.1 INTRODUCTION

To satisfy the need for a removable transducer according to the requirements expressed in chapter 1, the first idea was to fit gauges onto the definitive prosthetic metallic ankle. This device is worn by the patient between his prosthetic foot and the shank tube of the prosthesis. The main advantage of this approach was that it did not require a complete transducer. After a theoretical analysis of the prosthetic ankle / foot, a finite element analysis was made to test the strength and behaviour of the ankle. This analysis was also carried out to determine the best gauge locations.

3.2 DESCRIPTION OF THE PROSTHETIC ANKLE

Figure 3.1 shows the prosthetic ankle with its axle and the bolt to attach it to the foot.

The geometric shape of the ankle indicates that all loads acting on the ankle from the ground will pass through four points as shown in figure 3.2:

- from the axle (whose middle is the point O), the principal loads act on the ankle through the two lateral flanges (C_1 at the lateral side and C_2 at the medial side for a right foot in figure 3.2). This is particularly true when the shank tube is vertical at mid stance phase of the gait cycle.

- loads, from the posterior rubber bumper, act on the ankle at the posterior hollowed flange (point B in figure 3.2), when the ankle is in plantarflexion at early stance phase.

- loads, from the anterior rigid plastic ring, act on the ankle at the anterior flat flange (point A in figure 3.2), when the ankle is in dorsiflexion at toe off.

The captions of the figure 3.2 show all information used in the following

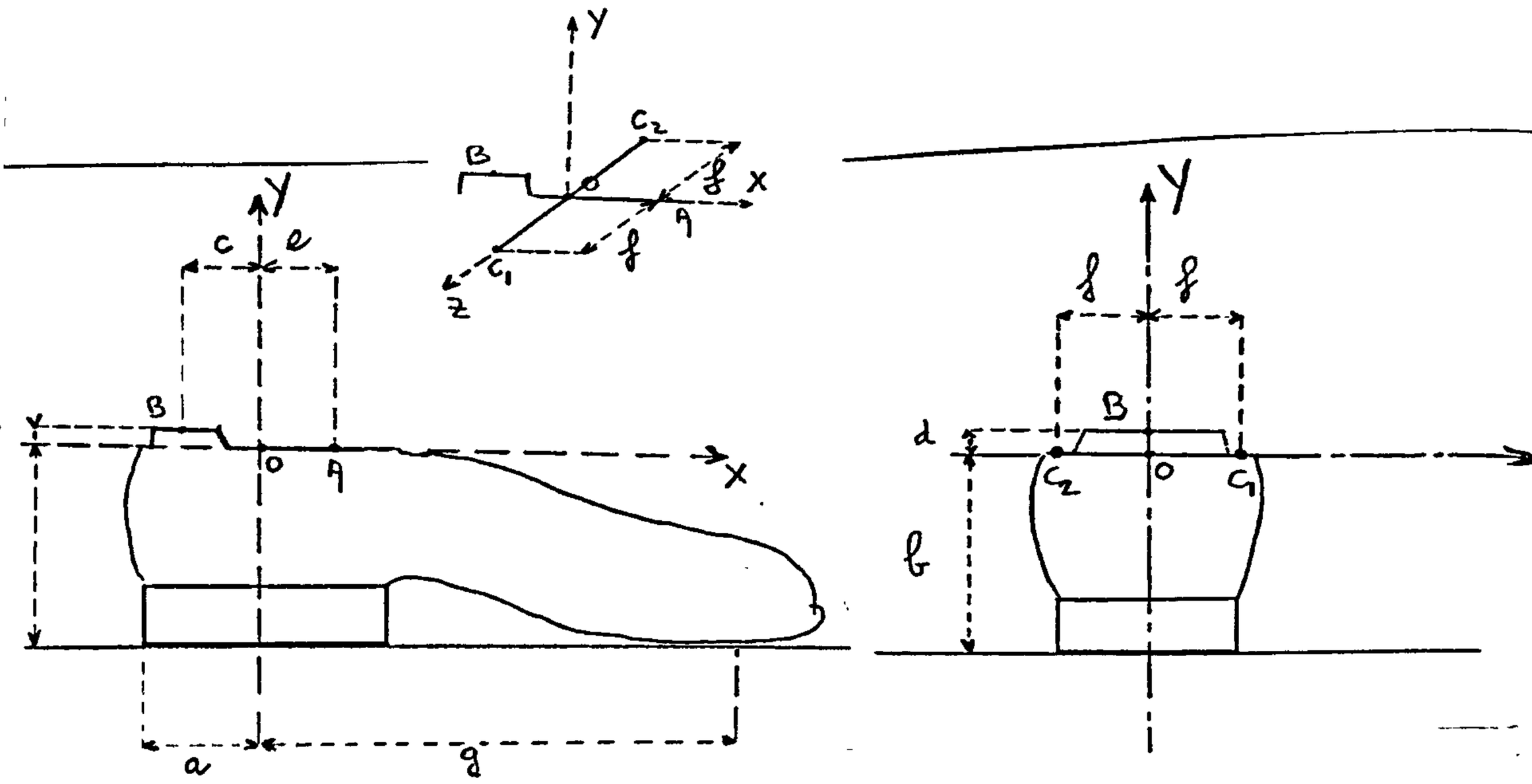

Figure 3.2: The four loading points; A, B, C_1, and C_2, having convention as follows (lateral and back view of a right foot):

1. ground actions on the footwear: $F_{ground\,/\,shoe}$ (F_x, F_y, F_z) in three orthogonal planes.
2. actions of the foot onto the ankle device at the front point A (A_x, A_y, A_z), at the rear point B (B_x, B_y, B_z) and at the two lateral flanges where the axis is fixed (C_{1x}, C_{1y}, C_{1z} in lateral and C_{2x}, C_{2y}, C_{2z} in medial position).
3. forces and bending moments hare named as follows:

point load A		point load C_1		point load C_2		point load B	
Fx_A	Mx_A	Fx_{C1}	Mx_{C1}	Fx_{C2}	Mx_{C2}	Fx_B	Mx_B
Fy_A	My_A	Fy_{C1}	My_{C1}	Fy_{C2}	My_{C2}	Fy_B	My_B
Fz_A	Mz_A	Fz_{C1}	Mz_{C1}	Fz_{C2}	Mz_{C2}	Fz_B	Mz_B

at each loading case, the following subscripts will be added:

A = foot flat (axial load)
H = heel - strike
T = toe - off

4. a is the distance in the X direction between the contact point of the shoe with the ground (at heel-strike) and the Y axis (through the centre of the ankle axis O) = 60 mm
5. b is the distance in the Y direction between the sole of the shoe and the centre of the ankle axis (O) = 75 mm
6. c is the distance in the X direction between the rear contact point of the ankle device on the artificial foot (B) and the centre of the ankle axis (O) = 35 mm
7. d is the distance in the Y direction between the rear contact point of the ankle device on the artificial foot (B) and the centre of the ankle axis (O) = 10 mm
8. e is the distance in the X direction between the front contact point of the ankle device on the artificial foot (A) and the centre of the ankle axis (O) = 35 mm
9. f is the distance in the Z direction between the ankle - axis connection (C_1 and C_2) and the centre of the ankle axis (O) = 21 mm
10. g is the distance in the X direction between the ground - foot contact point at toe - off and the centre of the ankle axis (O) = 160 mm for a standard footwear having 7 as size

theoretical analyses.

The material used for the prosthetic ankle is aluminium alloy (AS10GY33) and steel for the axle. They have characteristics shown in table 3.1.

3.3 THEORETICAL ANALYSIS OF THE ARTIFICIAL ANKLE / FOOT DEVICE

Before using any finite element analysis, it is necessary to study loads and equilibrium between the ground, the foot with its shoe and the shank tube. The prosthetic ankle device has a simple kinematic behaviour: it is a pivot turning around the single ankle axis, a « monoaxial artificial foot ». Hence, it will be easy to model the mechanical actions and interfacing connections onto the ankle device.

It is consequently necessary to study the static equilibrium of the entire assembly: shoe, foot, ankle and tube in three stance phase positions:

1. heel - strike; 2. flat foot; 3. toe - off.

The following assumptions are made:

1.All connections are point loads.

2.The ground force is on the back of the heel.

3.At mid stance, i.e., at foot flat, the force vector is along the Y axis

4.The force is at the front of the foot

5.It is assumed that there are no forces along the medio-lateral Z axis.

6.The footwear is of known dimensions.

3.3.1 Theoretical static equilibrium with foot flat

In static balance, one has: $\Sigma F = 0$ and $\Sigma M_O = 0$ with the middle of the ankle axis (O) as the reference point as shown in figure 3.3, in which the subscript A stands for axial. At foot flat, F_{xAA}, F_{zAA} and F_{xBA}, F_{zBA} are zero; F_{yC1A} and F_{yC2A} are equal between themselves relative to the reference point O = F_{yC12A}. Consequently, there are no moments about X and Z axes. Hence, the full set of equations is, with respect

	Ankle Aluminium Alloy AS10GY33	Ankle Steel Axle XC15
Young's modulus	$76 * 10^9$ Pa	$200 * 10^9$ Pa
Poisson's ratio	0.34	0.3
Density	2700 kgm^{-3}	7700 kgm^{-3}

Table 3.1: The properties of the material used for the Proteor® artificial ankle and axle.

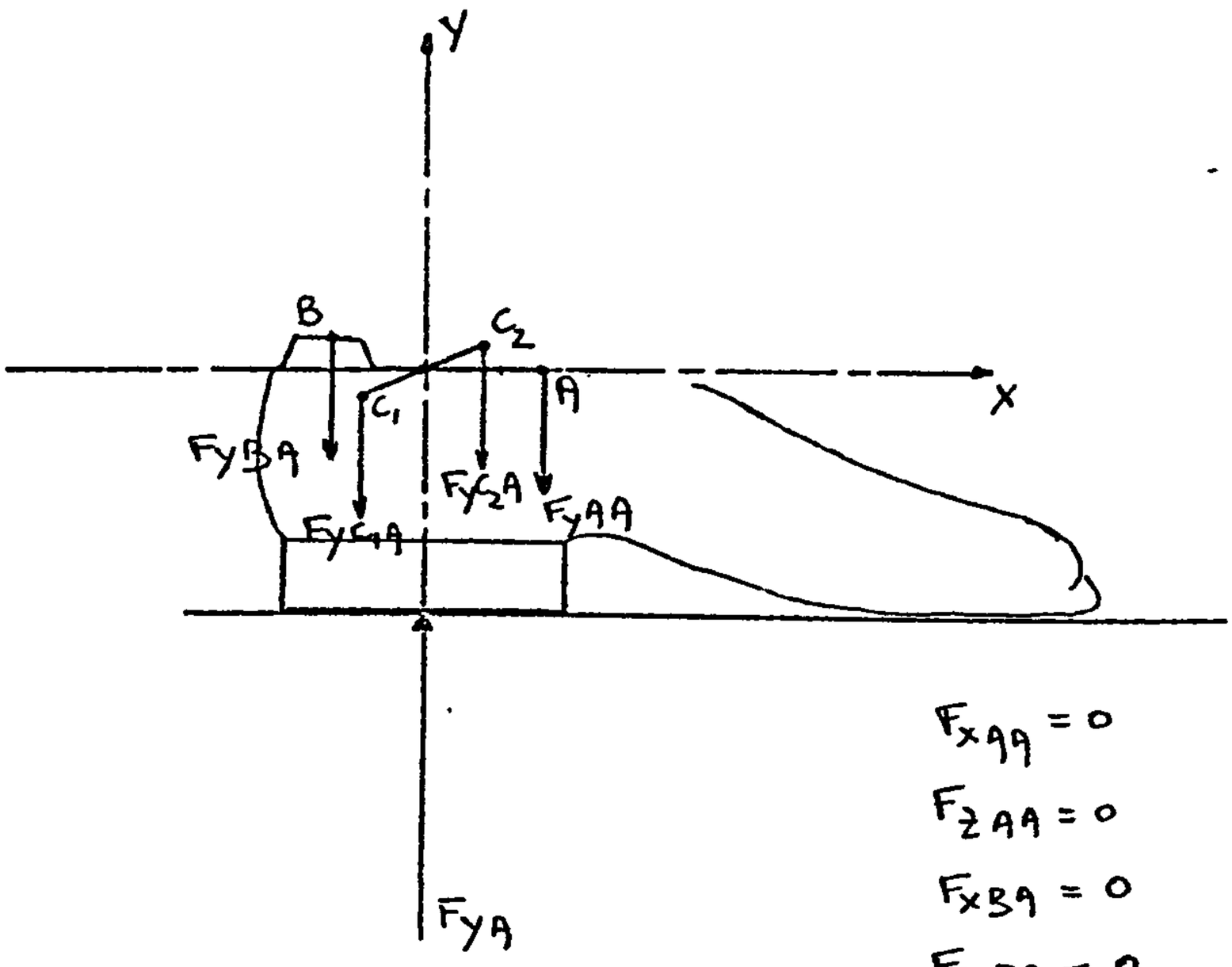

Figure 3.3: The foot flat loading case.

In figures 3.3, 3.4 and 3.5, the length of the different arrows are not proportional between themselves nor with the values of the represented forces.

to the axis positive directions (F_{yA} is positive upward) where the subscript A stands for axial:

$\Sigma F = 0$	$- F_{yC1A} - F_{yC2A} - F_{yAA} - F_{yBA} + F_{yA} = 0$	(3.1)
$\Sigma M_{o/x} = 0$	$(F_{yC1A} * f) - (F_{yC2A} * f) = 0$ hence, $F_{yC1A} = F_{yC2A}$	(3.2)
$\Sigma M_{o/y} = 0$		
$\Sigma M_{o/z} = 0$	$(F_{yBA} * c) - (F_{yAA} * e) = 0$ $F_{yBA} * c = F_{yAA} * e$ hence, $F_{yBA} = F_{yAA}$ since $c = e = 35$ mm	(3.3)

This set of three equations has four unknown values (F_{yC1A}, F_{yC2A}, F_{yAA} and F_{yBA}, but F_{yC1A}, F_{yC2A} and F_{yBA}, F_{yAA} are respectively equal). It is therefore possible to solve it. In practice, it means that axial load, called here F_{yA}, does not act only on the ankle axis. Transducers at each of the four points would be required to obtain this important axial load value. Moreover, in gait routine, the load is more complex than it is assumed, F_{yA} is not on Y axis and there will be:

1. a medio-lateral shear force Fz which introduces moments about the anterio - posterior X axis;

2. an anterio - posterior shear force Fx which introduces moments about the medio-lateral Z axis.

Therefore, all of these forces and moments have to be simultaneously measured.

3.3.2 Theoretical static equilibrium at heel - strike

The static balance equations with foot flat hold provided the inclination of the foot and the prosthetic shank tube is taken into account. At heel strike, this angle α is commonly 0.26 rad (15°) and this value will be thus be considered in the following

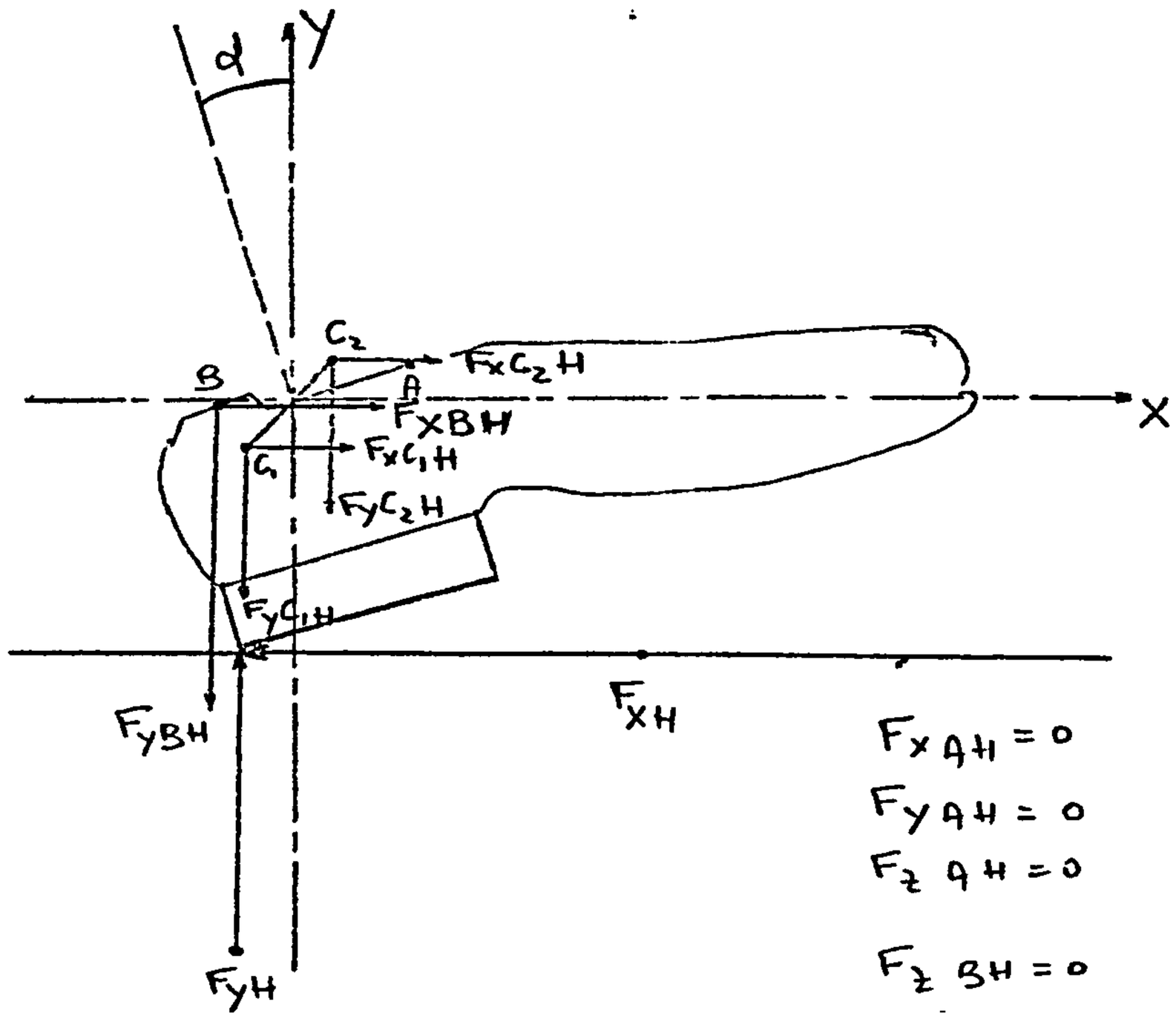

Figure 3.4: The heel strike loading case

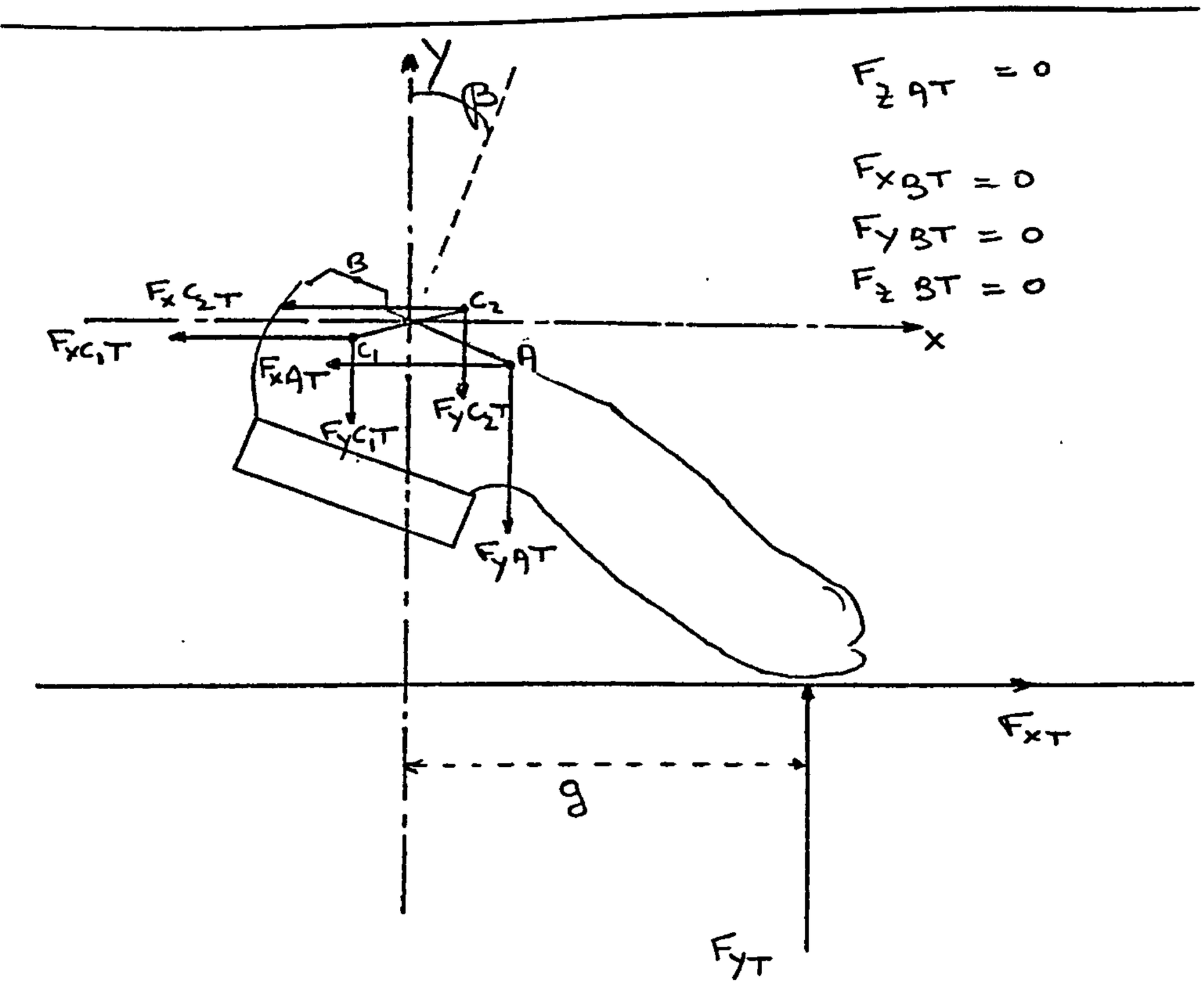

Figure 3.5: The toe - off loading case

calculations. In figure 3.4, the subscript H stands for heel - strike.

Because the ankle device is in plantarflexion, F_{xAH}, F_{yAH}, and F_{zAH} (A/P shear force, axial load and M/L shear force, at the front loading point A, respectively) are zero. By hypothesis, F_{xH} and F_{yH} have a value while F_{zH} is still equal to zero due to F_{yA} applied through the middle of the artificial ankle on the Y axis. Nothing else has changed. Respecting the positive axis directions, the whole set of equations becomes:

$\Sigma F = 0$	$F_{xC1H} + F_{xC2H} + F_{xBH} - F_{xH} = 0$ $- F_{yC1H} - F_{yC2H} - F_{yBH} + F_{yH} = 0$	(3.4)
$\Sigma M_{o/x} = 0$	$(F_{yC1H} * f) - (F_{yC2H} * f) = 0$ hence, $F_{yC1H} = F_{yC2H}$	(3.5)
$\Sigma M_{o/y} = 0$	$(- F_{xC1H} * f) + (F_{xC2H} * f) = 0$ hence, $F_{xC1H} = F_{xC2H}$	(3.6)
$\Sigma M_{o/z} = 0$	$(F_{yH} * \cos\alpha * a) + (- F_{xH} * \cos\alpha * a) + (F_{yBH} * c) + (F_{xBH} * d) = 0$	(3.7)

This set of three equations has four unknown values ($F_{yC1H} = F_{yC2H}$, $F_{xC1AH} = F_{xC2H}$, F_{xBH} and Fy_{BH}). It is therefore impossible to solve it. In practice, it means that the combined axial load (F_{yH}) and anterio - posterior shear force, named here as F_{xH}, are not transmitted only on the ankle axis. There is a sharing of the load between the rear flat flange (point load B) and the two points of the ankle axis (point load C_1 and C_2). Here also, three loading points will have a co-response. Therefore, it will not be easy to measure with enough accuracy these two important parameters of the gait using this shape of transducer.

3.3.3 Theoretical static equilibrium at toe - off

Due to the symmetry about the Z axis, the theoretical study was the mirror image of the one at heel - strike. The angle β between the vertical and the prosthetic shank tube was usually 0.34 rad (20°). Figure 3.5 shows the forces and moments balance.

	HEEL STRIKE	FOOT FLAT	TOE OFF
REAR FLANGE: LOADING POINT B	+	+	
ANKLE AXIS EXTERNAL: LOADING POINT C_1	+	+	+
ANKLE AXIS INTERNAL: LOADING POINT C_2	+	+	+
FRONT FLANGE: LOADING POINT A		+	+
Number of points under stress at each loading cases	**3**	**4**	**3**

Table 3.2: The different contact points and thus Wheatstone bridges where load was applied when the three main events of a stride occur.

	in literature	equations of equilibrium
Foot Flat		
F_x		≈ 0
F_y	0.9 * BW	618 N	$\Sigma Fy_{A,B,C1,C2} = 687$ N $Fy_{A,B,C1,C2} = 687/4 = 172$ N
F_z		≈ 0	≈ 0
Heel - Strike			
F_x	± 0.15 BW	- 103 N	$-F_y \sin\alpha = 213$ N
F_y	1.2 * BW	824 N	$F_y \cos\alpha = 795$ N
F_z	± 0.08 * BW	55 N	≈ 0
Toe - Off			
F_x	± 0.2 * BW	137 N	$F_y \sin\beta = 258$ N
F_y	1.1 * BW	755 N	$F_y \cos\beta = 709$ N
F_z	± 0.08 BW	- 55 N	≈ 0

Table 3.3: The theoretical numerical values found for a theoretical subject having a body mass of 70 kg (BW = 687 N; all forces are in N):

1. in literature (Plas *et al.*, 1979) for normal gait
2. applying the equations of equilibrium with the following lengths: c = e = 35 mm and f = 21 mm as shown in figure 3.2 (see sections 3.3.1, 3.3.2 and 3.3.3). The values for the angles α and β are respectively 15 and 20°.

Because both foot and ankle tend to be in dorsiflexion, there was no contact between the rear flange of the ankle and the rubber bumper of the foot. In other words, at the point B, there were neither loads nor moments. It is also important to notice that the front contact point between the flat flange and the rigid plastic ring was at the same level as the ankle axis. Using the same convention as above (the subscript T stands for toe - off), one has:

$\Sigma F = 0$	$- F_{xC1T} - F_{xC2T} - F_{xAT} + F_{xT} = 0$ $- F_{yC1T} - F_{yC2T} - F_{yAT} + F_{yT} = 0$	(3.8)
$\Sigma M_{o/x} = 0$	$(F_{yC1T} * f) - (F_{yC2T} * f) = 0$ hence, $F_{yC1T} = F_{yC2T}$	(3.9)
$\Sigma M_{o/y} = 0$	$(F_{xC1T} * f) - (F_{xC2T} * f) = 0$ hence, $F_{xC1T} = F_{xC2T}$	(3.10)
$\Sigma M_{o/z} = 0$	$(F_{yT} * \cos \beta * g) + (F_{xT} * \cos (\Pi/2 - \beta)) - (F_{yAT} * e) = 0$	(3.11)

Equations 3.2, 3.5, 3.9 and 3.6, 3.10 are equivalent because the entire device is in a similar position about the X axis. Here also, there are four unknown values ($F_{yC1T} = F_{yC2T}$, $F_{xC1T} = F_{xC2T}$, F_{xAT} and F_{yAT}) for three equations. Consequently, it is mathematically impossible to solve them. There is thus a sharing of loads between the ankle axis (point load C_1 and C_2) and the front flange of the prosthetic device (point load A). This introduces a major disadvantage.

In summary, it is possible to show in table 3.2, which points are in stress for each loading case.

3.3.4 Numerical Application

From Plas *et al.*, (1979), the numerical maximal values found during normal human gait were extracted. These values are shown in table 3.3 for a standard body mass of seventy kilograms.

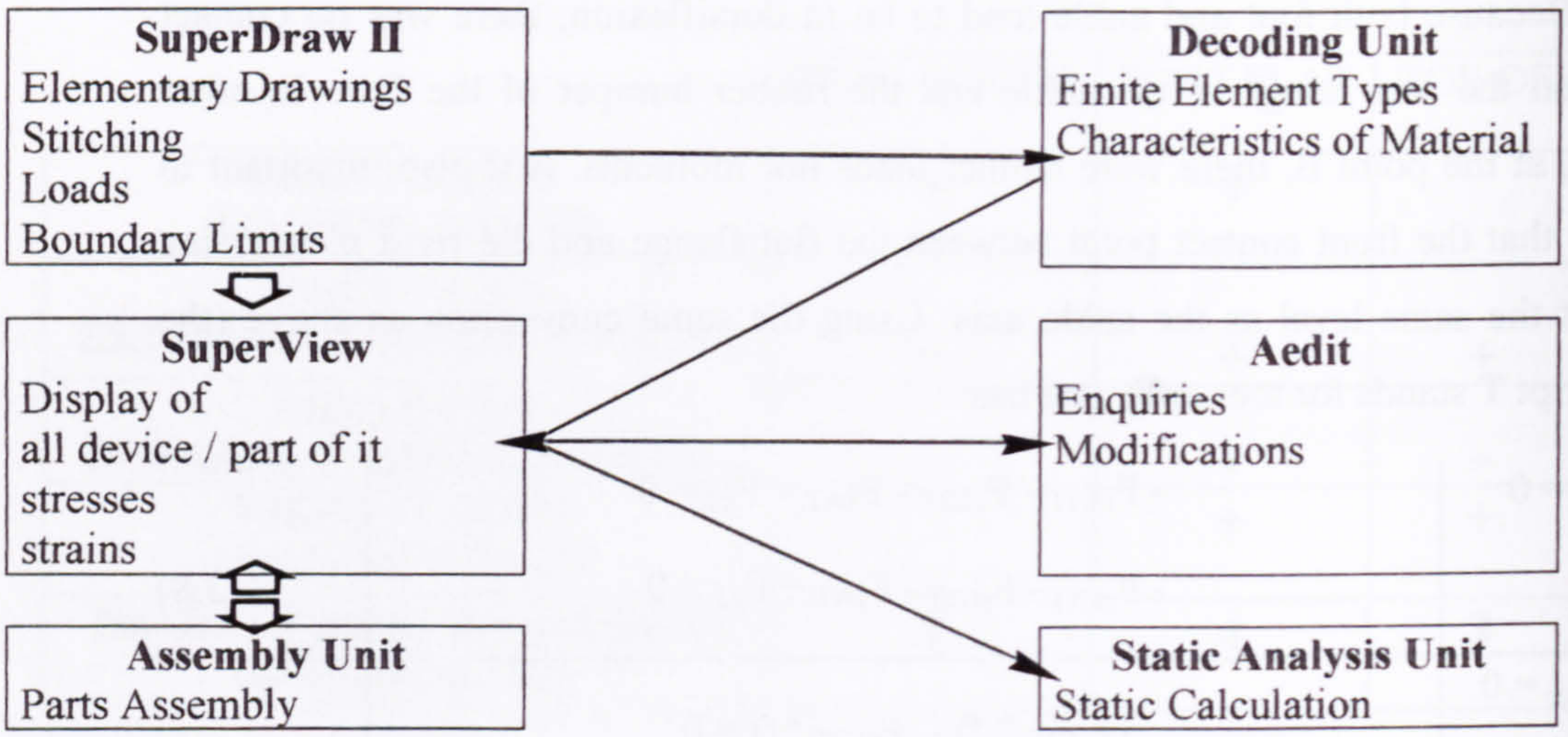

Table 3.4: Block diagram of Algor - CadSap

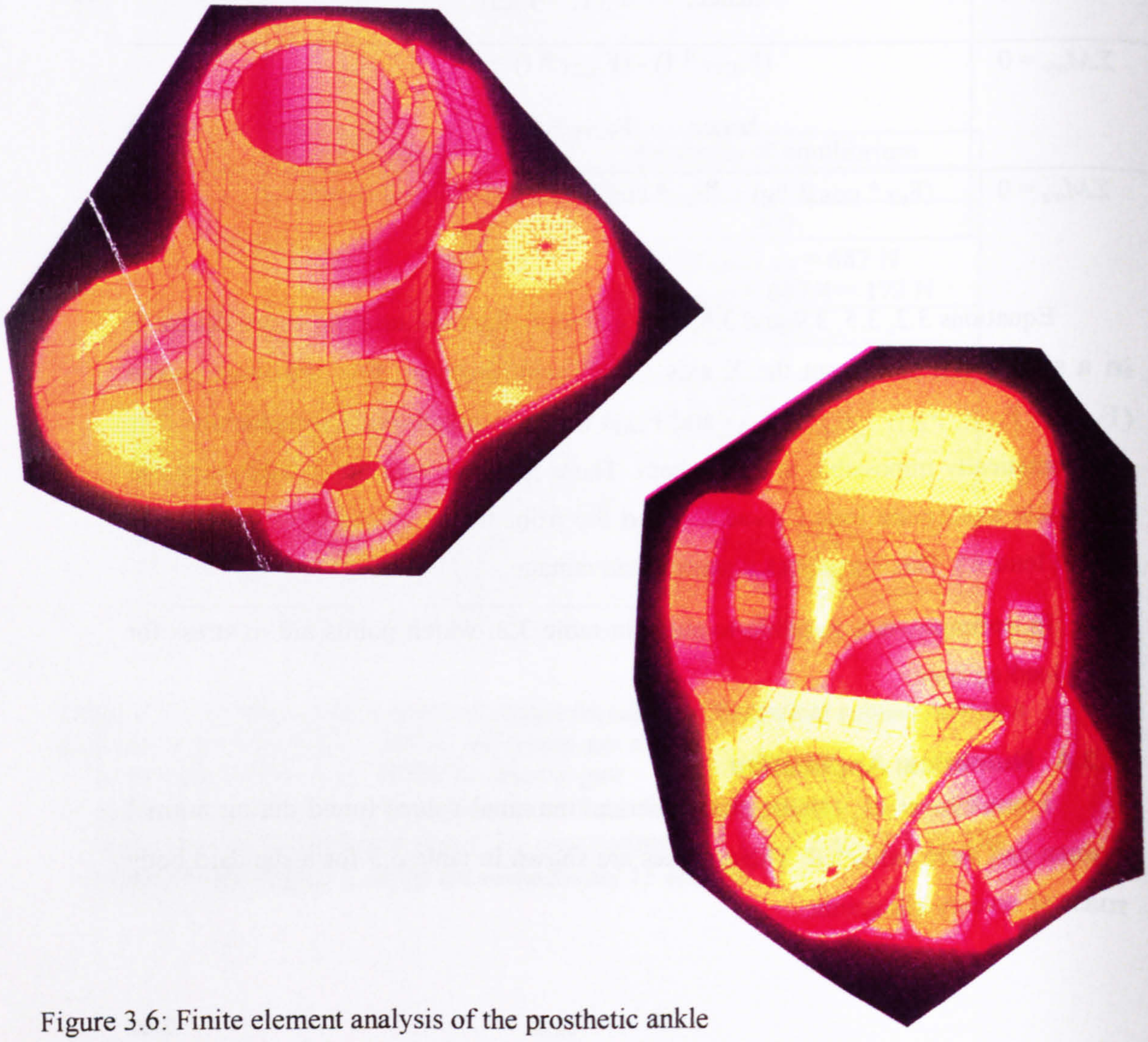

Figure 3.6: Finite element analysis of the prosthetic ankle

In practice, it is important to note that F_z (medio-lateral shear force) is not zero. It introduces some moment about the X axis, known, in physiotherapy practice, as pronation (external rotation) or supination (internal rotation) of the foot. These M/L shear forces along the Z axis are small in comparison with those along the two other axes.

Later, it will be interesting to compare all these forces with those given by the International Standard Organisation (ISO) for amputee proof tests and those measured by the transducer.

3.4 FINITE ELEMENT ANALYSIS OF THE ANKLE

The ankle device is geometrically complex; thus, the determination of the judicious place of the strain gauges was necessary. A judicious place could be defined as a location where stress is sufficiently high to be recorded by strain gauges, depending of the power supply and gain setting chosen. To determine the stress distribution, a finite element analysis was conducted using a commercial package called Algor-CadSap®[6], the French version of Algor®. Practically, the reasoning was to find where the stress was maximum for each loading case, and thus, to decide where the strain gauges might be fitted (i.e., the strain gauges must be positioned as close to the maximum stress areas as possible).

It was necessary to use six units:

1. SuperDraw II: CAD unit to model and define by the means of finite elements any structure in two or three dimensions;

2. Decoding Unit: to convert standard data in CadSap data plus definition of material characteristics;

3. AEdit: this unit reads and modifies any data as actions, nodes, materials;

4. Assemblage: this unit gathers the different parts of the device

---

[6]Algor-CadSap suppliers in France is: CADLM 9, rue Raoul Dautry 91190 Gif sur Yvette

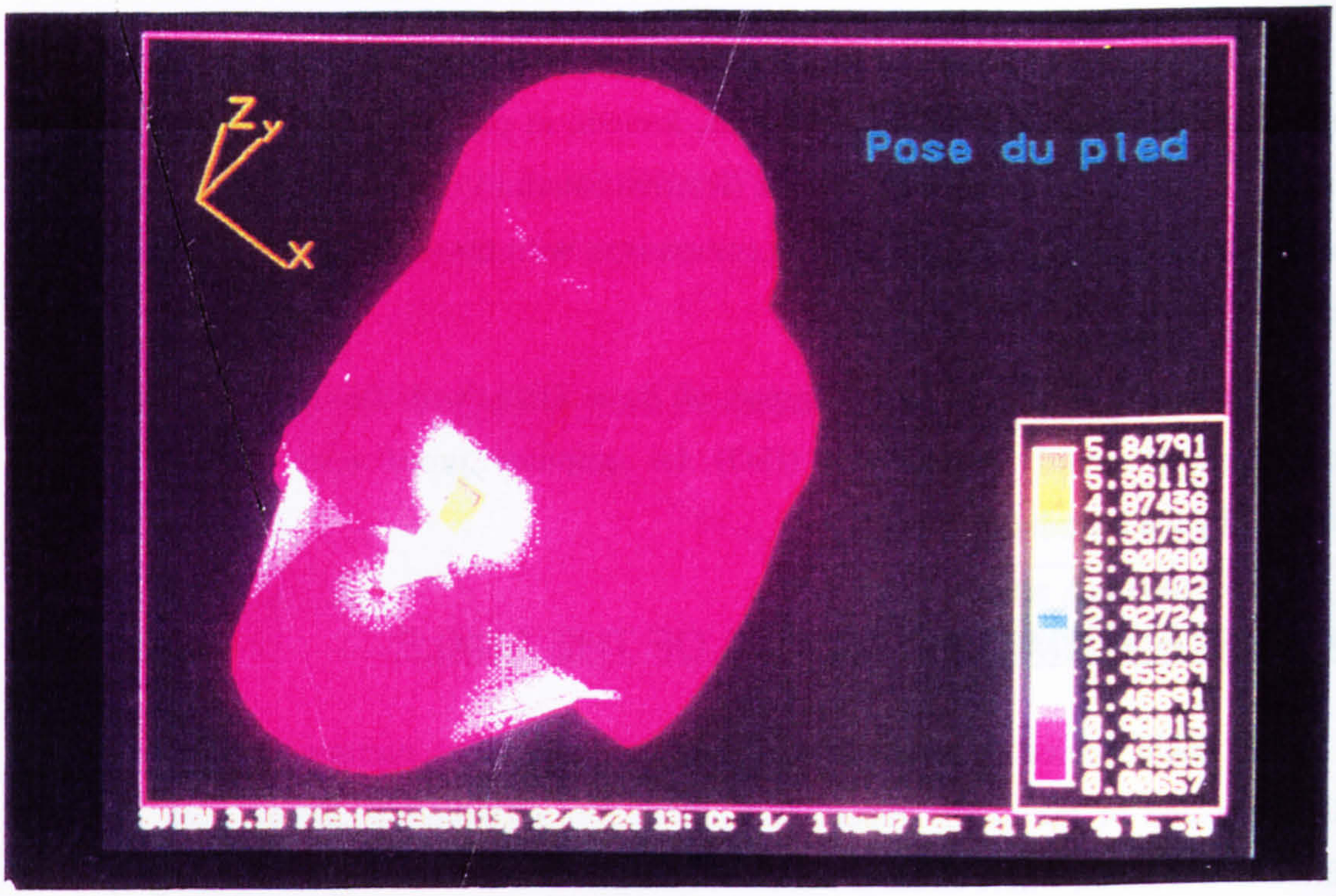

Figure 3.7: Finite element analysis of stresses at heel - strike (pose du pied). The exhibited values are stress, having $N.mm^{-2}$ as unit. The white parts on the lateral sides of the rear flat flange were under a stress of 3.9 $N.mm^{-2}$.

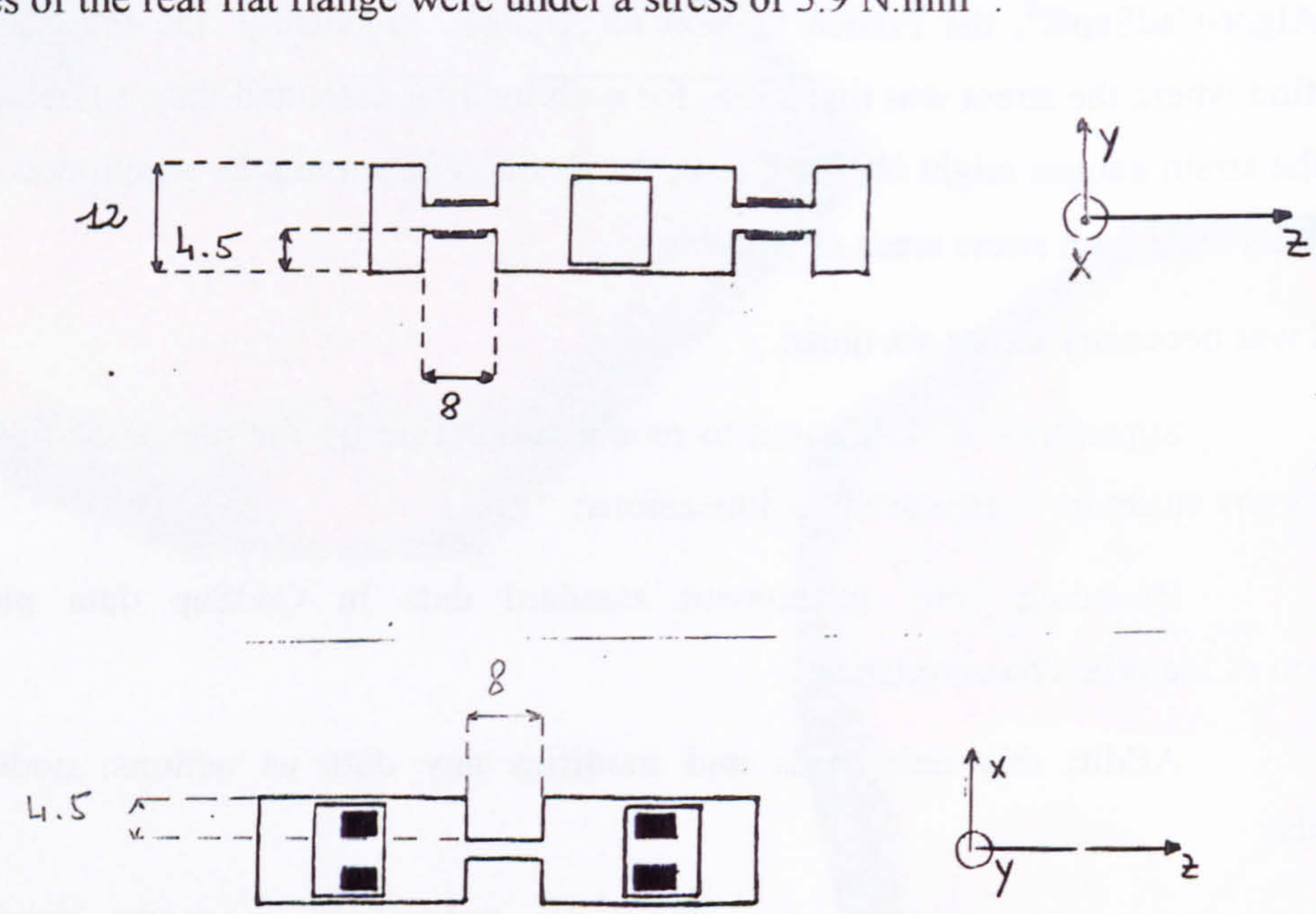

Figure 3.8: The artificial ankle axle
(lateral notches top; central notch bottom, all dimensions in mm).

modelled in the CAD unit;

5. Static Analysis: static calculation unit;

6. SuperView: this unit allows the visualisation of stresses and strains by the use of colour scales using Von Mises or Tresca criteria.

Table 3.4 shows the flow chart used for the modelling.

3.4.1 Design of the prosthetic ankle device

Because of the complexity of the device, it was necessary to divide it into ten parts called: part10, part20, ..., part100. To simplify the model, a piece of the shank tube has been put together. The boundary limit of this top part was an encastrement. It has been given the same material characteristics (Aluminium Alloy) as the ankle. The file corresponding to the tube is named part110, while the file named part100 represents the screw that holds the tube in position.

The AEdit unit showed that the ankle was represented by 1138 finite elements « brick » plus 1786 nodes as shown in figure 3.6, for example.

3.4.2 Results

The minimum microstrain value, that electrical strain gauges, (fitted in a full Wheatstone bridge with a power supply of 3 V and a gauge factor of 2), can record, could be estimated as $\varepsilon = 0.4$ μstrain for one computer unit (see equation IV.5, appendix 11.IV.3.3). It was therefore, necessary to evaluate at which level in value, stresses and strains were distributed throughout the artificial ankle (to transform stress into strain, see appendix 11.IV and properties of the material in table 3.1).

The results are shown in figure 3.7 for heel strike (plantarflexion). The calculated stresses were combined to give the Von Mises criteria (using Tresca criteria gave the same results). Figure 3.7 shows a stress of $\sigma = 3.9$ N.m^{-2} (for a unit load weight of 9.81 N), equal to $\varepsilon = 39$ μstrain on the lateral sides of the rear flat flange, on both sides of the rubber bumper calotte.

Using the equations for static equilibrium (see sections 3.3.1, foot flat; 3.3.2, heel- strike and 3.3.3, toe off) with the numerical values shown in table 3.3, it was

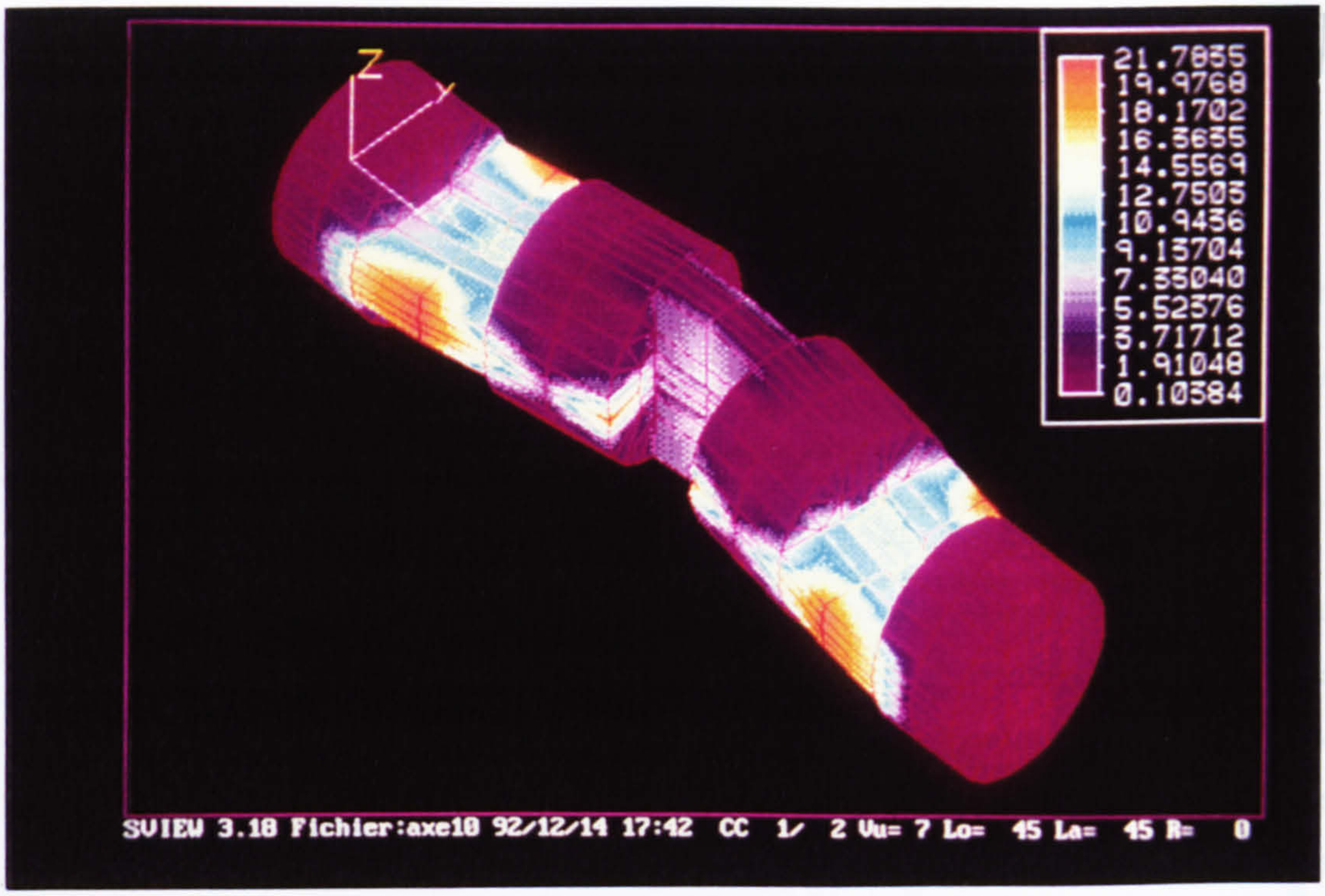

Figure 3.9: The ankle axis under an axial load using Van Mises criteria.

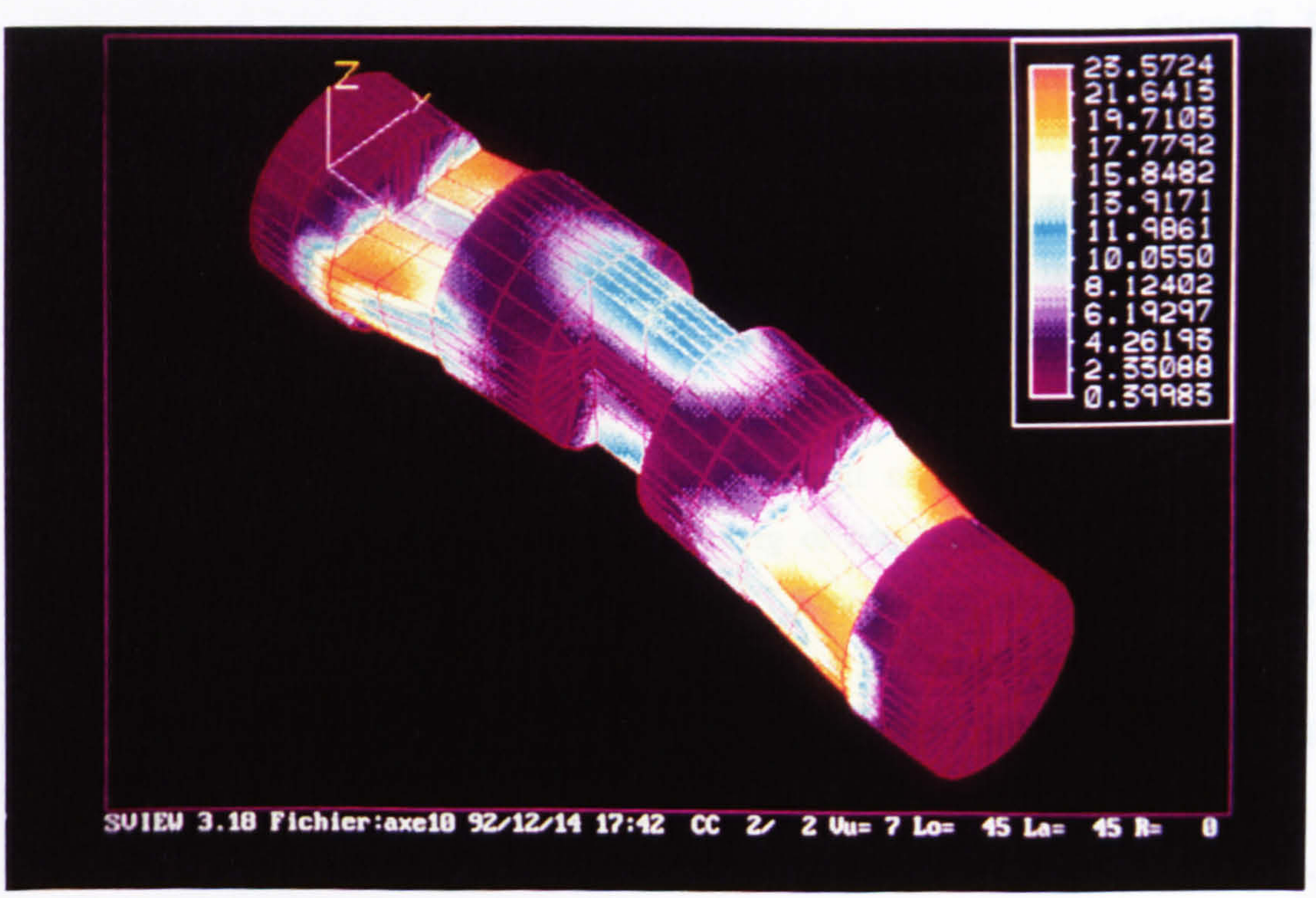

Figure 3.10: The ankle axis under anterio-posterior load.

possible to evaluate the stress where the proposed strain gauge bridges will be fitted. The mean maximum stress value was $\sigma = 1.5$ N.m^{-2}, equivalent to a strain of $\varepsilon = 15$ μstrain for a unit load weight of 9.81 N, (i.e., a mass of 1 kg). These results were found on the ankle axle bridges in foot flat, posterior flange bridges at heel-strike and anterior flange bridges at toe-off.

The results for toe - off were the same as above. Stress values were $\sigma = 1.5$ N.m^{-2} while strain values were 15 μstrain for an identical load case at each side of the front flat flange, where strain gauges have been glued.

All of these microstrain values showed that there were above the minimum required (0.4 μstrain per one computer unit) and thus, high enough to be recorded by a full bridge of electrical strain gauges

It should be noted that to obtain these results, it was necessary to make the front flange thinner (from 3 millimetres to 2 millimetres) and to cut the front shoulder. This was unavoidable but it made the prosthetic ankle transducer weaker than the standard ankle component (see section 3.6).

3.4.3 Design of the ankle axle

The ankle axle, made of steel, was machined with three planes looking like notches. The axle is shown in figure 3.8. These planes define some sections whose cross-sectioned area properties are known. The two lateral notches (8 mm * 4.5 mm each) are parallel to the X axis and perpendicular to the Y axis. These two lateral planes would have a response with both medio-lateral moments and axial load compression.

The central notch (8 mm * 4.5 mm) is parallel to the Y axis and perpendicular to the X axis, this plane could be gauged to measure the anterio - posterior shear force. The two sets of planes are at ninety degrees.

To define place, width and depth of the notches, a finite element model was made in the same manner as above for the ankle. Figure 3.9 shows the axle under axial load compression as a first loading case. The deformation in this direction is enough to have a suitable response from the gauges. The second loading case is

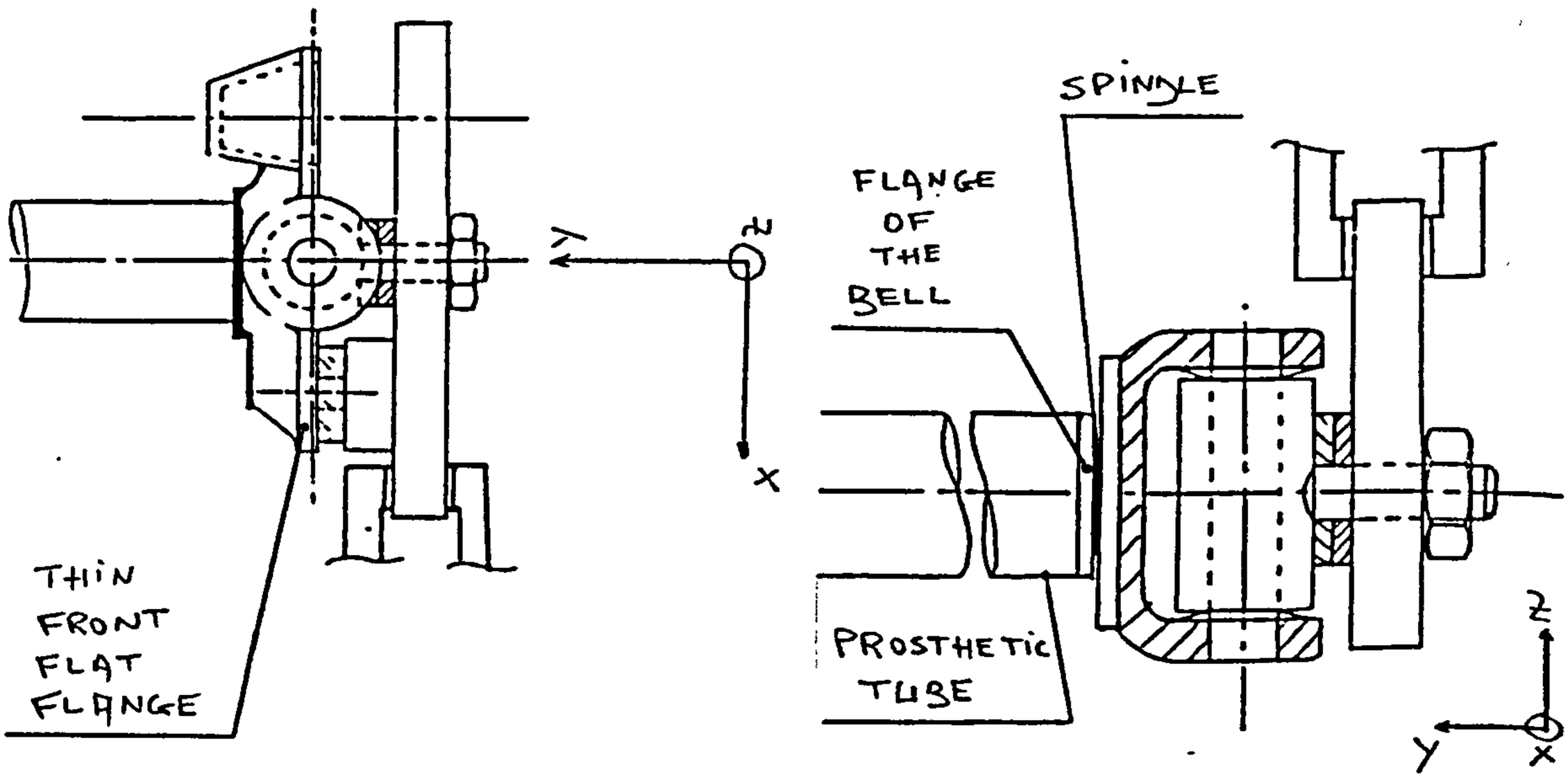

Figure 3.11: The set up for A/P and M/L bending moments calibration. The thin front flat flange; the flange of the bell and the spindle are shown.

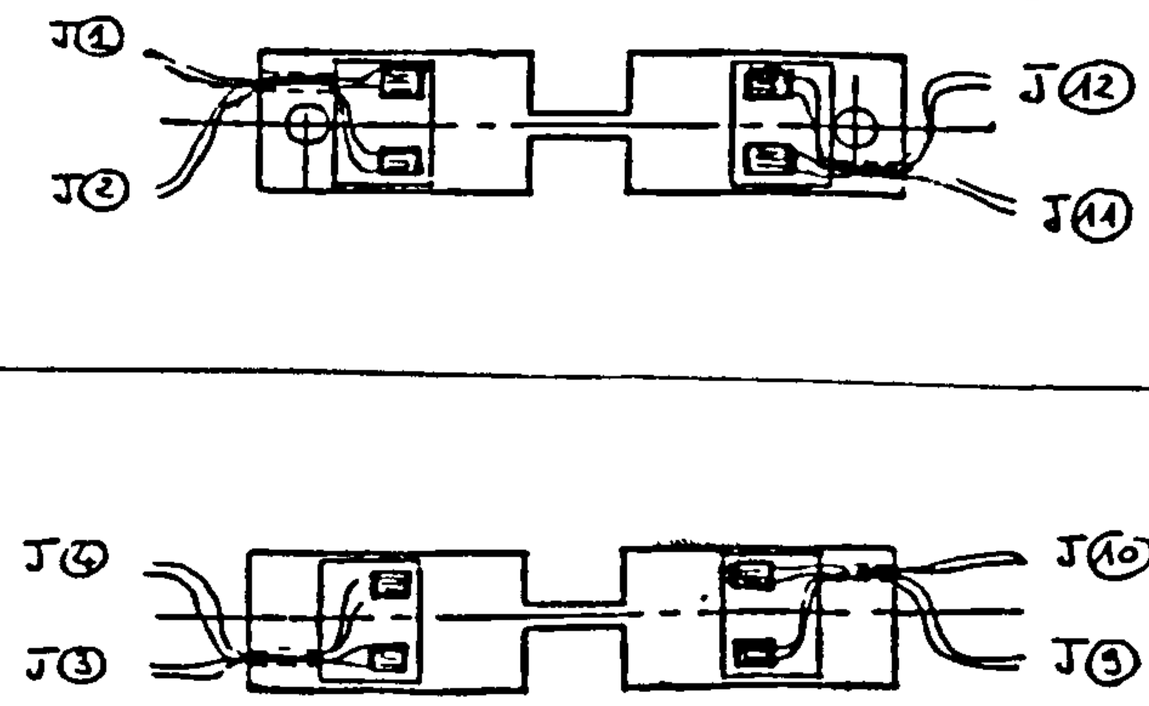

Figure 3.12: The final design of the ankle axle.

shown in figure 3.10: anterio - posterior shear force. The central notch did not respond enough: the deformation was insufficient to generate any signal in that particular channel, and thus the transducer had to be modified.

3.4.4 Final description of the ankle transducer

Figure 3.11 shows the final design of the ankle transducer, ready to be calibrated in A/P and M/L bending moments. The front flat flange was machined to be thinner and the shoulder was cut (see figure 3.1). On the front and rear flat flanges, at the places where gauges would be mounted, the aluminium surface was slightly machined: 1) to ensure that the two surfaces were strictly plane and parallel, 2) to be certain that the aluminium areas where gauges were fitted would provide a good quality contact surface.

Figure 3.12 shows the final design of the ankle axle after gauging. The central notch remained empty. The two lateral notches were provided for two full bridges measuring mainly the pylon axial load.

Figure 3.13 shows the solution adopted for the measuring of anterio-posterior shear force in order to replace the inefficient central notch of the ankle axis. A central and vertical shaft, concentric with the Y axis, covered with a "bell" on which the shank tube of the prosthesis reached down to load. This central axle was named the spindle, to avoid any confusion with the ankle axle. A space between the axis and the bell was left free to fit gauges on the spindle. All forces or moments, coming up from the ground or down from the prosthesis socket must be transmitted by through this spindle. Hence, it appears that the spindle will be sensitive to all forces and moments as well as to the anterio-posterior shear force Fx. This important comment will be exploited further when discussing the design of a new pylon transducer. However, at this time, only anterio-posterior shear gauges will be fitted on the spindle.

The protruding edge located at the bottom of the bell was designed so that, when the prosthetic shank tube was located on it, the previous height of the prosthesis was maintained.

A central bolt fixed the spindle onto the bell and it was only necessary to clamp

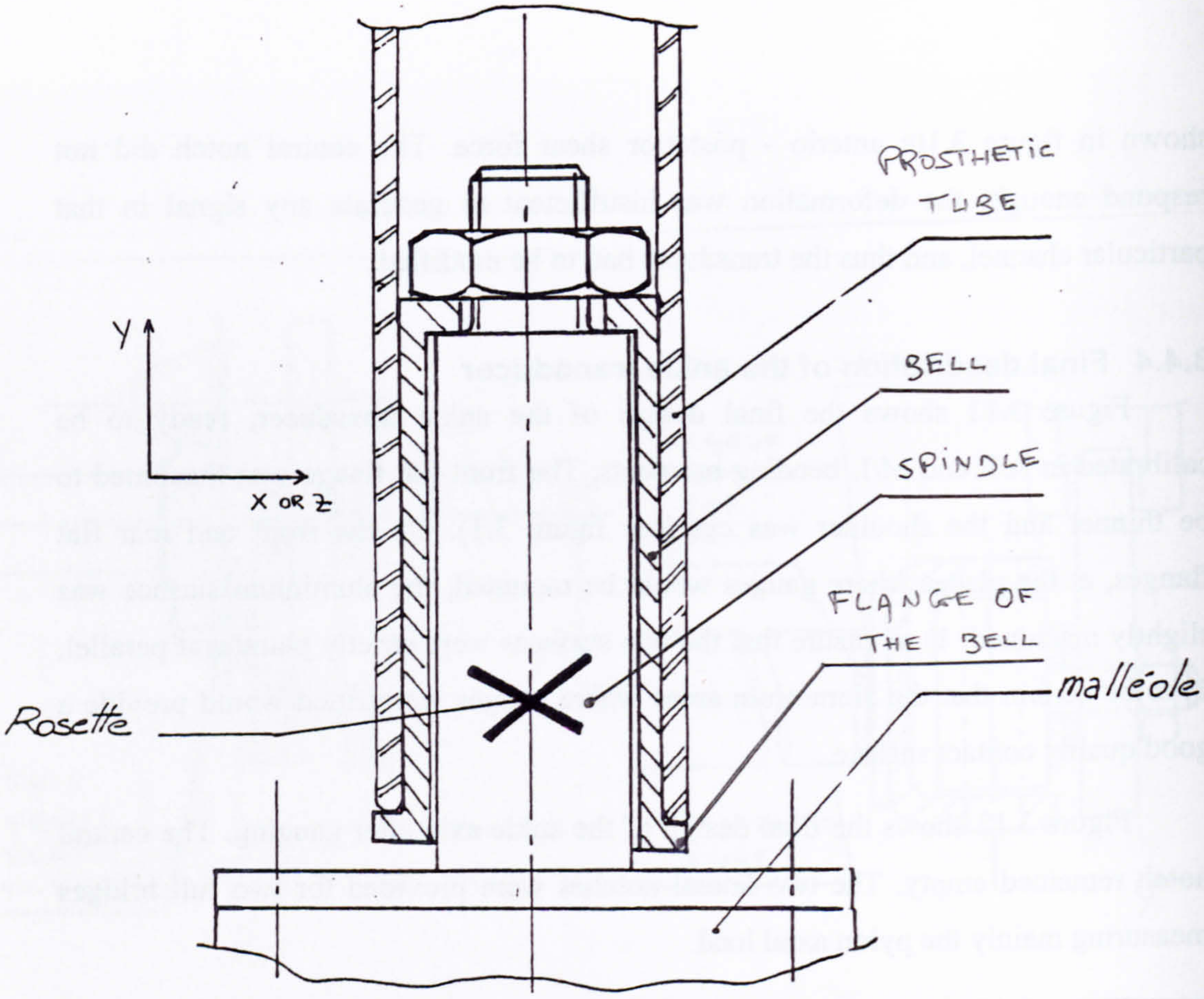

Figure 3.13: The central and vertical shaft (spindle) and the « bell » covered by the prosthetic shank tube.

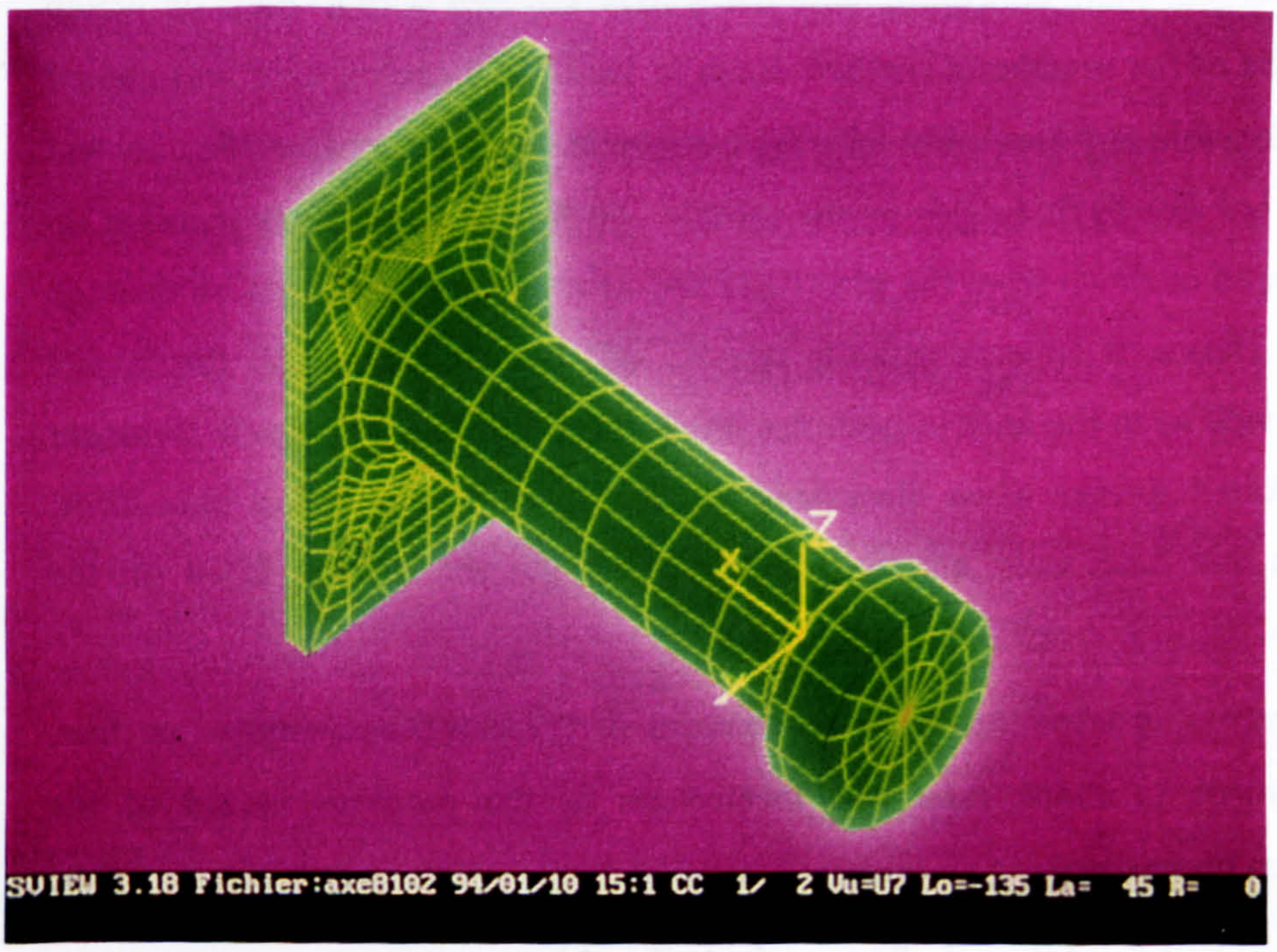

Figure 3.14: The finite element analysis of the spindle.

the prosthetic shank tube on the bell to assemble all the parts of the prosthesis. Figure 3.14 shows the finite element analysis of the spindle. It was necessary to machine two notches (3.5 * 20 mm) in the XY plane to increase its sensitivity for measuring fore and aft shear forces. The dimensions of the spindle are shown in figure 3.15.

3.4.5 Gauge location

Despite our requirements (i.e., a novel pylon transducer similar to the Strathclyde Pylon Transducer, designed by Berme *et al.*, 1975), the ankle transducer Model I could not, by design, record more than 5 channels. Because of the shape of the ankle part of the transducer and the design of the spindle (not totally cylindrical, see figure 3.15), no transverse torque gauges were fitted on this new device. It was, thus, not possible to measure the transverse torque (moment My about the Y axis) but this gait parameter exhibits usually a small value in amputee gait (a mean of 2 N m with the studied patients using two walking aids, see chapter 8). Therefore, neglecting the transverse torque was not considered important for clinical day to day practice. The lateral shear force Fz was also ignored.

All Wheatstone bridges were able to measure one and only one element of the gait, except two out of five. The lateral and medial ankle axle gauges recorded simultaneously the axial load (Fy) and the medio-lateral bending moment (Mx).

Figure 3.16 shows the location of the five Wheatstone bridges.

Two were on the front and the rear flanges of the ankle. They measured respectively the dorsiflexion moment (Mz positive) and plantarflexion moment (Mz negative). Two gauges were at both sides of the ankle axle, they measured axial load (Fy) and supination - pronation moments (Mx positive and negative). The last one is located on the spindle, it measured the anterio-posterior shear (Fx positive and negative).

In other words, with this first ankle transducer (Model I), it was possible to assess two forces and two moments among the six usual measures of kinetic studies, regularly recorded by any transducer. A summary is shown in the following table 3.5:

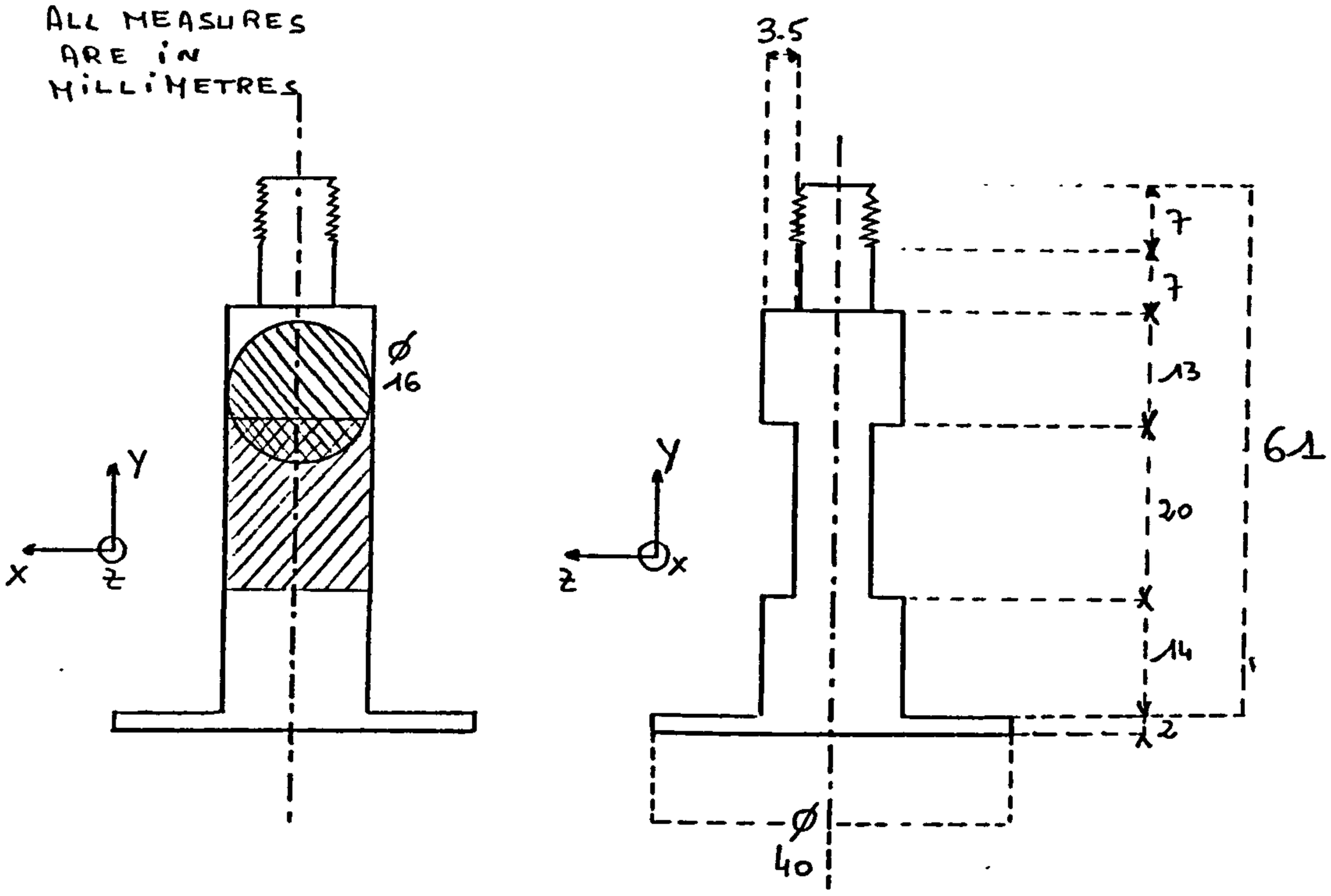

Figure 3.15: The final dimensions of the spindle.

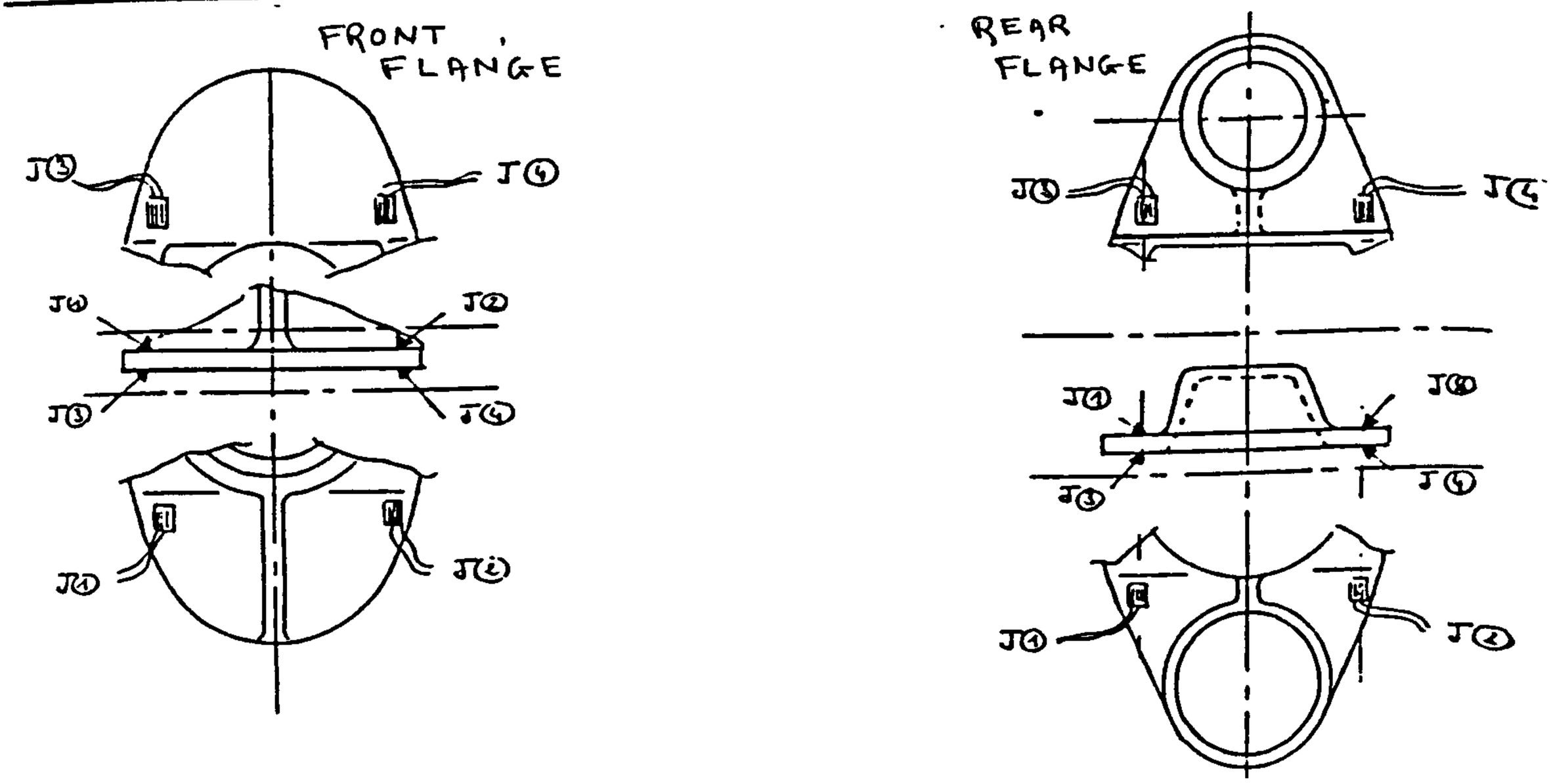

Figure 3.16: The gauges location on the ankle transducer.

Channel N°1	A/P shear forces	Fx + Fx -	rosette gauges on the spindle	
Channel N°2 Channel N°3	axial load	Fy	external gauges (ankle axis)	
			internal gauges (ankle axis)	
	M/L moments	Mx +	internal gauges external gauges	compression tension
		Mx-	internal gauges external gauges	tension compression
Channel N°4	A/P moments	Mz +	front flange gauges	
Channel N°5		Mz -	rear flange gauges	

Table 3.5: The five channels of the first new transducer: the channels 2 and 3 recorded simultaneously two load components (Fy and Mx). When Mx was positive, the internal Wheatstone bridge, situated on the artificial ankle axis, was in tension while the external was in compression.

It is important to notice that all forces and moments situated in the anterio - posterior plane XY are recorded. Winter & Sienko (1988) carried out a gait study of amputees taking only account of the gait parameters in anterio-posterior plane, because he had only a 2-D movement analysis system. Although, it was a limitation and that was the second drawback of this transducer design.

The gauges were French made[7] (PA-06-6060CA-350) for both the ankle and the spindle. Vishay - Micromesures[8] (EA-06-125PC-350) was the supplier of gauges for the steel ankle axis. These gauges are double and perfectly parallel between themselves. On the spindle, the rosette gauges have a resistance of 120 Ω, they are mounted at 45° about the X and Y axes. This geometry permits the fore - aft shear forces only to be recorded, independently of the moments.

All channels were in full Wheatstone bridges. The bridge voltages were 3 volts, recommended by the both companies for 120 and 6 V for 350 Ω gauges, taking account of the power dissipation of the aluminium. All amplifier gains were 500. A full explanation of the gauges, bridge voltage and gain settings will be presented and

---

[7]Société Européenne d'Extensométrie Appliquée (SEEA) 18, rue Françis Vovelle 28000 Chartres France

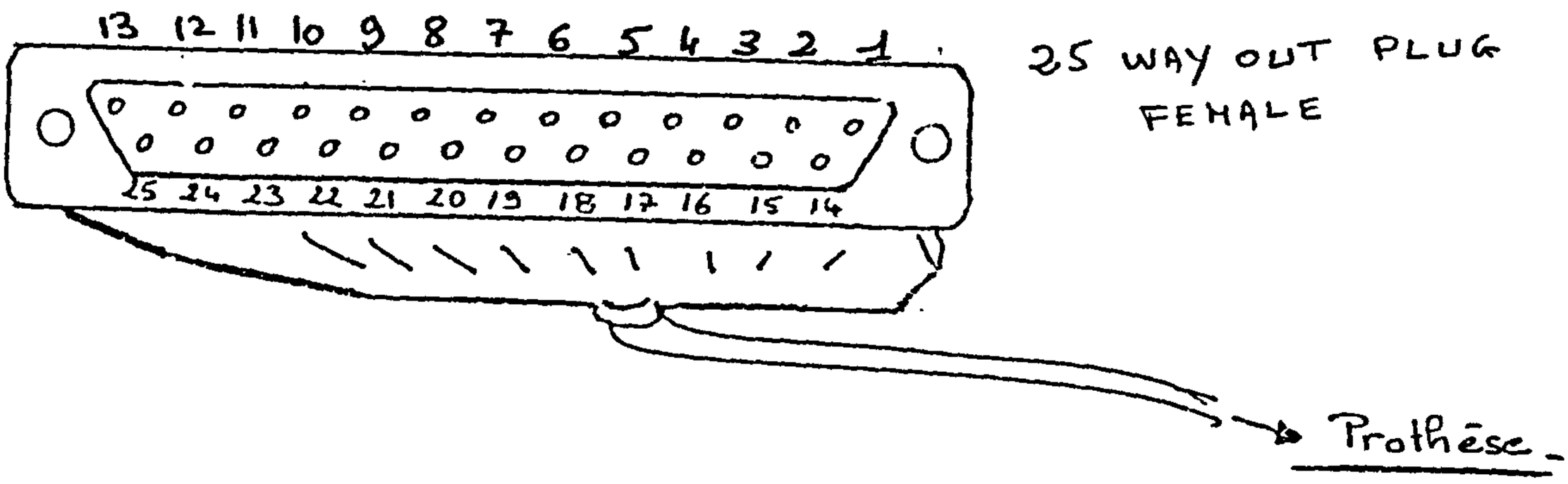

	PIN'S DISTRIBUTION	
FRONT GAUGES	9 - 23 10 - 22	± ve supply ± ve signal
BACK GAUGES	11 - 25 12 - 24	± ve supply ± ve signal
LATERAL AXIS	3 - 17 4 - 16	± ve supply ± ve signal
MEDIAL AXIS	5 - 19 6 - 18	± ve supply ± ve signal
SPINDLE GAUGES	7 - 21 8 - 20	± ve supply ± ve signal

Figure 3.17: The distribution of the pins

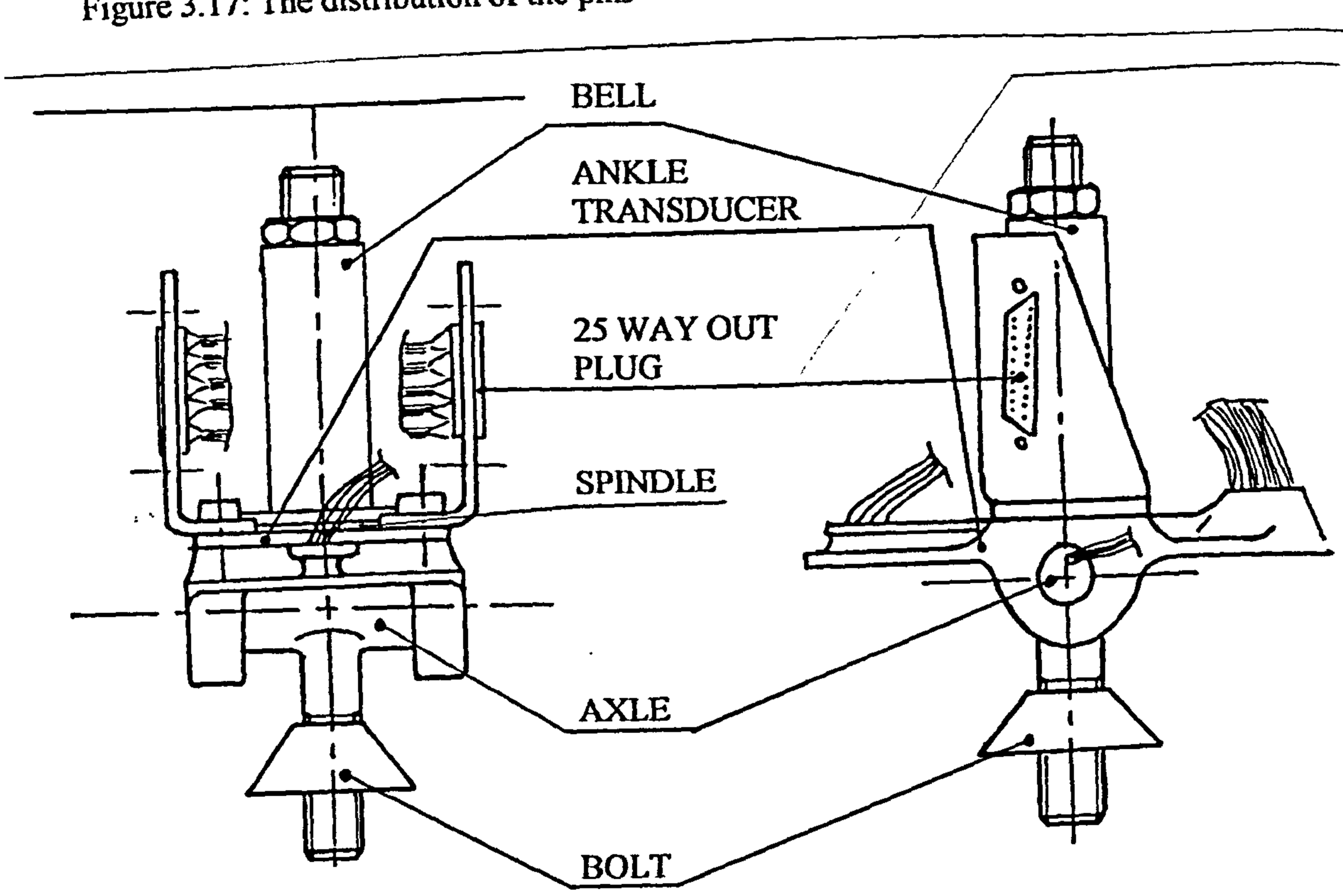

Figure 3.18: The final view of the ankle transducer.

described in chapter 4.

The output was through a 25 way plug. The pin connection diagram of the plug is shown in figure 3.17. Figure 3.18 shows the transducer fully assembled with the bolt that fixed it onto the artificial foot.

3.5 CALIBRATION

3.5.1 Introduction

A rigorous calibration was carried out on the new transducer. The technique used was to put one and only one known load on the transducer and then to record its response. This was necessary to convert forces (in N) or moments (in N m) input in computer units of the print out. These computer units have a linear relation with the electrical output of the transducer. When used with patients, it was possible to convert computer units back into N or N m.

A full description of transducer calibration will be given in chapter 6.

3.5.2 Amplifiers and recording system used

3.5.2.1 AMPLIFIERS

A set of eight identical amplifiers was supplied by the same French manufacturer of the strain gauges. Technical specifications of these amplifiers are given in appendix 11.III.1. When they were checked by means of an oscilloscope, their responses were stable, with no interference nor drifting. The fine balance was easy through a potentiometer while gross balance required the addition of some resistors. This task had to be done only once. In practical use, gauge circuits did not require more than fine adjustment. All the tests, performed with this pylon transducer, were conducted with a common bridge voltage of 3 volts, except 6 V for the 350 ς strain gauges fitted on the steel ankle axis, and a uniform gain of 500.

3.5.2.2 RECORDING SYSTEM

From the transducer and the amplifier box, a complete recording set was used. This data acquisition set had a configuration as follows: transducer → amplifier box

---

[8]Vishay - Micromesures 98, boulevard Gabriel Péri B.P. 51 92242

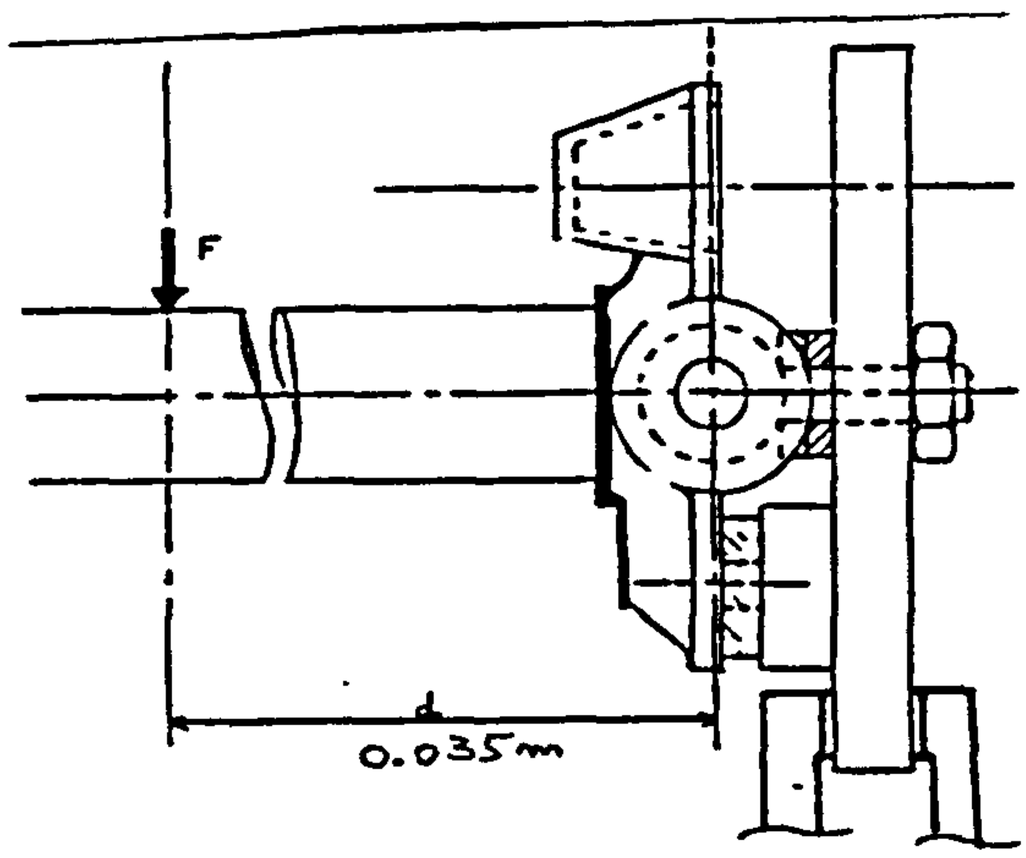

Figure 3.19: Pure Fx shear

	Mass in kg	Load Case in N
0 kg + shank tube + transducer + wires	0.344	3.374
+ steel wires and weight carrier	+ 0.770	10.928
weight n° A9	+ 10	109.028
weight n° A10	+ 10	207.128
weight n° A11	+ 10	305.228
weight n° A12	+ 10	403.328
weight n° A13	+ 10	501.428
weight n° A4	+ 5	550.478

Table 3.6: Load case for Fx shear force

Channel n°1	rosette gauges	shear main response
Channel n°2	lateral ankle axis gauges	secondary response in traction
Channel n°3	medial ankle axis gauges	secondary response in traction
Channel n°4	front flat flange gauges	secondary response in compression
Channel n°5	rear flat flange gauges	zero

Table 3.7: All responses with Fx positive

Channel N°1	Rosette gauges on the central spindle			
Loading Case in N	Fx +		Fx -	
	Trial No 1	Trial No 2	Trial No 3	Trial No 4
3.374	2002.3	2003.2	2001.9	2004.1
10.928	2008.3	2007.7	2006.2	2007.3
109.028	2065.6	2065.6	1947.9	1949.1
207.128	2123.4	2123.5	1889.2	1890.6
305.228	2181.9	2181.7	1831.5	1832.7
403.328	2240.2	2239.7	1773.1	1774.6
501.428	2299.1	2298.2	1714.3	1716.1
550.478	2327.5	2327.4	1687.7	1697.8
550.478	2328.1	2327.8	1688.1	1697.4
501.428	2299.4	2299.1	1714.3	1717.8
403.328	2241.1	2240.9	1773.1	1774.1
305.228	2183.1	2182.5	1831.1	1831.9
207.128	2124.7	2124.4	1889.7	1889.7
109.028	2066.7	2066.1	1974.6	1948.3
10.928	2008.5	2008.7	2005.7	2006.7
3. 374	2004.2	2003.9	2002.9	2002.1

Table 3.8: Main channel for A / P shear force

→ Amplicon A/D board PC 26AT® → Acquire data acquisition programme.

The analogic - digital board used was a high-speed 12-bit converter. It was easy to fit and use. Complete description and jumper selections of the A/D board are shown in appendix 11.III.2[9].

The data acquisition program Acquire version 1.8 (Philips, 1990) used is convenient software developed in the Bioengineering Unit. It allowed the recording of up to 16 channels of data. The user could choose the sampling frequency, (i.e. the speed at which data samples are collected). The duration of data collection depended on the sampling frequency and the memory capacity of the computer.

The results are given in computer units (cu) with the following convention:

$$4096 \text{ cu} = 10 \text{ V}$$

or

$$1\text{cu} = 2.44\ 10^{-3} \text{ V} = 2.44 \text{ mV} \qquad 1 \text{ mV} = 10^{-3} \text{ V} = 0.41 \text{ cu}$$

The data was stored in a special DOS file *.DAT. These files could not be set up within Acquire. We had to transfer them using a feature in Acquire called Export Data. This created an ASCII file with *.PRN as extension which allowed the data to be used in a commercial spreadsheet such as Microsoft Excel®. A numerical display and an oscilloscope were available in Acquire and it was possible to retrieve all the *.DAT files.

This friendly computer programme had a little bug when data are exported. The computer unit of the last channel in the last row had an error. Thus, it was necessary to record more data than required and then to erase the last line.

3.5.3 Following method

Details of calibration tests are presented in chapter 6. However, it is now sufficient to say that the dead-weight method, recommended by Magnissalis (1992) was used. Each loading case involved applying either a single force or moment. The

---

Malakoff Cedex France

Mass	Load	Fx +				
kg	in N	Test n°1				
			Regression Statistics			
0.344	3.37	2002.3	Multiple R	0.99998722		
1.114	10.93	2008.3	R Square	0.99997445		
11.114	109.03	2065.5	Adjusted R Square	0.99997263		
21.114	207.13	2123.4	Standard Error	0.63967187		
31.114	305.23	2181.9	Observations	16		
41.114	403.33	2240.2				
51.114	501.43	2299.1		*Coefficients*	*Standard Error*	
56.114	550.48	2327.5				
56.114	550.48	2328.1	Intercept	2001.47943	0.26348417	
51.114	501.43	2299.4	x1	5.81848994	0.00785971	
41.114	403.33	2241.1				
31.114	305.23	2183.1				
21.114	207.13	2124.7	*t Statistic*	*P-value*	*Lower 95%*	*Upper 95%*
11.114	109.03	2066.7	7596.203456	8.287E-51	2000.91430	2002.04454
1.114	10.93	2008.5	740.2932158	1.2196E-35	5.80163252	5.83534736
0.344	3.37	2004.2				

Table 3.9: Regression Analysis of the test N°1 for Fx +. The strain gauges were fitted on the spindle covered by the bell.

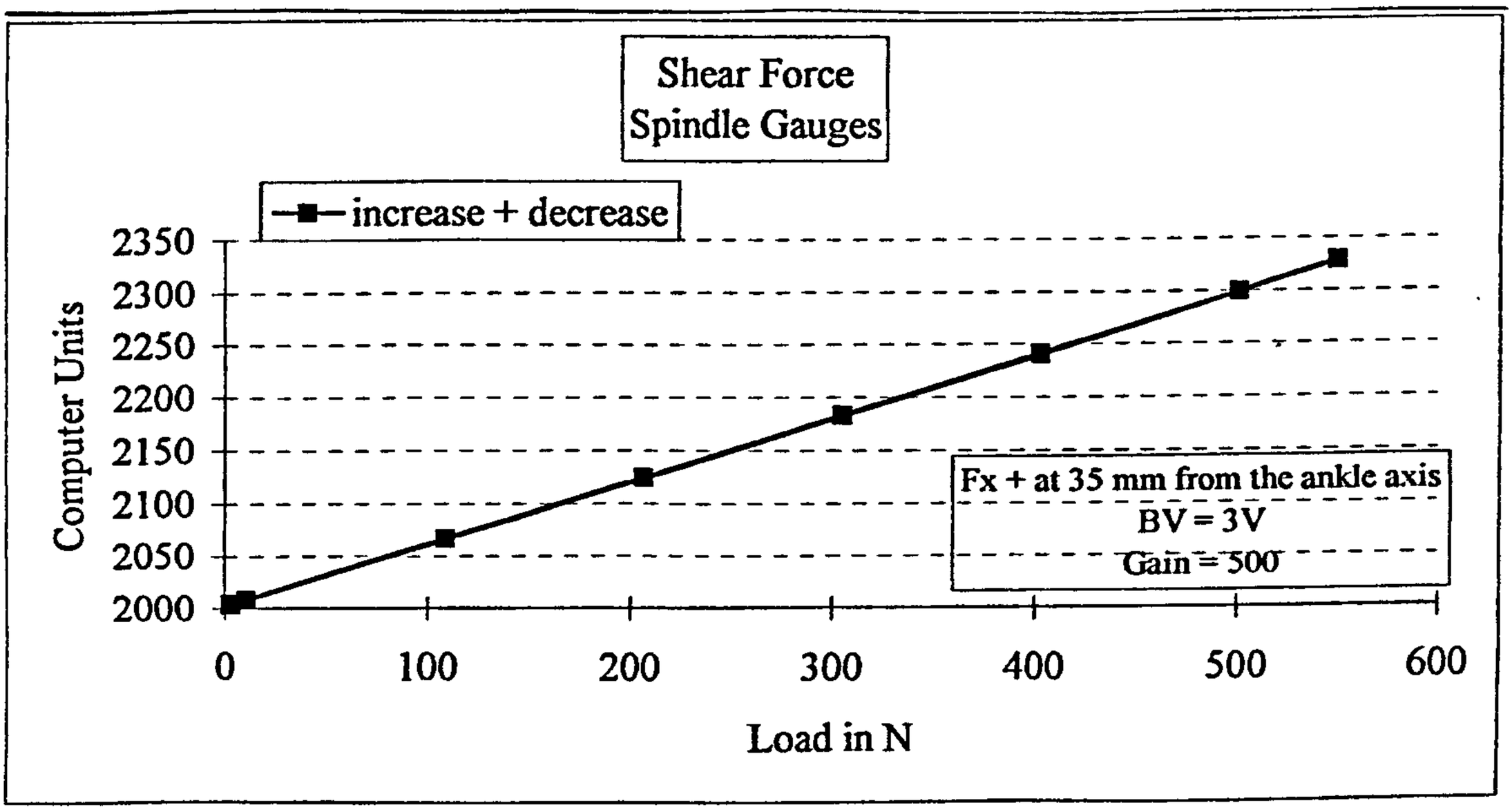

Figure 3.20: The test N°1 of A/P shear force Fx positive recorded from the spindle gauges: the traces are linear with no drifting.

transducer was bolted on a special heavy table, used as a bench, to have a static set - up. The operator had to wait until everything was stable before data was recorded over a period of 11 seconds at the sampling frequency of 1 Hz. This allowed the last second of recording to be cancelled thus avoiding the Acquire bug previously mentioned. Therefore, ten values (10 seconds at 1 Hz) were recorded for each loading case and it was possible to perform a statistical analysis of these values. For each set up and loading cases, four tests were conducted in two different days to ensure repeatability of results.

As an example, table 3.6 shows the results for an anterio-posterior shear force Fx. The set up was a cantilever configuration. All the weights used were calibrated by an authoritative calibration and test centre as shown in appendix 11.III.3. The force passed through the centre line of the spindle shear gauges at 0.035 m from the ankle axis, as shown in figure 3.19.

3.5.4 Results

Table 3.7 indicates all responses recorded in the Fx positive load case. That gives a glimpse of difficulties the transducer gave: all channels had a response and it was difficult to separate and analyse the individual values. These effects were recorded because the transducer had an asymmetrical shape. They were not cross - effects but secondary responses: it was impossible to cancel or to correct these values as it could be for cross – effects. A secondary response value must be added to the value of the main channel. For two load - cases Fx positive and positive, data from the rosette gauges on the spindle are presented in table 3.8 while table 3.9 illustrates the statistical regression analysis of one of these tests. A complete description of statistical analysis will be discussed in section 6.5. However, it is possible to note that the behaviour of this channel was sufficient as illustrated by figure 3.20 which is the graph of the typical load - case shown in tables 3.8 and 3.9: linearity (r - square = 0.999974, close to 1 which is the best). There was no hysteresis and no drifting or creeping when the load was maintained at full load more than ten minutes.

---

[9] The A/D board PC 26AT® supplier was Amplicon Liveline Ltd, Centenary Industrial Estate, Hollingdean Road, Brighton BN2 4AW, Great Britain.

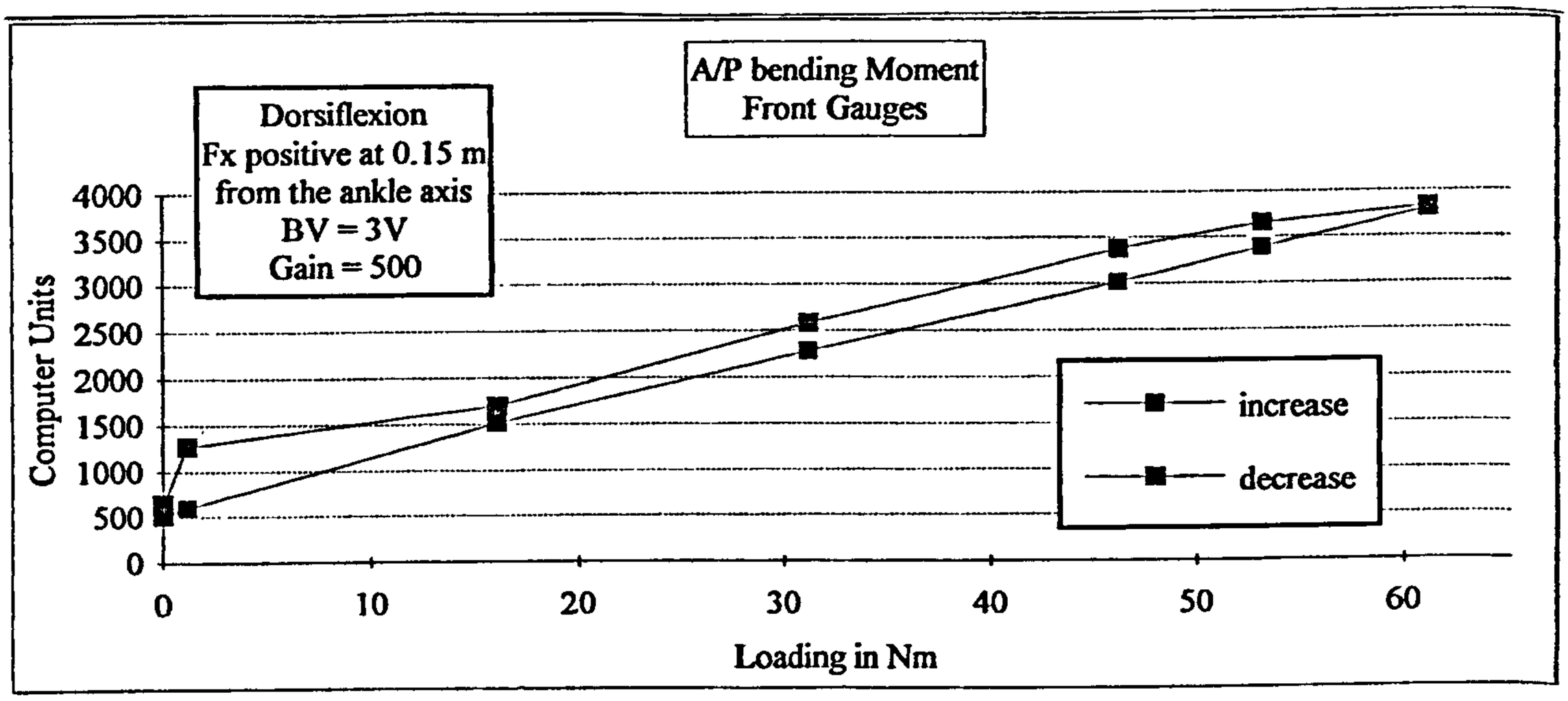

Figure 3.21: The traces from the front gauges responses in dorsiflexion (Mz +). It was a cantilever configuration. The loading point of the shear force Fx was at 0.15 m from the ankle axis.

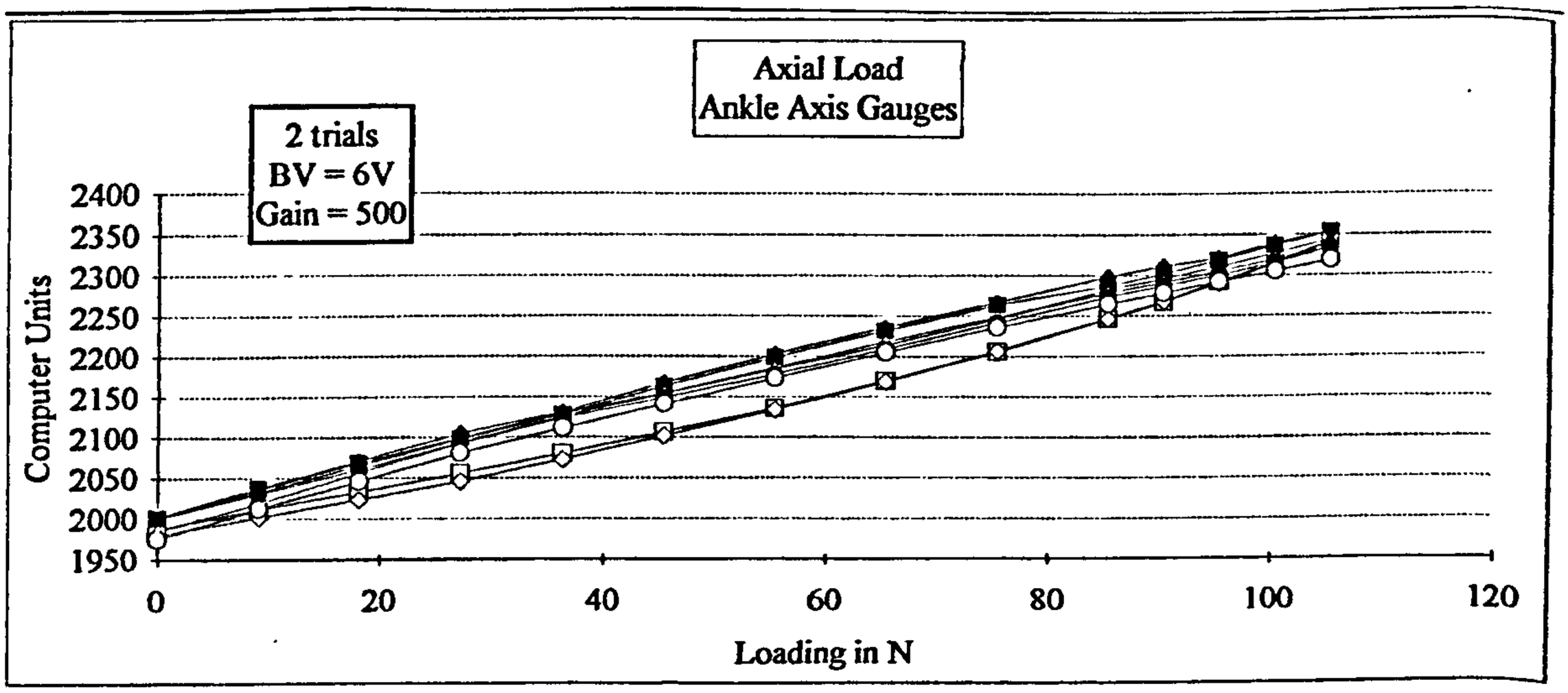

Figure 3.22: The traces from 2 trials in longitudinal axial load (Fy) showing the responses of the ankle axle gauges: hysteresis and drifting.

In other words, and this is an important comment for the next and definitive transducer: the behaviour of the gauges fitted on the axial spindle was linear with no hysteresis, no drifting and apparently no creeping. However, the performance of the other channels was not linear. As example, figure 3.21 shows the plot for channel No 4: the gauges fitted on the front flat flange. This test was performed to calibrate the Mz positive bending moment (dorsiflexion). It is obvious that there was a hysteresis, probably due to the material of the artificial ankle: the common aluminium alloy, on which the gauges were fitted. This seemed to exhibit a « memory » of the deflection. The same result was observed in Mz negative (plantarflexion) with the channel N°5 (the gauges fitted on the rear flat flange). Figure 3.22 displays the graph in Fy axial load recorded from the ankle axis gauges. Here also, there is a hysteresis and a drifting. The results were not as it was expected.

The full results of the calibration of this first ankle transducer, recorded from the five channels: front and rear flanges, external and internal axis, spindle Wheatstone bridges, are shown in appendix 11.III.4. These results are for in the following loading cases: A/P shear force and bending moments, axial load and M/L bending moments. No tests were performed with transverse torque (My) or M/L shear forces.

3.5.5 Comments

The results of this calibration allowed the author to draw several conclusions.

1. The geometry of this transducer was complex. The gauges were not in symmetrical locations about the reference point (centre of the ankle axis) and axes. This is why rendering of the results was difficult. It was impossible to account for the inconsistency of these responses by suggesting that they arose from cross-effects. In other words, for each load-case, there was one main response plus several secondary responses. These secondary responses occurred in some particular channel and were mixed with the main response of this channel. To separate these outputs, several hypotheses and assumptions were compulsory which introduced various uncertainties.

2. The material of which the artificial ankle device was built was inappropriate

4.2.2 Static proof test, cyclic test

Offsets corresponding to clause 6.1.5 and 7.2.6 of ISO 10328-3

Table 3: Test loading condition I

Reference Plane	Offsets			
	Direction	Value [mm]	Combined Value [mm]	Combined Angle [°]
Top*	f_T	132	182.6	-46.3
	o_T	-126.2		
Knee	f_K	52		
	o_K	-50		
Ankle	f_A	-32		
	o_A	30		
Bottom*	f_B	-48	66	-43.3
	o_B	45.2		

Test loading condition II

Reference Plane	Offsets			
	Direction	Value [mm]	Combined Value [mm]	Combined Angle [°]
Top*	f_T	24.3	53.3	-27.1
	o_T	-47.4		
Knee	f_K	71		
	o_K	-35		
Ankle	f_A	120		
	o_A	-22		
Bottom*	f_B	129.3	130.8	-81.4
	o_B	-19.5		

*) only for guidance in aligning test samples

4.2.3 Test forces

(see clause 3)

Table 4

	proof test force at attachement	static proof test force	static proof test force at failure		cyclic test force		
Loading condition	F_{pa} [N]	F_{sp} [N]	F_{su} [N] *ductile*	*brittle*	F_c [N]	$F_{max} = F_{min} + F_c$ [N]	Endurance No. of cycles
I	5376	2560	3328	4480	1280	1330	3×10^6
II	4830	2300	2990	4025	1150	1200	3×10^6

Figure 3.23: The ISO recommendations for static proof test. For the A/P bending moment positive (dorsiflexion) the values are as follows: $F_{sp} = 2560$ N with a lever arm of $f_A = 120$ mm at the ankle level.

for gauge testing. It had a non - elastic behaviour with hysteresis; so that, the accuracy of the transducer is very low.

3. The bell was attached to the spindle by means of only one central bolt about the Y axis. About this longitudinal axis, there is a torque. This moment is small in value but could be enough to generate a rotation of the bell round the spindle. The use of a locking washer seemed insufficient and the use of any adhesive was preventing the bell from being dismantled.

4. However, the spindle, although it was made in aluminium, gave sufficient accurate and linear responses. This is why the idea of the spindle with its bell will be taken up again for the second new definitive pylon transducer. Non-uniform contact between the bell and the pylon tube is suspected to take place.

3.6 STRENGTH MEASUREMENT

As previously stated, the front flat flange had to be made thinner to create a more sensitive channel response (see section 3.4.4). Therefore, this front part of the ankle transducer was weaker than that of a commercial prosthetic ankle. Hence, a stress study had to be undertaken to ensure that failure could not occur during patient tests.

The maximum stress on this front part of the ankle takes place when anterio-posterior moment (Mz) is positive. This occurs when the ankle is in dorsiflexion at the late stance phase of the gait cycle (just before toe - off).

The International Organisation for Standardisation, in its latest report (ISO 10328, 1993), recommends carrying out a static proof test for dorsiflexion at the ankle plane as shown in figure 3.23. More details concerning the ISO recommendations are shown in appendix 12.III.5.

loading condition $F_{sp} = 2560$ N

lever arm $f_A = 120$ mm

Hence, the positive dorsiflexion moment Mz is:

$$2560\,\text{N} * \frac{120}{1000} = 307.2\,\text{N.m}$$

Although these values are for prostheses for any user and the described design would be safe for elderly dysvascular amputees undertaking supervised tests (see chapter 8), a static failure test was considered as compulsory.

When the test was performed, with the same set up as that used for calibration (cantilever configuration, see section 6.3.4), a permanent bending deformation began to appear in few minutes and the transducer began to fail.

Therefore, it was definitively proved that a novel pylon transducer design was mandatory.

3.7 CONCLUSION

In this chapter, a description of a first new removable ankle transducer was shown. A full calibration was carried out. The results highlighted that the non - symmetrical shape of the transducer and the low quality of its material made it unsuitable for our purpose.

However, the shear rosette gauges fitted on the pivotal spindle, along the Y axis, behaved satisfactorily. They showed linearity, absence of hysteresis, repeatability and sensitivity. The spindle is also circular, i.e., symmetrical. All the required forces and moments went through it. This was why the idea to fit all the Wheatstone bridges on this central spindle under the bell seemed possible. About the choice of material, three considerations must be taken into account:

1. The design must be compatible with the ISO recommendations;

2. The strength of the must satisfy ISO requirements;

3. The mechanical properties of the material must be compatible with strain gauge technology.

The following chapter will present the design of a new definitive pylon transducer which takes the above requirements into account.

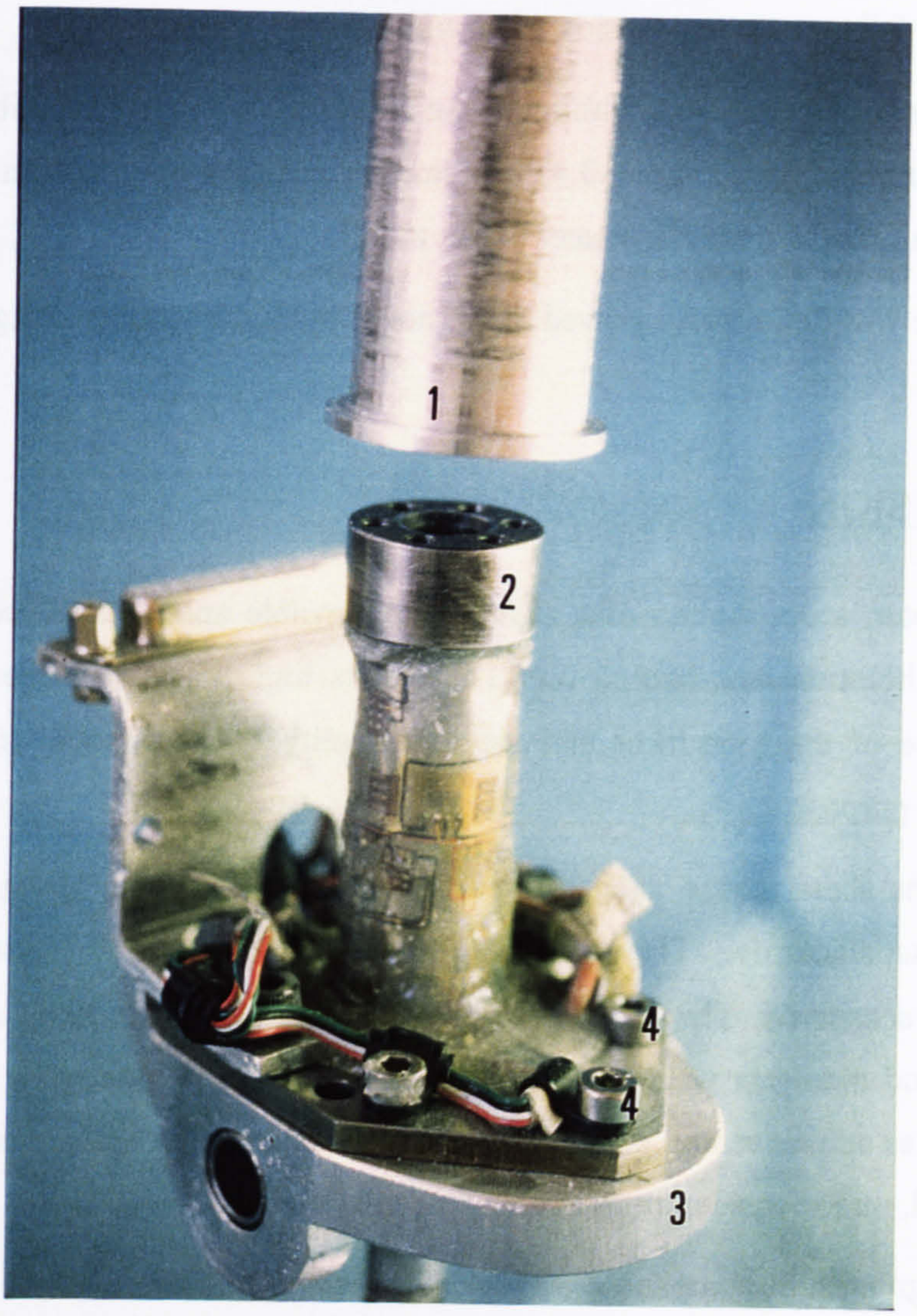

Figure 4.1: The three main parts of the new transducer plus the connecting cap screws between parts 2 and 3

1. the aluminium bell
2. the stainless-steel body of the transducer
3. the proximal component of the ankle joint
4. the connecting cap screws (2 out of 6 are shown)

4 OPTIMISATION OF TRANSDUCER SHAPE BY STRESS / STRAIN ANALYSIS

4.1 INTRODUCTION

Prior to manufacture of any new transducer, a precise theoretical study of the new device is advised. This must be done in two respects.

The first is to be sure that the transducer will be strong enough according to the International Organisation for Standardisation (ISO) recommendations. It was also necessary to consider the shape, dimensions and weight, in order to choose the most appropriate material. To reach this target, a stress - strain analysis (see section 11.IV) and a mechanical deflection study (see section 4.4) were conducted.

The second is to check the theoretical behaviour of the transducer. In other words, under a chosen load, the transducer shape should have a theoretical response large enough to be recorded by strain gauges. Therefore, a sensitivity investigation was undertaken. To achieve this aim, an investigation was made using temporary low cost strain gauges (see sections 4.5 and 4.6).

4.2 CHOICE OF THE MATERIAL

4.2.1 Description of the new transducer

Because the results of the gauges attached to the spindle, shown in figures 3.13 and 3.15, were accurate in the Model I transducer, the new definitive transducer was chosen to be similar in shape. The fundamental prerequisite was a symmetrical central spindle with sufficient room in height and diameter to allow bonding of the gauges. Therefore, the shape of the main body of the spindle was machined a circular shaft to fit inside a bell which, in turn, was fitted inside the standard prosthetic shank tube, as shown in figure 4.1. The space between the bell and the spindle was sufficient to allow the bonding of the gauges, the wires and the terminal blocks with the silicone rubber protective coat. The bell had to be fitted inside the standard shank tube of the prosthesis which is 26 mm internal diameter.

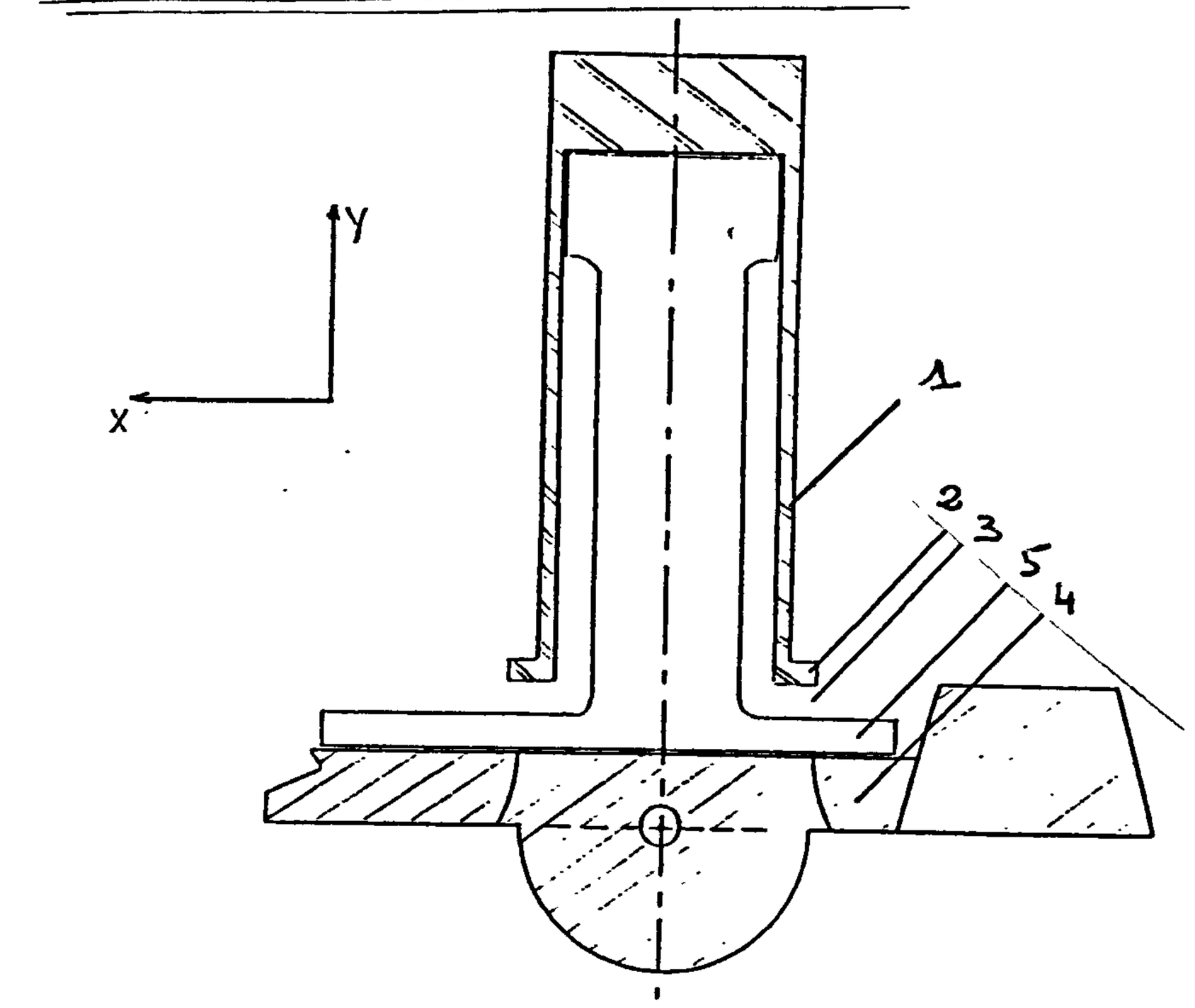

Figure 4.2: Four parts of the new transducer

1. The bell
2. Flange of the bell
3. Space (3.9 mm)
4. Connection saddle of ankle joint
5. Bottom flange of the transducer

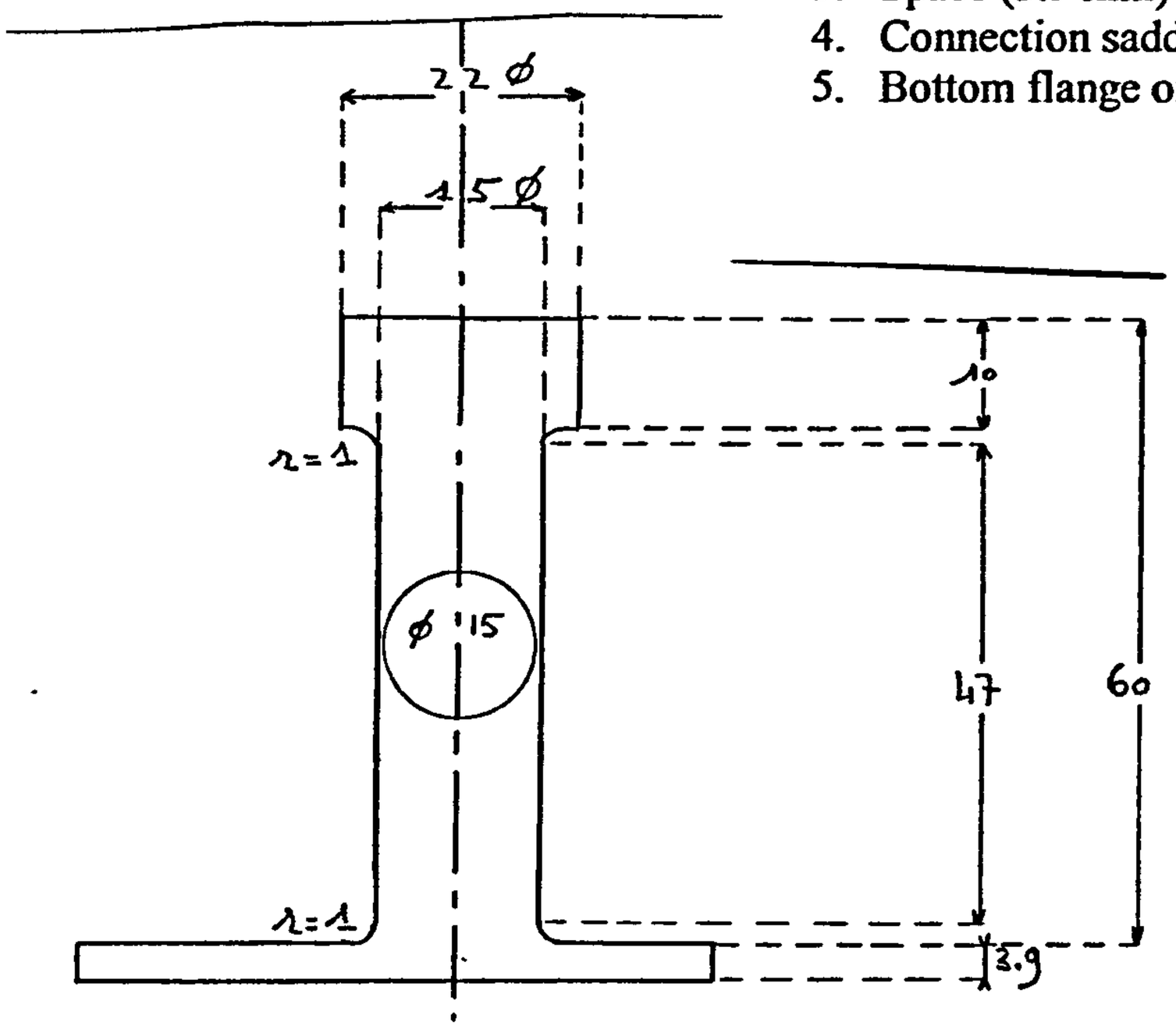

Figure 4.3: Details of the transducer spindle (all dimensions in mm)

The thickness of the bottom flange was prescribed by the available space between the ankle axis and the bottom end of the prosthetic shank tube. This distance was 18.8 mm and four parts could be included, as shown in figure 4.2:

1. *the bell*

2. *the flange of the bell* which has a thickness of 2 mm.

3. *the empty space between the bell and the bottom plate of the transducer*. This gap had to be sufficient to avoid any contact between the bottom edge of the bell and the top surface of the bottom flange of the transducer and enough to clear the wires connecting the gauges to the terminal blocks. The required minimum gap was estimated as 3.9 mm.

4. *the ankle connection saddle onto which the transducer is bolted.* This part linked the artificial foot with the prosthesis through the transducer. The thickness of this saddle had to be sufficient to transmit the loads developed. To decrease the weight of the apparatus, the chosen material, which was made after some stresses tests, (see below section 4.3) was a common aluminium alloy (BS 6082 T4). Therefore, the optimised thickness of this part was 9 mm (see section 4.4.3).

5. *the bottom flange of the transducer.* Because of the three lengths discussed above, this part of the new transducer required a dimension: 18.8 - (2 + 3.9 + 9) = 3.9 millimetres. Moreover, the chosen material had to be strong enough to transmit the applied loads with this small thickness.

Consequently, it was not possible to increase the thickness of this flat flange over 3.9 millimetres because when the shank tube of the prosthesis is loaded on the tube, the previous height of the prosthesis must be automatically respected (see appendix 11.II.4.4). However, this dimension was later found to be sufficient in all the conducted tests (see section 4.4.2).

Therefore, the choice of dimensions, as shown in figure 4.3, was dictated by the requirements and the general shape of the transducer, with all dimensions in millimetres.

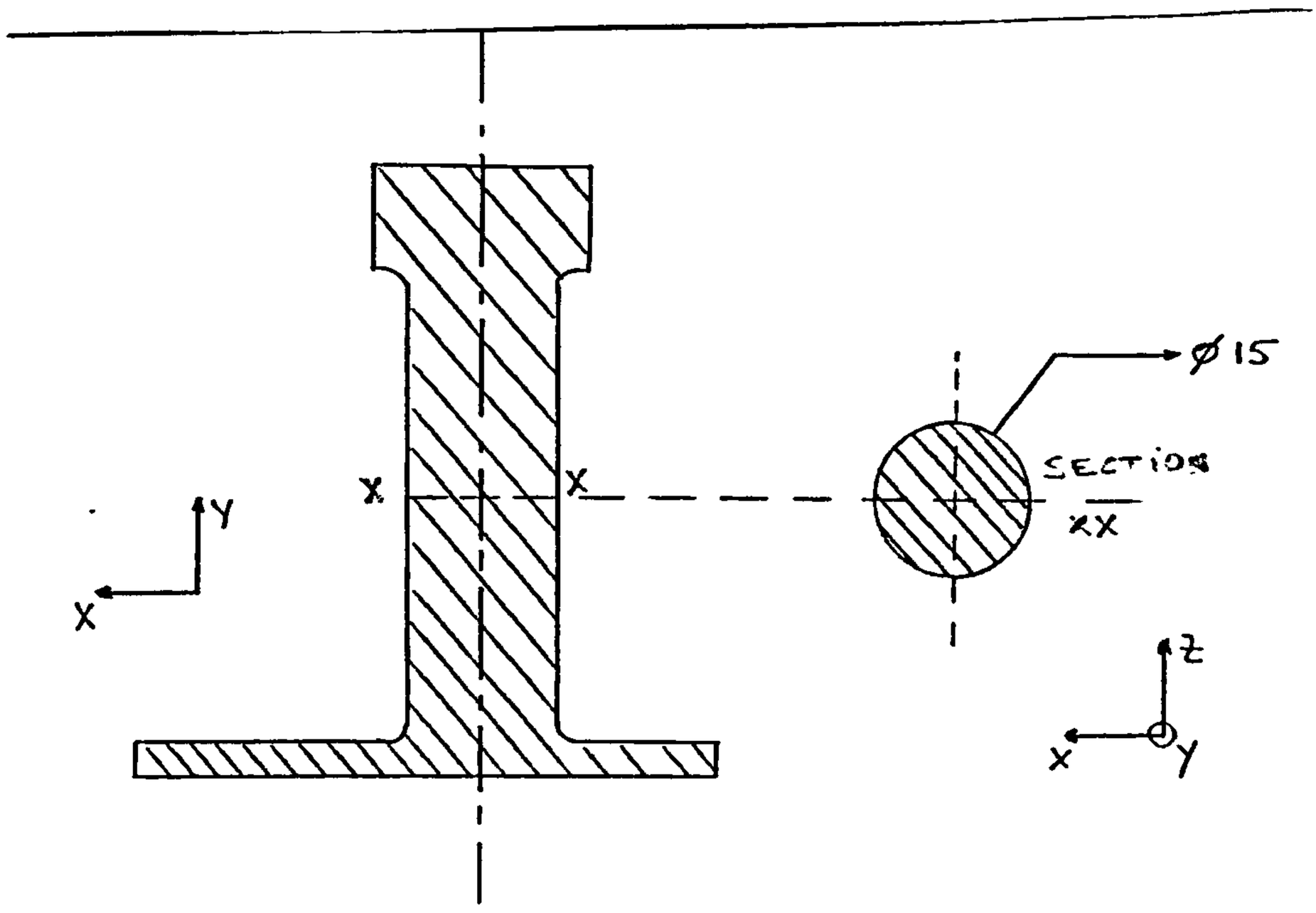

Figure 4.4: The solid spindle of the Model II

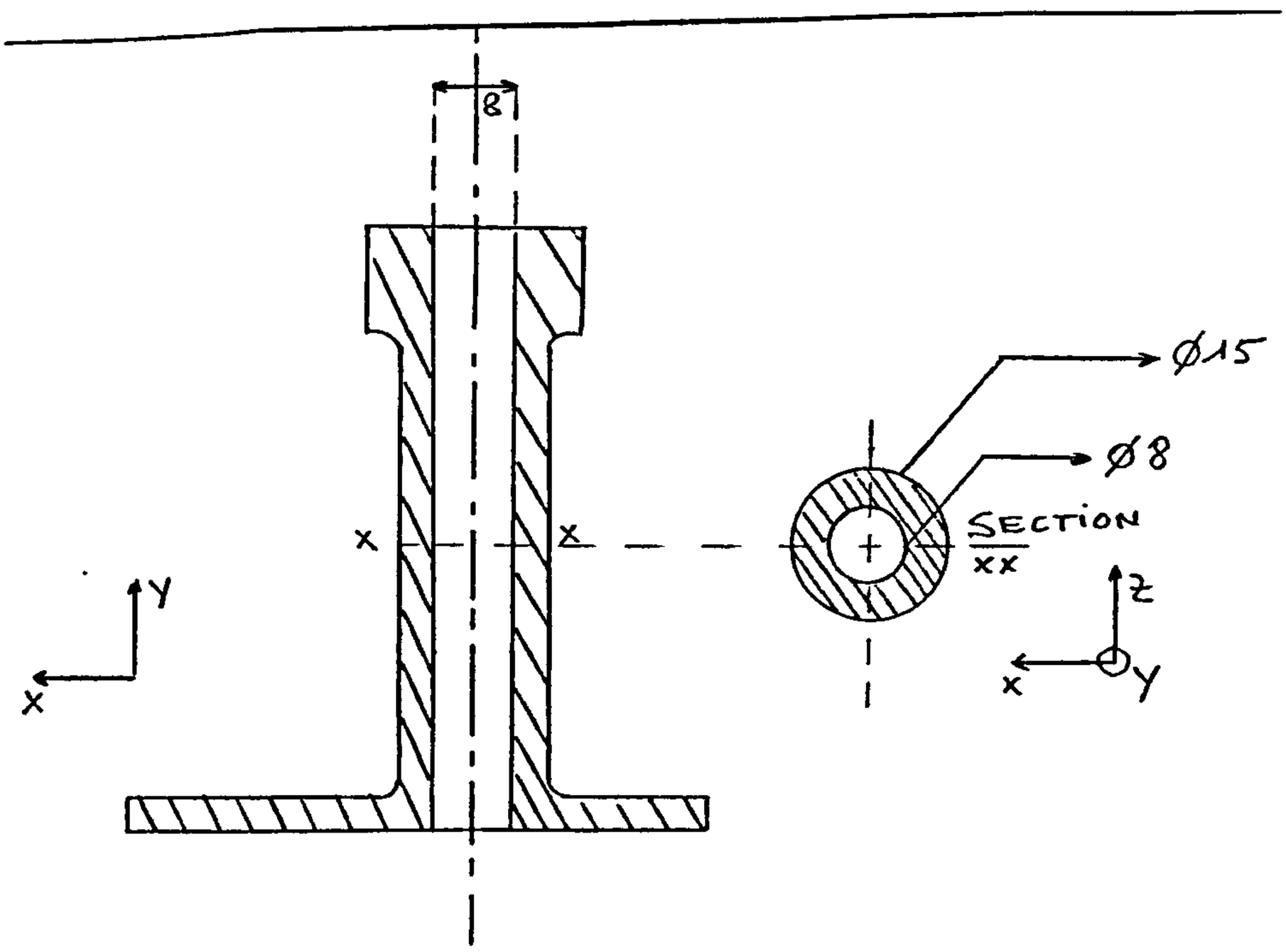

Figure 4.5: The hollow spindle of the model III

(all dimensions are in millimetres)

Two possibilities for the configuration of the spindle were conceivable, and both of them have been explored: a solid spindle to have a transducer stronger but probably less sensitive (Model II); a hollow spindle, along its full length, to increase the sensitivity (Model III). These two shapes are shown in figure 4.4 and 4.5. The choice of the material in which they have been built was made, following the ISO recommendations (ISO 10328-4, 1993): a stainless steel alloy as shown in appendix 11.IV.1. A thorough description of the two transducer samples built is given in the following section.

4.3 DESCRIPTION OF THE TWO PROTOTYPES OF THE NEW TRANSDUCER (MODEL II AND MODEL III)

Prior to the study of the mechanical properties of the new transducer, two samples of it were built. Both had the same principle: a bell interposed between the two components covers a spindle erected upon a flat flange. This flange is similar in the two samples and the aluminium ankle saddle that linked the transducer with the artificial foot is also identical in the two samples. Therefore, the only difference between the two units was the central spindle: the first (Model II) is solid and the second (Model III) is hollow. Therefore, a comparison between solid and hollow transducer is necessary. Nevertheless, there were some differences between the two prototypes:

- the solid transducer had already been heat treated for hardening while the hollow one was not. The latter was required to allow the possibility for modification of the shape. According to the specification of the company, 1) before hardening, the material should not be used and its Young's modulus of elasticity is only approximately known, although hardening does not affect Young's modulus significantly ($\approx 164 \times 10^3$ MPa); 2) after hardening. Changing the design of a hardened component would be very difficult and some special tools would have been needed.

- the top surface of the spindles and, consequently, the bells were not exactly the same in respect of the design of the cap screws. The solid spindle prototype was

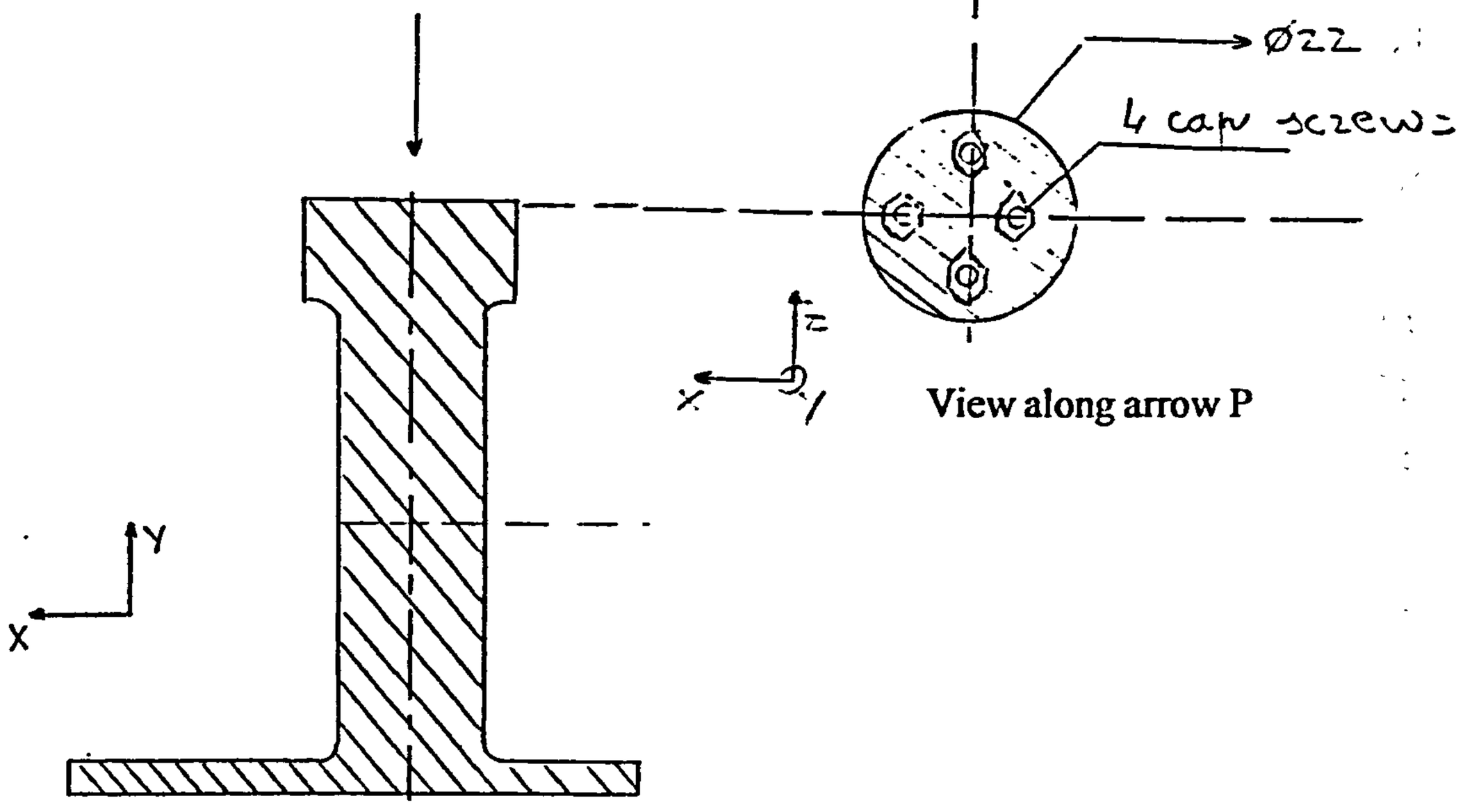

Figure 4.6: The solid spindle with four cap screws

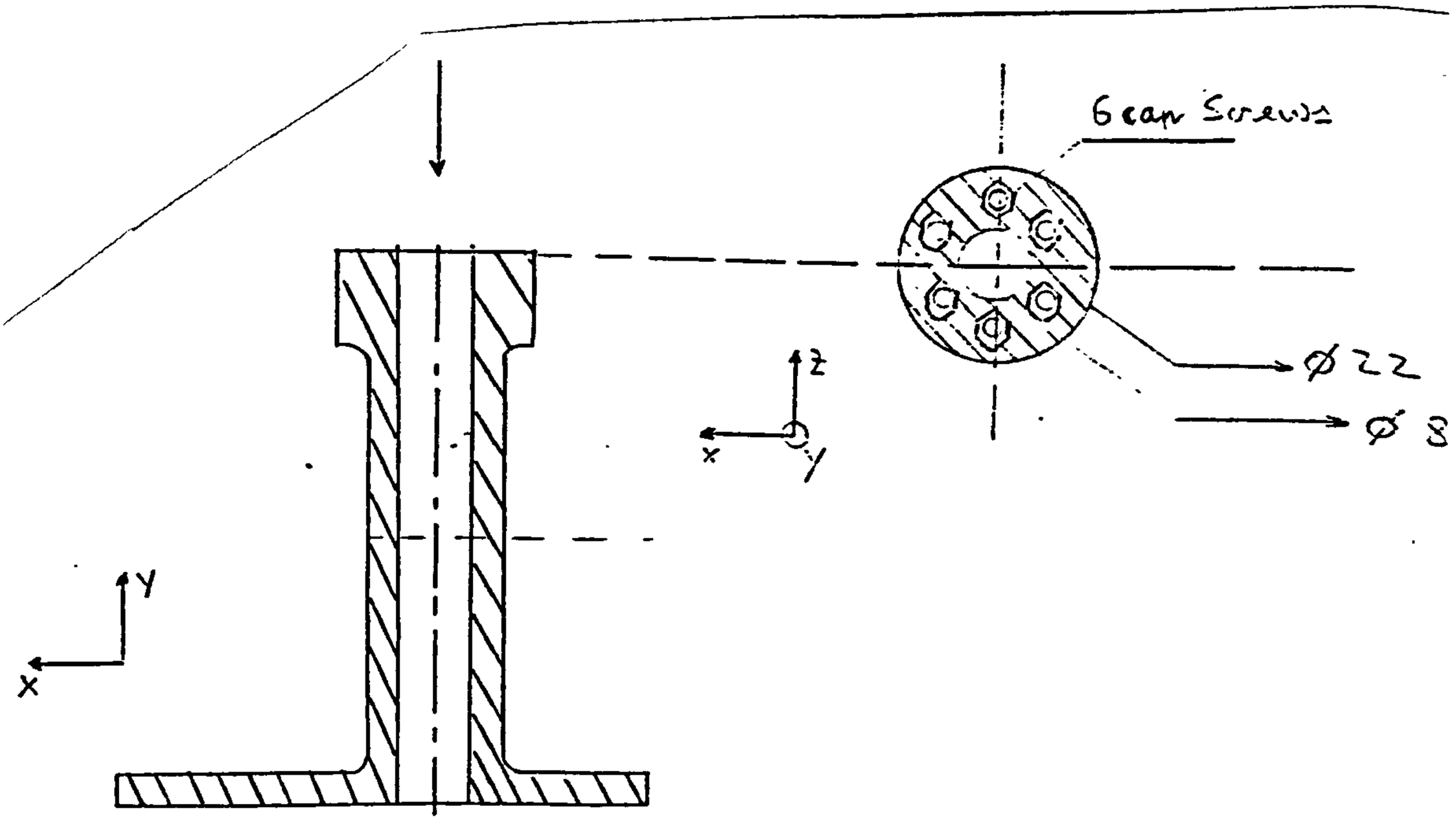

Figure 4.7: The hollow spindle with six cap screws (all dimensions in mm)

covered by a bell that was attached to it by four cap screws, two by two in X and Z directions. The hollow spindle prototype was covered by a bell that was attached to it by six cap screws (see complete description in the following section 4.8.2). All other dimensions, shape and material were exactly alike.

- the connection saddle of the ankle joint was not the same:

1) with Model II, it was designed from the Proteor® artificial ankle made of common aluminium (see description in appendix 11.II) and because of the modifications of the shape, this saddle was not strong enough. It introduced too much flexibility (see section 4.4) and it suffered permanent bending when a pulling out of the connecting cap screws (see No 4 in figure 4.1) proof test in A/P bending was performed (see section 4.4.2);

2) with Model III, the definitive connection saddle (see section 4.2.1) was used, it was more rigid and stronger than the Proteor® connection saddle.

Figure 4.6 shows the Model II of the new transducer while figure 4.7 shows the Model III. The mass of the solid spindle transducer Model II is 0.160 kg and 0.156 kg for the hollow Model III.

4.4 STUDY OF THE MECHANICAL BEHAVIOUR OF THE TWO PROTOTYPES

The study on the mechanical behaviour of the two transducer prototypes was carried out with four aims:

1. to choose the best configuration;
2. to verify the linearity of the two devices;
3. to investigate the behaviour of the aluminium bell;
4. to test the rigidity and strength of the aluminium ankle saddle and the cap screws (see n°4, figure 4.1) connecting it to the saddle: 1) designed from the Proteor® artificial ankle; 2) definitive connection ankle saddle designed after the previous test.

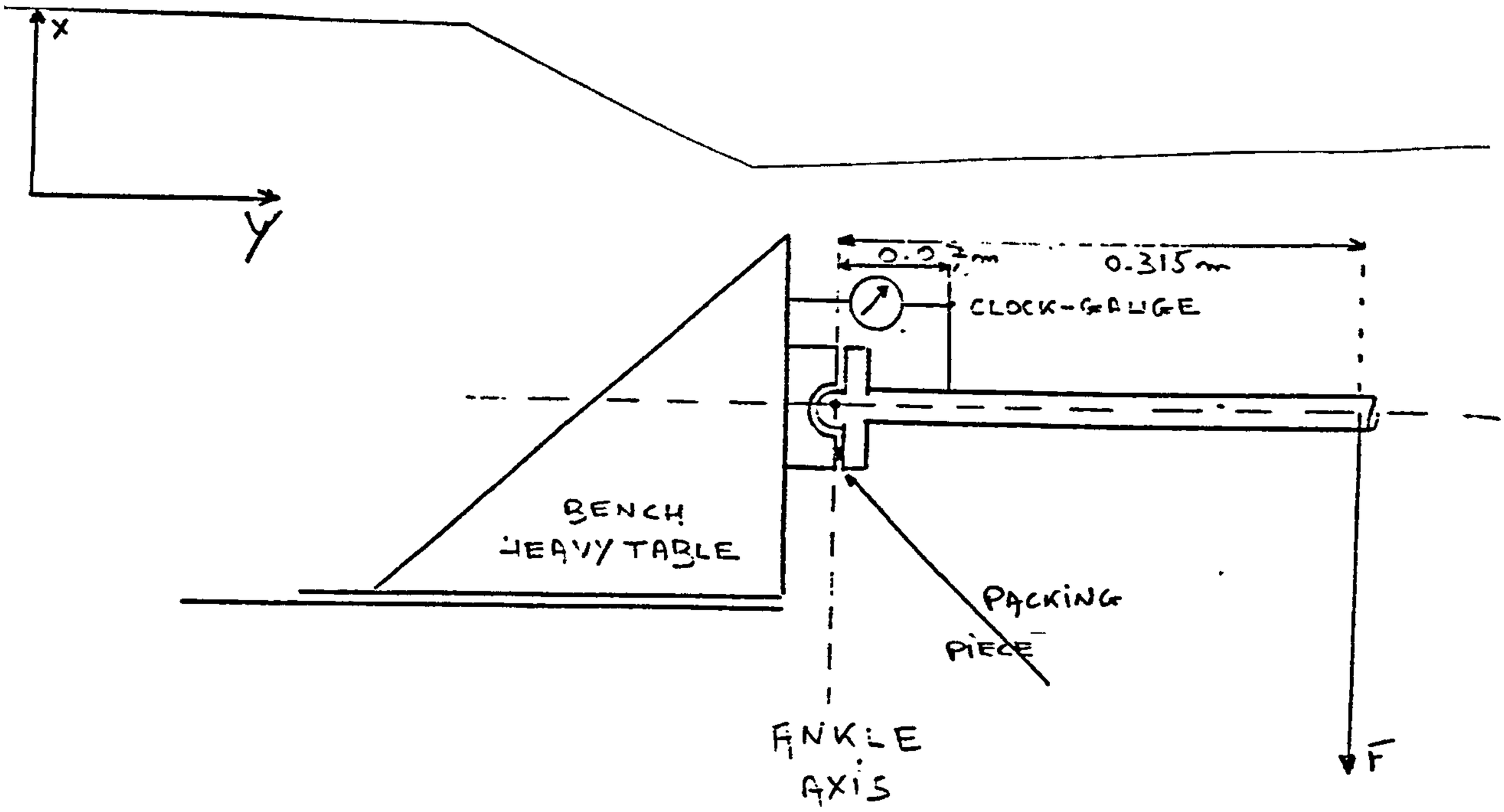

Figure 4.8: The set up for A/P bending moment tests with the lever arms and the clock-gauge

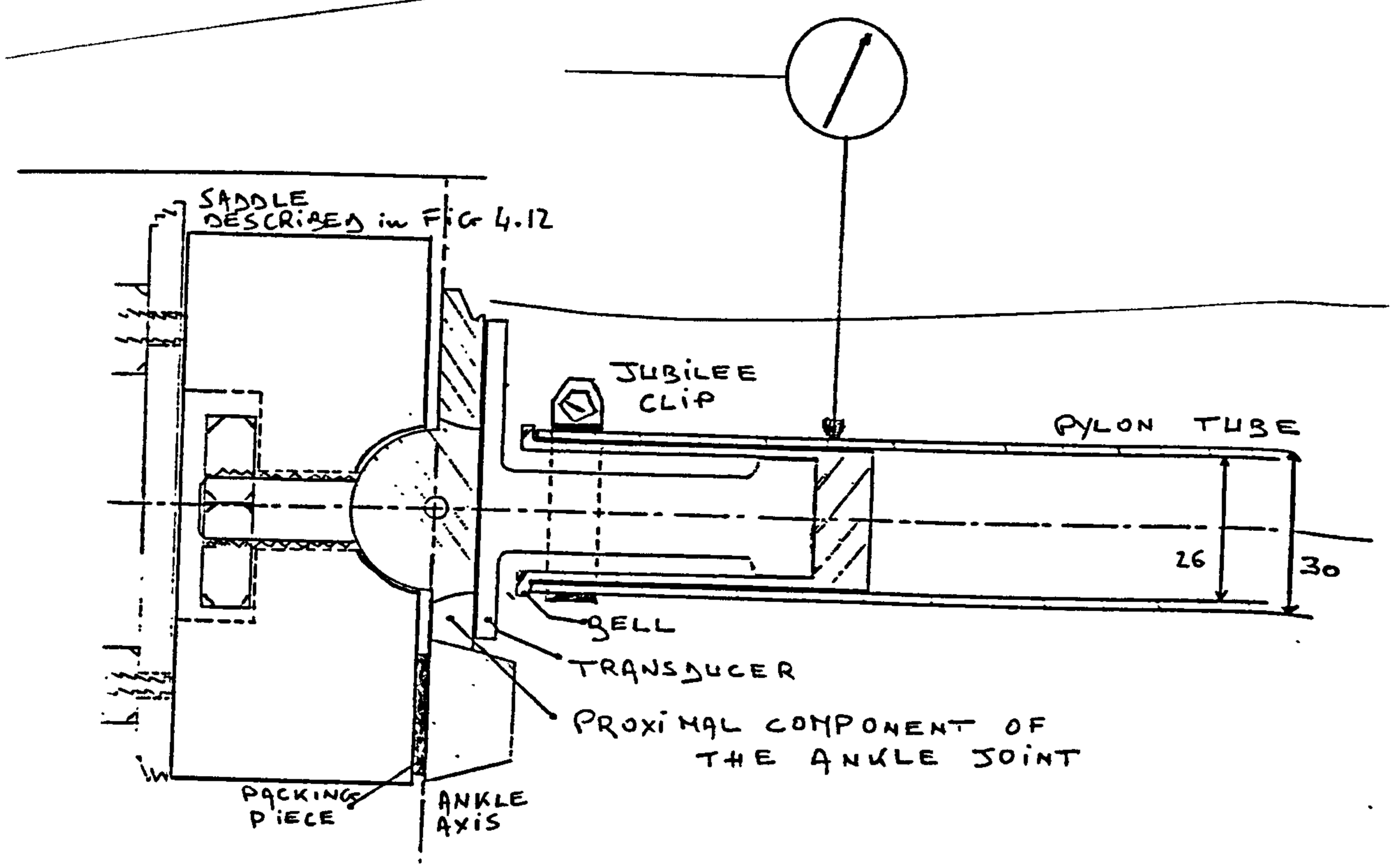

Figure 4.8a: Details of the set up of the transducer with the bell for A/P bending moments

A unique cantilever configuration has been used for the test which involved anterio-posterior and medio-lateral shear forces along X and Z axes combined with bending moments about the same two axes. Figure 4.8 shows the test arrangement used and gives the value of the lever arm (F at 0.315 m from the ankle axis). The standard aluminium tube that covered and loaded the bell had an external diameter of 30 mm and an internal diameter of 26 mm. It was the same tube as those used for the prosthetic shank. It had two opposite slits 3 cm in length. A jubilee clip was used to clamp the tube over the bell. This set up had the drawback of not being suitable for transmitting bending moment unless there is also a longitudinal force.

In order to measure the deflection, a mechanical clock-gauge has been used. In all trials, four tests were done, two the first day followed by two others the day after. Between the two series of tests, the equipment was dismantled. At each loading case, the result given by the clock-gauge was carefully checked and manually recorded. The divisions of the clock-gauge dial were one hundredths of a millimetre. One revolution of the pointer was equivalent to one millimetre. When the load was at its maximum, it was held constant for five minutes and any changes in the clock-gauge reading were recorded. Then an unloading phase was performed in which the load was reduced to zero. This procedure was the same as that used for calibration (see table 4.4, 4.5 and chapter 6). The choice of 0.07 m, which is small, from the ankle axis to the measurement point of the clock-gauge, was made because it gave the deflection of the transducer itself rather than that of the tube, because the tube was in contact with the proximal end of the transducer. The full set up for A/P loading tests is shown in figures 4.8 and 4.8a.

For the third goal, an attempt was made to eliminate the bell. A reverse bell was used as shown in figure 4.9. For robustness (this particular component will be used later in some validation tests, see chapter 7), this reverse bell was manufactured in steel rather than aluminium. This device ensured that the spindle of the transducer was totally free of any possible contact with the bell. Therefore, it was possible to compare the mechanical behaviour of the spindle whether covered by the bell or not. This reverse bell was used twice, once during the pilot test with temporary gauges (see below section 4.5) and secondly during the validation tests (see chapter 7).

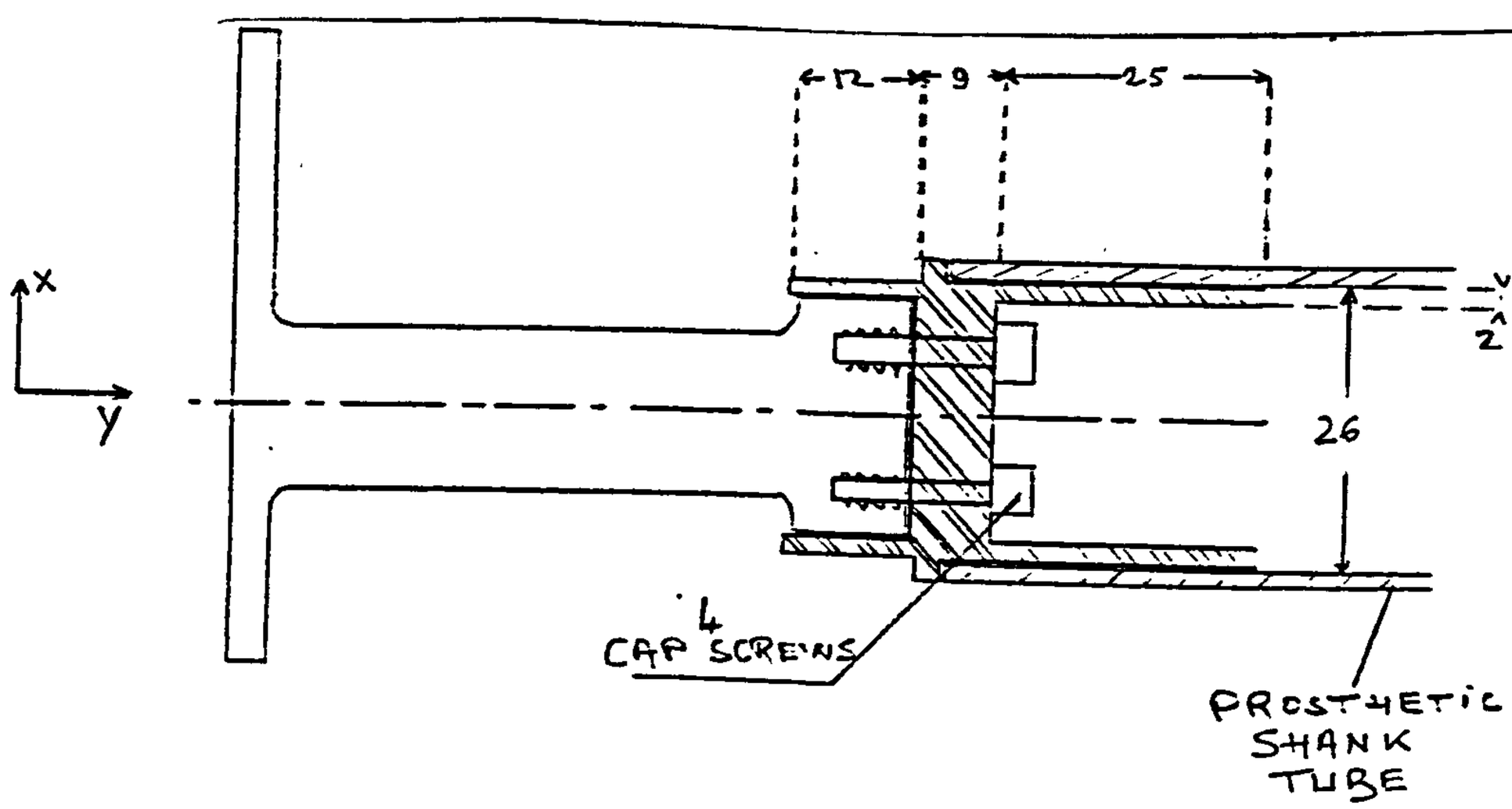

Figure 4.9: The reverse steel bell

For the fourth goal, a pulling out proof test of the connecting cap screws and a static test of the behaviour of both connection saddles was undertaken.

4.4.1 Linearity in deflection of the two models II and III

Only the major results are shown in this section, particularly those with positive bending moment which are of importance in prosthetic gait. It is common to find 100 N m at the end of the prosthetic stance phase, that is at toe off when the patients are pushing themselves up on their prostheses. The full numerical results are shown in appendix 11.IV.2.

Figure 4.10 shows the results when the prototype Model II having the solid spindle was loaded in anterio - posterior bending moment positive (Mz+, dorsiflexion). The deflections are plotted with the bell then with the reverse bell. The graph is linear. There is neither hysteresis nor creep at full load, over the 5 minutes period of constant load.

Figure 4.11 shows the plot of deflection against bending moments obtained from Model III with the hollow spindle. Using the reverse bell, the results are less linear with a crossing trace at 85 N m, probably due to a slipping of the clock-gauge or bell/tube slippage. The set up was the same as the one used for Model II but the loading cases were different. As stated, the device had not been yet heat treated at the time of the test. The maximum bending moment was limited to avoid overstressing. It was 145.7 N m instead of 269.4 N m for the solid device Model II.

The graphs appear linear for those the solid spindle and the bell. There was also neither hysteresis nor creep. However, looking at the two graphs (figures 4.10 and 4.11), it was evident that the two devices exhibited a significant difference in bending moment stiffness:

solid spindle (Model II)	1.17 mm for 145.7 N m
hollowed spindle (Model III)	0.53 mm for 145.7 N m

The author had expected the opposite result. This could be due 1) to the I value of each prototype: the ratio is 1.08 and it is not high enough to explain the difference

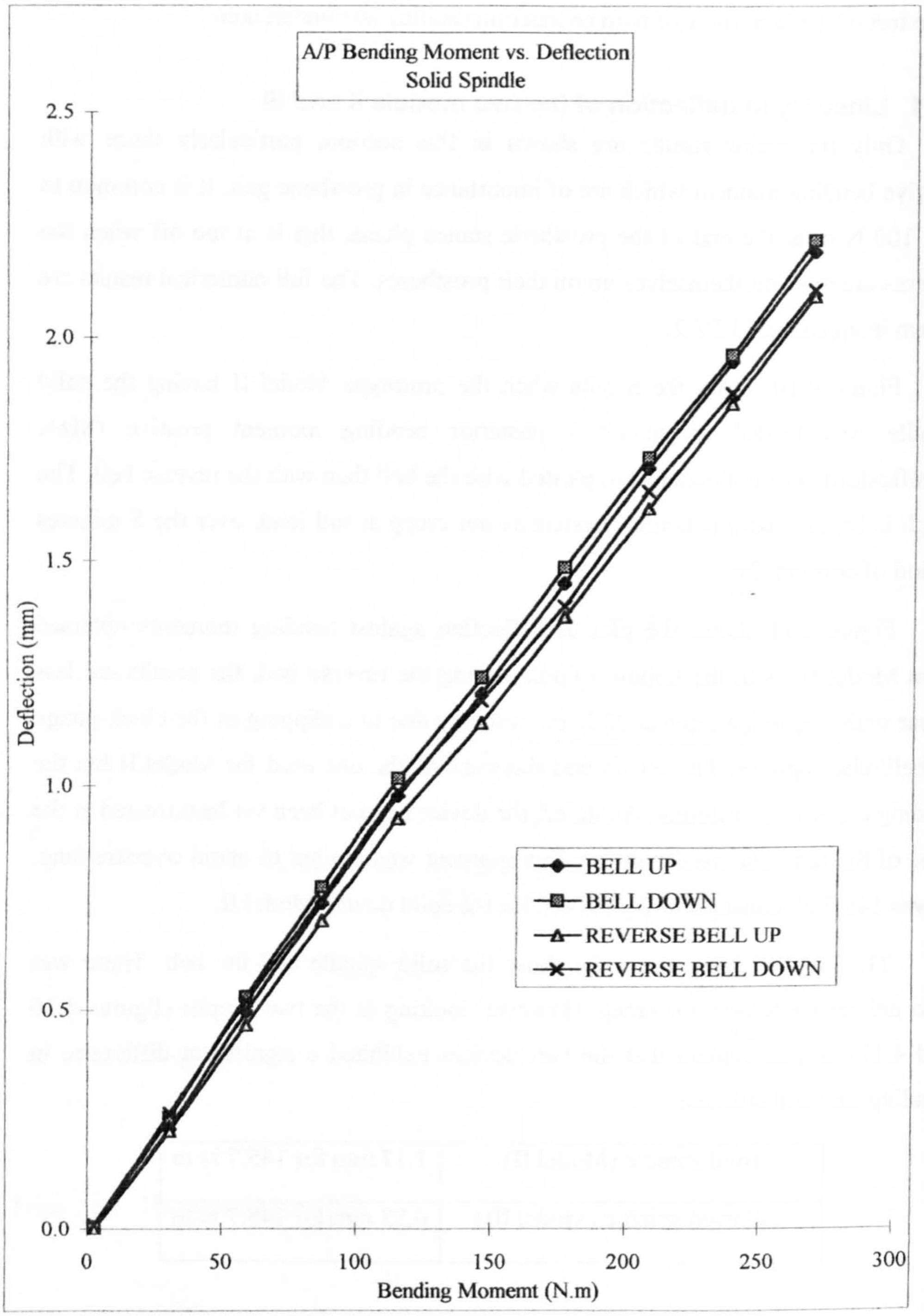

Figure 4.10: Graph showing the deflection of the solid spindle which is linear ($R = 0.99$). No hysteresis, no creep are seen from 4 tests with the bell and 4 tests from the reverse bell.

(see section 11.IV); 2) the difference in Young's modulus of elasticity of the material heat treated ($200x10^3$ MPa) or untreated ($\approx 164x10^3$ MPa); 3) mainly because the two connection saddles were not identical: the first (Model II, solid spindle), built from the Proteor® ankle, introduced more flexibility while the second (Model III, hollow spindle) was more rigid.

Therefore, the two devices (and the two set ups) were not the same: one had been heat treatmented and the cap screws attaching the bell and the spindles were not identical. Thus, it is not easy to compare the two devices.

It is important to note that the both prototypes seem to have a linear response. To make a conclusion about the linearity of Model II and Model III used with the bell; a regression analysis with the macro function Regress in Microsoft Excel™ has been made:

	R square in %	Slope of graphs 4.11 and 4.12 $mm.(N\ m)^{-1}$
solid spindle + bell (Model II)	99.82	0.008
hollow spindle + bell (Model III)	98.79	0.004

In this array, it is possible to see that R square is very high (nearly one) giving an indication of a very strong linear relation between the two variables: load and deflection. An R Square of 100 % would exhibit a perfect linear relation between the two variables. However, this is not necessary, the calibration need only be consistent, not necessarily linear.

4.4.2 Static proof test of the connection saddles

Concerning the fourth goal, a static proof test of 400 N m, during 75 minutes, was undertaken, following the recommendation expressed by the ISO committee. The set-up comprised the connection saddle designed from the Proteor® artificial ankle. This component showed some signs of overstress and weakness leading to a permanent bending and a pulling out of the connecting cap screws. Therefore, a new design was constructed of stronger material (see section 4.2.1). This new aluminium ankle saddle showed no signs of deformation or overstressing under a bending moment of 400 N m during 75 minutes. Therefore, this part of the transducer was

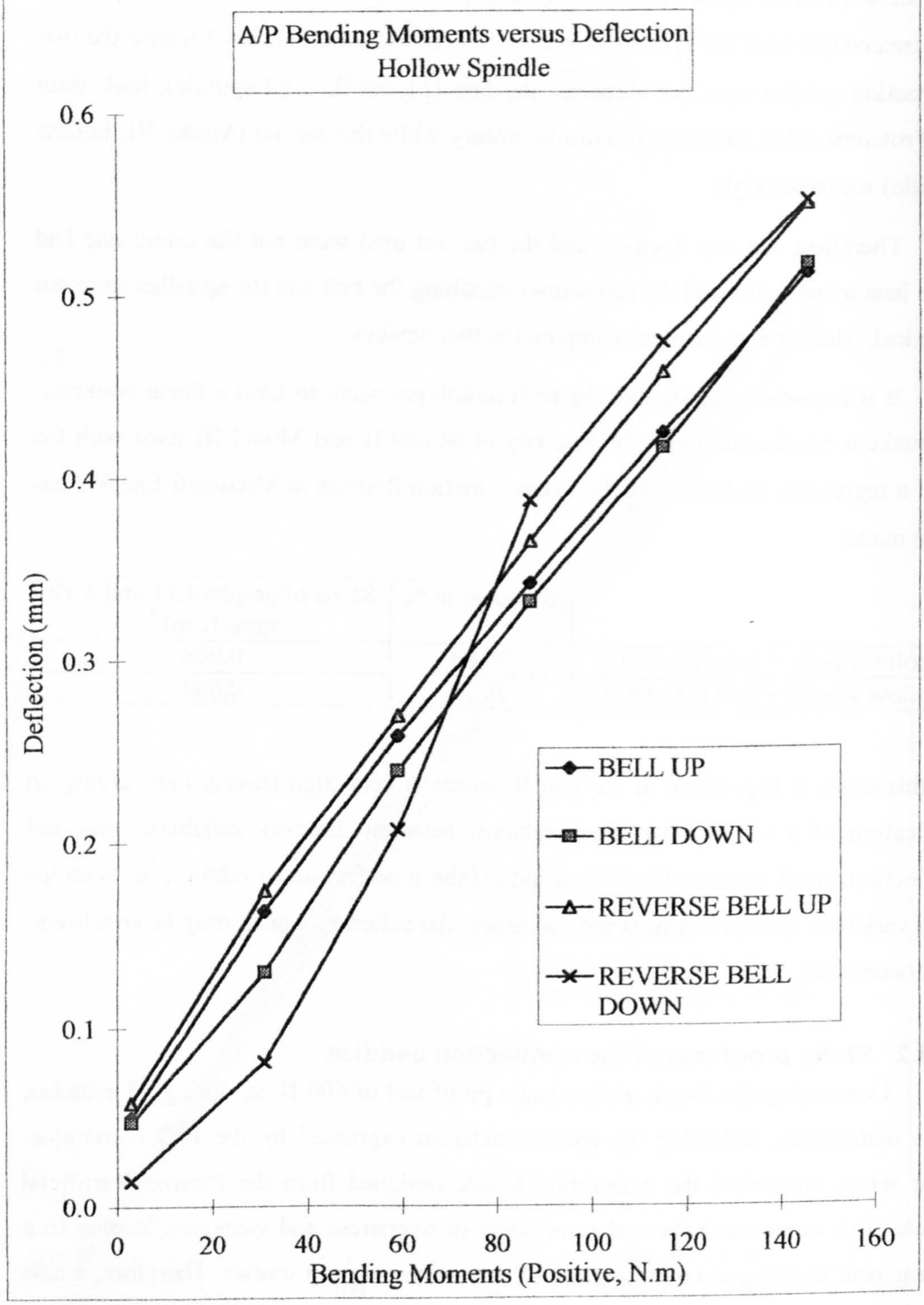

Figure 4.11: Graph showing the deflection which is not totally linear (R = 0.98) from 4 tests with the bell and 4 tests with the reverse bell. A small hysteresis but no creeping for the hollow spindle transducer are shown. The increase of the slope in one test has no evident explanation (see text).

proclaimed strong enough for our purpose.

4.4.3 Partial conclusion

The mechanical behaviour of the two prototypes were found to be linear. This confirmed the choice of the transducer material and shape.

The behaviour of the aluminium bell surrounding the spindle was found to be satisfactory. The curves obtained through the definitive aluminium bell versus the reverse bell were close enough to themselves to make any statistical study unnecessary. It has been therefore established that the bell does not entail any contact with the spindle.

In summary, the first goal was to determine the definitive profile of the spindle of the transducer. On the basis of the above linearity, hysteresis, creep and deflection, it was decided to use the hollow shape, Model III spindle. Thus, from now on, the hollowed single prototype Model III will be used as the only transducer. However, the clock gauge does not measure transducer deflection alone, but measures transducer + tube deflection. Furthermore, after heat treatment, any further modification of the component is prevented. Therefore, a complete study was undertaken to check the mechanical behaviour by means of temporary, low cost, strain gauges.

4.5 STUDY OF THE ELECTRICAL BEHAVIOUR OF THE CHOSEN TRANSDUCER (MODEL III)

In the following section, the electric behaviour of the Model III Villiers Pylon Transducer (VPT) using four low cost, temporary gauges is described.

The main goal of this preliminary study was to examine if this transducer had still a linear behaviour, without any hysteresis or creep. A check of the cross-talk levels was also conducted to verify the structure of the transducer and the accuracy of the gauge positioning. The new transducer was always affixed with the definitive connection saddle (see sections 4.2.1 and 4.4.2).

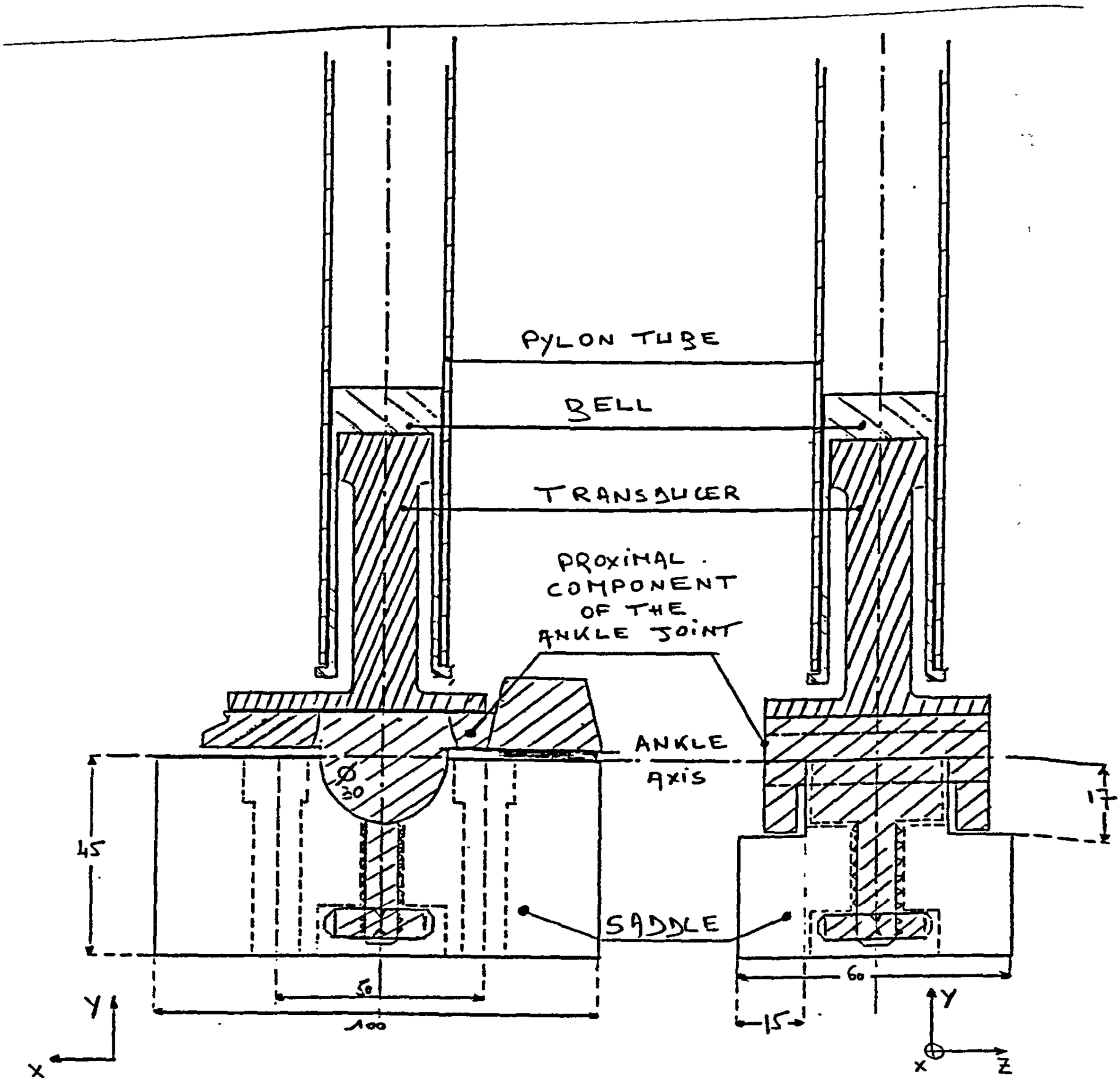

Figure 4.12: The special machined saddle for bending moment tests (the part without hatching)

The descriptions of the gauges, of the full Wheatstone bridges with output voltage and related equations are shown in appendix 11.IV.3.

4.6 TESTS DESCRIPTIONS

In all tests, the well-known dead-weight technique was used. Solomonidis (1989) and Magnissalis (1992) recommended this method rather than the use of an automatic loading test machine.

4.6.1 Set-up descriptions

4.6.1.1 BENDING MOMENT TEST IN ANTERIO-POSTERIOR PLANE: MZ

For the experimental tests concerning bending moment Mz, which was the main channel of the present study, a special machined saddle was used. It is shown in figure 4.12. This device allowed the transducer to be fixed securely on a special heavy steel table used as a bench base. The accuracy of the table alignment in the vertical and the horizontal plane was checked thoroughly by means of a large spirit level.

It was very important to check carefully with a spirit level if the transducer's ankle axis (Z direction) was perfectly horizontal. For that, a spirit level was laid on the top of the saddle and the adjustment was made by trial and error of the screws inside the holes of the heavy bench. The longitudinal axis of the transducer as defined by the prosthetic shank tube (Y direction), had to be accurately and perfectly horizontal before starting any loading, although a small deflection introduced a negligible error. For that, a range of metallic packing pieces was used. By trial and error, one of them was put between the top of the saddle and the flange of the transducer duraluminium base to have the Y axis correctly horizontal. A 180° rotation of the transducer was necessary to change between a positive and a negative result. Tests are completely described in section 6.3.4.

Figure 4.8 shows the set-up for the anterior-posterior bending moment test. It was a cantilever system that applied a combined shear force and bending moment to the transducer.

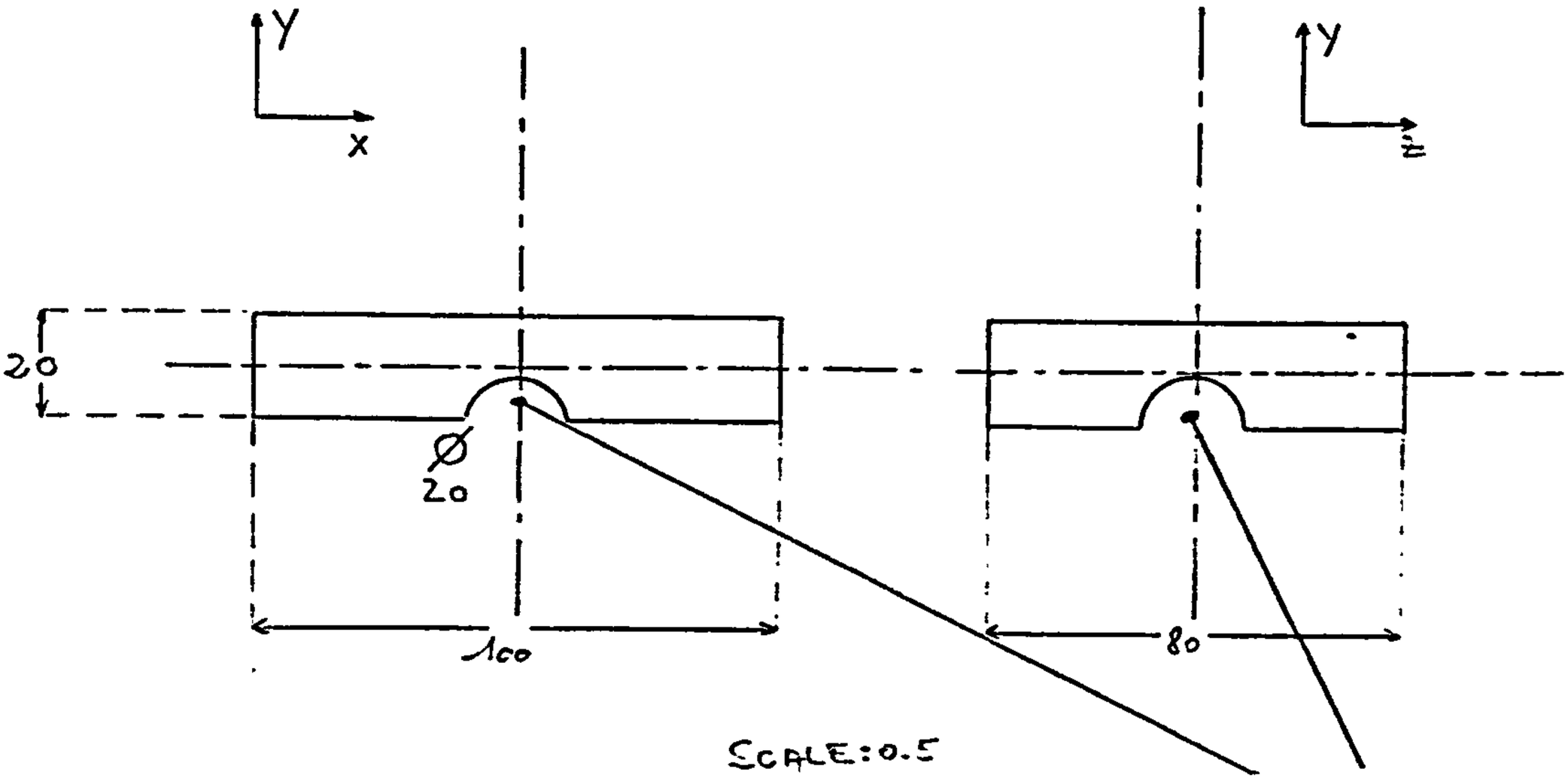

Figure 4.13: The special plate for axial load test with a spherical recess to suit steel ball

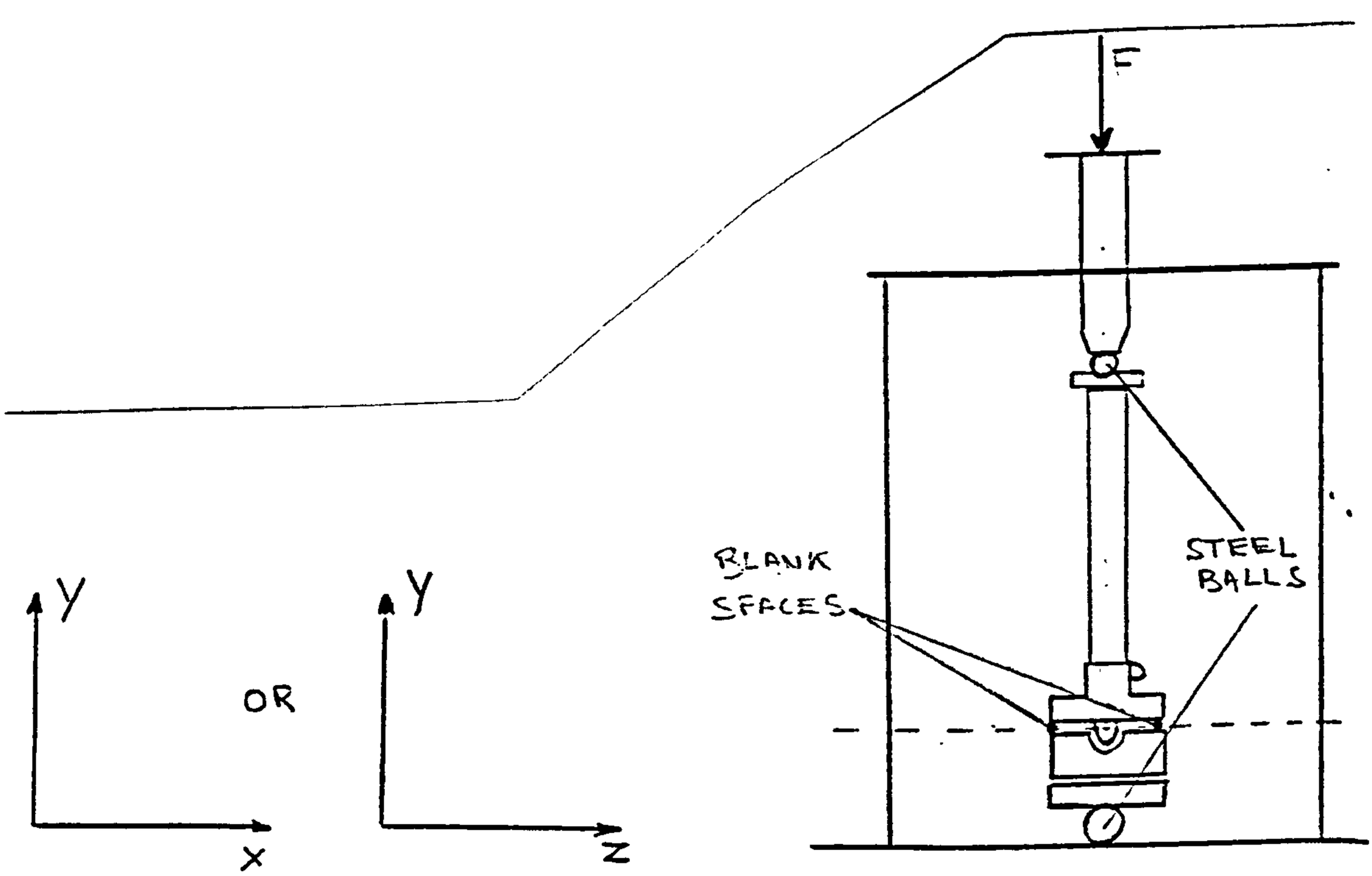

Figure 4.14: The set up for vertical axial load

4.6.1.2 BENDING MOMENT IN MEDIO-LATERAL PLANE: MX

For these moments, the transducer was rotated by 90° about the Y axis. The Z direction becomes vertical, the X direction horizontal.

As for anterio-posterior plane, it was very important to check accurately and carefully with a spirit-level and a plumbline if the transducer's ankle axis (Z direction) was perfectly vertical and the shank tube (the Y direction) horizontal before starting any loading. This was the same as above in A/P bending moment set-up: a cantilever system applying combined shear forces and bending moments.

4.6.1.3 VERTICAL AXIAL LOAD: FY

For the axial load Fy, a special device, reported by Lowe (1969) and described in section 6.3.2, was used. Loads were applied by means of weights on the top disc, resulting in compression of the transducer. It was important to check the alignment of the device to be sure that there was not any off-axis load. The vertical single axis through the loading point was guaranteed by steel balls at the interface between the transducer and the device.

Another special saddle was machined for these tests. This component was a simple steel plate with a spherical recess in its inferior surface as shown in figure 4.13. This cavity engaged with the bottom steel ball. This block was screwed onto the first saddle from which the central bolt had been removable as shown in figure 4.14.

During all loading tests, at each step, it was important to check if the flanges of the transducer remained horizontal because the transducer might lie only on its axis without any load on the two flanges. It was therefore possible that the transducer could tilt around the ankle axis. That could give some pressure onto one of the flanges introducing non-accuracy in the test with an off-axis load. This check was done at each loading case by sliding easily two sheets of rubber, having a thickness of one millimetre, between the saddle and the two flanges as shown in figure 4.15.

4.6.1.4 TORQUE IN TRANSVERSE PLANE: MY

For torque calibration, the same set-up as for the anterio-posterior bending moment was utilised. The transducer was securely screwed onto the heavy bench

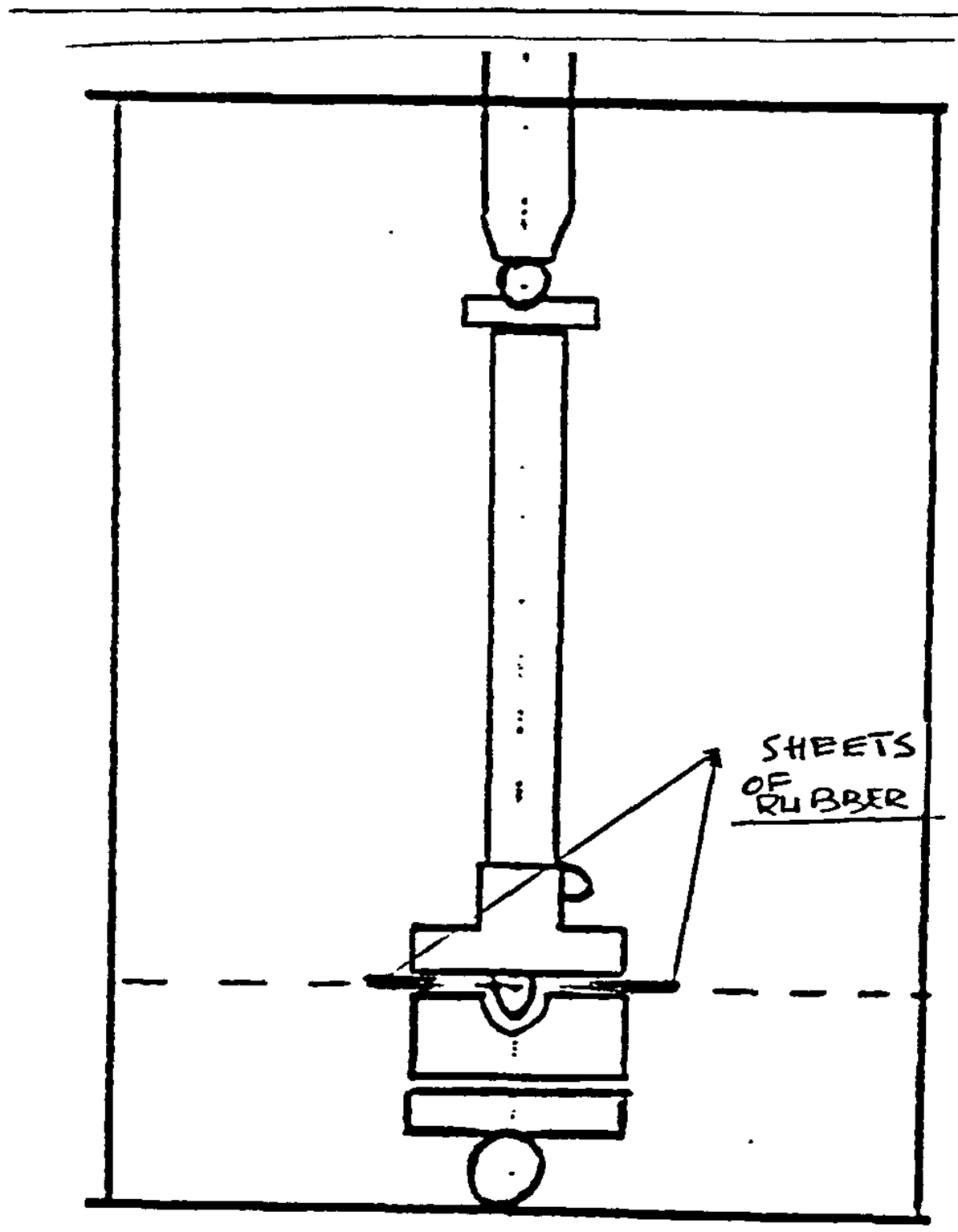

Figure 4.15: Two sheets of rubber are used to check the horizontality of the transducer leaver the two blank spaces between the two flanges of the transducer and the saddle empty.

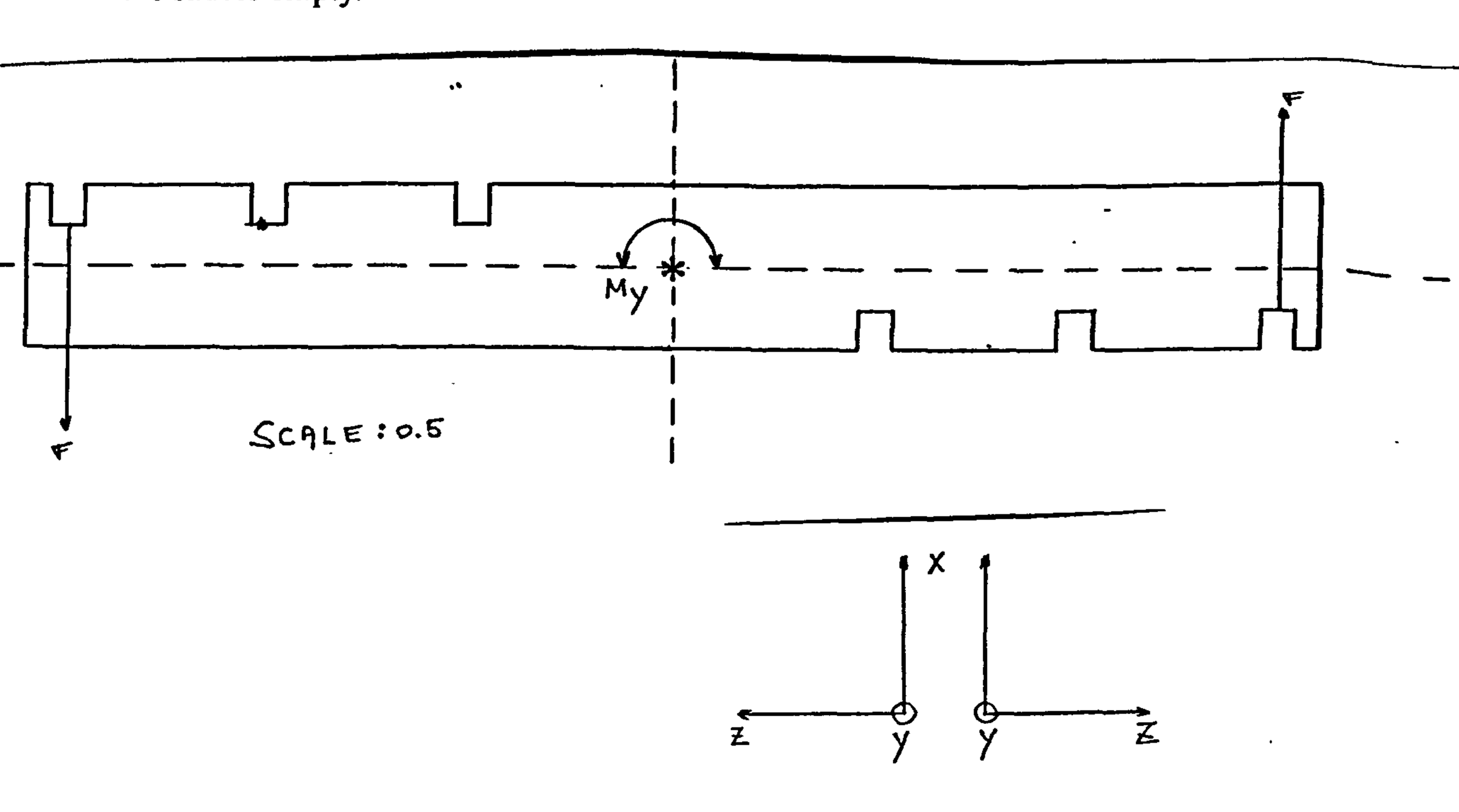

Figure 4.16: The machined torque bar

table with its two axes (Z ankle and Y longitudinal axis) in the horizontal plane. On the proximal end of the shank tube, a special machined bracket was fitted to support a horizontal bar. This bar has some notches situated at 5, 10 and 15 centimetres from the middle, which is the Y axis. The notches were machined to allow the coupling of the bar to cables for applying an upward and downward loads as shown in figure 4.16.

For the upwards load cable, a pulley was used to change the load direction: still strictly vertical but acting downwards. The two cables might be as parallel as possible (maximum accuracy ≈ 2°) to each other and they might be in the same perpendicular plane to the longitudinal axis of the transducer. It was important to put the same load on each side of the bar to ensure that no shear force was introduced. More information about uncertainties due to friction between the cable and the pulley is given in section 6.3.3.

4.6.2 Loading descriptions

For example, all the tests made in the anterio-posterior plane are shown in table 4.1 and the loading schedule in table 4.2. Each weight had a registration number and was calibrated by a certified test house (see section 3.5.3). For each test, the load was gradually increased in accordance with the load schedule shown in table 4.2. Some other tests were undertaken to check the possibility of any cross-effects. Among many reasons given in section 6.2, at this stage of the design of the new transducer, these cross-effects are due to inherent characteristics of the device, such as:

1. asymmetries of the device due to machining errors;
2. elastic deformations caused by the particular loading configuration;
3. minor differences in strain gauges alignment and gauge factor.

Obviously, because only one channel was fitted, it was impossible to record all the cross talks due to the misalignment of the gauges on the device (Magnissalis, 1992). However, it was essential to study the cross effects due to machining errors of the transducer before hardening and bonding any definitive expensive strain gauges. In other words, a recording of the temporary A/P bending gauges' cross effects was

A/P BENDING MOMENT		CHARACTERISTIC OF EACH TEST	COMMENTS maximum bending moment
Mz positive dorsiflexion	Test 0 Test 1 (fig 4.17) Test 2 (fig 4.17) Test 3 (fig 4.17)	F at 31.5 cm from axis Gain = 500	**140 Nm** Test 0 zero line = 2000 cu Test 1 to 3 zero line = 1000 cu
	Test 4 (fig 4.18)	F at 31.5 cm from axis Gain = 500	This test was made to check creep with a moment of **171 Nm** during 140 min
	Test 5 (fig 4.19)	F at 31.5 cm from axis Gain = 500	**140 Nm** In this test the reverse steel bell has been used to check the behaviour of the spindle without the usual aluminium bell
	Test 6	F at 16 cm from axis Gain = 500	**135 Nm**
	Test 7 Test 8	F at 31.5 cm from axis Gain = 200	**171 Nm** to check if the computer units are proportional with a gain of 500 versus a gain of 200
Mz negative plantarflexion	Test 9 (fig 4.17) Test 10 (fig 4.17)	F at 31.5 cm from axis Gain = 500	**85 Nm**
	Test 11	F at 16 cm from axis Gain = 500	**88 Nm**
	Test 12	F at 31.5 cm from axis Gain = 200	**85 Nm** to check if computer units are proportional with a gain of 500 versus a gain of 200

Table 4.1: The full range of tests done in anterio-posterior plane (see text for gain)

Loading Schedule	Mass in kg	Weights in N for axial load	Moments in Nm from the ankle axis	
			0.315 m	0.16 m
weight of carrier	0.88	8.88	***2.7***	1.4
20 lb. = 9.07 kg (A14)	9.95	97.65	***30***	15
20 lb. = 9.07 kg (A15)	19.02	186.63	***57***	29
20 lb. = 9.07 kg (A16)	28.09	275.61	***85***	44
20 lb. = 9.07 kg (A17)	37.16	364.58	113	58
20 lb. = 9.07 kg (A18)	46.23	453.56	140	72
10 kg (A4)	56.23	551.66	171	88
10 kg (A5)	66.23	649.76		104
10 kg (A6)	76.23	747.86		
10 kg (A7)	86.23	845.96		
10 kg (A8)	96.23	944.06		
10 kg (A9)	101.23	993.11		

Table 4.2: The different loading cases for bending moments (except torque) and axial load (in bold and italic letters and shaded cells: the four points shown in figure 4.17)

performed while axial load, M/L bending moments and torque were applied on the transducer.

The amplifier gain setting of 500 (Tests 1 to 6 and 9 to 11) was arbitrarily chosen following the one usually used with the Strathclyde Pylon Transducer (SPT), (Magnissalis, 1992). For checking amplifiers and the software « Acquire », Tests 7, 8 and 12 were performed with a different gain setting of 200.

4.6.3 Test procedures

All the tests had progressed in the same way as the calibration performed for the first ankle transducer (Model I) (see section 3.5.3). At each loading step, a computer output was recorded. The recorded value was transferred to another file in computer units per unit of applied load as explained in the above section 3.5. Four tests were carried out in two days and an arithmetical average was calculated. The final files are shown in appendix 11.IV.3. They represent the tests No1, 2 and 3 in dorsiflexion, i.e., Mz +, which is a bending moment positive about the Z axis and negative bending moment, i.e., plantarflexion, Mz-. After all these computer manipulations, plotting a graph was easy.

4.6.3.1 ANTERIOR-POSTERIOR BENDING MOMENTS

The positive and negative bending moments (Mz) about the Z axis in the fore - aft plane, are the main channel relatively to the fitted gauges described above.

According to the table 4.1, the tests N°1, 2 and 3 in dorsiflexion were made following the loading step shown in table 4.2 with the loading point at 0.315 m from the ankle axis.

When the maximum loading was applied, the load was maintained for five minutes and then a new record was taken to check for creep and drift. Then, a step by step return to zero load was performed.

Figure 4.17 shows the tests 1, 2 and 3 in positive bending moment Mz (dorsiflexion) and 9 and 10 in negative bending moment (plantarflexion). The transducer behaviour is linear (traces from tests 1 and 3 [Mz+] and 9 and 11 [Mz-] are totally overlapped, trace from test 2 is not), without any hysteresis nor drifting during the five minutes at full load. All these characteristics are shown in chapter 6

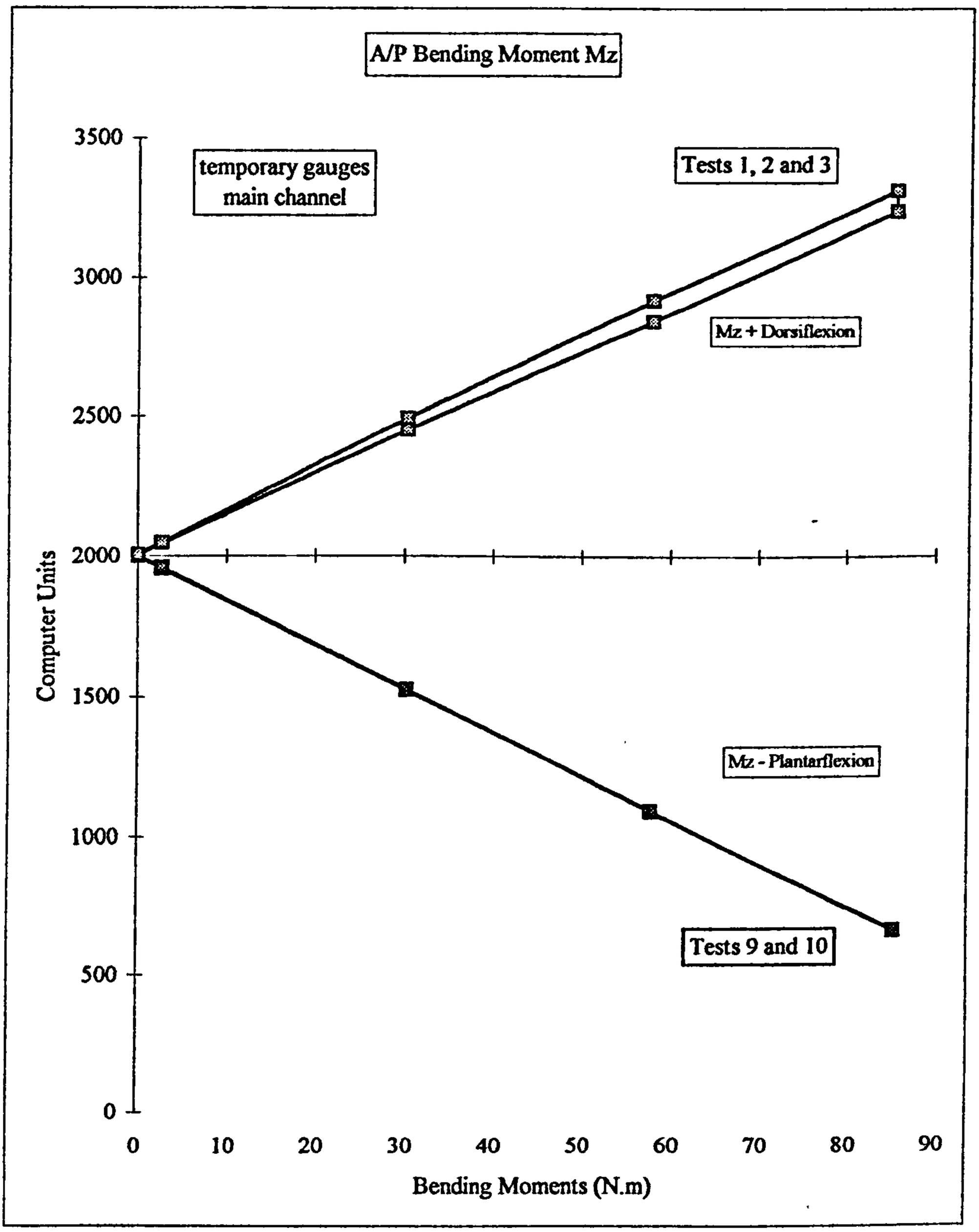

Figure 4.17: The graph of the results for A/P bending moments Mz (three tests in dorsiflexion Mz+ and two tests in plantarflexion Mz-) Some traces are totally overlapped. Due to symmetry reason in the graph, the traces in dorsiflexion were cut at 85 Nm to show a symmetrical result relative to plantarflexion.

during calibration tests of the transducer. Studying the results, it is possible to assert that, in this main channel, working with a gain of 500 and a bridge voltage of 3V:

• a positive bending moment of 140.6 N m gives a range of 2050 computer units. If these computer units are converted in millivolts, 5002 mV is found[10]. If these findings are normalised in computer units per unit N m, the sensitivity has an average value of 14.58 cu.$(N\ m)^{-1}$.

• a negative bending moment of 85.44 N m gives a range of 1337 computer units. If these computer units are converted in millivolts, 3262 mV is found. If these findings are normalised in computer units per unit N m, it gives an average value of 15.65 cu.$(N\ m)^{-1}$.

The following test (Test 4) was performed to check the new transducer for creep. It had the same set up as A/P bending moment with equivalent loading step (positive bending moment, Mz +) except a long stop of 140 min, at the maximum load of 551.6 N that is 171.01 N m.

It is easy to note that there was no creep: 3501 cu. starting the creep study at maximum load and 3503 cu. at the end of the 140 minutes stop. It is possible to notice that the test was done with the same gain and bridge voltage as above. The maximum value was 2502 computer units (3502 cu. – 1000 which was the zero line for the test 4), equal 6104 mV with an average normalised value of 14.63 cu.$(N\ m)^{-1}$. The results are shown in figure 4.18.

The following test (Test 5 in table 4.1) had the same characteristics as No 1 to 3 but the reverse bell made of steel (see figure 4.9) was fitted on the transducer for checking the behaviour of the spindle of the transducer without the usual aluminium bell.

Here also, it is possible to state that the behaviour of the steel transducer spindle is still linear, without any hysteresis. A single difference can be noticed: the number of computer units is higher than with the aluminium bell: a range of 2188 cu. instead of a mean value of 2044 cu. with the aluminium bell for the same load. That

---

[10]1 computer unit equals 2.44 millivolts (4096 cu. = 10 V), (see section 3.5)

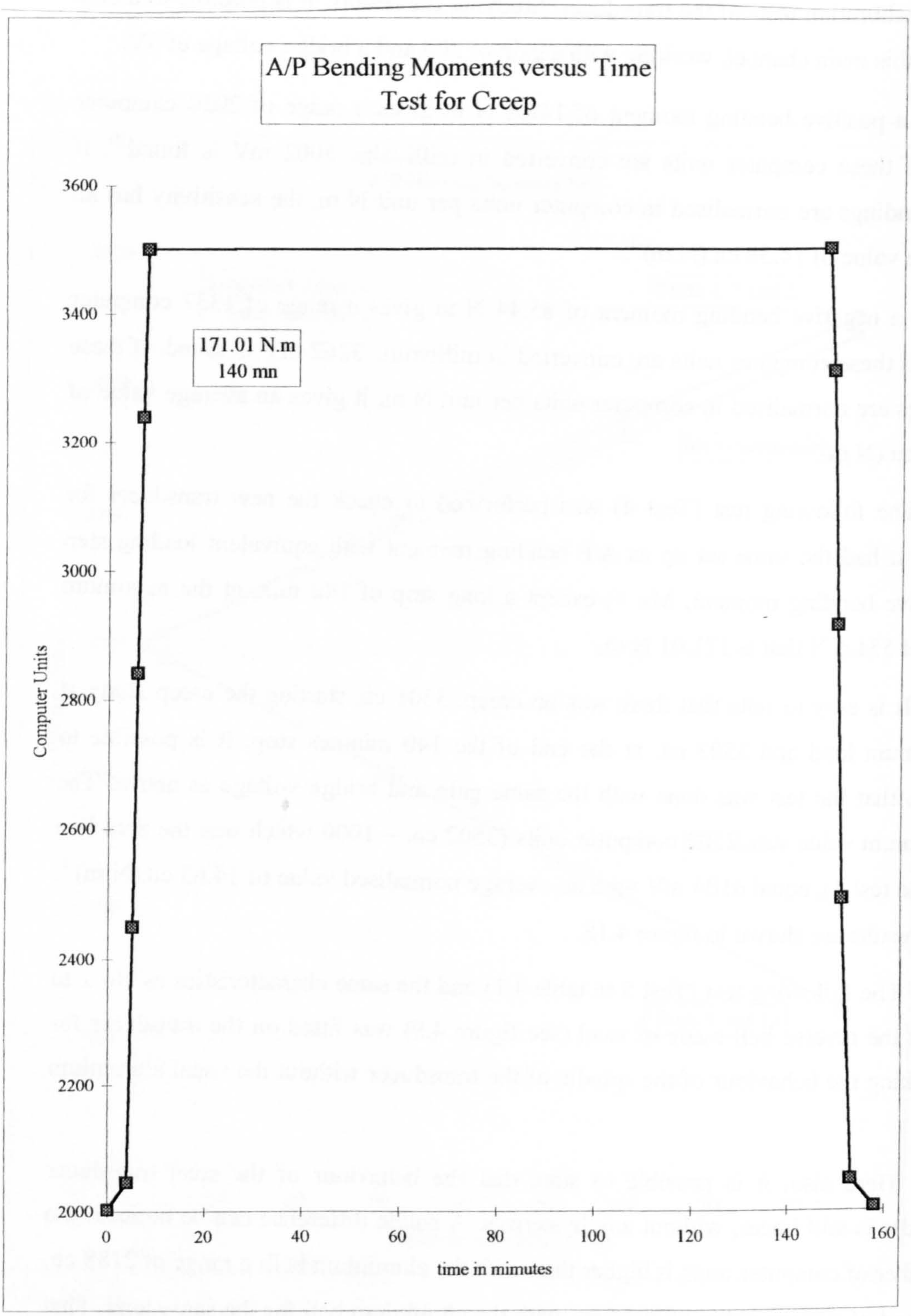

Figure 4.18: The bending moment results for creep (Mz+) at full loading (171 Nm) during 140 minutes

gives a difference of 7 %.

Figure 4.19 shows the graphs, it is important to pay attention to the linearity, the lack of hysteresis and drift.

The following tests (Tests 6,, 7 and 8) exhibited the same results. They are shown in appendix 11.IV.3.

At this stage, it was interesting to compare all the tests among themselves in respect of the output computer units. This comparison was made with all the tests having a gain of 500. The difference between maximum and minimum (in cu) was divided by the corresponding moment in N m, so that a normalised result in computer units for a unit N m was yielded.

- In positive bending moment: the test 0 (Mz+) was conducted to extend the sample with another range of computer units (software « Acquire » zero line at 2000 cu.). The difference between the maximum (13.47 cu.(N m)$^{-1}$, test 0 and 14.73 cu.(N m)$^{-1}$, mean tests 1 to 3 was only 1.26 cu.(N m)$^{-1}$ = 3.08 mV.(N m)$^{-1}$. This was very low and could correspond to noise. Moreover, all tests performed with a lever arm of 0.31 m had a very close result, a range of 14.49 to 14.73 = 0.24 cu.(N m)$^{-1}$. On the other hand, the single test N°6, using a lever arm of 0.16 m, had a range of results with tests using a lever arm of 0.315 m, more substantial. It was not easy to find a possible explanation. There might be cross sensitivity to shear force.

- In negative bending moment: the difference between the extremes was 15.67 and 14.76, that was 0.91 cu.(N m)$^{-1}$ = 2.22 mV.(N m)$^{-1}$ which looked very low. However, here also, there was a difference between the two tests having a lever arm of 0.31 m versus the test having a lever arm of 0.16 m. In both +ve and -ve bending moments, the sensitivity was decreased a little from a lever arm of 0.31 m to 0.16 m, about 9.35 % for positive moments and 6.16 % for negative moments. It is possible to summarise as follows:

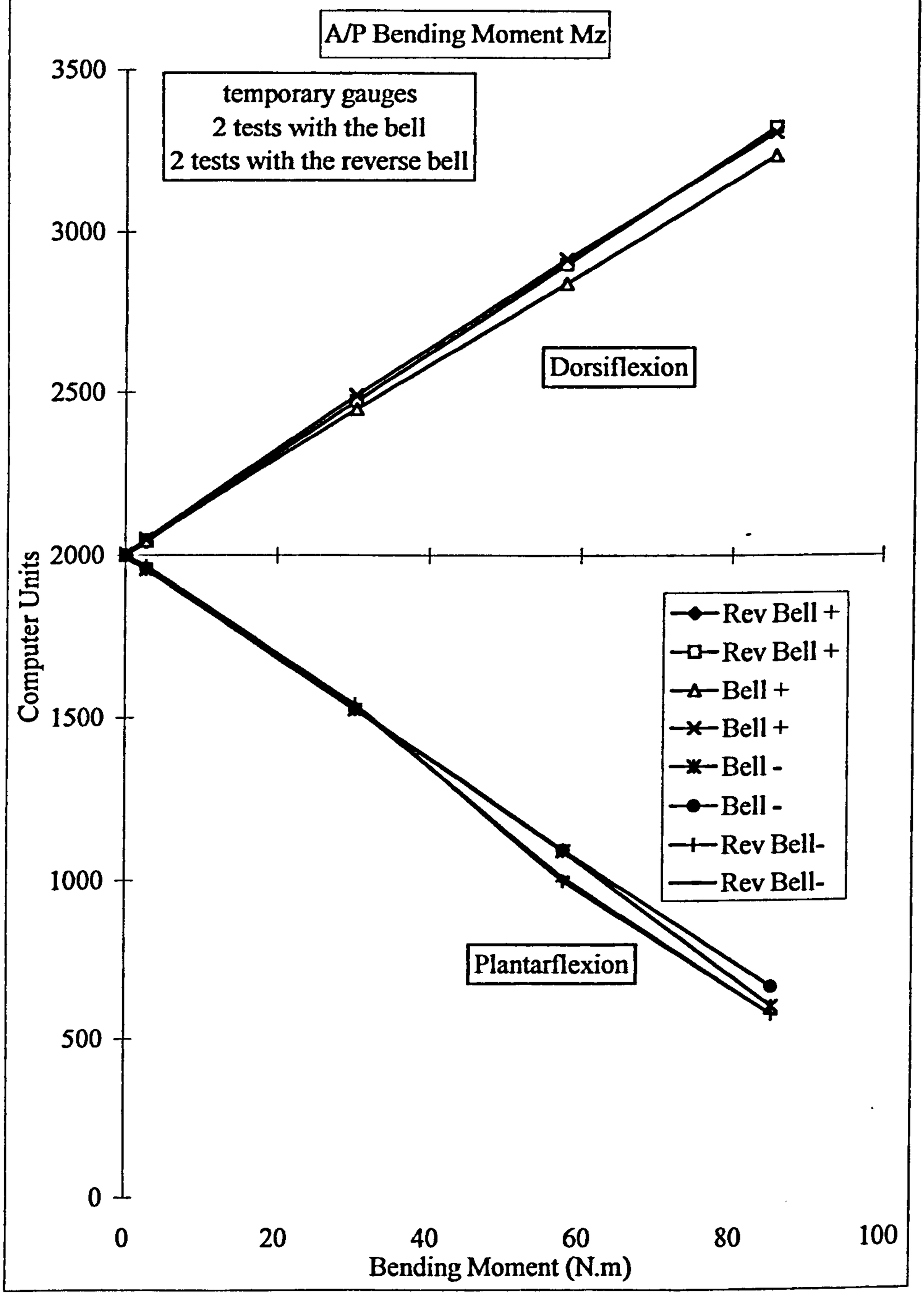

Figure 4.19: The A/P bending moment Mz results using the bell and the reverse steel bell (two tests in each direction).

	F at 0.16 m from ankle axis	F at 0.315 m from ankle axis	Difference in percentage
Dorsiflexion	+ve: 13.47 cu.(N m)$^{-1}$	14.73 cu.(N m)$^{-1}$	9.35
Plantarflexion	- ve: 14.76 cu.(N m)$^{-1}$	15.67 cu.(N m)$^{-1}$	6.16

There was a contrasted value in sensitivity between dorsiflexion and plantarflexion. The transducer was more sensitive in plantarflexion than dorsiflexion, whatever the lever arm:

- from plantar to dorsiflexion with a lever arm of 0.16 m: 1.29 cu.(N m)$^{-1}$ = 3.15 mV.(N m)$^{-1}$
- from plantar to dorsiflexion with a lever arm of 0.31 m: 0.94 cu.(N m)$^{-1}$ = 2.29 mV.(N m)$^{-1}$

Three reasons can be expressed: 1, low cost temporary gauges were used; 2, the set up was different; 3, the flat bottom flange of the transducer has not a symmetrical shape in the A/P plane (the front part is longer than the rear (see section 4.8.2). This could introduce more rigidity in the response of the assembly of pieces when a dorsiflexion bending moment was applied. These comments will be taken into account again in chapter 6 concerning the full calibration of the transducer with definitive gauges fitted on.

All these differences are very low by comparison with the full range of computer units: around 15 cu versus a range of more than 2000 cu. All the results are shown in table 4.3 and all the tables and figures are shown in appendix 11.IV.3.

At the end of this subsection, it is possible to make some preliminary conclusions:

1. the behaviour of the transducer is linear without any hysteresis;

2. its behaviour is perfectly elastic in the range of loading used;

3. in fore - aft bending moments, the sensitivity is enough to allow recording with the chosen gain settings and bridge voltage usually used with the Strathclyde Pylon Transducer (Magnissalis, 1992);

4. the outputs of the amplifiers and « Acquire » program are linear and

Test Number	minimal output in cu. (no load)	maximal output in cu. (variable loading)	difference between maximum and minimum	moment in Nm	numbers of cu. for 1 Nm	
DORSIFLEXION Mz +						
N 0	2001	4042	2041	140	**14.51**	+ ve
N 1	998	3040	2042	140	**14.52**	+ ve
N 2	998	3036	2038	140	**14.49**	+ ve
N 3	1001	3503	2502	171	**14.63**	+ ve
N 4	1003	3060	2057	140	**14.63**	+ ve
N 5	1003	3523	2520	171	**14.73**	+ ve
N 6	999	2823	1824	135	**13.47**	+ ve
PLANTARFLEXION Mz –						
N 9	1999	663	1336	85	**15.63**	- ve
N 10	2000	661	1339	85	**15.67**	- ve
N 11	2001	698	1303	88	**14.76**	- ve

Table 4.3: Normalised results in cu.$(N.m)^{-1}$ for positive and negative bending moments

proportional to the applied loads. A comparison between the experimental results and previous theoretical calculation is shown in appendix 11.IV.4.

4.6.3.2 THE CROSS - EFFECT STUDY

Ideally, when only one load corresponding to a particular channel is applied, it should be a non-zero output signal in only one channel. It is the definition of the main effect. However, in practical transducer utilisation, a single load introduces a response in all the six channels: one main effect and five interaction effects. They are called cross-talk effects. Therefore, their study was mandatory as shown in the following sections. A top - range transducer should have the lowest possible interaction effects. More details will be given in chapter 6.

In practice, one load and only one is applied in a different direction as the one corresponding to the main channel. That is: a medio-lateral bending moment, a vertical axial load and finally a torque were applied while recording from the anterio-posterior bending moment gauges. Because there was only one set of gauges, the study was not complete. The goal was only to record some interaction effects but the results can be interpreted to obtain the level of the interaction effects. Mainly, because it was not possible to compare the obtained cross-effects with each main channel, one by one. A study of these interactions will be conducted with the complete calibration of the new transducer (see chapter 6).

4.6.3.3 MEDIO-LATERAL BENDING MOMENTS

Thus, medio-lateral positive and negative bending moment tests were conducted to check the interaction effect on the anterio-posterior bending strain gauges (one test in positive and one in negative directions). The two tests had the characteristics shown in tables 4.4 and 4.5. The loading case succession was identical as those shown in table 4.2.

The results are shown in figure 4.20. They characterise the cross-talk level in both positive (Mx+) and negative (Mx-) medio-lateral bending moments. The cross-talk effect is symmetrical between positive and negative. It is linear without any hysteresis, creeping (but only during 5 min) or drifting: the up-load curve is superposed with the down-load one.

The positive cross-talk level is low: a maximum of 20.6 cu. (test 13) compared

M/L BENDING MOMENT		CHARACTERISTIC OF EACH TEST	MAXIMUM BENDING MOMENTS
Mx positive Mx negative	Test 13 Test 14	F at 0.315 m from axis Gain = 500	85 N.m

Table 4.4: Details of tests done in medio-lateral plane

WEIGHTS	MASS in kg	Moments with the loading point at 0.315 m from the ankle axis
0	0	0
weight of carrier	0.885	2.69 N.m
20 lb. = 9.07 kg (A14)	9.955	30.27 N.m
20 lb. = 9.07 kg (A15)	19.025	57.85 N.m
20 lb. = 9.07 kg (A16)	28.095	85.43 N.m

Table 4.5: Loading sequence used in the M/L bending tests

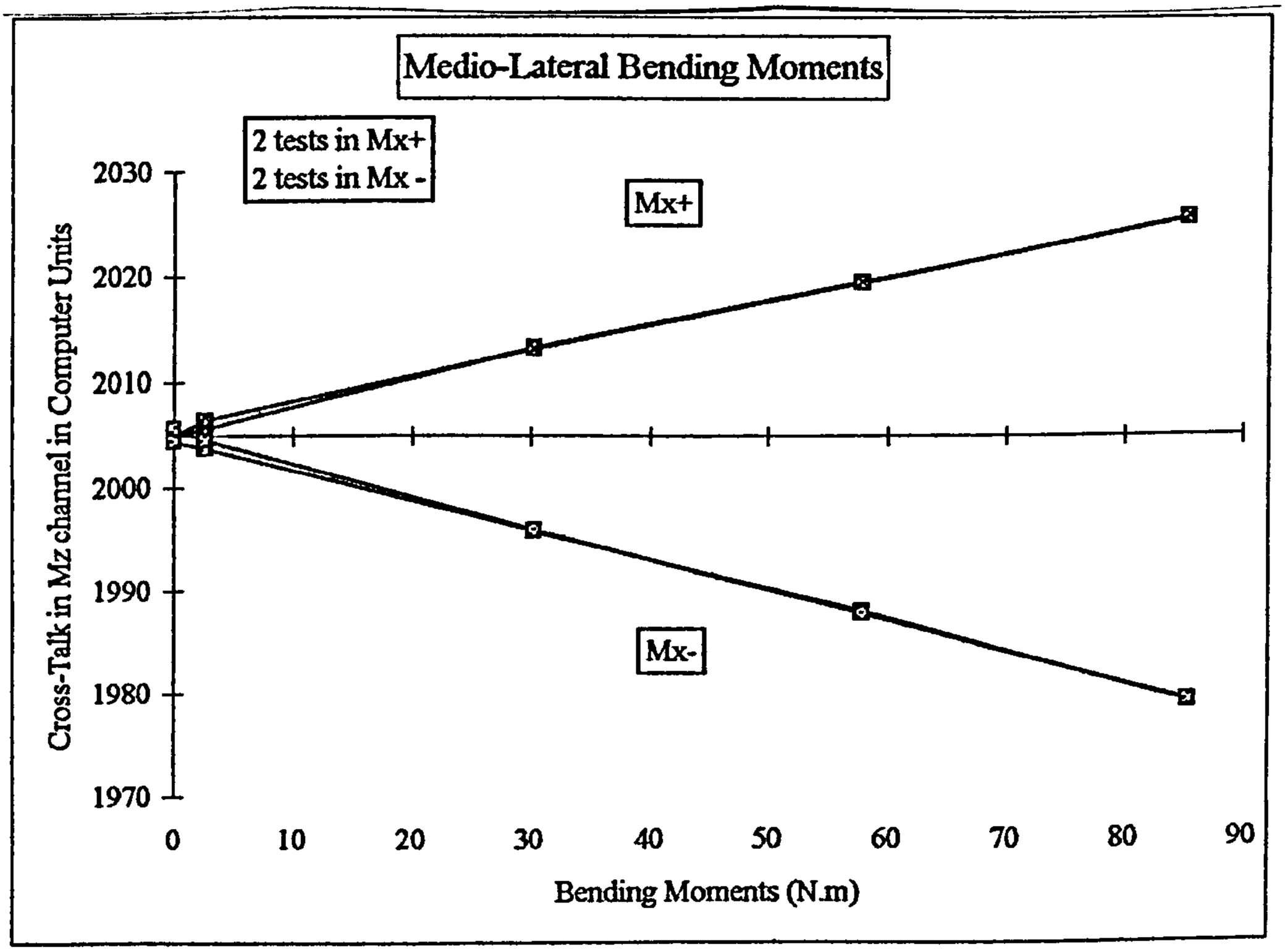

Figure 4.20: The cross-talk responses recorded in A/P bending gauges when M/L bending moments are applied (one test in each direction, Test 13 and 14).
The usual aluminium bell was used.

with a mean value of 1230 cu. in the main channel for the same moment when the anterio-posterior bending moment set up was used, therefore a ratio of 1.6 %.

In the negative loading case, it is also possible to notice a low cross-talk response: less than 25 cu (test 14) that exhibits a ratio of 1.9 %.

4.6.3.4 VERTICAL AXIAL LOAD

Exactly as in the medio-lateral plane, two axial load tests were performed to check the cross-talk effect. The full description of the device used is given in chapter 6. The maximum axial load was 993.11 N and the different loading schedules of the two tests are shown in table 4.2. The gain settings and the bridge voltage were equal to those in previous tests.

Figure 4.21 shows this cross talk when axial load is applied.

At the maximum load applied, the cross talk was very low: average value 12.7 cu. It was also important to note that the cross-talk curves were not linear, however, the values were small. It was, therefore, difficult to conclude anything among these possibilities: noise, wires or connection problems, amplifiers, and/or computer. This list is not exhaustive.

4.6.3.5 TRANSVERSE TORQUE

The bending moment in the horizontal plane (torque about the Y axis) tests were undertaken to check cross-talk effects using the set up described above (see sections 4.6.3.5 and 6.3.3). The maximum bending moment was 21.58 N m. Two different tests in My positive but only one in negative were conducted. The gain setting and the bridge voltage were the same as those in other tests.

The loading schedule is shown in table 4.6 while the figure 4.22 exhibits the results.

At the maximum torque applied, the same observation as the one made in axial load could be expressed. The cross-effect magnitude was low (My+ = 15 cu.; My- = 10 cu.) and the curves were not linear, with the same uncertainty about the origin as previously stated.

All of these interaction effects are shown in table 4.7. The cross - effects had a small magnitude, especially in medio-lateral bending and axial load. They were

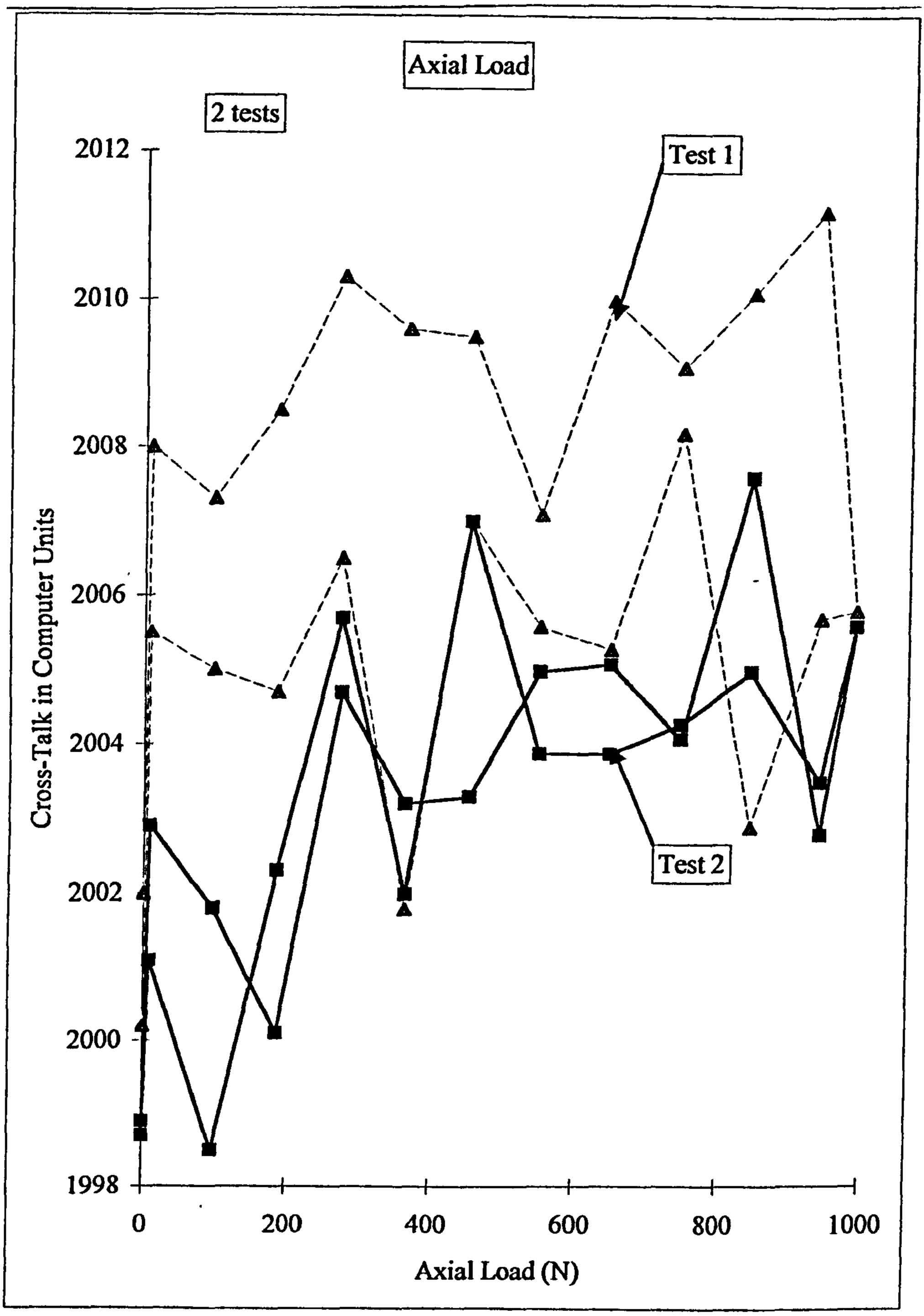

Figure 4.21: The cross-talk responses recorded in strain gauges fitted to record only the A/P bending moments when axial load is applied (2 tests have been conducted).

higher in torque (My). All these cross effects will be studied in chapter 6 (calibration procedure) and chapter 7 (static and dynamic validation of the Villiers Pylon Transducer).

In conclusion, the average cross-talk level in the five channels concerned was found to be as follows:

cross-talk level ≈ one per cent of main channel value

4.7 PARTIAL CONCLUSION

The work presented in this chapter provided many conclusions, which are:

1. The choice of the material from which the body of the transducer should be built was made following the ISO loading recommendations after a theoretical analysis of stresses and strains. The conclusion was to choose a special stainless steel, which, after heat treatment for hardening, had enough strength.

2. Two prototypes of the new transducer were built and were in competition with each other: one solid and the second hollowed. To decide between them, a mechanical analysis of the behaviour of the two samples was conducted. A study on deflection was managed. The conclusion was to choose the hollow prototype.

3. To confirm the decision, a full set of four low cost, temporary strain gauges was installed, in a full Wheatstone bridge, so that they recorded the anterio-posterior bending moments. The results were that the new transducer had a linear response, without any hysteresis nor creep.

4. To reinforce the confidence in the transducer's design, an interaction effect analysis was performed. The results showed a low level of interaction effects in all channels.

Therefore, both the definitive material and shape of the new transducer were confirmed. Thus, the following section provides a complete description of the new transducer.

Loading Schedule	Mass in kg	Bending Moments N.m loading point at 0.315 m from ankle axis
0	0	0
weight of carrier = 2 x 1 kg	2 x 1	2 x 0.981 = 1.9
2 x 5 kg (A4 and A5)	2 x 6	2 x 5.88 = 11.7
2 x 5 kg (A6 and A7)	2 x 11	2 x 10.79 = 21.6

Table 4.6: Loads applied in torque tests

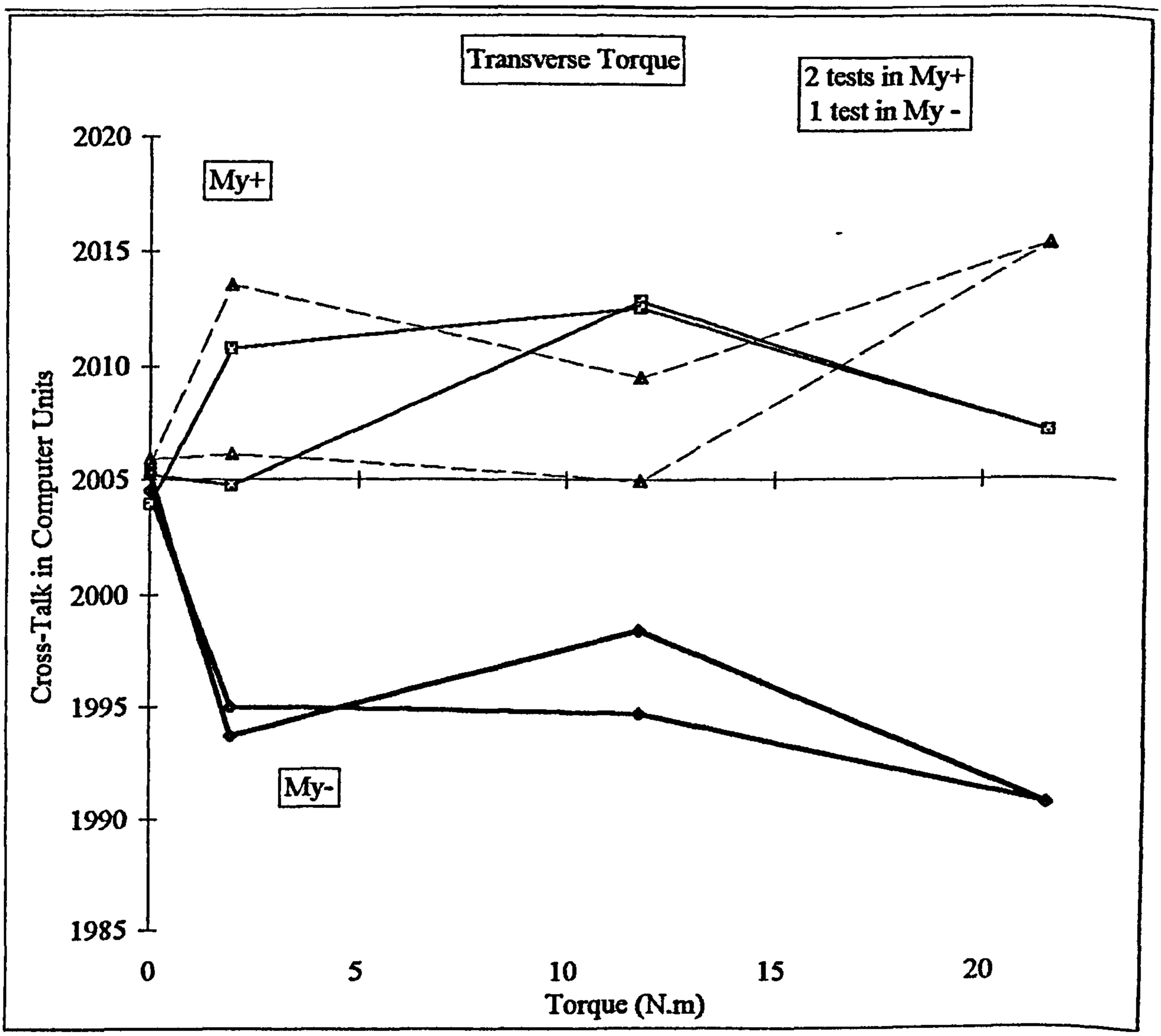

Figure 4.22: The cross-talk responses recorded in A/P bending gauges when transverse torque is applied (2 tests in positive and one test in negative direction).

4.8 FINAL DESCRIPTION OF THE NEW VILLIERS PYLON TRANSDUCER

4.8.1 Introduction

For the acquisition of kinetic data, concerning the loads applied during locomotion, the choice of a new, removable pylon transducer was made. Following the conclusions established in the previous section, the definitive shape of the new Villiers Pylon Transducer (VPT) was finalised. The work presented in these following sections has three goals:

- to make an extensive description of the definitive new device
- to describe the strain gauges used and to outline the disposal of the six full bridges around the body - test of the transducer
- to explain, by some theoretical consideration, how the strain gauges work, justifying the disposition of the strain gauge full bridges, their designations and the findings.

4.8.2 Description of the new pylon transducer

According to section 4.3 and after some theoretical and experimental analysis (see appendix 11.IV.3), it has been stated the design of the VPT. It is built in three parts. The gross outline is:

1. a circular aluminium bell, looking like a re - entrant cover, is installed inside the prosthetic tube. The prosthetic shank tube is loaded on this transducer's part by means of a flange. This flange is separated from the lower flange of the transducer by a gap of 3.9 mm (see section 4.2.1). This gap allows the bell to deform a little, under the action of stresses, under fore-and-aft, vertical and axial forces or moments. These loads are developed from the residual limb of the prosthetic user, via the socket and the distal tube, which covers completely the bell. It is mandatory to have the tube strongly connected to the bell.

Therefore, all loads are transmitted only by the transducer, resulting in strains, measured by the strain gauges. If these gauges are appropriately located and

Maximum Load	Channel	Main channel or Cross-talk	Computer unit	Computer unit per unit load	Computer unit per computer unit of main channel per unit load
171 N.m	Mz positive	Main channel	2513	14.69	1
85 N.m	Mz negative	Main channel	1339	15.67	1
85 N.m	Mx positive	Cross-talk	20.6	0.24	0.01
85 N.m	Mx negative	Cross-talk	25	0.29	0.02
993 N	Fy	Cross-talk	12.7	0.012	0.0008
21 N.m	My positive	Cross-talk	15	0.69	0.04
21 N.m	My negative	Cross-talk	10	0.46	0.03

Table 4.7: Results of the channel interaction effect

calibrated, it becomes possible to calculate the stresses and hence the values of the load actions.

2. the body of the transducer has a hollowed cylindrical shape. It is located inside the bell and is a push fit on its top part, having a 22 mm diameter. The middle and bottom parts are narrowed to 15 mm diameter. This 7 mm difference allows enough room between the body of the transducer and the bell to allow bonding of strain gauges and the pathway of the connecting leads. The test length of the transducer is extended through a base screwed on the third inferior part by the device.

3. an aluminium base to which the transducer is fastened, to join the transducer to the prosthetic foot.

4.8.2.1 THE ALUMINIUM BELL

Figure 4.23 shows the dimensions and the frame configuration adopted. The material is a common aluminium alloy (BS 6082 T4). The overall height is 64.5 mm, including the cap screws head thickness and fits into a normal prosthetic tube, of 26 mm inside x 30 mm outside diameter as dimensions. The bell is 61 mm long with six 3.5 mm holes for the cap screws which connect the bell to the transducer.

4.8.2.2 THE TRANSDUCER

Figure 4.24 shows the dimensions and the frame configuration adopted. The material was specified in the previous chapter. The stainless steel alloy used was heated at 480°C for one hour and cooled in air. The useful area for strain gauging and recording kinetics is 47 mm high and 47.12 mm in circumference.

At the transition between the measuring section and the flanges, there are radii of 1 mm at the top and 3.5 mm at the bottom to reduce stress concentration. The transducer has a lower flange, having an octahedral shape, which has six holes to connect with the aluminium base (see No 4 in figure 4.1). Two other threaded holes has been made in the flange to attach a bracket on which a 25 way terminal board is fixed (see figure 4.24, top and bottom).

4.8.2.3 THE ALUMINIUM BASE

Figure 4.25 shows the dimensions of the aluminium alloy base. The square hole allows the movement of the « T » part of the malleolus. The ankle axle is a

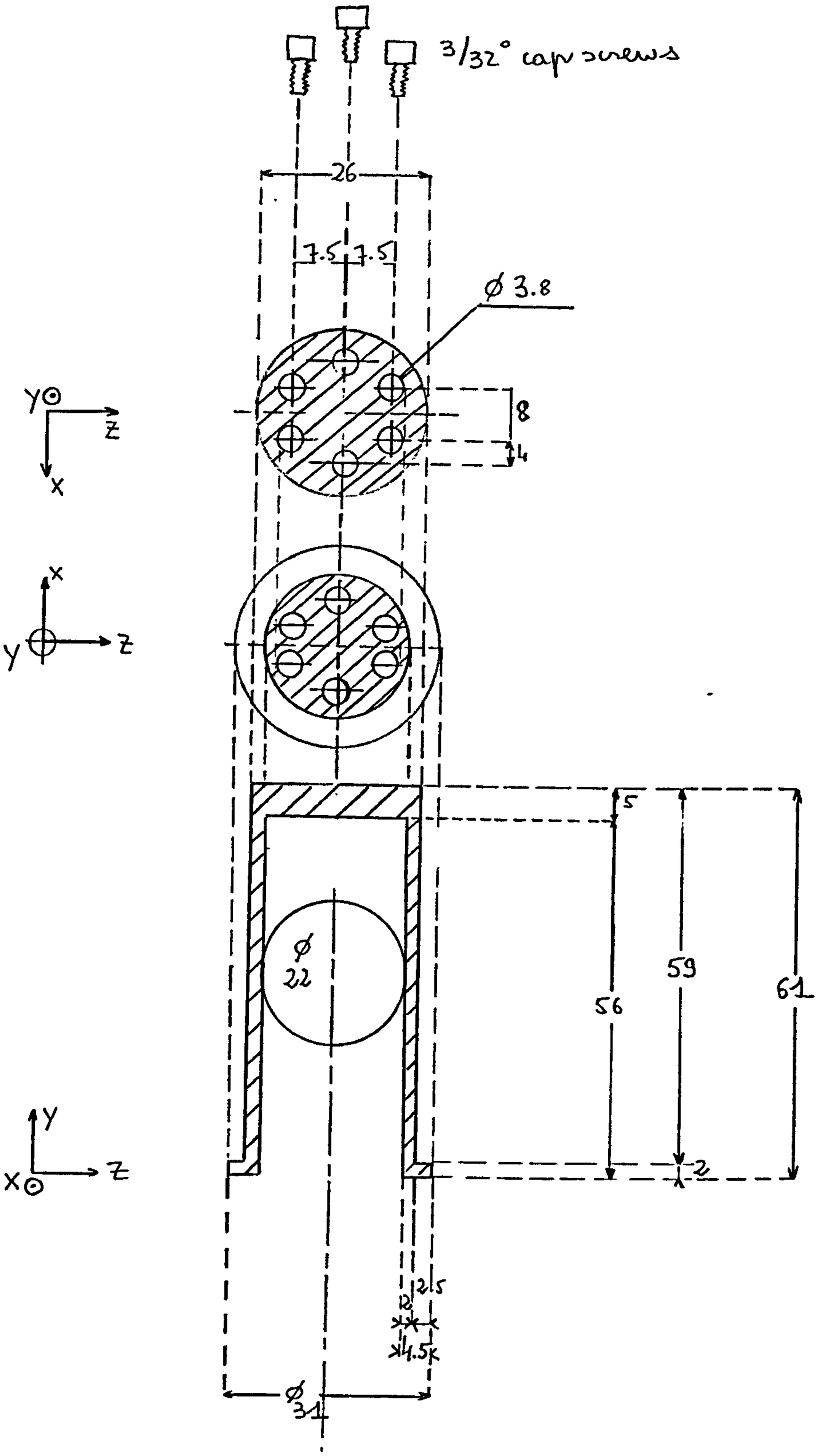

Figure 4.23: The aluminium bell (scale: full size)

commercially available ankle component. Two washers are separating the « T » from the prosthetic malleolus itself. They are used to reduce the friction of the components. The internal part of the « T » is covered with a thin layer of hard plastic foam (Teflon®) to decrease the friction coefficient between this part and the ankle axis itself. The lid of the hollow for the rear bumper is bolted on the aluminium base by the mean of two 6 x 6 mm cap screws.

The ankle axis coincides with the flat bottom part of the aluminium base.

This aluminium base was designed to be used with the mono axial foot most often used for the Villiers-Saint-Denis Rehabilitation Centre amputees. However, it will be easy to replace it, if necessary, if another artificial foot is brought into use.

4.8.2.4 THE SPECIAL RING TO CLAMP THE PROSTHETIC TUBE ON THE BELL

In day-to-day practice to test the greatest number of patients wearing their definitive prosthesis, it is not possible to split the prosthetic tube (see appendix 11.II). The tube is securely and strongly glued on the definitive socket, it is therefore impossible to remove it easily. Consequently, damaging the shank tube is unrealisable. It must go back to its previous state at the end of any gait assessment.

Thus, the problem was to clamp the circular prosthetic shank tube onto the circular bell, without any risk of damage to any of these elements. The tightening torque must be sufficiently high to avoid any sliding of the two parts relative to each other, especially due to the transverse torque. Fortunately, the value of the torque during the amputees' ambulation is lower than a maximum of 10 N m (see chapter 8) for the elderly, recent amputees tested in the Villiers-Saint-Denis Rehabilitation Centre.

Therefore, it was necessary to devise a special assembly. A newly designed ring was cut from the top part of a Proteor artificial ankle made of aluminium alloy, (see figures 3.1 and 4.26). The circular inner surface was filed down to be transformed into an oval-shape. The diameter of the intact part remained the same: 30 mm, which is the outer diameter of the prosthetic tube; while the diameter of the filed part was altered to become: 31.5 mm (arbitrarily chosen). When the ring is clamped, it distorts the prosthetic tube a little. This increases the clamping stress

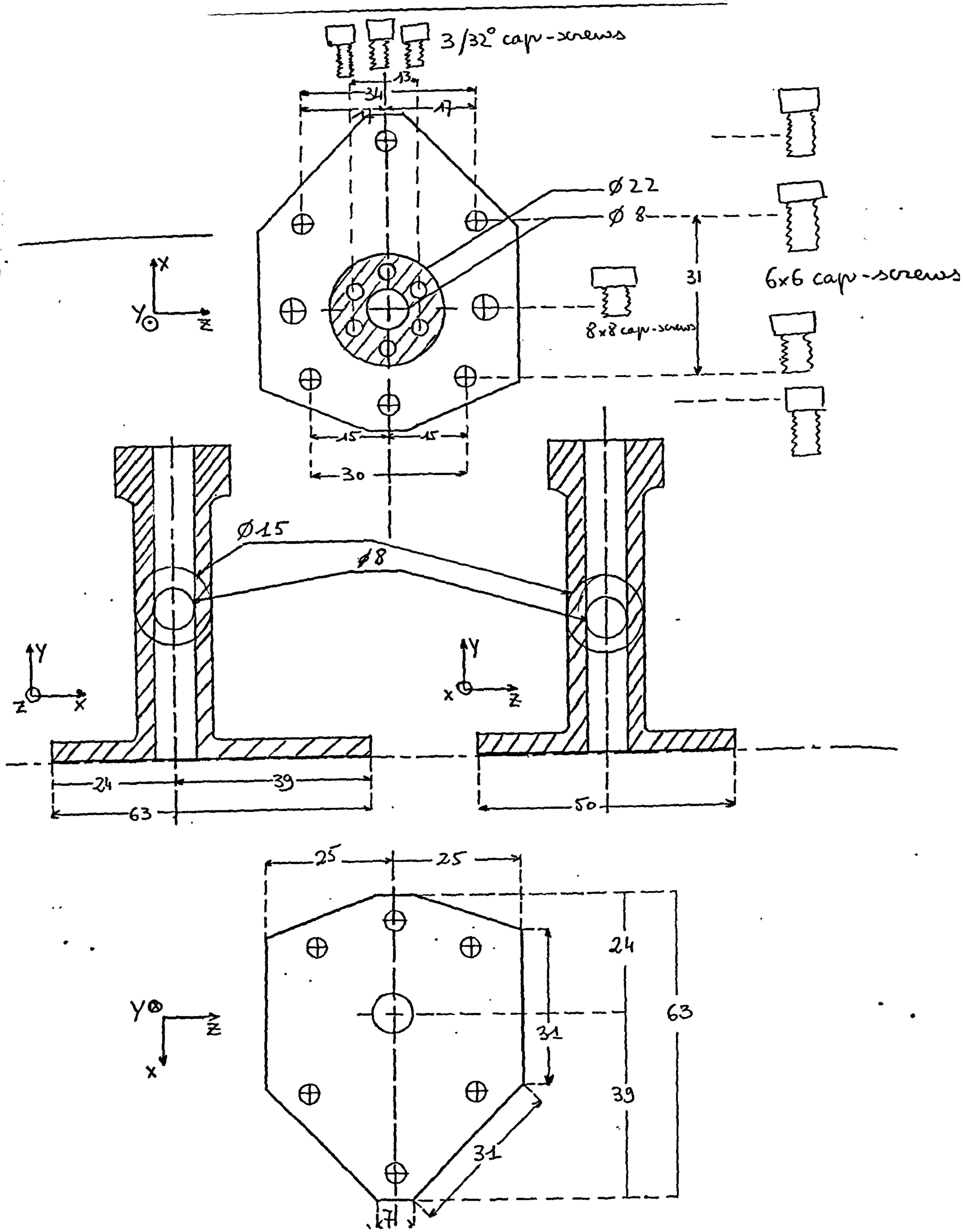

Figure 4.24: The body test of the transducer. The spindle was hollowed to improve axial from sensitivity for small increase in stress due to bending. (scale: full size)

between the two contact areas avoiding any tendency of sliding. When the test is finished, the ring is loosened and by its own elasticity, the prosthetic tube goes back to its previous shape. Therefore, it is possible to re-use it into the hole of the usual artificial ankle. A threaded metal rod, having a diameter of 6 mm, allows the ring to clasp the prosthetic tube onto the bell. To improve the binding strength and to ease the unscrewing of the nuts, a metallic collar, having a thickness of 5 mm, is used between the ring and one nut. The special ring was designed so that the clamping torsional strength is strong enough when the two brims of the ring become edge to edge.

To avoid any risk of randomised modification of the kinetic data due to the clamping of the prosthetic tube over the bell, the ring is always fitted in the same manner. The binding slot is fixed at the same place during each gait test: the slot is in the X axis direction with the metal screw, having the Z axis direction (see chapter 8). However, this grips the tube at an uncontrolled tightening torque which gives improved M/L bending moment Mx transmission although A/P bending moment Mz is greater (see chapter 9).

In summary, the new transducer has two main parts: an aluminium re-entrant cover, which is usually known as the « bell » and the transducer on which the strain gauges are bonded.

4.9 THE DESCRIPTION OF THE GAUGING

4.9.1 The choice of the gauges

Before choosing the gauges, some assumptions were made:

1. the new transducer has a circular gauging area similar to that of the Strathclyde Pylon Transducer (SPT) of Berme *et al.* (1975).

2. the expected findings are identical to those recorded by the SPT.

Consequently, the strain gauges should be similar to those fitted on the SPT. Moreover, the literature has provided, over a long period, strong recommendations about the strain gauge techniques (Murray & Stein, 1957). However, to corroborate

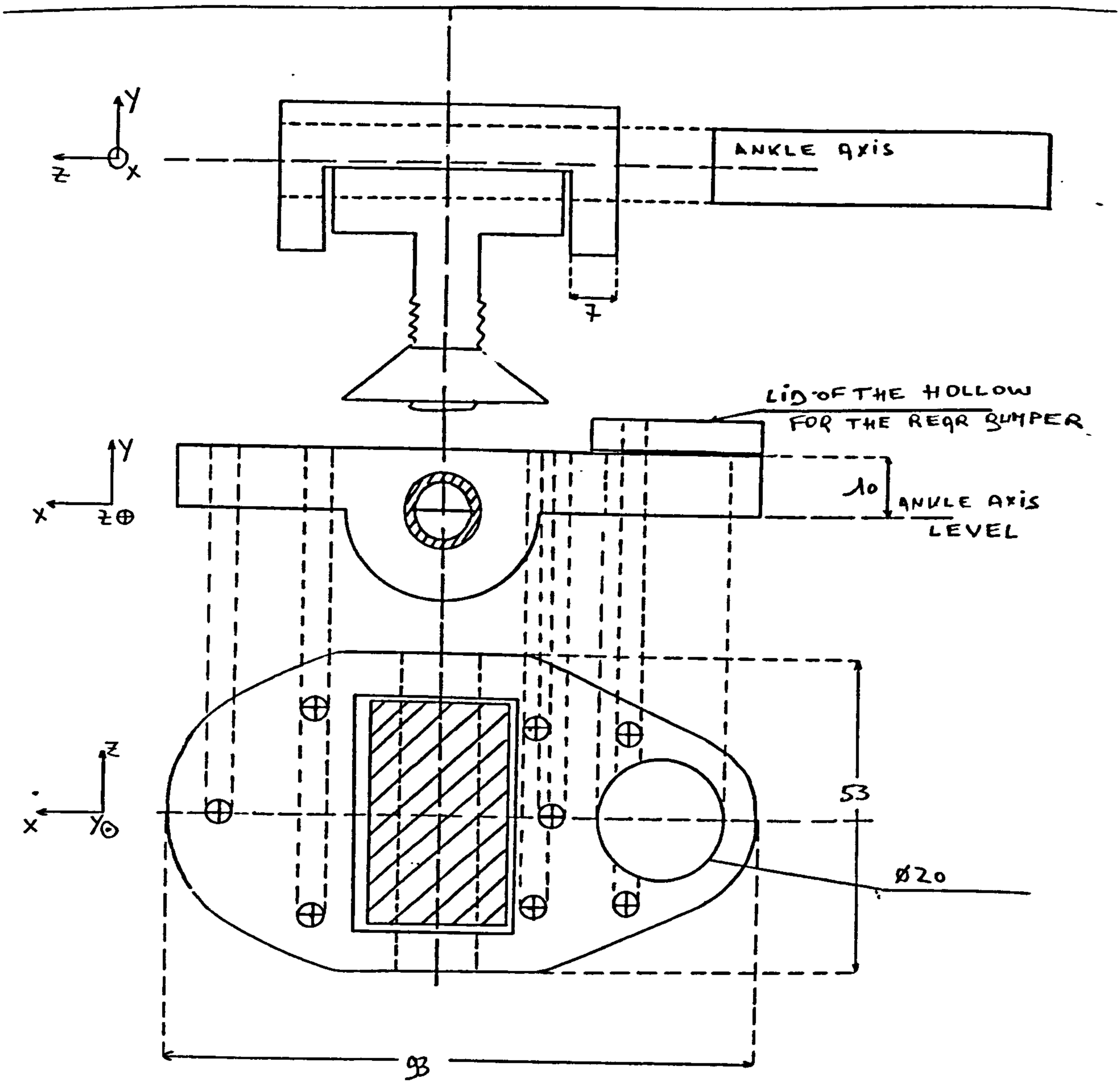

Figure 4.25: The aluminium base (scale: full size)

the decisions about the positioning and the wiring of the gauges, a qualitative analysis is an important prerequisite. Such an analysis is presented in sections 11.IV.4 and 11.IV.5.

Therefore, the chosen gauges were as follows:

• shear and torque: 2-Element 90° torque gauge, two for each channel, i.e., six gauges, each of them having an overall width of 2.92 mm. Hence, the total length is 17.52 mm.

• axial load: four general-purpose 90° « T » rosettes, having an overall width of 4.27 mm. Therefore, the total length is 17.08 mm.

• bending: dual pattern gauge used in back-to-back bending applications, two for each channel, that gives four gauges, each of them having an overall width of 3.81 mm. Consequently, the total length is 13.24 mm.

The gauges were compensated for stainless steel, although this was not necessary since the bridge circuits gave automatic temperature compensation. They were not encapsulated. The chosen resistance was 350 Ω. The high resistance allowed the strain gauge excitation level to be increased, as explained in detail in the following section. The full description of the gauges is given in table 4.8. The commercial supplier of the gauges is the Vishay Measurement Group.

Figure 4.27 shows the new Villiers Pylon Transducer (VPT) with gauges covered by a protecting coat of silicone rubber: 1 is transverse torque level (torque gauges are hidden), 2 is one of the axial gauges (at 330°), 3 is one of the shear gauges (at reference point, 0° corresponding to the X axis), 4 is one of the bending gauges (also, at reference point and badly shown).

4.9.2 The gauging

Hence, because of the decision made above, the total width of the gauges is 47.84 mm, over the available circumference (47.12 mm). So, it was impossible to arrange the gauging in a single line, although, this arrangement is claimed to be the best by Boenick *et al.* (1979) and Bray *et al.* (1990).

The gauge grouping designed by Berme *at al.*, (1975) for the SPT, i.e., two

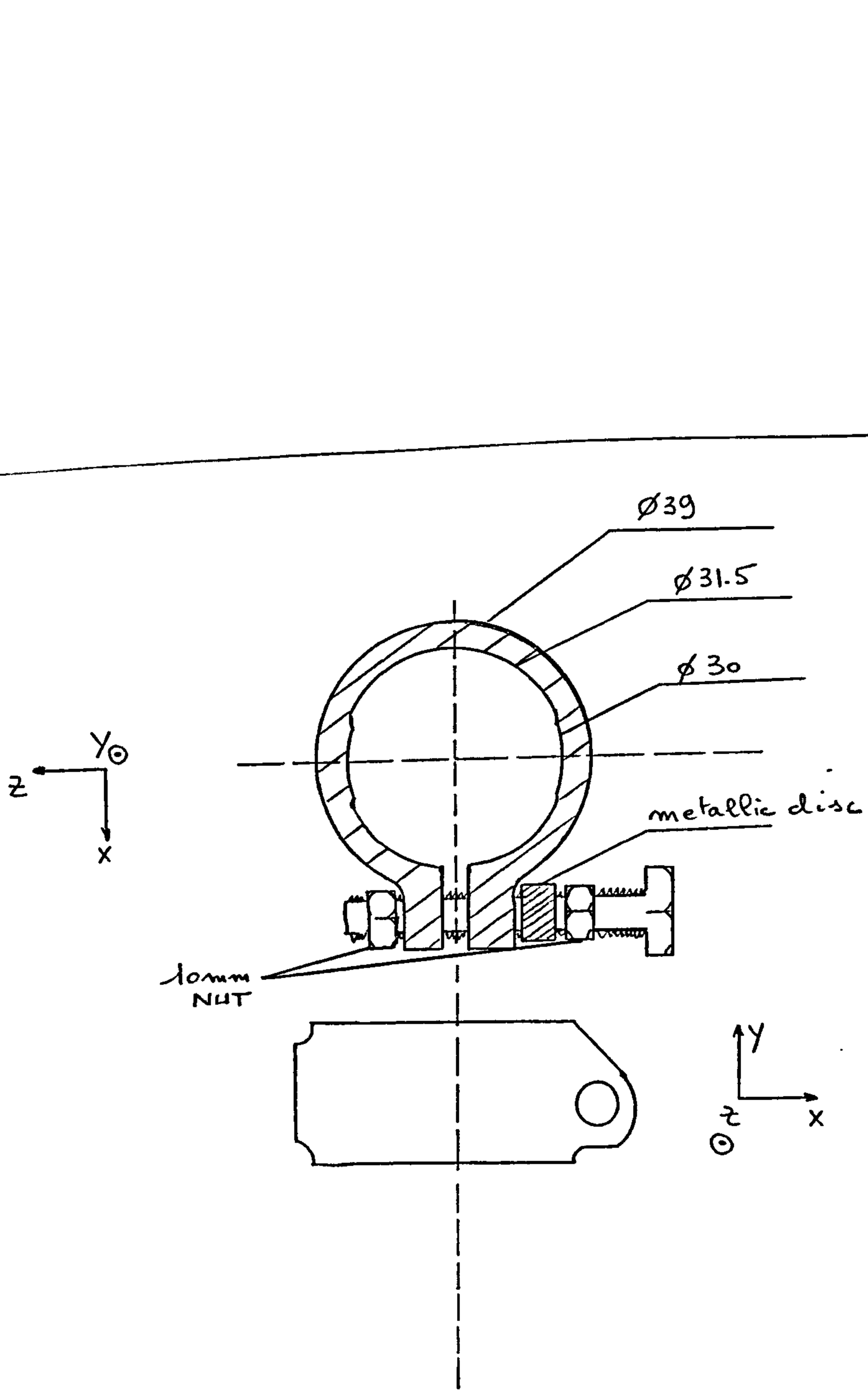

Figure 4.26: The specially made ring (scale: full size)

lines of strain gauges as shown in figure 2.10: one upper layer with, side by side, bending moments and axial load gauges ; the second with shear and torque gauges.

The thought process was: at the reference point 0°, which is the fore-and-aft direction (the X axis), there were two superposed gauges: one bending (3.81 mm) and one shear gauge (2.92 mm). These gauges being on both sides of the reference line, the maximum needed length was 3.81 / 2 = 1.9 mm. At 60° from the reference point, that is 47.12/6 = 7.85 mm, there were two superposed gauges: one axial load (4.27 mm) and one torque (2.92 mm). These gauges being on both sides of the 60° line, the maximum needed length was 4.27 / 2 = 2.13 mm. Hence, the maximum space needed for the gauges is 1.9 + 2.13 = 4.03 mm, which was less than the 7.85 mm available. Therefore, it was possible to put the strain gauges in two layers at 0° and 60°.

If the same approach was made for 60° axial load gauges and 90° bending moment gauges (47.12/12 = 3.92 mm), it was equally found 2.13 + 1.9 = 4.03 mm, which exceeded the 3.92 mm available. Therefore, it was not possible to gauge the sensor section of the new transducer in this way. Moreover, these estimations did not take account of the space needed by the wires, connections and terminals.

In conclusion, because of the shape and the available space around the sensor section of the new transducer, the gauging was performed in a single sector with four layers of full bridges.

For room reason and height available, there is an empty space of five millimetres maximum between the top of the sensor length of the new transducer and the upper level of gauges and five millimetres between the bottom flange of the new transducer and the lower layer of gauges.

Consequently, as a first approximation and recognising the limitations, the gauging area under study should be considered far enough from the ends of both the bottom and top flanges and therefore not subjected to any end-effects (see chapter 9).

Each layer is separated by a space having 3 mm (between the levels 2, 3 and 4) or 2.5 mm (between the level 1 and 2). The lay out of the new transducer, showing the central line at each level of gauges with the distance from the ankle axis, is given

	GAUGE DESIGNATION	Resistance in Ω	GAUGE LENGTH each section	OVERAL L LENGTH complete pattern	GRID WIDTH each section	OVERAL L WIDTH complete pattern
AXIAL LOAD	EA - 06 - 062TT - 350	350 ± 0.2 %	1.57	3.38	1.91	4.27
	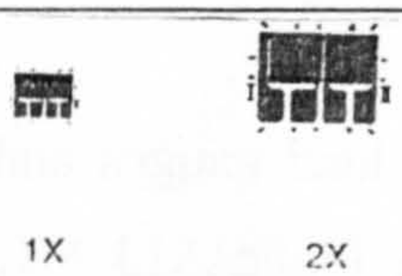 1X 2X					
BENDING MOMENTS	EA - 06 - 125PC - 350	350 ± 0.2 %	3.18	5.21	1.65	3.81
	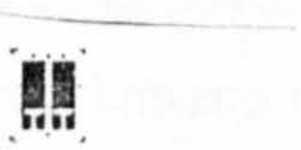					
SHEAR - TORQUE	EA - 06 - 062TV - 350	350 ± 0.2 %	1.57	4.45	1.40	2.92
	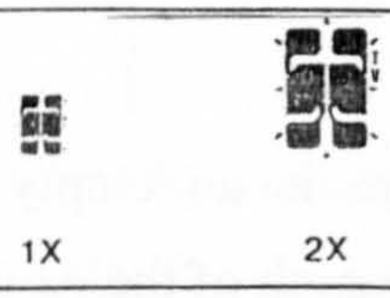 1X 2X					

Table 4.8: Strain gauge characteristics
(from Vishay Measurements Group Catalogue; p.29,30 and 43; all dimensions in millimetres)

in figure 4.28.

4.9.3 Description of the bridges

Each bridge is responsible for measuring one single component of the load acting upon the device (see section 3.4.5). The four layers of gauges are as close as the dimensions of the gauges permitted and the gauges are bonded using a heat curing epoxy adhesive.

When it was possible to definitively validate the full set up of the gauges, the wires and the whole connections, a protective coat, made of silicone rubber, was applied. It protects the gauges from any damage due to dust, water, contact or impact with other objects. It has also the advantage of being translucent and thus allowing inspection of gauges and wires for any checking needed.

The axial load is obtained using four 90-degree « T » 350 Ω rosette gauges equi-spaced around the periphery (60, 150, 240, 330 degrees). Therefore, each arm of the bridge has two serial gauges, that is each full bridge's arm consists of two resistance of 350 + 350 = 700 Ω. Hence, it will be feasible to double the bridge voltage to improve the sensitivity of this particular channel (see chapters 6 and 7).

The torque and shear loads are monitored using two 90-degree 350 Ω rosettes for each quantity, each aligned at 45° inclination from the longitudinal Y axis. Each full bridge consists of four resistances of 350 Ω.

The bending moments are monitored using two standard dual grid rosettes used in back-to-back bending applications for each quantity placed at 180° intervals around the periphery. Each full bridge consists of four resistances of 350 Ω. The gauges were fitted by a skilful technician, the tolerance on parallelism to transducer axis can thus be considered to be as small as possible but it was not controlled (see chapter 9).

4.9.4 The wiring of the full Wheatstone bridges

The wiring diagram of all strain gauges is shown in figure 4.29. V_o stands for the output voltage. The signal could be positive or negative. In the following pages, V_s stands for power supply or bridge excitation level.

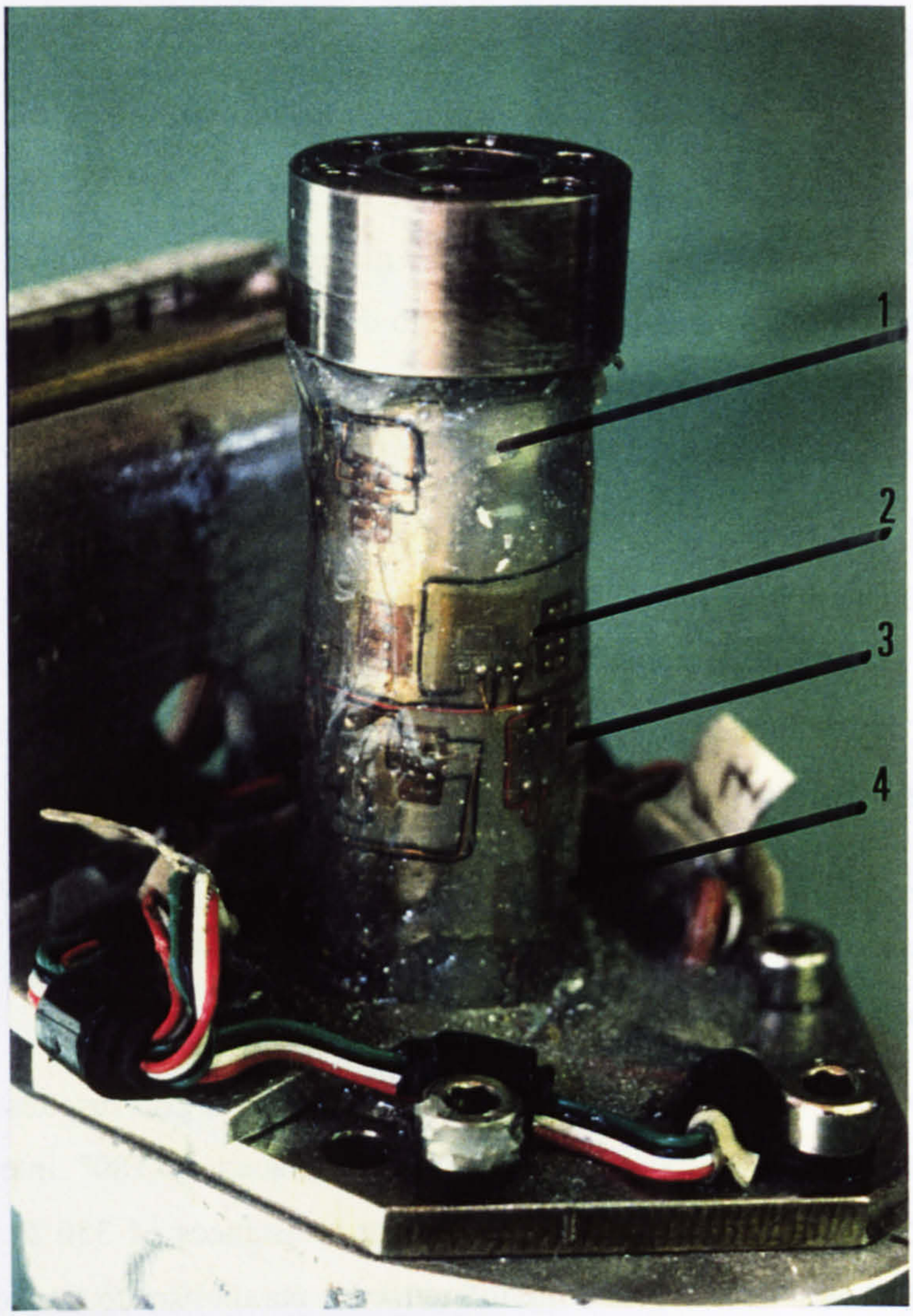

Figure 4.27: An antero-lateral view of the new Villiers Pylon Transducer.
The four levels are as follows:

1. transverse torque
2. axial load
3. shear
4. bending

The wiring diagram is essentially the same as the one used for the Strathclyde Pylon Transducer. Only for axial load Fy, it is different to a minor extent from the one used in the SPT as shown in figure 4.30. That was done to balance the resistance of the arm of the bridge. In fact, this wiring disposition introduces an asymmetric design in the bridge arms as shown in figure 4.31 that does not affect the Fy response but the interaction effect between the torque and the axial load increases. This consideration will be discussed in chapters 6 (calibration) and 7 (validation) of the Villiers Pylon Transducer.

Following the convention used by Berme *et al.* (1976), the full description of the wiring of all bridges is used:

conventional denomination	type of applied load
A	bending moment Mz
B	bending moment Mx
C	axial load Fy
D	frontal shear Fz
E	sagittal shear Fx
F	torque My

The final description of the strain gauges orientation, on the developed surface of the sensor section of the new transducer is shown in figure 4.32. The four levels of the strain gauges fitted on the gauging area are shown in the left part of figure 4.32. The orientation of each gauge and the respective direction of the grid are shown about the longitudinal Y axis in the central part of figure 4.32. The arrangement of the strain gauges, around the sensor section, about the transversal X and Z axes, is also shown in the right part of figure 4.32 (see appendix 11.IV.5 and 11.IV.6 for more details).

The bridge and pin connections with standardised wiring colours are shown in appendix 11.IV.7. A general view of the Villiers Pylon Transducer (VPT) is shown in figure 4.33.

To confirm the definitive locations of strain gauges onto the sensor section of the new VPT and to corroborate the taken decision about wiring, a theoretical qualitative and quantitative analysis of stresses and strains was an important

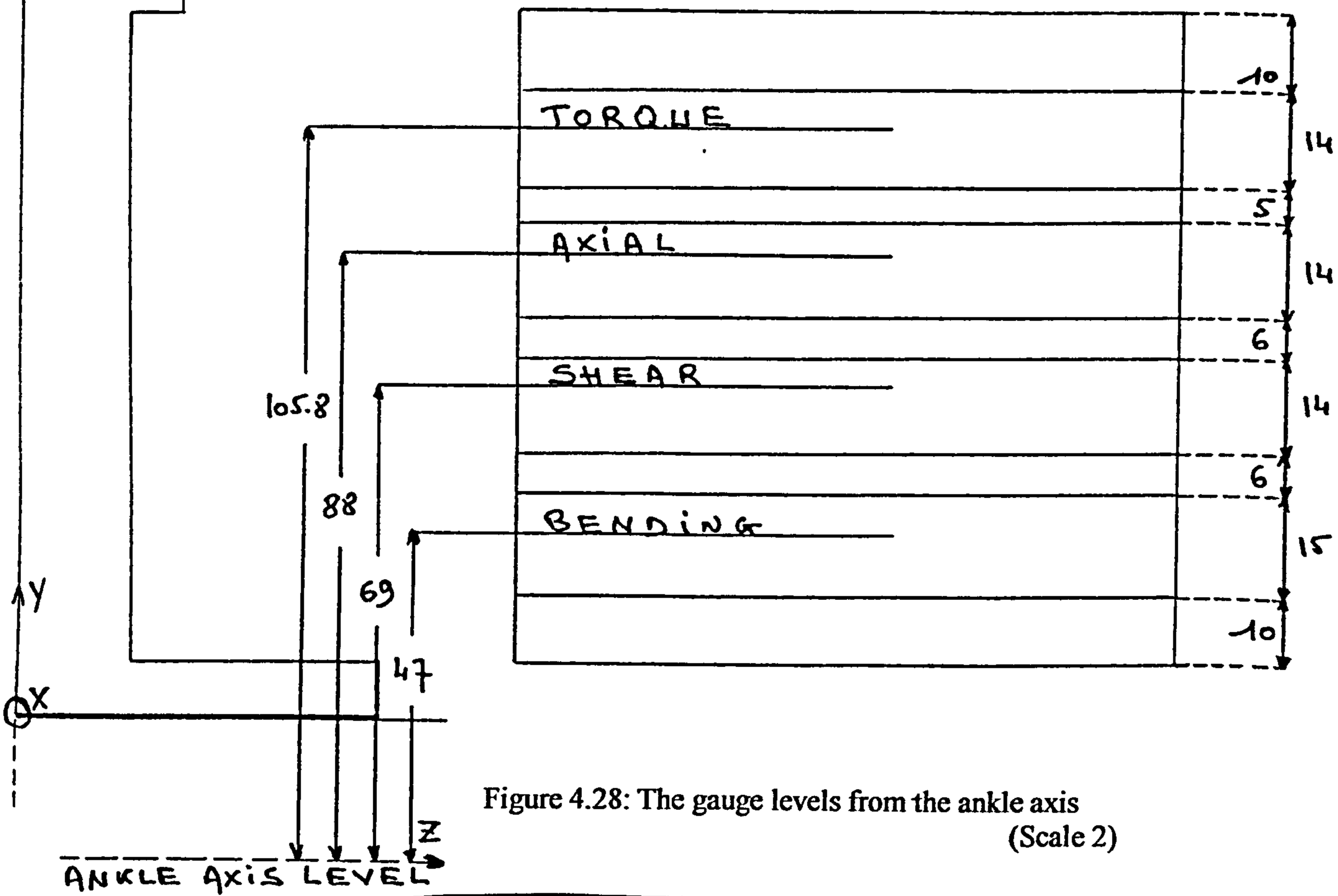

Figure 4.28: The gauge levels from the ankle axis
(Scale 2)

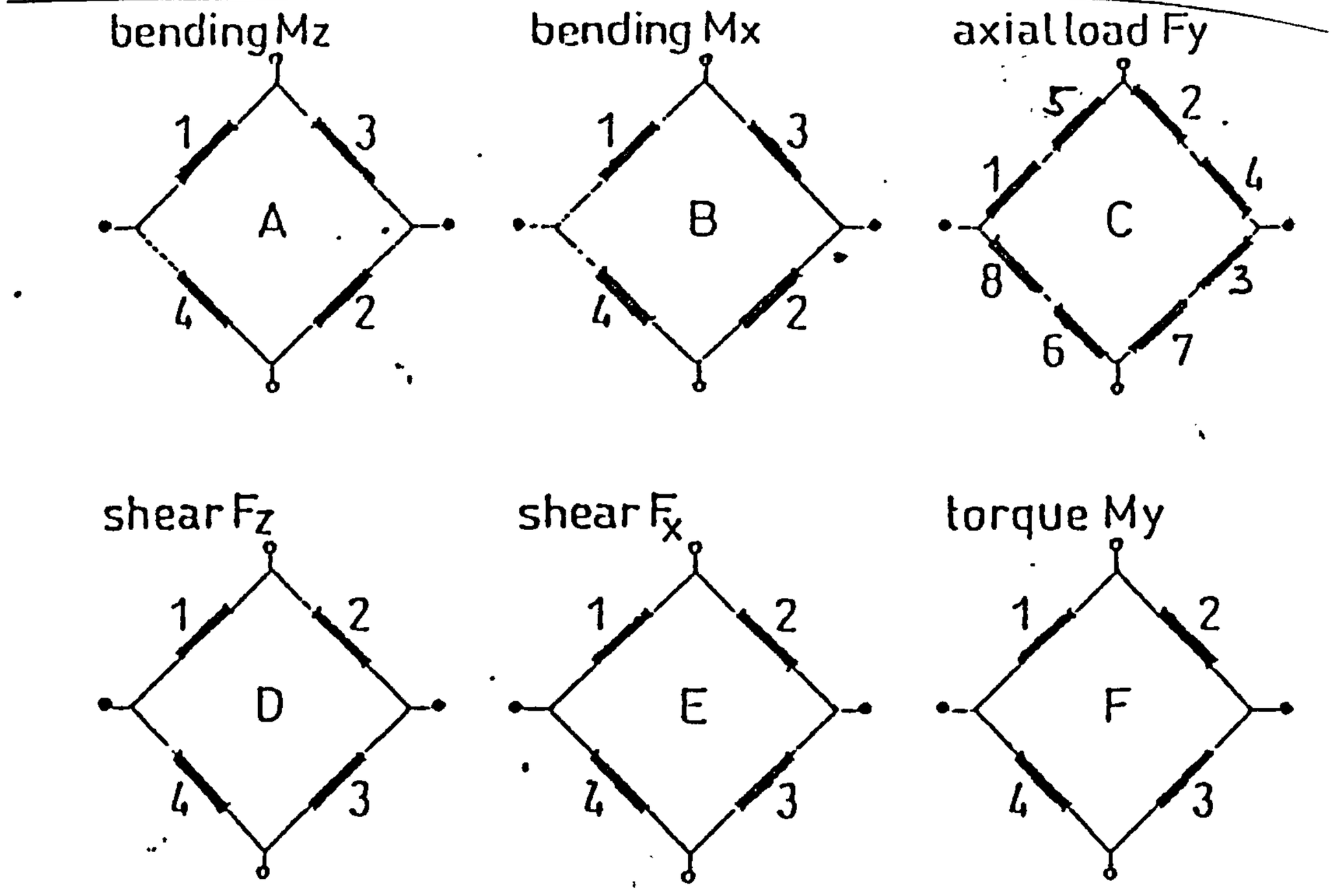

Figure 4.29: The wiring diagram of the six full bridges of the new VPT.

prerequisite.

The aim was to check and define the theoretical load-signal behaviour of the VPT to confirm the name of the different bridges and to assess the wiring diagram of each bridge gauge.

The target was to develop the logic of the strain responses, the calibration and the validation of the new transducer.

The ultimate target was to prove that the VPT could be considered to be equal to other transducers described in literature, especially the Strathclyde Pylon Transducer, despite:

- the design with the bell and the four layers of strain gauges,
- the small size of the gauging area,
- the non - symmetrical shape of the flat flange of the VPT.

In other words, the overall goal would be to assess the Villiers Pylon Transducer. This is done by stress and strain analysis using classical formulas, (Roark, 1954; Benham & Crawford, 1988). All these calculations are shown in appendices 11.IV.5 and 11.IV.6.

4.10 CONCLUSION

The work presented in this chapter was carried out in order

- to give a complete description of the new Villiers Pylon Transducer
- to describe all the bridges bonded on the surface of the new transducer and the gauges wiring
- to determine qualitatively and quantitatively the effects of various loading cases on the strain gauge bridges.

The system of gauging and bridge circuits were analysed and demonstrated theoretically to give signals from six channels uniquely related to the six load actions.

It was possible to demonstrate that a shear force (either Fx or Fz), an axial load

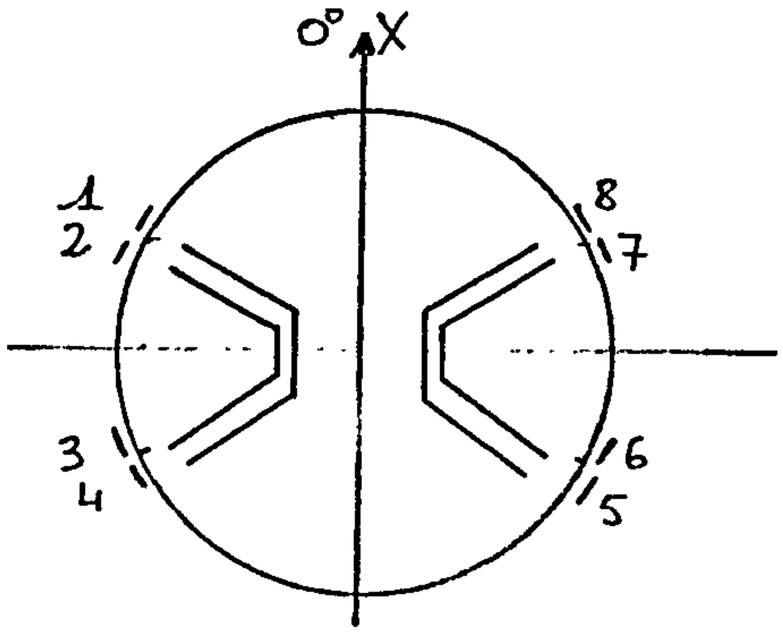

a) Strathclyde Pylon Transducer

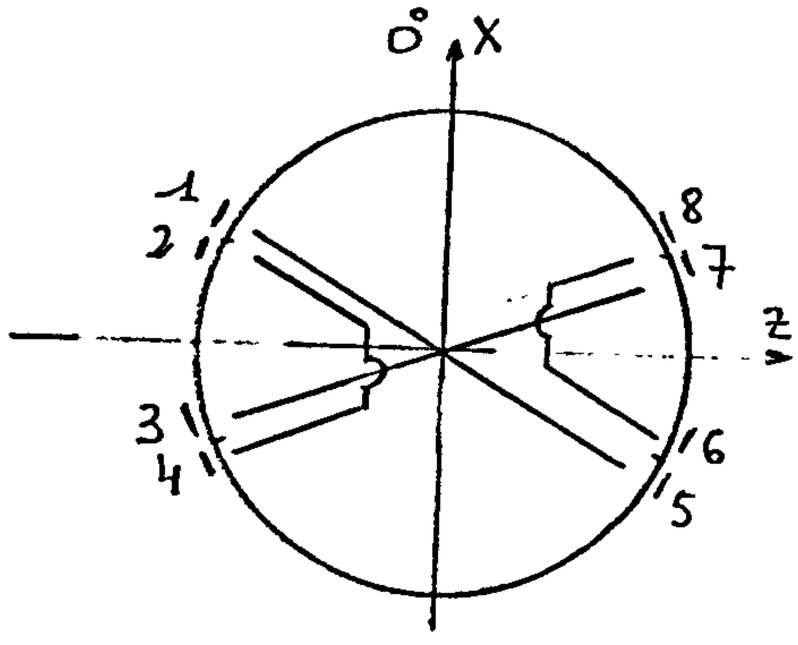

b) adopted wiring
for resistance reasons

Figure 4.30: Two possibilities of wiring the axial load bridge

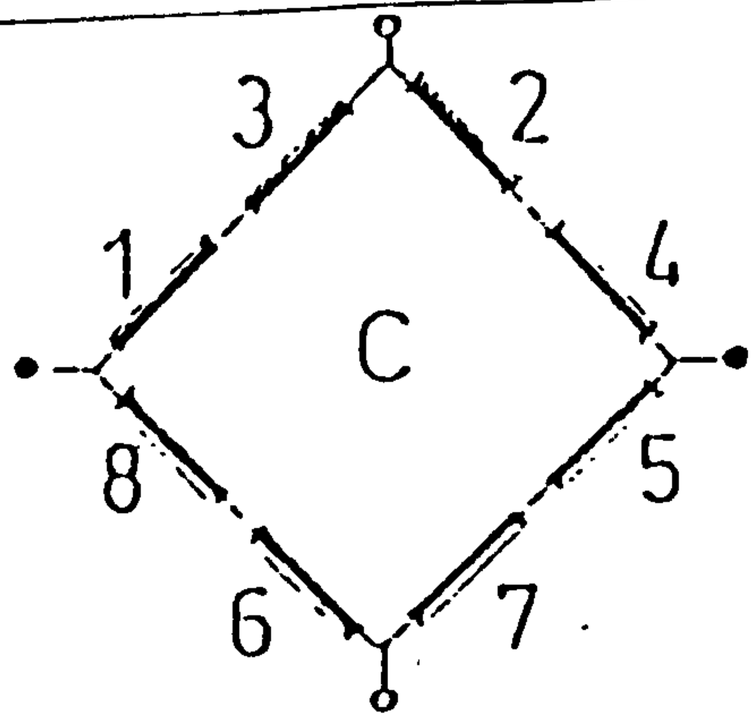

Axial load bridge
in the SPT
(Berme *et al.* 1975)

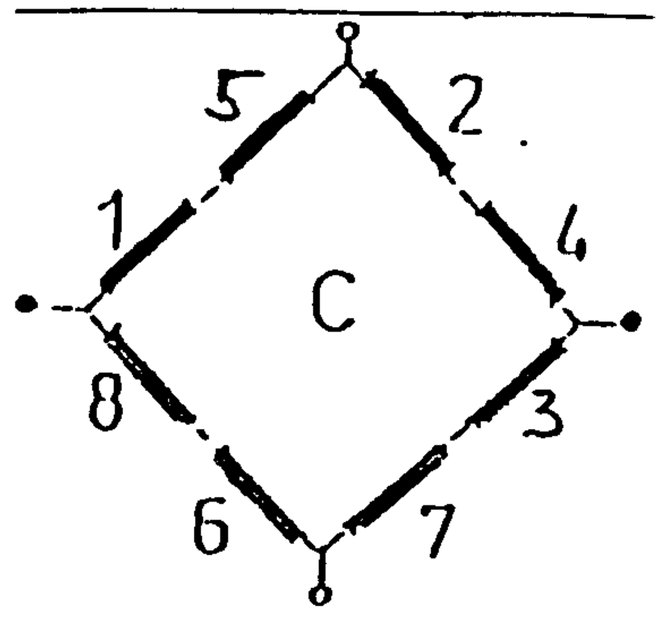

Axial load bridge
in the VPT

Figure 4.31: The Fy axial load bridge in the new VPT (horizontal plane)

Fy, a torque My and a bending moment (either Mx and Mz) are theoretically producing an output signal onto one and one bridge only, when applied individually. Thus, it was possible to give the name of individual loading cases at each bridge one by one.

The analysis depicts also that the new transducer has by-design (theoretically) no crossing interaction effects.

To use such a transducer, a full data acquisition system is needed. The following chapter will describe the two data acquisition systems used: the first with an umbilical cable and the second totally portable.

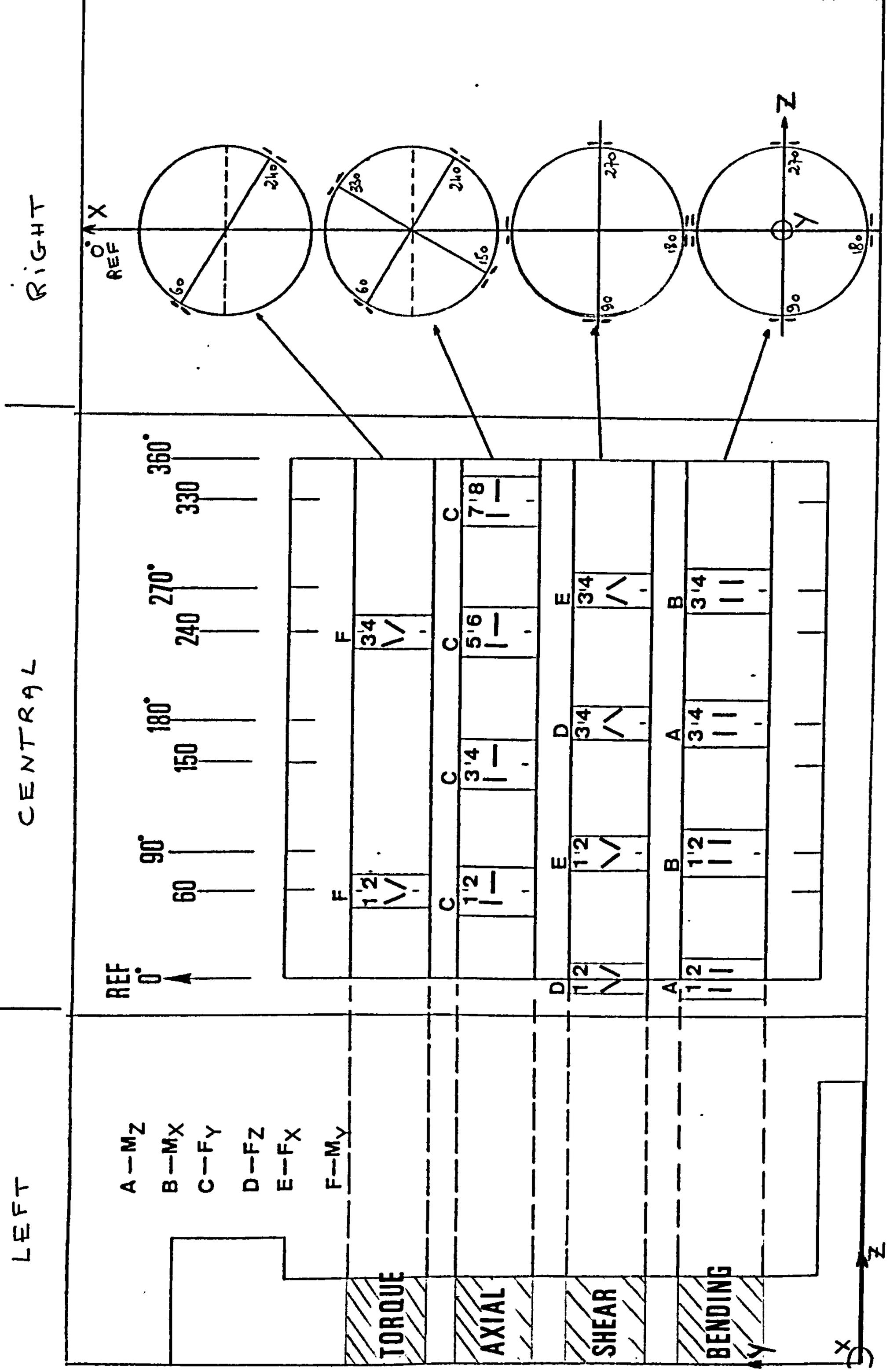

Figure 4.32: The gauges' orientation in two planes in cross-sectional and circumferential development views, (scale: 2).

5 DESCRIPTION OF THE EQUIPMENT USED

5.1 INTRODUCTION

To be able to use any transducer, a special data acquisition system is required. A broad description of such a system is invariably the same. There are two main parts:

1. a central unit which provides a power supply to the strain gauge bridges and an amplifier for the signals from the strain gauges. The power supply voltage is commonly 0 to 10 V while the amplifiers have generally gain settings from 50 to 3000. However, amplification can be undertaken using apreamplifier unit as close as possible to the strain gauge bridges and the output amplifier.

2. a storage and recording unit. For this purpose, two possibilities can be commonly found:

- To use directly, in real time, a computer having a specially designed program. In this case, the storage is through the RAM of the motherboard of the computer. Later, the recording is made on any floppy or hard disk. Obviously, the storage capacity and thus, the recording time (for a given sampling rate) depend of which range of computers is used and the software program. The advantage of such a system is not only its simplicity but also its accuracy due to both reliability of the RAM memory and computer device. The disadvantage is the need for a cumbersome cable between the amplifiers and the storage unit; except if expensive technology is used such as telemetry used by Boenick *et al.*, (1979).

- To use, first, a data storage unit and later, download the patient's test data to the computer. There are two main advantages in such a configuration, the storage capacity could theoretically be large, having the advantage of providing a long time period of recording (for a given sampling rate) and the storage unit could be portable. This recording technique has been developed in the Bioengineering Unit by Lovely (1981) and Pashalides (1989).

Figure 4.33: View of the new Villiers Pylon Transducer assembly with the bracket, socket and plug

Figure 5.1 shows the two approaches of data acquisition system in amputee gait assessment.

The different data acquisition systems successively used in this thesis had the two main arrangements with advantages and shortcomings of each of them.

5.2 THE FIRST DATA ACQUISITION SYSTEM

5.2.1 General description

The block diagram of the first data acquisition system used in this project is shown in figure 5.2

A brief survey has already been bestowed in section 3.5.2. It is essentially a complete central unit of eight identical electronic apparatus having two functions:

1. to provide an output voltage of ± 5 V as excitation level to the full bridges;

2. to amplify an input voltage coming from the strain gauge bridges, with a gain between 100 and 500.

The unit was supplied by a French company[11]. Six amplifiers were used for the six channels of the new Villiers Pylon Transducer (VPT), the last two amplifiers were devoted to the two instrumented walking aids (see section 5.4).

This central unit was linked to the VPT by means of a 25 way armoured long cable having a length of 25 metres which allowed the amputee under test to walk as freely as possible. This necessary and cumbersome cable had two main drawbacks: besides its bulk, it carried a very low voltage, output from the strain gauge bridges before any amplification. Therefore, the signal was susceptible to any electronic noise and artefacts, exhibiting a fluctuation in the calibration accuracy. This is why, when static tests were conducted to calibrate the new transducer, a short 25 way cable was used, being 2 metres long.

This central unit was connected to the host computer through an analogue -

---

[11]MI4, Micro-Ingénierie, 16, rue Francis Vovelle, 28000 Chartres, France.

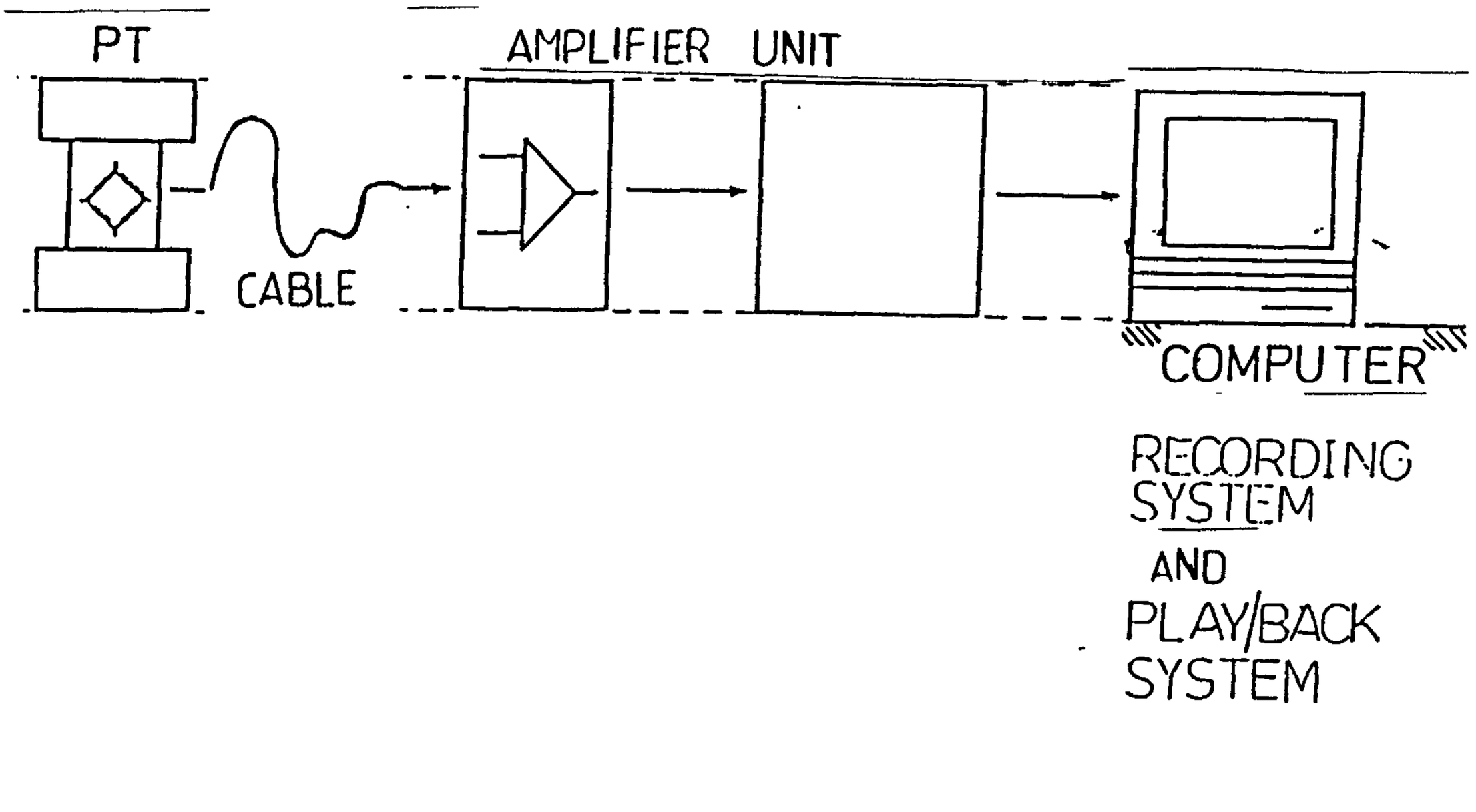

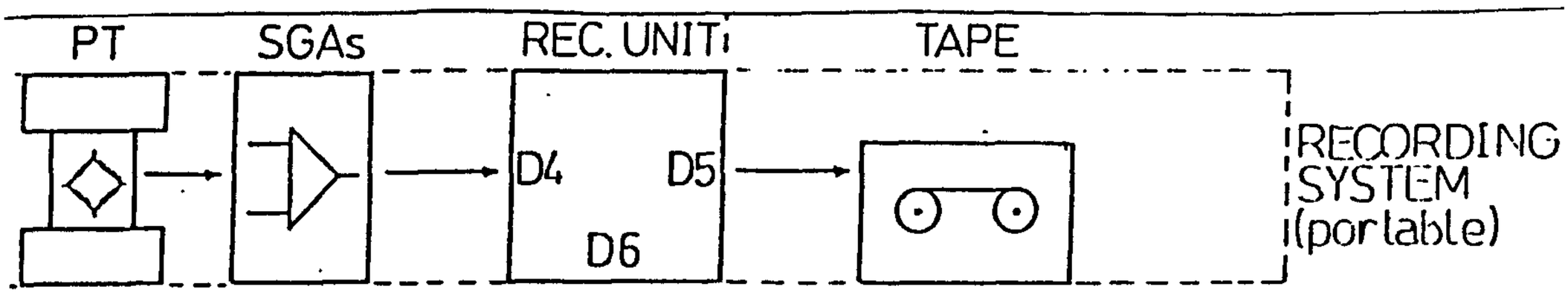

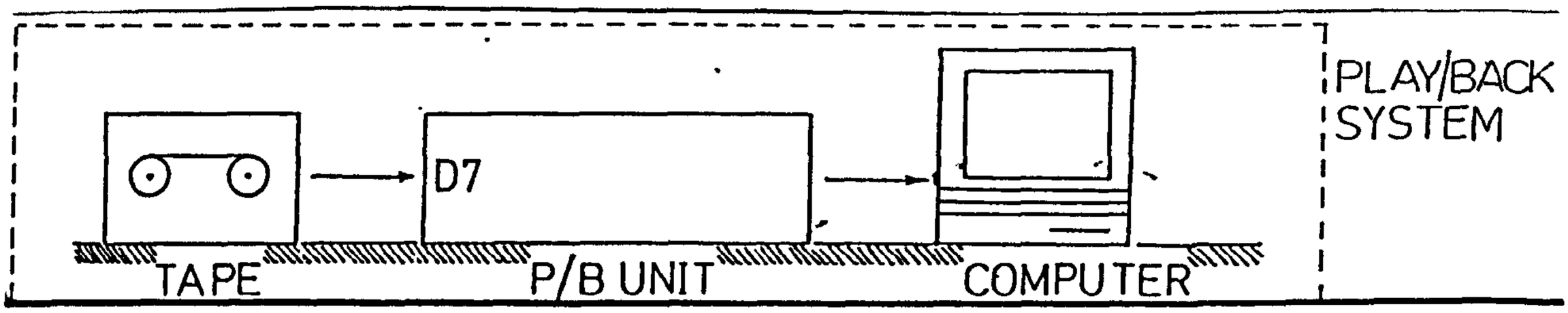

Figure 5.1: General description of two data acquisition systems widely used in the field of amputee gait analysis.

digital board Amplicon A/D board PC 26AT®[12], working at the high speed of 12 bits. The computer ran the program Acquire (Philips, 1990). All characteristics of the amplifiers are given in appendix 11.III.1, the A/D board in 11.III.2 and Acquire in section 3.5.2.2.

The main characteristic of Acquire is that the programme works only through positive computer units, e.g., from 0 to 4096. Thus, the middle range is approximately 2000 and this computer unit value was used as the zero level.

This full set of amplifiers and data acquisition system had two main advantages:

- its simplicity of using once the adjustments had been performed;
- its low cost, less than £200 per channel;

but two main disadvantages:

- as already stated, between the transducer and the amplifier box, there was a cable transmitting a very small voltage (from 0 to 500 mV). In a gait test, the patient must have enough space to walk. Thus, the cable used was 25 metres long, therefore, some loss of signal, increase of noise and accumulation of interference were inevitable. As previously stated, carrying the navel-like cable changes the gait behaviour of the patients and limits the size of the locomotion area.
- the Acquire programme had a stringent storage limitation which does not depend totally of the range of the applied computer: using six channels at the sampling frequency of 50 Hz, the maximum storage time was 109 seconds (81 seconds with 8 channels at 50 Hz), which is indeed too small and insufficient for the purpose of the research.

However, before buying the expensive data acquisition system described in section 5.3, a full range of tests were performed using this first system, having the target to verify and validate the reliability and accuracy of the new system. Moreover, these tests, conducted through this full set of amplifiers, had allowed the

---

[12]Amplicon Liveline Ltd, Centenary Industrial Estate, Hollingdean Road, Brighton BN2 4AW, Great Britain.

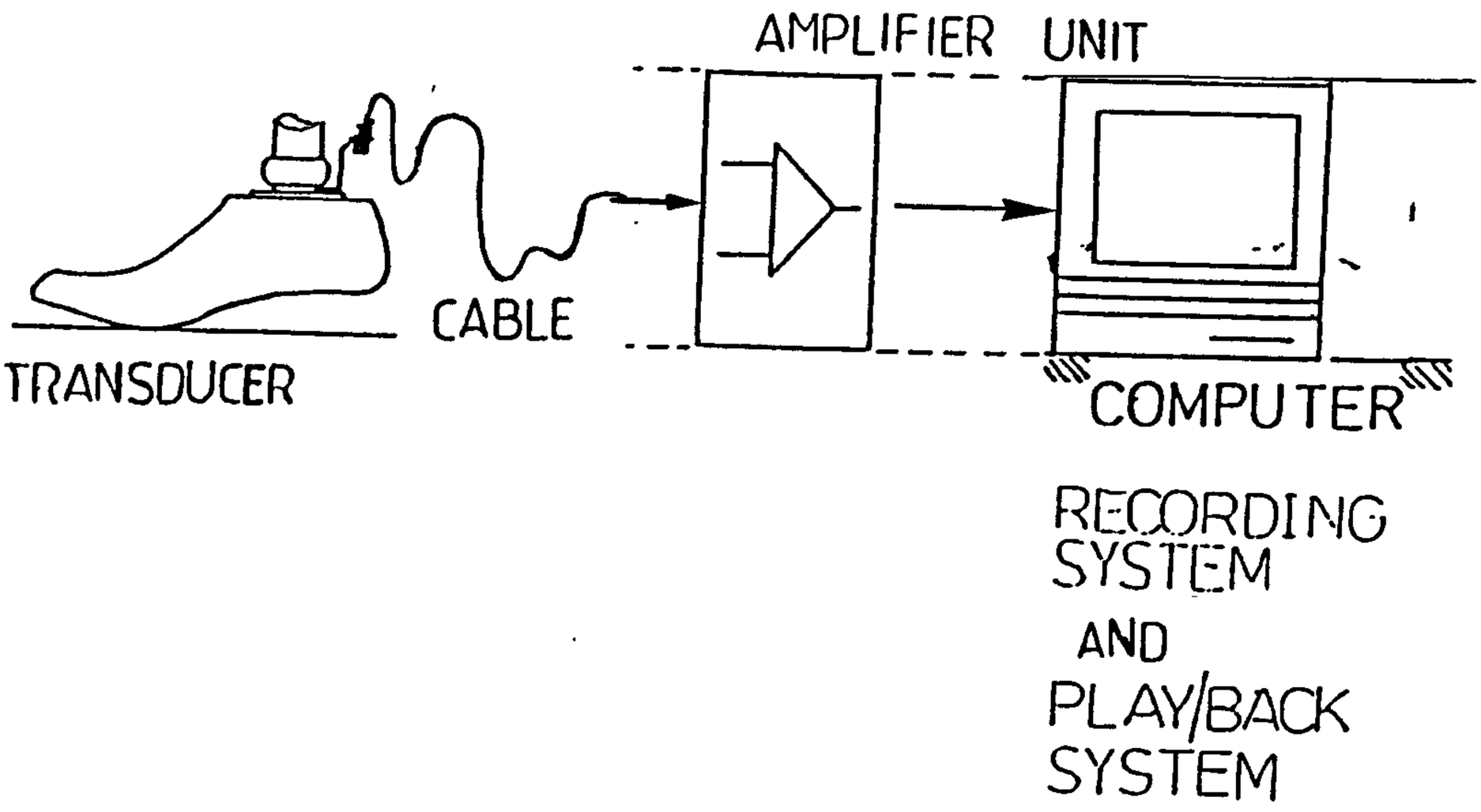

Figure 5.2: Description of the first data acquisition system.

calculation of the sensitivity of each channel. That was a mandatory procedure before the design of the needed signal-conditioning unit for the use of the definitive portable data acquisition system (see below section 5.3.2.1).

5.2.2 Adjustments of the new transducer

Two main adjustments had to be made before using the new transducer:

1. bridge excitation voltage levels
2. bridge balance to have an output of zero volt at the level of 2000 Acquire computer units.

5.2.2.1 THE CHOICE OF THE BRIDGE VOLTAGE

As stated in the previous section 5.5.1, a full bridge has to be supplied with an input voltage V_s, the choice of which is settled by the following considerations:

1. strain gauge grid area (gauge length x grid width)
2. gauge resistance
3. heat-sink properties of the mounting surface.

It is usual to say that the higher the bridge voltage, the better is the performance. However, it is important to realise that strain gauges are seldom damaged by excitation voltages considerably in excess of proper values. The usual result is performance degradation, rather than gauge failure and the problem therefore becomes one of meeting the total requirements of each particular installation.

Table 5.1 shows the grid area and the resistance of the chosen gauges previously described in table 4.8.

The supplier of the gauges provides a rough guide about optimising strain gauge excitation level with a separate plot for each main gauge resistance (Vishay Measurements Group, Tech Note, TN 502, 1979). It is shown in table 5.2. A meaningful statement must be made: even in gait assessment: the situation may be considered as static condition because of the very low frequency of any gait event as demonstrated by Antonsson & Mann (1985), especially with recent elderly amputees (commonly 38 step.min^{-1} = 0.63 Hz, see below the results of the conducted tests in

	GAUGE DESIGNATION	GRID AREA (mm^2)	GAUGE RESISTANCE (Ω)
AXIAL LOAD	EA - 06 062TT - 350	2.99	350
BENDING MOMENTS	EA – 06 125PC - 350	5.25	350
SHEAR & TORQUE	EA – 06 – 062TV - 350	2.20	350

Table 5.1: The chosen strain gauges with their grid area and resistance.

watts/in² *kilowatts/m²*

	Accuracy Requirements	EXCELLENT Heavy Aluminum or Copper Specimen	GOOD Thick Steel	FAIR Thin Stainless Steel or Titanium	POOR Filled Plastic such as Fiberglass/Epoxy	VERY POOR Unfilled Plastic such as Acrylic or Polystyrene
STATIC	High	2 — 5 *3.1 — 7.8*	1 — 2 *1.6 — 3.1*	0.5 — 1 *0.78 — 1.6*	0.1 — 0.2 *0.16 — 0.31*	0.01 — 0 02 *0.016 — 0.031*
STATIC	Moderate	5 — 10 *7.8 — 16*	2 — 5 *3.1 — 7.8*	1 — 2 *1.6 — 3.1*	0.2 — 0.5 *0.31 — 0.78*	0.02 — 0.05 *0.031 — 0.078*
STATIC	Low	10 — 20 *16 — 31*	5 — 10 *7.8 — 16*	2 — 5 *3.1 — 7.8*	0.5 — 1 *0.78 — 1.6*	0.05 — 0.1 *0.078 — 0.16*
DYNAMIC	High	5 — 10 *7.8 — 16*	5 — 10 *7.8 — 16*	2 — 5 *3.1 — 7.8*	0.5 — 1 *0.78 — 1.6*	0.01 — 0.05 *0.016 — 0.078*
DYNAMIC	Moderate	10 — 20 *16 — 31*	10 — 20 *16 — 31*	5 — 10 *7.8 — 16*	1 — 2 *1.6 — 3.1*	0.05 — 0.2 *0.078 — 0.31*
DYNAMIC	Low	20 — 50 *31 — 78*	20 — 50 *31 — 78*	10 — 20 *16 — 31*	2 — 5 *3.1 — 7.8*	0.2 — 0.5 *0.31 — 0.78*

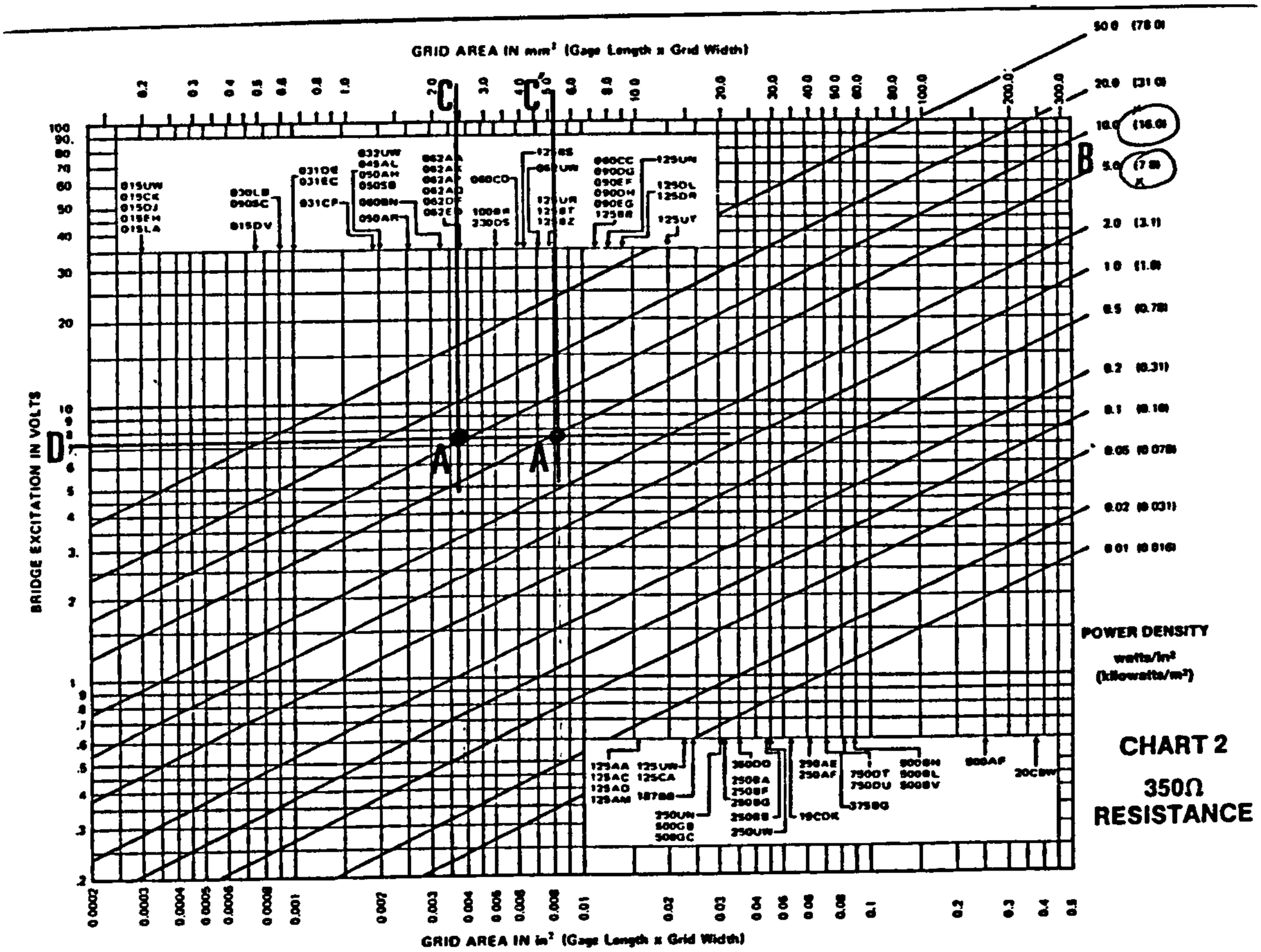

CHART 2

350Ω RESISTANCE

Table 5.2: Chart extracted from Vishay Measurement Group optimising strain gauge excitation levels (350 Ω resistance).

chapter 8). Hence, using the top part of the table 5.2, it is consequently easy to find the heat-sink conditions for a low accuracy (enough regarding our requirements) and for thick stainless steel in static condition: between 7.8 and 16 $kW.m^{-2}$ (line AB). Using the bottom double entry chart, having in mind that it should not be taken literally, it is thus elementary to find the best choice for the bridge voltage (grid area of 2.20 and 2.99 mm^2, line CA; grid area of 5.25 mm^2, line C'A; the axial load bridge is double, that is 700 Ω in each arm of the bridge): between 7 and 8 V (line AD; see figure 4.29).

Therefore, table 5.3 exhibits the bridge power supply used. It is important to note that, despite the difference in grid areas, the bending moment bridges and the shear - torque bridges had the same bridge excitation level. This was done for equilibrium reasons of the data acquisition system. This was also possible following the Vishay Technical Note TN 502, which gives a method for running performance tests for the experimental determination of maximum gauge excitation. Results showed that the normal bridge voltage on the tested strain gauges could be increased by 33 % without any adverse effects.

The adjustment of these bridge voltages was made by soldering some appropriate resistance between the two power supply wires: red (+ V_s) and black ($-V_s$) (see appendix 11.III.1).

5.2.2.2 THE CHOICE OF THE GAIN

The choice of the gain was made following the following assumptions:

⇒ the theoretical analysis, conducted in the previous chapter 4 (see section 4.6.3, table 4.3), showed that the expected responses had the same range per unit voltage and unit gain as those of the Strathclyde Pylon Transducer (SPT) designed by Berme *et al.* (1975).

⇒ the expected stresses applied on the VPT, on average, were of the same order as those of the SPT during different gait tests (Pashalides, 1989) and (Magnissalis, 1992).

⇒ the electrical study on the behaviour of the VPT performed by single use low cost strain gauges already demonstrated some useful results (see chapter 4).

	BRIDGE VOLTAGE (V)
AXIAL LOAD	10
BENDING MOMENTS	7.5
SHEAR & TORQUE	7.5

Table 5.3: The bridge voltage used

		GAIN SETTING
A/P SHEAR	Fx	400
AXIAL LOAD	Fy	1000
M/L SHEAR	Fz	400
M/L BENDING MOMENT	Mx	300
TORQUE	My	400
A/P BENDING MOMENT	Mz	100

Table 5.4: The six full bridges gain setting

	STRATHCLYDE PYLON TRANSDUCER designed by Berme *et al.* (1975) 120 Ω gauges		VILLIERS PYLON TRANSDUCER 350 Ω gauges	
	BRIDGE VOLTAGE V	GAIN SETTING	BRIDGE VOLTAGE V	GAIN SETTING
Fx	3	1000	7.5	400
Fy	6	2000	10	1000
Fz	3	1000	7.5	400
Mx	3	500	7.5	300
My	3	500	7.5	400
Mz	3	200	7.5	100

Table 5.5: Comparison between the SPT and the VPT. The system designation for co-ordinate axes from Berme *et al.*, (1975) have been adopted: the axes belong to the transducer and move with it (see section 2.6.3).

Therefore, the chosen gain settings are shown in table 5.4. Although the two transducers (SPT and VPT) had a similar application, the gains were not identical to those used in the SPT, but the design, the gauges and the bridge voltage were different as stated in table 5.5. The increase of the bridge power supply due to the higher strain gauge resistance allowed the gain setting to be decreased despite the lower expected level of sensitivity of the new transducer. This was especially important for the three forces. The decreased gain allowed the minimisation of drifting and electronic background noise.

Obviously, the possibility of eventually changing these gain settings was explored. Two possibilities could arise:

1. the full range of Acquire was not used, that is: not enough computer units to have a reliable accuracy in obtaining records

2. one response going over the capacity of the computer program, that is: one response came up (positive values) or down (negative values) beyond 2000 computer units.

However, all tests made later have confirmed that these gain settings were suitable.

5.2.2.3 THE BRIDGE BALANCE

It was stated above that the zero balance of all bridges was to be established at a level of 2000 computer units. Hence, it was mandatory to adjust the bridge equilibrium.

The amplifier box provides two ways for adjusting the bridge balance: a fine adjustment with a potentiometer (± 0.2 V) and a gross balance by means of a resistance soldered between two spikes (35 kΩ varied the zero by a value of 1 V). By making several attempts, it was possible to balance the six bridges (see appendix 11.III.1).

When tests are performed, it is usual to have slight drifting of the equilibrium point of each channel due to the heating of the bridges by the power supply. It was therefore necessary to adjust, between each test, the zero balance, this was done by means of the fine balance adjustment potentiometer.

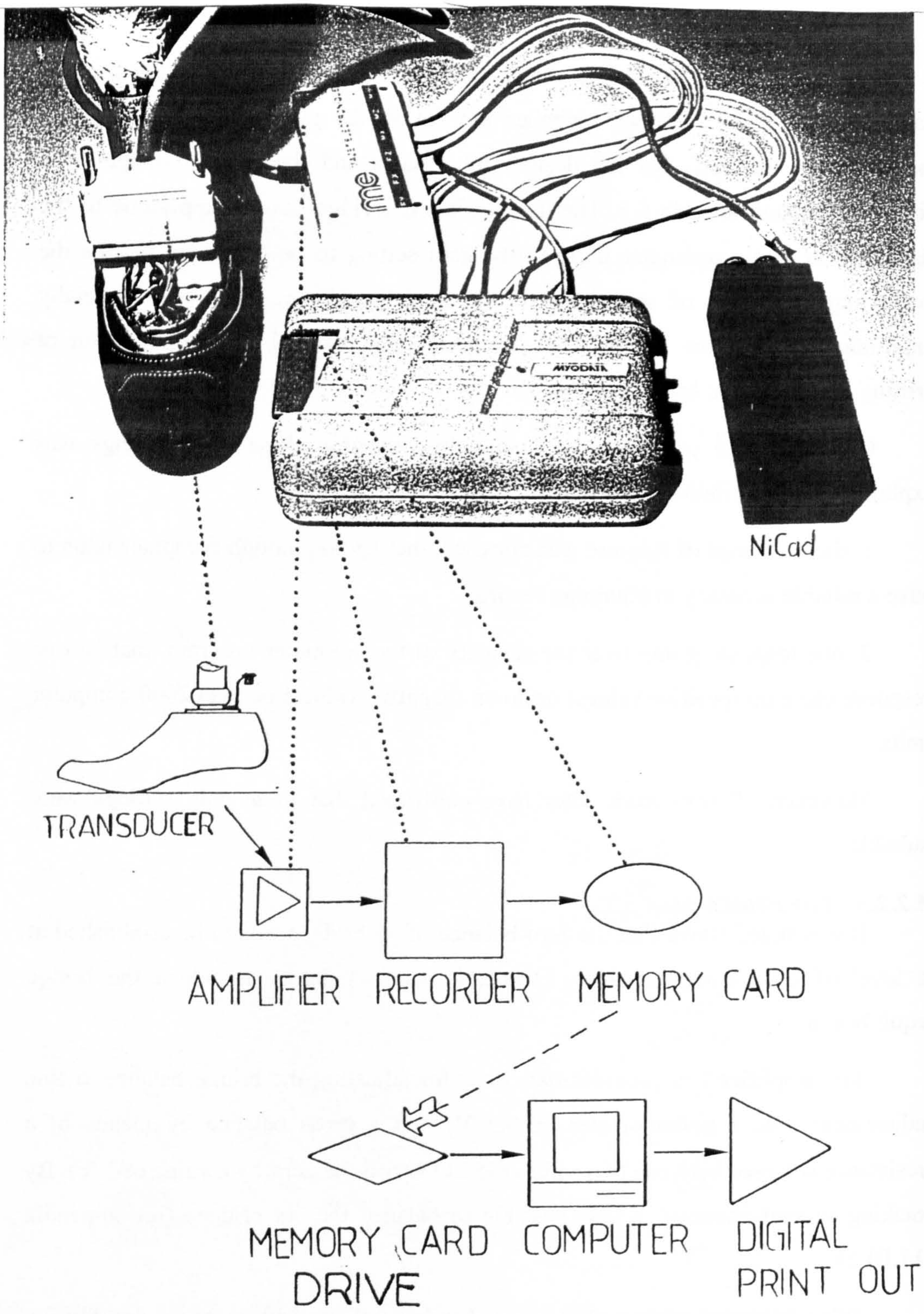

Figure 5.3: Block diagram of the data acquisition system: Myodata
solid arrow: physical connections by means of cables
dashed line: non-physical and time-shifted link
dotted lines: illustration of the portable data acquisition system

5.2.3 Using Acquire

This friendly computer software is working under DOS system. It can be used with a low range PC XT/AT and does not need any sophisticated device.

A numerical display is available and convenient to adjust one by one the fine balance of the six channels. An oscilloscope is also provided but simultaneously for four channels only. It is possible to choose the sampling frequency (from 0.001 Hz to 10000 Hz), but only two values were arbitrarily chosen (see section 5.3.2.3): 1 Hz in all static calibration tests and 50 Hz in all dynamic tests. Data are stored in numerical form and can be retrieved easily to be studied. It is possible to export data as ASCII files to use them in a usual spreadsheet such as Excel 4.0®.

5.2.4 Partial conclusion on the design of the first data acquisition system

The data acquisition system described above had enough advantages to be widely used in static tests. These tests were carried out to confirm the validity of the newly designed transducer.

Despite these usefulnesses, it was mentioned above the two main hindrances the system had. Therefore, efforts were made to find and use a fully portable data acquisition and recording system to allow the main purpose of the research to be conducted. Consequently, a new portable system is described in the following section.

5.3 THE DEFINITIVE PORTABLE DATA ACQUISITION SYSTEM

5.3.1 Introduction

As stated in chapter 1, the goal of the present work is to perform gait evaluation, produce a clinical and rehabilitation assessment tool, during the performance of daily activities of the amputees staying in a Rehabilitation Centre. This target needs not only the removable transducer described above but also a full portable data acquisition system. The chosen system belongs to the same class as the one described by Abu-Faraj *et al.*, 1997: a Holter-type, microprocessor - based,

VILLIERS PYLON TRANSDUCER
MYODATA AMPLIFIER BOX

INPUTS / OUTPUTS AMPLIFIER BOX

Channel n°1	**Fx**	pin n° 1	+ ve supply	red striped black
	A/P shear	pin n° 14	- ve supply	white striped blue
		pin n° 2	- ve signal	orange
		pin n° 15	+ ve signal	blue striped black
Channel n°2	**Fy**	pin n° 3	+ ve supply	white striped red
	axial load	pin n° 16	- ve supply	yellow striped blue
		pin n° 4	- ve signal	grey
		pin n° 17	+ ve signal	light blue
Channel n°3	**Fz**	pin n° 5	+ ve supply	yellow striped red
	M/L shear	pin n° 18	- ve supply	green
		pin n° 6	- ve signal	green striped brown
		pin n° 19	+ ve signal	red striped brown
Channel n°4	**Mx**	pin n° 7	+ ve supply	purple
	M/L moment	pin n° 20	- ve supply	pink
		pin n° 8	- ve signal	brown
		pin n° 21	+ ve signal	yellow
Channel n°5	**My**	pin n° 9	+ ve supply	white
	torque	pin n° 22	- ve supply	blue
		pin n° 10	- ve signal	black
		pin n° 23	+ ve signal	orange striped blue
Channel n°6	**Mz**	pin n° 11	+ ve supply	white striped green
	A/P moment	pin n° 24	- ve supply	yellow striped green
		pin n° 12	- ve signal	red striped blue
		pin n° 25	+ ve signal	red

Table 5.6: The pin connections of the 25-way input - output plug viewed from pins end

rehabilitation instrument for acquisition and storage of data.

Consequently, there were two possibilities:

1. using one of the portable data recording system available as the one designed by Pashalides (1989)

2. using a portable data recording system, commercially available

The first likelihood was not conceivable for several reasons such as:

- the impossibility of borrowing the device from the Bioengineering Unit over the long period of time
- the difficulty of fitting the system to the new transducer
- the non - 100 % - reliability of the recorder as already stated in chapter 2
- the old - fashioned storage system through a analogue tape recorder.

Therefore, the second possibility had to be considered.

5.3.2 The portable recording and data acquisition unit: Myodata

This is a commercial full system designed and supplied by a French company[13] and designed by a person with a Doctorate in Bioengineering (Ferrand, 1990).

It is built around a Motorola® MC 68000 processor and developed for EMG. It is multi-purpose, sufficient for use in the kinetic field for amputee gait study.

The general layout of the system is as follows:

Signals from the transducer level are conditioned by means of a small and lightweight six-channel signal-conditioning unit and then transmitted to a multiplexing and data storage unit housed within a belt pack. Power for the transducer, amplifiers, A/D board, processor and data storage is provided by a NiCad battery, also housed within the belt pack unit.

Figure 5.3 shows the block diagram of the Myodata system. The solid arrows show the cable connections while the dashed arrow indicates a non- - physical and

---

[13] Electronique du Mazet, route de Tence, 43520 Le Mazet-Saint-Voy, France

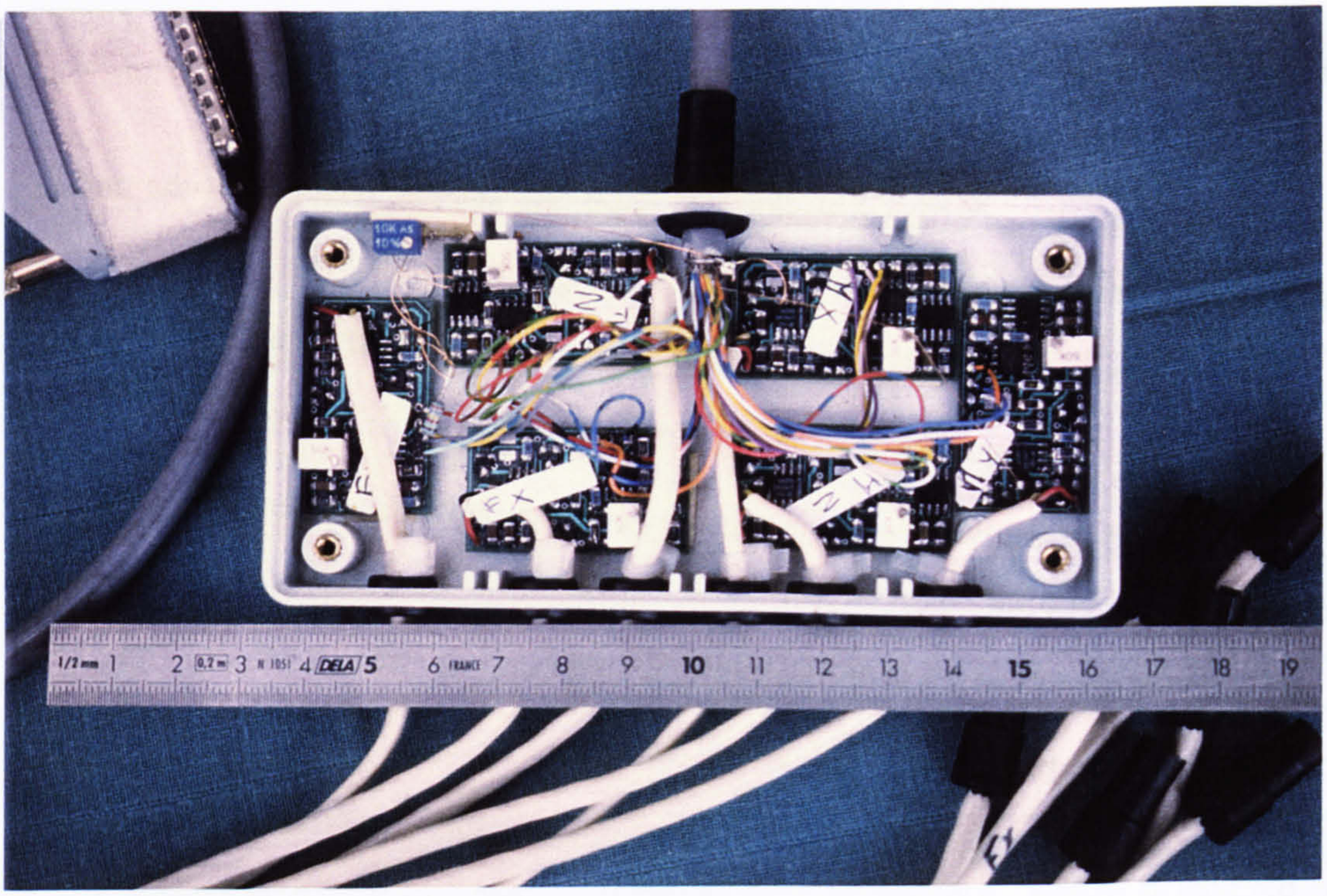

Figure 5.4: View of the internal components of the conditioning - signal unit.

	Sensitivity $mV * N^{-1}$ gain 1
SFx	$0.971 * 10^{-3}$
SFy	$0.432 * 10^{-3}$
SFz	$0.924 * 10^{-3}$
	$mV * (N.m)^{-1}$ gain 1
SMx	$175.33 * 10^{-3}$
SMy	$242.2 * 10^{-3}$
SMz	$172.82 * 10^{-3}$

Table 5.7: Channel sensitivities

		Range of measurement
A/P Shear Force	Fx	±100 N
Axial load	Fy	1500 N
M/L Shear Force	Fz	± 50 N
M/L Bending Moment	Mx	± 100 N.m
Transverse Torque	My	± 25 N.m
A/P Bending Moment	Mz	± 150 N.m

Table 5.8: Channel range of measurement extracted from ISPO, 1978.

time - shifted link between the memory card and its drive. The dotted lines display the name and the rank of each component into the portable data acquisition system.

5.3.2.1 THE SIGNAL CONDITIONING UNIT

As previously mentioned, a specific, small and lightweight six-channel signal-conditioning unit (looking like a preamplifier box) had to be built to harmonise the portable recorder with the new transducer.

The signal unit was a 13 cm x 6.5 cm x 2.5 cm box housing electronics for conditioning data from six channels. The mass with cables and sockets was 0.272 kg. The unit was designed to be connected to the six full Wheatstone bridge circuits of the new transducer. A 25-way plug connected the signal unit to the 25 sockets of the new VPT as shown in table 5.6. The unique 25 wires screened cable between the plug and the signal unit was 0.9 m long allowing the box to be worn in the patient's pocket. From the signal-unit to the recorder, there were six cables, one for each channel, having a length of 0.5 m and finishing by a four pin Binder plug.

Bridge balancing and amplification were performed by low-power surface mount solid state electronic circuitry on boards housed in the unit as illustrated in figure 5.4.

The mechanical housing of the signal-conditioning unit was designed to be lightweight and rigid but could be easily disassembled for access to the boards and to the potentiometers to balance the bridges. Only, the axial load Fy potentiometer was accessible through a hole in the plastic housing. This was done because this particular channel must have its offset regularly adjusted, presumably due to the high gain setting.

5.3.2.1.1 The choice of the bridge voltage

When it was time to design an amplifier box, the first step was to choose the bridge power supply. Because the same strain gauges full bridges as above were used, the same choice seemed evident. However, the Myodata was not able to provide a bridge voltage of 10 volts. The maximum was 8 volts. Thus, the accepted bridge voltages are shown in table 5.9.

		Bridge Voltage (V)
A/P Shear Force	Fx	7.46
Axial Load	Fy	8.04
M/L Shear Force	Fz	7.56
M/L Bending Moment	Mx	7.55
Transverse Torque	My	7.53
A/P Bending Moment	Mz	7.55

Table 5.9: The bridge voltages adopted in the portable data acquisition system.

		Channel Sensitivity in VN^{-1} or $VN.m^{-1}$	Transducer o/p signal in VV^{-1}	Bridge Voltage in V	Theoretical Amplifier Gain in VV^{-1}
A/P Shear Force	Fx	$0.971\ 10^{-6}$	$26.03\ 10^{-6}$	7.46	15 443
Axial load	Fy	$0.432\ 10^{-6}$	$81\ 10^{-6}$	8.04	4 629
M/L Shear Force	Fz	$0.924\ 10^{-6}$	$12.22\ 10^{-6}$	7.56	32 467
M/L Bending Moment	Mx	$175.33\ 10^{-6}$	$2\ 322\ 10^{-6}$	7.55	171
Transverse Torque	My	$242\ .2\ 10^{-6}$	$804.11\ 10^{-6}$	7.53	495
A/P Bending Moment	Mz	$172.82\ 10^{-6}$	$6\ 867\ 10^{-6}$	7.55	58

Table 5.10: Theoretical characteristics of the conditioning-signal unit. Here also, the system designation for co-ordinate axes from Berme *et al.*, (1975) have been adopted: the axes belong to the transducer and move with it (see section 2.6.3).

5.3.2.1.2 The choice of the gain

The second step and the main problem to solve are the selection of the gain. The gain of each channel had to be chosen following two contradictory requirements:

1. within the range of measures of any particular channel, the measured signal must take place within the full available scale; ***this supposes a high gain.***

2. despite the quality improvement of electronic components, the gain must not be too high, having the intent to minimise any drifting or background noise; ***this supposes a low gain.***

The maximum was usually 2000 as shown above in table 5.5, however, the actual quality improvement of electronic components allowed, in our days, to increase the gain setting up to 4000.

To calculate a particular gain, the first point was to establish the corresponding raw channel sensitivity, having the following units: $mV*N^{-1}$, gain 1 or $mV*(N\ m)^{-1}$, gain 1. For the new VPT, that was determined after the calibration made with the data acquisition system no 1, as shown in table 5.7 with « S » stood for Sensitivity (for more details, see calibration chapter 6). Knowing the channel sensitivity in $V*N^{-1}$ or $V*(N\ m)^{-1}$, the following method, in two steps, had been adopted to evaluate the amplifier gain:

- step 1: calculation of the transducer o/p signal using the following formula:

$$\frac{\text{Transducer o/p signal V}}{\text{Bridge Voltage}}\left[VV^{-1}\right]=\frac{\text{Channel sensitivity}\left[VN^{-1}\right]}{\text{Bridge voltage}\left[V\right]}*\text{Range of measure}\left[N\right] \tag{5.1}$$

- step 2: calculation of the amplifier gain using the following formula:

$$\text{Amplifier gain}\left[VV^{-1}\right]=\frac{\text{Recorder maximum input voltage}\left[V\right]}{\text{Transducer o/p signal}\left[V\right]} \tag{5.2}$$

The recorder had a maximum input voltage of 3 Volts and the maximum bridge voltage was 8 V (about recorder characteristics, see the following section 5.3.2.2).

Fx

TRANSDUCER CHARACTERISTICS

	Value	Units
Channel Sensitivity	$9.72\ 10^{-6}$	VN^{-1}
Transducer o/p Signal	$260.6\ 10^{-6}$	VV^{-1}
Range of measures	200	N
Bridge resistance	350	Ω

AMPLIFIER CHARACTERISTICS

	Value	Units
Amplifier Gain	1546	VV^{-1}
Interface Accrual	$11.53\ 10^{3}$	V
Bridge Voltage	7.46	V
Amplifier Sensitivity	$1.502\ 10^{-2}$	VN^{-1}
Amplifier consumption	2	mA

Fy

TRANSDUCER CHARACTERISTICS

	Value	Units
Channel Sensitivity	$0.997\ 10^{-6}$	VN^{-1}
Transducer o/p Signal	$186.1\ 10^{-6}$	VV^{-1}
Range of measures	1500	N
Bridge impedance	700	Ω

AMPLIFIER CHARACTERISTICS

	Value	Units
Amplifier Gain	2005	VV^{-1}
Interface Accrual	$16.12\ 10^{3}$	V
Bridge Voltage	8.04	V
Amplifier Sensitivity	$0.199\ 10^{-2}$	VN^{-1}
Amplifier consumption	2	mA

Fz

TRANSDUCER CHARACTERISTICS

	Value	Units
Channel Sensitivity	$9.33\ 10^{-6}$	VN^{-1}
Transducer o/p Signal	$123.4\ 10^{-6}$	VV^{-1}
Range of measures	100	N
Bridge impedance	350	Ω

AMPLIFIER CHARACTERISTICS

	Value	Units
Amplifier Gain	3215	V/V
Interface Accrual	$24.3\ 10^{3}$	V
Bridge Voltage	7.56	V
Amplifier Sensitivity	$2.99\ 10^{-2}$	VN^{-1}
Amplifier consumption	2	mA

Table 5.11: The full characteristics of the channels representing the three forces

The range of measurement for each channel was chosen following the maximum values typically found in amputee gait analysis studies and in accordance with the consensus figures reached in plenary session at Heathrow conference (ISPO, 1978), as shown in table 5.8.

Hence, the results on the theoretical gain setting are shown in table 5.10. Each appraisal gain setting for the three forces was far above the usual limit used in amputee gait assessment (rarely above 2000). Consequently, it was decided to divide by ten the gain of the two shear force channels and to limit at 2000, the gain of the axial load Fy. This way of doing had obviously the drawback to decrease the raw signal magnitude but, because a calibration matrix was always used (see chapter 6). This disadvantage could be easily compensated studying processed data. Therefore, the gains, used in the Myodata acquisition and storage data system, can be summarised as follows:

		Bridge Voltage in V (± 0.001 V)	Applied Gain Setting in VV^{-1} (± 5 units)
A/P Shear	Fx	7.46	1550
Axial load	Fy	8.04	2000
M/L Shear	Fz	7.56	3210
M/L Bending Moment	Mx	7.55	170
Torque	My	7.53	490
A/P Bending Moment	Mz	7.55	60

The mean accuracy of ± 5 units of these gains are attested by both the designer and the supplier.

To completely characterise one particular channel, the recorder evaluates and shows the interface accretion:

$$\text{Interface accretion}\,[V] = \text{Amplifier gain}\,\left[VV^{-1}\right] * \text{Bridge voltage}\,[V] \qquad (5.3)$$

and the amplifier sensitivity:

$$\text{Amplifier output}\,\left[VN^{-1}\right] = \frac{\text{Interface accretion}\,[V] * \text{Transducer gain}\,\left[VV^{-1}\right]}{\text{Range of measure}\,[N]} \qquad (5.4)$$

Mx

TRANSDUCER CHARACTERISTICS

	Value	Units
Channel Sensitivity	$175.33\ 10^{-6}$	$V(N.m)^{-1}$
Transducer Gain	$2322\ 10^{-6}$	VV^{-1}
Range of measures	100	N.m
Bridge impedance	350	Ω

AMPLIFIER CHARACTERISTICS

	Value	Units
Amplifier Gain	174	VV^{-1}
Interface Accrual	$1.313\ 10^{3}$	V
Bridge Voltage	7.55	V
Amplifier Sensitivity	$3.048\ 10^{-2}$	$V(N.m)^{-1}$
Amplifier consumption	2	mA

My

TRANSDUCER CHARACTERISTICS

	Value	Units
Channel Sensitivity	$242.2\ 10^{-6}$	$V(N.m)^{-1}$
Transducer Gain	$804.11\ 10^{-6}$	VV^{-1}
Range of measures	25	N.m
Bridge impedance	350	Ω

AMPLIFIER CHARACTERISTICS

	Value	Units
Amplifier Gain	493	VV^{-1}
Interface Accrual	$3.72\ 10^{3}$	V
Bridge Voltage	7.53	V
Amplifier Sensitivity	$11.99\ 10^{-2}$	$V(N.m)^{-1}$
Amplifier consumption	2	mA

Mz

TRANSDUCER CHARACTERISTICS

	Value	Units
Channel Sensitivity	$172.8\ 10^{-6}$	$V(N.m)^{-1}$
Transducer Gain	$6867\ 10^{-6}$	VV^{-1}
Range of measures	300	N.m
Bridge impedance	350	Ω

AMPLIFIER CHARACTERISTICS

	Value	Units
Amplifier Gain	59	VV^{-1}
Interface Gain	$0.445\ 10^{3}$	V
Bridge Voltage	7.55	V
Amplifier Sensitivity	$1.023\ 10^{-2}$	$V(N.m)^{-1}$
Amplifier consumption	2	mA

Table 5.12: The full characteristics of the channels representing the three bending moments

or

$$\text{Amplifier output}\left[VNm^{-1}\right]=\frac{\text{Interface accretion}\left[V\right]*\text{Transducer gain}\left[VV^{-1}\right]}{\text{Range of measure}\left[Nm\right]} \quad (5.5)$$

Therefore, the full set up characteristics of the three channels representing forces are shown in table 5.11. Table 5.12 exhibits the full characteristics of the three channels representing bending moments. Any gain has the unit of VV^{-1}, any sensitivity has the unit of VN^{-1} or $V(N\,m)^{-1}$ and any accrual has the unit of V.

Therefore, the conditioning-signal unit, which has six-channel amplifiers and bridge power supply unit and thus can balance the six full Wheatstone bridges, is presently totally described. It works with a portable recorder that will be outlined in the next section.

5.3.2.2 THE PROGRAMMABLE PORTABLE RECORDING UNIT

As previously stated, the portable recording unit was designed round about a Motorola® MC 68000 processor with appropriate peripherals and custom-written software. The A/D board has a resolution of 12 bits.

The device is mounted in a plastic case having a dimension of 180 x 115 x 61 mm and a mass of 0.650 kg. The total mass is of 1.350 kg including batteries and belt. That is lower than the equivalent system described by Sanders *et al.* (1995) which has a mass of 2.4 kg but about the same range of another fully portable acquisition and storage data rehabilitation instrument described by Abu-Faraj *et al.* (1997) which is 1.250 kg. For reliability and lightweight reasons, CMS and CMOS technology is used.

A 4 Mbytes PCMCIA flash card was used for data storage (10, 20 or 40 Mbytes memory cards are also available). The system collected data for 1 hour and 8 minutes using the eight channels at the sampling frequency of 64 Hz with a 4 Mbytes card. This recording duration was considered sufficient relative to the test specifications stated in chapter 1. Moreover, the tests performed in chapter 8 had a maximum duration of 10 to 15 minutes, due to the weakness and general status of the patients of the Villiers-Saint-Denis Rehabilitation Centre.

The main specifications of the Myodata are shown in table 5.13. The

Maximum Channels	8 channels
Data Storage	PCMCIA Type I Flash: 4 or 10 Mbytes
Band Width	Direct Current 0 to 800 Hz
Maximum Sample Rate ≈ 2.56 x Band Width	16 to 2048 point s^{-1}
PC Interface	1 serial port
Data Transfer Rate	9600 bit s^{-1}
External Memory Card Drive Data Transfer Rate	35 kbyte s^{-1}
4^{th} order Butterworth Filter cut-off frequency	6,12, 50, 100, 200, 400 or 800 Hz

Table 5.13: The main specifications of the Myodata

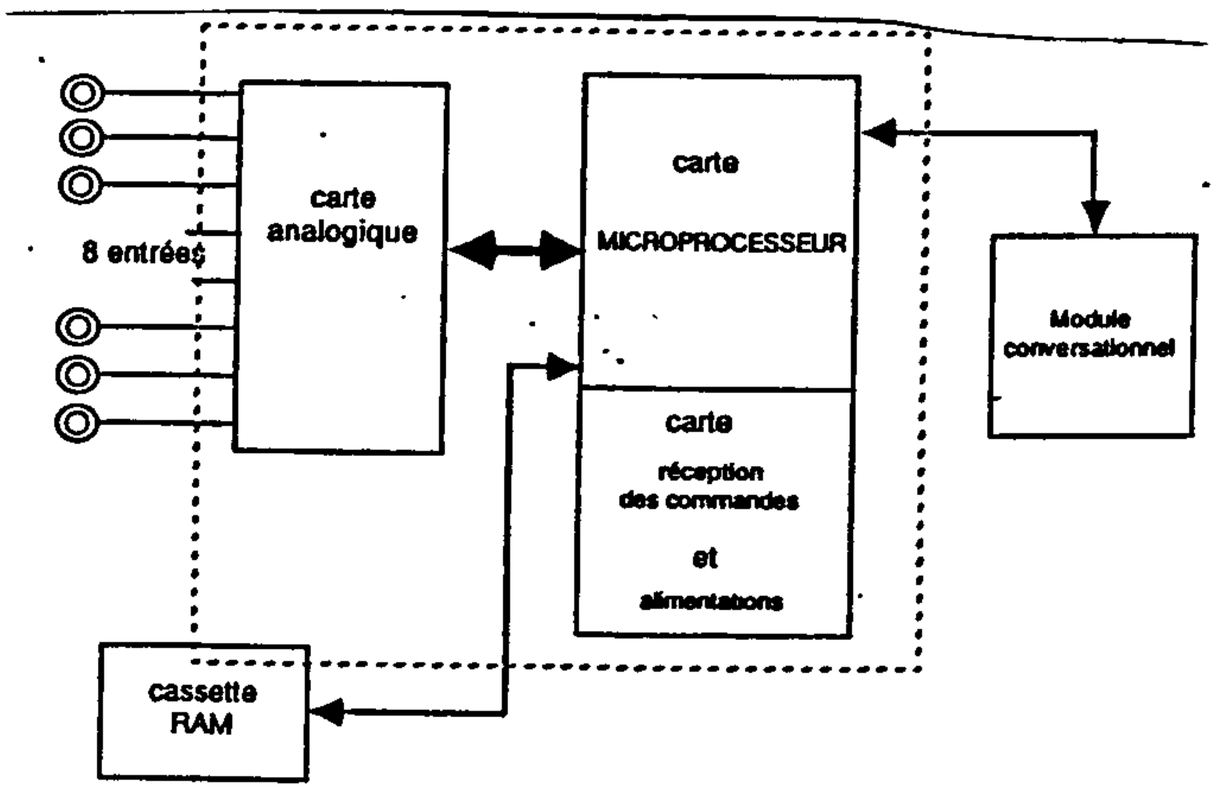

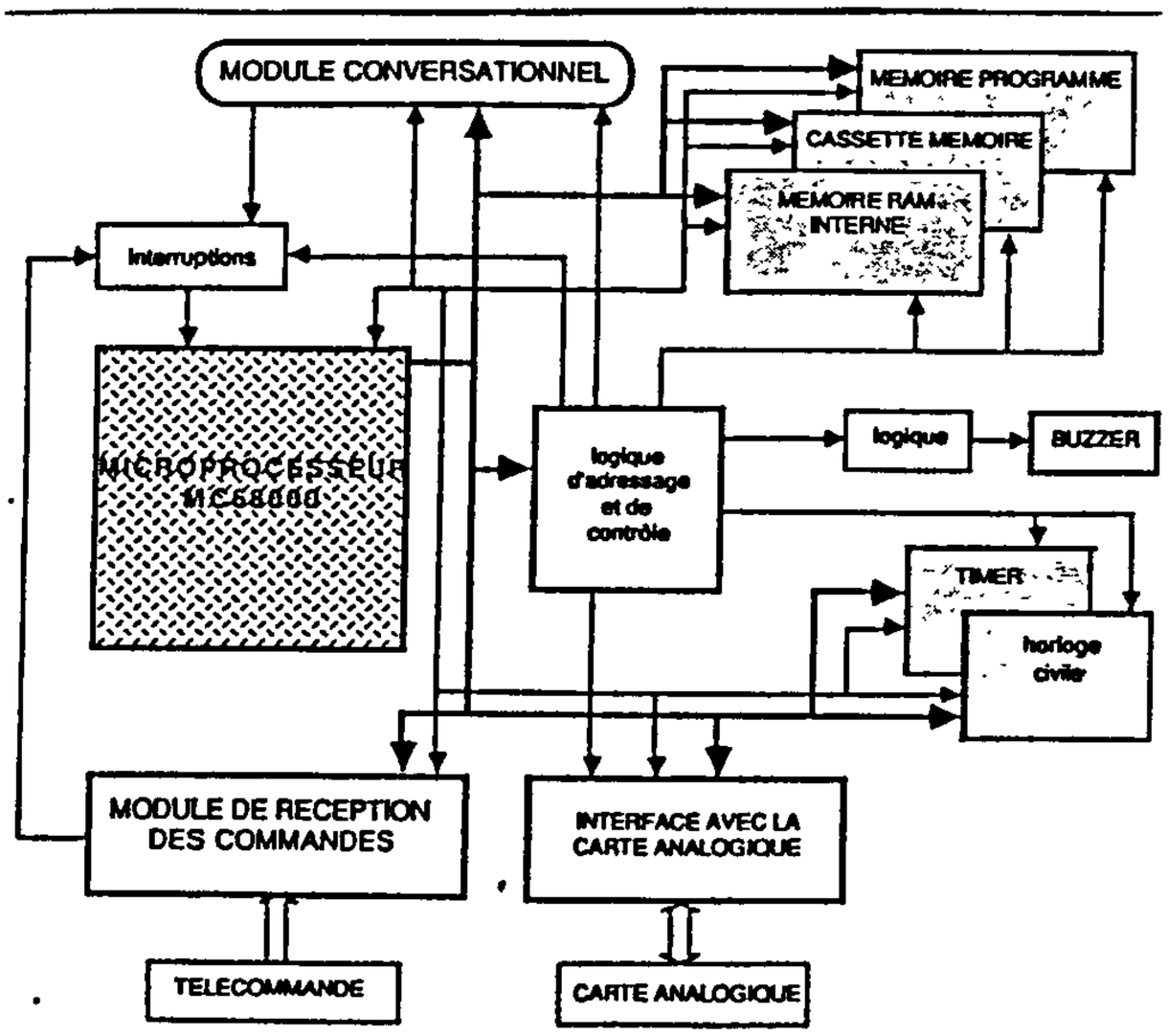

Figure 5.5: Block diagram of physical parts and electronic boards of the recorder (extracted from Ferrand, 1990)

instrumentation synopsis of the recorder is shown in figure 5.5.

Therefore, the system is fully portable: subjects carry it in a belt pack and ambulate freely without disruption to their usual gait pattern. This characteristic is fundamental regarding the main requirement settled in chapter 1.

5.3.2.3 USING THE PORTABLE MEASUREMENT SYSTEM: MYODATA

Before any recording, the system had to be configured through a serial port of a basic host computer (PC or notebook, minimum configuration 386 SX 25, standard RS232 and basic serial cable DB 15 pins - DB 9 pins). There were three possibilities:

1. to create a new configuration,

2. to use a configuration already stored in the Myodata,

3. to load in the Myodata a configuration already made and stored onto the hard disk of the host computer.

This step runs a DOS® program named CONFMYO.BAT® and was required when the recording unit was used for the first time with a new device such as the Villiers Pylon Transducer.

This configuration file gave to the data acquisition unit some values in the following order:

1. band width from which the sampling rate is settled;

2. number of selected channel (8 inputs were used because of the six channels of the new pylon transducer and the two channels for the assistive walking devices);

3.following by the number of each channel, in order:

- transducer characteristics such as: transducer gain, internal gain of the Myodata (see below for more details), accuracy (double or simple), transducer units, transducer name
- range of measure and transducer sensitivity
- balancing bridge viewing the signal trace of one particular channel (i.e., it is impossible to see more than one channel on the same screen).

The Myodata acquisition system allows the choice of accuracy for each test:

Band Width	25 Hz
Sampling Rate	64 values s^{-1}
Cut Off Frequency	6 Hz
Number of Channels	8
Transducer o/p signal	Particular o/p signal of each channel
Recorder Internal Gain	1
Accuracy	double
Transducer Unit	V
Transducer Name	SFx, SFy, SFz, SMx, SMy, SMz, CaRi and CaLe for each channel
Range of Measurement	particular range in N or N.m of each channel
Transducer Sensitivity	particular value in VN^{-1} or $V(N.m)^{-1}$ of each channel

Table 5.14: Characteristics of the usual configuration file
(CaRi and CaLe stand respectively for Right and Left walking aids).

1. usual default « double » accuracy in which raw data are stored as 12 bits form and each value is equal to two bytes

2. a « simple » accuracy in which raw data are stored as 8-bit form, each value having one byte.

The latter possibility expands the memory space twice and thus the available recording time. Because of the battery time available and patients weakness, this possibility had never been used. In all tests presented in this thesis, the usual default « double » accuracy was chosen.

The transducer was then declared: « install » and the created configuration file stored in the host computer hard disk for further use. This configuration file has the following extension: *.TYP.

The next step was to start the recording. The Myodata needed some more information, such as the memory card size loaded into the unit and some comments about the test. The unit selected automatically the recording duration.

The usual configuration file used in this work, named MYOGAIT2.TYP, has characteristics as shown in table 5.14.

In the processing of any time-varying data, no matter what their source, the following sampling theorem must not be violated: "the process signal must be sampled at a frequency at least twice as high as the highest frequency present in the signal itself" (Winter, 1994). If any signal is sampled at too low a frequency, it is subject to errors called aliasing. Thus, Winter (1994) recommends a minimum of 24 Hz as sample rate for movements such as walking. Concerning the frequency content of gait, Antonsson & Mann (1985) have established a mean of 15 Hz. Krebs (in Craik & Oatis, 1995, p. 337) quoted as evident that normal gait has some kinematic components with frequencies of 10 to 30 Hz. Therefore, according to these authors, a minimum of 30 Hz or even more as sample rate would be chosen.

The two sample rates just around and above 30 Hz, available in the portable recording unit are as follows, with a multiplying coefficient given by the company:

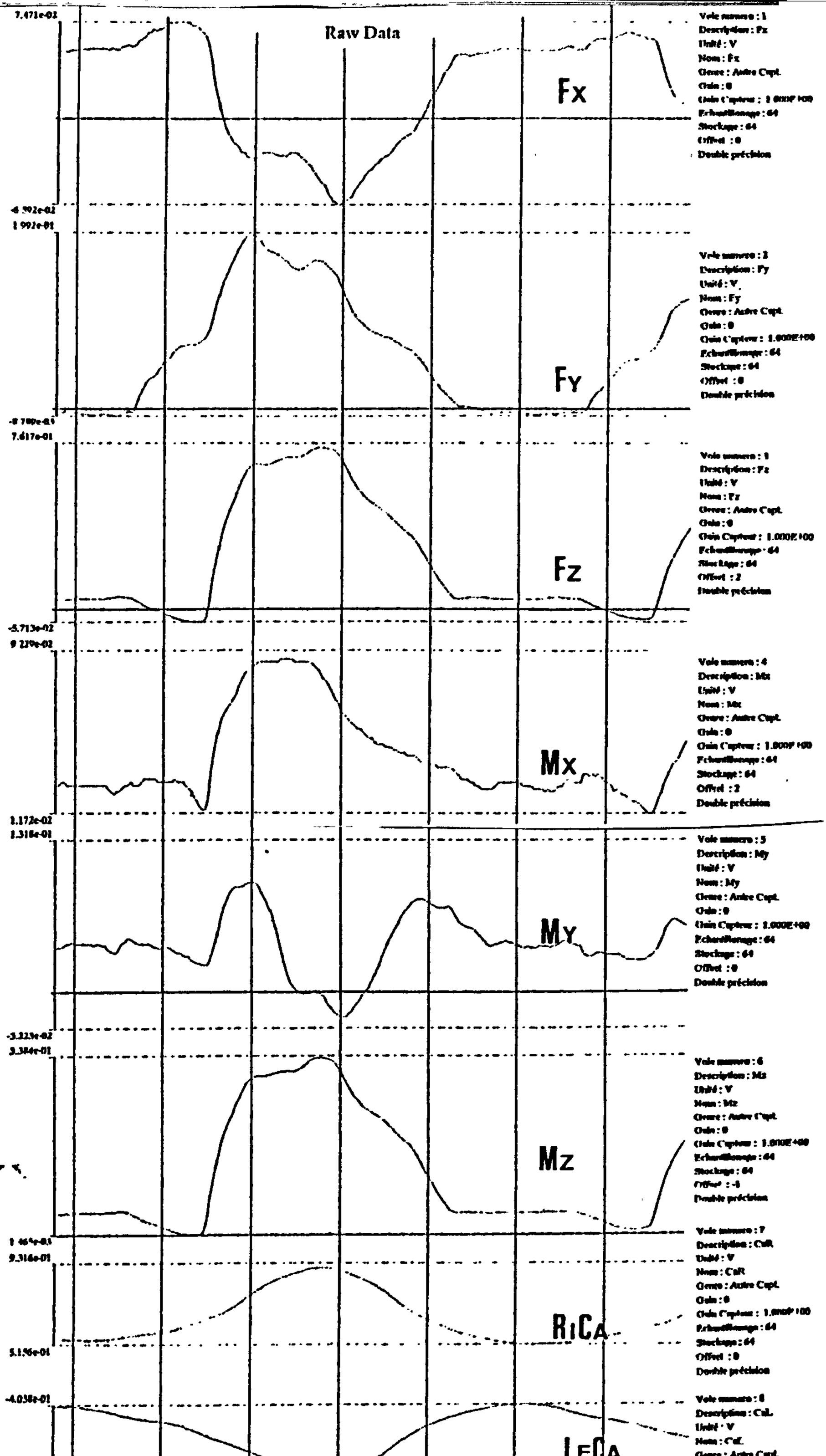

Figure 5.6: Raw data of a transtibial amputee using two sticks (see text for explanation).

Band Width Hz	multiplying coefficient	Sampling Rate Hz
6	2.66	16
12	2.66	32
25	2.56	64

The sample rate of 16 was too low, 32 could be possible, but some minor errors at the peaks could appear even if the major pattern was maintained. Hence, the sampling rate of 64 Hz was chosen because it was the typical rough estimated rate found in the gait assessment for kinetics in the amputees' field. For example, the sampling rate was 60 Hz in Pashalides (1989) portable recording system. This sampling rate of 64 Hz provides a cut - off frequency of the 4th order Butterworth low pass filter of 6 Hz.

When the test was finished, data were transferred into the host computer through the external memory card drive (data transfer rate: 35 Kbyte.s^{-1}, see table 5.13). Data were stored onto the PC or the notebook under the form of a special file having *.IMG as extension. Whatever the recording time was, transferred data were full memory card size. In other words, one hour eight minutes of recording represents 4 Mb as stated above, if the test is only ten minutes as example, the 4 Mb have to be transferred, blocking the computer hard disk with full of zero digits, impossible to delete.

This *.IMG raw data file can be visualised on the screen by means of a Windows® software named MYOPRO.EXE®. This friendly program provides a full range of tools for working on the traces. As a model, figure 5.6 shows the raw data of a transtibial patient walking during one step with two sticks on a flat vinyl floor.

From top to bottom, it is possible to identify:

1. the six channels recorded from the transducer: A/P shear force, Fx; Axial load, Fy; M/L shear force, Fz; M/L bending moment, Mx; Transverse Torque, My and A/P bending moment, Mz;

2. the right stick axial force (Channel 7 named CaRi, positive) and then the left stick axial force (Channel 8 named CaLe, negative).

The units are volts versus time. For each channel, the maximum and minimum values in V are shown on the left part of the figure and visualised by means of dotted lines. A solid line indicates the zero values of each channel

Beside the different traces: a broad description of the eight channels is provided such as (with the French equivalent, in bracket): number (Voie numéro), name (Description), unit (Unité in V), internal gain of the recorder (1.000E+00), sampling rate (Echantillonage 64Hz), storage rate (Stockage, 64Hz), offset and accuracy (Double précision).

The solid vertical lines display the time equivalent in 0.5 s.

The *.IMG files could not be used in another software such as a spreadsheet. It had to be converted in ASCII file having *.TXT as extension. This could be done manually by MYOPRO.EXE® but for each channel separately. This was a source of mixing channels and therefore the task had to be conducted very conscientiously.

The complete description of a test with a patient will be given, with more details, in chapter 8.

5.3.3 Partial conclusion about the definitive portable data acquisition system

Despite its price (≈ £9000), the Holter - type, microprocessor - based, rehabilitation instrument for acquisition and storage data has many advantages:

1. fully portable
2. lightweight, reliable, accurate
3. totally in accordance with the requirements established in chapter 1
4. sufficiently flexible to be used later for EMG, ECG, electrogoniometer, accelerometer.

The main disadvantage, for the research presently conducted, is the export data tool which is difficult, pains-taking to use and encourages mistakes. Some other commercial package could solve the problem. The second disadvantage, inherent to this conception of data acquisition system, is that traces cannot be viewed in real time for analysis and checking.

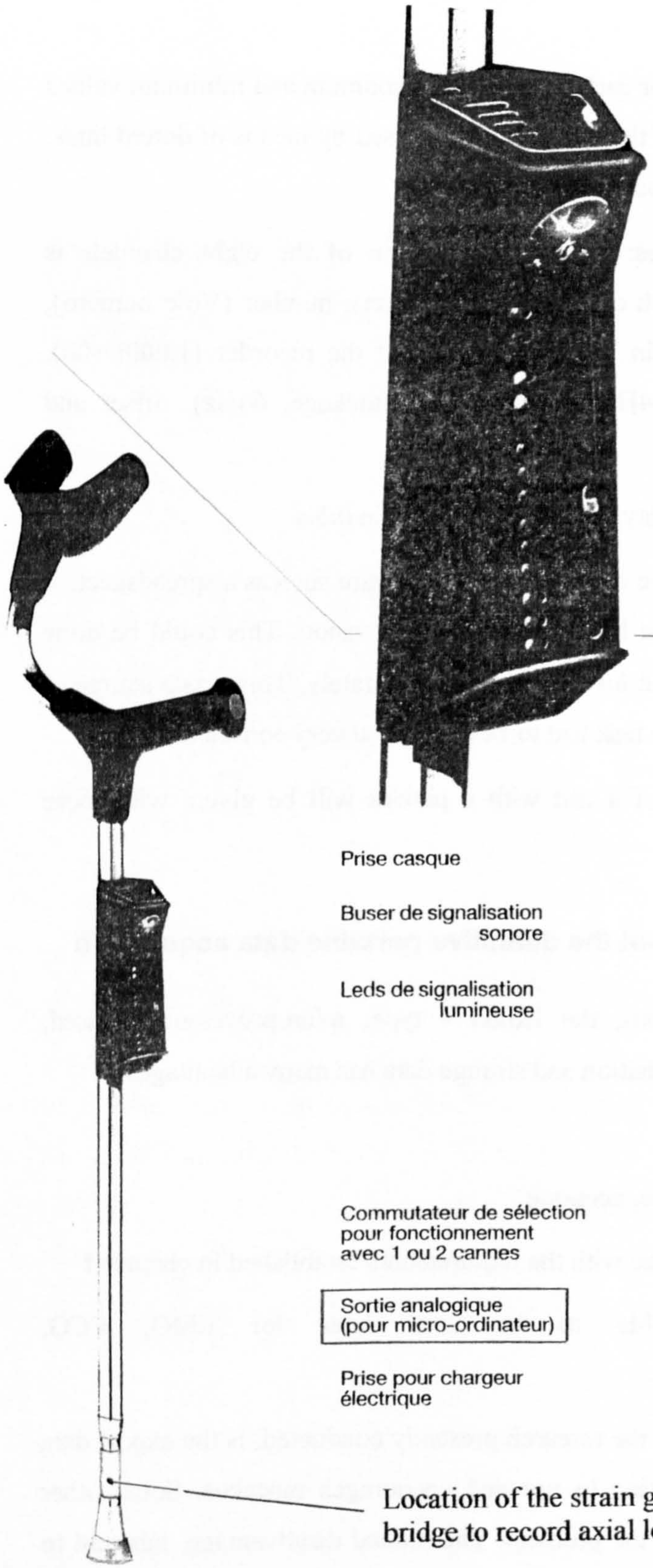

Figure 5.7: General view of the instrumented walking assistive device

5.4 THE INSTRUMENTED ASSISTIVE WALKING DEVICES

5.4.1 Introduction

Because tests carried on patients who are recent amputees, having a fragile residual limb with still a wound not yet healed and pain, subjects must have a stick - assisted gait. Therefore, it was mandatory to use instrumented walking aids.

Because the portable acquisition system makes up eight channels on which six of them were used by the transducer, only two channels were available, thus a single one per stick. Hence, the choice of which force or moment might be recorded had to be made. The requirements were established by the following thoughts.

Several instrumented walking sticks have been described in the literature, some could measure axial load force, bending moments and transverse moment (Seireg *et al.*, 1968; Winter *et al.*, 1993) or only axial and two shear forces (Opila *et al.*, 1987). Despite these possibilities, most papers (Ely & Smidt, 1977) emphasise the axial load on the walking sticks. Hence, it seemed obvious to choose the axial load as the single channel for measurement.

5.4.2 Description

The instrumented walking canes are commercially available[14]. They are used in orthopaedic rehabilitation. They include an analogue output able to be directly connected to the recorder. To allow length adjustment, the shaft is strain - gauged at the end nearest to the floor. The four strain gauges are arranged in a full Wheatstone bridge arrangement. Two extruded aluminium rods — the top one bearing the handle, the bottom one having the strain gauges — slide on each other. That allows the adjustment subjects' aids, individually, to the height of the ulna styloid to the floor, with the elbow flexed between 15° and 30°. The general view of the instrumented walking aid is illustrated in figure 5.7.

A plastic box is put on the top shaft under the handle. This box covers batteries and two potentiometers providing the possibility to adjust the response level of the

---

[14]Dynatronic, Domaine de St-Ruff, Route de Beaumont, 26000 Valence, France

	Conventional Name	Channel Number
A/P Shear Force	Fx	1
Axial load	Fy	2
M/L Shear Force	Fz	3
M/L Bending Moment	Mx	4
Transverse Torque	My	5
A/P Bending Moment	Mz	6
Right stick (for the subject)	CaRi	7
Left stick (for the subject)	CaLe	8

Table 5.15: The configuration of the portable data acquisition unit.

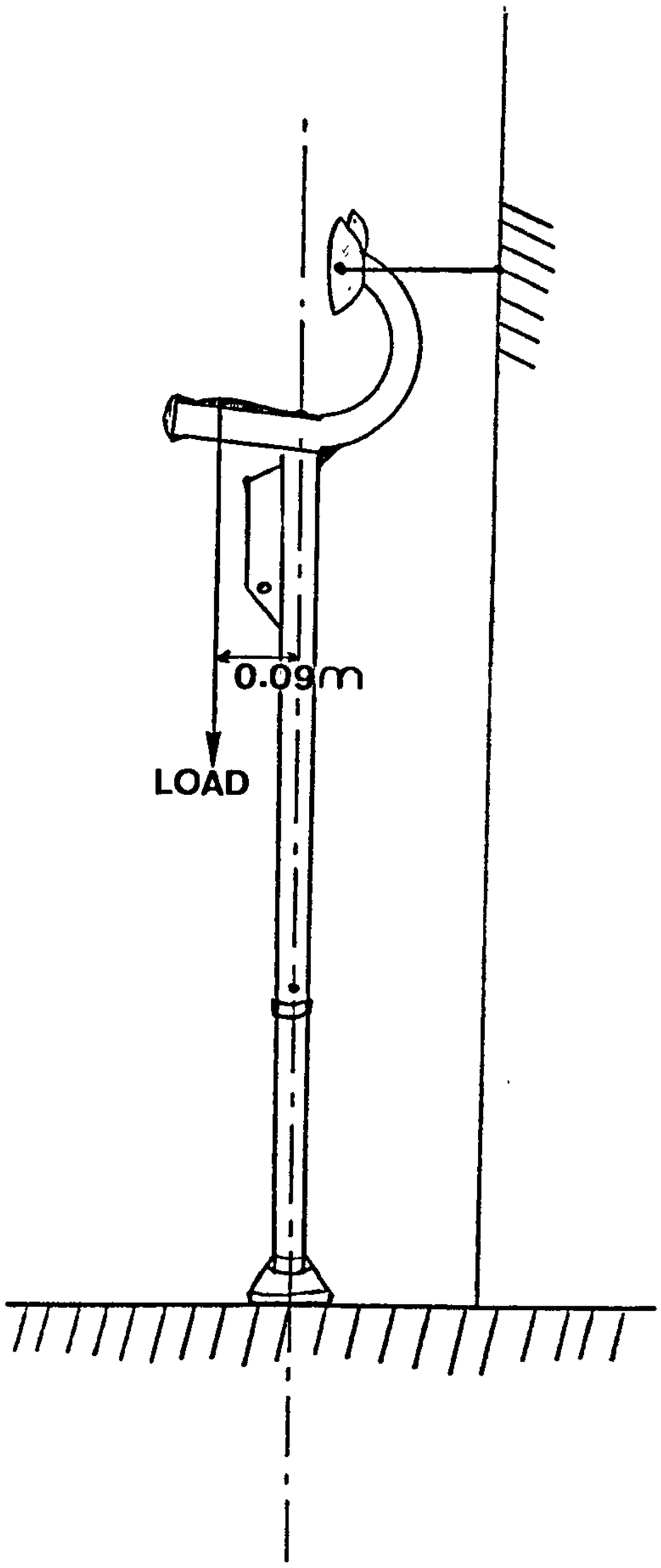

Figure 5.8: The set up for the calibration of the walking aids.

device according to the subject using the stick (weight, one or two sticks, permitted load level following the prescription of the orthopaedic surgeon). Therefore, the response of the walking aids could vary for an identical axial load and thus, performing an accurate calibration is impossible.

In this thesis, these two potentiometers were thus arbitrarily fixed in one position, in the middle range. This allowed the calibration of the two devices to be performed with accuracy: a unique response is provided by the instrumented walking aids for each axial load value. In this instrumented stick, there was no possibility to correct the bridge balance.

5.4.3 Calibration of the two assistive walking devices

The first point was to label each stick: left and right relative to the side of the subject.

To minimise errors, the portable data acquisition system was utilised. The six first channels were connected to the new transducer as in a gait assessment test. Channel number 7, named CaRi, was connected to the right (for the subject) stick while channel number 8, named CaLe, was connected to the left (for the subject) stick. Thus, the configuration of the recording unit is shown in table 5.15 (see above characteristics of the calibration file MYOGAIT2.TYP):

This arrangement is used in the remainder of this thesis.

Each stick was fitted as shown in figure 5.8. The bottom shaft was vertically positioned with accuracy by means of a plumbline and a spirit level. The bottom end was blocked on the floor and the top end at the level of the forearm counter-load. Loads were applied by means of a weight-carrier suspended under the stick handle through a steel cable, positioned on the handle at nine centimetres from the vertical shaft. This distance is the mean area of the handle on which the subject's hand is pushing at the maximum.

For accuracy reasons, the method used was the dead-weight technique (see more details in chapter 6). Normalised weights were used (see section 3.5.3 and table III.2).

Table 5.16: The calibration of the right walking assistive device: four tests with mean values, median, standard deviation and confidence level (95%). The statistical analysis and the linear regression of the mean values versus the applied load are shown. The corresponding graph of the mean values is shown in figure 5.9.

Right	**Cane**								
Loading Mass	Applied Load	Test N°1	Test N°2	Test N°3	Test N°4	Mean	Median	Standard Deviation	Confidence Level
kg	N	mV	mV	mV	mV	mV			95%
0.0	0.0	-301.62	-298.77	-299.65	-300.61	-300.16	-300.13	1.23	1.20
0.7	7.3	-268.42	-265.84	-264.99	-266.12	-266.34	-265.98	1.46	1.44
5.0	49.1	-86.55	-86.30	-86.37	-86.48	-86.42	-86.43	0.11	0.11
9.2	90.2	87.01	86.63	88.92	87.56	87.53	87.28	1.00	0.98
14.3	140.1	300.73	300.37	301.70	299.85	300.66	300.55	0.78	0.76
19.3	189.6	526.77	523.15	525.37	524.13	524.85	524.75	1.57	1.54
24.4	239.2	760.41	753.51	755.69	757.24	756.71	756.46	2.90	2.84
24.4	239.2	759.57	753.30	755.73	756.23	756.21	755.98	2.58	2.53
19.3	189.6	527.69	523.00	526.58	525.11	525.59	525.85	2.03	1.99
14.3	140.1	314.90	315.41	313.01	316.07	314.85	315.15	1.32	1.29
9.2	90.2	91.01	89.56	87.12	88.59	89.07	89.08	1.64	1.60
5.0	49.1	-89.12	-88.13	-87.59	-88.13	-88.24	-88.13	0.64	0.63
0.7	7.3	-265.04	-263.66	-267.73	-267.48	-265.98	-266.26	1.96	1.92
0.0	0.0	-298.79	-298.87	-295.45	-299.31	-298.11	-298.83	1.78	1.75
Regression Statistics									
Multiple R	0.999748324								
R Square	0.999496712								
Adjusted R Square	0.999454771								
Standard Error	2.053016362								
Observations	14								
Analysis of Variance									
	df	*Sum of Squares*	*Mean Square*	*F*	*Significance F*				
Regression	1	100445.5027	100445.5027	23831.18706	3.66697E-21				
Residual	12	50.57851417	4.214876181						
Total	13	100496.0812							
	Coefficients	*Standard Error*	*t Statistic*	*P-value*	*Lower 95%*	*Upper 95%*			
Intercept	0								
x1	0.228644638	0.001481113	154.373531	1.3316E-22	0.22541757	0.231871706			

When the set-up was correctly installed and carefully checked, the data acquisition system was switched on and a ten minutes wait was observed to stabilise the bridges. The configuration file used for the recording unit was MYOGAIT2.TYP as described above. Thus, the sampling rate was 64 Hz. When the unit was ready, several loading-unloading cycles were run as follows:

- four times with one loaded cane (the right then the left one)
- two times with the two canes simultaneously loaded.

Between each cycle, the set up was dismounted and re–set up again for the following test. Various lengths of canes were used.

Some validation tests were performed. They are presented in appendix 11.V.1.

Each test was a series of twelve load cases. At each load case, a stop of 15 seconds was observed. Full load was maintained for one minute to record any drifting. Therefore, the full test was about a minimum of 225 seconds which represented 225 x 64 = 14 400 digits.

At the end of the test, the file was converted in ASCII file and data were processed into the Excel 4® spreadsheet which has a maximum size of 16 384 rows.

The method used to process data was as follows: at each loading case, a chain of 100 digits was randomly chosen. These 100 digits were summarised and divided by 100 finding the average value. This mean value was finally transferred in another file for statistical data process.

5.4.4 Calibration results

Results are presented in two frameworks: tables 5.16 and 5.17 represent respectively the four tests of the right and the left canes, with statistical data processing. The tables concerning the two assistive walking devices, simultaneously recorded, are shown in appendix 11.V.1. The statistical regression analysis shows a linearity of the two devices (R square = 0.84 and 0.99 having a maximum of 1). Mean and median values are closed. Standard deviation and confidence level are small (concerning statistical analysis, see more details in the following section 6.5).

Left	Cane								
Loading Mass	Applied Load	Test N°1	Test N°2	Test N°3	Test N°4	Mean	Median	Standard Deviation	Confidence Level
kg	N	mV	mV	mV	mV	mV			95%
0.0	0.0	117.05	123.00	127.49	135.77	125.83	125.25	7.89	7.73
0.7	7.3	93.76	101.10	106.91	113.14	103.73	104.01	8.27	8.10
5.0	49.1	-33.50	-26.15	-19.24	-15.76	-23.67	-22.70	7.85	7.69
9.2	90.2	-168.75	-164.13	-154.66	-152.31	-159.96	-159.39	7.77	7.61
14.3	140.1	-343.02	-338.41	-329.02	-325.84	-334.07	-333.71	8.00	7.84
19.3	189.6	-523.52	-514.30	-502.29	-503.89	-511.00	-509.09	9.90	9.70
24.4	239.2	-705.42	-701.85	-685.49	-688.31	-695.26	-695.08	9.84	9.64
24.4	239.2	-697.45	-696.07	-678.66	-681.14	-688.33	-688.60	9.80	9.61
19.3	189.6	-509.43	-508.42	-492.16	-488.63	-499.66	-500.29	10.80	10.59
14.3	140.1	-334.78	-340.69	-321.88	-316.18	-328.38	-328.33	11.31	11.08
9.2	90.2	-170.12	-165.68	-155.29	-152.60	-160.92	-160.48	8.33	8.17
5.0	49.1	-32.91	-26.18	-18.01	-13.04	-22.53	-22.10	8.79	8.61
0.7	7.3	109.30	110.19	118.02	141.97	119.87	114.10	15.24	14.94
0.0	0.0	120.09	127.36	136.20	137.94	130.40	131.78	8.29	8.12

Regression Statistics	
Multiple R	0.920120742
R Square	0.84662218
Adjusted R Square	0.769699103
Standard Error	34.43373773
Observations	14

Analysis of Variance	*df*	*Sum of Squares*	*Mean Square*	*F*	*Significance F*
Regression	1	85082.21139	85082.21139	71.75801801	2.08333E-06
Residual	13	15413.86982	1185.682294		
Total	14	100496.0812			

	Coefficients	*Standard Error*	*t Statistic*	*P-value*	*Lower 95%*	*Upper 95%*
Intercept	0					
x1	-0.358688041	0.02568021	-13.96748884	1.30257E-09	-0.41416675	-0.303209332

Table 5.17: The calibration of the left walking assistive device: four tests with mean values, median, standard deviation and confidence level (95%). The statistical analysis and the linear regression of the mean values versus the applied load are shown. The corresponding graph of the mean values is shown in figure 5.9.

Figure 5.9 represents the graph of the calibration tests of the two walking aids. The offset was adjusted to zero. Two points must be highlighted:

1. due to a wiring connection, the right cane has a positive response while the left cane has a negative response

2. the two devices were bought independently, with an interval of several months. This is why the linearity of the results recorded from the left cane is poorer than those from the right cane (left R Square 0.84 versus 0.99 for the right R square) and they have a different level of sensitivity (difference ≈ 28 %) as follows:

	Sensitivity in $mV.N^{-1}$	Sensitivity in $N.(mV)^{-1}$
Right Cane (Channel 7)	4.41	0.227
Left Cane (Channel 8)	3.42	0.292

The regression analysis, performed through the spreadsheet Excel® and shown in tables 5.16 and 5.17, exhibits the slope of the regression line (x1 coefficient).

The mean value when no load was applied on each walking aid gives the offset coefficient:

$$\text{Right Cane} \quad 300.16 + 298.11 = 598.27 / 2 = \mathbf{297.135} \tag{5.6}$$

$$\text{Left Cane} \quad 125.83 + 130.40 = 256.23 / 2 = \mathbf{128.115} \tag{5.7}$$

These coefficients must be used to process raw data.

Therefore, the two following equations will be used supplementary of the calibration matrix of the new transducer (see section 6.7), they are as follows:

for the right cane (channel 7 named CaRi)

$$X = 0.2286 (Y + 297.135) \tag{5.8}$$

and for the left cane (channel 8 named CaLe)

$$X = -0.3587 (Y - 128.115) \tag{5.9}$$

in which X is the loading case in N and Y the recorded output in mV.

From equations 5.8 and 5.9, it was easy to convert output (expressed in mV) into axial load (having N as unit). This was done with a sufficient accuracy regarding

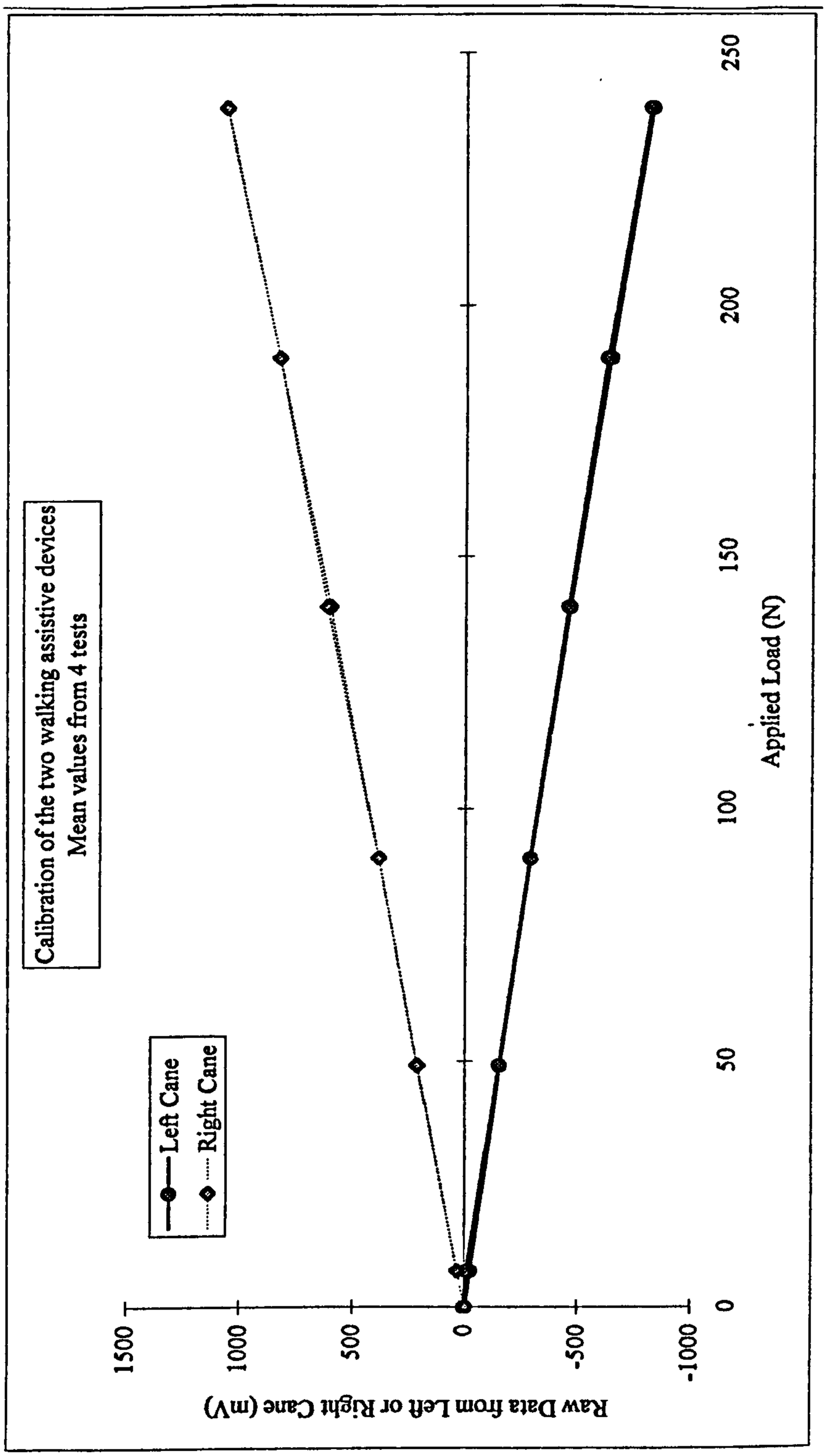

Figure 5.9: The graph of the mean values (see tables 5.16, right cane and 5.17, left cane) calculated from 4 calibration tests separately performed with the two walking assistive devices. The offset coefficients have been applied to have 0 mV when a load of 0 N was applied: + 297.135 for the right cane and –128.115 for the left cane (see text for more explanation).

the linearity of the two instrumented canes with neither hysteresis nor drifting during the usual duration of any test with recent lower limb amputees.

In the different patients' tests recorded and presented in chapter 8, a walking aid such as a cane or a stick is expected to record an average value of 300 N as axial load force. A sufficient accuracy could therefore be estimated at the level of 5 % = 15 N for our requirements in such a project. These 15 N gave for the right walking aid a mean output of 3.4 mV and 4.3 mV for the left. During the calibration tests performed, the gap between applied and predicted loads had always a value inferior than 3 mV. Thus, the two instrumented walking aids were proclaimed to have a sufficient accuracy.

5.4.5 Validation tests and results of the two assistive walking devices

To confirm the calibration tests undertaken and presented above, some static validation tests were conducted. They are presented in the following section.

The procedure followed was to apply a unique known load on the walking assistive device as shown in figure 5.8. Then, to move the stick backward as shown in figure 5.10, applying the same unique known load, offset from the stick axis. The counter-load was applied on the forearm ring. Two series of tests were conducted. Because of the rod of the stick, it was not possible to move the stick frontward. For bending moment reasons, it was also not possible to load the stick laterally.

The two sticks were simultaneously loaded and recorded: channel 7 for the right stick and channel 8 for the left stick. The six channels of the new Villiers Pylon Transducer were also concurrently recorded to avoid any possibility of errors. Thus, the set-up was as it was in a gait assessment test (identical gain setting and sampling frequency). It was therefore possible to compare two values of the same load:

1. the theoretical value of the load calculated by the means of a trigonometric analysis: sin 0.30/0.79 = 0.3797. Hence, the angle is 22°.31 and cosine 22°31 is 0.9251.

2. the predicted value given by the assistive walking devices through the portable data acquisition system after applying equations 5.8 and 5.9.

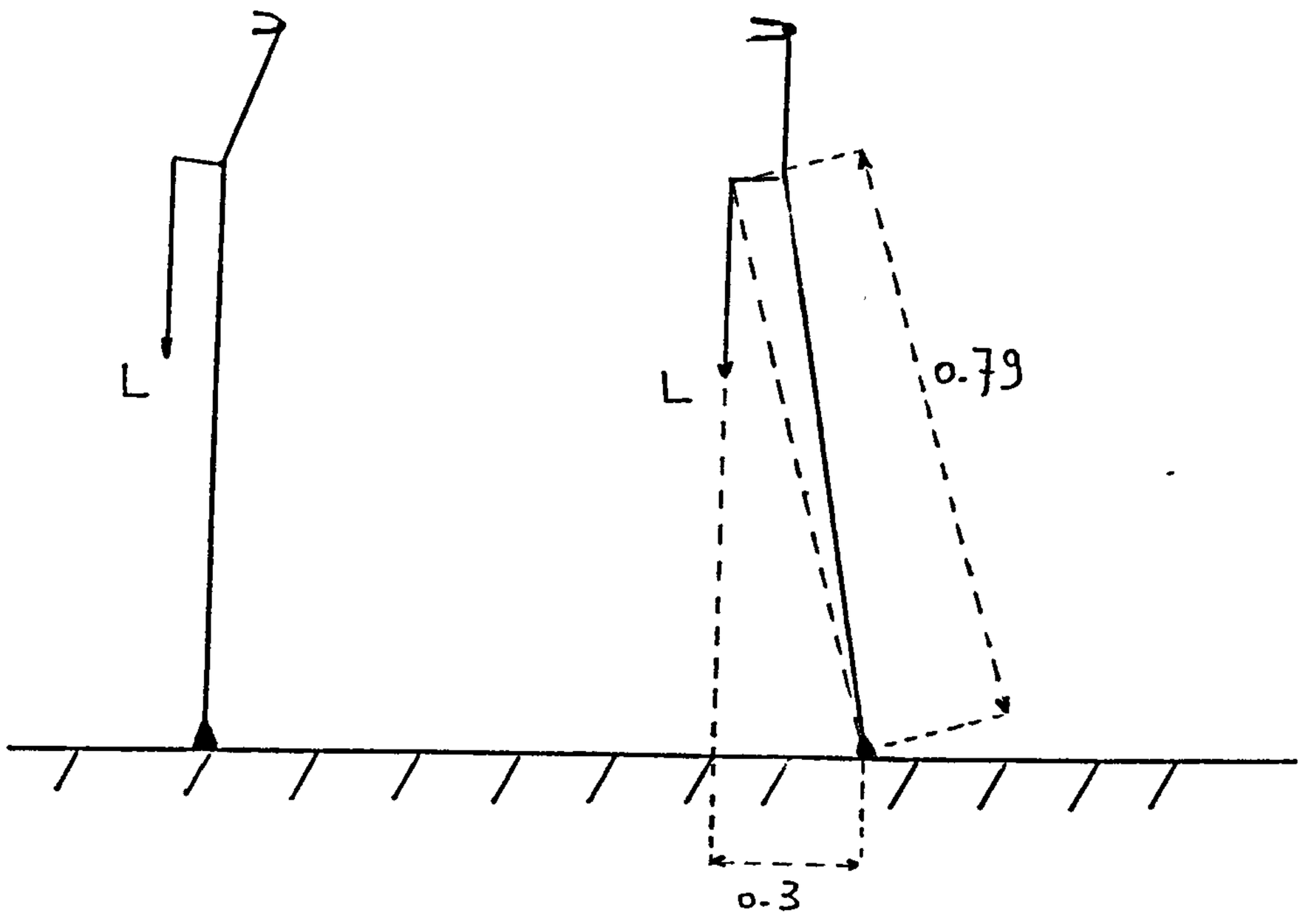

Figure 5.10: The set up of the validation tests performed to verify the calibration undertaken with the two walking assistive devices.

All dimensions are in metres.

$$\sin \frac{0.30}{0.79} = 22°31 = 0.3797$$

$$\cos 22°31 = 0.9251$$

The different load case and results are shown in appendix 11.V.2.

The conclusions are as follows: the right walking assistive device exhibits results with an average increase of 2.92 % while the left stick gives results with an average increase of 3.3 %, as shown in table V.1.

However, the behaviour of the two sticks is linear as shown in figure 5.11. It shows as solid bold line the recorded values when the rod of the walking devices was vertical as it was during calibration tests and as solid thin line the recorded values when the walking device was oblique backward. Neither of there are drifting nor was hysteresis present during a short time gap looking like a step. The test duration was also too short to notice any creep.

5.5 SUMMARY

This chapter has described the two data acquisition systems used during this work.

The first system was not portable. The recordings were made in real time through a computer. This system was used to make a first calibration of the new transducer. This calibration enabled calculation of the sensitivity of each channel of the new transducer.

The second system presented is definitive. It is fully portable and allows storage and recording of 8 channels of data during a sufficiently long time with a high enough sampling rate. The channel sensitivities, established by means of the previous data acquisition unit, have granted to design the characteristics of the amplifiers newly built.

This chapter has described the two instrumented walking aids used during this work.

The two walking aids are instrumented to measure only one force in each: the axial load. A full calibration was conducted. The calibration results have allowed the possibility of readily convertion from raw data to processed data by means of two equations. These equations were established after a regression analysis. Nevertheless,

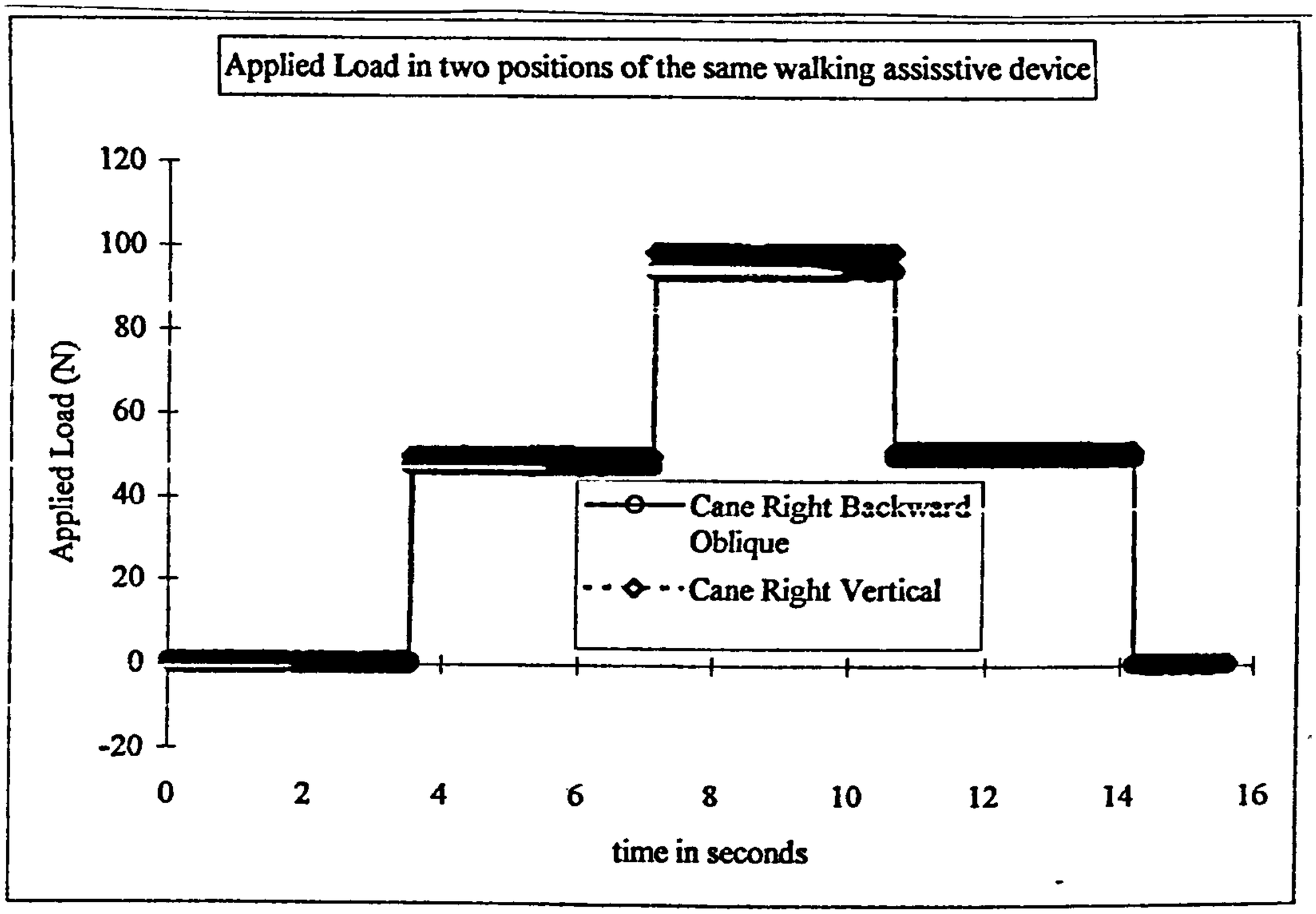

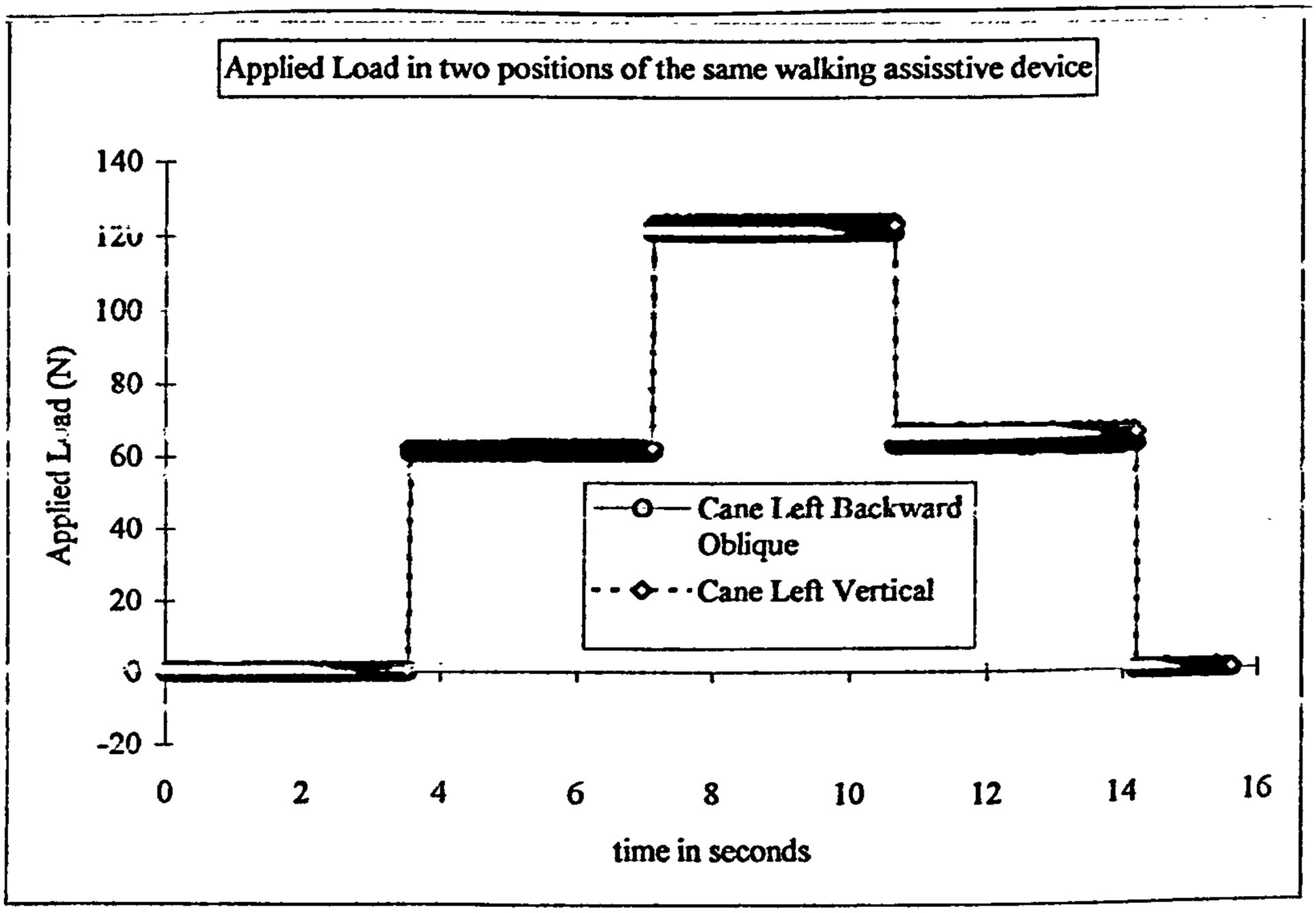

Figure 5.11: The validation tests of the two walking assistive devices: bold line, the shaft of the cane was vertical; thin line, the shaft of the cane was positioned backward as shown in figure 5.10. Right cane, top; left cane, bottom. Two tests were performed in each configuration.

the cross-sensitivity to bending of such a device was not investigated and thus a degree of uncertainty may be present. In this respect, further research should be undertaken (see chapter 9).

However, the two instrumented walking aids have a sufficient linear response, with a negligible hysteresis and no drifting. Therefore, they appear to have sufficient accuracy for the aim of the work presented later.

In chapter 4, the new Villiers Pylon Transducer was described. In the above sections, two data acquisition systems were outlined. Through the utilisation of these devices, it will be possible to calibrate the new Villiers Pylon Transducer to use it with accuracy and reliability during amputee tests. Therefore, a complete detailed calibration, thoroughly and carefully conducted, will be presented in the following sections.

6 THE NEW VILLIERS PYLON TRANSDUCER CALIBRATION

6.1 INTRODUCTION

No piece or scientific equipment such as a new transducer can be used without that equipment being calibrated. All calibration must be between measured input quantities and final output data. A careful calibration is thus, needed to convert the raw output signals of the transducer into meaningful mechanical quantities (forces in N and moments in N m). This conversion is achieved from the response of the transducer to any load, which is raw data in computer units (cu), reflection of electrical tension variation. The principle of calibration is to apply one and only one known load onto a mechanical system containing the transducer and then recording the one and only output signals set of the six channels. Hence, the basic principles of a reliable and accurate calibration are:

- ❖ All loading forces and moments must be as isolated as much as possible.
- ❖ All loading forces and moments must be accurately known in intensity and direction.
- ❖ Tests must be repeated several times and the mean should be considered as an image of the reality (with statistical precautions).

The objective is the compilation of a mathematical relationship between load and computer units or voltage. As far as calibration of transducers is concerned, two mathematical approaches: one linear and one non-linear are advocated. The choice depends on the accuracy required and it has been proved that the non-linear models contribute to the accuracy rather marginally (Magnissalis, 1992). Furthermore, some authors have stated: « a second order calibration curve is not necessarily done if the first order calibration curve is linear ». (Bray *et al.*, 1990, p. 26). Therefore, considering the accuracy required for the amputee gait tests, the static conditions of measures (even in human gait) and low strains applied to the transducer, the non-linear approach is not necessary. It would introduce sophisticated calculations,

$$SFx = m_{11}Fx + m_{12}Fy + m_{13}Fz + m_{14}Mx + m_{15}My + m_{16}Mz$$

$$SFy = m_{21}Fx + m_{22}Fy + m_{23}Fz + m_{24}Mx + m_{25}My + m_{26}Mz$$

$$SFz = m_{31}Fx + m_{32}Fy + m_{33}Fz + m_{34}Mx + m_{35}My + m_{36}Mz$$

$$SMx = m_{41}Fx + m_{42}Fy + m_{43}Fz + m_{44}Mx + m_{45}My + m_{46}Mz$$

$$SMy = m_{51}Fx + m_{52}Fy + m_{53}Fz + m_{54}Mx + m_{55}My + m_{56}Mz$$

$$SMz = m_{61}Fx + m_{62}Fy + m_{63}Fz + m_{64}Mx + m_{65}My + m_{66}Mz \qquad (6.4)$$

Table 6.1: The set of equations used for calibration. The prefix S stands for Signal. It shows that it is raw data.

$$[M] = \begin{bmatrix} m_{11} & m_{12} & m_{13} & m_{14} & m_{15} & m_{16} \\ m_{21} & m_{22} & m_{23} & m_{24} & m_{25} & m_{26} \\ m_{31} & m_{32} & m_{33} & m_{34} & m_{35} & m_{36} \\ m_{41} & m_{42} & m_{43} & m_{44} & m_{45} & m_{46} \\ m_{51} & m_{52} & m_{53} & m_{54} & m_{55} & m_{56} \\ m_{61} & m_{62} & m_{63} & m_{64} & m_{65} & m_{66} \end{bmatrix} \qquad (6.7)$$

Table 6.2: The desired coefficients m_{ij} of the calibration square matrix [M]

source of useless wasting time and equipment. Moreover, it is important to note that the non-linear approach, also called, second-order models have never been adopted in the field of prosthetics. The interested reader concerning second order models can obtain more information from Magnissalis (1992).

6.2 LINEAR APPROACH

The linear approach is the most common method for calibrating transducers. Many researchers have used it (Lowe, 1969; Berme *et al.*, 1976; Jones, 1976; Grant-Thomson, 1977; Lovely, 1981; Lawes, 1982; Pashalides, 1989; Runcinam, 1993). This method was discussed by Berme (1990) and very well explained by Magnissalis (1992) and it is only repeated in summary to understand the following sections.

The linear model assumes that each signal can be expressed as a linear equation between itself and the applied load:

$$(signal)_i = \sum_{j=1}^{6} m_{ij} \times (load)_j \qquad (6.1)$$

where the coefficients m_{ij} are the quantities to be determined. This equation is the same type as a linear regression equation. When i = j, equation (6.1) represents the main effect and in all other cases the coefficients correspond to the five cross-effects and ideally should be zero.

By definition, a non-zero output signal is called a main effect when and only when a load corresponding to that particular channel is applied. In practice, however, in the presence of one single load component, all six channels may respond: one main effect and five interaction effects. This introduces the study of six output signals for each loading case in the calibration procedure. These effects are due to inherent characteristics of the transducer, which could be an addition of:

- asymmetries of the device due to machining errors, even with the highest limits of engineering practice being observed;
- misalignment of the gauges on the transducer (Paul 1949);

$$
\begin{array}{llllll}
m_{11}=\frac{SFx}{Fx} & m_{12}=\frac{SFx}{Fy} & m_{13}=\frac{SFx}{Fz} & m_{14}=\frac{SFx}{Mx} & m_{15}=\frac{SFx}{My} & m_{16}=\frac{SFx}{Mz} \\
m_{21}=\frac{SFy}{Fx} & m_{22}=\frac{SFy}{Fy} & m_{23}=\frac{SFy}{Fz} & m_{24}=\frac{SFy}{Mx} & m_{25}=\frac{SFy}{My} & m_{26}=\frac{SFy}{Mz} \\
m_{31}=\frac{SFz}{Fx} & m_{32}=\frac{SFz}{Fy} & m_{33}=\frac{SFz}{Fz} & m_{34}=\frac{SFz}{Mx} & m_{35}=\frac{SFz}{My} & m_{36}=\frac{SFz}{Mz} \\
m_{41}=\frac{SMx}{Fx} & m_{42}=\frac{SMx}{Fy} & m_{43}=\frac{SMx}{Fz} & m_{44}=\frac{SMx}{Mx} & m_{45}=\frac{SMx}{My} & m_{46}=\frac{SMx}{Mz} \\
m_{51}=\frac{SMy}{Fx} & m_{52}=\frac{SMy}{Fy} & m_{53}=\frac{SMy}{Fz} & m_{54}=\frac{SMy}{Mx} & m_{55}=\frac{SMy}{My} & m_{56}=\frac{SMy}{Mz} \\
m_{61}=\frac{SMz}{Fx} & m_{62}=\frac{SMz}{Fy} & m_{63}=\frac{SMz}{Fz} & m_{64}=\frac{SMz}{Mx} & m_{65}=\frac{SMz}{My} & m_{66}=\frac{SMz}{Mz}
\end{array}
\tag{6.8}
$$

Table 6.3: The form of all coefficients m_{ij} of the matrix [M], equal to the ratio of signals [S] with forces and bending moments [L]

- elastic deformations which normally change the properties and shape of the transducer;
- differences in the resistance and gauge factor of gauges in the various bridge circuits;
- non uniformity of gauge adhesives.

Equation (6.1) may be written in the form of a vector [L] for the six load components while the six output signals are given the form of a vector [S]:

$$[L]=\begin{bmatrix} Fx \\ Fy \\ Fz \\ Mx \\ My \\ Mz \end{bmatrix} \qquad (6.2)$$

$$[S]=\begin{bmatrix} SFx \\ SFy \\ SFz \\ SMx \\ SMy \\ SMz \end{bmatrix} \qquad (6.3)$$

then using equation (6.1), the whole set of equations is shown in table 6.1, which can also be written in a simpler form:

$$[S]=[M][L] \qquad (6.5)$$

Hence,

$$[M]=\frac{[S]}{[L]} \qquad (6.6)$$

in which the square matrix [M] (6 rows * 6 columns) is a column vector of the desired coefficients m_{ij} and [L] the loading case in N or N m. Coefficients m_{ij} have subscript as shown in table 6.2.

The first subscript i (same value in row) represents the sum of cross-effects for one output signal, while the second subscript j (same value in column) stands for interfering effects for one particular channel.

$$[C]=\begin{bmatrix} c_{11} & c_{12} & c_{13} & c_{14} & c_{15} & c_{16} \\ c_{21} & c_{22} & c_{23} & c_{24} & c_{25} & c_{26} \\ c_{31} & c_{32} & c_{33} & c_{34} & c_{35} & c_{36} \\ c_{41} & c_{42} & c_{43} & c_{44} & c_{45} & c_{46} \\ c_{51} & c_{52} & c_{53} & c_{54} & c_{55} & c_{56} \\ c_{61} & c_{62} & c_{63} & c_{64} & c_{65} & c_{66} \end{bmatrix} \qquad (6.13)$$

Table 6.4: The inverted matrix [C] = $[M]^{-1}$

$$\begin{bmatrix} Fx \\ Fy \\ Fz \\ Mx \\ My \\ Mz \end{bmatrix} = \begin{bmatrix} c_{11} & c_{12} & c_{13} & c_{14} & c_{15} & c_{16} \\ c_{21} & c_{22} & c_{23} & c_{24} & c_{25} & c_{26} \\ c_{31} & c_{32} & c_{33} & c_{34} & c_{35} & c_{36} \\ c_{41} & c_{42} & c_{43} & c_{44} & c_{45} & c_{46} \\ c_{51} & c_{52} & c_{53} & c_{54} & c_{55} & c_{56} \\ c_{61} & c_{62} & c_{63} & c_{64} & c_{65} & c_{66} \end{bmatrix} \begin{bmatrix} SFx \\ SFy \\ SFz \\ SMx \\ SMy \\ SMz \end{bmatrix} \qquad (6.14)$$

Table 6.5: The matrix form equation of [C]

The diagonal coefficients of matrix [M] represent the primary transducer signal (main effect when coefficients i and j are equal) and the off-diagonal coefficients are the transducer cross-effects.

Therefore, all the coefficients m_{ij} of matrix $[M]=\frac{[S]}{[L]}$ have the form of equation 6.8 shown in table 6.3.

It is important to note that interfering signals for each particular channel are distributed in columns. The resulting six output signals for each loading case could be analysed using linear regression to determine the corresponding six components of a column of the matrix [M].

As the output signals from the data capture equipment are in mV converted by the A/D board into computer units and loading forces are in N or bending moments in N m, the m_{ij} terms have the following units:

$$m_{ij}=\frac{(mV)_i}{(N)_j} \qquad m_{ij}=\frac{(mV)_i}{(Nm)_j} \tag{6.9}$$

or

$$m_{ij}=\frac{(cu)_i}{(N)_j} \qquad m_{ij}=\frac{(cu)_i}{(Nm)_j} \tag{6.10}$$

It is important to note that, in amputee gait tests, the provided numbers are the output signals in computer units and what we require to know are the six components of the load applied onto the transducer at each particular instant of the gait cycle. So, in equation (6.5), we record [S] and we would like to know [L]. It is therefore necessary to change the form of equation (6.5), multiplying it by $[M]^{-1}$, the inverse of [M]. Hence:

$$[M]^{-1}*[S]=[M]^{-1}*[M]*[L]$$

or

$$[M]^{-1}*[S]=[L]$$

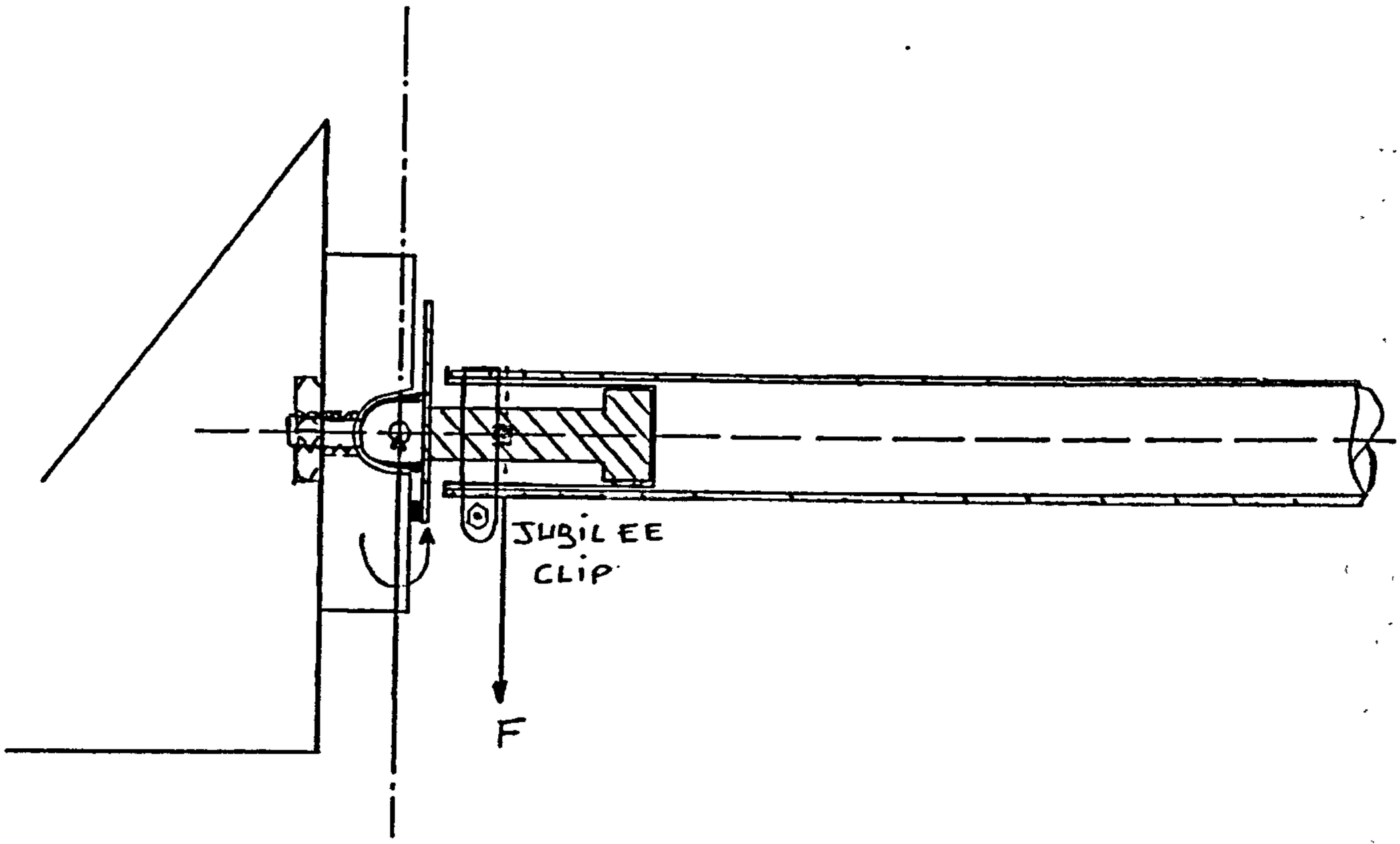

Figure 6.1: The set up for shear force calibration.

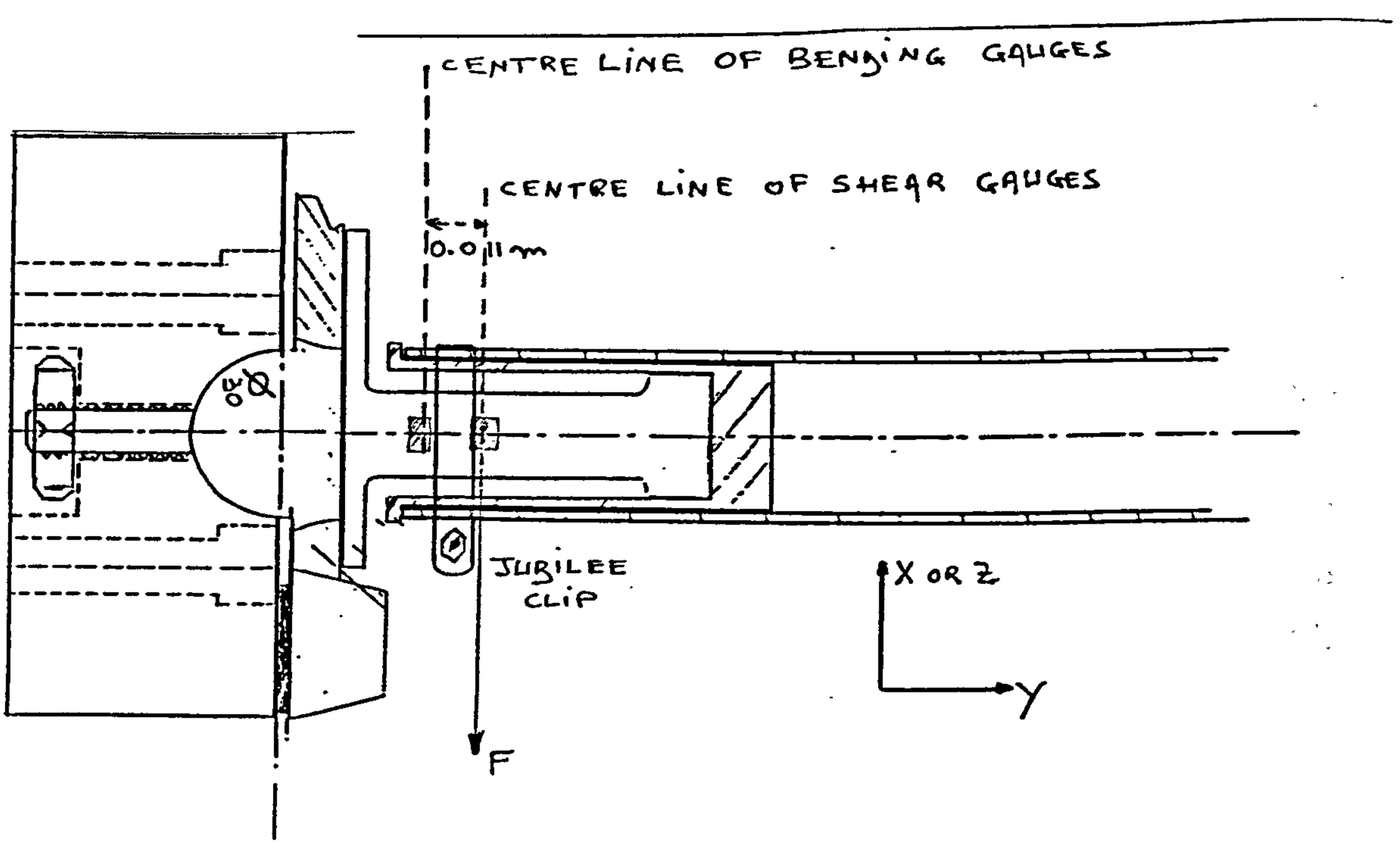

Figure 6.2: The position of the steel cable relative to the centre line of the shear and bending gauges. The lever arm (0.011 m) of the bending moments is shown. It has the same value in Fx or Fz set-ups.

or

$$[L] = [C] * [S] \qquad (6.11)$$

in which $[C] = [M]^{-1}$ is called the calibration matrix for the transducer (Solomonidis, 1989). [C] is a matrix and a complete set of constantly. Therefore, the active load in a particular channel is then equal to the calibration constant times signal [S] which is the main signal from that channel minus the sum of all the interfering signals (Grant-Thomson 1977).

This statement can be written as:

$$[L] = [C] \times \left[\begin{matrix} \text{observed} \\ \text{channel} \\ \text{signal} \end{matrix} - \sum (b * \text{other channel signals}) \right] \qquad (6.12)$$

in which « b » is a constant expressing the proportion of interference in that channel caused by the loading of some other channel.

The calibration constants contained in $[C] = \frac{1}{[M]}$ are the slope of the line relating the bridge output signal to the applied load. These constants are obtained by experimental methods. The constant m_{11} to m_{16} are also obtained from experimental analysis of the transducer. They are the ratio of the interfering signal level in the channel of interest (SFx, ..., SMz) to the main channel from which they came (Fx, ..., Mz), as shown in table 6.3.

For inverting the matrix [M], a specialised mathematical computer programme named MathCad 4.0® has been used (see more information in 6.6.3).

The matrix [C] is of the form shown in table 6.4. This gives the matrix form equation shown in table 6.5.

Here also, the diagonal coefficients of the matrix represent the main channels (when coefficients i and j are equal, i.e. c_{11}, c_{22}, etc.) and the off-diagonal coefficients are cross-effects.

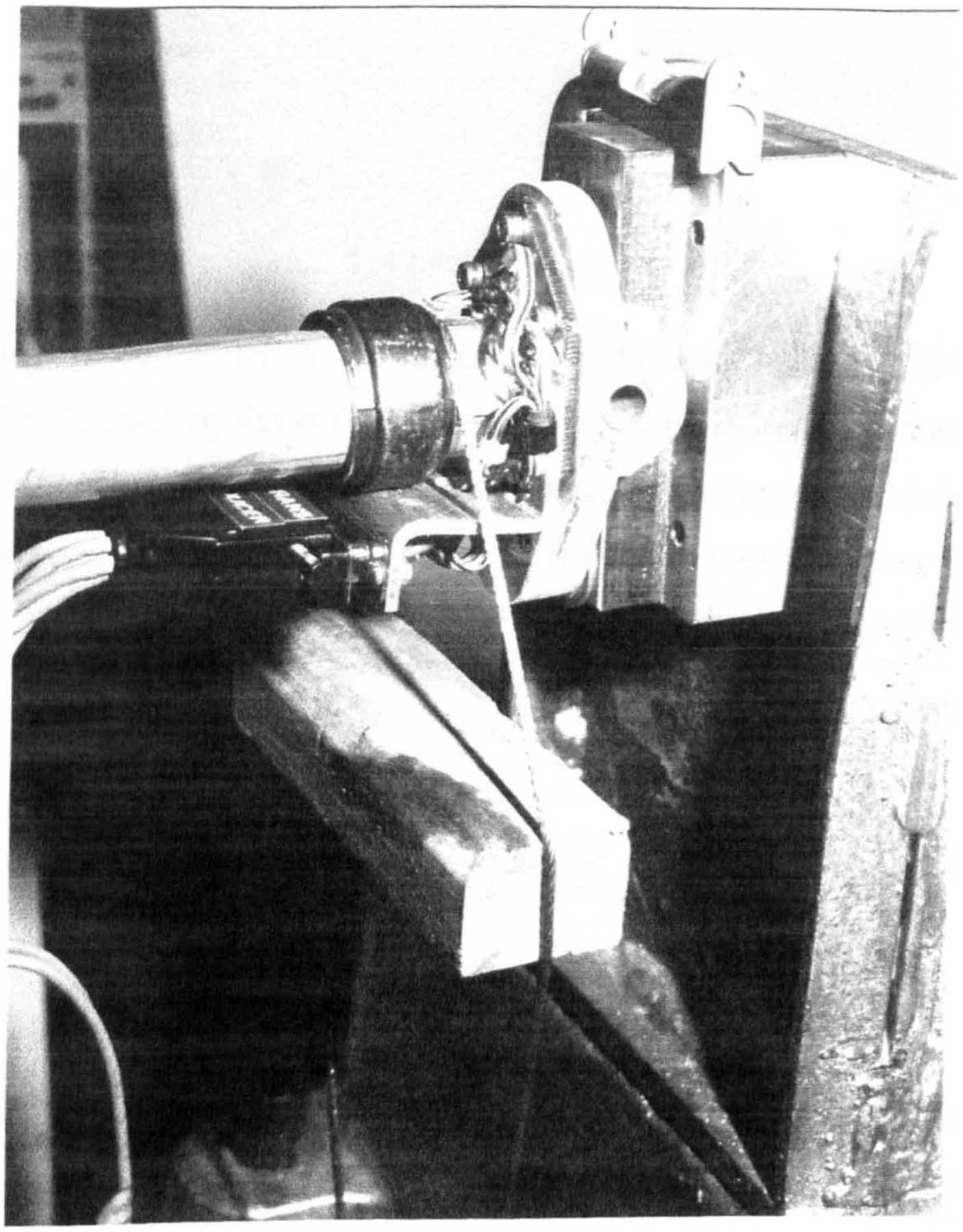

Figure 6.3: The set up for shear force Fx positive calibration. To avoid any friction between the steel cable and the plug of the transducer, a complementary piece of wood was fitted as shown in figure 6.3a to push away the steel cable from the bracket of the plug.

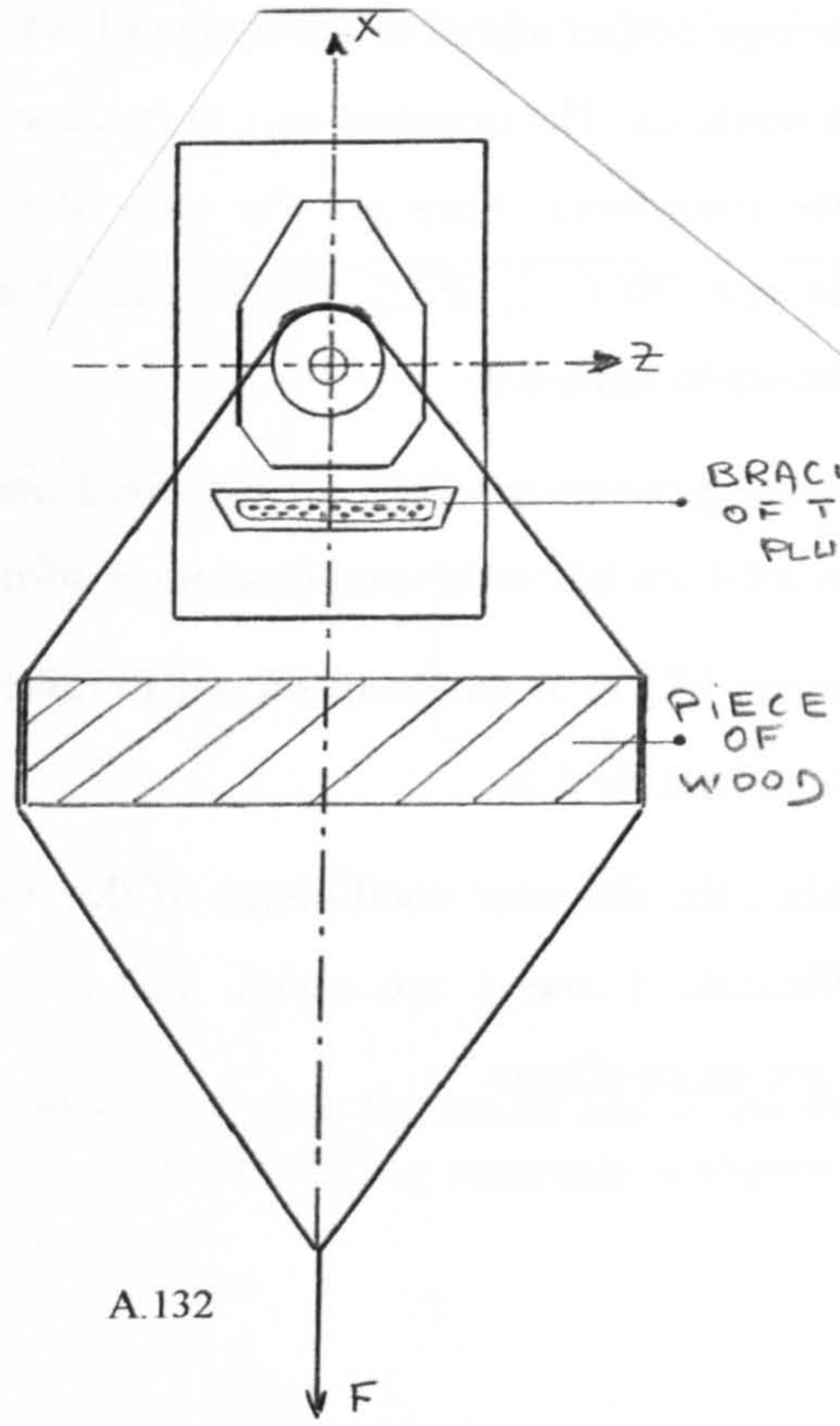

Figure 6.3a: Detail of the set up for shear force Fx positive calibration.

Units are those of the inverted matrix $[M]^{-1}$ and it is easy to understand that, at this stage, the index notation for i and j can be interchanged without any risk of errors, so:

$$c_{ij} = \left(m_{ij}\right)^{-1} = \frac{(N)_j}{(mV)_i} \qquad c_{ij} = \left(m_{ij}\right)^{-1} = \frac{(Nm)_j}{(mV)_i} \tag{6.15}$$

or

$$c_{ij} = \left(m_{ij}\right)^{-1} = \frac{(N)_j}{(cu)_i} \qquad c_{ij} = \left(m_{ij}\right)^{-1} = \frac{(Nm)_j}{(cu)_i} \tag{6.16}$$

When all is said and done, the final step for calibrating a transducer is to build up the calibration matrix, i.e., studying 36 graphs and finding 36 coefficients, six for each of the six loading configurations. These coefficients are the slopes of the linear regression lines, therefore, in the following section 6.6.2, a discussion about statistical linear regression analysis will be undertaken. However, before this stage, a study of the raw data and raw calibration curves is necessary to detect:

- any lack of repeatability, linearity, and hysteresis;
- any drift or creep.

6.3 DESCRIPTION OF TESTS

In a previous section, the importance of applying one load component only during calibration was noted. This is why, in all tests, we used the dead-weight technique. Solomonidis (1989) and Magnissalis (1992) recommend this method rather then a loading machine such as an Instron®. These researchers proved that Instron® technique introduces undesirable and unquantifiable friction effects, which put the accuracy of some tests under question. Moreover, Bray *et al.* (1990, p. 260-261) have established a hierarchy based on the values of measurement uncertainty currently observed in different types of machines. They found that dead-weight machines (with a relative uncertainty of 2 to $5 * 10^{-5}$) will occupy the first place then dead-weight lever- or hydraulic-amplification machines (uncertainty of 1 to $5 * 10^{-4}$)

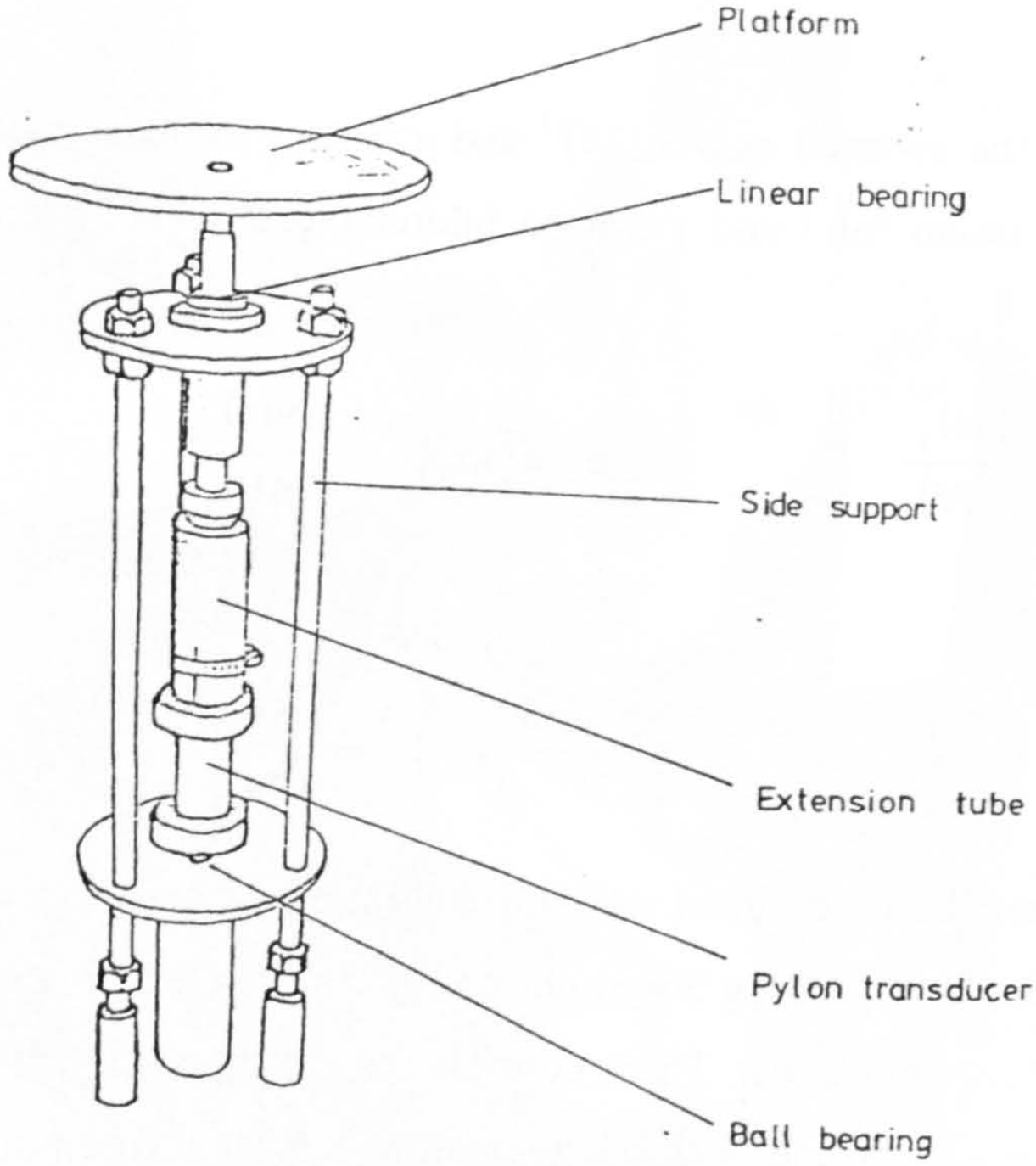

Figure 6.4: Axial Load weight-carrier (from Lowe, 1969)

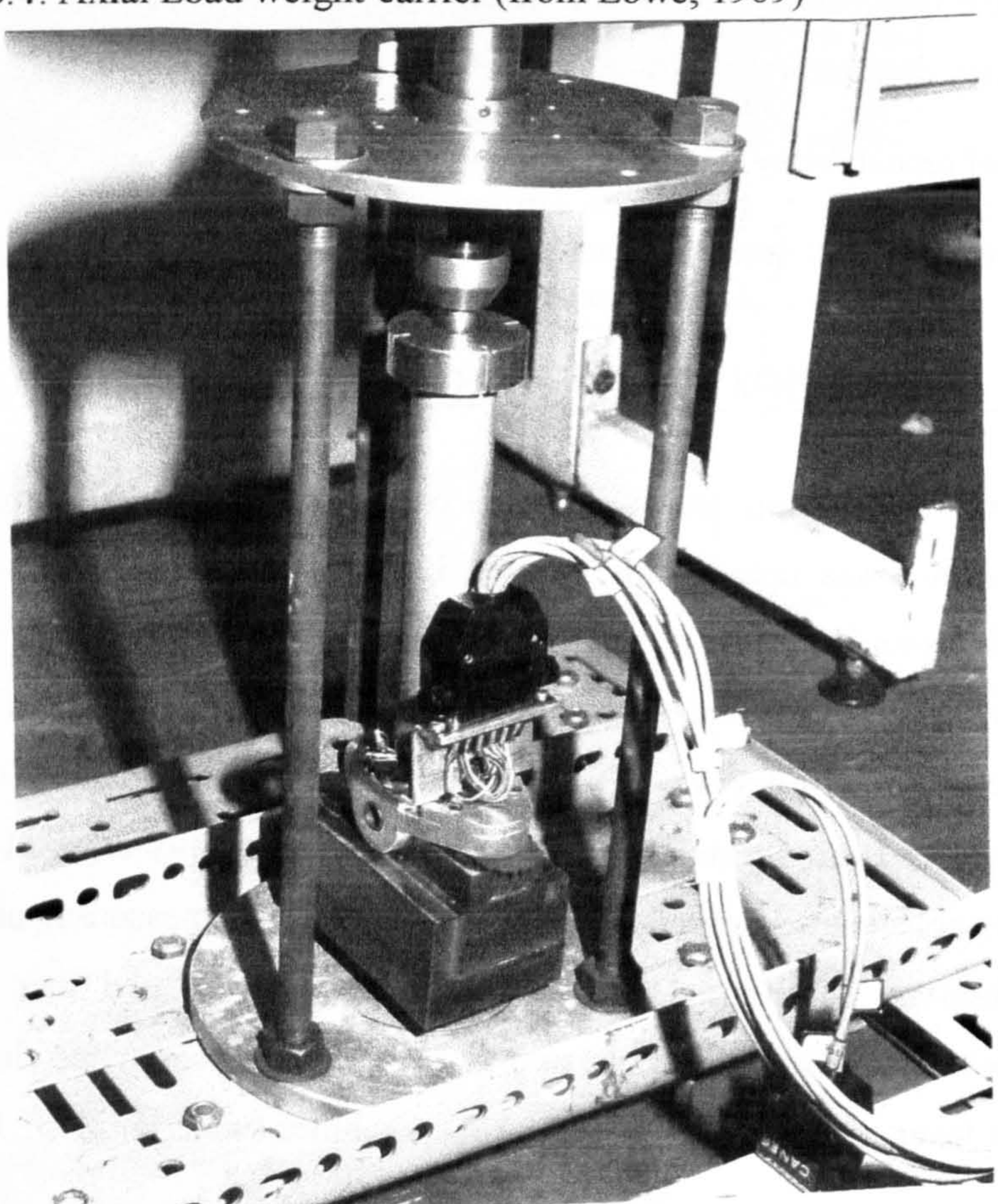

Figure 6.5: The set-up for axial load calibration adapted for the purpose

follow, and finally materials testing machines will be found at the bottom, with an uncertainty ranging from 0.5% to 1% and 2% with normal machines.

The individual set-up designed and built for each loading case is reported as follows:

6.3.1 Shear Force Fx and Fz

The principle described by Grant-Thomson (1977) and Lawes (1982) was used. The full description of the set-up has been given in a previous chapter (see sections 3.5.3 and 4.4). The bell that covers the transducer was used as a re-entrant drum. The pure shear force was applied by means of suspended weights. The positioning of the steel-cable on the plane crossing the four Fx or Fz shear force gauges attempted to eliminate almost all bending moments as shown in figure 6.1. However, the associated small bending moments were not equal to zero. They are respectively:

Mz in the Fx set-up

Mx in the Fz configuration.

The lever arm was the distance between the steel wire location and the bending gauges' centre line plane, i.e. 0.011 m, as shown in figure 6.2. This lever arm was equivalent in both set ups (shear forces Fx and Fz). At the maximum test load, this gave a non-unimportant bending moment. Its importance and how to use it as an interaction effect will be seen in the following section.

In Fx shear, weights were suspended along the X axis and gave a combination of Fx shear force and Mz bending moment.

In Fz shear, weights were suspended along the Z axis and gave a combination of Fz shear force and Mx bending moment.

The apparatus was securely attached on the heavy table, which was described previously. It was most important that the set-up be as rigid as possible. Axis positions, mainly X-axis and Z-axis, were carefully checked by means of a spirit level and a plumbline. The set-up is shown in figure 6.3.

When the set-up was correctly assembled, the amplifier box was switched on, and a 10 minutes wait was necessary until zero drifting had stopped while a

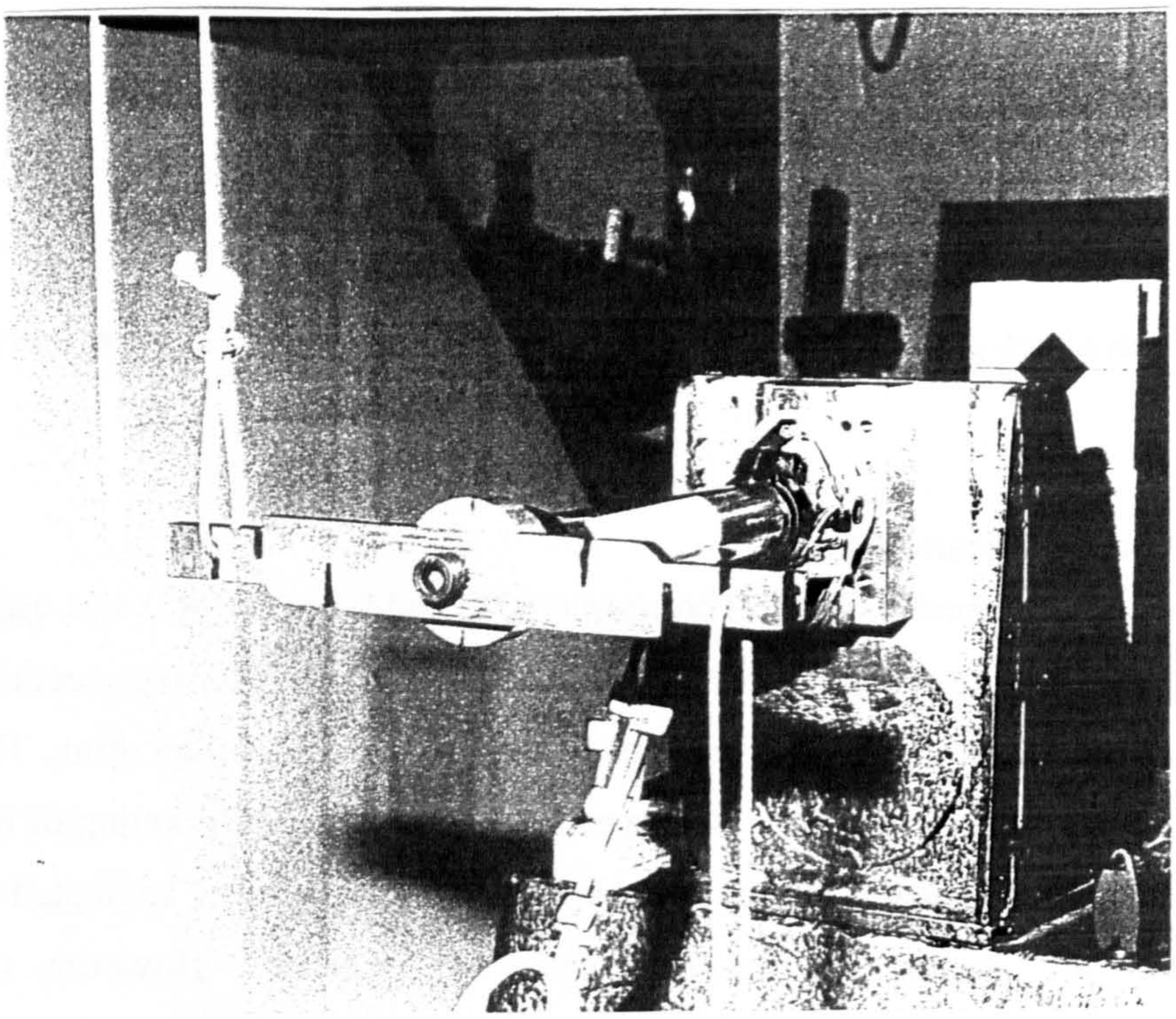

Figure 6.6: The set up for transverse torque calibration

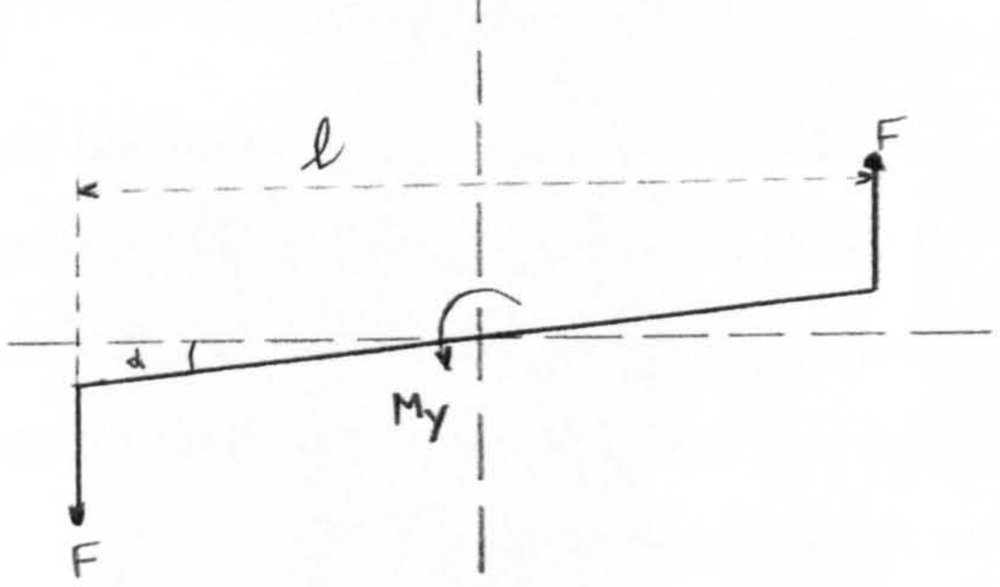

Figure 6.7a: My = 2Flcosα

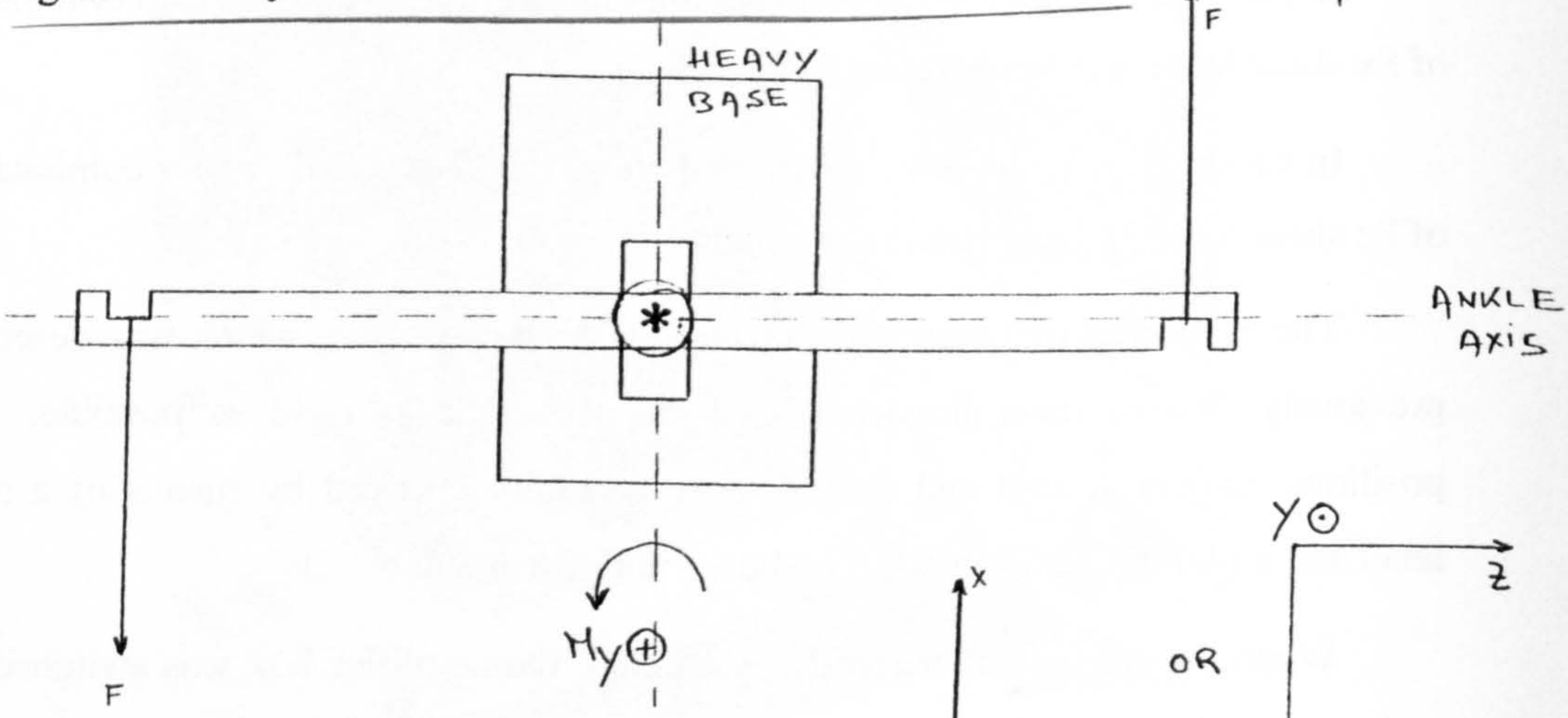

Figure 6.7: Transverse torque (My) calibration

stabilised temperature was developed between gauges and mounting surface. The bridges were then balanced. Offsets were controlled and values were adjusted at a level of 2000 computer units which was the zero level balance (see description of Acquire data capture program in chapter 5). The stability was re-checked. Tests were now carried out by a putting series of suspended weights on the cable by means of a weight-carrier. Exactly as it was done for the first transducer (Model I, see section 3.5), at each loading condition, the six output signals were recorded for eleven seconds at the sampling frequency of 1 Hz to be sure of having a stabilised signal. When the loading cycle was at its maximum, a five minutes period was allowed and a new recording was made at the end of it. This procedure was used to detect any possible creep. Then an unloading cycle was performed going back to zero.

The loading-unloading cycle was then repeated twice the first day and twice the following day. Between these two series of tests, the set-up was dismantled to avoid possible repetition of the setting error. At the end of each test, any zero drift was recorded and the amplifier output re-zeroed. When the four tests were completed, the data were manipulated according to a procedure described in section 6.4.

A 90° rotation of the transducer was necessary to change the loading from Fx to Fz. At each new position, all the procedures were fully repeated. When the transducer was positioned in one direction, it was necessary to rotate it by 180° to make Fx positive and Fx negative then Fz positive and negative, i.e., rotating the transducer with respect to the loading tube allowed calibration in both positive and negative directions. A total of sixteen tests were performed, four for each configuration. All results are shown in appendix 11.VI.1.

6.3.2 Axial Load Calibration Fy

As for the first transducer (Model I, see section 3.5.3), the device shown in figure 6.4, first reported by Lowe (1969) was used. This device has been used by many researchers who used the dead-weights method for calibrating transducers (Lovely, 1981; Lawes, 1982 and Pashalides, 1989). It is only necessary to remind the reader that loads were applied by means of weights on the top platform disc,

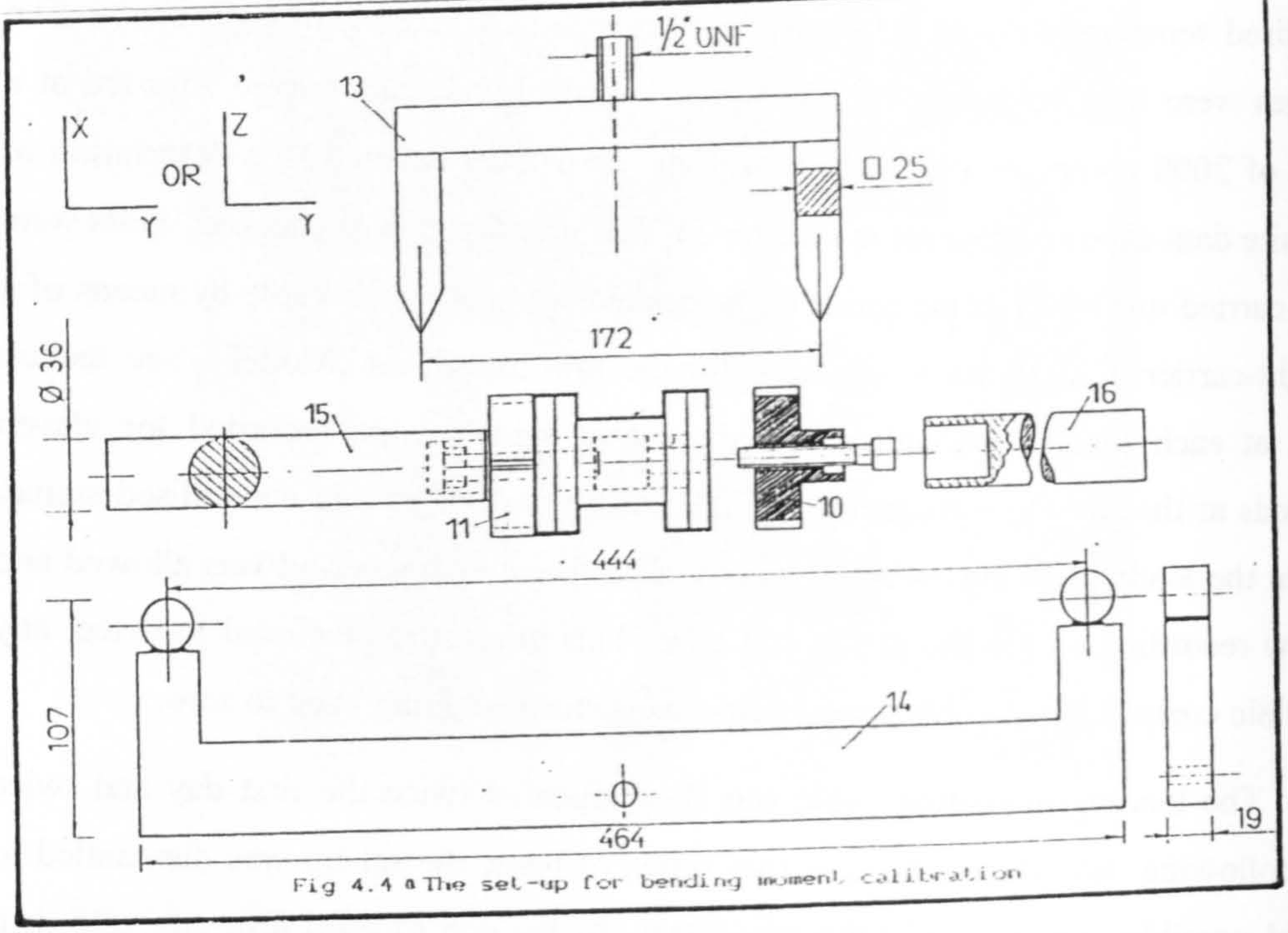

Figure 6.8: The four points configuration for bending moments
(extracted from Magnissalis, 1992)

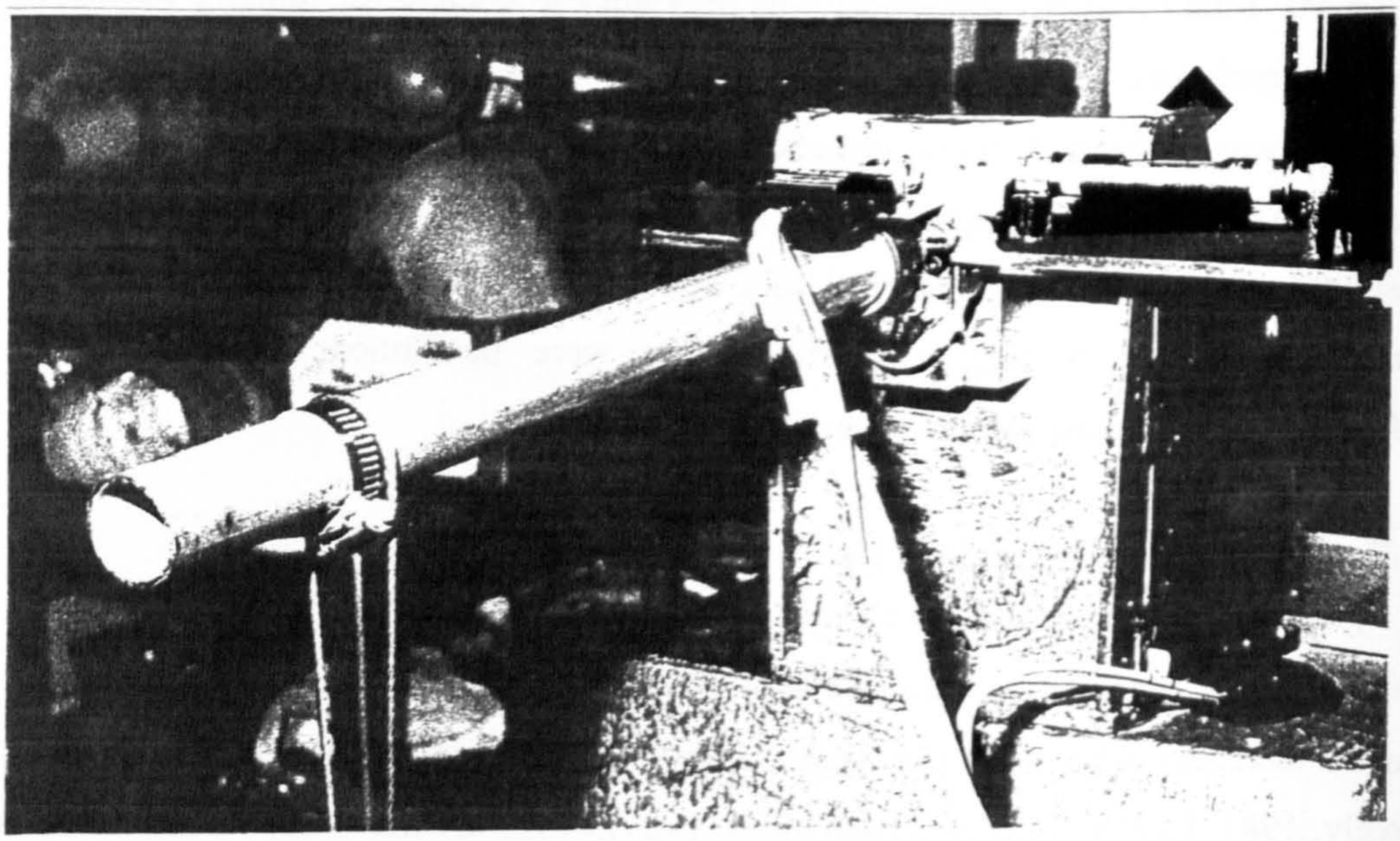

Figure 6.9: The set up for bending moment calibration (Mz positive: Dorsiflexion)

resulting in compression of the transducer. Location of the line of action of the load with a minimum uncertainty was mandatory, if even only moderately accurate results were aimed at. This location of loading points was guaranteed by the use of steel balls at both interfaces between the transducer and the device. This convenient ball-and-socket device set up for load application was also used by Dubois *et al.* (1980) calibrating the ONERA 300 kN multicomponent dynamometer, quoted by Bray *et al.* (1990). The set-up is shown in figure 6.5. The test procedure was the same as for shear force except for the loading progression. The maximum load was 1039.4 N. As above, four tests were conducted in two successive days and the results are shown in appendix 11.VI.2.

6.3.3 Transverse Torque Calibration My

The description of the torque set-up is shown in section 4.6.1.4. Using the set-up shown in figure 6.6 and described in figure 6.7: the transducer was securely fitted on the heavy table and a specially machined bar applies the torque by means of a system of pulleys and cables. The components had to be controlled accurately by means of a plumbline to avoid any Mx bending moment or Fy axial load. Magnissalis (1992) noted that due to friction in the path followed by the cable through the pulley, the two branches of the cable did not eventually transmit the same force. The one, which was directly connected to the transverse bar, transmits a greater force. Therefore, the pulley introduced some errors in load values, owing to cable bending and bearing friction. No attempt was made to overcome this problem of friction. Bray *et al.* (1990) stated that keeping the load uncertainty below 1 % might not be easy. Weights must be equal in order to provide a zero shear load. It is necessary to tighten securely the bar onto the tube at the top of the transducer to avoid any rotation of the bar. This could introduce some error in My calculation since angles between cables and bar may not be 90°. This is why it was very important to check the horizontality of the bar by means of a spirit level at each successive loading step, to maintain the cosine of the angle α equal to one (see figure 6.7 and equation 6.17). This is why, also, it was impossible to go higher than 10.7 N m in applied torque. That is the middle of the maximum value — about 20 N m — (ISO 10328-4, 1993) usually observed in amputee tests with very active transfemoral

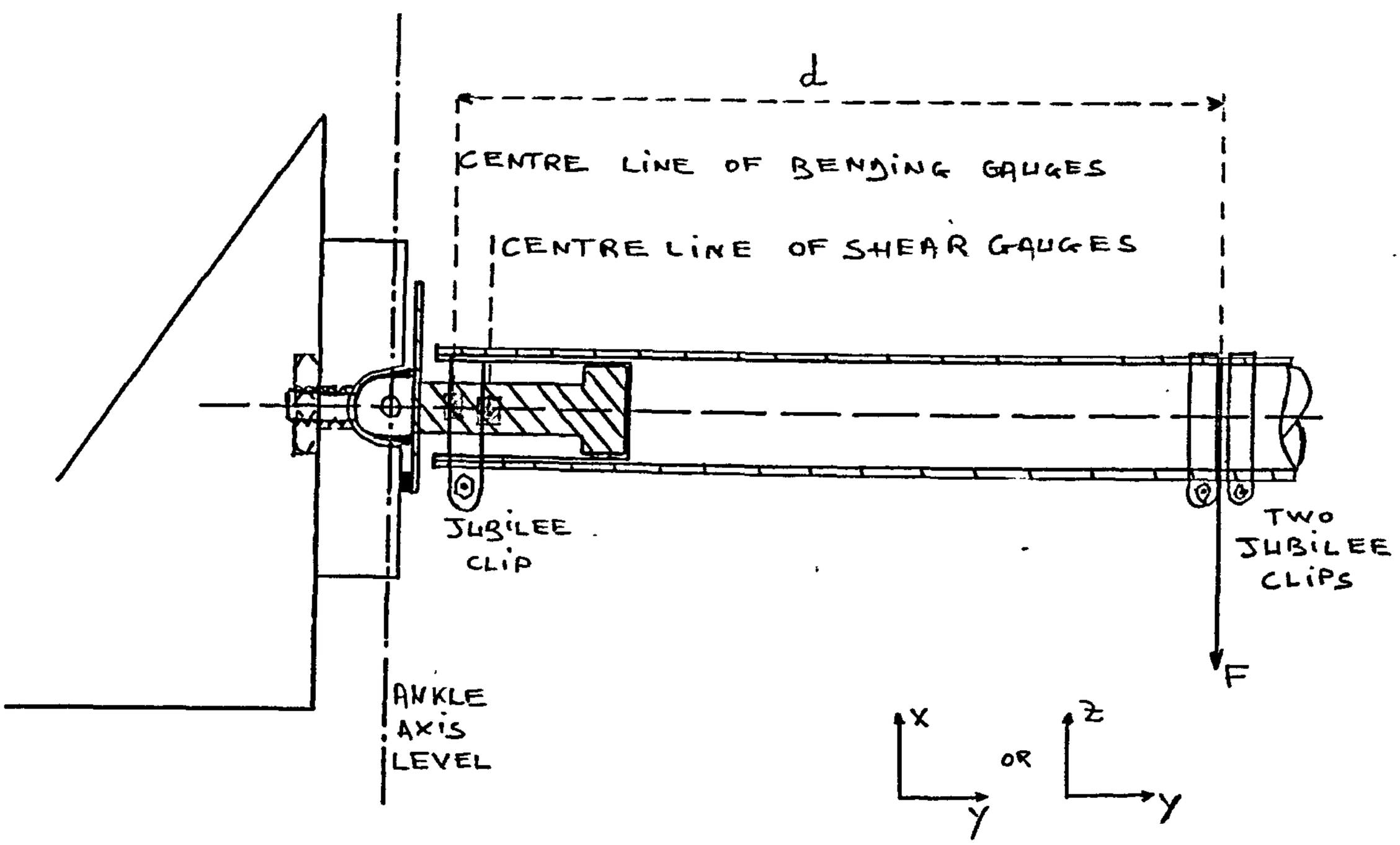

Bending Moment = F.d

Shear force = F

Figure 6.10: Combined Mz bending moment and Fx shear force.

subjects (Pashalides, 1989). However, 10.7 N m seemed high enough for an accurate calibration according to Lawes (1982), particularly for elderly PVD recent amputees tested in this work. The loading procedure was the same for My negative and My positive. The lever arm for calculating the applied torque was 0.1 m, (i.e.: l = 0.1 m, see fig. 6.7), hence:

$$\text{Applied Torque in N m} = (\text{Applied Load in N}) * l\,(\text{in m}) * \cos\alpha \quad (6.17)$$

As above, in each situation, four tests were made in different days. The complete results of the tests performed are given in appendix 11.VI.3.

6.3.4 Bending Moments Calibration Mx and Mz

For bending moments calibration, there are two solutions: the first one concerns the application of a pure bending moment to a pylon transducer. Cunningham & Brown (1952) and Grant-Thomson (1977) used it and more recently, it was used by Magnissalis (1993) with an Instron® mechanical testing machine. This technique was a four point loading configuration, which gives a pure bending moment in the middle section. It is shown in figure 6.8, extracted from Magnissalis (1992). The second method for performing this calibration (but it does not produce a pure bending moment, see section 6.4.4.1) was more widely used. It was a cantilever configuration (Lowe, 1969; Lovely, 1981; Lawes, 1982; Pashalides, 1989), a full description is given in section 6.4.4. Jones (1976) used both methods: cantilever loading for a long pylon and four points loading for a short pylon. Both methods are acceptable and produce identical results (Lovely 1981).

A similar set-up as that for shear force calibration was used. An aluminium shin tube, identical to a prosthetic shank tube, was fitted at one end of the transducer onto the re-entrant bell while the other end of the transducer was securely screwed on the heavy bench table. The horizontality of the axis (Fy and Fz for A/P bending moment; Fy and Fx for M/L bending moment) was accurately checked by means of a spirit level. That gave a cantilever system. The weights were suspended by means of a cable and a weight-carrier as shown in figure 6.9. This method of loading applied a combined shear force and bending moment. This introduces two unknown factors in each calibration equation. Therefore, having two loading combinations utilising two

Pure Shear	Force	Positive		Main	Channel	Fx			
Load applied									
along X axis		*MEAN*	*MEDIAN*	*1/2 SD*	*CONFIDENCE*	*MEAN*	*MEDIAN*	*1/2 SD*	*CONFIDENCE*
at 0.0355 m		*4*			*INTERVALS*	*4*			*INTERVALS*
from ankle axis		*tests*			*LEVEL*	*tests*			*LEVEL*
					95%				*95%*
Loading mass	Loading								
kg	N	**SFx**				**SFy**			
0.0	0.0	2001.3	2001.3	0.4041	0.3961	1999.2	1999.1	0.5916	0.5798
0.8	7.6	2002.2	2002.3	0.4349	0.4262	1998.9	1998.9	0.8185	0.8021
9.8	96.6	2016.3	2016.3	0.4509	0.4419	1999.1	1999.2	1.3077	1.2815
18.9	185.5	2030.3	2030.2	0.4796	0.4700	1998.9	1998.9	1.6176	1.5852
28.0	274.5	2044.5	2044.4	0.5909	0.5791	1999.2	1999.1	1.5130	1.4827
37.1	363.5	2058.4	2058.4	0.4655	0.4562	1999.8	1999.7	1.4765	1.4469
46.1	452.5	2072.8	2072.9	0.3862	0.3785	1999.7	1999.7	1.5406	1.5097
46.1	452.5	2072.8	2072.9	0.3862	0.3785	1999.7	1999.7	1.5406	1.5097
37.1	363.5	2058.6	2058.7	0.5188	0.5084	1999.1	1999.0	1.7597	1.7245
28.0	274.5	2044.5	2044.5	0.4031	0.3950	1998.5	1998.6	1.7173	1.6829
18.9	185.5	2030.4	2030.4	0.5228	0.5123	1998.3	1998.3	1.7935	1.7576
9.8	96.6	2016.4	2016.4	0.5228	0.5123	1997.9	1997.9	1.7991	1.7631
0.8	7.6	2002.3	2002.3	0.5354	0.5247	1997.4	1997.4	2.1432	2.1003
0.0	0.0	2001.2	2001.1	0.5315	0.5209	1997.2	1997.2	2.4116	2.3633
		MEAN	*MEDIAN*	*1/2 SD*	*CONFIDENCE*	*MEAN*	*MEDIAN*	*1/2 SD*	*CONFIDENCE*
		4			*INTERVALS*	*4*			*INTERVALS*
		tests			*LEVEL*	*tests*			*LEVEL*
Loading mass	Loading				*95%*				*95%*
kg	N	**SFz**				**SMx**			
0.0	0.0	1998.7	1998.8	1.4095	1.3813	2000.1	1999.9	0.3500	0.3430
0.8	7.6	1998.7	1998.8	1.2806	1.2550	2000.2	2000.2	0.2986	0.2926
9.8	96.6	1998.7	1998.6	1.2261	1.2016	1999.9	1999.7	0.5679	0.5565
18.9	185.5	1998.7	1998.6	1.4259	1.3974	1999.5	1999.5	0.2944	0.2885
28.0	274.5	1998.8	1998.6	1.3988	1.3708	1999.3	1999.2	0.4796	0.4700
37.1	363.5	1998.8	1998.8	1.3525	1.3254	1998.7	1998.8	0.6000	0.5880
46.1	452.5	1999.1	1998.9	1.5716	1.5402	1998.0	1998.0	0.7365	0.7218
46.1	452.5	1999.1	1998.9	1.5716	1.5402	1998.0	1998.0	0.7365	0.7218
37.1	363.5	1999.1	1999.1	1.4434	1.4145	1998.6	1998.6	0.5228	0.5123
28.0	274.5	1998.8	1998.6	1.2275	1.2029	1999.2	1999.2	0.7228	0.7084
18.9	185.5	1999.0	1998.8	1.2675	1.2422	1999.4	1999.3	0.3403	0.3335
9.8	96.6	1999.1	1999.0	1.4408	1.4119	1999.9	1999.9	0.3317	0.3250
0.8	7.6	1998.8	1998.8	1.4818	1.4522	2000.1	2000.1	0.4031	0.3950
0.0	0.0	1998.8	1998.8	1.4491	1.4201	2000.1	2000.1	0.3162	0.3099
		MEAN	*MEDIAN*	*1/2 SD*	*CONFIDENCE*	*MEAN*	*MEDIAN*	*1/2 SD*	*CONFIDENCE*
		4			*INTERVALS*	*4*			*INTERVALS*
		tests			*LEVEL*	*tests*			*LEVEL*
Loading mass	Loading				*95%*				*95%*
kg	N	**SMy**				**SMz**			
0.0	0.0	1999.3	1999.3	0.2062	0.2020	2000.9	2000.9	0.1633	0.1600
0.8	7.6	1999.1	1999.1	0.2646	0.2593	2001.3	2001.2	0.2517	0.2466
9.8	96.6	1999.8	1999.5	2.6671	2.6137	2007.4	2007.4	0.2082	0.2040
18.9	185.5	1999.4	1999.2	2.7379	2.6830	2013.4	2013.4	0.1708	0.1674
28.0	274.5	1998.7	1998.9	2.0320	1.9914	2019.4	2019.3	0.3775	0.3699
37.1	363.5	1999.0	1998.8	1.4364	1.4077	2025.3	2025.3	0.2872	0.2815
46.1	452.5	1999.1	1998.7	1.6217	1.5893	2031.8	2031.8	0.2646	0.2593
46.1	452.5	1999.1	1998.7	1.6217	1.5893	2031.8	2031.8	0.2646	0.2593
37.1	363.5	1998.7	1998.4	1.3429	1.3160	2025.5	2025.6	0.2828	0.2772
28.0	274.5	1998.7	1998.2	1.6543	1.6212	2019.4	2019.4	0.3304	0.3238
18.9	185.5	1998.8	1998.4	1.5979	1.5659	2013.2	2013.2	0.2160	0.2117
9.8	96.6	1999.1	1999.1	0.2630	0.2577	2007.4	2007.4	0.1291	0.1265
0.8	7.6	1999.4	1999.4	0.3416	0.3347	2001.1	2001.1	0.2062	0.2020
0.0	0.0	1999.3	1999.4	0.3162	0.3099	2000.6	2000.6	0.3403	0.3335

Table 6.6: Raw data, simultaneously recorded in the six channels when positive A/P shear forces were applied, with descriptive statistics.

cantilever lengths were necessary to have a set of two equations with two unknown quantities, easy to solve. The weights were suspended by means of a steel cable at a distance of 0.2 m and 0.3 m from the bottom flange of the transducer which was precisely $d_1 = 0.215$ m and $d_2 = 0.315$ m from the ankle axis. These distances d_1 and d_2 were meticulously measured. To be sure that the steel cable was always at the proper location, avoiding any slipping, distances d_1 and d_2 were marked out by means of two jubilee clips (only one is shown in figure 6.9). These lever arms were chosen arbitrarily. This gave a combination of Fx-Mz and Fz-Mx for both bending and shear. In each combination, the shear force remained constant because it was independent of the moment arm, bending moments alone were changing.

For combined Fx and Mz calibration, the weight was suspended along the X axis of the transducer as it is shown in figure 6.10. From equation 6.4, the six output signals could be expressed as:

$$SMz_1 = m_{61}Fx + m_{62}Fy + m_{63}Fz + m_{64}Mx + m_{65}My + m_{66}Mz_1$$

$$SMz_2 = m_{61}Fx + m_{62}Fy + m_{63}Fz + m_{64}Mx + m_{65}My + m_{66}Mz_2 \qquad (6.18)$$

where Mz_1 and Mz_2 were respectively the bending moments Mz corresponding to levels $d_1 = 0.215$ m and $d_2 = 0.315$ m.

For combined Fz and Mx calibration:

$$SMx_1 = m_{41}Fx + m_{42}Fy + m_{43}Fz + m_{44}Mx_1 + m_{45}My + m_{46}Mz$$

$$SMx_2 = m_{41}Fx + m_{42}Fy + m_{43}Fz + m_{44}Mx_2 + m_{45}My + m_{46}Mz \qquad (6.19)$$

where Mx_1 and Mx_2 were respectively the bending moment Mx corresponding to levels $d_1 = 0.215$ m and $d_2 = 0.315$ m. All the results are shown in appendix 11.VI.4.

6.4 RAW DATA STUDIES IN EACH LOADING CASE

Before any statistical analysis could be performed, it was necessary to make an in-depth study of raw data and raw calibration curves. This procedure was necessary in order to quantify any possible lack of repeatability and / or combined errors in linearity and hysteresis.

Maximum Load Applied	SFx	SFy	SFz	SMx	SMy	SMz
452.46 N	72.1	0.3	0.7	1.4	1.6	32.2

Table 6.7: In A/P shear force Fx (main channel), the difference in computer units between no loading and maximum loading, with an average calculation between SFx + and SFx - results (mean raw data from 4 tests).

SFx	0.159 cu	for 1 N Gain 400
	$0.398\ 10^{-3}$ cu	for 1 N Gain 1
	$0.971\ 10^{-3}$ mV	for 1 N Gain 1

SFx	6.27 N	for 1 cu Gain 400
	$1.56 * 10^{-2}$ N	for 1 cu Gain 1
	$0.64 * 10^{-2}$ N	for 1 mV Gain 1

Table 6.8: The results from A/P shear force Fx (main channel) expressed in computer units (cu) per N, Gain 1 (top) or in N per cu, Gain 1 (bottom), using the results found after the calibration study of each channel respectively.

	Fx	Fy	Fz	Mx	My	Mz
Fx	**452.5 N**	1.7 N	4.6 N	0.06 N.m	0.04 N.m	4.2 N.m

Table 6.9: From A/P shear force Fx (main channel, bold letters), the apparent loads when a shear force of 452.5 N was applied.

SMz	6.47 cu	for 1 N.m Gain 100
	$6.47\ 10^{-2}$ cu	for 1 N.m Gain 1
	$15.8\ 10^{-2}$ mV	for 1 N.m Gain 1

SMz	0.13 N.m	for 1 cu Gain 100
	$0.13\ 10^{-2}$ N.m	for 1 cu Gain 1
	$5.3\ 10^{-4}$ N.m	for 1 mV Gain 1

Table 6.10: The results of A/P bending moment from A/P shear force Fx (main channel) expressed in cu or mV per N.m (top) or in N.m per cu or mV (bottom).

6.4.1 Shear force Fx

Table 6.6 shows the calibration data obtained in averaging four tests in positive Fx shear force. This table is only presented as a sample for all the channels (Fx to Mz). All results and tables are shown in appendixes 11.VI.1 to 11.VI.4. The table presents data in columns, which are respectively:

- loading mass in kilograms;
- loading forces in N representing the Fx loading schedule (1 kg = 9.81 N);
- the six mean output signals in computer units: SFx, SFy, SFz, SMx, SMy, SMz; followed by columns of descriptive statistics such as the median which should be as close to the mean as possible to have a symmetrical data distribution, the standard deviation which should be as small as possible, i.e. raw values are ± ½ standard deviation and finally the confidence intervals at the level of 95 % which should also be as small as possible and at least inferior to the exhibited standard deviation (Weiss, 1995, p. 414).

The main channel is the first column SFx. The other columns are cross-effects.

The difference in computer units between no-load and maximum load is shown in table 6.7. For the maximum values, an averaged calculation between Fx negative and positive was calculated (see 11.VI.1).

Indeed, the four cross-effects SFy, SFz, SMx and SMy had a low value (for example: 0.97 % between SFx and SFz, these two channels having the same gain). It was possible to liken them to noise but a statistical analysis should be performed later to conclude at which level of cross-effects they were.

Regarding the sixth channel SMz, its response was relatively high because the shear force set-up forms a cantilever design. Later, it should be necessary to take into account this important interaction.

It was possible to study the sensitivity of both Fx and Mz channels. Moreover, it should be interesting later to compare the Mz sensitivity in the present combination and the one having Mz as main channel (see section 6.4.6.1). For a load of 452.47 N and a gain of 400, SFx was 72.09 computer units. Having 2.442 mV for one

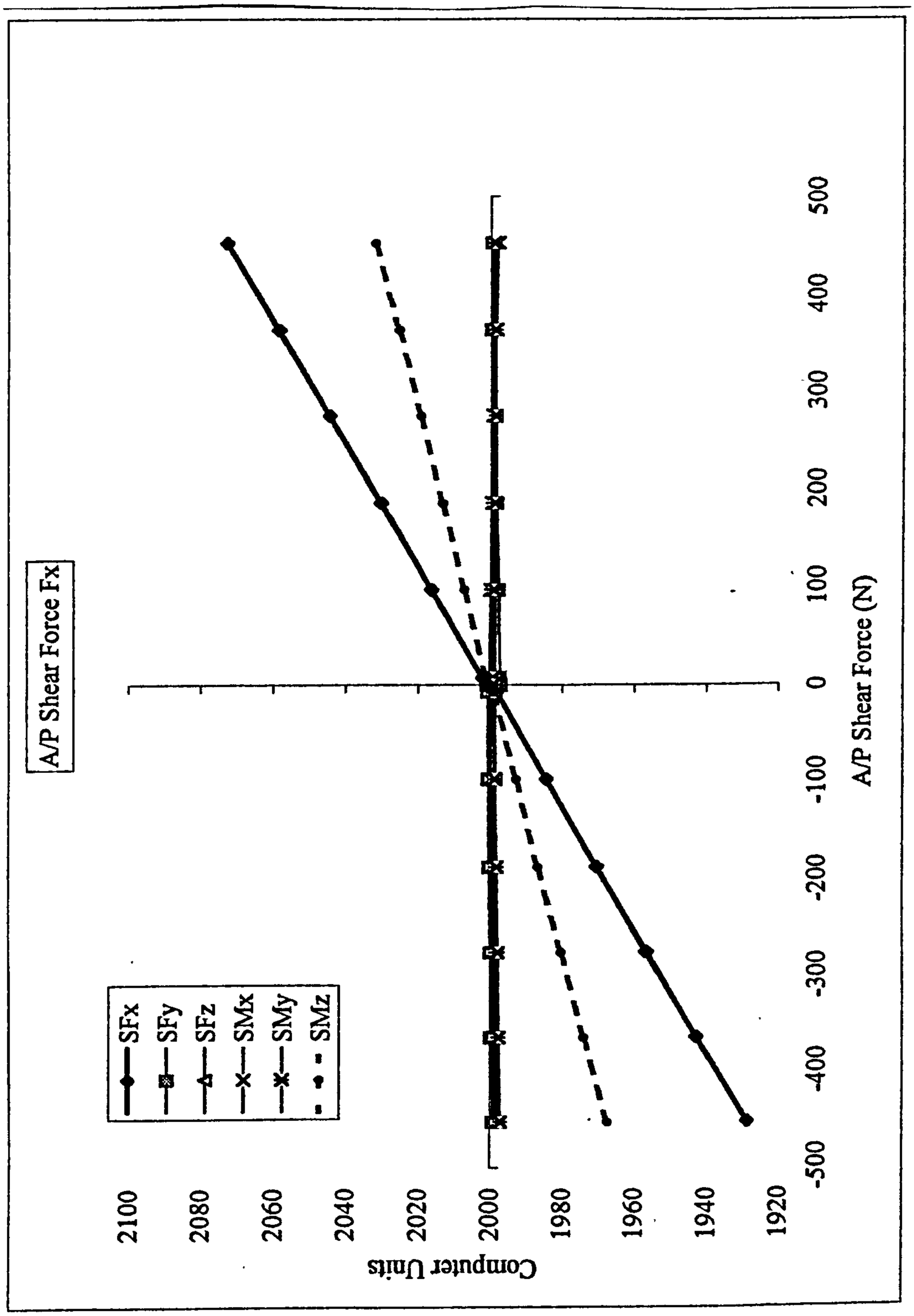

Figure 6.11: Pure A/P shear force Fx (main channel) with the associate A/P bending moment Mz and the corresponding four cross-effects (mean raw data from 4 tests).

computer unit, it was possible to express the results relative to 1 N with a gain of 1 in both computer units and millivolts. This could be shown comparing force versus computer units or millivolts as shown in table 6.8.

Having raw data for a unity of applied force and gain 1 allows comparing the sensitivity of different transducers: section 6.6.4 shows such a comparison between the Villiers Pylon Transducer and the Strathclyde Pylon Transducer.

This method also allowed the comparison of cross-effects in N of the two forces — Fx being the main channel in bold letter — and N m, the two bending moments Mx and Mz plus torque My, using results found after the calibration study of each channel respectively (see table 6.9).

For a load of 452.47 N multiplied by the lever arm which was 0.011 m (distance between the centre line of shear gauges and the centre line of bending gauges), the Mz bending moment was 4.97 N m, relatively close to 4.2 N m found using the Mz calibration results (see section 6.4.6). For a gain of 100, SMz is 32.185 computer units.

Hence, the results of such an A/P bending moment Mz channel when an A/P shear force was applied are shown in table 6.10, with the appropriate units. These values will be discussed later in the section concerning Mz bending moment calibration (see section 6.4.6).

It is now necessary to study plots of graphs of Fx raw data. For all channels, the graph, shown in figure 6.11, indicates four important properties of the transducer in that main channel Fx:

1. linearity: all curves are straight lines both when loading and unloading;

2. no hysteresis: i.e., when a loading-unloading cycle is made, the increasing and decreasing curves are exactly superimposed;

3. no drifting at maximum load and all curves return to zero

4. adequate repeatability that it is possible to check plotting the four tests on the same graph. All curves of each test are superimposed on one another.

Maximum Load Applied	SFx	SFy	SFz	SMx	SMy	SMz
1039.37 N	1.15	184.02	3.2	2.48	1.63	11.73

Table 6.11: In axial load Fy (main channel), the difference in computer units between no loading and maximum loading (mean raw data from 4 tests).

SFy	0.177 cu	for 1 N Gain 1000
	$0.177 * 10^{-3}$ cu	for 1 N Gain 1
	$0.432 * 10^{-3}$ mV	for 1 N Gain 1

SFy	5.64 N	for 1 cu Gain 1000
	$5.64 * 10^{-3}$ N	for 1 cu Gain 1
	$2.31 * 10^{-3}$ N	for 1 mV Gain 1

Table 6.12: The results from axial load Fy (main channel) expressed in computer units (cu) per N, Gain 1 (top) or in N per cu or mV, Gain 1 (bottom).

	Fx	Fy	Fz	Mx	My	Mz
Fy	7.2 N	**1039.4 N**	21 N	0.1 N.m	1.63 N.m	1.6 N.m

Table 6.13: From axial load Fy (main channel), the apparent loads when an axial load of 1039.4 N was applied, using the results found after the calibration study of each channel respectively.

6.4.2 Axial Load Fy

The numerical results from this channel are shown in appendix 11.VI.2. They have the same form as table 6.6. The main channel is now column SFy, which is the channel 2.

As was done in the case of Fx, the mean maximum raw data from 4 tests are presented in table 6.11.

The cross-effects for the two shear forces SFx, SFz and the three bending moments SMx, SMy and SMz were very low. Later, it should be possible to confirm this conclusion by a statistical analysis.

For an axial load of 1039.37 N, SFy response in computer units was 184.02, therefore the sensitivity is shown in table 6.12. As above, the comparison between force versus computer units or millivolts is shown in table 6.12.

This allows the comparison of the cross-effects in N, the two shear forces Fx and Fz plus the main channel axial load Fy in bold letter and N m, the two bending moments Mx and Mz plus the transverse torque My (see table 6.13).

Studying plots of axial load raw data, the four important properties expressed in Fx shear force were found again: linearity, lack of hysteresis and drifting with a good repeatability, as shown in figure 6.12.

6.4.3 Shear Force Fz

Exactly in the same way, it was possible to study Fz shear force (all tables are shown in appendix 11.VI.1). The chart, which is now familiar, is shown in table 6.14.

For a shear force Fz of 452.47 N, SFz response in computer units was 68.5. The sensitivity is shown in table 6.15.

It was possible to note that calibration values in Fx and Fz were very close which was logical taking into account that both channels had the same configuration in gauges and bridges. Gauges power supply and amplifier gain settings were also equal.

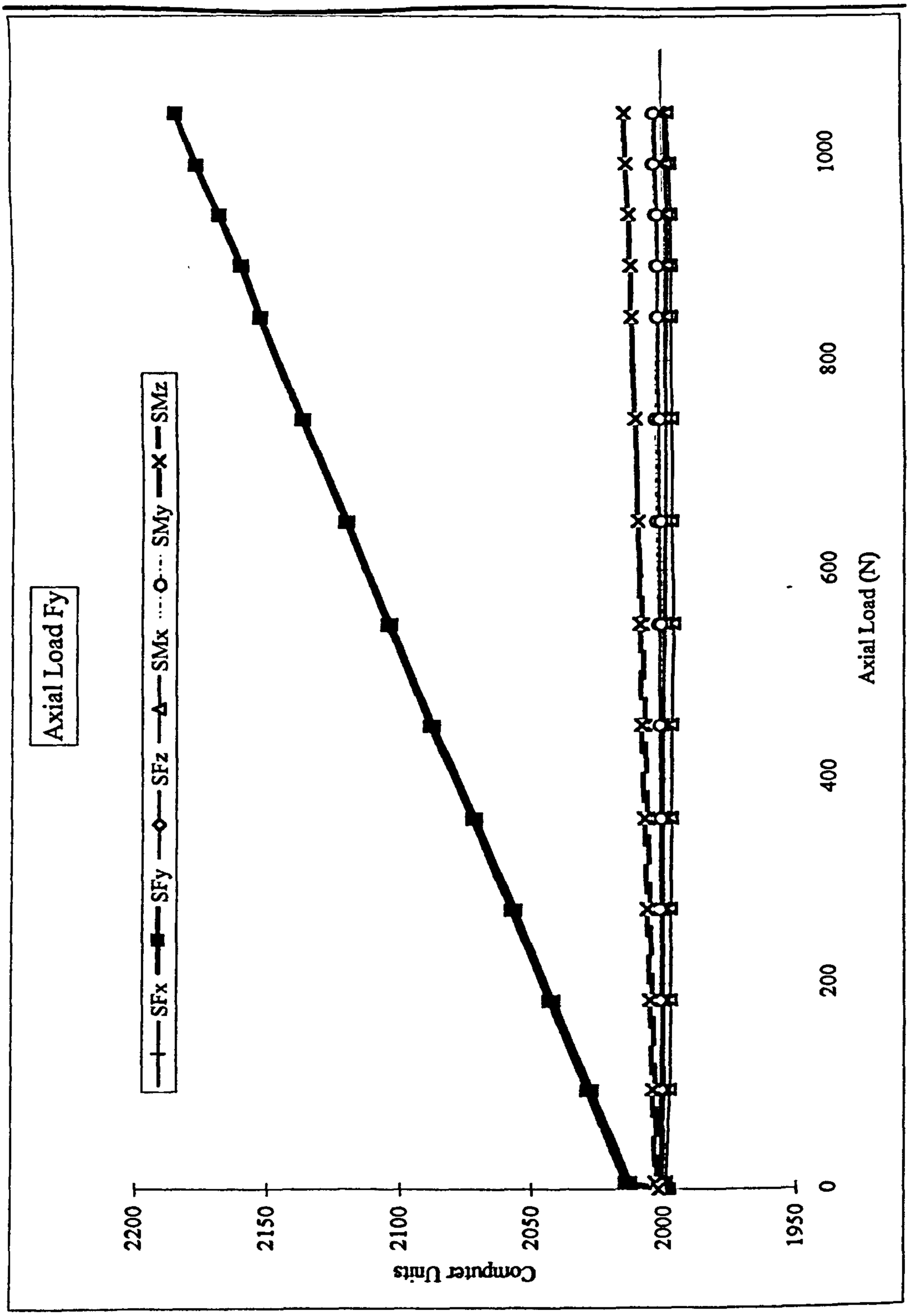

Figure 6.12: Pure Fy axial load main channel and the five corresponding cross-effects (mean raw data from 4 tests).

It was also possible to make a chart of Fz shear force in N versus one computer unit (see table 6.15). It is now possible to compare cross-effects in both N and N m as shown in table 6.16.

The Fz set-up was identical to the Fx one, except that the transducer was rotated ninety degrees about the Y axis. Exactly as above in Fx, Fz shear force, with a load along Z axis, a small bending moment Mx appeared. It was equal to 452.47 N * 0.011 m = 4.97 N m, close to 4.8 N m found using the Mx calibration results (see section 6.4.4). For a gain of 300, SMx response was 104.18 cu as shown in table 6.17. These values will be discussed in section 6.4.4.

It was also important to note that SMx was around three times more than SMz for the same bending moment. This was consistent because gains were three times more: 100 for Mz channel versus 300 for Mx channel.

As above in Fx and Fy, the graphs of all channel curves simultaneously plotted are shown in figure 6.13. It gives same conclusions about properties of the transducer in that particular channel. Gauges give a response whose characteristics are: linearity, no hysteresis, no drift and good repeatability.

6.4.4 Bending Moment Mx

Following the same approach as in other channels, it was possible to study raw data in averaging four tests. The whole set of tables are shown in appendix 11.VI.4: positive and negative bending moments Mx with two different lever arms $d_1 = 0.215$ m and $d_2 = 0.315$ m. Consequently, the third column of each chart is bending moment applied about the X axis. To change from positive value to negative one, it was sufficient to rotate the entire device to 180° around the Y axis.

As in Fx and Fz channels, the Mx cantilever set-up gave a mixing of Fz and Mx. This combination allowed to find the real coefficient for Mx — m_{44} — and Fz — m_{43} — according to the rules defined in the previous section about the cantilever system using equation (6.19).

Maximum Load Applied	SFx	SFy	SFz	SMx	SMy	SMz
452.47 N	0.17	2.42	68.5	104.18	1.28	0.5

Table 6.14: In M/L shear force Fz (main channel), the difference in computer units between no loading and maximum loading, with an average calculation between SFz + and SFz – results (mean raw data from 4 tests).

SFz	0.151 cu	for 1 N Gain 400
	$3.78 * 10^{-4}$ cu	for 1 N Gain 1
	$9.24 * 10^{-4}$ mV	for 1 N Gain 1
SFz	6.61 N	for 1 cu Gain 400
	$1.66 * 10^{-2}$ N	for 1 cu Gain 1
	$0.67 * 10^{-2}$ N	for 1 mV Gain 1

Table 6.15: The results from M/L shear force Fz (main channel) expressed in computer units (cu) per N, Gain 1 (top) or in N per cu or mV, Gain 1 (bottom).

	Fx	Fy	Fz	Mx	My	Mz
Fz	1.1 N	13.6 N	**452.5 N**	4.8 N.m	0.03 N.m	0.06 N.m

Table 6.16: From M/L shear force Fz (main channel), the apparent loads when a shear force of 452.5 N was applied, using the results found after the calibration study of each channel respectively.

SMx	20.9 cu	for 1 N.m Gain 300
	$6.9\ 10^{-2}$ cu	for 1 N.m Gain 1
	$16.8\ 10^{-2}$ mV	for 1 N.m Gain 1
SMx	0.047 N.m	for 1 cu Gain 300
	$1.59\ 10^{-4}$ N.m	for 1 cu Gain 1
	$6.5\ 10^{-5}$ N.m	for 1 mV Gain 1

Table 6.17: The results of M/L bending moment Mx from M/L shear force Fz (main channel) expressed in cu or mV per N.m (top) or in N.m per cu or mV (bottom).

Table 6.18 shows the found values. Some values are omitted to make the chart more readable. All are shown in appendix 11.VI.4. This table gives the opportunity to make four important comments:

- It is difficult to understand why there was a difference from double (SFy) to triple (SMy) between positive and negative positions of the transducer in axial load and torque. Finding coefficients m_{42} and m_{45} for matrix [M] will compelled to do averaging.

- The cantilever configuration introduced a small traction along Y axis. That was noticed when test descriptions were made. This is why, when SFy was quite important, the SFy sign was negative. However, the sign should be negative in both cases. A careful study of the signs of all coefficients will be expressed later.

- In Fz, there was no evident reason that this channel did not respond with the equivalent magnitude when the lever arm was changing, even more so that bending moments were close between themselves. Finding coefficient m_{43} for matrix [M] will compelled to do averaging.

- The Fx channel should not have any response in that cantilever configuration and there was one. Coefficient m_{41} will take this cross-effect into account.

These comments bring to the fore that the three forces are very sensitive with the set-up. The transducer has very small dimensions and a minor misalignment in the set-up gives unforeseen responses. However, these responses are repeatable and they do not affect the quality of the transducer. The influence of the set-up will be highlighted in the following chapter 7 concerning the validation of the Villiers Pylon Transducer.

In the main channel Mx, the sensitivity was equivalent whatever the lever arm was: 21.10 cu. per N when lever arm was 0.215 m and 21.98 cu when lever arm was 0.315 m. Averaging these sensitivities in each lever arm, then between themselves per unit, the chart becomes more simple (see table 6.19)

It was also possible to make a chart of Mx bending moment in N m versus 1 computer unit or 1 mV (see table 6.20). These small calculations were only done to

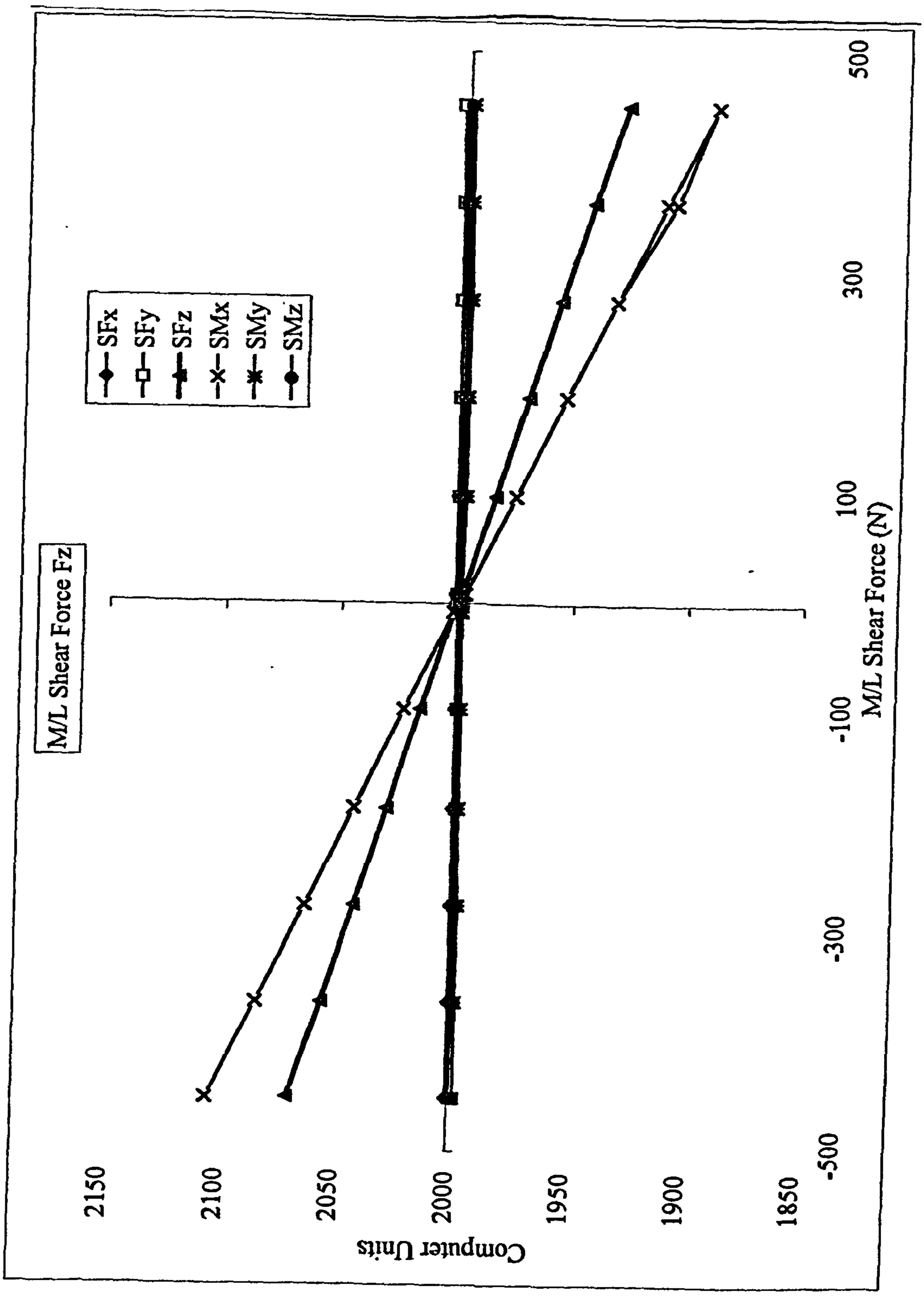

Figure 6.13: Pure M/L shear force Fz (main channel) with the associate M/L bending moment Mx and the corresponding four cross-effects (mean raw data from 4 tests).

compare channels between themselves and calibration data from other researchers. As example, the cross-effects in N or N m are shown in table 6.21.

It was important to evaluate the cross-talk levels in percentage per unit gain. Dividing any cross-effect channels by the main one and multiplying by 100 gave:

SFx	SFy	SFz	SMx	SMy	SMz
4.085 %	0.303 %	2.034 %	100 %	0.323 %	0.662 %

The maximum cross-effect is thus about 4 %; indeed this value is not very high and it should be easy to compensate it for using the calibration matrix [C].

However, as it was previously noted in section 6.3.4, the main cross-effect is in Fx channel, which is not logic. It was shown in the previous chapter 4 that Fx gauges, diagonally located in Z plane should be: the upper one in tension, the lower one in compression and the bridge should be balanced but obviously, the Fx bridge was not.

Magnissalis (1992) made a similar calibration using four points method. This researcher found a maximum cross-effect in Fy channel with a percentage of 2.55. Lovely (1982) used a cantilever configuration and his results exhibited a maximum cross-effect in Fz channel with a percentage level of 9 %. It was important to note that in a cantilever configuration, it was logic to have a Fz response in Mx main channel. This Fz cross talk might be called « associate response » rather than cross-effect. Other researchers showed a rough estimate of cross-effect levels. Thus, it is possible to say that in this channel, the Villiers Pylon Transducer has an acceptable behaviour regarding the requirements expressed in chapter 1.

If all channel curves are plotted on a same graph as shown in figures 6.14a (lever arm d1 = 0.215 m), and 6.14b (lever arm d2 = 0.315 m), same conclusions as above could be made. The behaviour of the transducer is correct in that particular channel.

6.4.4.1 MATRIX COEFFICIENTS CALCULATION

In section 6.3.4 concerning bending moment tests descriptions, it was noted that a cantilever method laid down to resolve a set of two equations with two unknown variables finding matrix calibration coefficients, hence, from equation 6.19.

Lever arm	Maximum Bending Moment Mx	Bending Moment sign	SFx	SFy	SFz	SMx	SMy	SMz
d_1 0.215 m	88.7 N.m	+ or -	101	- 26	62	1872	12	4
		+		12			- 3.2	
d_2 0.315 m	89.3 N.m	+ or -	108	- 28	42	1964	13	4.5
		+		14			- 5	

Table 6.18: The maximum values recorded in the six channels when a maximum M/L bending moment Mx was applied (in computer units), , with an average calculation between SMx + and SMx – results (mean raw data from 4 tests).

Average Sensitivity		SFx	SFy	SFz	SMx	SMy	SMz
in Mx channel	$[cu*(N.m)^{-1}] * 10^{-3}$ per unit gain	2.9	0.2	1.4	71.8	0.2	0.5
	$[mV*(N.m)^{-1}] * 10^{-3}$ per unit gain	7.08	0.48	3.41	175.3	0.48	1.22

Table 6.19: The sensitivity found in the six channels when a maximum M/L bending moment Mx of 88.7 or 89.3 N.m was applied.

SMx	0.046 N.m	for 1 cu Gain 300
	$1.53 * 10^{-4}$ N.m	for 1 cu Gain 1
	$0.62 * 10^{-4}$ N.m	for 1 mV Gain 1

Table 6.20: The results from M/L bending moment Mx (main channel) expressed in N.m per cu or mV, Gain 1.

	Fx	Fy	Fz	Mx	My	Mz
Mx Main channel positive	677 N	79 N	277 N	**89.35 N.m**	0.12N.m	0.58 N.m

Table 6.21: From M/L bending moment Mx (main channel), the apparent loads when a bending moment of 89.35 N.m was applied, using the results found after calibration study of each channel respectively.

$$SMx_1 = m_{43}\, Fz + m_{44}\, Mx_1$$

$$SMx_2 = m_{43}\, Fz + m_{44}\, Mx_2 \qquad (6.20)$$

If the measured values for SMx, Fz and Mx from numerical tables shown in appendix 11.VI.4 are replaced in these equations taking the same numbers in both lever arms for Fz = 185.54 N because shear force is independent of the lever arm. For Mx, its value is equal to 58.44 N m if the lever arm is $d_2 = 0.315$ m and 39.86 N m when the lever arm is $d_1 = 0.215$ m.

Regarding output signals, the difference between the measured number in both lever arm and the measured number with a zero load, was noted. This measured number was closed to 2000, which was the zero in Acquire programme. In Mx positive and $d_1 = 0.215$ m as lever arm, one had: 2843.8 - 2000.3 = 843.5 for SMx_1; with $d_2 = 0.315$ m as lever arm, it was: 3286.9 - 1999.9 = 1287 for SMx_2.

Thus, using equation (6.20), for Mx positive, the following set of equations was established. A positive sign close to the m suffix indicates that it was the positive configuration:

lever arm = 0.215 m	$843.5 = m_{43+} * 185.54 + m_{44+} * 39.89$
lever arm = 0.315 m	$1287 = m_{43+} * 185.54 + m_{44+} * 58.44$

It was easy to solve these two equations and the results were:

$$m_{43+} = -0.594$$
$$m_{44+} = 23.908$$

It was necessary to perform the same task in Mx negative, using the same equation (6.20):

lever arm = 0.215 m	$-842.4 = m_{43-} * 185.54 + m_{44-} * 39.89$
lever arm = 0.315 m	$-1285.4 = m_{43-} * 185.54 + m_{44-} * 58.44$

This gave:

$$m_{43-} = 0.594$$
$$m_{44-} = -23.884$$

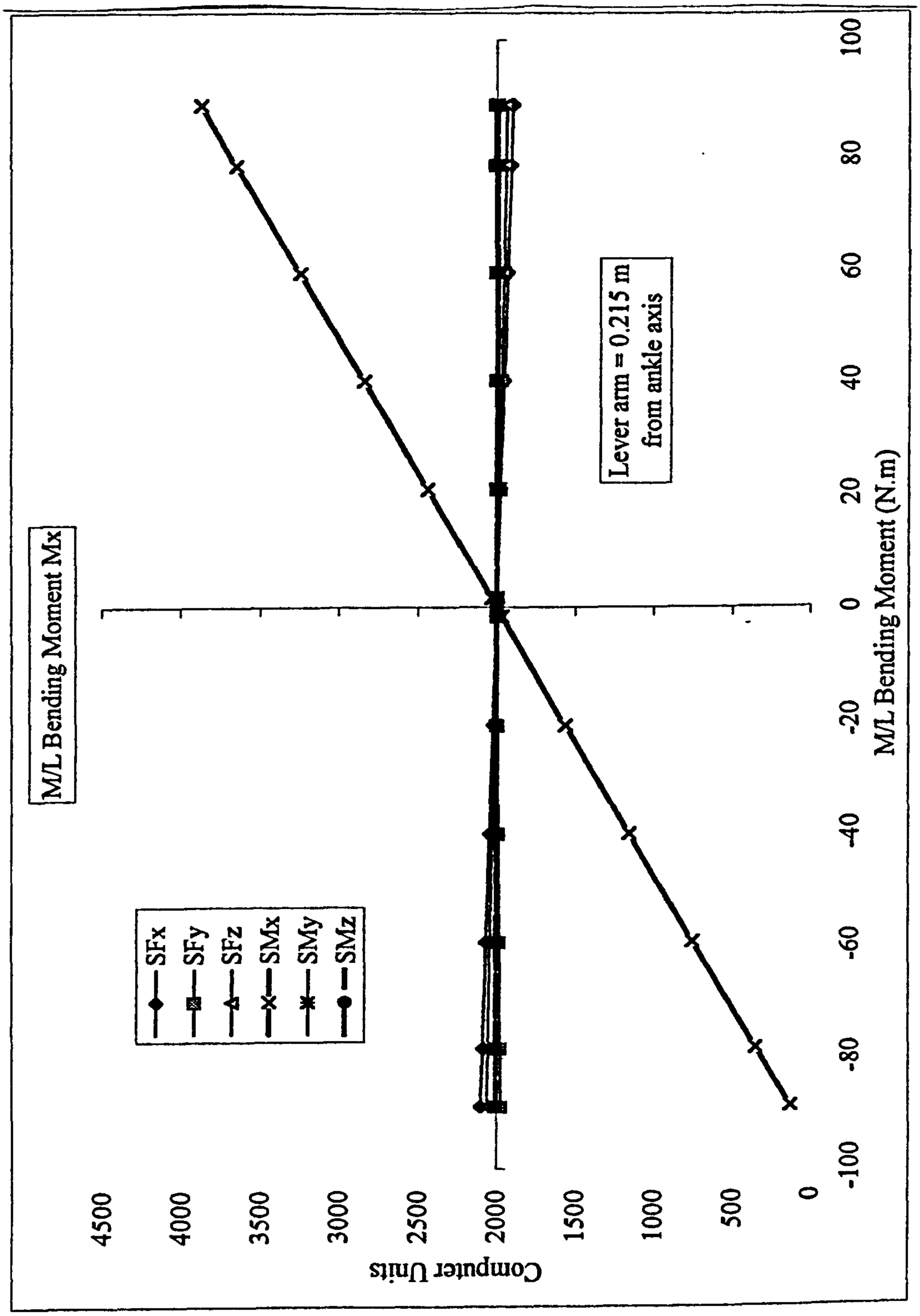

Figure 6.14a: Pure M/L bending moment Mx (main channel) with a lever arm of 0.215 m from the ankle axis and the five corresponding cross effects (mean raw data from 4 tests).

Now, it was possible to average these values finding two out of the thirty-six coefficients of the definitive matrix [M]:

$$m_{43} = 0.594$$
$$m_{44} = 23.896$$

There are no signs with the coefficient suffixes because these numbers are used in both set-ups, positive and negative. These two coefficients will be found again in section 6.6.1 when matrix [M] should be discussed.

The discussion concerning the coefficient signs will be performed in the same section 6.6.1.

6.4.5 Torque My

Using the same methodology as Mx channel, raw data are studied in a chart showing the averaging results in four tests. Tables are shown in appendix 11.VI.3. There is two series of results: My positive and negative. Table 6.22 shows the main results, which are given in computer units.

The average maximum values between positive and negative, simplified for 1 N m and gain 1, in computer units and in millivolts, with the transverse torque My main channel in bold letters type, are shown in table 6.23. It is also possible to make a chart of My torque in N m versus one computer unit (table 6.24).

Table 6.25 shows the cross-effects in N or N m when a maximum transverse torque of 10.7 N m was applied. It is obvious that there is a problem in axial load Fy interaction effect. As in Mx channel, it is interesting to evaluate the cross-effects in percentage per unit gain, using the same way of doing:

Fx	Fy	Fz	Mx	My	Mz
1.29 %	5.64 %	0.07 %	1.46 %	100 %	7.52 %

It is also stimulating to check and to compare the cross-effects results from other researches, with the transverse torque as main channel in italic bold letters:

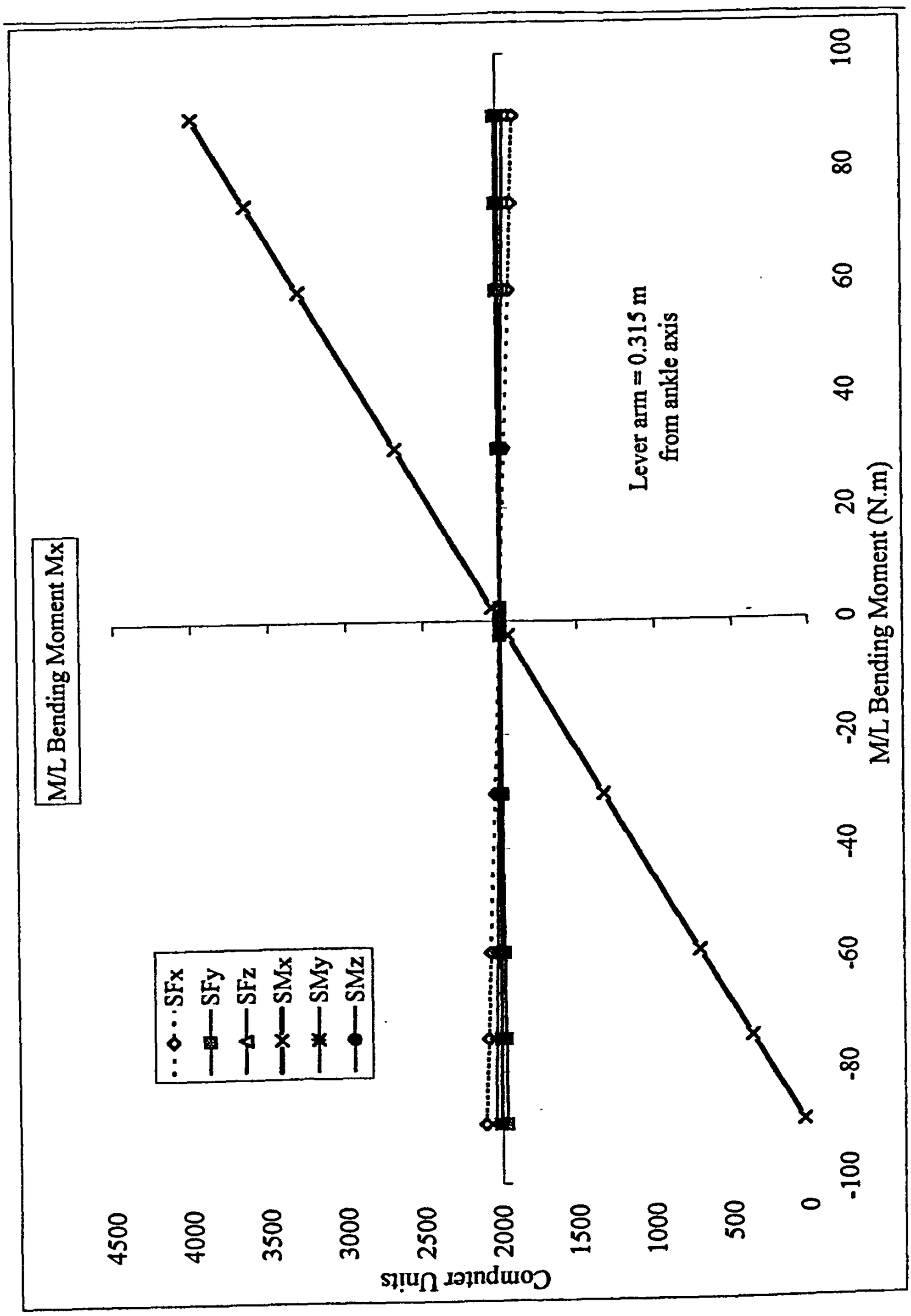

Figure 6.14b: Pure M/L bending moment Mx (main channel) with a lever arm of 0.315 m from the ankle axis and the five corresponding cross effects (mean raw data from 4 tests).

	Fx	Fy	Fz	Mx	*My*	Mz
New VPT	1.29 %	5.64 %	0.07 %	1.46 %	***100 %***	7.52 %
SPT Magnissalis (1992)	11 %	0.51 %	2.73 %	0 %	***100 %***	2.73 %
Lovely (1982)	1.14 %	0.09 %	1.01 %	1.46 %	***100 %***	4.39 %

It is possible to note that in Magnissalis (1992) with the Strathclyde Pylon Transducer, maximum cross talk was in Fx channel. Its level was 11 % for a torque of 10.99 N m. In Lovely (1981) with the same transducer, the maximum was in Mz channel with a magnitude of 4.39 %. Obviously, in the VPT, there is a cross-effect rather important in both channels Fy and Mz. Understanding the Fy interaction problem will take place in section 7.3.4.

Concerning the plots of all the channel curves on a same graph (see figure 6.15), the conclusion is that the transducer has a linear (despite the small inflexion when torque is closed to zero), no hysteresis and good repeatability behaviour in this particular channel.

6.4.6 Bending Moment Mz

The same procedure as in Mx channel was used to study raw data, averaging four tests (all tables are shown in appendix 11.VI.4). The lever arms were identical (0.215 m and 0.315 m) as those in Mx tests. The chart is identical as in M/L bending moment Mx except the third column in which the bending moments were applied about Z axis while loading were applied along X axis. Rotating the transducer of 180° around Y axis was sufficient to move from Mz positive to Mz negative. Mz positive represents a dorsiflexion of the artificial ankle in relation to the leg, while Mz negative is a plantarflexion. In amputee's tests, dorsiflexion (Mz positive) has a maximum value of 100 to 150 N m (ISO 10328-4, 1993; Pashalides, 1989).

The set-up was a cantilever method, which gave a mixing of Fx and Mz. Having two lever arms allowed to calculate matrix coefficients for Mz — m_{66} — and Fx — m_{61}— following the same method used in Mx bending moment as shown in section 6.4.4. The results are shown in table 6.26.

	Maximum Torque = 10.704 N.m	SFx	SFy	SFz	SMx	SMy	SMz
My positive		0.9	61	0.3	8	425	10
My negative		0.5	59	0.3	1.35	425	6

Table 6.22: The maximum results in computer units found in transverse torque My (10.704 N.m) (mean raw data from 4 tests).

	SFx	SFy	SFz	SMx	**SMy**	SMz
$[cu*(N.m)^{-1}]\ 10^{-3}$ per unit gain	1.3	5.6	0.1	1.4	**99.2**	7.5
$[mV*(N.m)^{-1}]\ 10^{-3}$ per unit gain	3.2	13.6	0.2	3.4	**242.2**	18.3

Table 6.23: The average maximum values per 1 N.m and gain 1

SMy	0.025 N.m	for 1 cu Gain 400
	$6.25 * 10^{-5}$ N.m	for 1 cu Gain 1
	$2.56 * 10^{-5}$ N.m	for 1 mV Gain 1

Table 6.24: The maximum values found in the main channel My per 1 cu and gain 1.

	Fx	Fy	Fz	Mx	My	Mz
My Main channel positive	4.4 N	338 N	1.9 N	0.2 N.m	**10.7 N.m**	1.3 N.m

Table 6.25: The cross-effects in N or N.m recorded when a maximum transverse torque of 10.7 N.m was applied, using the results found after calibration study of each channel respectively.

This chart is a mirror picture of Mx channel (see table 6.18). The values in Mz channel were around the third as those in Mx channel which was logic regarding amplifier gain: 300 in Mx channel and 100 in Mz channel. In other channels, same comments as those in Mx channel could be expressed. The full chart for cross sensitivity is shown in appendix 11.VI.4.

The average sensitivity per unit follows the same approach as above in section 6.4.4; it is shown in table 6.27.

It is also possible to show a chart of the Mz bending moments in N m versus one computer unit, as shown in table 6.28. The chart showing the cross-effects in N or N m when a maximum bending moment was applied in the main channel Mz, is presented in table 6.29.

In percentage per unit gain (from table 6.27), it is:

SFx	SFy	SFz	SMx	SMy	SMz
2.252 %	0.225 %	4.23 %	0.098 %	0.324 %	100 %

In this channel Mz, as in Mx, the maximum cross-effect is about 4 % ; this is not very high and compensation by using calibration matrix [C] should be possible.

Other researchers data show a maximum cross-effect in Fz: 5.33 % with a bending moment of 33.35 N m (four points method: Magnissalis, 1992) and 9.39 % with a bending moment of 119 N m (cantilever method Lovely, 1982).

Putting these two channels side by side with the main channels in italic bold letters, it should be possible to note that there is an illogical response of the transducer:

		SFx	SFy	SFz	**SMx**	SMy	**SMz**
Mx channel	$[cu * (N_3 m)^{-1}]10^{-}$ gain 1	2.93	0.22	1.46	***71.79***	0.23	0.4
Mz channel	$[cu * (N_3 m)^{-1}]10^{-}$ gain 1	1.59	0.16	3	0.07	0.23	***70.8***

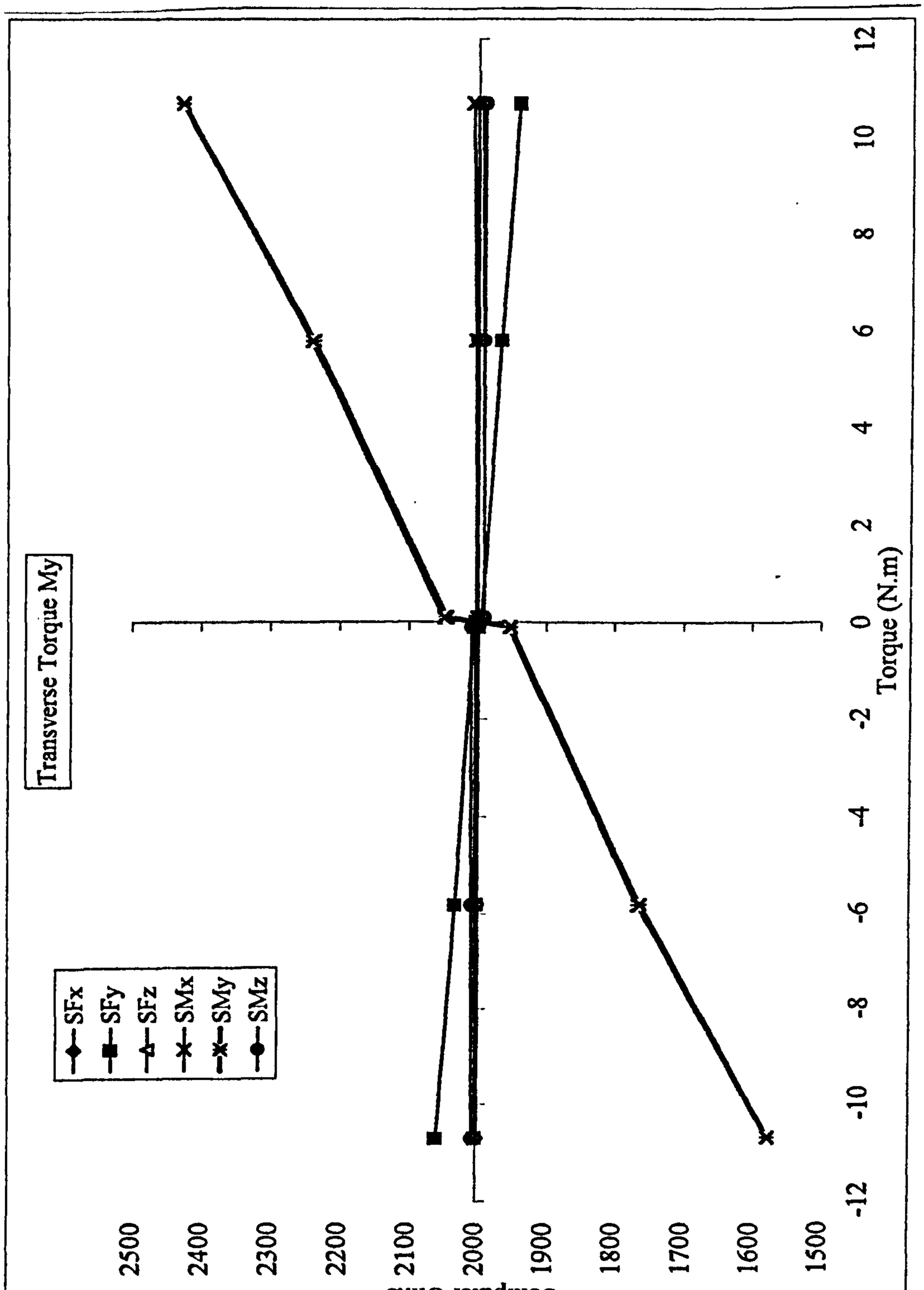

Figure 6.15: The pure transverse torque My main channel with the five corresponding cross effects (mean raw data from 4 tests).

As it was said in section 6.4.4, the Mx cantilever set-up gave a mixing of Fz and Mx, whereas Fx response was higher than Fz which was unexpected. The same comment could be done in Mz channel: Fx value should be higher than Fz and it was the opposite. Although this characteristic of the Villiers Pylon Transducer, each channel was the inverted view of the other one with linearity, it might be possible to correct them using the calibration matrix [C]. All researchers who documented transducer calibration (Grant-Thomson, 1977; Lovely, 1982; Lawes, 1983; Pashalides, 1989; Magnissalis, 1992) found the opposite logic pattern of cross-effects. Two hypothesis were made about these surprising responses:

1. a crossing wire or a mixing gauges
2. a misalignment of gauges

Studying several times, the body test of the Villiers Pylon Transducer through a microscope, it was found that the second hypothesis might be possible: a misalignment of Fx gauges of about 2 degrees along Y axis could explain this illogical response. To illustrate this point, Pople (1980), quoted by Miles and Tanner (1990) considered the measurement of thrust on a shaft subjected to a torque-to-thrust ratio of 7.5:1: one degree of gauge misalignment with the shaft axis led to an error of 53 % in the measurement of thrust. The data of other researcher (Little, 1990) showed how a systematic error of 2 % could result from a deviation of only 0.05 mm in embedding a strain gauge at a distance of 2.55 mm from the neutral axis in a cantilever bend test. Considering the small size of this new transducer with shear and bending gauges in two levels, some tiny misalignments were inevitable and not amazing.

However, these cross talks are not very high; the transducer has always a linear response. Therefore, offsetting them should be possible.

The plots of all the channel curves on a same graph allows to observe that the behaviour of the Wheatstone bridges is good in all the channels, concerning linearity, hysteresis and creep (figure 6.16a, lever arm 0.215 m; 6.16b, lever arm 0.315 m).

Lever arm	Maximum Bending Moment	Bending Moment Sign	SFx	SFy	SFz	SMx	SMy	SMz
d_1 0.215 m	88.70 N.m	+ or -	67	0.3	103.7	2	7.3	615.65
		+		- 13.3				
d_2 0.315 m	89.35 N.m	+ or -	47	0	110.7	2	9	646.1
		+		- 15.7				

Table 6.26: The maximum values recorded in the six channels when a maximum A/P bending moment Mz was applied (in computer units) , with an average calculation between SMz + and SMz – results (mean raw data from 4 tests).

Average Sensitivity in Mz channel		SFx	SFy	SFz	SMx	SMy	SMz
	[cu * $(N.m)^{-1}$] 10^{-3} per unit gain	1.595	0.16	3	0.07	0.23	70.85
	[mV * $(N.m)^{-1}$] 10^{-3} per unit gain	3.89	0.39	7.32	0.17	0.56	173

Table 6.27: The sensitivity found in the six channels when a maximum A/P bending moment Mz of 88.7 or 89.35 N.m was applied.

SMz	0.13 N.m	for 1 cu Gain 100
	$1.38 * 10^{-3}$ N.m	for 1 cu Gain 1
	$0.56 * 10^{-3}$ N.m	for 1 mV Gain 1

Table 6.28: The results from A/P bending moment Mz (main channel) expressed in N.m per cu or mV, Gain 1.

	Fx	Fy	Fz	Mx	My	Mz
Mz Main channel positive	295 N	88 N	731 N	0.1 N.m	0.2 N.m	**89.3 N.m**

Table 6.29: From A/P bending moment Mz (main channel), the apparent loads when a bending moment of 89.35 N.m was applied, using the results found after the calibration of each channel respectively.

6.4.6.1 MATRIX COEFFICIENTS CALCULATION

As in Mx, a matrix coefficient calculation is needed (see section 6.4.4.1), from equation 6.18:

$$SMz_1 = m_{61}\, Fx + m_{66}\, Mz_1$$

$$SMz_2 = m_{61}\, Fx + m_{66}\, Mz_2 \qquad (6.21)$$

By substituting the measured values, it is possible to express, in positive configuration:

SMz_1 = 276.3 (reading output signals - 2000.7), at 185.54 N as loading mass which gives 39.89 N m as bending moment with a lever arm of 0.215 m

SMz_2 = 423 (reading output signals - 2000.6), at 185.54 N as loading mass which gives 58.44 N m as bending moment with a lever arm of 0.315 m. Thus, with a positive sign close to the m suffix indicating positive configuration:

lever arm = 0.215 m	$276.3 = m_{61+} * 185.54 + m_{66+} * 39.89$
lever arm = 0.315 m	$423 = m_{61+} * 185.54 + m_{66+} * 58.44$

Solving this set of equations:

$m_{61+} = -0.211$
$m_{66+} = 7.908$

In negative position, it comes:

lever arm = 0.215 m	$-277.9 = m_{61-} * 185.54 + m_{66-} * 39.89$
lever arm = 0.315 m	$-423 = m_{61-} * 185.54 + m_{66-} * 58.44$

Hence,

$m_{61-} = 0.184$
$m_{66-} = -7.822$

Averaging these values to use them in matrix [M], it could be possible to write:

$m_{61} = 0.198$
$m_{66} = 7.865$

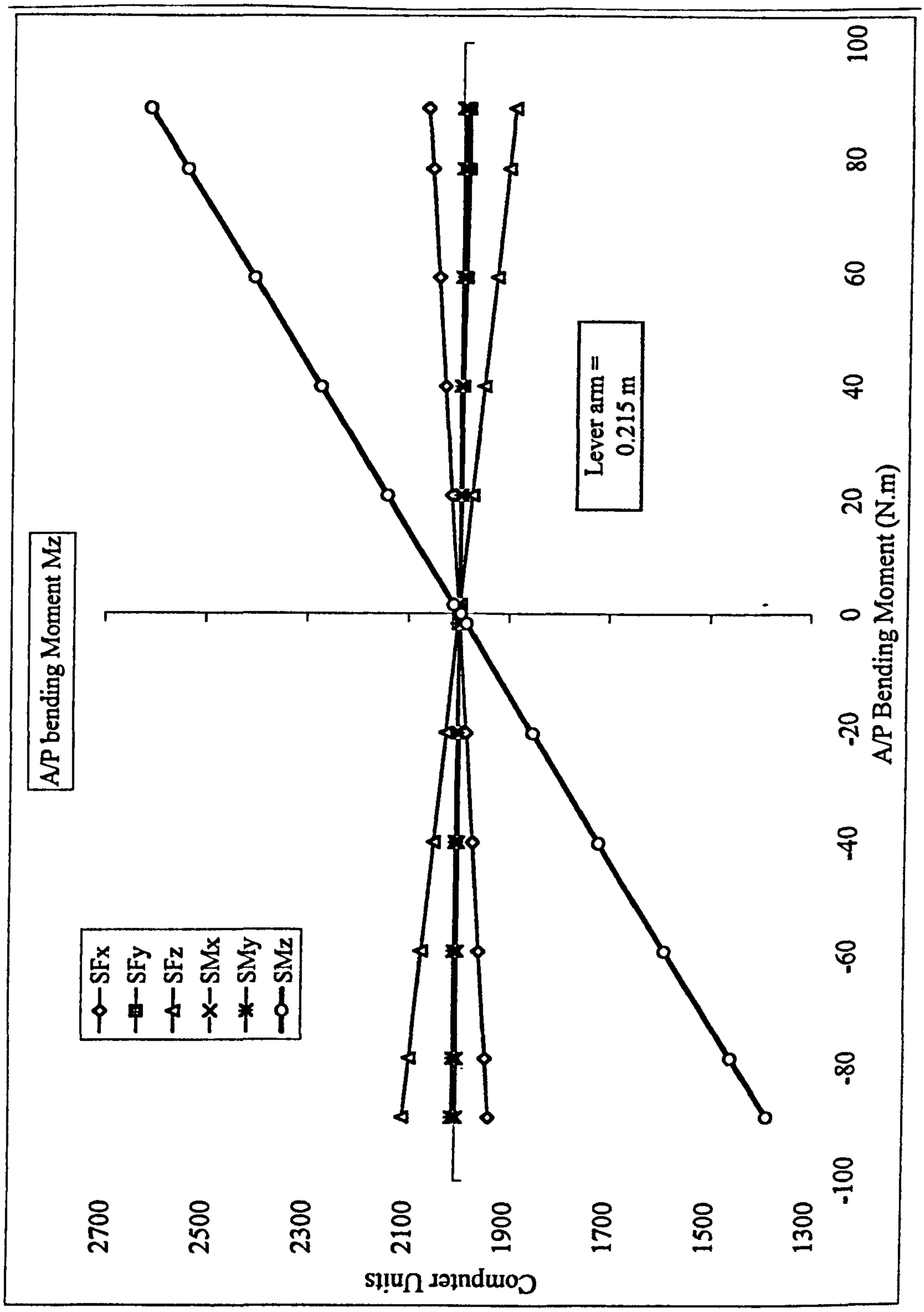

Figure 6.16a: Pure A/P bending moment Mz (main channel) with a lever arm of 0.215 m from the ankle axis and the five corresponding cross effects (mean raw data from 4 tests).

As previously stated in section 6.4.4.1, there were not any signs with the coefficient values. A complete discussion will be conducted in section 6.6.3, concerning the signs used in matrices [M] and [C].

6.4.7 Summary and Discussion

Since all loads were purely applied in one and only one direction, the output signals recorded on Acquire programme during each test, corresponding to one main effect and five cross-effects caused by the particular load applied, could be studied.

All the sensitivities of the Villiers Pylon Transducer are shown in table 6.30 in N or N m per computer units or millivolts with current gain, unit gain and bridge voltage 1. Table 6.31 shows the sensitivities of the VPT in computer units or millivolts per unit force or moment with both current gain and unit gain. The last column of these two tables expresses these sensitivities in one volt as Wheatstone full bridge voltage, making transducer's comparison easier.

Signals were recorded in computer units versus the corresponding load in N or N m, with a linear relation between computer units and millivolts (see section 3.5.2):

$$1 \text{ computer unit} = 2.442 \text{ mV}$$

$$1 \text{ mV} = 0.409 \text{ computer unit}$$

The coefficients m_{ij} of matrix [M] shown in equation 6.4 can be derived by regression of the data, i.e., fitting the linear regression line:

$$signal_i = m_{ij} * load_j$$

Therefore, a full presentation of this statistical analysis is shown in the following section.

6.5 STATISTICAL ANALYSIS OF CALIBRATION RAW DATA

In transducer calibration, there are an independent, controlled, known variable X (the loading case) and a dependant, response, unknown variable Y (the output signals) (Chatfield, 1981). A regression analysis is to study the relationship between these two variables. It is possible to find a regression equation between X and Y. An

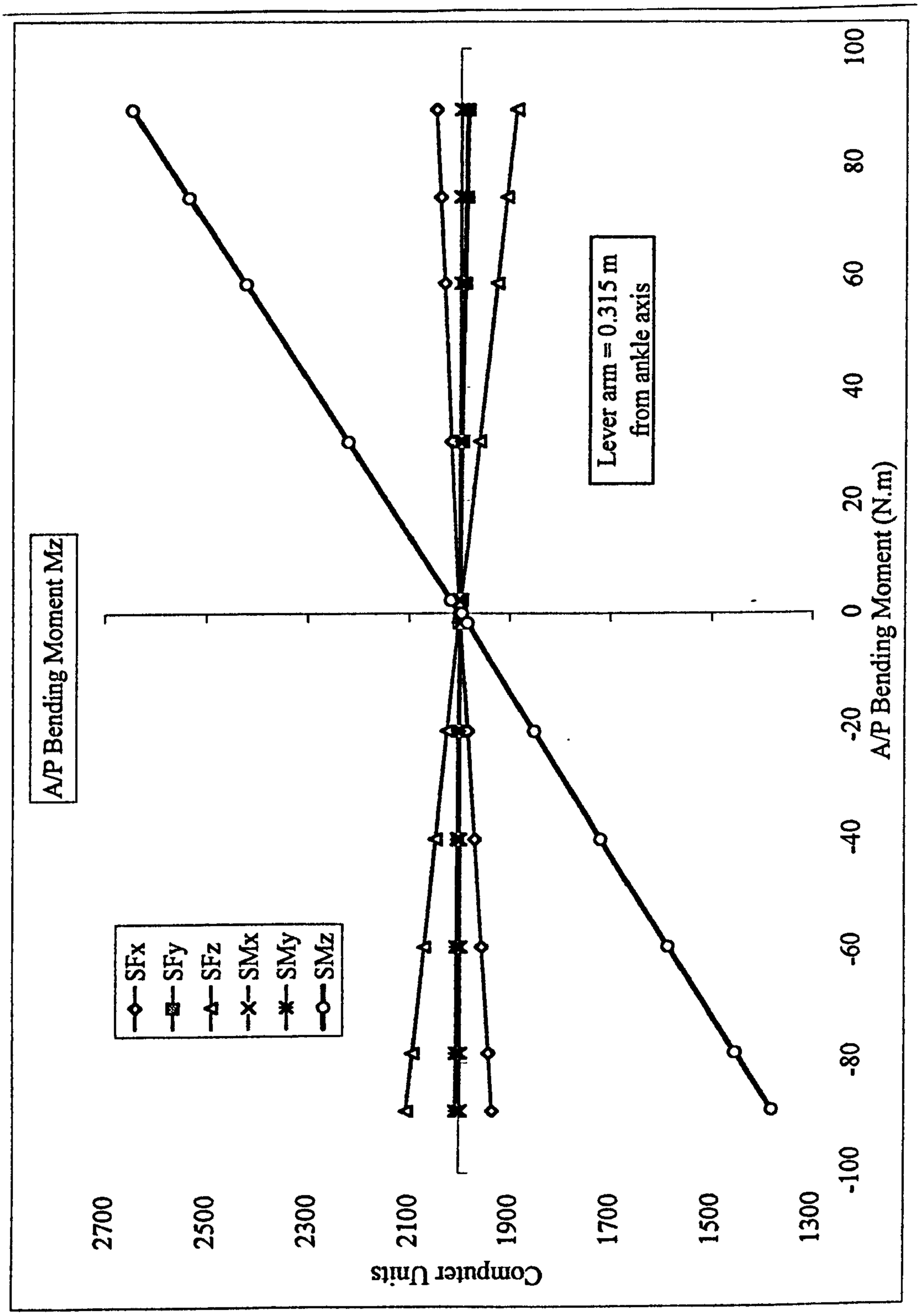

Figure 6.16b: Pure A/P bending moment Mz (main channel) with a lever arm of 0.315 m from the ankle axis and the five corresponding cross effects (mean raw data from 4 tests).

important feature is that this regression equation is linear, namely, that it is of the form:

$$Y = b_0 + b_1X$$

where b_0 and b_1 are constants, they are called the regression coefficients (Freund, 1992):

- b_1 is called the slope of the linear regression line
- b_0 is the Y-intercept

The regression line is the straight line that best fits a set of data points according to the least-squares criterions (Weiss, 1995). To find the regression equation, a special macro was used in the spreadsheet software Microsoft Excel 4®. This programme calculates, the two-regression coefficients b_0 and b_1. It also shows the coefficient of determination r^2 (r-square). The r-square value only gives information on the amount of the output signal variation explained by the applied load component. In other words, r-square reflects the linearity of the two variables but it does not show the magnitude of the predicted load. If r-square is equal to one, then all observed points lie exactly on a straight line. If it is equal to nought, the slope of the regression line is zero. Therefore the closer the coefficient of determination r-square is to one, the closer the points lie to an exact straight line (Chatfield, 1981). Thus, knowing and studying r-square is necessary but not sufficient. This is why Excel® programme shows additional statistical calculation, mainly the p-value of 95 % as chosen threshold between acceptable and non-acceptable coefficient.

In general practice, the task is to find an estimation of b_0 and b_1. The intercept value b_0 is only used to verify that the linear regression line is starting from zero for both axes. What it is of paramount importance is: for each pair of data one has the slope b_1 which is one of the coefficient of the matrix [M], i.e., the six output signals are regressed against each loading case. The question is now about which coefficients b_1 should be retained. The decision must be made on statistical grounds.

	Sensitivity $N * cu^{-1}$ full gain	Sensitivity $N * cu^{-1}$ gain 1	Sensitivity $N * (mV)^{-1}$ gain 1	Sensitivity $N * (mV)^{-1}$ gain 1 bridge voltage 1
SFx	6.27	$1.56 * 10^{-2}$	$6.38 * 10^{-3}$	$8.51 * 10^{-4}$
SFy	5.64	$5.64 * 10^{-3}$	$2.31 * 10^{-3}$	$2.31 * 10^{-4}$
SFz	6.61	$1.66 * 10^{-2}$	$6.75 * 10^{-3}$	$9.00 * 10^{-4}$
	$N.m * cu^{-1}$ full gain	$N.m * cu^{-1}$ gain 1	$N.m * (mV)^{-1}$ gain 1	$N.m * (mV)^{-1}$ gain 1 bridge voltage 1
SMx	0.046	$1.53 * 10^{-4}$	$0.62 * 10^{-4}$	$8.26 * 10^{-6}$
SMy	0.025	$0.62 * 10^{-4}$	$0.25 * 10^{-4}$	$3.33 * 10^{-6}$
SMz	0.13	$13.8 * 10^{-4}$	$5.65 * 10^{-4}$	$0.75 * 10^{-4}$

Table 6.30: Sensitivities in N or N.m per computer unit, full gain, gain 1 and gain 1 plus bridge voltage 1.

	Sensitivity $cu * N^{-1}$ full gain	Sensitivity $cu * N^{-1}$ gain 1	Sensitivity $mV * N^{-1}$ gain 1	Sensitivity $mV * N^{-1}$ gain 1 bridge voltage 1
SFx	0.159	$0.398 * 10^{-3}$	$0.971 * 10^{-3}$	$0.129 * 10^{-3}$
SFy	0.177	$0.177 * 10^{-3}$	$0.432 * 10^{-3}$	$0.432 * 10^{-4}$
SFz	0.151	$0.378 * 10^{-3}$	$0.924 * 10^{-3}$	$0.123 * 10^{-3}$
	$cu * N.m^{-1}$ full gain	$cu * (N.m)^{-1}$ gain 1	$mV * (N.m)^{-1}$ gain 1	$mV * (N.m)^{-1}$ gain 1 bridge voltage 1
SMx	21.1	$70.3 * 10^{-3}$	$171.75 * 10^{-3}$	$22.90 * 10^{-3}$
SMy	39.71	$99.2 * 10^{-3}$	$242.42 * 10^{-3}$	$32.32 * 10^{-3}$
SMz	7.05	$70.5 * 10^{-3}$	$172.16 * 10^{-3}$	$22.95 * 10^{-3}$

Table 6.31: Sensitivities in computer unit per N or N.m, full gain, gain 1 and gain 1 plus bridge voltage 1.

Magnisalis (1992) discussed and recommended the way it was used. This researcher expressed the following recommendation: it is considered statistically more sound to base any decisions on either of the p-values, than on the r-square value of the regression model. This procedure will be shown below, in section 6.6.2.

6.6 DATA PROCESSING

As explained in the previous chapter 4, the procedure for each load was identical. After exporting data from Acquire to an Excel® spreadsheet file, the eleventh row was erased and then an arithmetic mean value of the ten rows remained was calculated: sum of ten values divided by ten. This value was transferred in a new file with the corresponding loading case, opposite each other.

When data processing of the four tests was finished, a descriptive statistic (mean value, median, standard deviation and confidence interval) was performed. This gave the final raw data, ready to the next step of statistical processing. Some of them were presented in the previous chapter 4. The next stage was for statistical analysis and steps were as follows:

1. put the loading case in one column and the mean recorded output signals in an other column, opposite each other into an Excel® spreadsheet file;

2. assume that the loading case column is the variable X (known variable) and the mean value of recorded output signals column is the variable Y (unknown variable);

3. choose the value of 95 % as the threshold;

4. make the statistical analysis by means of Regression Analysis Tools in Excel®;

5. study the coefficient of determination (r-square). It may be the closer to one as possible (currently 0.9999 * 100 as result in percentage, in main channel data).

This procedure was done for the six loading case and then, a chart was built exhibiting the 6 * 6 = 36 coefficients of matrix [M] (m_{11}, ..., to m_{66}) and the statistical analysis of data, as shown in table 6.32. The results consist of the

coefficients	mean	st. error	p-value	r-square
mij	cui / N,Nmj	cui / N,Nmj		(%)
		under load Fx		
m11	0.1574334	0.0002087	0.000	99.9979
m12	0.0033590	0.0007214	0.002	65.8109
m13	0.0014765	0.0001920	0.025	61.6417
m14	-0.0025875	0.0002400	0.004	71.1111
m15	-0.0042807	0.0002483	0.000	96.0956
m16	0.0700189	0.0001870	0.000	99.9913
		under load Fy		
m21	0.0014506	0.0000736	0.000	93.2808
m22	0.1689965	0.0017053	0.000	99.7157
m23	-0.0027256	0.0001008	0.000	96.3096
m24	-0.0019708	0.0006259	0.004	26.1507
m25	0.0018251	0.0002248	0.000	70.1855
m26	0.0110048	0.0002436	0.000	98.6469
		under load Fz		
m31	-0.0009180	0.0001916	0.000	65.9122
m32	0.0043203	0.0003916	0.000	91.0896
m33	0.1510992	0.0002426	0.000	99.9969
m34	-0.2333959	0.0009705	0.000	99.9683
m35	0.0021109	0.0006646	0.024	43.0349
m36	0.0001612	0.0002422	0.436	6.0944
		under load Mx		
m41	-1.1765420	0.0008521	0.000	99.9994
m42	0.2295117	0.0064126	0.000	98.8726
m43	-0.5944277	0.0011516	0.000	99.9954
m44	23.8962630	0.0089414	0.000	99.9997
m45	-0.0966207	0.0028184	0.000	92.5480
m46	-0.0458795	0.0005885	0.000	99.6084
		under load My		
m51	0.1184490	0.1879072	0.465	9.7301
m52	-5.3124401	0.2095330	0.000	99.0739
m53	0.0256275	0.0585865	0.693	4.0101
m54	0.4431425	0.0684446	0.049	66.5815
m55	37.6657494	1.3824076	0.000	99.1982
m56	-0.2570624	0.3565310	0.499	8.0924
		under load Mz		
m61	0.1980000	0.0010021	0.000	99.9965
m62	-0.0793407	0.0066465	0.173	52.9347
m63	-1.2062831	0.0012752	0.000	99.9988
m64	-0.0205910	0.0016182	0.000	93.3977
m65	-0.0910521	0.0058046	0.000	95.1114
m66	7.8650000	0.0038361	0.000	99.9999

Table 6.32: Statistical analysis of the calibration data.

following columns: the mean values of the coefficients (slope, b_1; b_0 is not shown); the standard errors of the coefficients (both have $cu_i * N^{-1}$ or $(N\ m)^{-1}{}_j$ as unit); the p-value of the coefficients (three decimal places only) and the r-square (in percentage) of the fitted lines. As shown in table 6.32, the fitted lines explain more than 99 % (r-square) of the variation of the main effects, giving an indication of a very strong linear relation between the two variables. The anticipated statistical significance of the derived coefficients is proved by the zero p-value. Most of them have a multiplying factor of 10^{-35}.

6.6.1 Signs of the mean values

Studying signs of the mean values is the utmost importance to establish the matrix [M] to use accurately the inverted calibration matrix [C], because the sign of a cross-effect coefficient in [M] modifies the result of [C].

The rule used for the sign study is as follows: « when a response in main channel is positive, the signs of all cross-effect responses must be considered and it is essential to keep them » (Solomonidis, 1989).

When output signals are close to zero, a positive sign is accepted.

Results are presented in table 6.33, with main channel in bold type and point screen.

6.6.2 P-value statistical analysis

It was now time to study which coefficients b_i should be retained according to the procedure recommended by Lovely (1981) and Magnissalis (1992): a p-value statistical analysis. This was done as follows (Weiss, 1995):

- Step 1: read the p-value and use it to perform a hypothesis test using the p-value approach:
- Step 2: state the null and alternative hypothesis

H_0: μ = mean coefficient is negligible

H_a: μ = mean coefficient is not negligible

- Step 3: decide on the significance level, $\alpha = 0.05$ at 95 %

	SFx	SFy	SFz	SMx	SMy	SMz
Fx	+	+	-	-	+	+
Fy	+	+	+	+	-	-
Fz	+	-	+	-	+	-
Mx	-	-	-	+	+	-
My	-	+	+	-	+	-
Mz	+	+	+	-	-	+

Table 6.33: The sign of the mean values used in the calibration matrix [M].

- Step 4: read the p-value on the spreadsheet screen
- Step 5: if p-value $\leq \alpha$, then reject H_0 ; otherwise, do not reject the hypothesis.

In other hand, if p-value ≥ 0.05, we did not reject H_0 so, mean coefficients were negligible, i.e., = 0.

Doing this procedure, it is easy to see in table 6.32 which coefficients exhibit a high p-value (≥ 0.05). These coefficients could thus be considered negligible. Therefore, the coefficient m_{36}, m_{51}, m_{53}, m_{56} and m_{62} were considered zero. Obviously, these last coefficients also exhibited very low t-ratios (not shown in table 6.32, but given by the programme), which were less than the value provided by tables for a level of 95 % (Gilbert, 1988).

Most of the coefficients of the cross-effects however, were non-zero. They exhibited p-values ≤ 0.05, which did not allow to be considered negligible, and therefore they might be taken into account as derived. These coefficients, as expected, also exhibited t-ratios higher than the values provided by tables. At the same time, as shown, the r-square values were not high, or even very poor for some coefficients (less than 50 %): m_{24} and m_{35}. Although these regression lines exhibited poor linearity it was not considered statistically correct to assume that the corresponding coefficients were zero and therefore they were taken into account with their calculated values (Magnissalis, 1992).

6.6.3 Calibration matrices [M] and [M]$^{-1}$ = [C]

According to the theoretical matrix 6.7 (see section 6.2), it is now possible to put up the 6 * 6 coefficients square matrix [M], as shown in table 6.34. The six rows exhibit the corresponding coefficients to each channel (respectively Fx, Fy, Fz, Mx, My, Mz) while the six columns exhibit the same channels succession. Thus, diagonal coefficients represent the main effect mean values and the off-diagonal coefficients are the transducer cross-effect mean values.

Using a mathematical computer software MathCad 4.0®, matrix [M] was inverted to matrix [C] = [M]$^{-1}$ with a determinant equal to 26.7678408.

0.15743342	0.00335898	0.00147653	-0.00258754	-0.00428068	0.07001892
0.00145058	0.16899649	-0.00272563	-0.00197076	0.00182514	0.01100482
-0.00091797	0.00432034	0.15109925	-0.23339587	0.00211090	0.00000000
-1.17654197	0.22951169	-0.59442768	23.88826297	-0.09662071	-0.04587951
0.00000000	-5.31244009	0.00000000	0.44314249	37.66574936	0.00000000
0.19800000	0.00000000	-1.20628309	-0.02059104	-0.09105211	7.86500000

Table 6.34: The calibration matrix [M], having as units: cu_i / N or N.m_j

6.38953	0.11575	-0.41191	0.00330	-0.00054	0.05755
0.03965	5.92640	-0.04589	0.00093	0.00026	-0.00804
0.46439	-0.09394	6.85256	-0.06700	-0.00060	0.00392
-0.32629	-0.05690	-0.14929	0.04335	0.00014	-0.00260
0.00943	0.83653	-0.00471	-0.00037	0.02658	-0.00110
0.06147	0.02699	-1.07427	0.01037	0.00039	0.12594

Table 6.35: The inverted matrix [C] = $[M]^{-1}$, having as units: N or N.m_i / cu_j

Table 6.36: These matrices are for a bridge voltage (BV) and a gain settings (GS) of:

		BV	GS
Channel 1	Fx	7.5	400
Channel 2	Fy	10.0	1000
Channel 3	Fz	7.5	400
Channel 4	Mx	7.5	300
Channel 5	My	7.5	400
Channel 6	Mz	7.5	100

To compute the determinant and inverse of the square matrix [M], the programme decomposed it into a lower-triangular matrix L and an upper-triangular matrix U, such as:

$$[M] = L * U$$

This is called the LU decomposition of the matrix. The determinant of the original matrix is simply the product of the diagonal elements of U, the upper-triangular matrix in the LU decomposition. To compute the inverse, the programme solves the equation M * vj = ej where e is a vector with a one in element j and a zero in all other elements. The solution vectors for each j form the columns of the inverse matrix (MathCad 4.0®, User's Guide, 1993, p. 431).

Calibration matrix [C] is shown in table 6.35. It is also of the form of a 6 * 6 square matrix as the theoretical matrix equation shown above (6.13), see section 6.2. In addition to tables 6.34 and 6.35, the corresponding bridge voltages and gain settings are shown in table 6.36.

6.6.4 Comparison with the Strathclyde Pylon Transducer

It is not easily possible to compare the calibration matrices from other transducers: units, bridge voltages and gain settings are not equivalent. Moreover, the comparison of different transducers must be conducted carefully, avoiding any nonsense. Nevertheless, it is possible to compare the sensitivities of the main effects (diagonal coefficients of matrix [M]) of two transducers: the Strathclyde Pylon Transducer (SPT) designed by Berme, *et al.* (1975) and the Villiers Pylon Transducer. The calibration matrix of the SPT is extracted from Solomonidis (1989), reported by Magnissalis (1992), using dead-weight method. The SPT is widely used in lower limb prosthetic field since many years. Table 6.37 shows a comparison of these two pylon transducers.

Globally, the ratio between the two sensitivities is more or less about two: the new VPT is less sensitive in Fx and Fz but more in Fy than the SPT. It is globally twice more sensitive for the three bending moments. This is probably due to its thickness.

	Villiers Pylon Transducer	*Strathclyde Pylon Transducer*
	$mV * N^{-1}$ per unit gain bridge voltage 1	$mV * N^{-1}$ per unit gain bridge voltage 1
SFx	$1.29 * 10^{-4}$	$3.31 * 10^{-4}$
SFy	$0.43 * 10^{-4}$	$0.21 * 10^{-4}$
SFz	$1.23 * 10^{-4}$	$3.16 * 10^{-4}$
	$mV * N.m^{-1}$ per unit gain bridge voltage 1	$mV * N.m^{-1}$ per unit gain bridge voltage 1
SMx	$0.23 * 10^{-1}$	$0.11 * 10^{-1}$
SMy	$0.32 * 10^{-1}$	$0.13 * 10^{-1}$
SMz	$0.22 * 10^{-1}$	$0.09 * 10^{-1}$

Table 6.37: The comparison of the sensitivities of two pylon transducers

$$Fx = \textit{6.38930 SFx} + 0.11575\ SFy - 0.41191\ SFz + 0.00330\ SMx - 0.00054\ SMy + 0.05755\ SMz$$

$$Fy = 0.03965\ SFx + \textit{5.92405 SFy} - 0.04589\ SFz + 0.00093\ SMx + 0.00026\ SMy - 0.00804\ SMz$$

$$Fz = 0.46439\ SFx - 0.09394\ SFy + \textit{6.85256 SFz} - 0.06700\ SMx - 0.00060\ SMy + 0.00392\ SMz$$

$$Mx = -0.32629\ SFx - 0.05690\ SFy - 0.14929\ SFz + \textit{0.04335 SMx} + 0.00014\ SMy - 0.00260\ SMz$$

$$My = 0.00943\ SFx + 0.83653\ SFy - 0.00471\ SFz - 0.00037\ SMx + \textit{0.02658 SMy} - 0.00110\ SMz$$

$$Mz = 0.06147\ SFx + 0.02699\ SFy - 1.07427\ SFz + 0.01037\ SMx + 0.00039\ SMy + \textit{0.12594 SMz}$$

Table 6.38: A set of 6 equations to be used in a spreadsheet for processing data from raw data

Some validation tests, using simultaneously the two pylon transducers, have been undertaken. They are presented in section 7.4, named static validation tests using simultaneously two pylon transducers. To evaluate and to compare these two transducers, some patient tests with the two pylon transducers simultaneously fitted on the same artificial limb were conducted and shown in section 7.6, named dynamic validation tests.

6.6.5 Using calibration matrix [C]

The calibration matrix [C] is used into a complete set of 6 equations as shown above in equation (6.4). Hence, table 6.38 shows the six equations in which the main channels are in bold italic type. Using this set of equations in a spreadsheet like Excel® or in any similar programme is easy, as explained in section 8.2.3.

6.7 CALIBRATION RESULTS USING THE PORTABLE DATA ACQUISITION SYSTEM

Because a portable data acquisition system (described in section 5.3), having different gain settings and bridge voltages, will be used later in all the performed tests, another full calibration was mandatory.

The performed procedure was identical as above. Therefore, only the results are now presented. The main difference was that the portable data recorder exhibited the results directly in voltage, instead of computer units.

Thus, the coefficients m_{ij} had the following unit: mV_i / N or N m_j as shown in the headings of table 6.39, showing the statistical analysis of the calibration data using the portable data acquisition system (same presentation as table 6.32).

The signs of the mean values are presented under the form of a chart, with main channel in bold type and point screen. The rule used was the same as the one shown in section 6.6.1.

coefficients	mean	standard error	p-value	r-square
m_{ij}	mV_i / N or N.m_j	mV_i / N or N.m_j		(%)
under load Fx				
m_{11}	1.50846	0.0010582	0.000	99.9995
m_{12}	0.00083	0.0496721	0.961	00.2741
m_{13}	0.08763	0.0040296	0.000	98.1325
m_{14}	0.00447	0.0006737	0.000	83.0526
m_{15}	0.01529	0.0013447	0.000	93.4931
m_{16}	0.13298	0.0011031	0.000	99.9381
under load Fy				
m_{21}	0.00825	0.0004813	0.000	92.7502
m_{22}	0.86646	0.0009711	0.000	99.9971
m_{23}	0.02793	0.0008235	0.000	98.0401
m_{24}	0.00092	0.0004487	0.049	15.7227
m_{25}	0.00378	0.0008789	0.000	44.6901
m_{26}	0.00619	0.0004599	0.000	88.7532
under load Fz				
m_{31}	0.01062	0.0047622	0.056	41.5485
m_{32}	0.05742	0.0516221	0.298	15.0226
m_{33}	3.24649	0.0205401	0.000	99.9719
m_{34}	0.37926	0.0022054	0.000	99.9763
m_{35}	0.00372	0.0282486	0.898	00.2469
m_{36}	0.00005	0.0007613	0.940	00.0836
under load Mx				
m_{41}	9.98818	0.0683463	0.000	99.9648
m_{42}	7.50153	0.4708304	0.000	97.1286
m_{43}	1.14501	0.0944549	0.000	99.9832
m_{44}	35.73444	0.0860052	0.000	99.9998
m_{45}	0.44501	0.1193246	0.045	72.6318
m_{46}	0.00811	0.0078385	0.094	87.7581
under load My				
m_{51}	1.10377	0.1291593	0.001	87.5408
m_{52}	63.86476	2.7830097	0.000	99.0631
m_{53}	1.35071	0.9040832	0.281	08.0194
m_{54}	1.14648	0.1273767	0.016	97.5630
m_{55}	136.42109	2.0052473	0.000	99.8913
m_{56}	0.41939	0.0527264	0.004	79.5902
under load Mz				
m_{61}	0.56231	0.0336729	0.000	99.9888
m_{62}	2.65351	0.3511176	0.000	83.7561
m_{63}	22.49432	0.0689499	0.000	99.9957
m_{64}	0.07905	0.0175881	0.127	62.6887
m_{65}	0.67891	0.1136221	0.003	79.7304
m_{66}	12.71181	0.0114598	0.000	99.9998

Table 6.39: The statistical analysis of the calibration data using the portable data acquisition system.

	SFx	SFy	SFz	SMx	SMy	SMz
Fx	+	-	+	+	+	-
Fy	+	+	+	+	+	-
Fz	-	+	+	+	-	+
Mx	+	+	+	+	-	+
My	+	-	-	+	+	+
Mz	-	+	+	-	-	+

Therefore, table 6.39 shows data processing and statistical analysis of such a calibration. The same comments as those expressed above could be highlighted. The following coefficients could be neglected (p-value ≥ 0.05): m_{12}, m_{31}, m_{32}, m_{35}, m_{36}, m_{46}, m_{53} and m_{64}.

According to the matrix (6.7), (see section 6.2), it was possible to put up the 6 * 6 coefficients square matrix [M], as shown in table 6.40. The inverted calibration matrix $[M]^{-1} = [C]$ is shown in table 6.41. The corresponding bridge voltages and gain settings are also shown in table 6.42.

As previously stated in section 6.6.5, the calibration matrix [C] is used into a complete set of equations extracted from the theoretical equation (6.4). This set of equations is shown in table 6.43 in which the six main channels are in bold italic type.

6.8 DISCUSSION

The work presented in this chapter provided many conclusions, which are presented in this final section.

1. The choice was made to use the dead-weight method for the calibration of the Villiers Pylon Transducer, applying one load and only one at one time and adopting the linear approach for the calibration model, as it was recommended by former researchers. Coefficients m_{ij} were derived, with the decision based on the p-values of the statistical analysis.

1.50846	0.00000	-0.08763	0.00447	0.01529	-0.13298
-0.00825	0.86646	0.02793	0.00092	-0.00378	0.00619
0.00000	0.00000	3.24649	0.37926	0.00000	0.00000
9.98818	7.50153	1.14501	35.73444	0.44501	0.00000
1.10377	63.86476	-1.35071	-1.14648	136.42109	-0.41939
-0.59137	-2.65351	22.49432	0.00000	0.67891	12.71181

Matrix [M]

Units: mV_i / N or $N.m_j$

Table 6.40: The 6*6 calibration matrix when the portable data acquisition system is used.

0.66431	0.00582	0.02190	-0.18748	-0.00947	-0.00610
0.02712	**1.14981**	0.02841	-0.24314	-0.53958	0.21879
-0.03023	-0.00630	**0.30804**	-0.00015	0.00456	-0.54548
0.00023	0.00003	-0.00327	**0.02801**	0.00020	0.00577
-0.00010	0.00003	0.00000	-0.00006	**0.00731**	-0.00040
0.00690	-0.00049	0.00021	-0.00183	0.00040	**0.07811**

Matrix [C] = $[M]^{-1}$

Units: N or $N.m_i$ / mV_j

Table 6.41: The inverted calibration matrix when the portable data acquisition system is used.

		BV	GS
Channel 1	Fx	7.46	1546
Channel 2	Fy	8.04	2005
Channel 3	Fz	7.56	3215
Channel 4	Mx	7.55	174
Channel 5	My	7.53	493
Channel 6	Mz	7.55	59

Table 6.42: The bridge voltage (BV) and gain settings (GS) used in the matrices shown in table 6.40 and 6.41.

Fx = ***0.66431 SFx*** + 0.00582 SFy + 0.02190 SFz - 0.18748 SMx - 0.00947 SMy - 0.00610 SMz

Fy = 0.02712 SFx + ***1.14981 SFy*** + 0.02841 SFz - 0.24314 SMx - 0.53958 SMy + 0.21879 SMz

Fz = - 0.03023 SFx - 0.00630 SFy + ***0.30804 SFz*** - 0.00015 SMx + 0.00456 SMy - 0.54548 SMz

Mx = 0.00023 SFx + 0.00003 SFy - 0.00327 SFz + ***0.02801 SMx*** + 0.00020 SMy + 0.00577 SMz

My = -0.00010 SFx + 0.00003 SFy + 0.00000 SFz - 0.00006 SMx + ***0.00731 SMy*** - 0.00040 SMz

Mz = 0.00690 SFx - 0.00049 SFy + 0.00021 SFz - 0.00183 SMx + 0.00040 SMy + ***0.07811 SMz***

Table 6.43: The complete set of six equations to use in a spreadsheet to convert raw data recorded through the portable data acquisition system into processed data.

2. Despite a lot of efforts made to minimise all cross-effects, some of them could not be totally eliminated, especially with the three moments:

- Fx in Mx main channel
- Fy in My main channel
- Fz in Mz main channel

These cross-effects probably are due to three main reasons (in descending order):

- misalignment on some gauges, in particular the Fx shear gauges but this was inevitable with so little room onto such a small gauging area;
- high deflection of both the transducer with its aluminium bell and shin tube;
- some defects in the calibration set-ups, i.e., particularly pulleys and cables in My.

However, this does not affect the global mechanical performance of this pylon transducer, but results in N or N m must be corrected using the inverted calibration matrix [C]. A discussion about these interactions will be re-opened in the following chapter 7, concerning the validation tests.

These interactions did not depend on the amplifiers and recording system used, because they were identical when both data acquisition systems were used.

In the following chapter 7, the conducted validation tests will establish the validity of the set of equations shown in table 6.43.

In chapter 8, an explanation concerning how this set of equations was used through a macro-command of a spreadsheet to exhibit the processed data of all conducted tests will be provided.

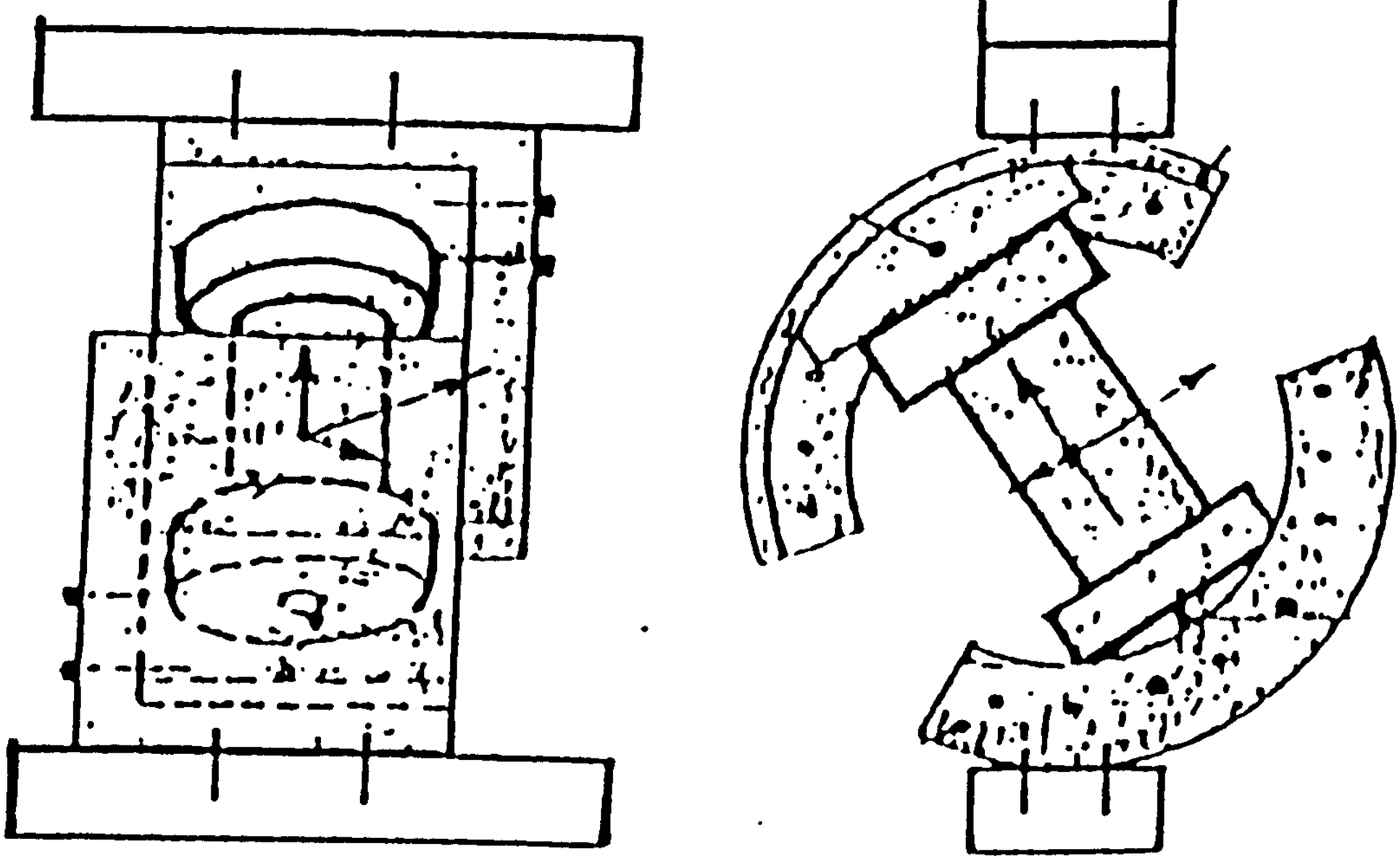

Figure 7.1: The versatile device used for calibration matrix evaluation and designed by Magnissalis (1992)

7 VALIDATION TESTS OF THE CALIBRATION MATRIX APPLIED ON THE NEW VILLIERS PYLON TRANSDUCER

7.1 INTRODUCTION

When a calibration matrix from a new designed transducer is obtained through calibration tests, it is always necessary to check its prediction ability, by applying combined known loads and moments on the transducer. This procedure is known as the validation of the calibration matrix.

In other words, there are two reasons for conducting a validation procedure. For both calibration matrix and transducer, the validation procedure means:

- to apply various load configurations on the transducer: applied load
- to measure the output signals of the transducer through the calibration matrix: predicted load.

By comparison of these values, through statistical study such as a regression analysis, the prediction ability of the new transducer accompanying calibration matrix can be estimated.

For the validation tests, two ways of loading were considered:

a) the first approach was static, using firstly a versatile device specially conceived by Magnissalis (1992), secondly the bench heavy table used for calibration (see chapters 4 and 6) with the new transducer alone followed by the same apparatus and the Strathclyde Pylon Transducer (SPT) designed by Berme *et al.* (1975) assembled in series along a shaft.

b) the second approach was dynamic, testing simultaneously the two transducers (SPT and VPT) fitted on the prosthesis of a transfemoral patient walking in the gait laboratory.

7.2 STATIC TESTS WITH SPECIAL DEVICE

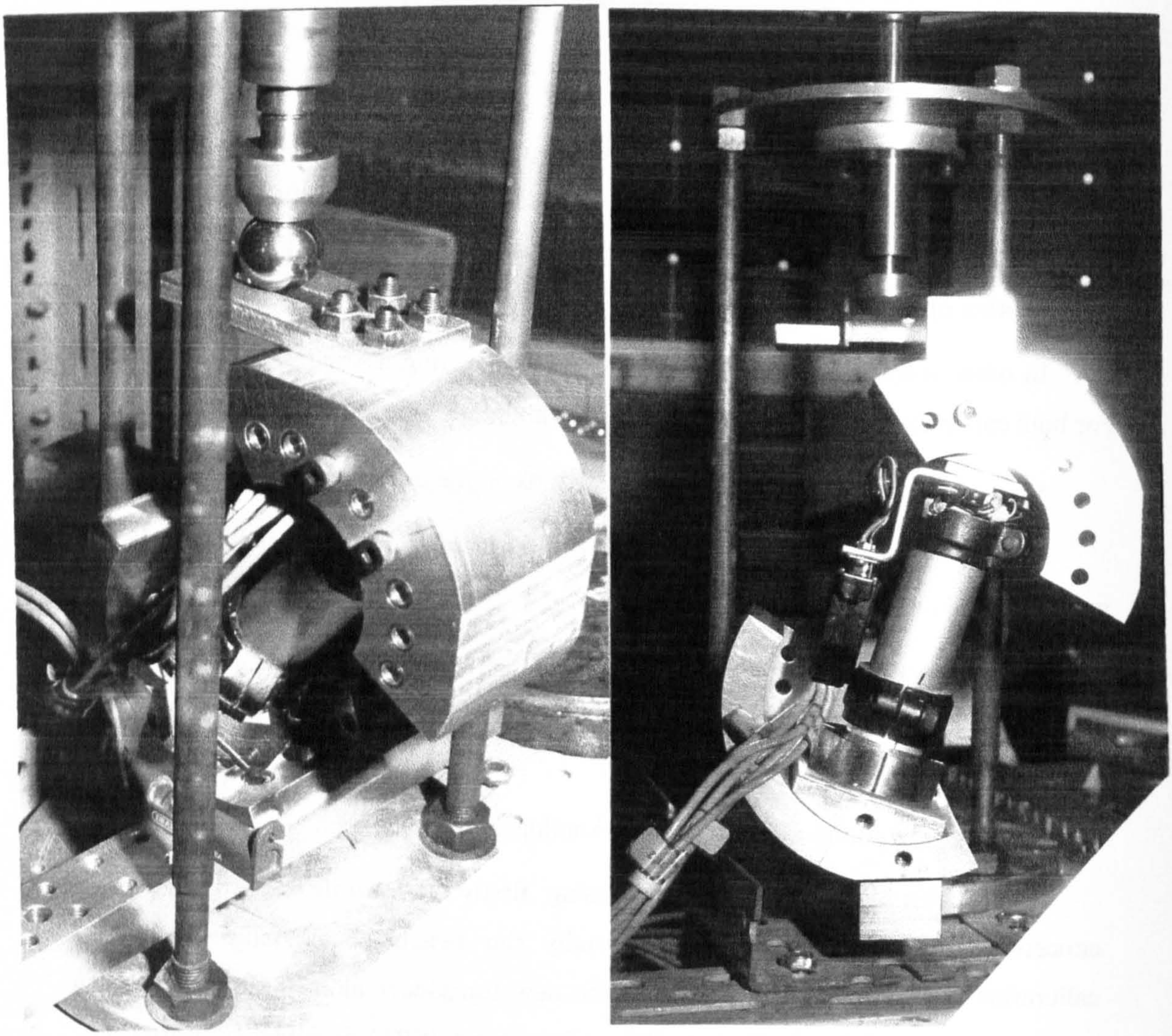

Figure 7.2: A general view of the set-up using the special device designed by Magnissalis (1992): semi-front and lateral view.

7.2.1 Description of the device used

The device developed by Magnissalis (1992) to validate the calibration matrix of the Strathclyde Pylon Transducer (SPT) allows the generation of three forces and three moments through the application of one single load wherever it is produced, such as an Instron® machine or dead - weight load. The analytical description of the componentry is given in Magnissalis (1992).

The device is made of two semi-circular flanges, each of them fitted on both sides of the pylon transducer. The componentry with the pylon transducer was calculated to be inscribed in a circle. In other words, the Magnissalis device has been developed for the Strathclyde Pylon Transducer, with its dimension as shown in figure 7.1.

For another transducer, having different dimensions, the device was not any longer inscribed in a circle but in an ellipse. Therefore, it was still possible to use it and it worked but less efficiently. This important drawback had prevented the measurement of torque. It also introduced an off - axis load about the X axis, source of problems such as eversion and inversion. This device generated another particularity: the theoretical angle Θ_z shown by the device was not easy to measure accurately. It had to be checked by measuring precisely the whole dimensions of the set-up by the means of a plumbline and a protractor. Thus, some errors, due to parallax, could appear. Another important consequence of the particular shape of the device was its non-reversibility. In other words, when the transducer was turned from plantar to dorsiflexion, the bending moment lever arm was not the same, because it was designed for a different length of transducer.

Figure 7.2 shows a front and lateral view of the set-up. The Villiers Pylon Transducer (VPT) was used with the bell covered with an aluminium tube (0.1 m long) as prosthetic shank tube. Because there was no torque (see in section 7.2.2 the direction of the loading force vector), the use of any jubilee clip or clamp collar was not necessary. The aluminium artificial ankle was removed and substituted by an aluminium plate to link the transducer with the flange of the Magnissalis's device. However, the bottom flange of the transducer was bolted in the same way as in calibration (see section 6.3.1). To avoid any slipping, two pieces of sandpaper were

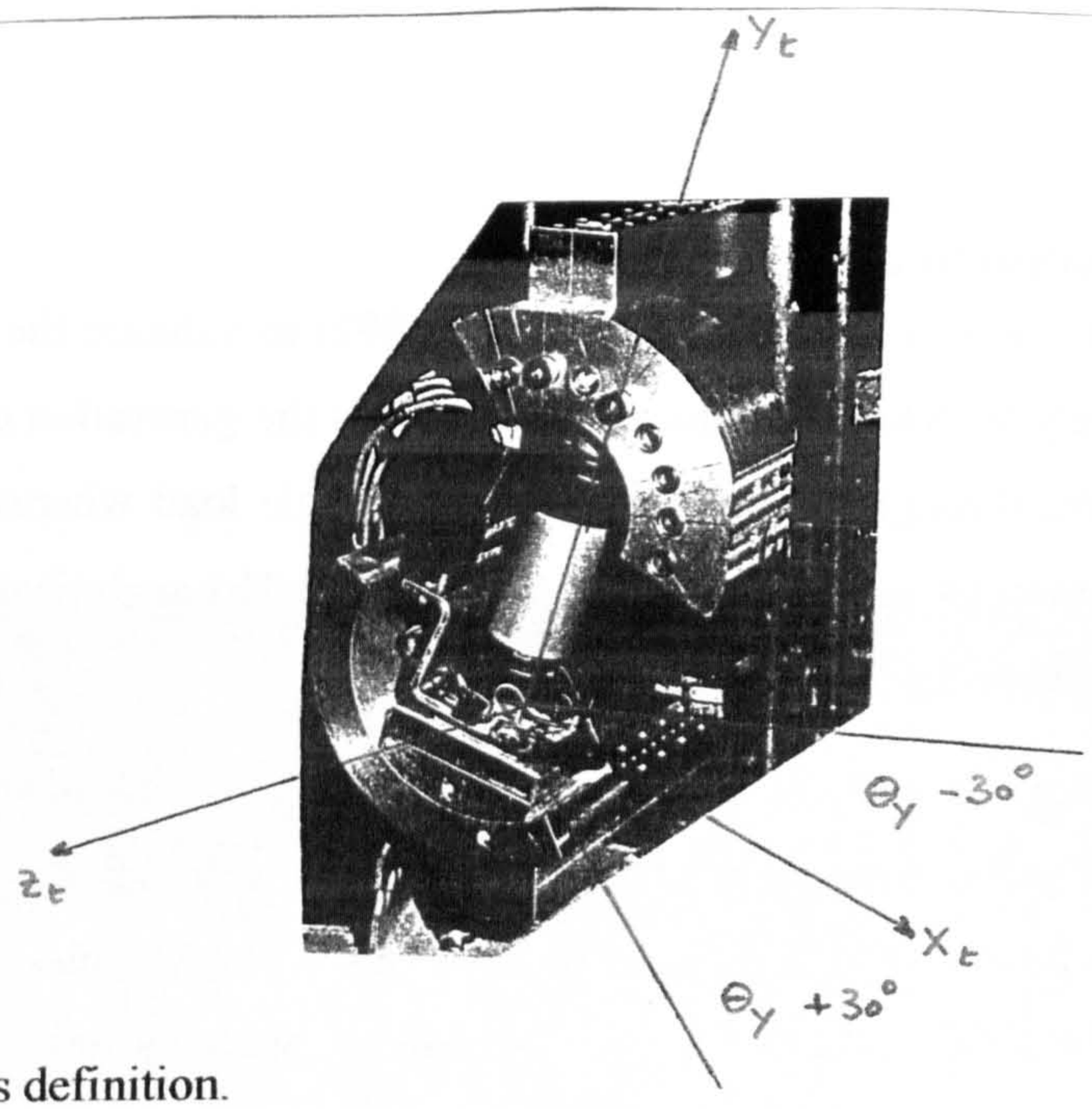

Figure 7.3: Θ_y and its definition.

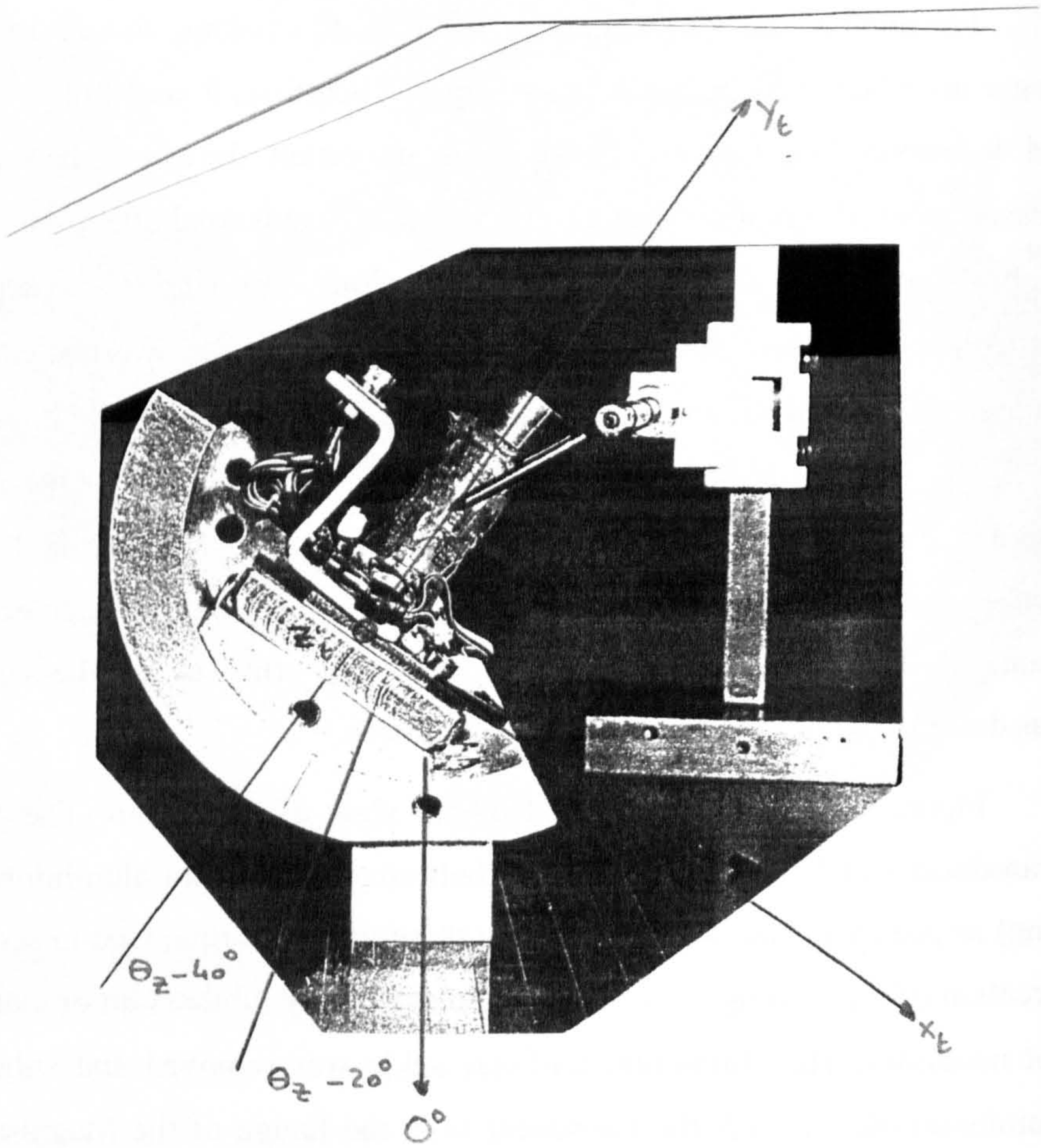

Figure 7.4: Θ_z and its definition.

placed between the top and bottom contacting surfaces. At each step, the set-up was carefully checked by the means of a plumbline and a spirit level.

The device was able to represent different positions. Two angles could be implemented:

as shown in figure 7.3: Θ_y with two options: 0 and $\pm \approx 30°$

as shown in figure 7.4: Θ_z with three options: 0, $\pm \approx 20°$ and $\pm \approx 40°$, merging these options, there were theoretically fifteen possibilities of combined load as shown in table 7.1. All of them were not explored because in practice, in tests with patients, some angles such as $\Theta_z \pm 40°$ were never recorded.

The angle Θ_y was a rotation about the longitudinal Y axis of the transducer. It was thus the representation of an internal or external rotation of the artificial foot. The angle Θ_z was a rotation about the medio - lateral Z axis of the transducer, it was thus the representation of dorsi and plantar flexion. Applying the right hand rule for a right foot, the sign convention was the following (see chapter 2):

Θ_y	positive	internal
	negative	external
Θ_z	negative	plantarflexion
	positive	dorsiflexion

Positive and negative signs depended on the origin of the Y axis and on the point of view of the observer. The convention was: the origin of the Y axis was the middle of the artificial axis and the observer was viewing the device from the distal part to the proximal, i.e., the foot was always in the foreground.

The loading combinations shown in table 7.1 were sufficient, regarding one requirement met: for the validation to be as reliable as possible the way by which the loads were to be applied on the transducer should be similar to the mode of the loads applied in practice. Consequently, Θ_z, which represented dorsi and plantar flexion, had sufficient magnitude with $\pm 20°$. With respect to Θ_y, which represented lateral or medial rotation about the longitudinal Y axis, it also was of sufficiently high magnitude with $\pm 30°$.

		$\Theta_y = -30°$		
$\Theta_z = -20°$		$\Theta_z = 0$		$\Theta_z = 20°$
external rotation plantar flexion		external rotation		external rotation dorsi flexion

		$\Theta_y = 0°$		
$\Theta_z = -40°$	$\Theta_z = -20°$	$\Theta_z = 0°$	$\Theta_z = 20°$	$\Theta_z = 40°$
plantar flexion			dorsi flexion	

	$\Theta_y = 30°$	
$\Theta_z = -20°$	$\Theta_z = 0°$	$\Theta_z = 20°$
internal rotation plantar flexion	internal rotation	internal rotation dorsi flexion

Table 7.1: The different possibilities of the explored combined load.

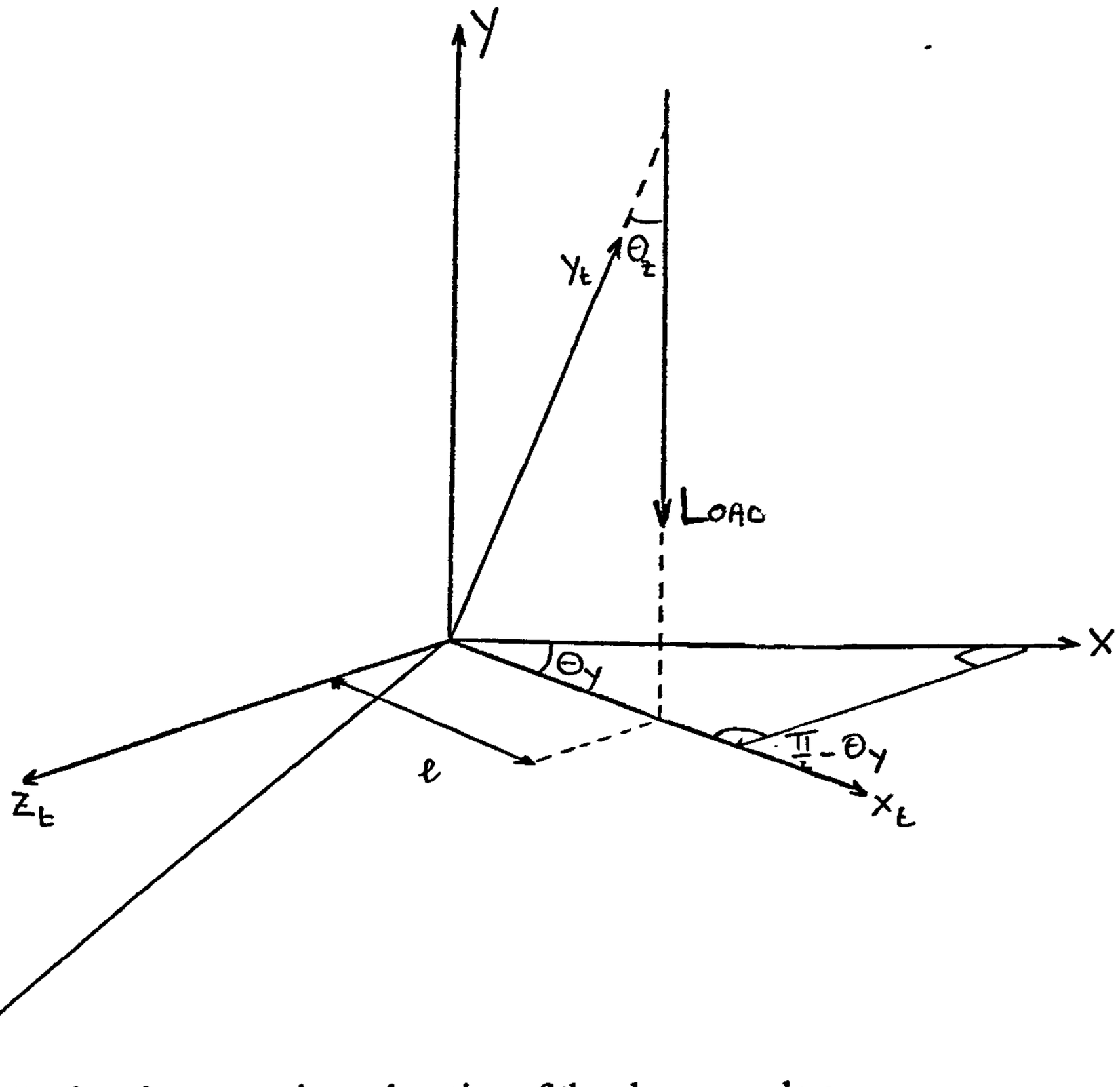

Figure 7.5: The trigonometric explanation of the chosen angles:
External Rotation, Θ_y was negative.
Dorsiflexion, Θ_z was positive.

7.2.2 Mathematical considerations

Referring the two figures 7.3 and 7.4, it is possible to show through figure 7.5 that, by trigonometry, the projection of the unique force vector about the three transducer axes F_x, F_y, F_z, was:

$$F_x = L \sin \Theta_z \cos \Theta_y \tag{7.1}$$

$$F_y = L \cos \Theta_z \tag{7.2}$$

$$F_z = L \sin\Theta_z \cos\left(\frac{\pi}{2} - \Theta_y\right) \tag{7.3}$$

$$M_x = L (\mathit{1} \sin \Theta_y) \sin \Theta_z \tag{7.4}$$

$$M_y = 0 \tag{7.5}$$

$$M_z = L (\mathit{1} \cos \Theta_y) \sin \Theta_z \tag{7.6}$$

where L = magnitude of the applied load transmitted through the bell as in calibration tests described in chapter 6;

1 = magnitude of the lever arm which was the distance between the line of action of the applied load and the centre line of the bending moment gauges. This lever arm *1* was the same for the A/P bending moment gauges (Mz) and the M/L bending gauges (Mx). When the angle of dorsi flexion Θ_z was 20°, the lever arm *1* = 0.023 m (when Θ_z was 40°, *1* = 0.042 m). When the angle of plantar flexion Θ_z was 20°, the lever arm *1* = 0.004 m and 0.012 m with Θ_z = 40°. These values were scrupulously checked for each set-up by the means of a plumbline and a square set.

Considering the small value of the different lever arms and the set-up configuration, both applied M/L and A/P bending moments were lower values relative to those found in practice (4 N m versus 10 N m in Mx and 7 N m versus 70 N m in Mz). These two bending moments were therefore cautiously checked and analysed.

The line of action of the applied load was always in a vertical plane containing

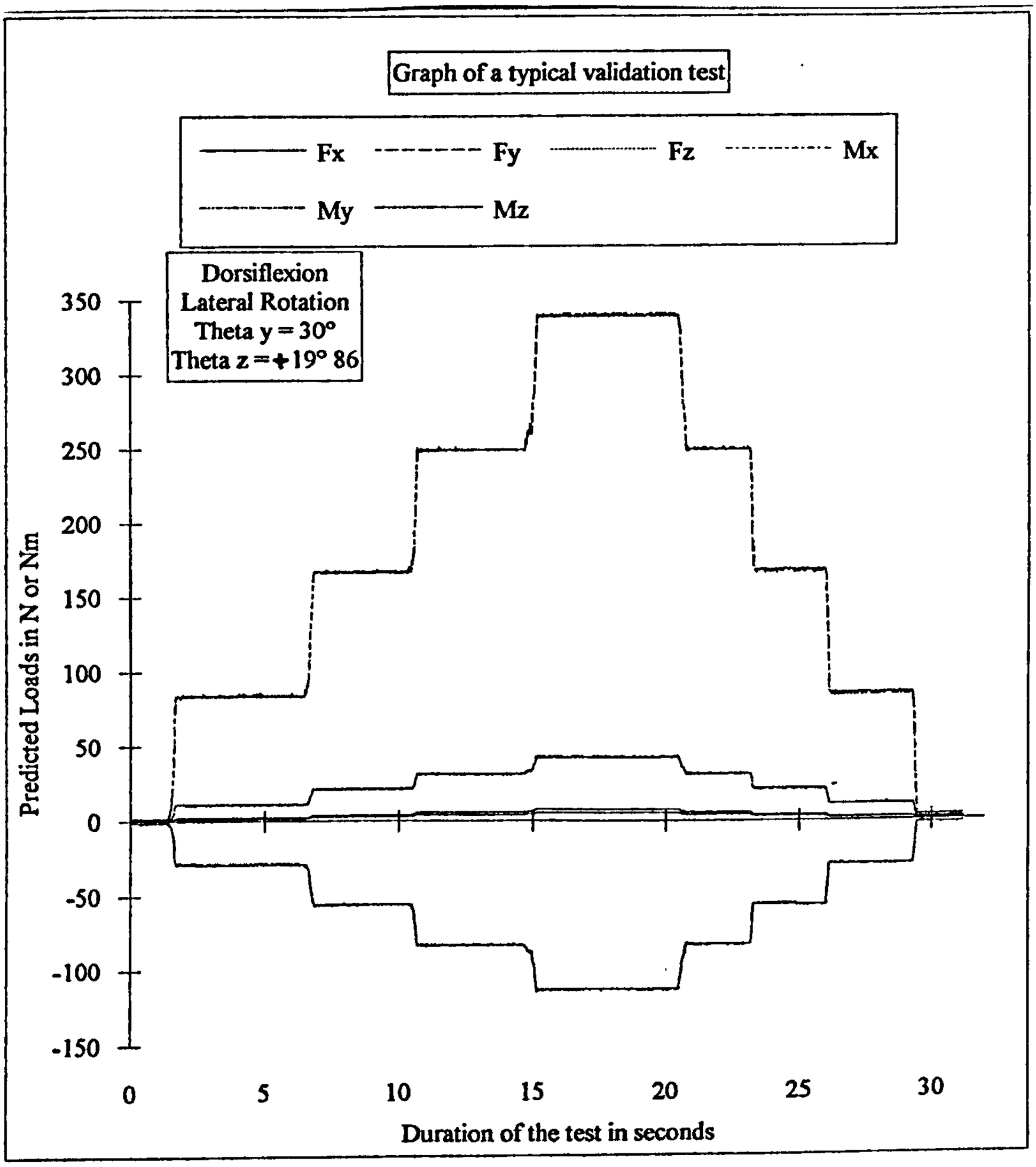

Figure 7.6: Typical Validation Test: All channels were simultaneously recorded

Predicted Value									
Fx in N	-1.2	-29.1	-55.4	-83.7	-113.3	-83.9	-56.1	-29.3	-1.2
Fy in N	1.3	83.8	167.4	249.1	340.7	249.2	167.6	83.8	1.6
Fz in N	1.12	11.08	20.82	31.12	41.87	30.59	20.69	10.92	0.69
Mx in N.m	0.81	1.81	2.81	3.81	4.97	3.86	2.85	1.85	0.81
My in N.m	0.05	0.04	0.01	0.00	-0.01	0.00	0.02	0.03	0.05
Mz in N.m	0.01	1.75	3.6	5.34	7.4	5.34	3.6	1.86	0.12

Table 7.2: Predicted load expressed by the VPT through portable data acquisition system and calibration matrix (from figure 7.6)

the Y_t axis of the transducer, thus, there was never any torque. The applied M_{yt} value should be always equal to zero.

Therefore, the magnitude of the applied values was known and it was easy to compare them with the predicted load values exhibited by the new transducer through the portable data acquisition system and calibration matrix [C], calculated in the previous section 6.7 (see table 6.43).

7.2.3 Description of the tests

All tests presented below were performed in an identical manner. For each of the investigated possibilities among those given above, two series of tests were monitored:

1. one test with the transducer and the two assistive walking devices switched on. In this case, the portable data acquisition unit was configured as it was described in chapter 5. That is, with MYOGAIT2.TYP as configuration file having a sampling rate of 64 Hz. This way of performing the test offered the possibility to check the transducer in the most realistic routine because it is the configuration that will be used later in all tests made with patients for gait assessment.

The disadvantage was the relative high sample rate for a static test and thus the large number of unnecessary samples to study. A loading - unloading cycle was commonly 80 seconds, which represented a large amount of 5120 rows to study. This is why another solution was adopted, as follows:

2. one test with the transducer alone using a Myodata configuration file named VALIDAT.TYP in which all parameters were the same as in MYOGAIT2.TYP except two items:

a) only six channels of the portable data acquisition system corresponding to the transducer outputs were used

b) the sampling rate was reduced to the minimum level allowed by the recording unit, that is: 16 Hz (bandwidth = 6 Hz, see more details in chapter 5).

This allowed the elimination of any interaction between the walking devices and the VPT and to check if the sampling rate was changing the shape of the traces

	Fx			Fy			Fz		
Loading Weight in N	Applied in N	Predicted in N	Mean Diff. in %	Applied in N	Predicted in N	Mean Diff. in %	Applied in N	Predicted in N	Mean Diff in %
7.84	-2.3	-1.2	n.s.	7.37	6.3	n.s.	1.33	1.12	n.s.
96.82	-28.4	-29.1	2.5	91.1	88.8	-2.5	16.41	11.08	-32.5
185.8	-54.5	-55.4	1.7	174.8	172.4	-1.4	31.49	20.82	-33.9
274.77	-80.7	-83.7	3.7	258.5	253.1	-2.1	46.57	31.12	-33.2
372.87	-109.43	-113.3	3.5	350.9	345.7	-1.5	63.20	41.87	-33.8
274.77	-80.7	-83.9	3.9	258.5	254.2	-1.7	46.57	30.59	-34.3
185.80	-54.5	-56.1	2.9	174.8	172.6	-1.3	31.49	20.69	-34.3
96.82	-28.4	-29.3	3.2	91.1	88.8	-2.5	16.41	10.92	-33.5
7.84	-2.3	-1.2	n.s.	7.37	6.6	n.s.	1.33	0.69	n.s.

	Mx			My			Mz		
Loading Weight in N	Applied in N.m	Predicted in N.m	Mean Diff. in %	Applied in N.m	Predicted in N.m	Mean Diff. in %	Applied in N.m	Predicted in N.m	Mean Diff in %
7.84	n.s	n.s	n.s	0	0.05	0	- 0.15	0.01	n.s
96.82	n.s	n.s	n.s	0	0.04	0	1.81	1.75	n.s
185.8	n.s	n.s	n.s	0	0.01	0	3.47	3.6	n.s
274.77	n.s	n.s	n.s	0	0.00	0	5.14	5.34	n.s
372.87	n.s	n.s	n.s	0	0.01	0	6.98	7.4	-6.0
7.84	n.s	n.s	n.s	0	0.05	0	5.14	5.34	n.s
96.82	n.s	n.s	n.s	0	0.03	0	3.47	3.6	n.s
185.80	n.s	n.s	n.s	0	0.02	0	1.81	1.86	n.s
274.77	n.s	n.s	n.s	0	0.00	0	0.15	0.12	n.s

Table 7.3: Applied and Predicted Loads of the test described in section 7.2.4.1 with the mean difference (Diff.) in percentage (n.s = not significant)

$\Theta_z = 19° 86$	$\sin \Theta_z = 0.339$	$\cos \Theta_z = 0.941$	$l = 0.023$ m
$\Theta_y = -30°$	$\sin \Theta_y = -0.5$	$\cos \Theta_y = -0.866$	$\cos\left(\frac{\pi}{2} - \Theta_y\right) = \sin\Theta_y = 0.5$

Table 7.4: Numerical values for applied loads L in the test described in section 7.2.4.1

and the magnitude of the results. The complete results are shown in appendix 11.VII.1.

Between each test, the whole set-up was dismantled. The loading process was the dead-weight method. The weight-carrier was similar to the one used in the axial load calibration test (see section 6.3.2). The loading cases were as follows:

Applied Load	Loading Mass in kg	Loading Weight in N
Weight Carrier	0.8	7.84
20 lb. (A14)	9.87	96.82
20 lb. (A15)	18.94	185.80
20 lb. (A17)	28.01	274.77
10 kg (A9)	38.01	372.87

A loading-unloading cycle was performed for all tests. At each loading level, a thirty seconds stop was observed except at full loading level in which a two minutes stop was observed. When the test was completed, data were transferred into the host computer under the form of a special Myodata file, named *.IMG. From this file and for each channel, five seconds (5 x 16 = 80 samples), randomly chosen, of each loading case were carried into a sequence of 66 usual ASCII raw data files. As example, for four loading cases, that gave:

Loading Cases	Denomination of transferred files
0	Fx_1, Fy_1, Fz_1, Mx_1, My_1, Mz_1.TXT
7.84 N	Fx_2, Fy_2, Fz_2, Mx_2, My_2, Mz_2.TXT
.../...	
372.87 N	Fx_6, Fy_6, Fz_6, Mx_6, My_6, Mz_6.TXT
.../...	
0	Fx_{11}, Fy_{11}, Fz_{11}, Mx_{11}, My_{11}, Mz_{11}.TXT

At full loading case, the 5 seconds transferred were taken from the end of the two minutes stop, to ensure recording stabilised values.

This being done, the 66 files were merged in six raw data files named Fx, Fy, ..., Mz .TXT. Finally, these 6 raw data files were analysed through two Excel® macro-sheets: MYOGAIT2.XLM (when the two walking sticks were used, sampling frequency 64 Hz) and MYOGAIT01.XLM (when no walking aids were used,

	Mean Difference in %	Comments
Fx A/P Shear	≈ 3 %	the predicted load is always higher than applied; mean difference in % is positive
Fy Axial Load	from ≈ - 2.5 to - 1.3 %	1. the predicted load is always lower than applied; mean difference in % is negative 2. the accuracy increases for higher loads applied
Fz M/L Shear	≈ - 33 %	1. the predicted load is always lower than applied; mean difference in % is negative 2. the difference seems linear (quotient of the two values is always from 1.48 to 1.52 (see section 9.7)
Mx M/L Bending Moment	not significant	the applied moments were too small to express some accurate comments
My Torque	≈ 0 %	
Mz A/P Bending Moment	≈ 6 %	the accuracy was sufficient for an applied moment higher than 6 N.m (10 % of the value found in practice)

Table 7.5: The mean difference in percentage between applied and predicted loads with appropriate comments in one validation tests.

sampling frequency 16 Hz). These macro-sheets are fully described in chapter 8. The data files derived from the different tests carried out for any particular loading case were reduced to size average values for each loading case.

7.2.4 Results

7.2.4.1 SAMPLE TEST FULLY DESCRIBED: TEST COMBINING DORSIFLEXION AND EXTERNAL ROTATION OF THE FOOT

One example is fully detailed in the following paragraphs, the whole set of results and analytical data are shown in appendix 11.VII.2.

Figure 7.6 shows a graph of a typical validation test. It was a combined load in the anterio - posterior plane with a rotation about the Y_t axis of the transducer. The angle Θ_y = - 30° was negative, hence it was an external rotation. The angle $\Theta_z = \sin^{-1}$ $\frac{52}{153} = \sin^{-1} 0.339 = 19° 87$ was positive, hence it was a dorsiflexion. The lever arm for bending moments was 0.023 m. In this configuration, the described test was the one performed by the VPT and the two assistive walking devices switched on, at the sampling frequency of 64 Hz. The difference of the predicted values between 0 N and 7.84 N (weight-carrier) was not sufficient to be seen on the traces. Hence, the zero value was erased. The traces started with the weight-carrier loading case. The spreadsheet file was composed of 30 seconds multiplied by a sampling frequency of 64 Hz = 1920 rows. If one row was randomly chosen for each loading case, that gave the table 7.2 which shows the numerical values extracted from figure 7.6 to facilitate the reading.

From equations 7.1 to 7.6, it was thus possible to calculate applied loads being compared with the predicted loads shown in table 7.2. Studying the two bending moments Mx and Mz, it appeared that the applied values in such channels were smaller than the values found in practice (50 % in Mx and 90 % in Mz). The applied values lower than 4 N m in Mx and 6 N m in Mz were thus erased and not considered sufficiently accurate for any comment and conclusion. Therefore, the full results of the chosen example are shown in table 7.3, with numerical values of the chosen example in table 7.4. Table 7.3 has also a column named « mean difference in % » to justify the conclusions stated in the following paragraphs. Mean differences in

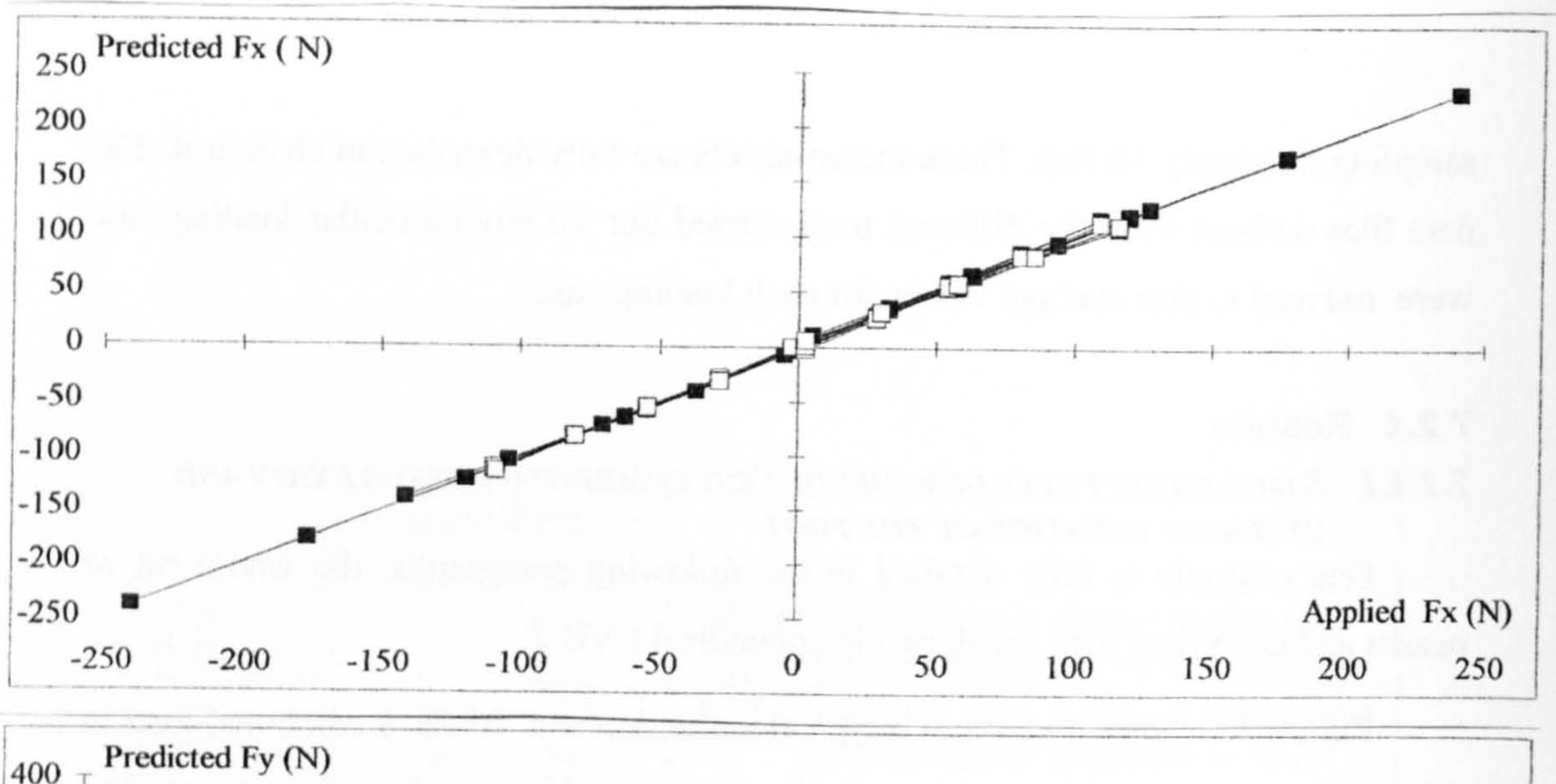

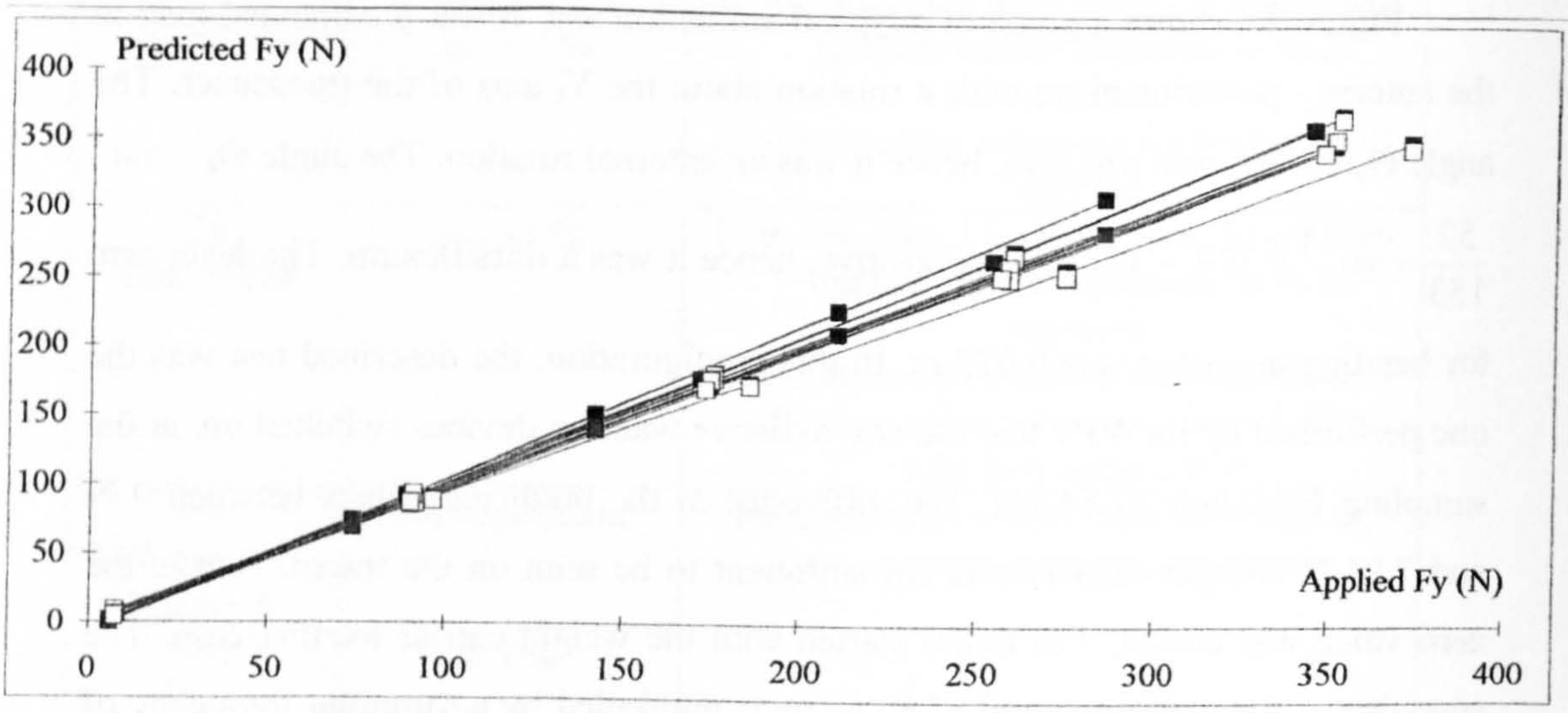

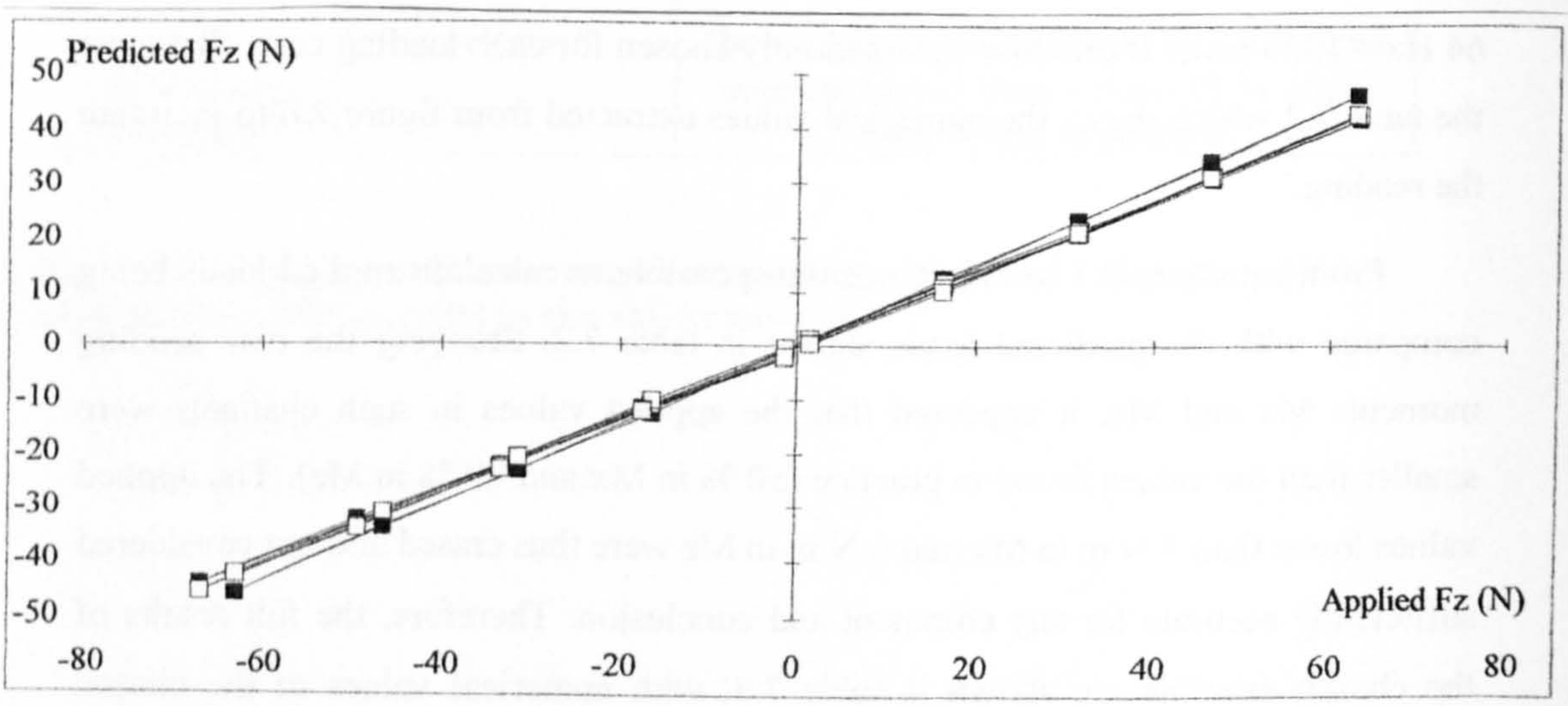

Figure 7.7: Predicted versus Applied A/P (Fx) and M/L (Fz) Shear Forces and Axial Load (Fy). Four tests for each graphs: two in dorsiflexion and two in plantarflexion (see numerical values in appendix 11.VII.1). The traces are linear.

percentage were calculated using the following formula, in which a positive result showed a predicted value higher than applied and the opposite when the result was negative:

$$\frac{\text{predicted load - applied load}}{\text{applied load}} \times 100 \qquad (7.7)$$

From table 7.3, the first comments they were possible to express are shown in table 7.5. In other words, the mean accuracy of the Villiers Pylon Transducer is high, except in M/L shear force Fz, and sufficiently high for any gait assessment. This was particularly verified in the A/P plane: Fx shear force, Fy axial load and Mz bending moments. These three channels were thoroughly studied in the conducted tests with patients in chapter 8. The conducted test could not show any accurate answer about M/L bending moment Mx and none for transverse moment. The VPT appeared to be inaccurate in M/L shear force Fz, but because of the low values, it was not important for the current investigation. However, the non-accuracy of this particular channel remained linear. A unique and efficient correcting factor could thus be established from all these validation tests. The other tests, shown in appendix 11.VII.2, performed in dorsiflexion, internal rotation, plantarflexion and both rotations, dorsi and plantarflexion without rotations allowed to express identical conclusions.

To corroborate these comments, a summarised analysis of all tests made, such as plantar and dorsiflexion with and without any rotation, are now shown. The results are presented in a way so that inferences about the prediction ability of the calibration matrix can be drawn. In figure 7.7 and 7.8, the predicted load values are plotted against the actual applied load components. Three important remarks about these figures can be made.

1. The ideal pattern would be a straight line with unit slope and zero intercept, as shown in figures 7.7 and 7.8. A linear regression of the data gives the following:

(predicted Fx) = 0.48769 + 0.99702 x (applied Fx) in N (7.8)
(predicted Fy) = - 4.39947 + 1.00518 x (applied Fy) in N (7.9)
(predicted Fz) = - 0.28468 + 0.67596 x (applied Fz) in N (7.10)
(predicted Mx) = 0.04652 + 1.07471 x (applied Mx) in N m (7.11)
(predicted Mz) = - 0.13454 + 0.97916 x (applied Mz) in N m (7.12)

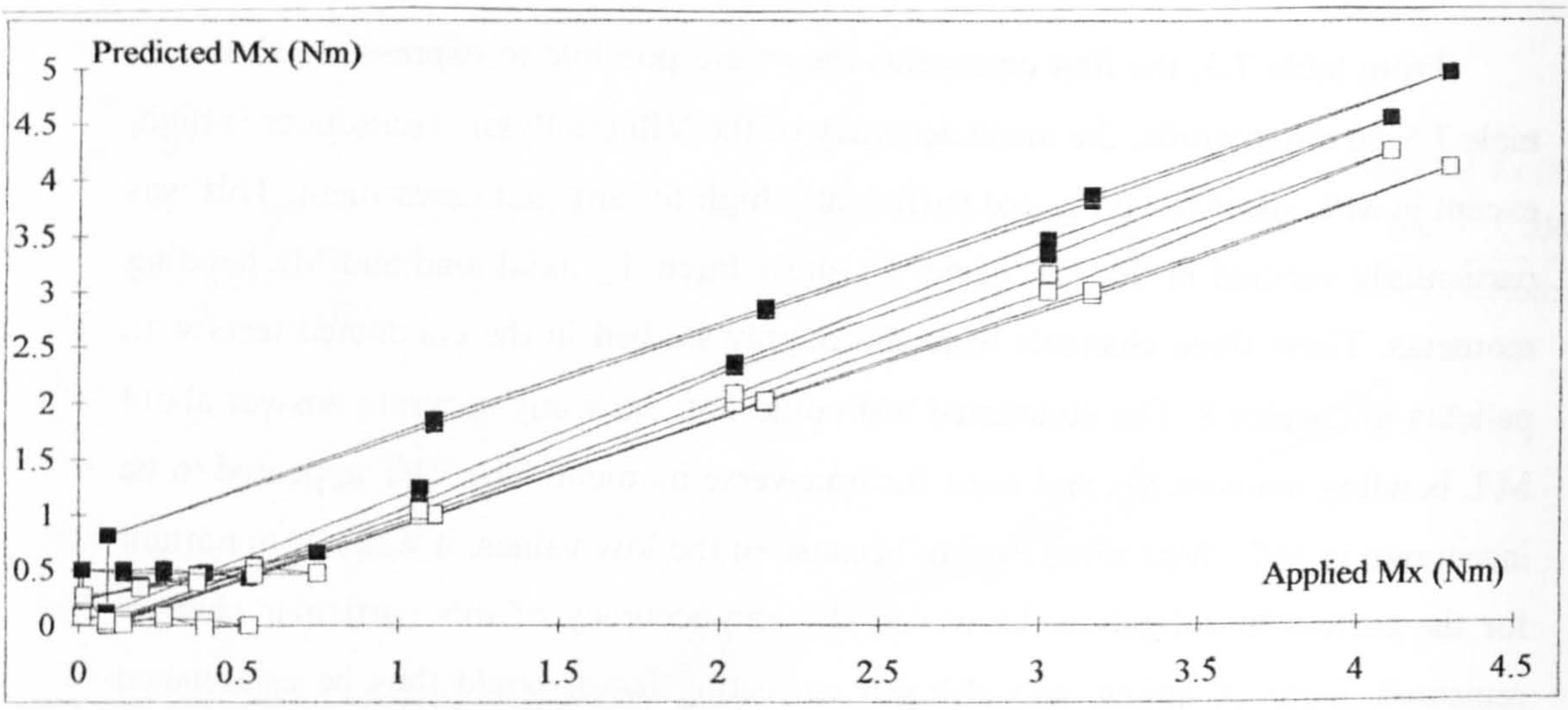

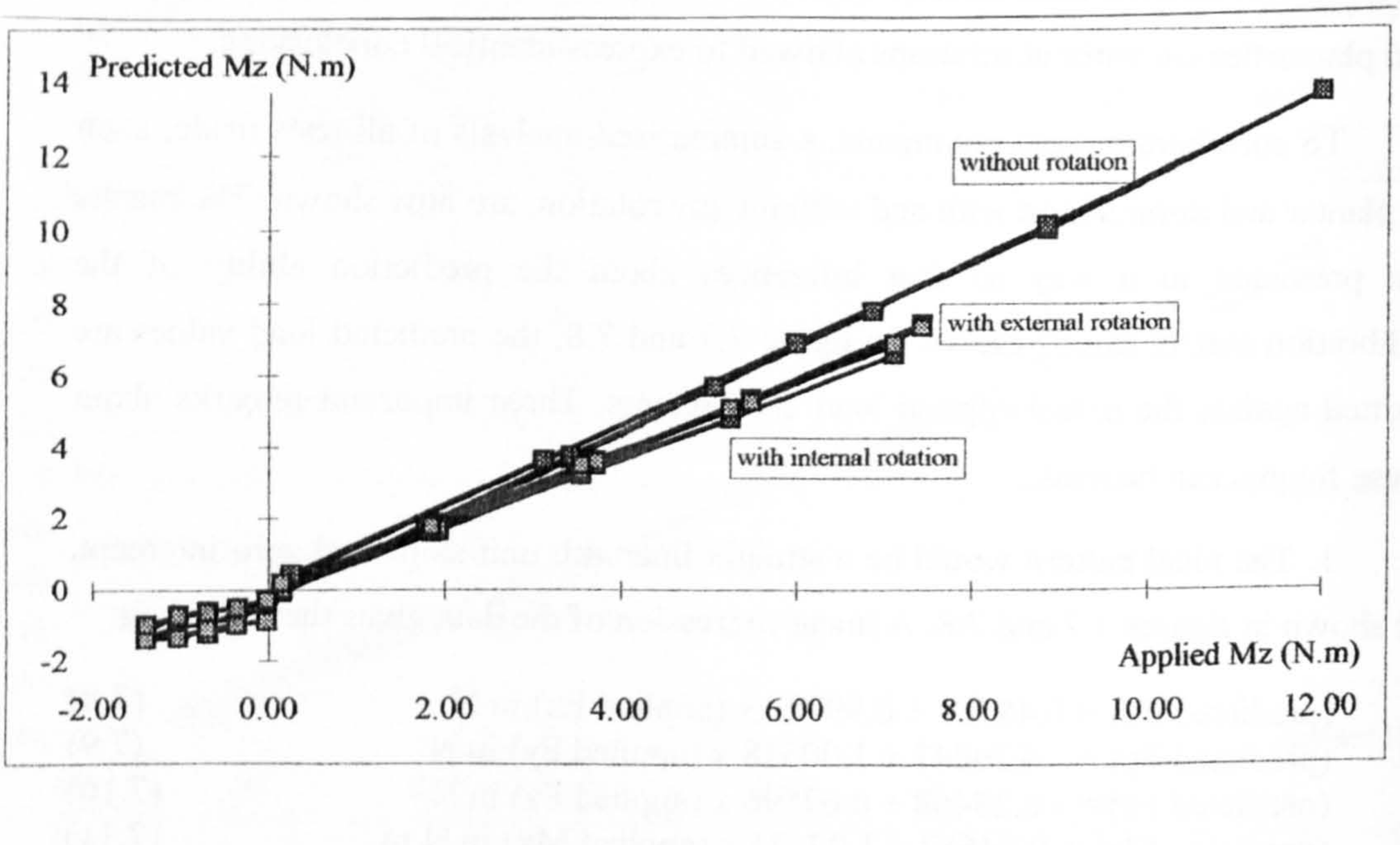

Figure 7.8: Predicted versus Applied Positive Moments in four tests in M/L bending moment Mx (top) and A/P bending moment Mz (bottom), with and without rotation.

Indeed, the intercepts were close to zero except in Fy, but - 4 N is not significant regarding the average value usually exhibited by such a channel in practice. The slopes were close to unity except in Fz. On the other hand, as indicated by the r-square values, these equations satisfied the plotted data by more than 99 %, the only exception being the equation for Fy where the value for r-square was poorer (98.6 %). The complete statistical regression studies of the data are shown in appendix 11.VII.

When applied bending moments were very low, that is less than 4 N m (Mx) and 6 N m (Mz) because a so small lever arm, results were inaccurate and could be combined with noise. This was particularly true for A/P bending moment Mz in plantarflexion, as shown in appendix 11.VII.2, when the lever arm was about 4 and 12 mm. Consequently, the calculated errors were established cancelling the two first and last load cases, as recommended by Magnissalis (1992). They are as follows (table 7.6):

load component	calculated prediction error in percentage
for Fx over 20 N	2.3
for Fy over 50 N	2.0
for Fz over 20 N	31.9
for Mx over 4 N m	not calculated
for Mz over 6 N m	6

Table 7.6: The calculated prediction error exhibited by the VPT in static tests using a special rig.

The thresholds for the three forces were chosen according to the recommendation of Magnissalis (1992). However, concerning the two moments, the thresholds were lower (4 and 6 N m instead of 10) than in Magnissalis (1992) because of the low level of these bending moments when the tested subjects had an assisted gait (usually, Mx was < 10 N m and Mz < 70 N m, see chapter 8).

These calculated prediction error from the VPT will be compared later (see section 7.5) with those from the SPT and studied by Magnissalis (1992). The torque channel My is not shown because in all conducted tests until now, applied torque was 0, it was therefore impossible to plot any results. The torque study will be described

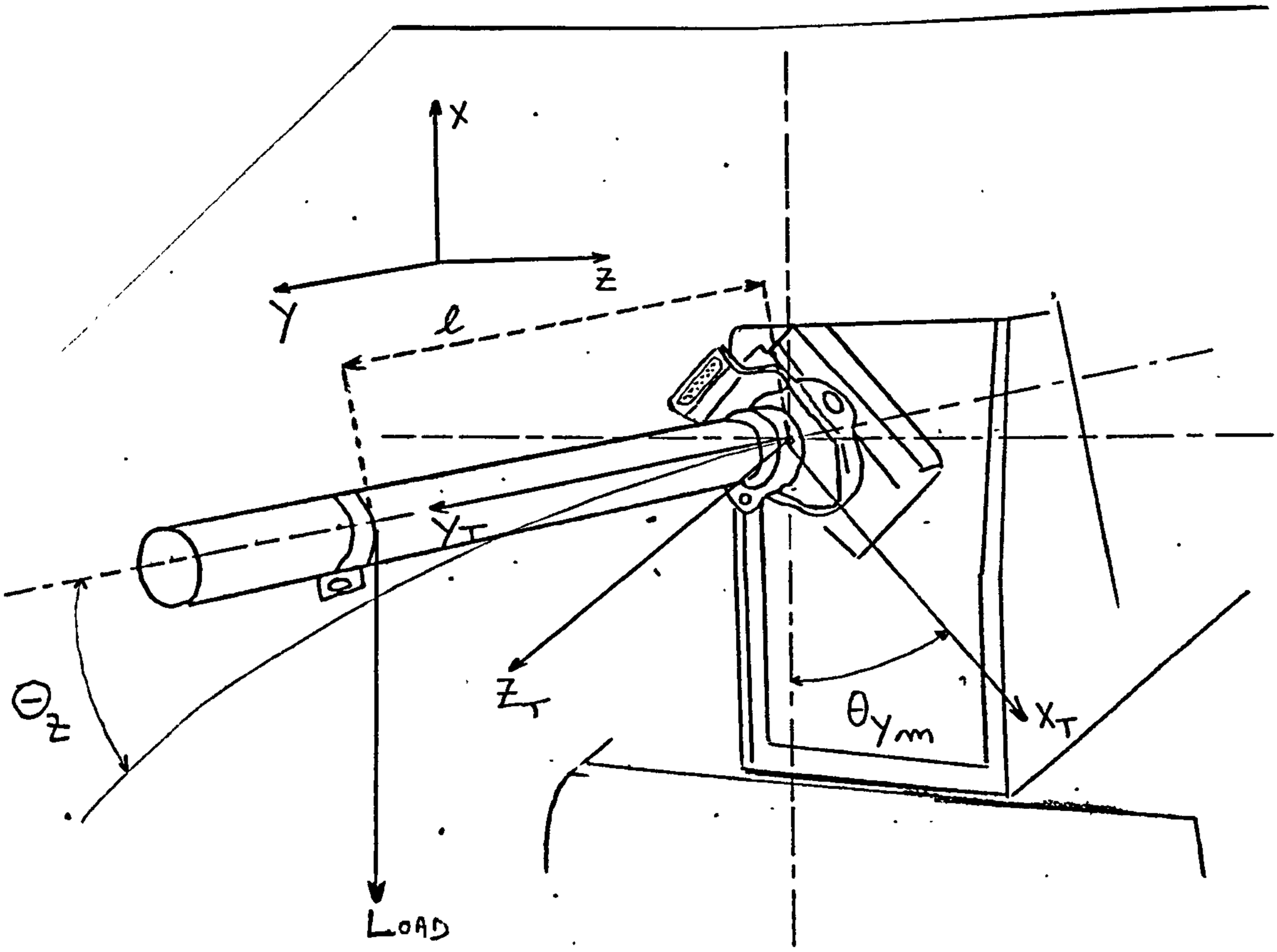

Figure 7.9: The set-up and different angles using the bench table. The transducer was located for a test in dorsiflexion (Θ_z positive) and internal position (Θ_y positive) for a right foot. The deflection Θ_z was measured by means of a clock-gauge.

in section 7.3.4.

7.3 STATIC TESTS WITH BENCH TABLE

7.3.1 Description of the bench heavy table and tests made

It was the same device as the one used for calibration tests (see section 6.3). With the same set-up as for calibration, it was possible to study combined shear and bending moments as shown in figure 7.9. This set-up had the main drawback to generate tension in the longitudinal channel Fy with low values. This created uncertainties with unexpected results. This is why this channel was not considered when the results were being discussed. A mechanical clock-gauge was used to measure the deflection and thus the corresponding angle with usual uncertainty in accuracy (see section 4.4). This set-up similarly allowed the torque My to be applied to perform a validation of both transducer and calibration matrix in this particular channel.

7.3.2 Mathematical considerations

Relatively to the transducer and the middle of the artificial ankle axis and following the caption shown in figure 7.9, it was necessary and sufficient to define one angle and a lever arm *l* to calculate the wanted applied forces and moments:

1. Θ_y represents the angle, about the longitudinal Y axis, contained into the transverse plane, between the transducer X_T axis and the absolute fore - aft X direction.

2. *l* represents the distance between the application point of the applied load and the central line of the corresponding gauge bridges of the transducer.

Consequently, the applied loads were as follows, having L as load:

$$Fx = L \cos \Theta_y \quad (7.13)$$

$$Fy = \text{not considered} \quad (7.14)$$

$$Fz = L \sin \Theta_y \quad (7.15)$$

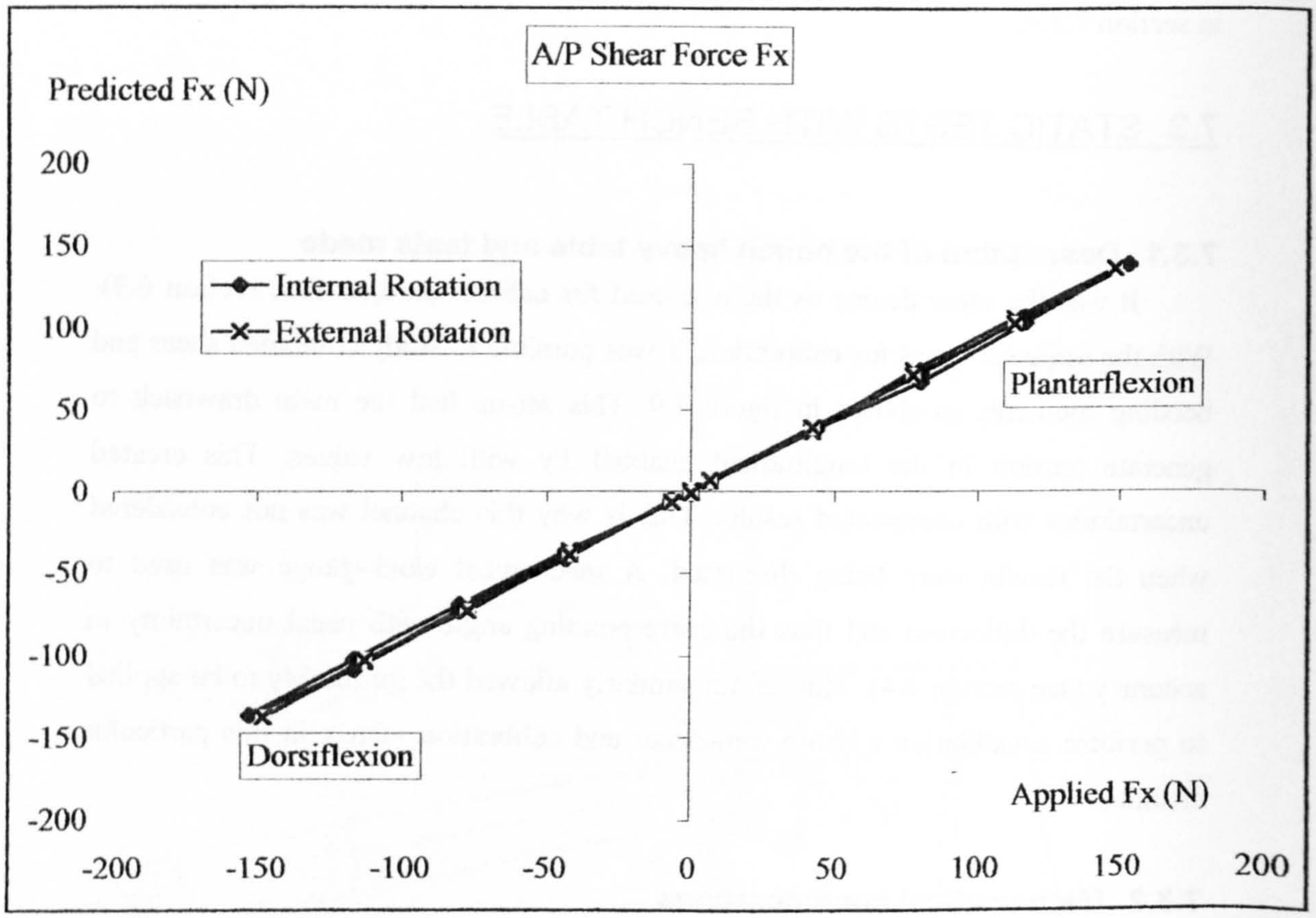

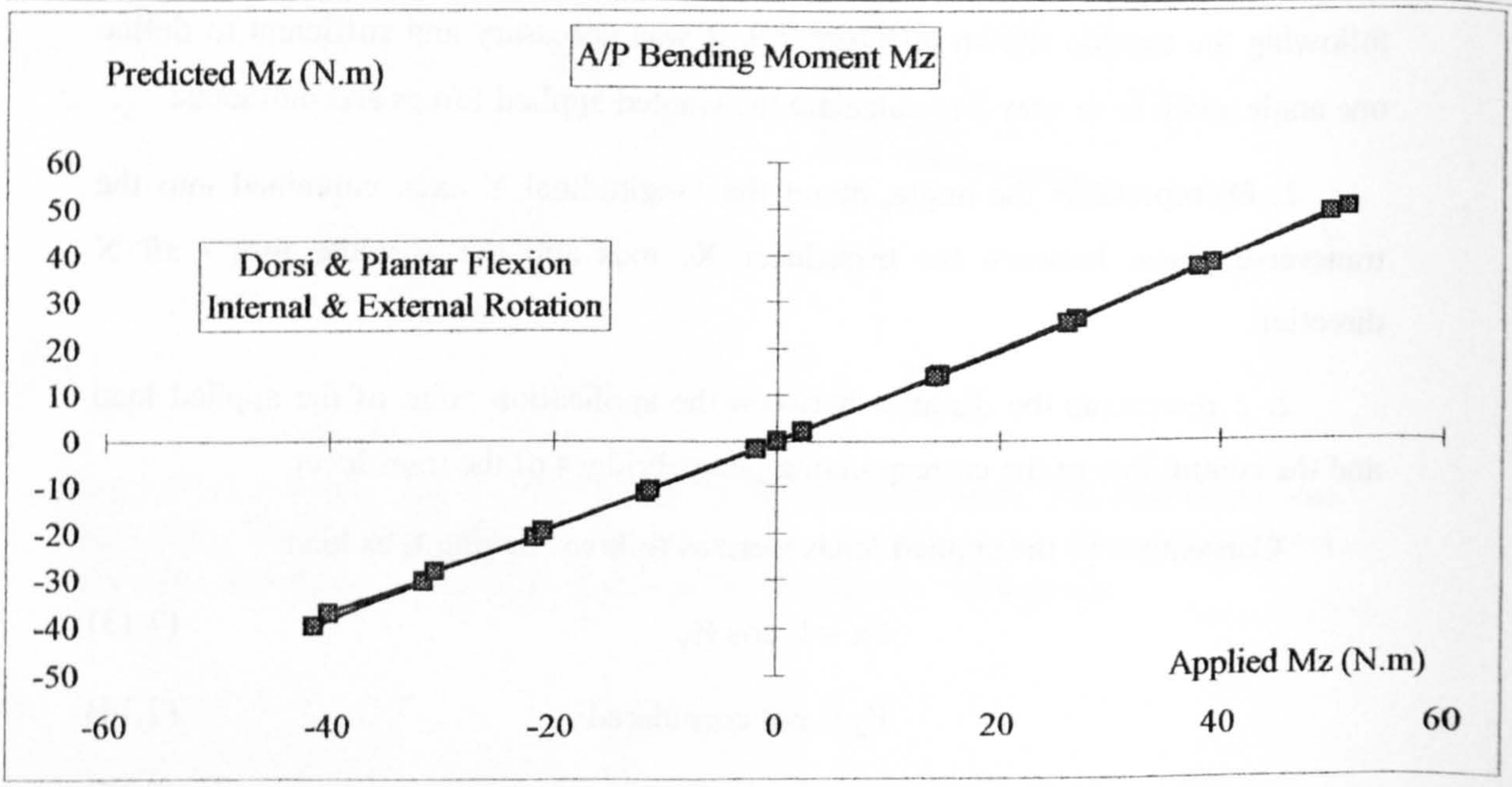

Figure 7.10a: Predicted and Applied forces and moments, in the anterio – posterior plane, using the bench table

$$Mx = L\,(\,l \sin \Theta_y\,) \tag{7.16}$$

$$My \approx 0 \tag{7.17}$$

$$Mz = L\,(\,l \cos \Theta_y\,) \tag{7.18}$$

7.3.3 Loading cases and results

The tests were planned to be carried out at two lever arms l = 0.271 (plantarflexion) and 0.337 m (dorsiflexion). The two values of the angle Θ_y were chosen according to the possibility of the bench table and the shape of the transducer aluminium base: - 42° (external rotation) and 44° (internal rotation).

Applied Load	Loading Mass in kg	Loading Weight in N
Weight Carrier + Steel Cable	0.950	9.32
5 kg (A4)	5.950	58.37
5 kg (A5)	10.950	107.42
5 kg (A6)	15.950	156.47
5 kg (A7)	20.950	205.52

A loading - unloading cycle was performed for each test. Four different loading configurations were tried and full analytical data from these tests are shown in appendix 11.VII.3. Figures 7.10a (Fx and Mz, the A/P plane) and 7.10b (Fz and Mx, the M/L plane) show the plotted diagrams of these tests. Internal and external rotations are mixed in one diagram for each shear forces (Fx and Fz) and bending moments (Mx and Mz). As previously stated (see section 7.2.4.1, these charts exhibit the linear behaviour of each channel rather than their prediction ability to display the predicted loads versus the applied loads with a slope coefficient of 1.The calculated errors are as follows (table 7.7) with the same precautions as already stated:

load component	calculated prediction error in percentage
for Fx over 20 N	11.8
for Fy	n.s.
for Fz over 20 N	6.7
for Mx over 3 N m	2.7
for Mz over 7 N m	0.3

Table 7.7: The calculated prediction error exhibited by the VPT in static tests using the bench table.

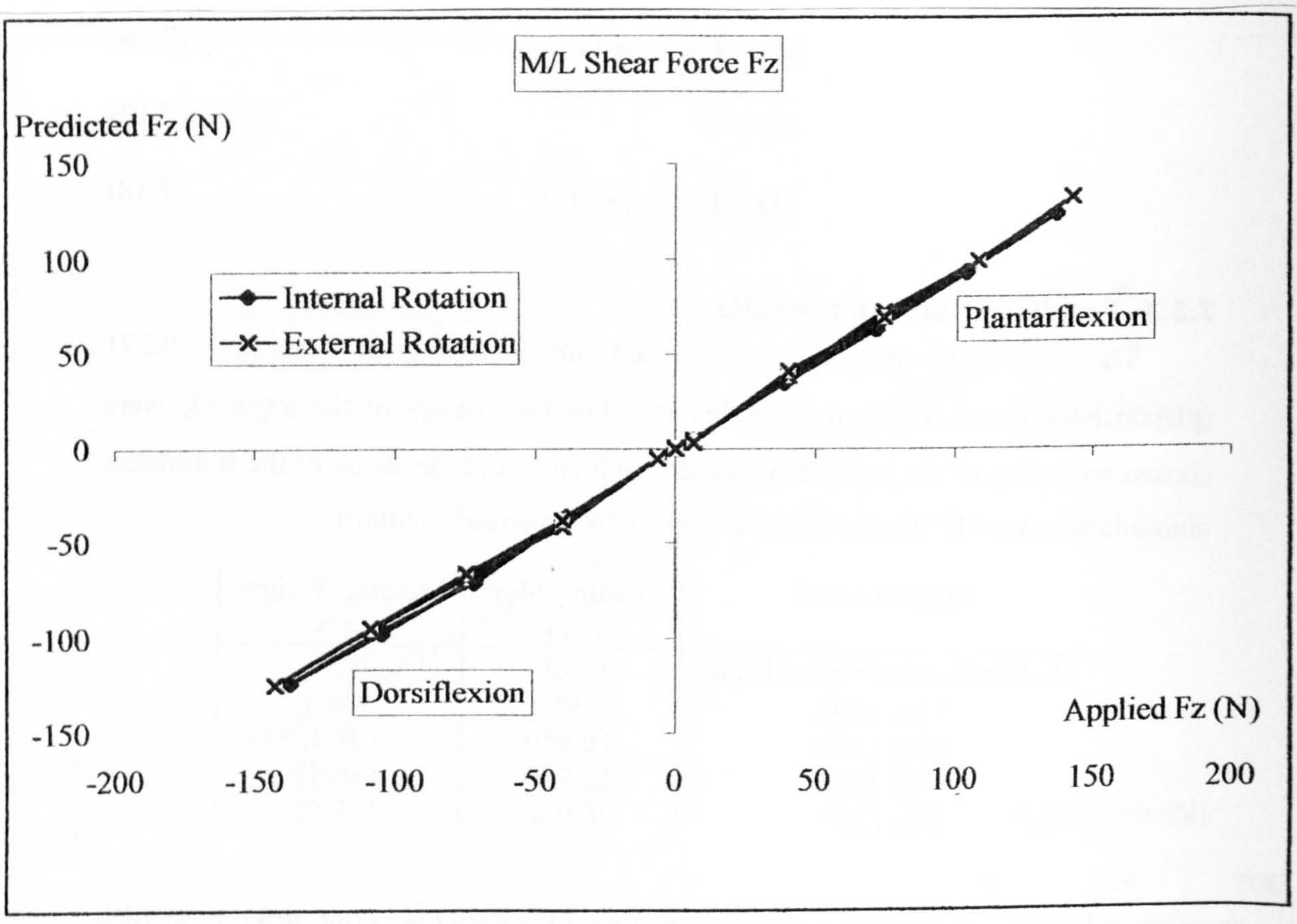

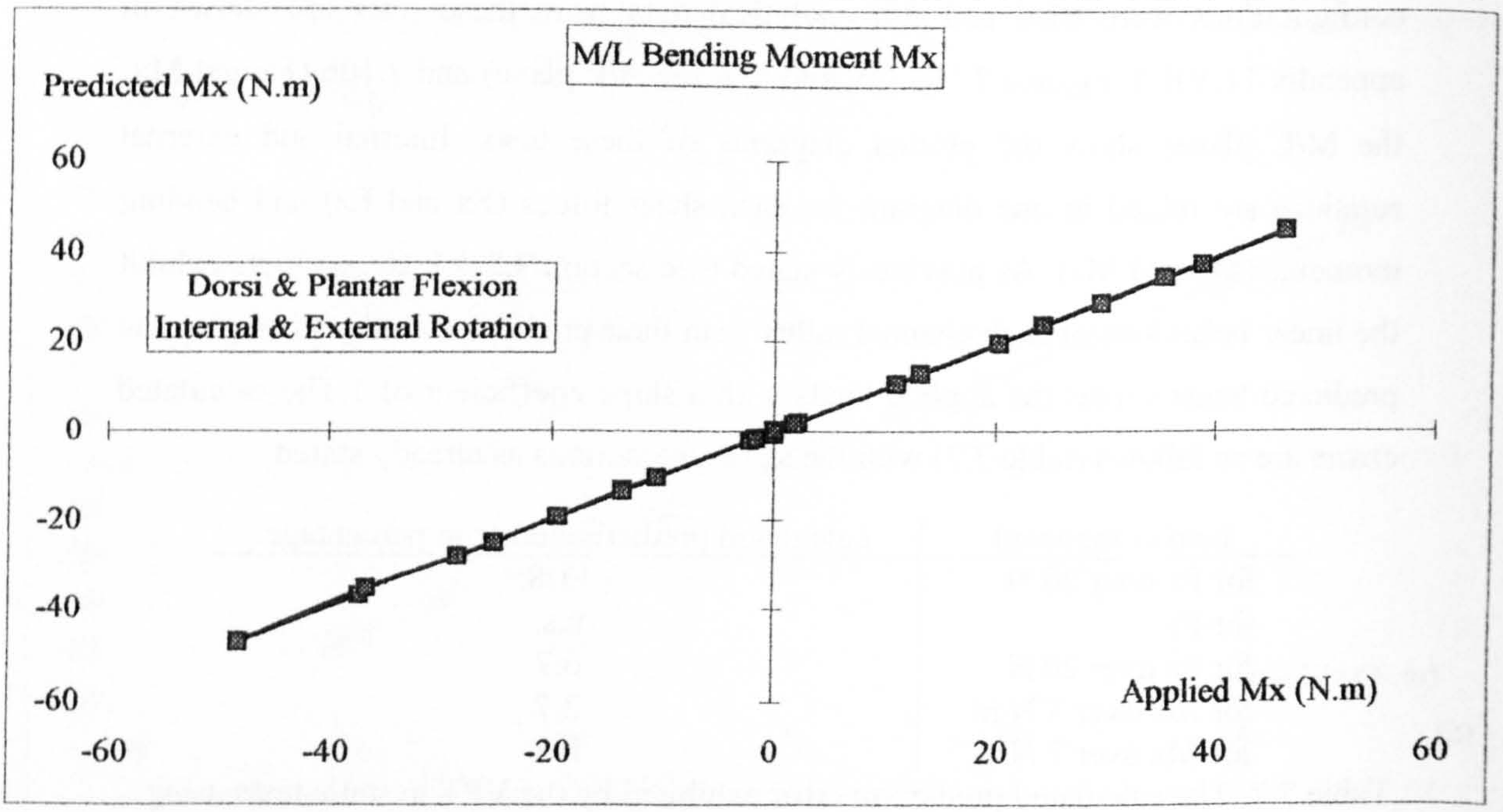

Figure 7.10b: Predicted and Applied forces and moments, in the medio – lateral plane, using the bench table

The thresholds were chosen according the recommendations expressed by Magnissalis (1992), as previously stated in section 7.4.2, table 7.6.

All of these predicted errors were improved in this configuration relatively to those found with the first series of tests, except for the A/P shear Fx. Without any satisfactory explanation, this set-up (especially in dorsiflexion with an internal rotation) disrupted the results in this particular channel. The following tests with two transducers, having one of them used as standard, have tried to find the answer. One explanation could be the asymmetric shape of the base of the VPT (an irregular octahedral contour, see section 4.8.2.2.).

7.3.4 Torque study

To study torque My, the same set-up as the one applied for calibration was used (see section 6.3.3). The first tests were performed with the Villiers Pylon Transducer alone then another series of tests were undertaken with simultaneously two transducer, the SPT and the VPT being fitted together (see below section 7.4.5). In such a configuration, the responses of all channels should be 0, except the torque channel My. Following the previous section 6.3.3, the applied torque was:

$$\text{Applied Torque in Nm} = (\text{Applied Load in N}) * 0.1\,\text{m} \qquad (7.19)$$

Hence:

Description	Loading Mass in kg	Loading Weight in N	Torque in N m
Weight Carrier + Steel Cable	1.804	17.7	1.76
5 kg (A4) + 5 kg (A5)	11.804	116	11.61
5 kg (A6) + 5 kg (A7)	21.804	214	21.42

As usual, one loading-unloading cycle was performed for positive and negative situation. Analytical data are shown in appendix 11.VII.4. To complete the above figures 7.7 (the 3 forces, equations 7.8 to 7.10) and 7.8 (only two bending moments out of 3, equations 7.11 and 7.12) with the transverse torque channel, the predicted load values, through calibration matrix [C] (table 6.41) are plotted against the actual applied loads. It is shown in figure 7.11. As previously stated, the ideal pattern would

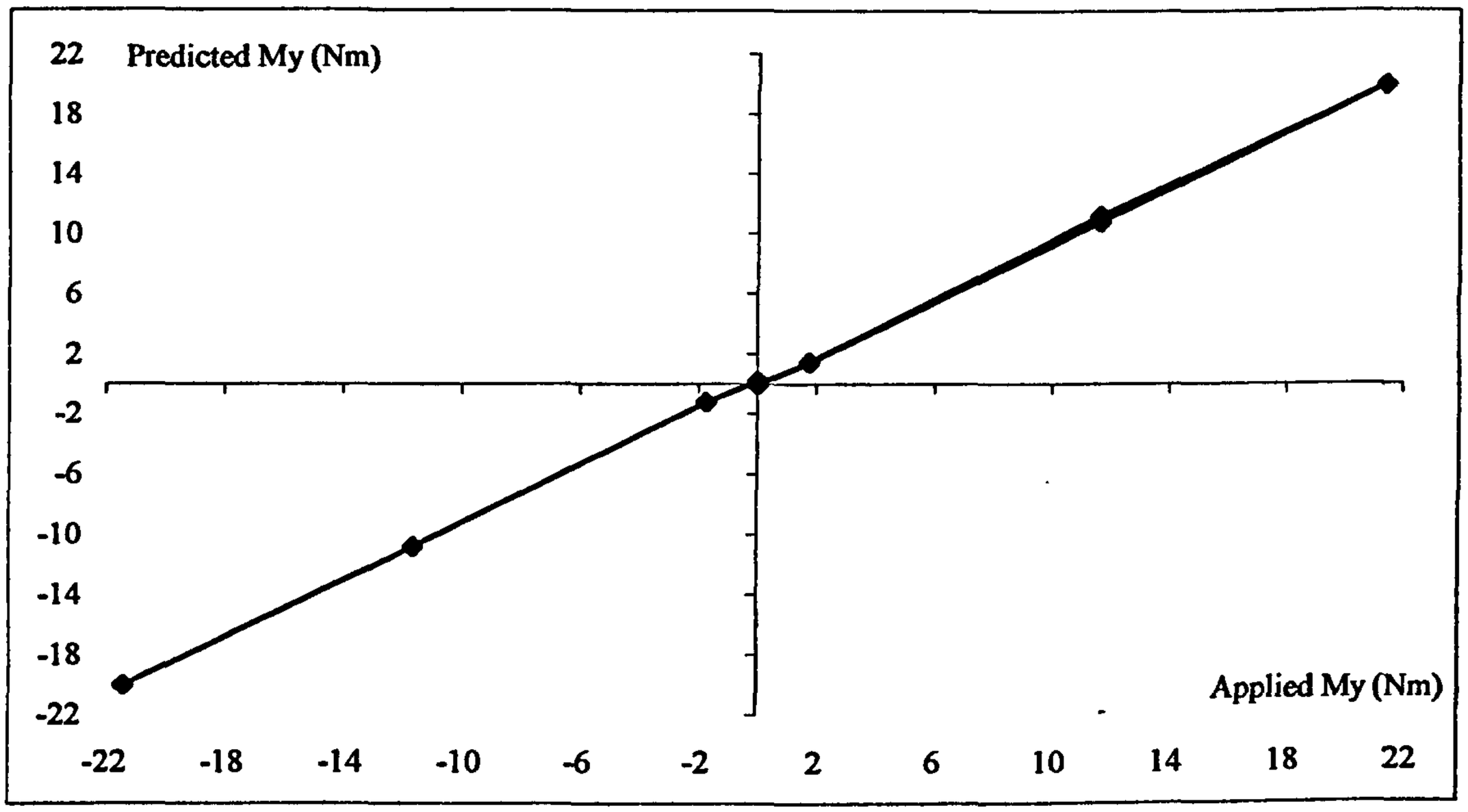

Figure 7.11: Predicted versus Applied torque moment

				Torque Positive	Torque Negative
Loading Weight in N	Applied Torque in ± N.m	Predicted Torque in N.m	Applied Fy in N	Predicted Fy in N	Predicted Fy in N
0	0	0.04	0.0	0	0.6
17.7	1.76	1.32	0.0	29.8	-27.9
116	11.61	10.82	0.0	211.49	-208.3
214	21.42	20.02	0.0	388.96	-387.5
116	11.61	11.02	0.0	214.82	212.7
17.7	1.76	0.67	0.0	34.82	-35.7
0	0	0.03	0.0	5.95	-3.1

Table 7.9: Applied versus Predicted results (mean from two tests in positive and negative direction) in torque and in axial load channel when torque was applied

be a straight line with unit slope and zero intercept. A quantitative evaluation of the pattern shown could be obtained by linear regression of the data. The result was as follows:

(predicted My) = 0.03714 + 0.98517 * (applied My) in N m (7.20)

Indeed, the intercept was close to zero and the slope was close to unity. On the other hand, as indicated by the r-square value, this equation satisfied the plotted data by more than 99.9 %. The complete statistical study of the torque data is shown in appendix 11.VII.4. The calculated errors are as follows, having in mind that the application of equation 7.7 is a non sense when theoretical applied load is zero. Hence, the subtraction predicted - applied is a better reflect of this particular channel:

load component	calculated prediction error in percentage	average subtraction applied - predicted in N or N m
for Fx	n.s.	0.585
for Fy	n.s.	388
for Fz	n.s.	2.63
for Mx	n.s.	0.145
for My over 0.88 N m	6.11	
for Mz	n.s.	0.235

Table 7.8: The calculated prediction error in transverse moment (torque) exhibited by the VPT in static tests using the bench table.

Studying these results, there is obviously a problem in this particular channel. All predicted values are close to the applied ones except in Fy axial load channel. The predicted responses of such an axial load channel should be 0 and they are shown in table 7.9. When torque is positive, Fy interaction is negative and it is the opposite when torque is negative. Each interaction is the mirror image of the other. A suggested explanation could be as follows:

- the mixing of axial load gauges into the arms of the Wheatstone bridge of such a channel (due to the necessity of an equilibrium of the bridge's arms in gauges' resistance), but the strain gauge theory shows that the places of the strain gauges in each arm of the bridge does not matter.

- it also could be possible to mention a problem of gauge orientation or gauge adhesion, but a theoretical analysis showed that a misalignment of 18° is necessary to

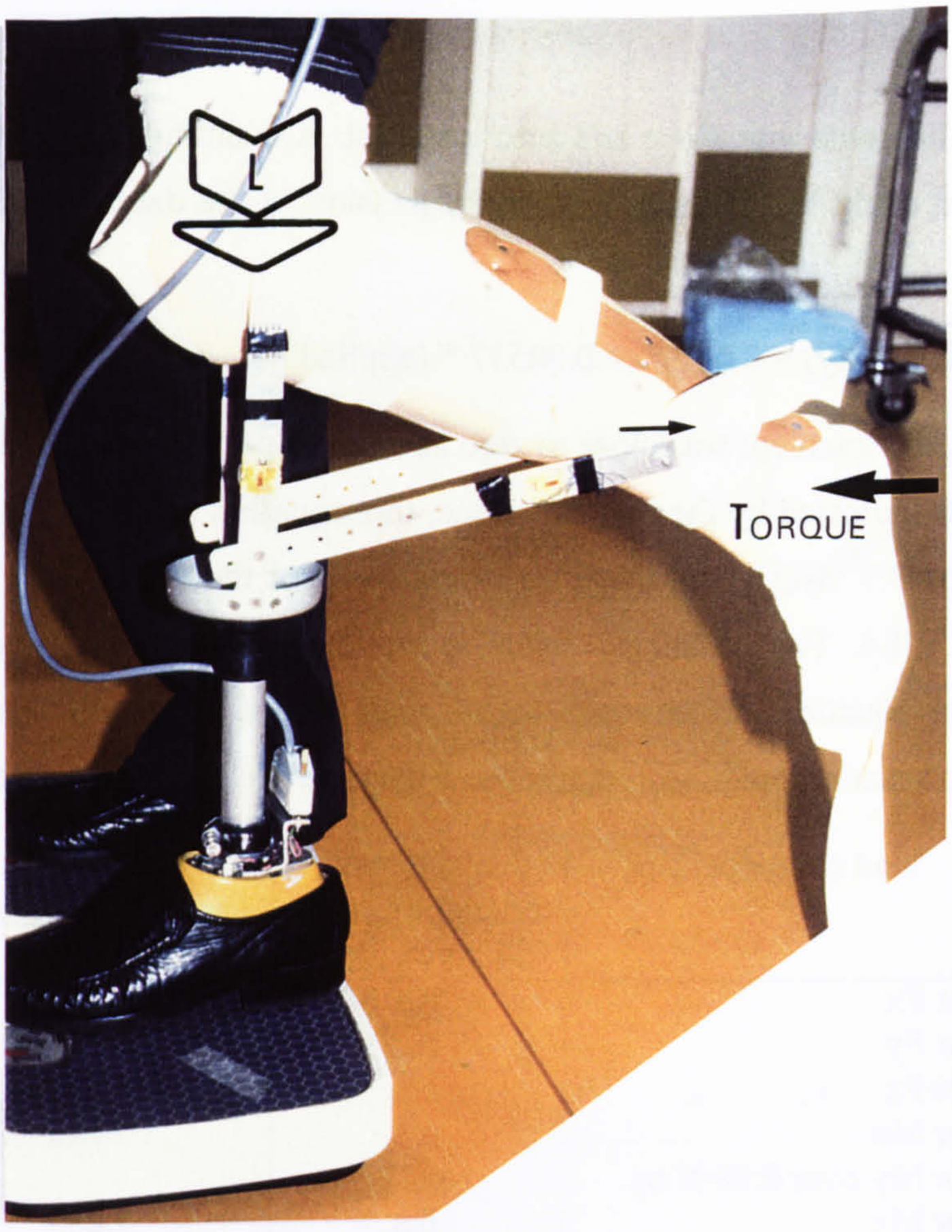

Figure 7.12: The use of a kneeling prosthesis loaded on a simple bathroom scale to check interaction effects between torque and axial compression

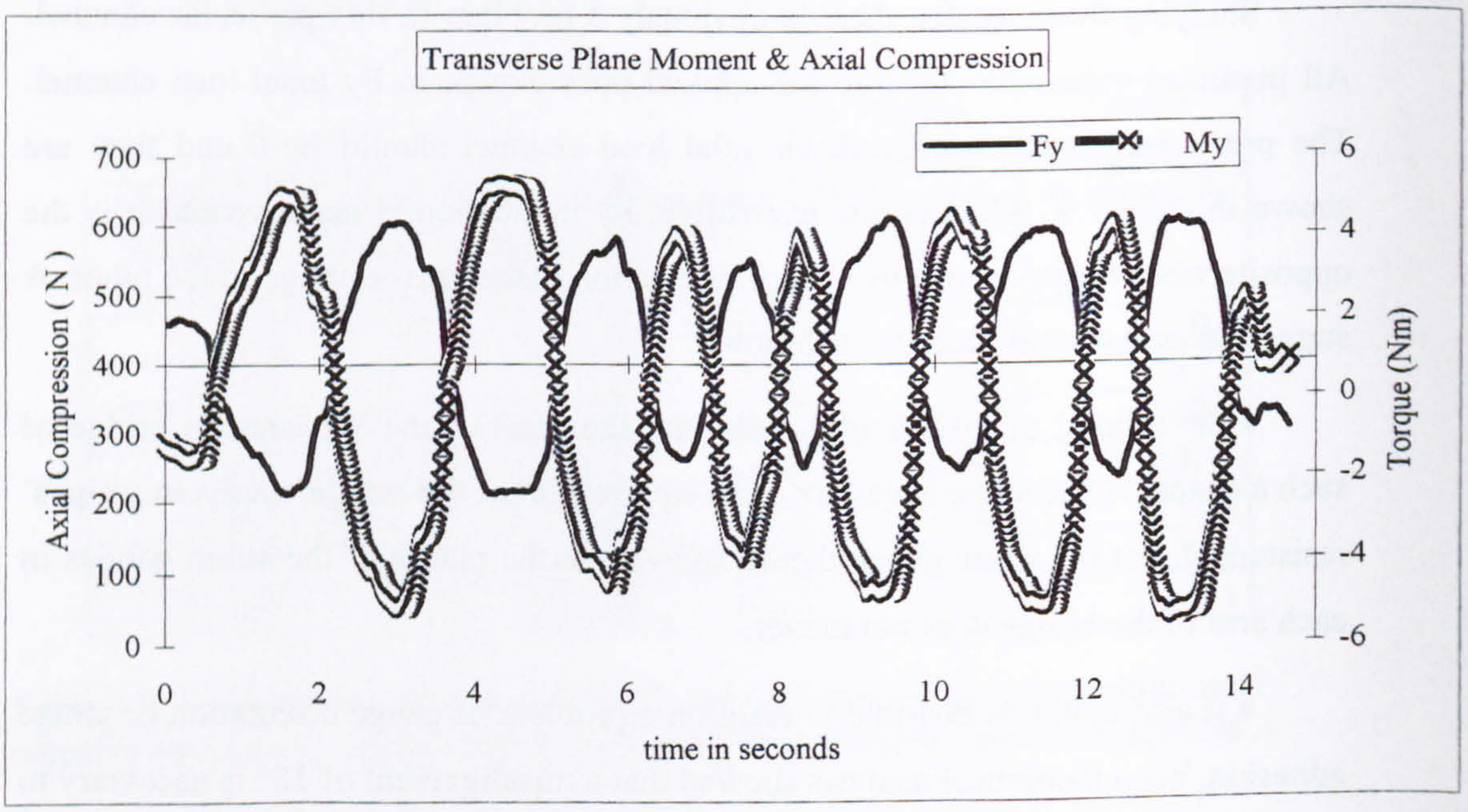

Figure 7.13: Results of the kneeling prosthesis test

express such a Fy axial load cross-effect. A so high level of misalignment could not be seen through a microscope checking and thus, this possibility should not be mentioned.

However, the important fact is the stability, the linearity and the repeatability of this main interaction which can therefore be corrected.

7.3.4.1 CHECKING OF TORQUE AND AXIAL COMPRESSION INTERACTION - EFFECTS

To check the results predicted above (that is, ± 1 N m torque = ± 40 N axial compression), another test was undertaken using a kneeling prosthesis fitted on a non amputated subject as shown in figure 7.12. The subject was standing up on two bathroom scales (130 kg capacity) into parallel bars. He had to load his artificial foot of about 30 kg (294 N) then 40 kg (392 N). When this was done, the following task was performed:

- an operator pushed manually the prosthetic socket towards external or internal horizontal direction (see horizontal arrows in figure 7.12) introducing torque at the maximum allowed before any slipping of the shank tube covering the VPT and clamped by means of the special ring described in section 4.8.2.

Figure 7.13 shows the results of the trial where the subject loaded his artificial foot by 392 N as axial compression and the operator was passively pushing the socket in both torque negative and positive direction. When a torque moment was applied, the predicted level of the axial compression Fy was changing although it should not. The ratio between torque and axial compression was the following, with a relatively large order of uncertainty due to the possibility of an uncontrolled M/L bending moment:

- when a full range of passive torque was used:

$$\pm 5 \text{ N m (torque)} = \pm 200 \text{ N (axial compression)}$$

- when the subject applied himself the torque:

$$\pm 2 \text{ N m (torque)} = \pm 100 \text{ N (axial compression)}$$

Therefore, the ratio found above was corroborated and later in this work, an uncertainty of 40 N in axial compression Fy should be applied at each level of 1 N m

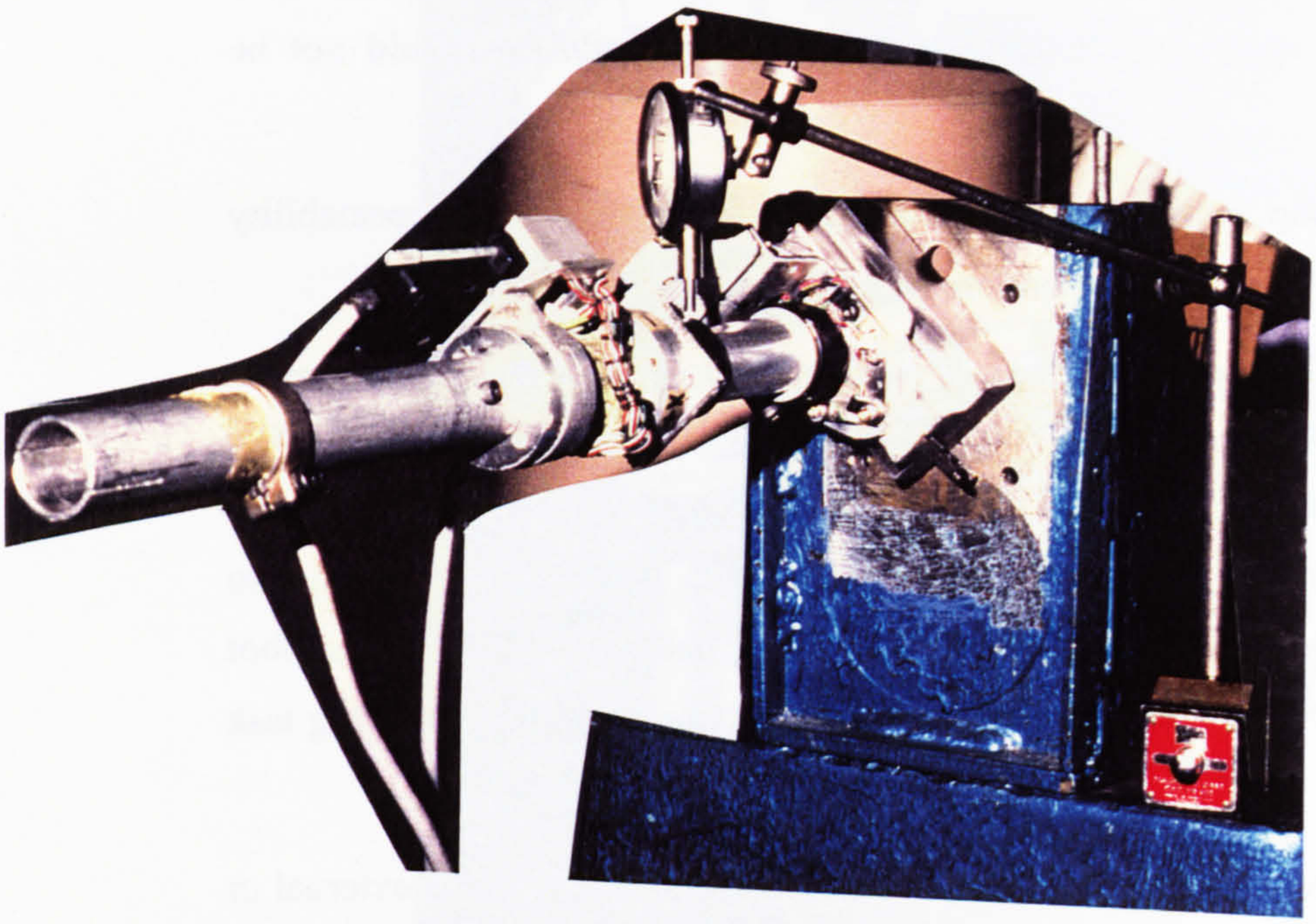

Figure 7.14: The general view of the two pylon transducers used concurrently: A/P bending moment positive in dorsiflexion with an internal rotation about the Y axis. The clock-gauge, to measure deflection, is shown.

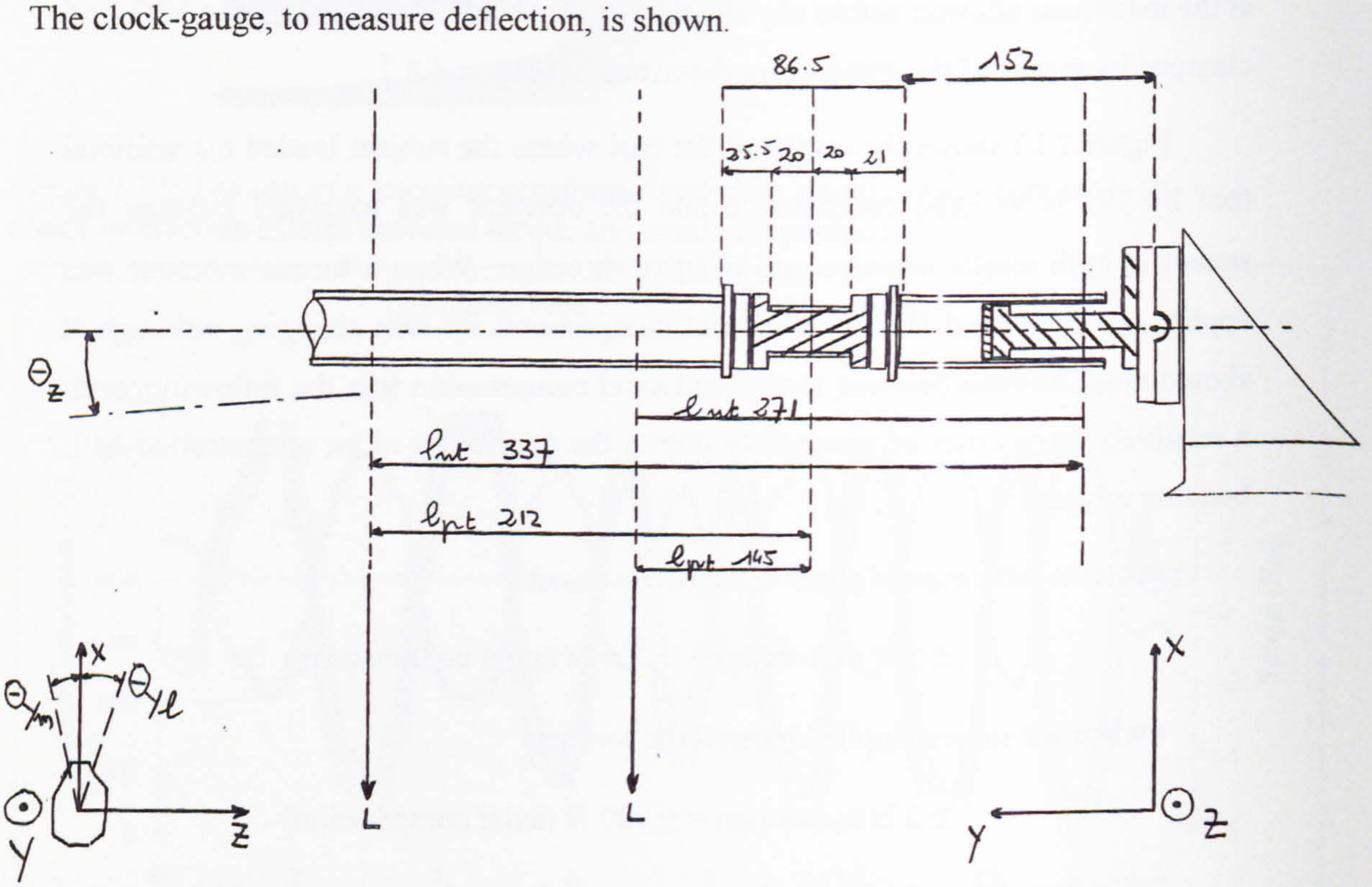

Figure 7.15: The set-up for using simultaneously the two pylon transducers in static tests. The VPT was fitted as it was when the tests with patients were performed, i.e., with the bell.

torque, increasing when torque is negative and decreasing when positive. However, it is shown in chapter 8 when amputee gait tests are described that the mean torque was usually lower than 1.5 N m in relation with the use of the walking aids and thus the axial load Fy was not exceedingly over or underestimated.

7.4 STATIC VALIDATION TESTS USING SIMULTANEOUSLY TWO TRANSDUCERS

7.4.1 Description of the set-up with data acquisition systems used

The set-up is shown in figure 7.14. The Villiers Pylon Transducer with the bell (VPT) was attached to the bench bracket and the Strathclyde Pylon Transducer (SPT) was in turn attached to the VPT. The SPT was used as standard. An aluminium tube was the final part of the set-up. A jubilee clip was used to locate accurately the position of the steel cable for suspending the weights. The bending moments created a small response in axial load Fy which was negligibly small. However, this set up was not a satisfactory connection for transmitting bending moment without application of axial load (see chapter 9). For maximum bending moments, it was not considered in the conclusion concerning the VPT.

For recording data from the VPT, the portable data acquisition system was used. The six channels were simultaneously recorded at the sampling frequency of 16 Hz avoiding the collection of an unnecessary large amount of data. Gain settings and bridge voltages were identical to those permanently used in all tests (see section 5.3.2). The calibration matrix [C] established in the previous chapter 6 was used (see tables 6.41 and 6.43).

For recording data from the SPT, a set of six amplifiers was used and monitored using the Acquire program. Gain settings, bridge voltages and calibration matrix were those established by Ni Ling (1996). They are shown in appendix 11.VII.5. Data were recorded at a sampling frequency of 16 Hz and then transferred to a spreadsheet.

As an example, raw data recorded simultaneously from the two transducers, for three loading cases, are presented in appendix 11.VII.5.

Description	Loading Mass in kg	Loading Weight in N	**Plantar Flexion**	**Dorsi Flexion**
			$\Theta_{yext} = 34°$ $\Theta_{yint} = -33°$	$\Theta_{yext} = 42°$ $\Theta_{yint} = -30°$
0	0	0	lever arm in m external or internal rotation $l_{nt} = 0.271$ $l_{pt} = 0.145$	
Weight Carrier + Steel Cable	0.950	9.32		
5 kg (A4)	5.950	***58.37***		
5 kg (A5)	10.950	***107.42***		
5 kg (A6)	15.950	***156.47***		
5 kg (A7)	20.950	***205.52***		

Table 7.10: The different load cases and angles when using the two transducers together. The loading weights in bold italic letters and shadowed cells were those taken into account to establish the mean differences shown in tables 7.11a to 7.11d.

7.4.2 Mathematical considerations

Referring to the set-up shown in figures 7.14 and 7.15, two angles were necessary to describe the combined applied loads, similarly to figure 7.9. The notation used is as follows:

1. Θ_y was the angle about the longitudinal Y axis of the devices comprised between the vertical loading line and the fore - aft X axis of both transducers. The subscript was « l » when the whole set-up was rotated in the external negative direction (always for a right artificial foot of a theoretical subject, see section 7.2.1) and « m » when the rotation was internal and positive. Therefore, the right hand rule might be applied for bending moment signs.

2. *l* was the lever arm for bending moments: between on the one hand the application point of the load and on the other hand the bending gauge level of the VPT and the middle line of the SPT. The subscript was « nt » for the VPT and « pt » for the SPT.

Hence, with L as applied load, equations are as follows:

$$Fx = L \cos \Theta_{yl \text{ or } ym} \tag{7.21}$$

$$Fy = \approx 0 \tag{7.22}$$

$$Fz = L \sin \Theta_{yl \text{ or } ym} \tag{7.23}$$

$$Mx = l_{nt \text{ or } pt} (Fz) \quad = l_{nt \text{ or } pt} \times L \sin \Theta_{yl \text{ or } ym} \tag{7.24}$$

$$My \approx 0 \tag{7.25}$$

$$Mz = l_{nt \text{ or } pt} (Fx) \quad = l_{nt \text{ or } pt} \times L \cos \Theta_{yl \text{ or } ym} \tag{7.26}$$

7.4.3 Description of the tests

In each configuration, two series of tests were carried out, having the following characteristics, shown in table 7.10. The angle $\Theta_{yl \text{ or } ym}$ and the lever arm $l_{nt \text{ or } pt}$ were changed to increase the opportunity of discovering any wrong response. The full analytical data and results are shown in appendix 11.VII.5.

7.4.4 Results

Tables 7.11a, 7.11b, 7.11c and 7.11d are the summaries of the results. In all columns, the results are shown in percentages: equation (7.7) was applied. The best results should be as close to zero as possible. The comments are made using the

	Villiers Pylon Transducer		Strathclyde Pylon Transducer	
	mean difference [(pred - app)/app] in %	comment	mean difference [(pred - app)/app] in %	comment
Fx	- 7.3	pred. values lower than app.	-0.7	n.s.
Fy		not considered		not considered
Fz	-24	pred. values lower than app.	1.8	pred. values close and higher than app.
Mx	-1.6	pred. values close and lower than app.	-3.8	pred. values close and lower than app
My	-0.27	n.s.	0.43	n.s.
Mz	-2.2	pred. values close and lower than app.	1	pred. values close and higher than app

Table 7.11a: Comparison of the performance of the Villiers Pylon Transducer with that of the Strathclyde Pylon Transducer (pred. = predicted ; app. = applied).

A heavy bench table was used. The abbreviations are as follows: pred. stands for predicted ; app. for applied

The set-up was in dorsiflexion and external position of the foot ($\Theta y = 42\ °$)

	Villiers Pylon Transducer		Strathclyde Pylon Transducer	
	mean difference [(pred - app)/app] in %	comment	mean difference [(pred - app)/app] in %	comment
Fx	7	pred. values higher than app.	-2.2	pred. values close and lower than app.
Fy		not considered		not considred
Fz	-7.4	pred. values close and lower than app.	3.2	pred. values close and higher than app.
Mx	9.7	pred. values close and higher than app	2.3	pred. values close and higher than app
My	-0.04	n.s.	0.27	n.s.
Mz	-6.1	pred. values close and lower than app.	0.1	n.s.

Table 7.11b: Comparison of the performance of the Villiers Pylon Transducer with that of the Strathclyde Pylon Transducer.

The set-up was in dorsiflexion and internal position of the foot ($\Theta y = -30°$)

following thresholds:

1. a (predicted - applied) difference lower than 0.99 % is described to be « non significant (n.s.) » in relation to the expected mean accuracy of the set-up

2. a (predicted - applied) difference between 1 and 9.99 % is described to be « close » with predicted values higher or lower than those applied

3. a (predicted - applied) difference above 10 % is described to be « higher » or « lower » than those applied.

In all calculations, the two first and the last rows were not considered. This was due to the low level of applied loads, which gave inaccurate responses. Therefore, the mean difference in percentage was established from eight loading and unloading cases (see in table 7.10, the loading weights in bold italic letters and shaded cells).

Regarding the results of the VPT versus the SPT, some considerations could be voiced:

- The Fx channel of the VPT had lower prediction ability in an external rotation than in internal. No rational explanation could be found, even more so since the other static tests conducted did not exhibit any differences. However, this difference was not so high that it jeopardised the accuracy of the VPT. The SPT had a very good prediction response.

- The Fy channel was not considered because the VPT is not able to record the axial load when the set-up is in tension.

- The Fz channel had lower prediction ability in an internal position than in an external. The difference between the two positions was smaller than in the Fx channel. However, here also, no rational explanations could be found, even more so since the other static tests (see section 7.4.2) did not exhibit any differences. In two configurations out of four (see tables 7.11b and 7.11d), the predicted values were close to the applied loads and even once the VPT showed better results than the SPT (see table 7.11d).

Regarding these results, an alignment problem in the set-up could be evoked, particularly in A/P and M/L shear forces (Fx and Fz). Consequently, it is possible to

	Villiers Pylon Transducer		Strathclyde Pylon Transducer	
	mean difference [(pred - app)/app] in %	comment	mean difference [(pred - app)/app] in %	comment
Fx	-13.7	pred. values lower than app.	1.4	pred. values close and lower than app.
Fy		not considered		not considered
Fz	-7.4	pred. values lower than app.	3.3	pred. values higher than app.
Mx	18.6	pred. values close and higher than app	10.2	pred. values close and higher than app
My	0.11	n.s.	-0.07	n.s.
Mz	-14.1	pred. values lower than app.	-13.6	pred. values lower than app.

Table 7.11c: Comparison of the performance of the Villiers Pylon Transducer with that of the Strathclyde Pylon Transducer.

The set-up was in plantarflexion and external position of the foot ($\Theta y = 34°$)

	Villiers Pylon Transducer		Strathclyde Pylon Transducer	
	mean difference [(pred - app)/app] in %	comment	mean difference [(pred - app)/app] in %	comment
Fx	67.2	pred. values far higher than app.	3.3	pred. values close and higher than app.
Fy		not considered		not considered
Fz	10.1	pred. values higher than app.	3.0	pred. values close and higher than app.
Mx	25.4	pred. values higher than app	18.2	pred. values higher than app
My	-0.05	n.s.	-0.12	n.s.
Mz	-22	pred. values lower than app.	-18.5	pred. values lower than app.

Table 7.11d: Comparison of the performance of the Villiers Pylon Transducer with that of the Strathclyde Pylon Transducer.

The set-up was in plantarflexion and internal position of the foot ($\Theta y = -33°$)

state that the set-up used was not accurate enough to study the three forces

- The bending moment Mx channel had a better prediction ability in the Villiers Pylon Transducer than the three force channels. Both devices exhibited a predicted value higher than the applied, except in dorsiflexion and lateral position.

- The My channel had a very good prediction ability in the two transducers. There was no applied torque, neither of the transducers indicated torque which was satisfactory.

- The Mz channel had high prediction ability in all configurations. When the predicted value of the Villiers Pylon Transducer was higher than applied (i.e., above 10 %), it was the same for the Strathclyde Pylon Transducer, thus the set-up could be used.

The summary (in percentage) of predicted loads versus applied loads in the two pylons is shown in table 7.12. The thresholds were chosen according to the recommendations expressed by Magnissalis (1992).

Globally, it is possible to say that the Villiers Pylon Transducer predicts lower values than those predicted by the Strathclyde Pylon Transducer.

7.4.5 Torque study

The set-up used has been previously described in chapter 6 and was identical. The Strathclyde Pylon Transducer was only inserted between the Villiers Pylon Transducer and the torque loading mechanism. Two series of tests were conducted applying both negative and positive torque. Analytical data are shown in appendix 11.VII.6. The differences between predicted and applied loads are shown in table 7.13. Equation 7.7 was applied to estimate the average difference in percentage .

The results are consistent except in two cases. As already stated above, the new VPT exhibits lower predicted values in axial load Fy. The mean difference is about ± 175 % (± 36 N for each 1 N m in torque)..

Hence, in the torque static set-up, the best channels for cross-effects are the two A/P and M/L bending moments, followed by the two A/P and M/L forces. The axial load channel must not be considered for reason given above. Concerning the

Load Component	Villiers Pylon Transducer	Strathclyde Pylon Transducer
for Fx over ± 20 N	12	1.9
for Fy	n.s.	n.s.
for Fz over ±20 N	15	8.1
for Mx over ± 3 N.m	14	7
for My	≈ 0	≈ 0
for Mz over ± 7 N.m	12	8

Table 7.12: The calculated prediction error (in percentage) expressed by both transducers, simultaneously recorded in static tests.

	Torque Negative		Torque Positive	
	VPT	SPT	VPT	SPT
	mean difference	mean difference	mean difference	mean difference
Fx	0.21	-1.06	1.22	2.46
Fy	175.94	-0.37	-173.96	-2.27
Fz	-2.46	-8.93	1.53	10.65
Mx	-0.08	-0.20	0.07	-0.04
My	-6.45	-1.63	-7.01	1.87
Mz	0.67	0.75	-0.81	-1.07

Table 7.13: Average difference in percentage between predicted and applied loads in torque for the VPT and the SPT.

main torque channel My, the Villiers Pylon Transducer predicts lower results than applied with a difference of about 15 %.

7.5 PARTIAL CONCLUSION FROM STATIC VALIDATION TESTS

Following the different tests performed in both configurations (see sections 7.2, 7.3 and 7.4) and the results shown in tables 7.14 and 7.15, a partial conclusion can already be drawn as follows:

1. In all validation tests and all channels, the predicted lines resulting from applied loads were linear. The Villiers Pylon Transducer was linear with combined loads as it was for calibration with one single load.

2. The Villiers Pylon Transducer had a good pattern for the three moments in all validation tests performed: an intercept coefficient comprised between - 0.31 and 1.19 (the best being zero) and a slope between 0.87 and 1.17 (the best being one). Averaging slopes and intercepts, as shown in table 7.15, exhibit that the A/P bending moment is the best channel about the prediction ability of the calibration matrix [C], followed by the M/L bending moment Mx and at least the torque My.

3. Concerning the three forces, shear force Fx, medio-lateral shear force Fz and axial compression Fy had a slope close to unity and a small intercept (± 3 N) relatively to the high level of values at the ankle joint during amputee locomotion (commonly, Fx = 2 N and Fy = 10 N for 1 kg of subject's body mass).

Tables 7.6, 7.7, 7.8 and 7.12 show the Villiers Pylon Transducer mean calculated prediction errors in static tests, having in mind that Fz channel is less accurate when load component is lower than 30 N.

However, this calculation of the percentage error is not considered appropriate for all the data acquired because many of the applied load components appear with small values and thus percentage errors could be misleading. As can be seen in table 7.16, an interrogation mark is shown in Mx and My values. Magnissalis (1992) has excluded the torque component from the statistical analysis.

Villiers Pylon Transducer using special device (see section 7.2) (predicted Fx) = 0.48769 + 0.99702 x (applied Fx) in N (predicted Fy) = - 4.39947 + 1.00518 x (applied Fy) in N (predicted Fz) = - 0.28468 + 0.67596 x (applied Fz) in N (predicted Mx) = 0.04652 + 1.07471 x (applied Mx) in N.m (predicted Mz) = - 0.13454 + 0.97916 x (applied Mz) in N.m
Villiers Pylon Transducer using bench table in torque (see section 7.3.4) (predicted My) = 0.03714 + 0.98517 x (applied My) in N.m
Villiers Pylon Transducer using bench table without any rotation (see appendix 11.VII) (predicted Fx) = - 0.02784 + 1.00110 x (applied Fx) in N (predicted Fy) = - 2.49598 + 1.02741 x (applied Fy) in N (predicted Mz) = - 0.31988 + 1.17123 x (applied Mz) in N.m
Villiers Pylon Transducer using bench table with medial or lateral rotation (see section 7.3.3) (predicted Fx) = 0.53518 + 0.91199 x (applied Fx) in N (predicted Fz) = 0.789256 + 0.907851 x (applied Fz) in N (predicted Mx) = - 0.09665 + 0.97093 x (applied Mx) in N.m (predicted Mz) = 0.32664 + 0.96146 x (applied Mz) in N.m
Villiers Pylon Transducer studied with Strathclyde Pylon Transducer on the bench table (see section 7.4.3) INTERNAL (predicted Fx) = 11.12817 + 1.52507 x (applied Fx) in N EXTERNAL (predicted Fx) = 2.89809 + 0.77481 x (applied Fx) in N (predicted Fz) = 1.90069 + 0.99553 x (applied Fz) in N (predicted Mx) = - 0.25765 + 1.09495 x (applied Mx) in N.m (predicted My) = 0.37724 + 0.98526 (applied My) in N.m (predicted Mz) = 1.19347 + 0.87749 x (applied Mz) in N.m

Table 7.14: The results of the different performed tests after linear regression statistical analysis

(predicted Fx) = 3.3853 + 1.0775 x (applied Fx) in N (predicted Fx) = - 3.4477 + 1.0162 x (applied Fx) in N (predicted Fz) = 1.3824 + 0.9802 x (applied Fz) in N (predicted Mx) = - 0.1026 + 1.0468 x (applied Mx) in N.m (predicted My) = 0.3743 + 0.9852 x (applied My) in N.m (predicted Mz) = 0.2664 + 0.9973 x (applied Mz) in N.m

Table 7.15: The mean results averaging slope and intercept from all the performed tests in static.

As shown in table 7.15, the correcting factors (slope, close to the unity) of each channel and calculated from a linear regression analysis are as follows:

(real applied value Fx) in N	[(predicted Fx) - 3.3853] * 1.0775^{-1}	(7.29)
(real applied value Fy) in N	[(predicted Fy) + 3.4477] * 1.0162^{-1}	(7.30)
(real applied value Fz) in N	[(predicted Fz) - 1.3824] * 0.9802^{-1}	(7.31)
(real applied value Mx) in N m	[(predicted Mx) + 0.1026] * 1.0468^{-1}	(7.32)
(real applied value My) in N m	[(predicted My) - 0.3743] * 0.9852^{-1}	(7.33)
(real applied value Mz) in N m	[(predicted Mz) - 0.2664] * 0.9973^{-1}	(7.34)

7.6 DYNAMIC TESTS

The main idea was to use simultaneously two transducers fitted in series on the shank tube of a transfemoral amputee: the Villiers Pylon Transducer (VPT) and the Strathclyde Pylon Transducer (SPT) used as standard.

7.6.1 Description of the set-up, the subject and the different tests

Figure 7.16 shows the set-up. The VPT was at its usual place, i.e., at the artificial ankle level and the SPT was just above. The distance L, between the origin points of the two pylon transducers, was 0.155 m. The data from the VPT were recorded through the portable data acquisition system described in section 5.3.2. The SPT was linked to a set of amplifiers by means of an umbilical cable 15 metres long. It was thus not possible to walk outside the gait laboratory because of the cable between the SPT and its data acquisition system. Thus, the patient was not able to step freely. Consequently, all tests have been made in the gait laboratory, the subject walking on a flat vinyl floor.

The patient was selected to be very active, having a Day activity score about + 30 (Day, 1981) and walking without any assistive aids. He was a 36 year old male, having a period since amputation of 16 years. His right amputation was due to trauma. He wore a quadrilateral contact socket, without any suspension belt. He used an Otto Bock® safety knee. Because of the VPT, he had to wear a Proteor®

load component	calculated prediction error VPT	calculated prediction error SPT
for Fx over 20 N	2.35 %	5.3 %
for Fy over 50 N	2.05 %	3.5 %
for Fz over 20 N	28.42 %	16.9 %
for Mx over 3 N.m	7.75 % ?	4.4 % over 10 N.m
for My over 0.6 N.m	4.83 % ?	
for Mz over 7 N.m	6.08 %	2.4 % over 10 N.m

Table 7.16: Comparison of the prediction errors resulted from the validation tests from Villiers and Strathclyde Pylon Transducers (concerning the SPT, the results are extracted from Magnissalis, 1992, p 110A).

monoaxial foot which was not his usual artificial foot (Otto Bock Dynamic Foot®).

The subject was asked to walk in a straight line in the gait laboratory. The gait rate of the patient was as regular as possible. This was done to avoid the main drawback of such a set-up: the lack of any electronic congruous system between the two transducers. During tests, arrangements were made to ensure that the same stride was being analysed for the two pylons. Matching the instant of the two heel-strikes was manually done using the computer screen. Two series of tests were conducted. The first (trials n°1 and n°2) was identical to those conducted with patients in this work (see chapter 8), that is with a sampling frequency of 64 Hz for both transducers. During the last series (trial n°3), a sampling frequency of 2048 Hz has been used for the VPT without any changing for the SPT. This test has been performed to verify if the filtering cut-off frequency which is linked with the sampling frequency in the portable data acquisition system generated a shrinking of the results (see section 5.3.2).

Considering the fitting of the two transducers on the prosthesis, the three forces and the transverse torque My were equal. Since the position in the leg of the two transducers was different, the two moments Mx and Mz were different. If the SPT was fitted at the same position as the VPT (i.e., at the artificial ankle level), the M/L (Mx_{VPT}) and A/P (Mz_{VPT}) bending moments would be:

$$Mx_{VPT} = Mx_{SPT} + Fz_{SPT} * L \tag{7.35}$$

$$Mz_{VPT} = Mz_{SPT} + Fx_{SPT} * L \tag{7.36}$$

with L being the distance between the origin point of the two transducers, equal to 0.155 m, as shown in figure 7.16. These two equations were used to compare the A/P and M/L bending moments results recorded from the two pylons as shown in table 7.17b.

7.6.2 Results

Analytical data of all the tests undertaken are presented in appendix 11.VII.7. From trial no 2, processed data of all mixed channels of the same three strides,

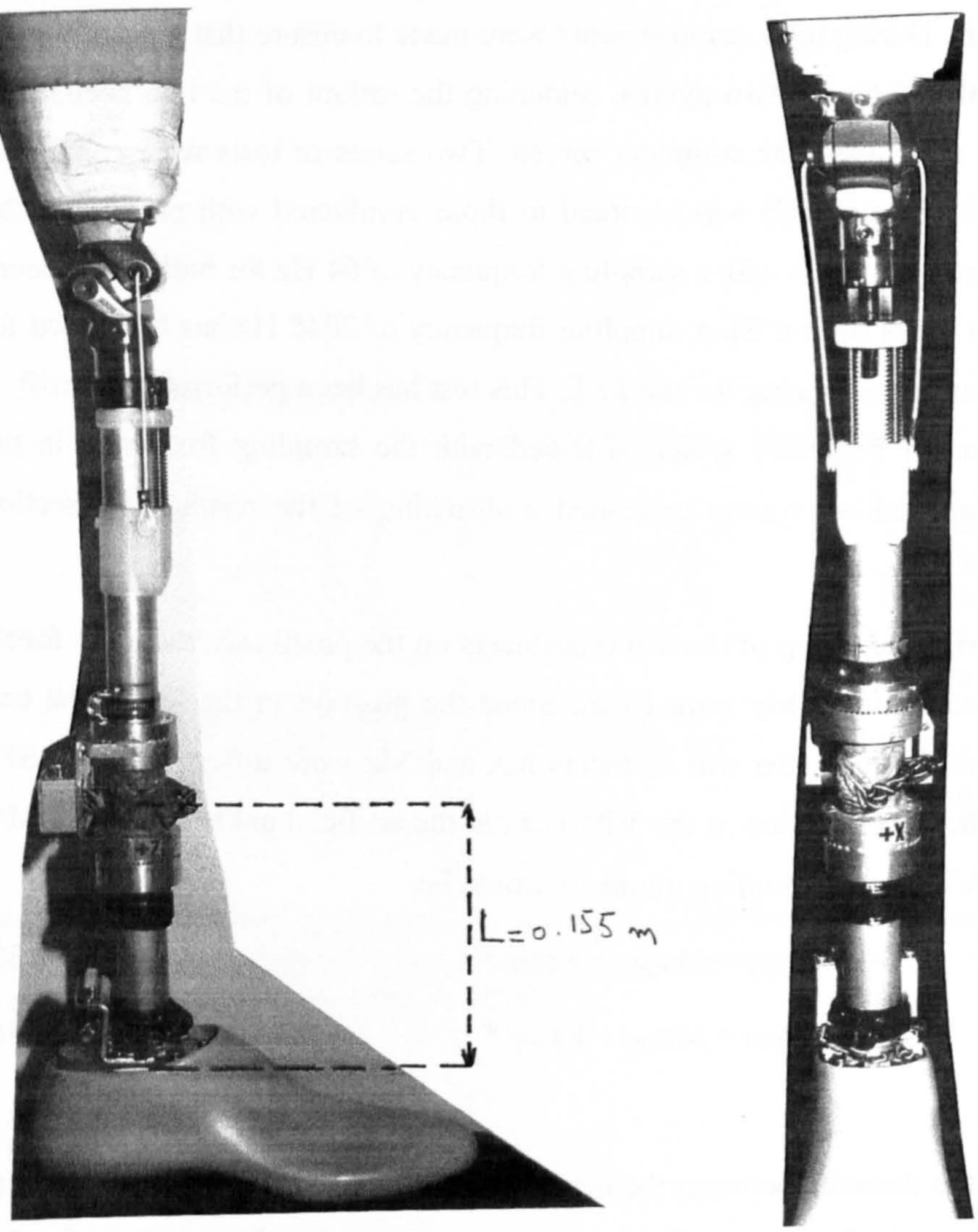

Figure 7.16: The two transducers fitted on a transfemoral prosthesis

randomly chosen, recorded from both transducers are shown as example in figure 7.17. These traces are shown before applying any factors (see section 7.7.1) but obviously after applying the calibration matrix shown in section 6.7 for the Villiers Pylon Transducer. For the Strathclyde Pylon Transducer, the applied calibration matrix is shown in table 11.VII.16 (see appendix 11.VII.5). Only one example, from trial no 1, is shown in figures 7.18a, b and c and is fully detailed. The three forces are shown as follows: 7.18a, A/P shear force Fx; 7.18b, axial load Fy and 7.18c, M/L shear force Fz. The three bending moments are shown in figures 7.19a (Mx), b (My) and c (Mz). These graphs represent the processed data of two strides, randomly chosen among eleven. They exhibit simultaneously the traces recorded from the two transducers. From the two trials no 1 and 2, two other strides recorded simultaneously by both transducers were randomly chosen and are presented and discussed in appendix 11.VII.7.

The six channels (figures 7.18 and 7.19) are shown on the same page, as follows (from top to bottom):

- raw data in millivolts versus time;
- after applying the calibration matrices (see section 6.7 and table 6.43 for the VPT and table 11.VII.16 for the SPT), in N or N m versus time;
- after applying both the calibration matrices respectively to each pylon transducer plus the factors calculated and shown in section 7.8.1 (see table 7.20) only on the Villiers Pylon Transducer.

From trial no 3, because of the high sampling frequency of 2048 recorded values per second, (see section 5.3 for more details), the raw data from the two transducers were different and thus computed separately. Processed data were different: eleven strides for the SPT but only two for the VPT (the test is completely described in appendix 11.VII.7). This was due to the limit of the spreadsheet: two strides at 2048 Hz as sampling frequency with a gait rate of 1.46 s.stride^{-1} were equal to 6000 rows which was the maximum of Excel 4®.

The maximum values could be summarised as shown in table 7.17a. The first important comment is to note that the trial n°3, having a sampling frequency of 2048

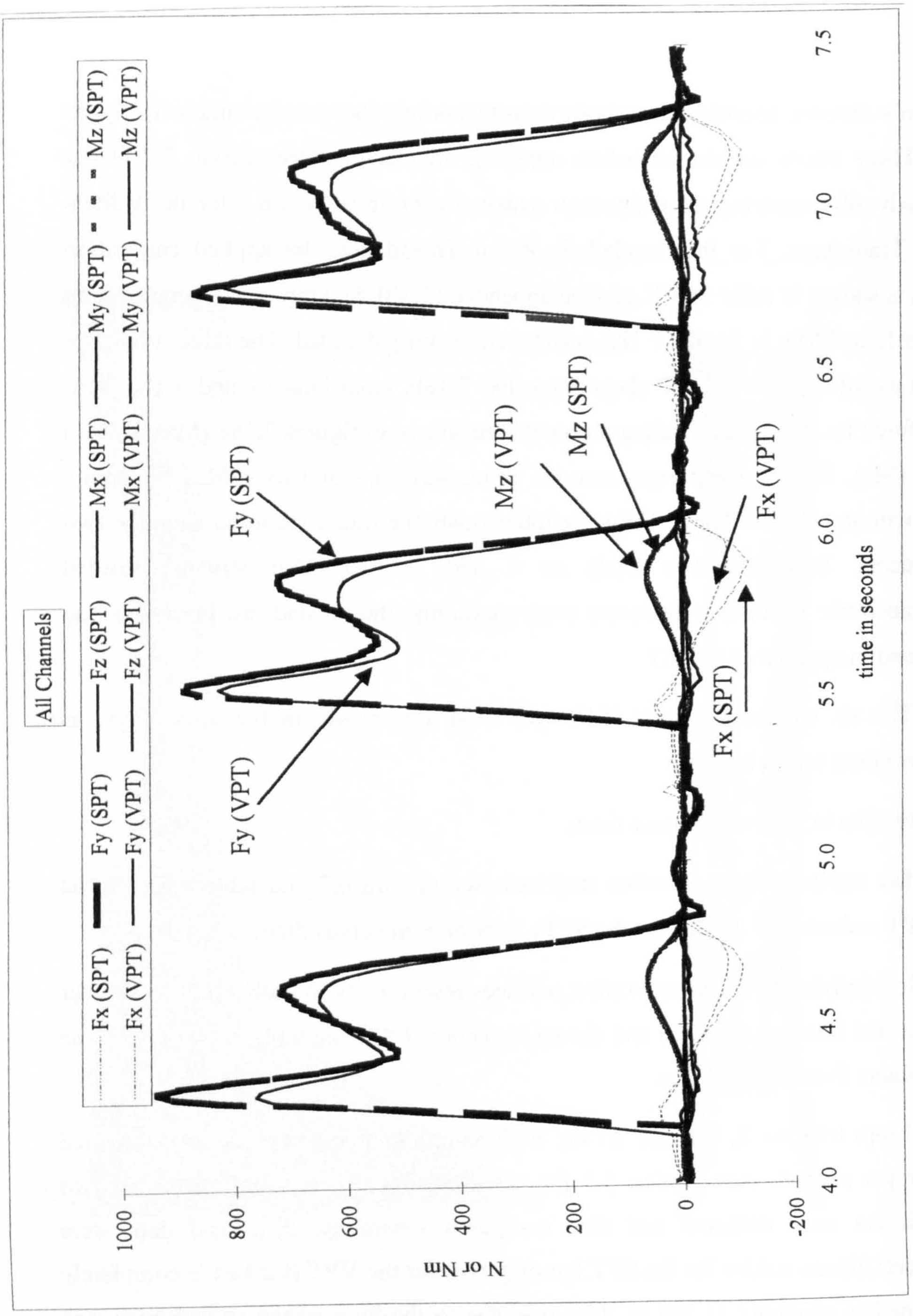

Figure 7.17: Processed data of all the six channels from the same three strides recorded from the Strathclyde Pylon Transducer (SPT) and the Villiers Pylon Transducer (VPT). Axial loads Fy, A/P shear forces Fx and A/P bending moments Mz (recorded from the two pylon transducers) are labelled. These three gait components are those studied in chapter 8. The three other components of the gait have a small magnitude and they thus, cannot be observed easily on the graph. The same scale is used to evaluate the respective magnitude of the different values of the gait parameters.

Hz for the VPT, does not exhibit any difference in comparison with the two others. In other words, the filtering cut-off had no effect on the processed data. Therefore, the demonstration that the chosen sampling frequency of 64 Hz, with a cut-off frequency of 6 Hz (see section 5.3.2) was an accurate choice, was proved.

The differences in percentage were calculated following the equation:

$$\left(\frac{\text{maximum (VPT)} - \text{maximum (SPT)}}{\text{maximum (SPT)}}\right) * 100 \qquad (7.37)$$

From equation 7.37, it is easy to see that when the difference in percentage is negative, the SPT predicted a response higher than the VPT. The opposite is also possible. A negative percentage was the case in all channels. However, a small shifting in the matching of the heel strikes could result in some bias in the comments made. Table 7.17b shows the results recorded from the A/P and M/L bending moments applying equations 7.35 and 7.36 (shadowed cells). The percentage results were established between the recorded results of the VPT and the results calculated from the SPT (named SPT corrected). This task was undertaken to compare these two channels, despite the different positions in the prosthetic shank tube of the two transducers. From table 7.17b, it is possible to express the following main significance: the VPT recorded lower values than SPT. The gap was from a maximum of 73 % in M/L bending moment Mx positive to a minimum of 4 % in A/P bending moment Mz negative. However, these results and comments must be expressed prudently because the maximum values from the two transducers were not recorded simultaneously. A mean time interval of 0.1 s was observed between maximum values from the VPT and those from the SPT.

Averaging the results from the six channels in three tests is shown in table 7.18. The M/L bending moment Mx was the worst channel, but, as stated above, the comparison between the two transducers must be done cautiously

All signs were negative, when the Villiers Pylon Transducer was compared with the Strathclyde Pylon Transducer. Hence, the new transducer predicted lower values than those from the Strathclyde Pylon Transducer (from 8 % to 53 %). Predicted Mx values from the new Villiers Pylon Transducer were 26 to 53 % lower

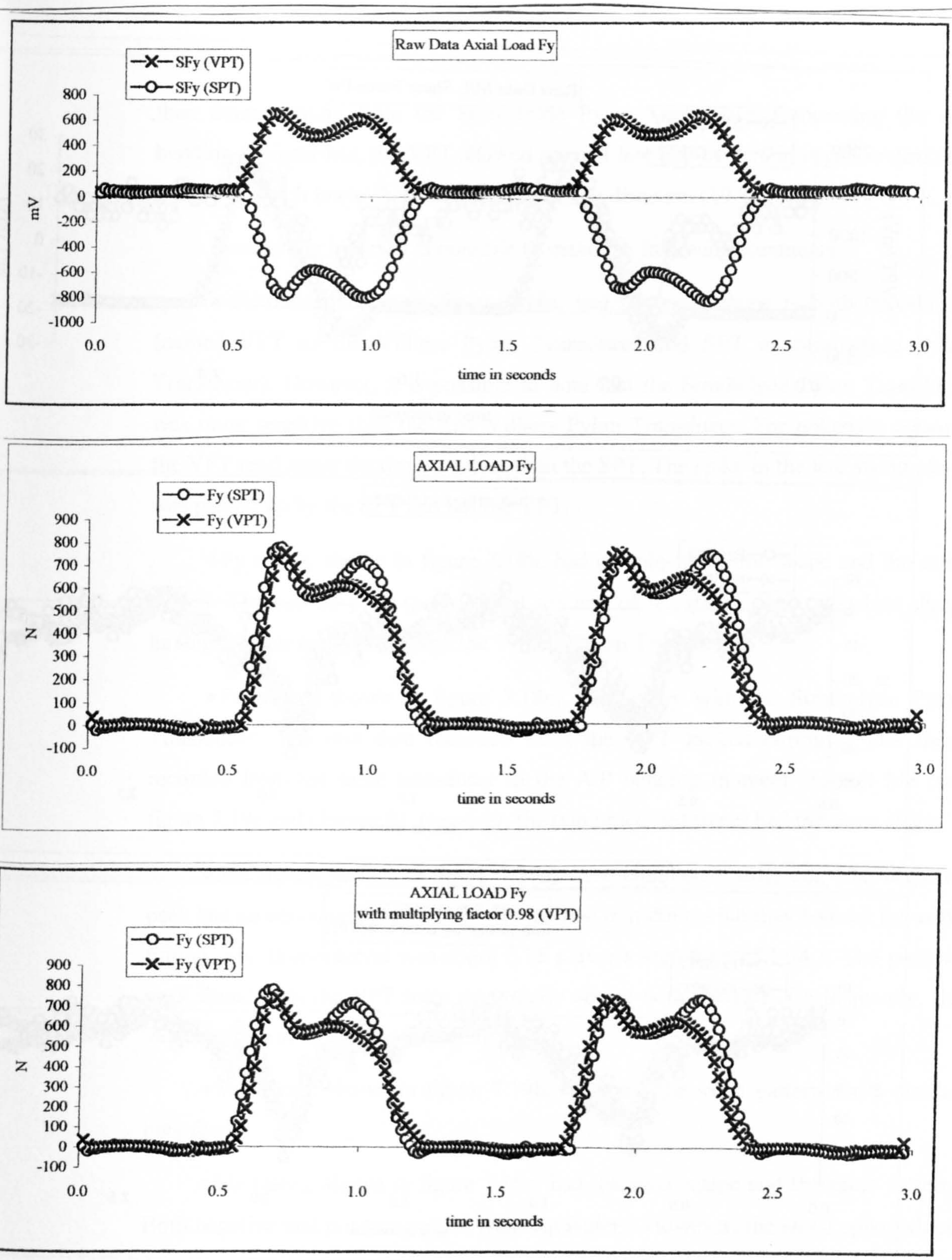

Figure 7.18b: The axial load Fy using simultaneously the two transducers: raw data (top); after applying the cross-sensitivity matrices (see section 6.7 and table 11.VII.16) (middle); after applying the cross-sensitivity matrices plus the factors established in section 7.8.1 only on the VPT (bottom)

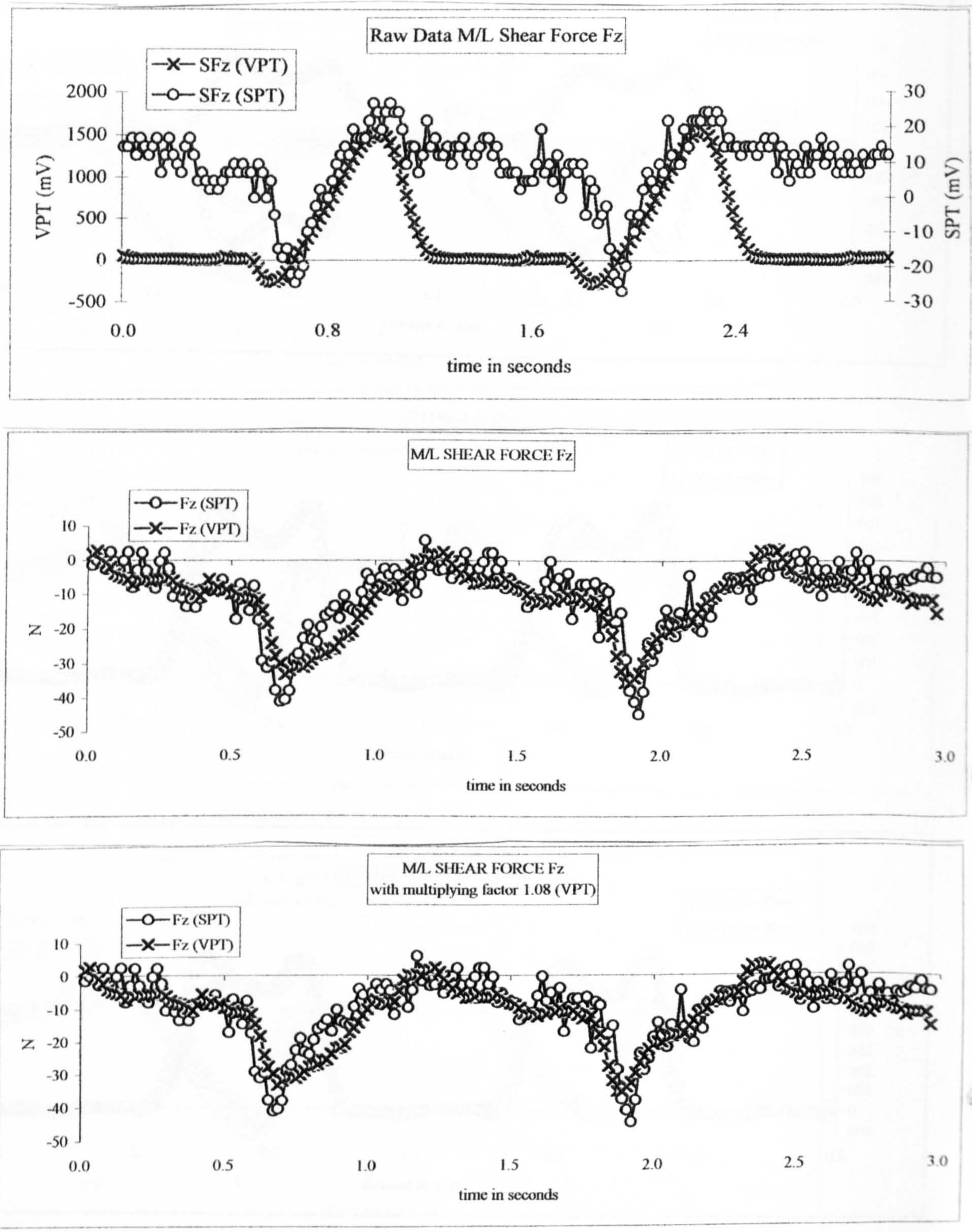

Figure 7.18c: The M/L shear force Fz using simultaneously the two transducers: raw data (top); after applying the cross-sensitivity matrices (see section 6.7 and table 11.VII.16) (middle); after applying the cross-sensitivity matrices plus the factor (1.08) established in section 7.8.1 only on the VPT (bottom)

than those coming from the Strathclyde Pylon Transducer. Concerning the A/P bending moment Mz, the VPT showed a small low gap of 8 % in negative direction but it was much lower than the SPT in positive direction (19 %).

Concerning traces, it is possible to make the following comments:

• Fx traces, shown in figure 7.18a, had the same shape in both transducers (named VPT as the Villiers Pylon Transducer and SPT as Strathclyde Pylon Transducer). However, it is possible to note that the Strathclyde Pylon Transducer was more sensitive than the new Villiers Pylon Transducer. For unknown reasons, the VPT read lower maximum values than the SPT. The spike in the late swing phase was picked up by the SPT and not the VPT.

• Fy traces, shown in figure 7.18b, had globally the same shape and the same values. The second peak (push-off) at the end of the stance phase was less sharp, having a lower magnitude, with the Villiers Pylon Transducer.

• Fz traces, shown in figure 7.18c, were noisy with the Strathclyde Pylon Transducer. The raw data recorded from the VPT looked curiously like those recorded from the same transducer in the A/P bending moment channel Mz (see figure 7.19c and chapter 9). However, the two processed traces had the same shape.

• Mx traces, shown in figure 7.19a, were completely different. The negative peak had an equivalent magnitude with the two transducers but they had not the same timing. The time-interval was about 0.38 s over a step time of 1.34 s. The positive peak found with the VPT trace was totally absent with the SPT. Consequently, the values' gap was found important: 30 %.

• My traces, shown in figure 7.19b, exhibited the same pattern and a similar magnitude.

• Mz traces, shown in figure 7.19c, had the same shape and the same pattern. Both negative and positive values were equivalent. However, the small spike which depicted the knee locking was sharper with the SPT (2.37 N m) than with the VPT (1.02 N m). The difference was small but it looked like that the VPT was less sensitive than the SPT when an event was short (refer to Fx spike, top of the page).

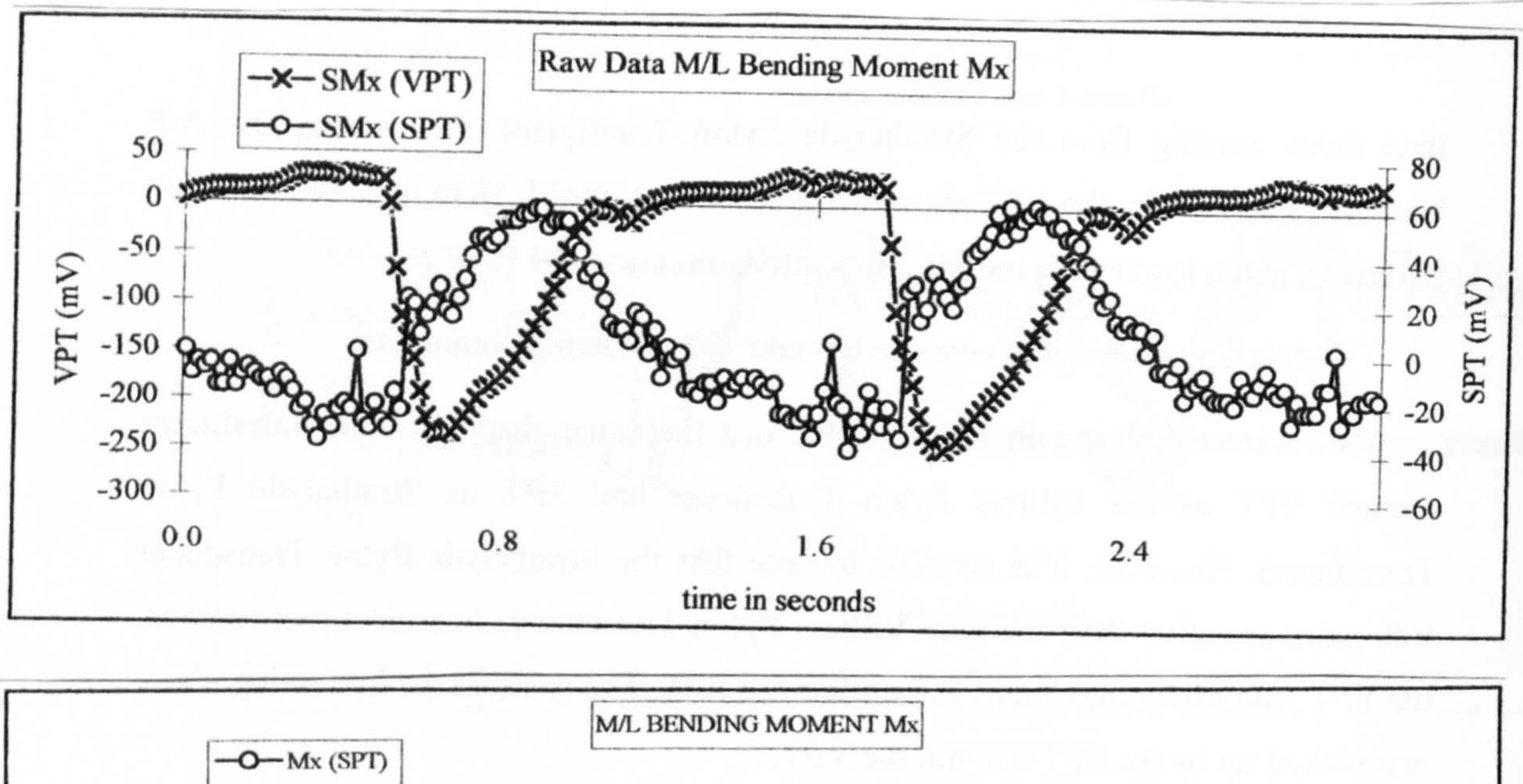

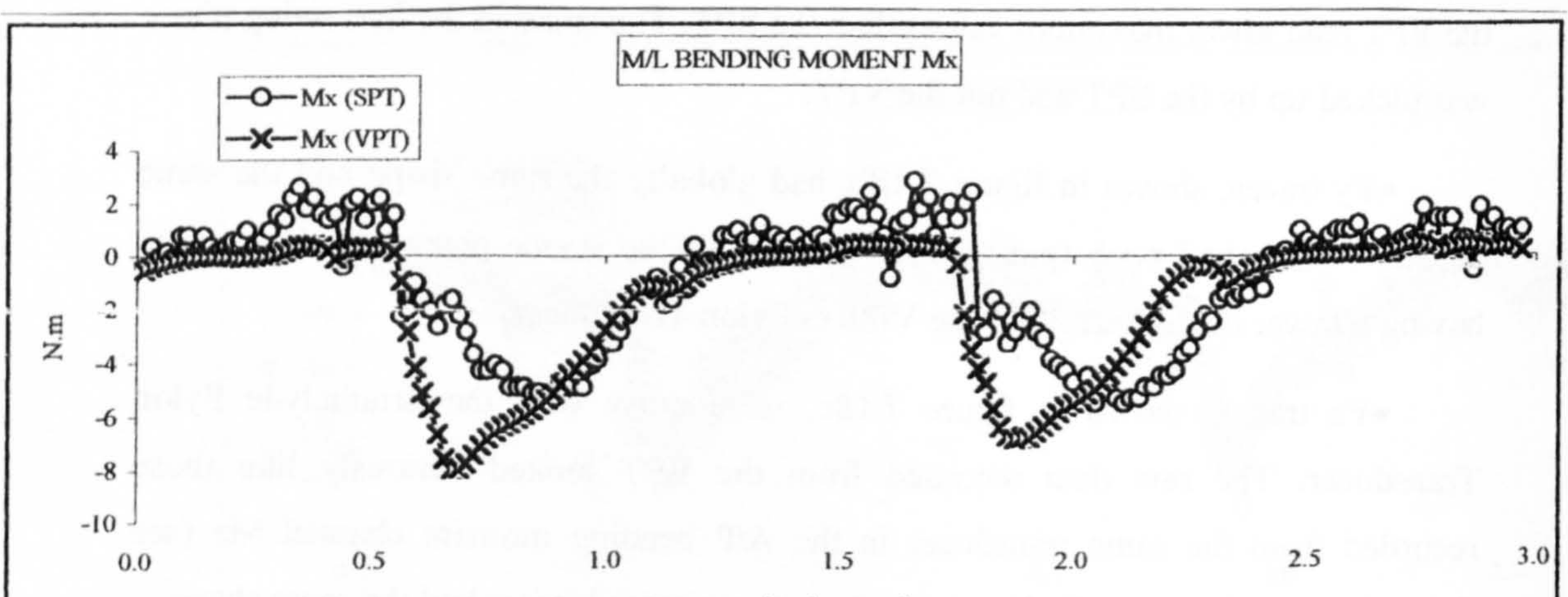

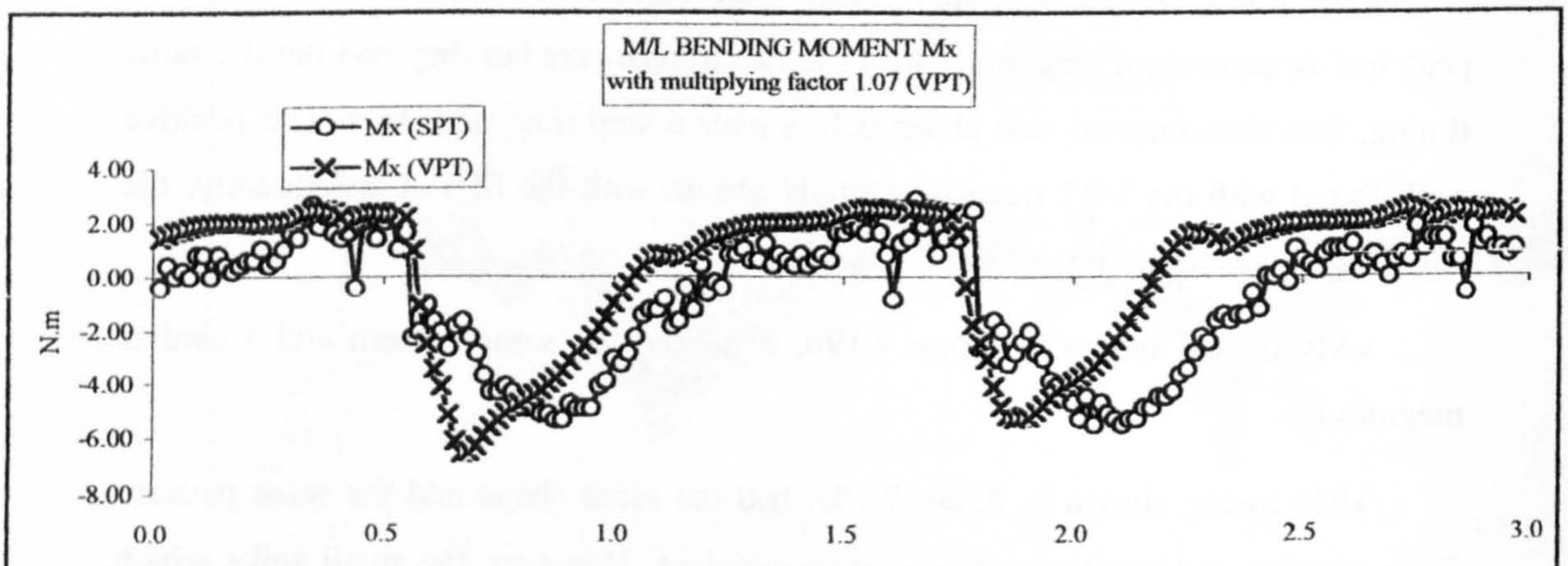

Figure 7.19a: The M/L bending moment Mx using simultaneously the two transducers: raw data (top); after applying the cross-sensitivity matrices (see section 6.7 and table 11.VII.16) (middle); after applying the cross-sensitivity matrices plus the factors established in section 7.8.1 only on the VPT (bottom)

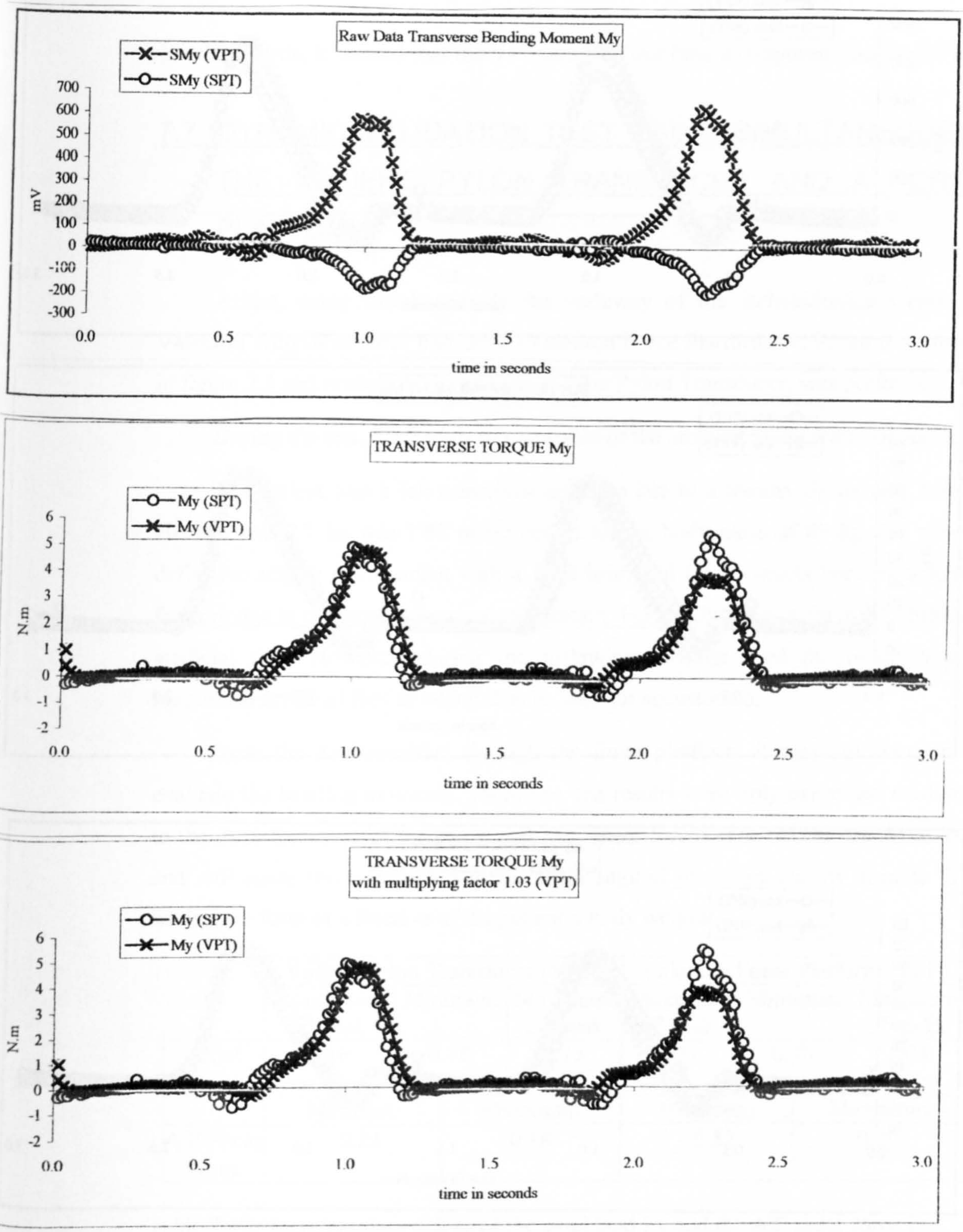

Figure 7.19b: The transverse bending moment My using simultaneously the two transducers: raw data (top); after applying the cross-sensitivity matrices (see section 6.7 and table 11.VII.16) (middle); after applying the cross-sensitivity matrices plus the factor (1.03) established in section 7.8.1 only on the VPT (bottom)

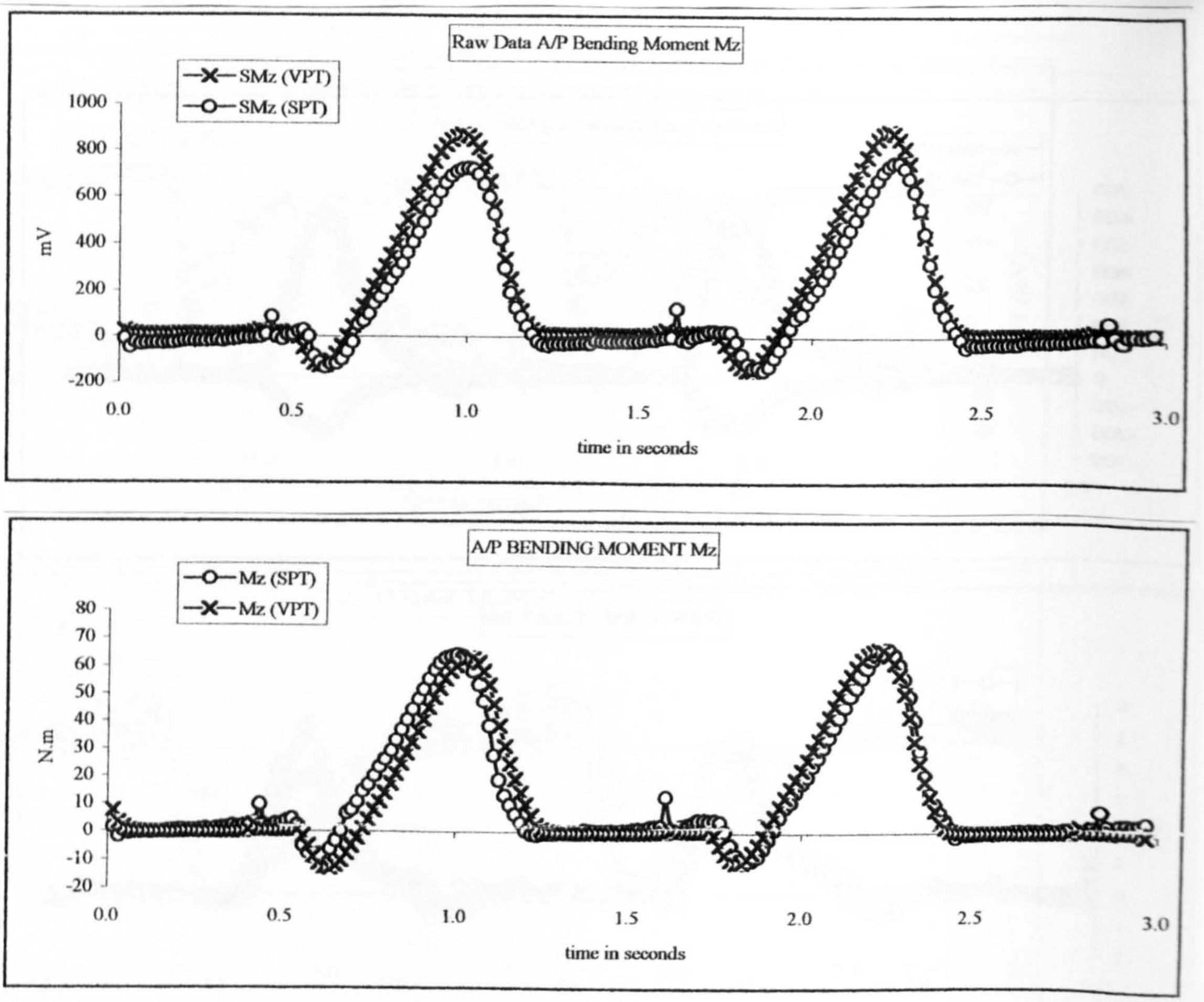

Figure 7.19c: The A/P bending moment Mz using simultaneously the two transducers: raw data (top); after applying the cross-sensitivity matrices (see section 6.7 and table 11.VII.16) (middle); after applying the cross-sensitivity matrices plus the factor established in section 7.8.1 only on the VPT (bottom)

In other words, it seemed that the VPT had a slower time as response than the SPT.

7.7 DYNAMIC VALIDATION TEST USING SIMULTANEOUSLY THE VILLIERS PYLON TRANSDUCER AND A FORCE PLATFORM

A test, using simultaneously the walkway of the Rehabilitation Centre of Valenton with three force platforms (Valenton Force Platform, VFP, see description in figure 2.3 and section 2.3.3) and the Villiers Pylon Transducer, was performed.

During the test, three trials of one stride of the amputated leg were conducted.

The patient was a left transtibial amputee due to a trauma six months before. His age was 25, he was 1.88 metre height with a body mass of 89 kg. He wore a definitive acrylic resin socket with a PTB brim and thigh corsets because a femur fracture due to the same trauma as amputation. He usually wore a Protéval Multiflex artificial foot. However, during the following test, he used the usual Protéor monoaxial artificial foot to which thus he was not accustomed.

From the data recorded through the force platform, it was not possible to evaluate the bending moments. Therefore, the results were only expressed relatively to the three forces: axial load, A/P and M/L shear forces. The two forces (axial load and A/P shear force) recorded in the main sagittal plane are shown in table 7.19 having the form of a fraction of the patient's body weight:

	Villiers Pylon Transducer (VPT)			Valenton Force Platform (VFP)		
	Maximum 1st peak	Minimum	Maximum 2nd peak	Maximum 1st peak	Minimum	Maximum 2nd peak
Axial Load	1.16	0.78	1.15	1.21	0.70	1.04
	Minimum		Maximum	Minimum		Maximum
A/P Shear Force	- 0.24		0.18	- 0.52		0.20

Table 7.19: The maximum values of the axial load Fy and the A/P shear force Fx recorded from the Villiers Pylon Transducer (VPT) and the Valenton's force platform (VFP) for the same stride of a left transtibial patient. The results are expressed in a fraction of the body weight of the patient (873 N).

Test N°1:

	VPT				SPT			
	maximum negative	maximum positive	Mx and Mz corrected see equations 7.35 & 7.36		maximum negative	maximum positive	maximum negative VPT vs. SPT in %	maximum positive VPT vs. SPT in %
Fx	-105.72	42.17			-126.19	48.55	- 16	- 13
Fy		909.1				995.6		- 8
Fz	-32.44	9.7			-32.13	8.24	- 1	17
My	-0.55	7.07			-0.99	8.45	- 44	- 16

Test N°2:

	VPT				SPT			
	maximum negative	maximum positive	Mx and Mz corrected see equations 7.35 & 7.36		maximum negative	maximum positive	maximum negative VPT vs. SPT in %	maximum positive VPT vs. SPT in %
Fx	-103.94	51.78			-117.54	44.41	- 11	16
Fy		779.21				809.88		- 3
Fz	-21.34	6.76			-24.59	5.96	- 4	13
My	-0.30	4.77			-0.45	5.41	- 15	- 11

Test N°3 (Sampling Frequency of 2048 Hz for the VPT and 64 Hz for the SPT):

	VPT				SPT			
	maximum negative	maximum positive	Mx and Mz corrected see equations 7.35 & 7.36		maximum negative	maximum positive	maximum negative difference in %	maximum positive difference in %
Fx	-99.85	37.84			-100.34	46.96	0	- 19
Fy		781.44				784.32		0
Fz	-17.51	12.61			-14.95	13.38	- 17	- 6
My	-0.05	3.25			-0.08	3.08	- 12	- 5

Table 7.17a: Three tests with the Villiers Pylon Transducer and the Strathclyde Pylon Transducer fitted on the same transfemoral prosthesis and simultaneously recorded, before applying any correction factors.

These results were not totally comparable because of the inclination of the prosthesis relatively to the vertical in the A/P plane. However, the angle might not be estimated over 20° (but it was not measured or controlled). The multiplying factors were thus closed to 1 (cos 20 = 0.93, for the axial load) or small (tang 20 = 0.36 for the A/P shear force). When the maximum values of these two forces were recorded, it could be expected that the prosthesis was vertical. Hence, no multiplying factors might be applied to the results. The traces are shown in the following figures:

Figure 7.20 shows the A/P shear force Fx traces recorded from the VPT (top) and from the VFP (bottom). The values expressed by the VPT were calculated after applying the factors established in the following section 7.8.1. The sign convention was the same and the force platform expressed an offset: the flat part of the Fx trace (A/P shear force = 0, at mid stance phase) was not on the horizontal axis. The offset could be evaluated as a mean value of 0.1 BW. However and despite this offset, the traces coming from the same stride and simultaneously recorded from the VPT and the Valenton's force platform were similar in shape and values except the minimum. There were - 0.24 BW (VPT) and - 0.52 BW (VFP), but a multiplying factor of tg 20 = 0.36 had to be applied: -0.52 BW x 0.36 = 0.19 BW (VFP), to compare with the 0.24 BW recorded from the VPT;

Figure 7.21 shows the axial load Fy traces recorded from the VPT (top) and the VFP (bottom). The maximum angle between the vertical axis of the force platform and the longitudinal axis of the Villiers pylon transducer could be estimated as 20° (0.35 rad). Therefore, a correcting factor having a maximum value of cos 20 = 0.93 might be applied, especially in early and late stance phase. This angle and its variation could explain the minor difference in shape between the two traces. The VFP trace was more vertical in early stance than VPT. The VFP second peak also expressed a lower value than the one recorded from the VPT. However and despite this angle, it is obvious that the two traces are globally similar in shape and values.

Figure 7.22 shows the M/L shear force Fz recorded from the VPT (top) and the VFP (bottom). The general shape of the two traces was similar. However, the traces showed a main difference: the M/L shear force recorded from the VPT (at the ankle level) crossed over the zero line but the M/L shear force recorded from the VFP did

	VPT			SPT			
	maximum negative	maximum positive	Mx and Mz corrected see equations 7.35 & 7.36	maximum negative	maximum positive	maximum negative VPT vs. SPT corrected in %	maximum positive VPT vs. SPT corrected in %
Test N°1							
Mx	-10.72	6.82	-7.21	0.38	-9.97	1.42	- 28	-73
Mz	-17.07	67.09	-18.4	47.3	-20.93	64.99	- 12	- 27
Test N°2							
Mx	-9.46	2.54	-3.79	1.24	-5.51	1.84	- 31	- 32
Mz	-12.81	66.48	-13.7	53.2	-14.28	62.37	- 4	- 14
Test N°3							
Mx	-5.29	4.21	-4.31	1.77	-5.46	3.93	- 21	- 54
Mz	-15.49	70.01	-16.6	57.2	-18.12	69.91	- 8	- 18

Table 7.17b: Three tests in M/L and A/P bending moments, after calculations concerning Mx and Mz (using equations 7.35 and 7.36) to compare the given results of the VPT with those calculated from the SPT
(VPT vs. SPT corrected, in percentage).

	maximum negative VPT vs. SPT in %	maximum positive VPT vs. SPT in %
Fx	-9	-5
Fy		-4
Fz	-12	-14
My	-11	-17
	maximum negative VPT results vs. SPT calculated	Maximum positive VPT results vs. SPT calculated
Mx	- 26	- 53
Mz	- 8	- 19

Table 7.18: Summary of the mean results recorded from the VPT and the SPT (after calculations concerning Mx and Mz).

not. It was always negative under the zero line. However, the toe out angle of the prosthetic foot was not measured and thus the traces were not accurately comparable.

It is thus proved that the Villiers Pylon Transducer exhibits results, sufficiently similar in shape in the sagittal plane, as those recorded from the Valenton's force platform. The difference showed in the medio-lateral plane could be due to three factors: 1) the toe out angle of the prosthetic foot, 2) the sloppiness of the foot wear and/or 3) the slipping of the artificial foot into the patient's shoe.

7.8 DISCUSSION

7.8.1 Followed method to calculate the amending factors

Regarding all the tests performed to validate the calibration matrix [C] (see table 6.41), the use of correcting factors (mean slope of the linear regression analysis calculated from the performed tests and close to the unity) was found compulsory, despite the fact that a calibration matrix should avoid such a factors. Merging the different static and dynamic tests, the method to establish these factors was as follows:

1. Fx: the dynamic test was found more accurate (for set-up reasons) and thus a factor of 1.07 was calculated (by means of a linear regression analysis) from the maximum values recorded through the two pylon transducers (see equation 7.29).

2. Fy: all the tests exhibited the same accurate response, thus following the equation 7.30, a factor of 0.98 was calculated.

3. Fz: averaging the static tests (see equation 7.31) and the dynamic tests, a factor of 1.08 was calculated.

4. Mx: averaging the static tests (see equation 7.32 and table 7.15) and the dynamic tests, a factor of 1.07 was calculated.

5. My: for set-up reasons, the dynamic tests were found more accurate than static tests and thus a factor of 1.03 was calculated.

6. Mz: averaging the static tests (see equation 7.34 and table 7.15) and the dynamic tests, a factor of 0.99 was calculated.

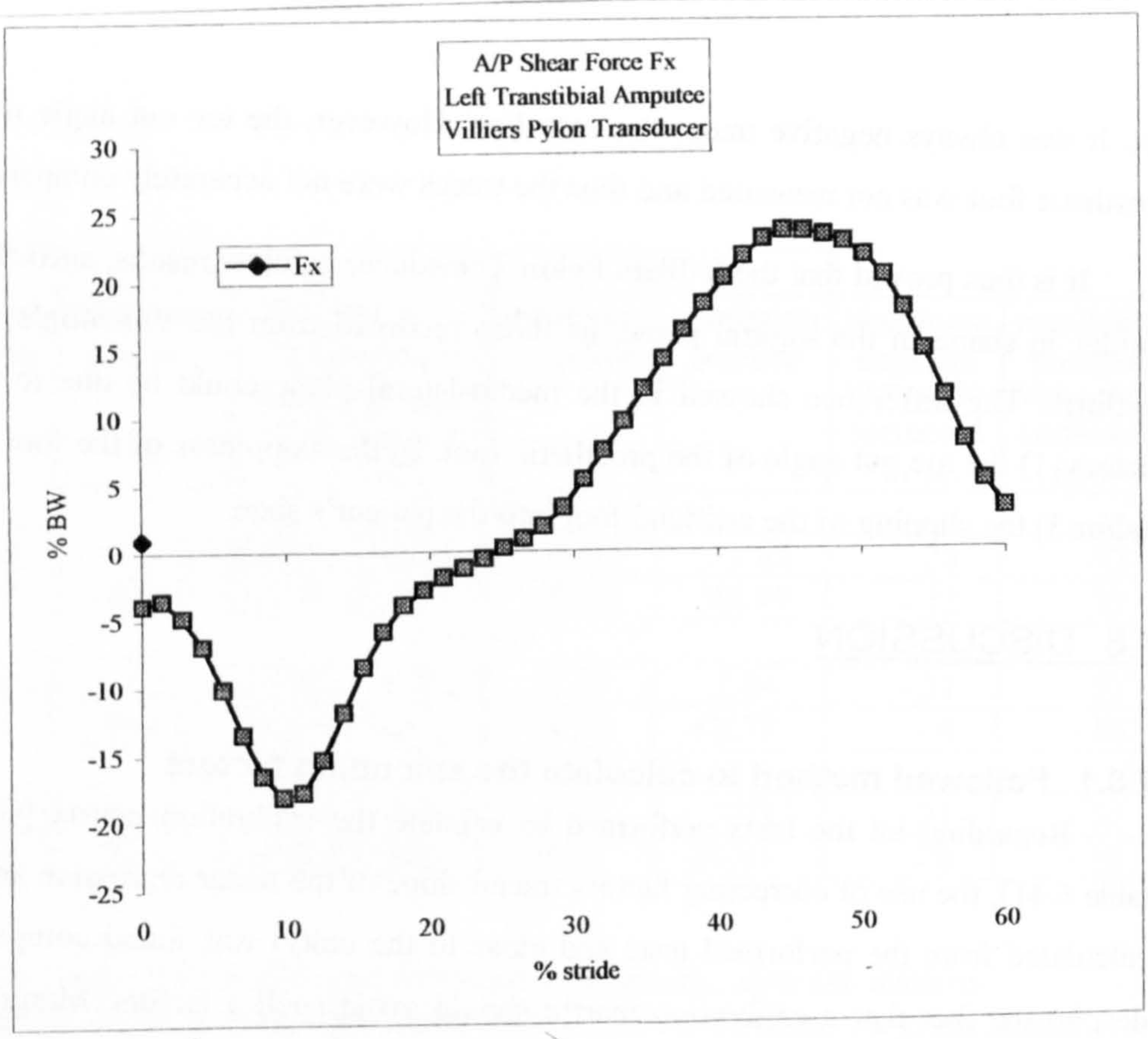

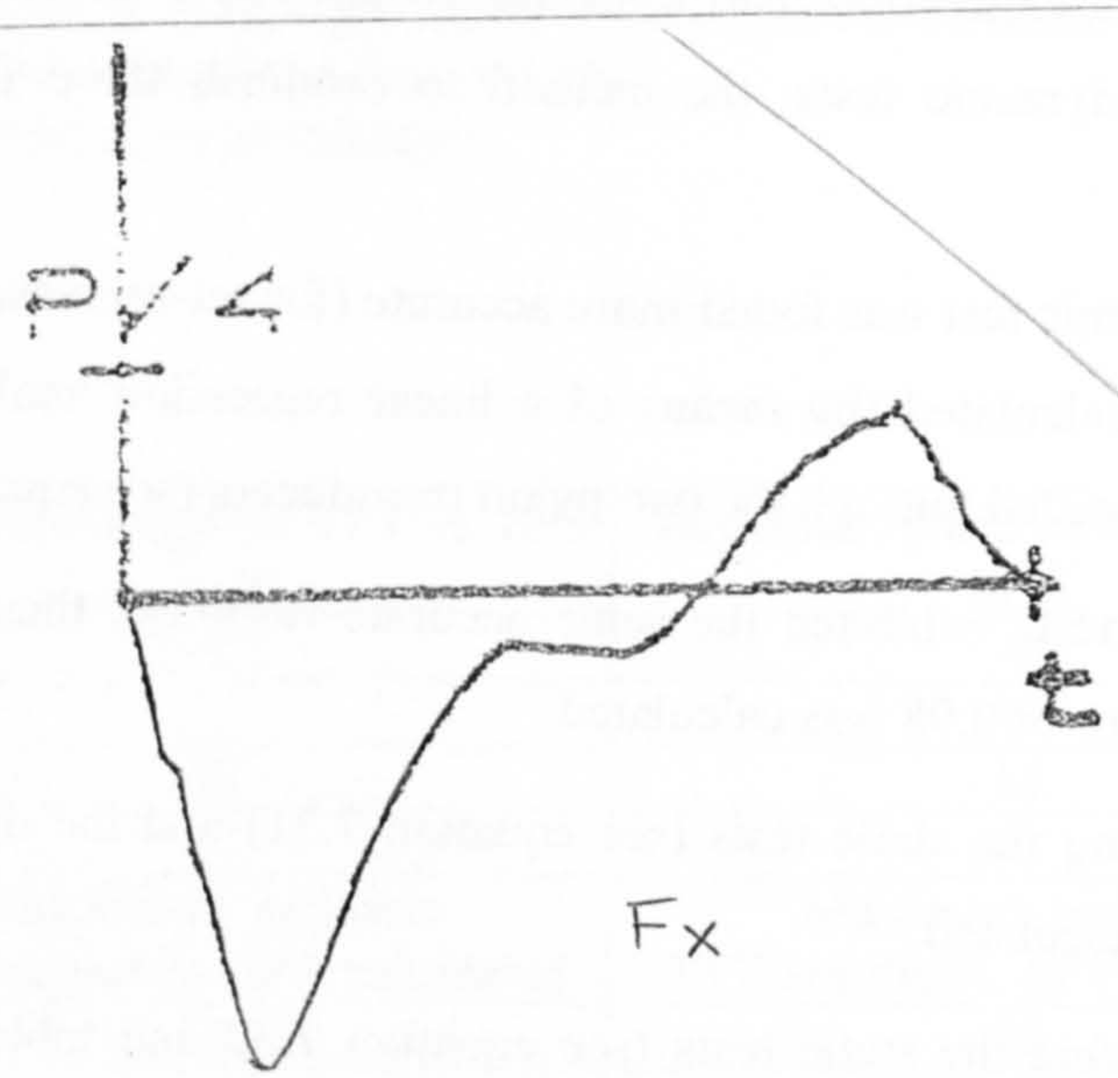

Figure 7.20: The A/P shear force traces recorded from the Villiers Pylon Transducer (top) and the Valenton's force platform (bottom). The two traces were recorded simultaneously from the same stride of a left transtibial amputee. In the bottom figure, the conventions are as follows: in abscissa, t = 60 % of stride; in ordinate: P/4 = 25 % of BW.

The VPT values were calculated after applying the factors shown in table 7.20. See text for explanations concerning the reference axis of the two systems, which were not identical.

Therefore, the factors to be applied in all the tests presented in chapter 8 and to be used in addition with the calibration matrix [C] described in chapter 6 are the followings:

Fx	1.07	Mx	1.07
Fy	0.98	My	1.03
Fz	1.08	Mz	0.99

Table 7.20: The factors to be used in addition with the calibration matrix of the Villiers Pylon Transducer.

7.8.2 Verification of the correcting factors

To verify the relevance of the correcting factors established in the previous section, figures 7.23a, b and c (the three forces) and 7.24a, b and c (the three moments) show 9 strides extracted from the trial no 1. More than two strides are shown to be sure that the correcting factors are applicable with accuracy and reliability in all the phases of the gait cycle. In each figure, the traces without and with applying the correcting factors are shown.

Except in the M/L bending moments Mx and Mz (and this is logic since the two pylons were fitted in different position on the artificial leg), the traces recorded from the two pylon transducers are often so close and even superimposed that they are difficult to separate. The same types of graphs showing the different recorded trials are shown in appendix 11.VII.7.

Figure 7.25 shows the M/L and A/P bending moments of the same nine strides of figures 7.23 and 7.24. To establish the Villiers Pylon Transducer traces (denoted VPTT, the second T stands for theoretical) equations 7.35 and 7.36 were applied to transform the SPT results at the middle of the artificial leg into theoretical VPT results as they should be at the ankle level. This way of doing was applied in order to compare the two pylons despite the two different positions they had in the artificial leg.

The three shapes of the traces were similar. The two pylon transducers showed thus the same trend in these two particular channels. The positive and negative maximum values are shown in table 7.21:

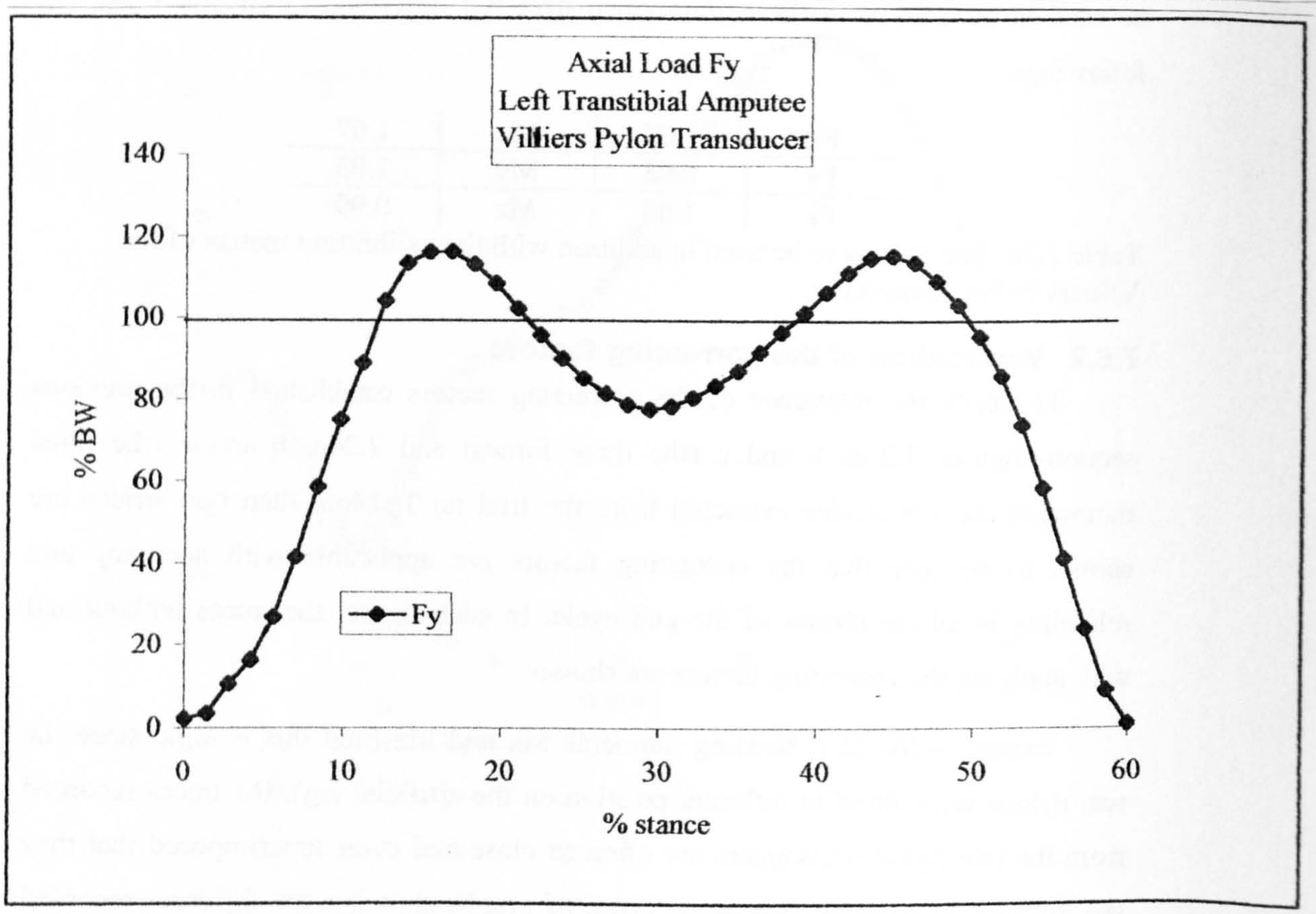

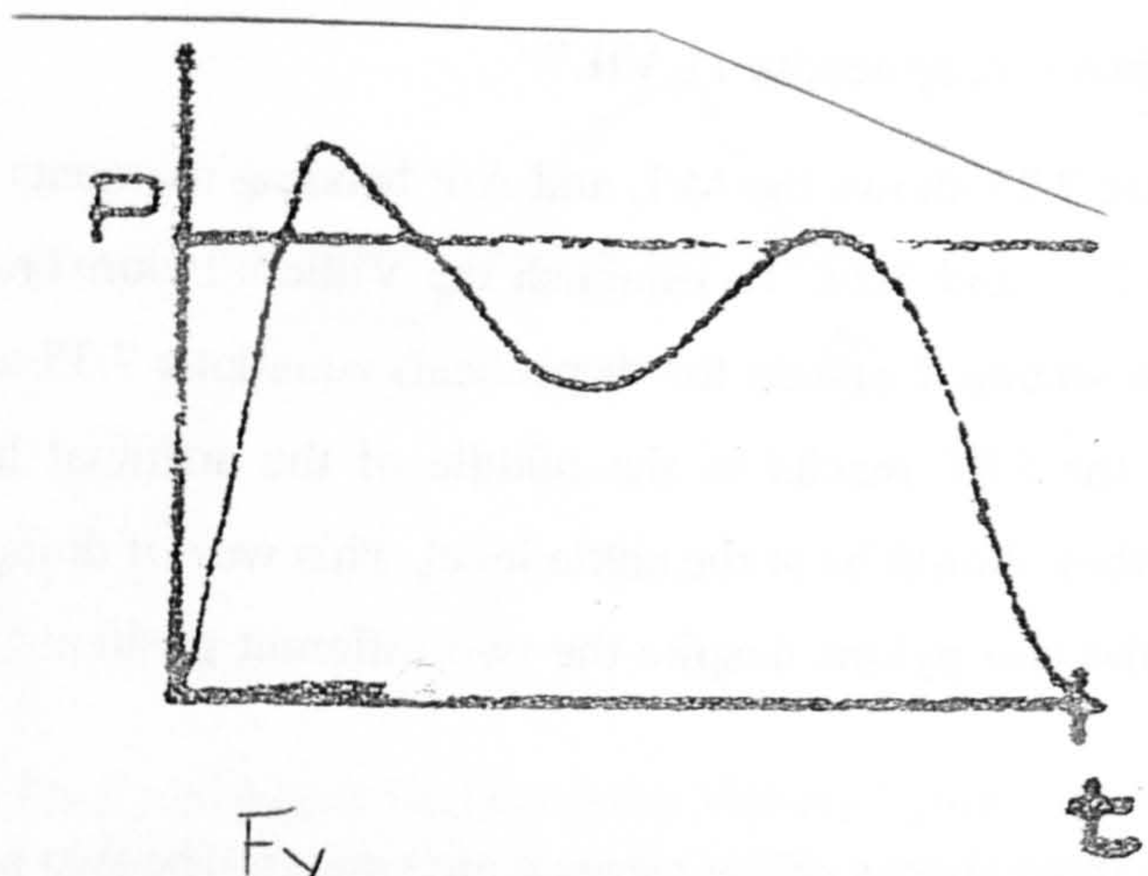

Figure 7.21: The axial load traces recorded from the Villiers Pylon Transducer (top) and the Valenton's force platform (bottom). The two traces were recorded simultaneously from the same stride of a left transtibial amputee. In the bottom figure, the conventions are as follows: in abscissa, t = 60 % of stride; in ordinate: P = 100 % of BW.

	VPT Recorded		VPT Calculated		SPT Recorded	
M/L Bending Moment Mx in N m	7.3	-11.5	2.61	-14.2	2.64	-9.9
A/ P Bending Moment Mz in N m	66.42	-16.9	49.1	-18.5	64.9	-20.9

Table 7.21: The negative and positive maximum values in M/L and A/P bending moments: recorded from the Villiers Pylon Transducer (calibration matrix and correcting factors being applied); calculated values from the Strathclyde Pylon Transducer results; recorded from the Strathclyde Pylon Transducer (calibration matrix being applied).

The difference in percentage between the values recorded from the VPT and those calculated from the SPT recorded values is the following (table 7.22):

	((VPT Recorded – VPT Calculated) / VPT Calculated) *100	
M/L Bending Moment Mx Difference in %	179	- 23
A/ P Bending Moment Mz Difference in %	- 19	- 8

Table 7.22: The difference in percentage between the maximum values recorded from the VPT and those calculated from the SPT recorded values.

The results showed a large gap in the positive direction of the M/L bending moment Mx (shaded cell). However, since this maximum value was calculated following the equation 7.35 in which the noisy Fz_{SPT} was considered, this gap could not thus be considered totally accurate. As example, it was possible to establish a gap of 0.37 % to – 2269 % in a time interval of 5/100 of second. Moreover, this channel was not considered important in the gait evaluation tests conducted and presented in the following chapter 8.

7.9 CONCLUSION

The work presented in this chapter was conducted to establish a full set of methods by which users of the new Villiers Pylon Transducer can be confident in the calibration matrix they use and results it gives.

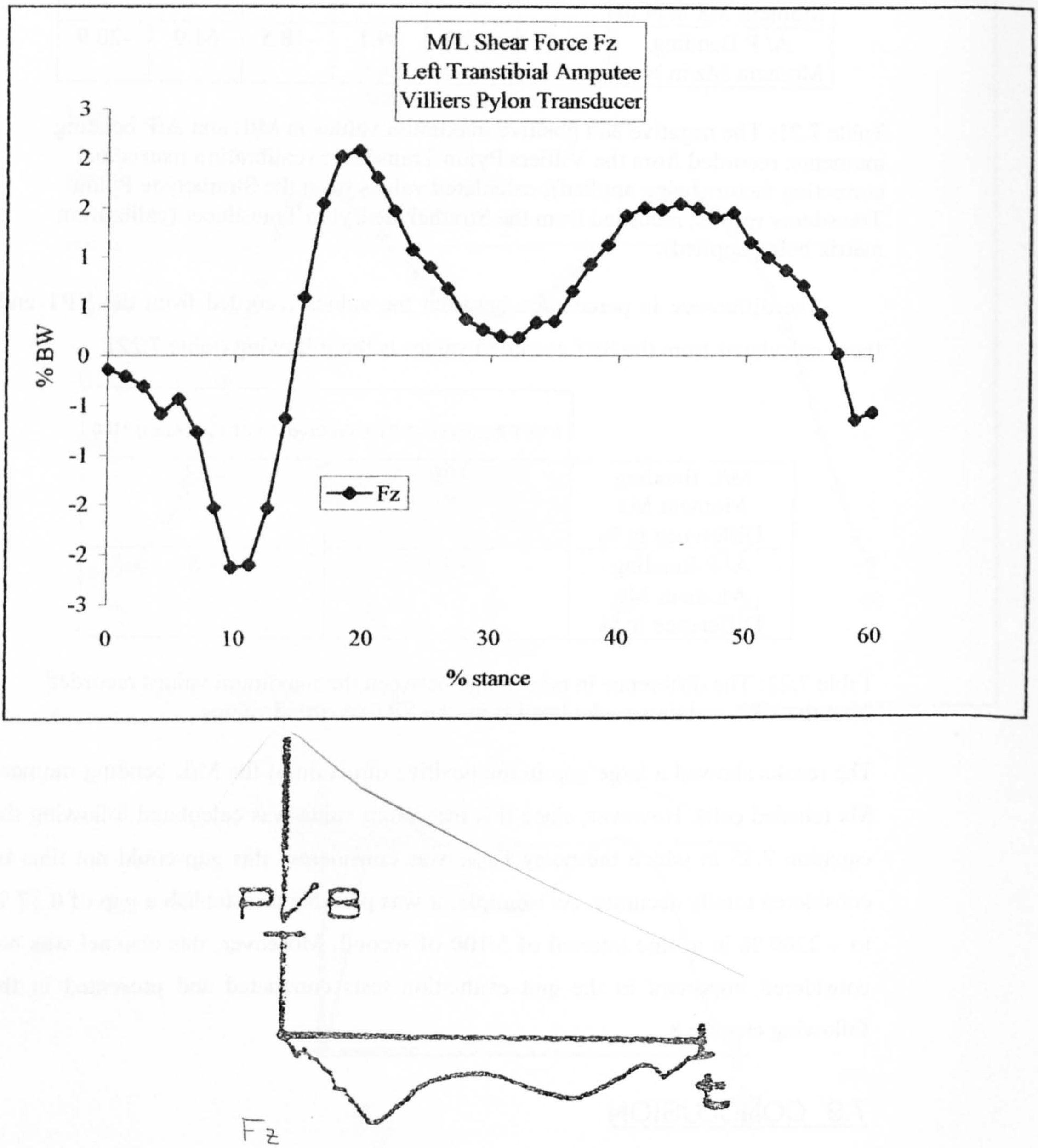

Figure 7.22: The M/L shear force traces recorded from the Villiers Pylon Transducer (top) and the Valenton's force platform (bottom). The two traces were recorded simultaneously from the same stride of a left transtibial amputee. In the bottom figure, the conventions are as follows: in abscissa, t = 60 % of stride; in ordinate: P/8 = 12.5 % of BW.

1. A combined static method was developed using tools such as a calibration rig and a static bench table. Some tests were undertaken on just the Villiers Pylon Transducer and some others with both the VPT and the Strathclyde Pylon Transducer being used as standard. The static method allowed an exploration of the six channels with their interaction-effects.

2. A dynamic method was described. From a gait test with the two transducers fitted on a transfemoral prosthesis, a comparison of the processed data could be made. Because these tests were performed in a configuration close to the day to day set-up used when amputees' gait assessments are conducted, these results seemed to be more reliable than those using the bench table. These tests and the associated set-up could be considered more « genuine and/or accurate ».

The different methods proved to be a useful tool for the calibration matrix [C] evaluation. They exhibited the good linearity of the new transducer. However, some drawbacks could be recognised which are reported here.

1. The special validation rig developed by Magnissalis (1992) had been designed for the Strathclyde Pylon Transducer. It was not entirely satisfactory to use this device with the Villiers Pylon Transducer, due to its different dimensions. This was a limitation in performing some of the tests: there was no possibility of combined torque with other loads. This also introduced some uncertainties because some of the lever arms were so small that the corresponding bending moments were smaller than the full range of the appropriate channels. Therefore, some loading configurations could not be completely explored.

2. The set-up, using the heavy bench table, introduced a tension in the axial load instead of compression. Consequently, this particular channel Fy was not considered.

3. The static set-up, using the heavy bench table with the two transducers was a chain of many different devices linked with aluminium tubes and clamped with jubilee clips. Therefore, the set-up was not perfectly accurate and a lack of confidence had been found in the results.

4. The dynamic tests, using simultaneously the two transducers, had the

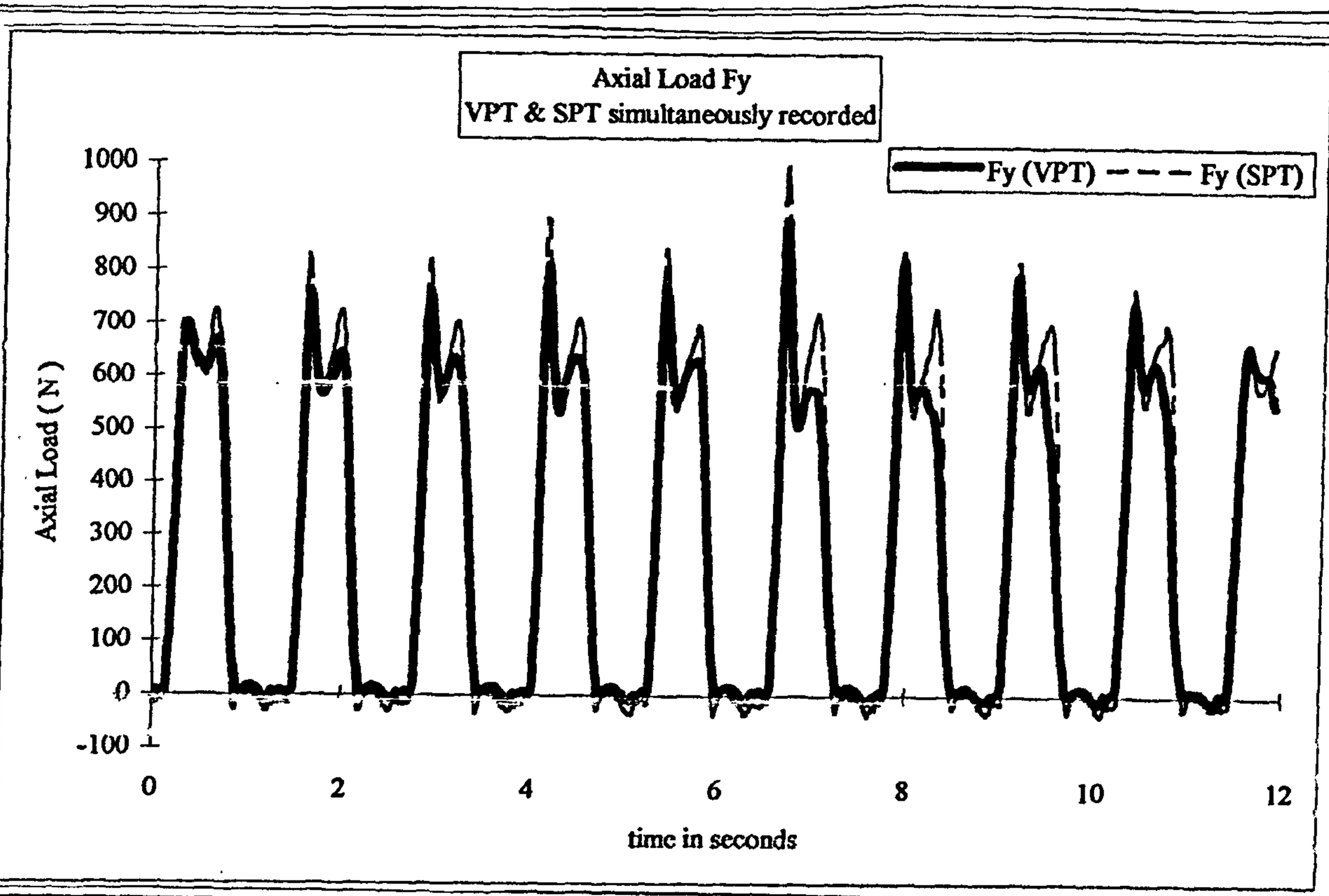

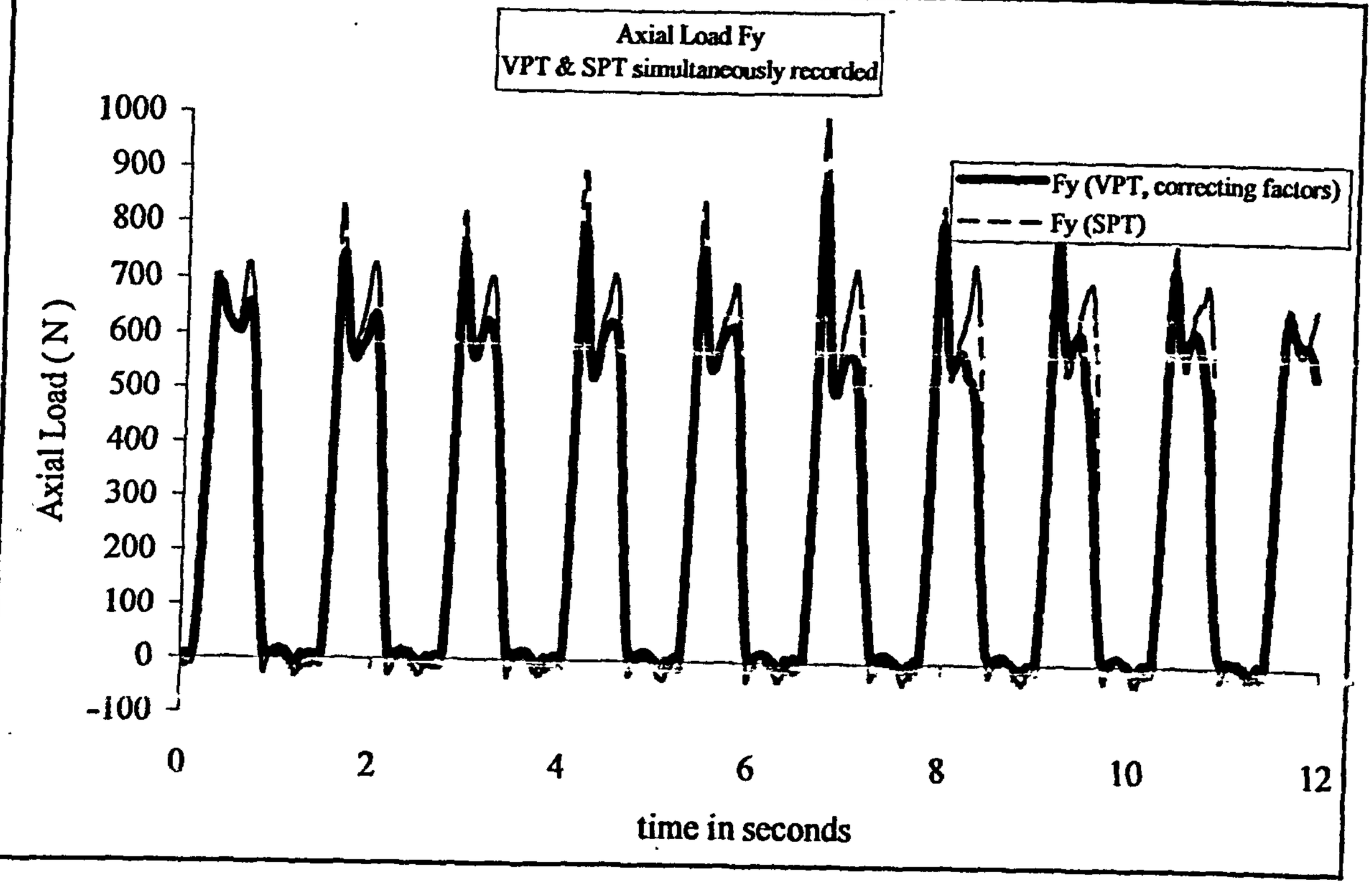

Figure 7.23b: The axial load Fy using simultaneously the two transducers: after applying the cross-sensitivity matrices only (see section 6.7 and table 11.VII.16) (top); after applying the cross-sensitivity matrices plus the factor established in section 7.8.1 (see equation 7.38) only on the VPT (bottom)

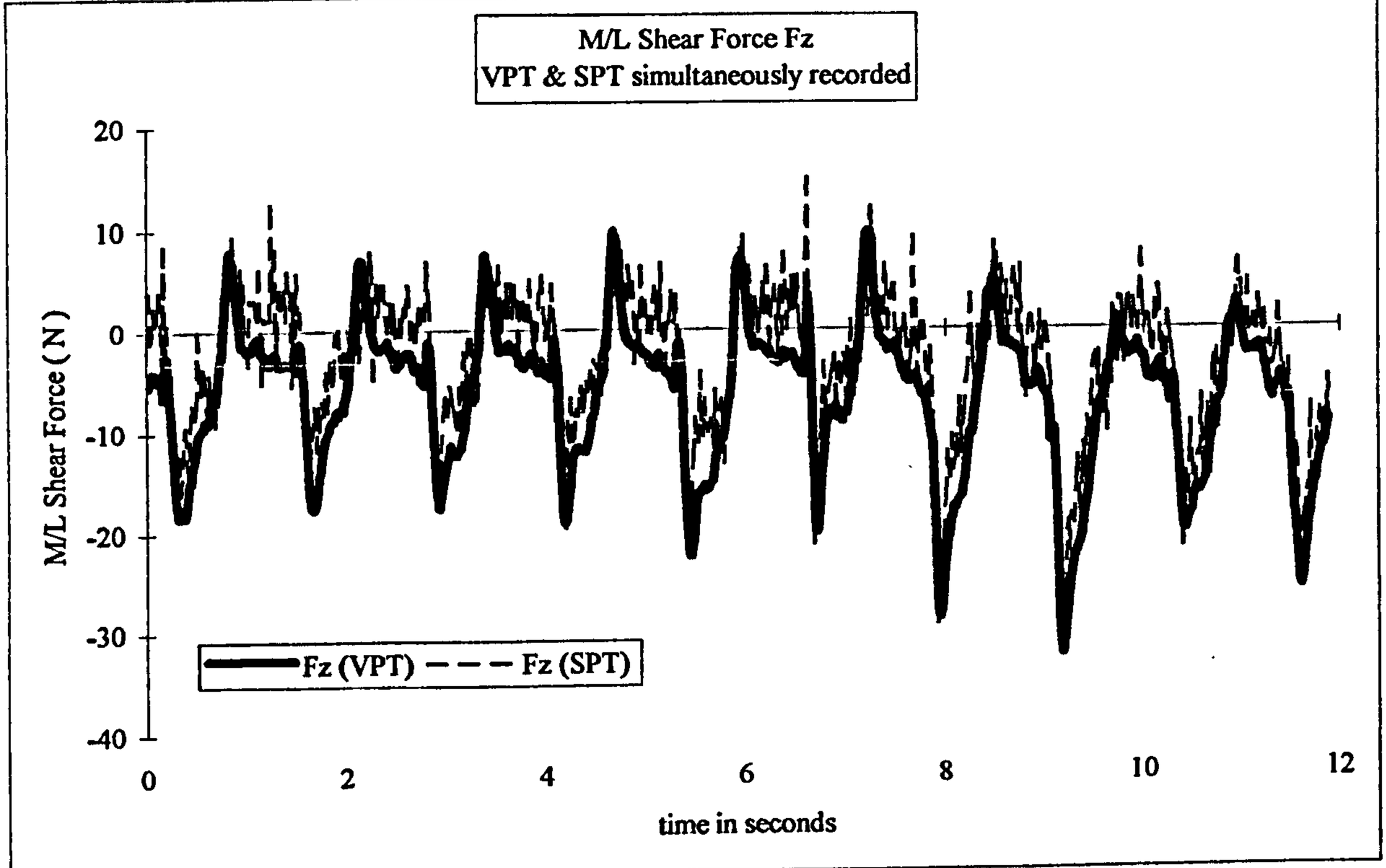

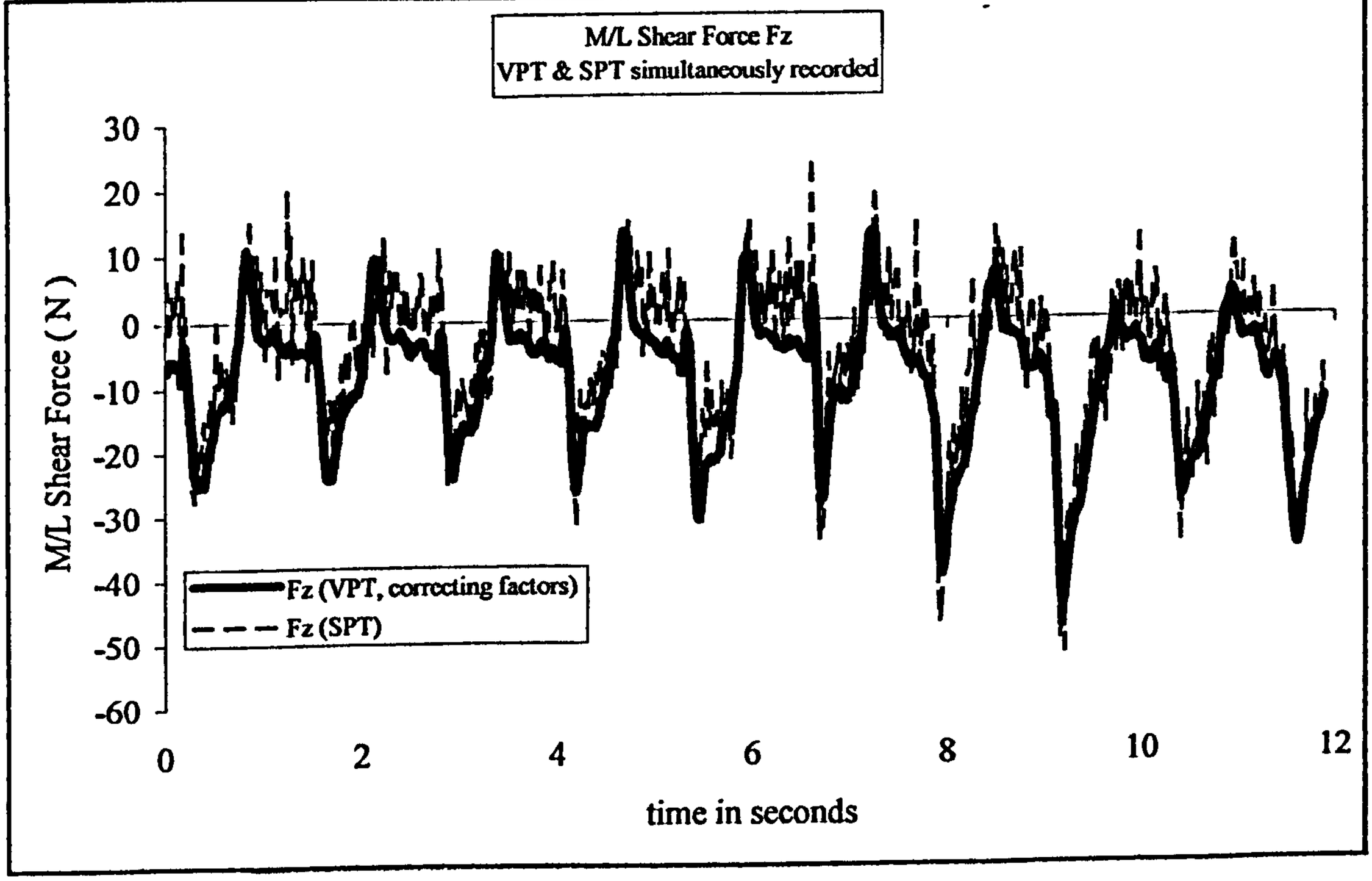

Figure 7.23c: The M/L shear force Fz using simultaneously the two transducers: after applying the cross-sensitivity matrices only (see section 6.7 and table 11.VII.16) (top); after applying the cross-sensitivity matrices plus the correcting factor established in section 7.8.1 (see equation 7.38) only on the VPT (bottom)

main drawback that the two devices were not electronically linked and it was difficult to align each gait event from each transducer.

5. The dynamic tests, using simultaneously a force platform and the VPT, showed an accurate correlation between the different results, despite the difference in reference axes.

Following all these comments, the static tests with the two transducers couple together were considered to have a certain degree of uncertainty. On the contrary, the dynamic tests, with the two transducers used in a realistic way, were considered accurate enough to give confidence to the user. All this having said and done, conclusions could finally, be drawn as follows:

The validation tests for the calibration matrix [C] under study resulted in the calculation of the prediction errors, which however could not be attributed to the calibration matrix with confidence, for reasons discussed above. These results of such errors were as follows:

- low for the shear force Fx and axial compression Fy (2.35 % and 2.05 %, respectively);
- high for the bending moments Mx and Mz (7.75 % and 6.08 % respectively);
- middle range for the transverse torque My (4.83 %)
- larger for the shear force Fz than the two other forces (28.42 %).

This introduced a main discussion about these last two errors:

1. M/L shear force Fz, despite many efforts, no satisfactory explanation was found. It could be a misalignment problem of the gauges, hidden when the transducer was used in a pure static configuration such as a calibration set-up. It could be a dynamic interaction effect between M/L shear force gauges and A/P bending moment gauges: the raw traces of these two particular channels were too similar for one not to be suspicious about them (see section 11.VII.7.2).

2. In transverse torque, the explanation could be the following: 1) a mixing of axial load gauges between each arm of the Wheatstone bridge, 2) a

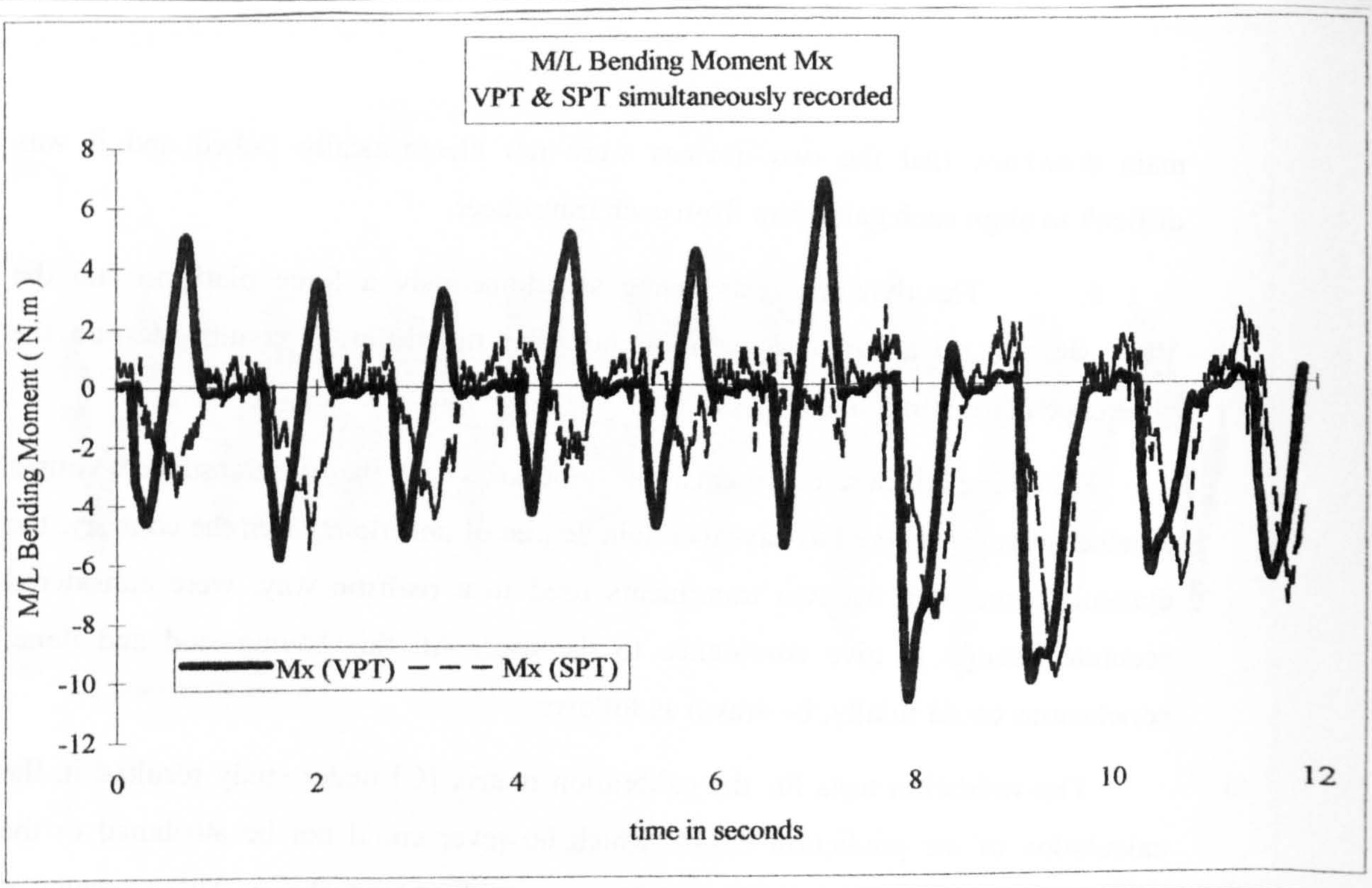

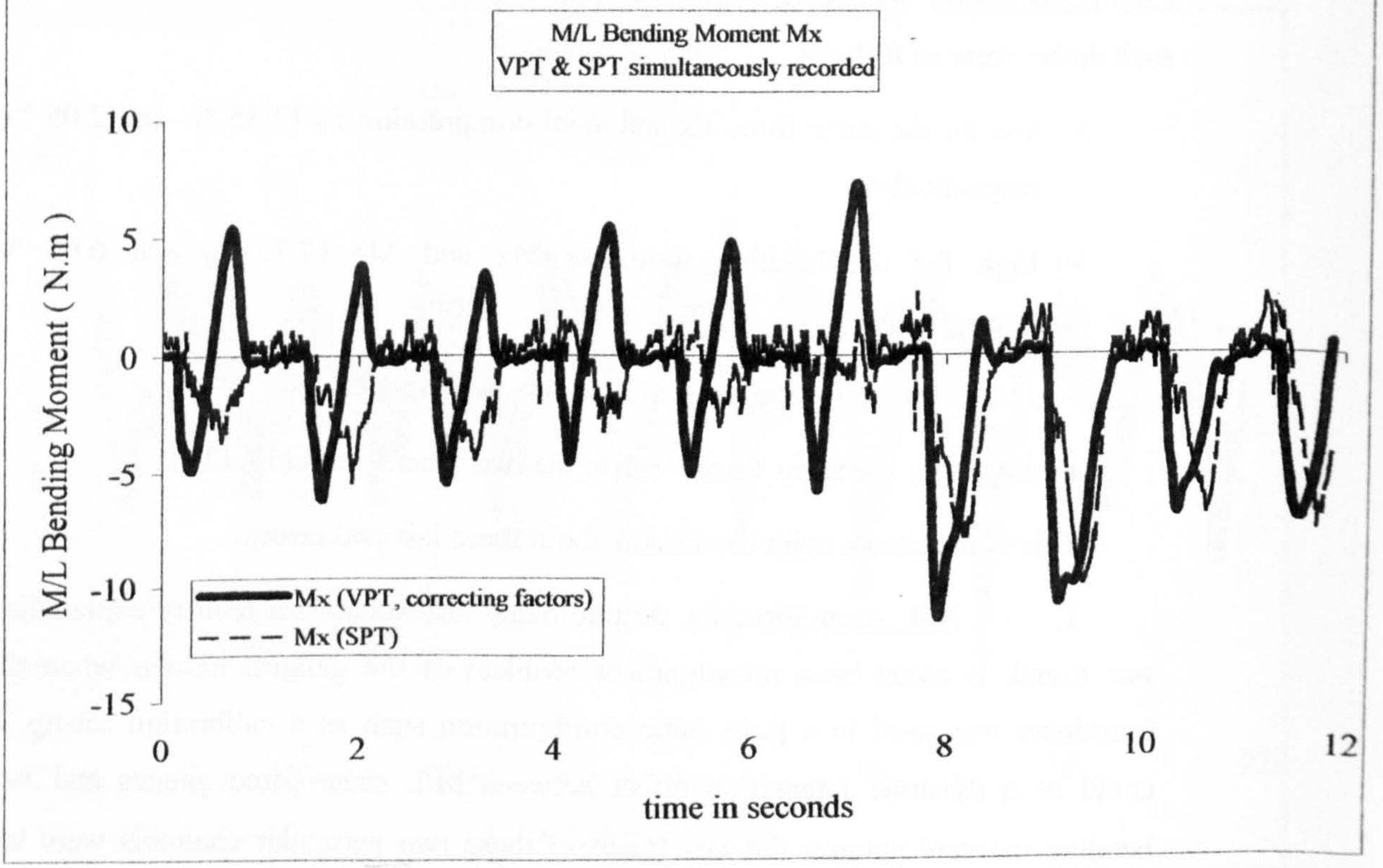

Figure 7.24a: The M/L bending moment Mx using simultaneously the two transducers: after applying the cross-sensitivity matrices only (see section 6.7 and table 11.VII.16) (top); after applying the cross-sensitivity matrices plus the factors established in section 7.8.1 (see equation 7.38) only on the VPT (bottom). Since the position in the leg of the two pylons was different, the moments were different.

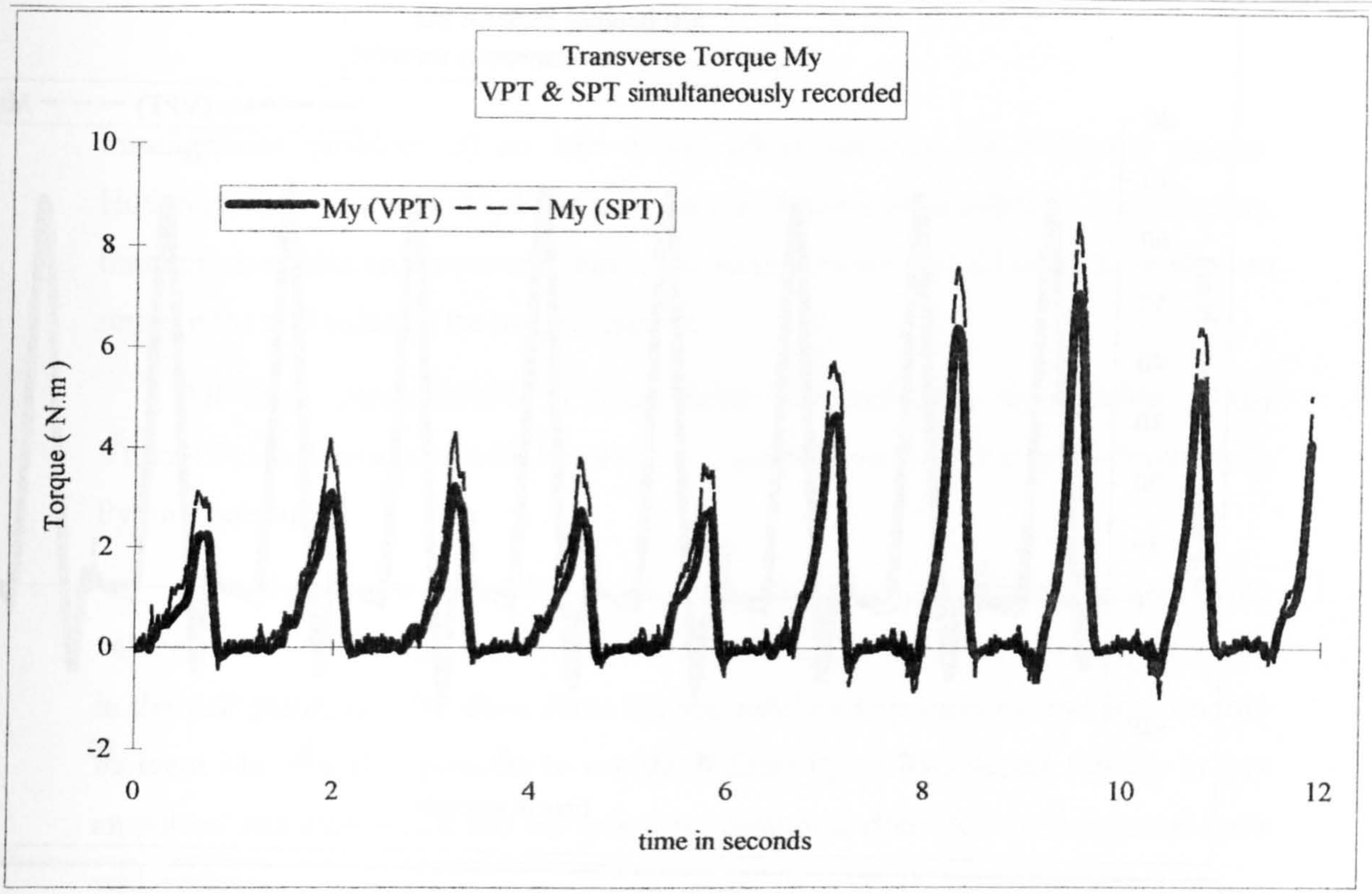

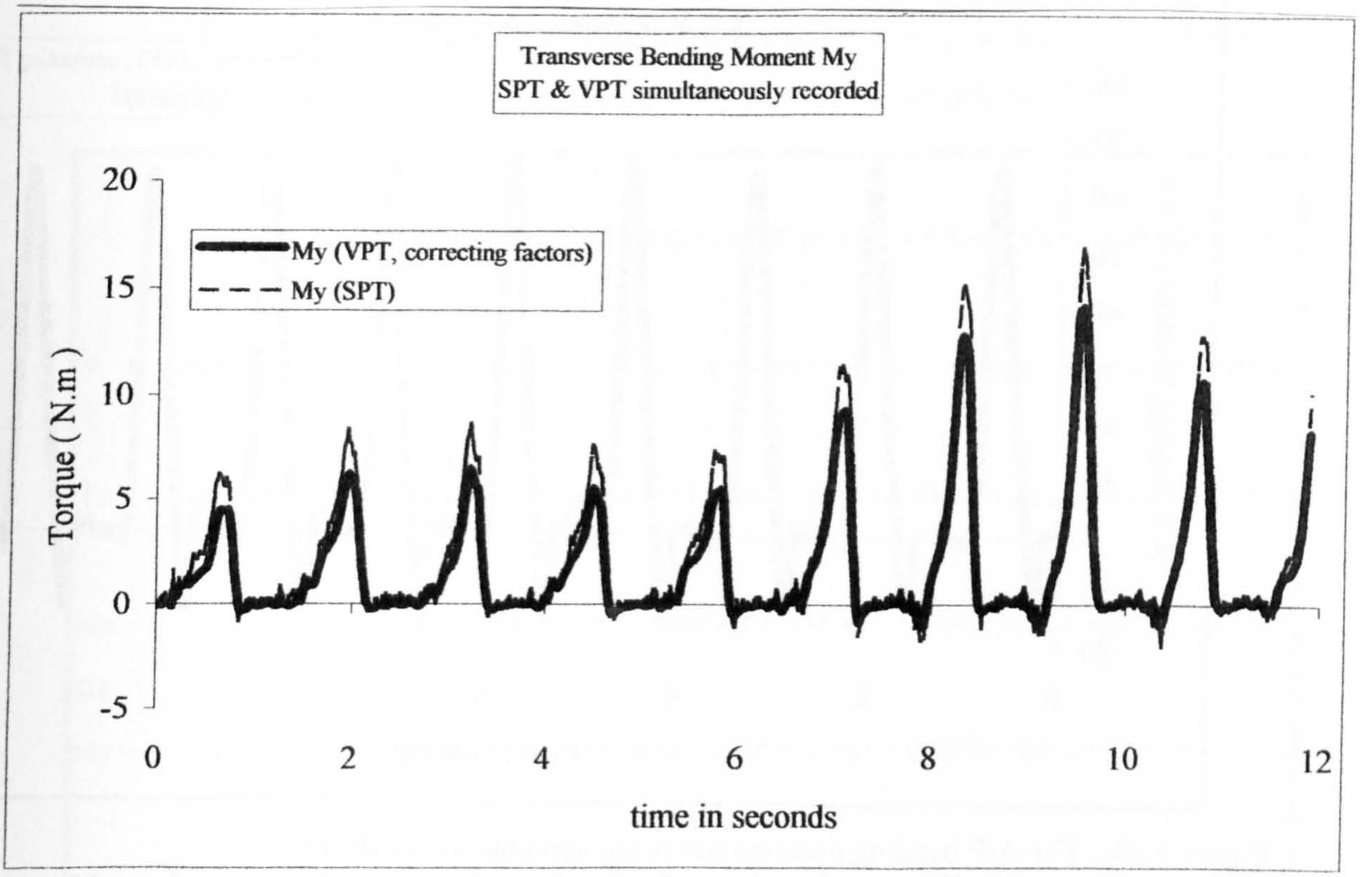

Figure 7.24b: The transverse bending moment My using simultaneously the two transducers: after applying the cross-sensitivity matrices only (see section 6.7 and table 11.VII.16) (top); after applying the cross-sensitivity matrices plus the factor established in section 7.8.1 (see equation 7.38) only on the VPT (bottom).

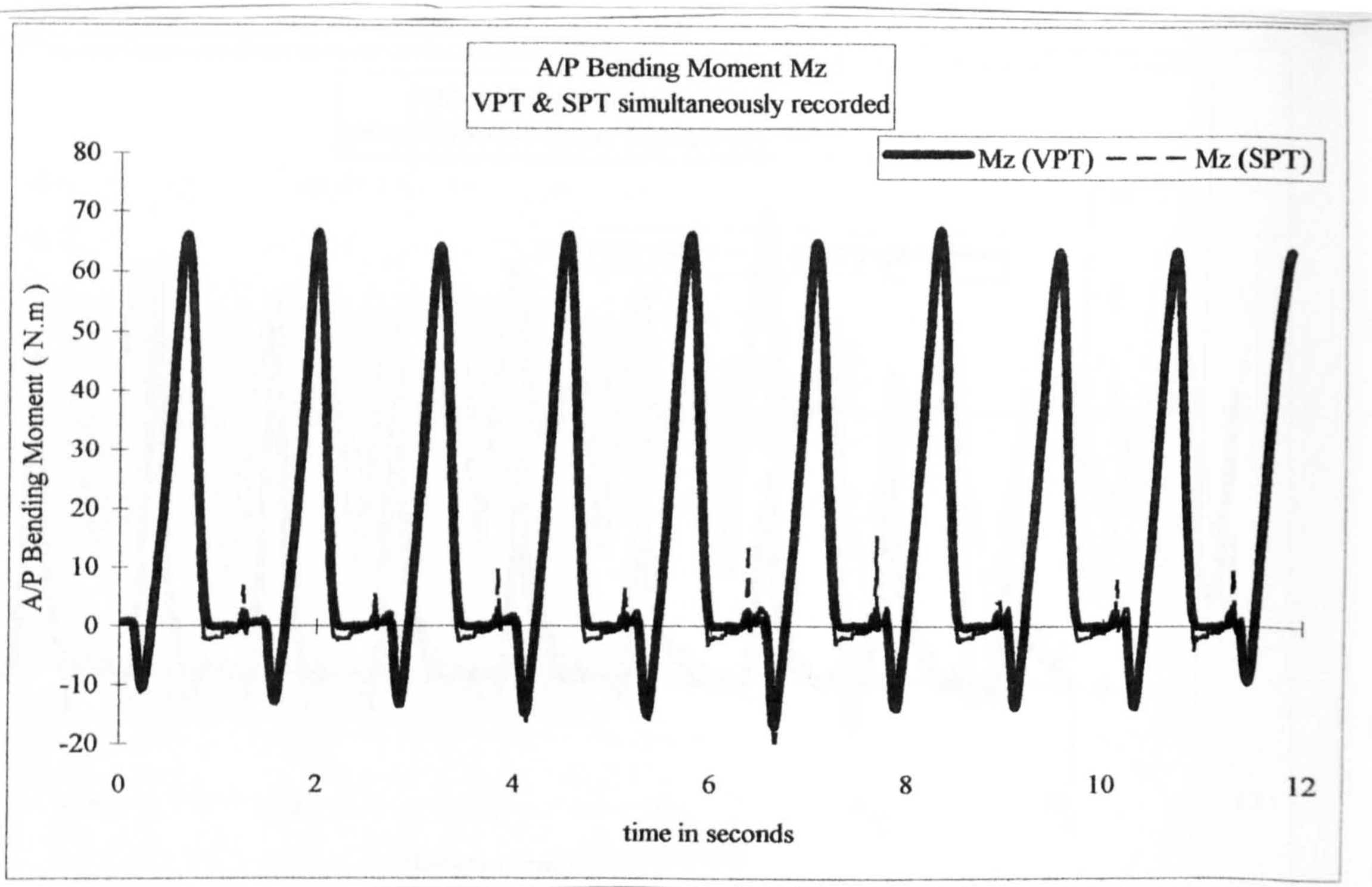

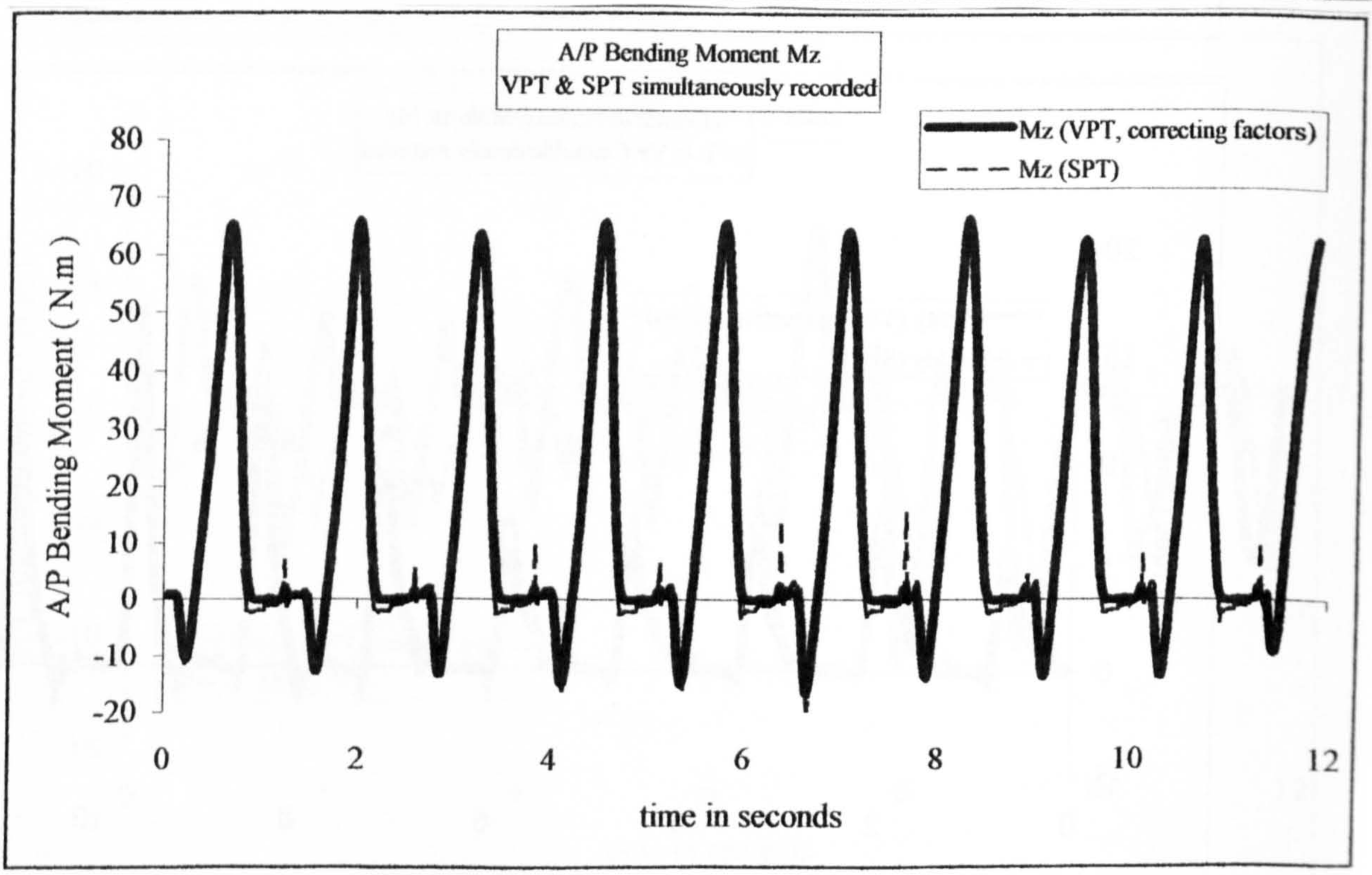

Figure 7.24c: The A/P bending moment Mz using simultaneously the two transducers: after applying the cross-sensitivity matrices only (see section 6.7 and table 11.VII.16) (top); after applying the cross-sensitivity matrices plus the factor established in section 7.8.1 (see equation 7.38) only on the VPT (bottom). Since the position in the leg of the two pylons was different, the moments were different.

misalignment problem, 3) an inter-action effect between the Poisson's gauges. However, more research should be necessary to discovery the solution. Nevertheless, these cross effects are linear and thus, a correcting factor of 1.03 must be applied to retrieve the real value of the torque channel.

All these tests exhibited a linear behaviour and good repeatability of the Villiers Pylon Transducer with however, a lower response relative to the Strathclyde Pylon Transducer.

Nevertheless, the new VPT is able to predict, with a sufficient accuracy, the values usually found and recorded in clinical gait assessment. This is particularly true in the A/P plane, i.e., the shear force Fx, the axial compression Fy and the bending moment Mz. It is thus possible to use the Villiers Pylon Transducer for day to day amputees' gait assessment and the following chapter 8 describes the conducted tests with patients.

The final form of the set of equations, extracted from equation 6.4 and shown in table 6.43 (see section 6.7), is consequently as follows (equations 7.38):

$$
\begin{aligned}
Fx = {} & (\mathbf{0.66431\ SFx} + 0.00582\ SFy + 0.02190\ SFz - 0.18748\ SMx - 0.00947\ SMy + 0.0061\ SMz)*1.07 \\
Fy = {} & (0.02712\ SFx + \mathbf{1.14981\ SFy} + 0.02841\ SFz - 0.24314\ SMx - 0.53958\ SMy + 0.21879\ SMz)*0.98 \\
Fz = {} & (-0.03023\ SFx - 0.0063\ SFy + \mathbf{0.30804\ SFz} - 0.00015\ SMx + 0.00456\ SMy - 0.54548\ SMz)*1.08 \\
Mx = {} & (0.0023\ SFx + 0.00003\ SFy - 0.00327\ SFz + \mathbf{0.02801\ SMx} - 0.0002\ SMy + 0.0577\ SMz)*1.07 \\
My = {} & (-0.0001\ SFx + 0.00003\ SFy + 0.0000\ SFz - 0.00006\ SMx + \mathbf{0.00731\ SMy} - 0.0004\ SMz)*1.03 \\
Mz = {} & (0.0069\ SFx - 0.00049\ SFy + 0.00021\ SFz - 0.00183\ SMx + 0.0004\ SMy + \mathbf{0.07811\ SMz})*0.99
\end{aligned}
\tag{7.38}
$$

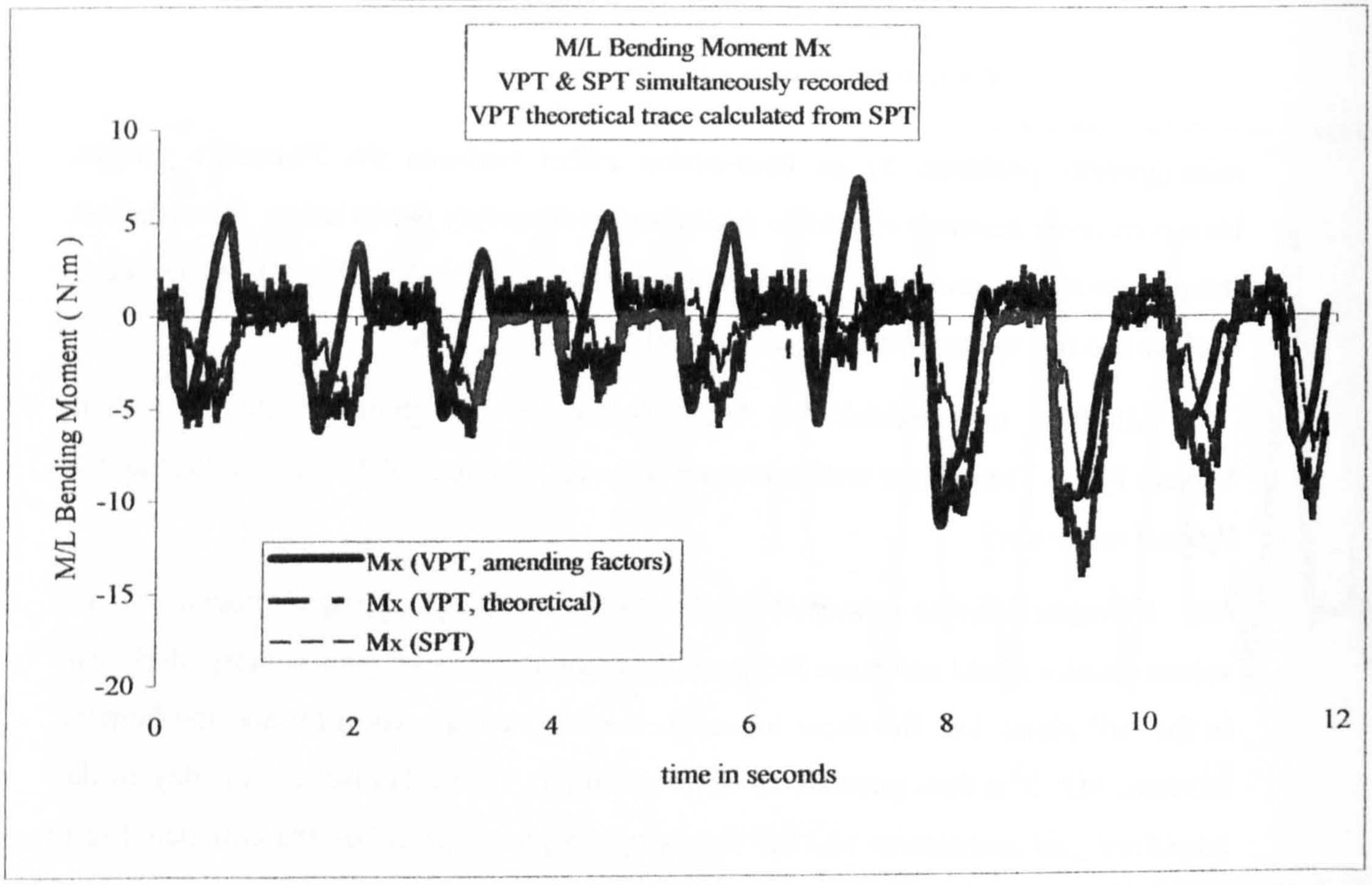

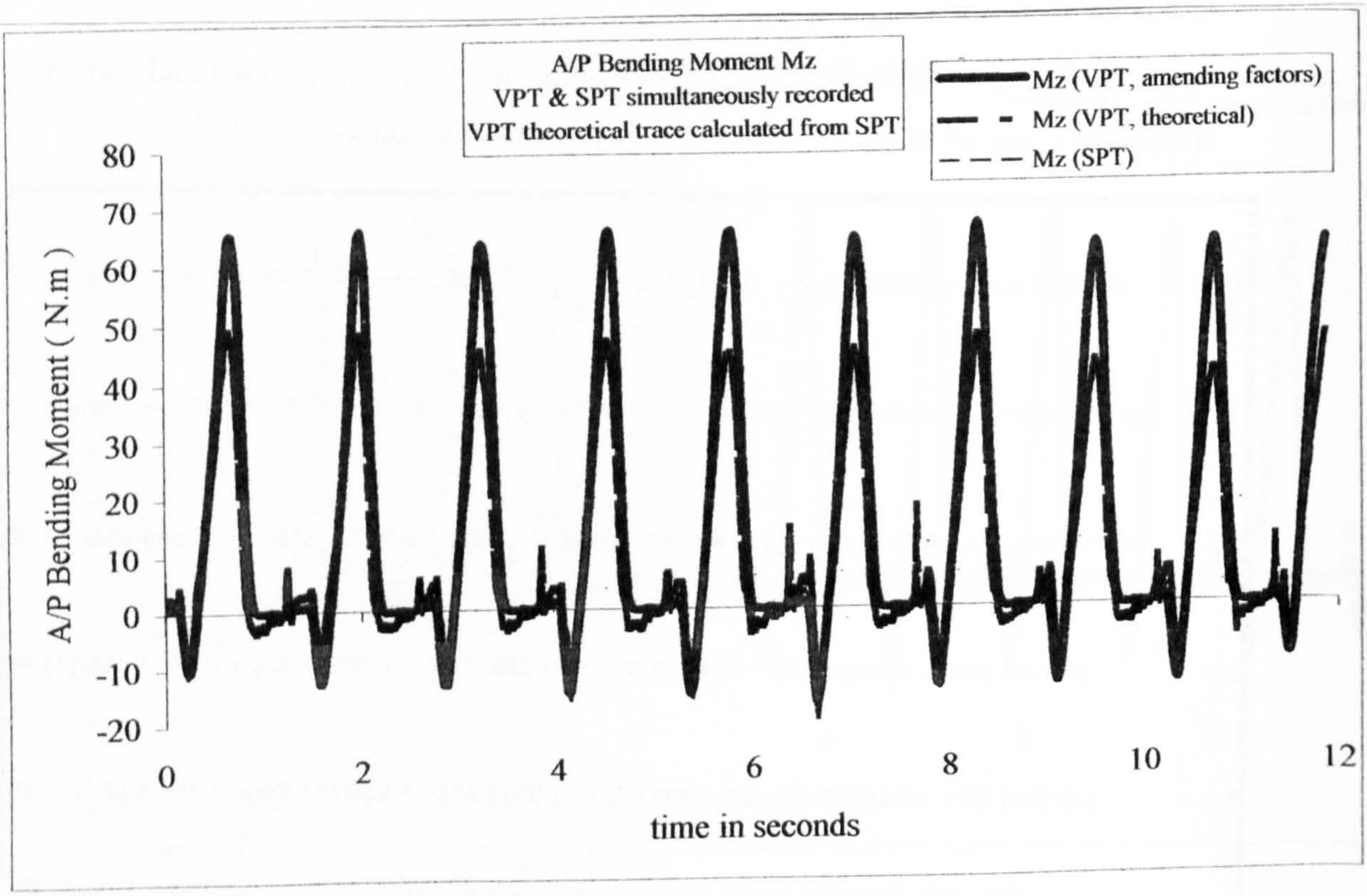

Figure 7.25: The M/L (Mx, top) and A/P (Mz, bottom) bending moments. The SPT traces are the same as those in figures 7.23 and 7.24. There are two VPT traces: 1) the same as those in figures 7.23 and 7.24; 2) theoretical traces calculated applying equations 7.35 and 7.36 to convert SPT values from the middle of the artificial tube to the ankle level. The VPT theoretical traces, calculated from SPT values, are completely superimposed with those recorded from the SPT.

Equations 7.38 were used in all the performed tests shown in chapter 8 to convert raw data expressed in volts into meaningful processed data expressed in N or N m. From both calibration and validation tests, the accuracy of such a transformation was found enough for the goals, aims and requirements established in chapter 1. The following chapter 8 shows the undertaken tests and performed results. A thorough discussion of the results is conducted.

Figure 8.1: A patient (TTR13) is wearing the transducer, the portable data acquisition system and the instrumented walking devices.

8 TESTS, RESULTS AND DISCUSSION

8.1 INTRODUCTION

Prior to showing and discussing the results from the tests performed, a description of the management and checklist of any conducted tests is necessary, together with data on treatment. As an example, one transtibial patient has been selected to illustrate the test and data treatment shown in the following sections. This unique patient will be followed all along the data processing. She was chosen because she perfectly portrayed the selected and studied series, as explained below in section 8.3. This patient, fitted with all the equipment, is shown in figure 8.1.

Prior to starting the test itself, a patient's checklist was required, the prosthetic technical aspect and data treatment of the test, and the research aims themselves, as shown in sections 8.2 and 8.3.

8.2 THE PROGRESS OF THE TESTS PERFORMED

The test subjects wearing their artificial limbs had to be selected with the following prosthetic respects in mind:

1. the patient might be able to walk soundly and safely with two sticks or two canes for a sufficient time and distance;

2. the prosthetic shank tube might have an internal diameter of 26 mm with an external of 30 mm;

This was common for transtibial patients whatever the sockets were but unusual for transfemoral patients fitted with a Plaster of Paris socket. In this case, a telescopic tube was fitted instead of a 26/30 tube. On the other hand, transfemoral amputees fitted with an acrylic resin socket were usually provided with a standardised 26/30 shank tube.

3. the artificial tube might be deep enough, i.e., it might have a base length of

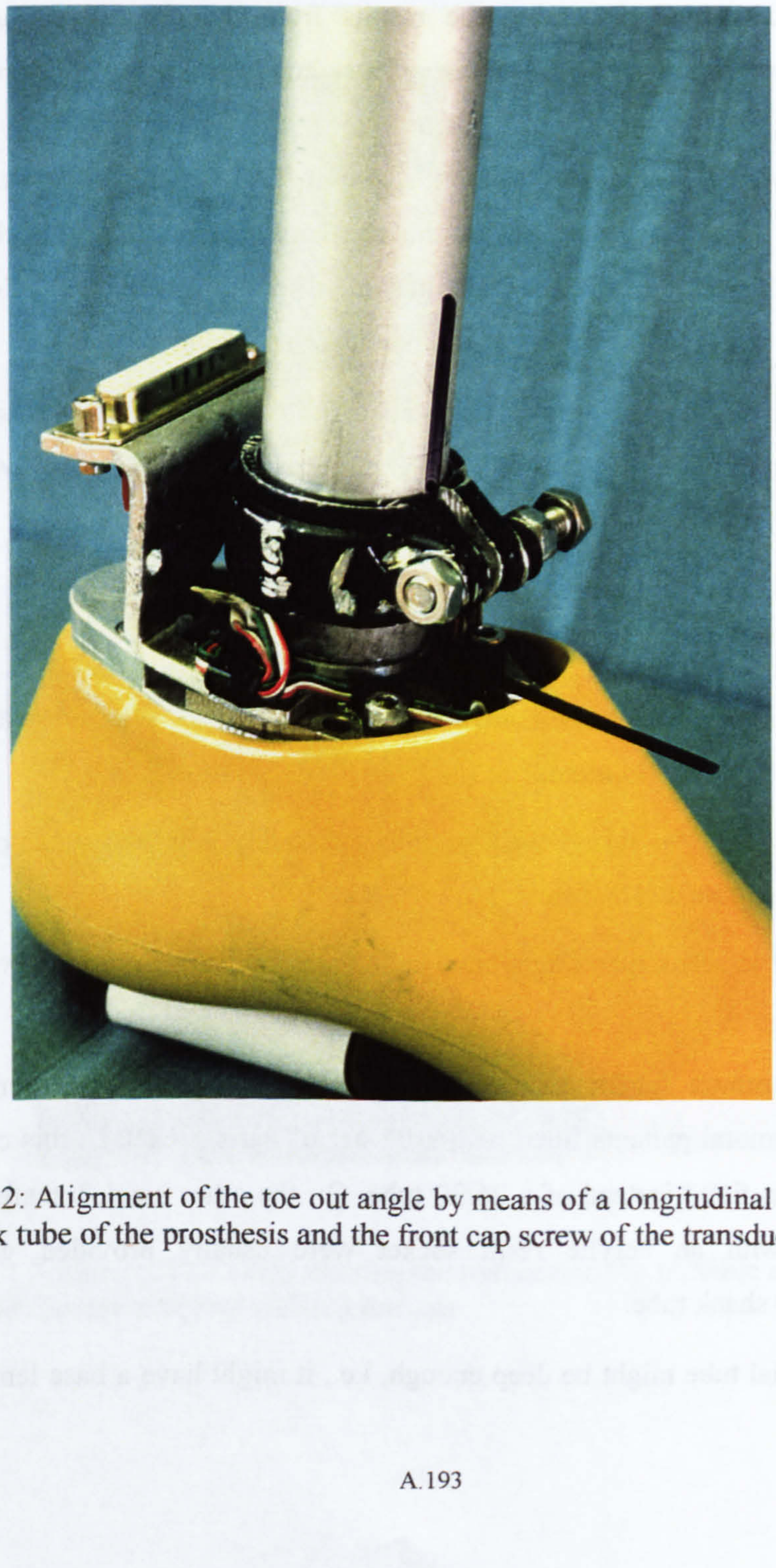

Figure 8.2: Alignment of the toe out angle by means of a longitudinal line drawn on the shank tube of the prosthesis and the front cap screw of the transducer.

70 mm minimum, or preferably 75 mm to ensure that no load could be applied on the top of the bell of the transducer (see section 4.8.2).

This prevented application to transtibial amputees with too long a residual limb. However, it was also possible to find the artificial shank tube partly full of acrylic resin or fibreglass and therefore unsuitable for fitting the pylon transducer within it.

4. the socket and the alignment of the prosthesis were assumed to be checked accurately by a skilful prosthetist;

5. The patients wore their usual shoes. The patient's footwear required a structure to avoiding any slipping on the equipment fitted. It was usually a simple tape around the usual patient's shoe and the top part of the artificial foot (not shown in figure 8.1). This "shoe - sloppiness - check" was only executed through the skill of the physiotherapist. There was no technical and accurate assessment of the tested subjects' shoes.

As previously mentioned (see sections 1.2 and 1.3), characteristics, such as age, time gap from amputation day, type of prosthesis worn or gait pattern of the patients were included in the studied series. Clinical aspect of the desired research is explained in the following section 8.3.

8.2.1 Patient's consent

Once, the subject was selected by the therapist, the assent of the patient was obtained. To have a valid contract between the therapist and the tested subject, it was necessary to explain thoroughly what was the aim of the study and how the tests were managed. Because, there was no foreseeable risk or invasive technique such as X-ray or injection, this agreement was oral. According to French laws, a formal consent form with double signatures from patient and witness was not mandatory.

The subject might be advised of the following considerations with a vocabulary adapted to elderly "basic" patients:

- the prosthetic foot will be removed from the artificial shank tube during the test. It will be subsequently brought to the exact position as it was previously;

Figure 8.3: The patient TTR13 had her socket laid down on a stool with the artificial foot free to allow the different offset adjustments.

• an other artificial ankle (i.e., the transducer), having a small extra mass of 0.24 kg will replace the prosthetic ankle;

• some wires will link the new fitted ankle with the recording device through a junction box fitted in the pocket of the subject;

• the recording box (≈1.5 kg) will be fitted onto a waist-belt and worn by the patient as shown in figure 8.1;

• the waist-belt could make the patient warmer with perspiration making him uncomfortable. This is particularly true in summer;

• the usual walking aids used by the patient will be replaced by other devices having the same configuration and exactly the same height and weight, these devices will be connected to the recording box by means of wires;

• all the equipment is not fragile and nothing serious could damage the equipment — the therapist who escorts the subject all along the test will take care of the equipment —;

• the test is made for research on how the patient is walking and it is not conducted to measure any extra performance, consequently the patient has to walk exactly as he usually does.

Therefore, it was important to be aware that the test did not impose any additional efforts or over-stresses to the patient, in relation to what he did usually in day-to-day gait training. Consequently, formal medical advice was not required. The extra mass of the transducer, relative to the removed artificial ankle joint, could not be considered enough to impose an extra load.

It was usual to inform the patient that his results, after data treatment, will be shown and explained to him. The range of these explanations depended on the intellectual level of the patient and the interest he found in such research. It was also necessary to convince the patient that the results were used with no reference to his name. It was similarly important to guarantee the patient that any refusal to participate or withdrawal from the study will in no way affect his present and / or future treatment at the Hospital of Villiers-Saint-Denis. In other words, no pressure

PATIENT INFORMATION **Date:**

Name		First Name
Amputation Level:	AK BK	Amputation Side
Stump Length	(mm)	Activity Level
Cause of Amputation		Date of Amputation
Body Mass	(kg)	Age
Body Height	(m)	Sex

PATIENT COMMENTS	Pain
Gait Pattern	Prosthesis

PROSTHESIS INFORMATION

Type of Prosthesis	Knee Unit (AK only)
Type of Socket	Information on shoes
Suspension Type	Prosthesis Mass (kg)

TRIAL INFORMATION **File Name:**

Trial N°	Terrain	M1
Equipment used		M2
Distance Walked (m)		M3
		M4

Comments

Trial N°	Terrain	M1
Equipment used		M2
Distance Walked (m)		M3
		M4

Comments

Trial N°	Terrain	M1
Equipment used		M2
Distance Walked (m)		M3
		M4

Comments

Table 8.1: The information chart carried out for each patient. The activity level of the patient was determined through the skilful and the patient's knowledge of the physiotherapist.

might be put on the patient to force him to give his agreement.

However, to avoid any risk of refusal, it was important to explain to the patient that the duration of his stay-in the Rehabilitation Centre did not depend of results expressed by his test. For example, several patients were afraid that if they had "bad" results, showing a "bad" gait pattern, they would have to stay-in longer than they expected before any discharge from the Rehabilitation Centre, to improve their gait.

The last important consideration needed was to inform the patient that the duration of the test should be 1.5 hour maximum. Thus, the patient might be free of any medical appointment or family visit during this time and a strong co-operation with medical and nurses staff was required, especially for diabetic patients.

8.2.2 Successive stages of a gait evaluation test

8.2.2.1 BEFORE STARTING

Once the subject was selected and his consent obtained, a procedure, having 8 steps, had to be followed:

1. The socket of transtibial amputees was usually doffed to make the patient more comfortable when the artificial foot was removed. The socket of a transfemoral patient was not doffed but the prosthetic shank tube was laid on a stool. However, these rules were not absolute and through an agreement with the patient, another arrangement could be found.

2. A careful and accurate location, by means of ballpoint lines, of the position of the artificial foot relative to the prosthetic shank tube was made in both coronal and horizontal planes. A transverse line was drawn following the top part of the artificial ankle to check the prosthesis height. A longitudinal line was plotted following a cast line on the Proteor® artificial ankle to check the toe-out angle. So that, the foot could be fitted at the exact position it was before, bringing back the prosthesis to its previous alignment.

3. The footwear was removed. The exact position of the artificial ankle bolt within the prosthetic foot was marked by means of a pen point to be sure that the tightening torque on the transducer's bolt will be as it was before dismantling. The artificial ankle could now be removed from the prosthetic foot and the transducer

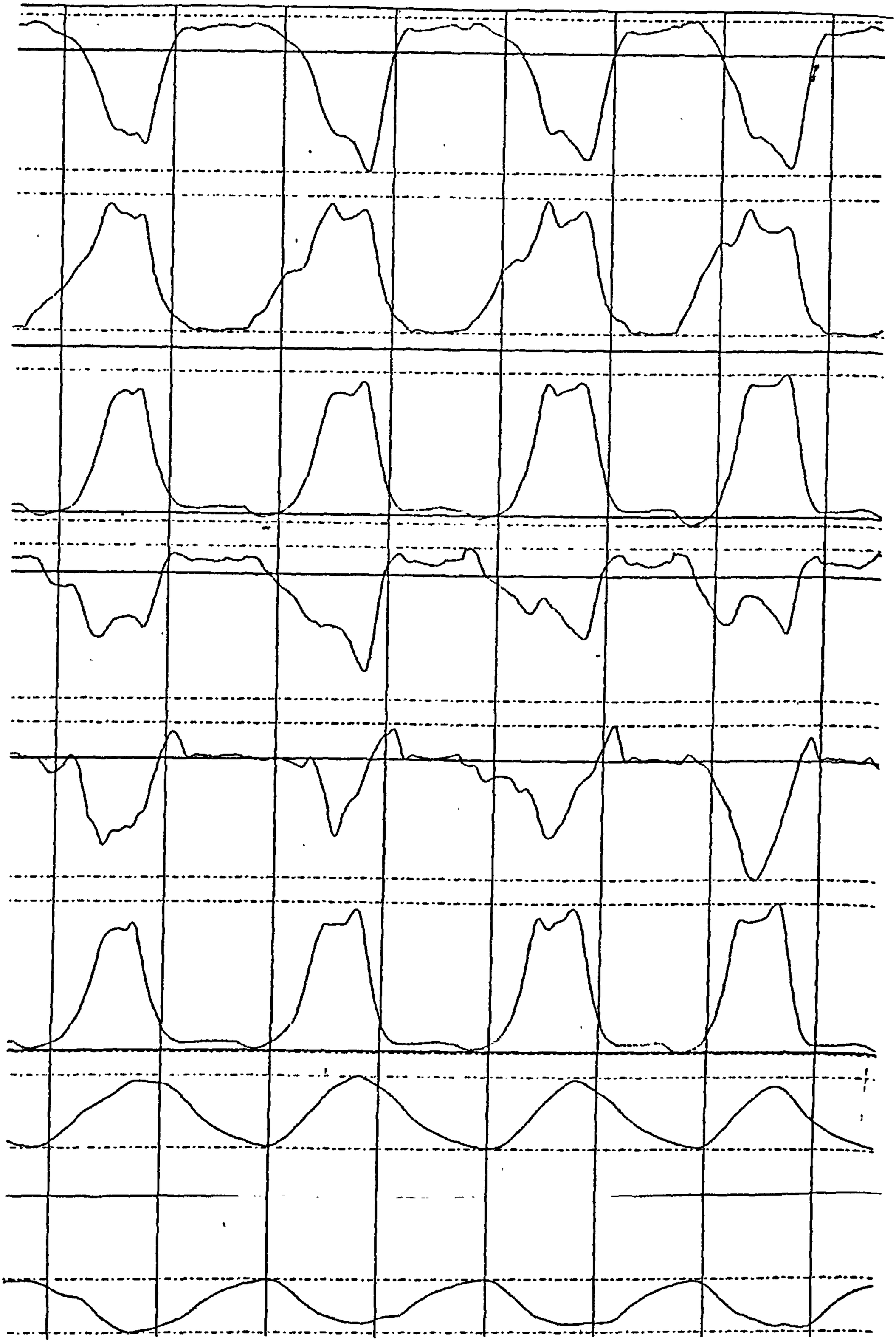

Figure 8.4: Raw data of the same transtibial patient (TTR13), from up to bottom, the 6 components of the gait (Fx, Fy, ..., Mz), the right and the left stick (see figure 5.6).

took its place. Then, the transducer's bolt was tightened at the same tightening torque, which was assessed by means of the traced line. It was important to do this job properly to fasten both artificial foot and ankle with the same force, applying the same stress on the plastic front ring and the rear rubber bumper (see description in appendix 11.II.4.2 and figure II.25). Then, the footwear was put on again.

4. The next task was to fit the special shank clamp described in section 4.8.2.4 and figure 4.26 on the prosthetic shank tube. The location of the clamp might be always the same: 2 centimetres from the bottom end of the prosthetic shank tube having the slit of the clamp aligned with the longitudinal line traced when the task 2 was undertaken. The bell and the transducer were now fitted inside the structure of the prosthesis until the bottom flange of the bell was in contact with the prosthetic shank tube. The toe-out angle of the artificial foot had to be carefully checked as follows: the longitudinal pen line marked on the prosthetic shank tube (task 2) might be laid out in line with the front cap screw of the bottom flange of the transducer (see figure 4.1), as shown in figure 8.2.

Here also, the tightening torque of the shank clamp was important: the two edges of the slit might be closed so that they contacted without any stress. This was accomplished having two targets:

a) to avoid any risk of artificial foot rotation caused by the transverse torque My about the Y axis, although the value of this moment was small (see section 4.8.2 and results in section 8.5, 8.7 and 8.8);

c) to have, throughout all the tests performed, an equivalent compression force (not recorded and never controlled) onto the bell of the transducer through the artificial shank tube.

The socket could then be donned.

5. The Myodata recording box with the power supply battery was now fitted onto the trunk of the subject by means of a waist-belt. The belt might not be over - tightened, avoiding any breathing discomfort to the patient. Two shoulder belts, crossed in the patient's back, were fitted to avoid any slipping of the equipment. The recording box had to be situated high enough from the subject's abdomen to ward off

Name **Test N°**

First Name

Trial N° **Date**

Amputation Level & Side Socket

Sticks Canes

Ground Source File

Gait Rate (s.stride^{-1}):

Beginning Time
Finishing Time Duration

Offset Factors	Row Number
Fx	My
Fy	Mz
Fz	CaRi
Mx	CaLe

BW + Prosthesis: (kg)

File Name .XLS	Directory C:/	Folder	page to print
Processed Data			
Processed Data in % of BW			
Processed Data in % of N or N.m			

Comments:

Table 8.2: The test information chart performed at each test for all patients.

any risk of pulling out the wires from the recording box when the patient was sitting, through an excessive fold of the wires and four pin Binder plugs.

6. The 25-way plug on the cable from the signal-conditioning unit was plugged into the socket of the transducer. Then, the six cables, corresponding to each channel of the transducer, were assembled in correct order (respectively from Fx to Mz, channel 1 to 6) onto the Myodata box. A slit on both plug and socket avoided any positive - negative error impossible (see description of the portable data acquisition system in section 5.3.2).

7. The height of the instrumented walking aids was now adjusted by comparison with those used by the patient. They were connected to the recorder: right stick (for the right side of the patient) in channel 7 and left stick in channel 8. The two sticks were labelled to avoid any confusion. The power supply battery cable was now connected to the recorder (see description in section 5.4).

8. The PCMCIA memory card was then plugged onto the recorder, which had to be linked (through a 25/9 serial cable) to the computer. Therewith, the recorder and the sticks were switched on, the patient having the prosthetic socket (for a transtibial patient) or the artificial shank tube (for a transfemoral amputee) sat on a stool, as shown in figure 8.3, to adjust the channel offsets.

The patient was now ready for the test. Before starting, the operator required to:

a) check the six transducer channels' offsets;

b) program the recorder.

Once the program CONFMYO.BAT was running, it was necessary to adjust the bridge balance of each channel. The traces of each channel, one by one, were viewed on the computer screen, which was used as an oscilloscope. The trace of any particular channel might overlap the zero line. However, an important comment has to be made: as previously stated (see chapter 1): the equipment was developed to be used in day-to-day physiotherapy practice. In other words, waiting and wasting time was difficult. It was not, therefore, usual to delay until a stabilised temperature was developed between gauges and mounting surface. The consequence was that the

Time	SFx	SFy	SFz	SMx	SMy	SMz	SCaRi
00.0	5.57E-02	4.54E-02	7.18E-02	1.61E-02	5.86E-03	3.37E-02	6.83E-01
00.0	5.57E-02	4.40E-02	7.32E-02	1.61E-02	4.40E-03	3.52E-02	6.75E-01
00.0	5.71E-02	4.40E-02	7.62E-02	1.61E-02	4.40E-03	3.52E-02	6.69E-01
00.0	5.86E-02	4.40E-02	7.76E-02	1.61E-02	4.40E-03	3.66E-02	6.64E-01
00.1	5.86E-02	4.40E-02	7.91E-02	1.47E-02	2.93E-03	3.66E-02	6.58E-01
00.1	5.86E-02	4.40E-02	7.91E-02	1.61E-02	1.47E-03	3.81E-02	6.52E-01
00.1	6.01E-02	4.40E-02	7.76E-02	1.61E-02	0.00E+00	3.81E-02	6.48E-01
00.1	6.01E-02	4.40E-02	7.62E-02	1.76E-02	0.00E+00	3.81E-02	6.42E-01
00.1	6.01E-02	4.54E-02	7.47E-02	1.90E-02	0.00E+00	3.81E-02	6.37E-01
00.1	6.01E-02	4.69E-02	7.32E-02	1.90E-02	1.47E-03	3.81E-02	6.33E-01
00.2	6.01E-02	4.69E-02	7.18E-02	2.05E-02	2.93E-03	3.66E-02	6.28E-01
00.2	5.86E-02	4.83E-02	6.89E-02	2.05E-02	4.40E-03	3.81E-02	6.23E-01
00.2	5.71E-02	4.83E-02	6.74E-02	2.05E-02	7.32E-03	3.66E-02	6.20E-01
00.2	5.57E-02	4.98E-02	6.74E-02	2.05E-02	8.79E-03	3.52E-02	6.15E-01
00.2	5.57E-02	4.98E-02	6.45E-02	2.05E-02	1.03E-02	3.52E-02	6.11E-01
00.2	5.57E-02	4.98E-02	6.45E-02	2.05E-02	1.17E-02	3.37E-02	6.08E-01
00.3	5.57E-02	4.98E-02	6.45E-02	2.05E-02	1.17E-02	3.52E-02	6.05E-01
00.3	5.57E-02	4.98E-02	6.45E-02	2.05E-02	1.17E-02	3.52E-02	6.02E-01
00.3	5.57E-02	4.98E-02	6.45E-02	2.05E-02	1.17E-02	3.52E-02	5.98E-01
00.3	5.86E-02	5.27E-02	5.71E-02	2.34E-02	5.86E-03	3.37E-02	5.95E-01
00.3	6.01E-02	6.01E-02	3.81E-02	2.20E-02	1.47E-03	2.64E-02	5.92E-01
00.3	6.15E-02	7.03E-02	2.34E-02	2.20E-02	1.47E-03	2.20E-02	5.89E-01
00.3	6.30E-02	7.76E-02	8.79E-03	2.20E-02	2.93E-03	1.76E-02	5.86E-01
00.4	6.30E-02	8.35E-02	-4.40E-03	2.34E-02	2.93E-03	1.47E-02	5.83E-01

Table 8.3: An example of the raw data in volts of the same patient (TTR13).
For size reason, the SCaLe row, corresponding to the left walking aid, is not shown.

offsets of each channel had to be checked and corrected again later, between trials, when data were processed (see the following section 8.2.3). The offset of the two instrumented assistive walking devices could not be adjusted.

When this offset checking was performed, the subject always sat in the position shown in figure 8.3. Therefore, there were no forces or bending moments, except a small (but never quantified) positive shear force Fx with a negative bending moment Mz, due to the weight of the prosthetic foot added with the transducer and the footwear. These two quantities were considered as inconsequential relative to the average values of 1) the expected shear force Fx and bending moment Mz, 2) the accuracy, 3) the reliability of both requirements and aims.

Once this was done, the recorder had to be programmed. The programme asked the operator to give the name of the subject and the size of the memory card. Other information, such as date, number and name of each channel were provided automatically. When this was achieved, a white start button was pushed and a green light flashed on the recorder indicating that the recording was starting.

8.2.2.2 DURING THE TEST

A standard test was regularly divided into three (it could be four) trials according to the needs of the therapist, the capability of the patient and his level of amputation.

→ Trial 1: The operator asked the patient to stand up, putting the signal-conditioning unit in the patient's pocket. At that time, the patient started to walk freely, having his usual behaviour such as gait rate, positioning of feet, upper limbs and sticks, to be familiarised with the equipment. This first "limbering-up" trial was generally carried out in the physiotherapy room, on a vinyl flat floor (see the ground in figure 8.1). After this stage, the patient sat down to rest and during it, the information shown in table 8.1 was collected. The duration of such a rest was variable, depending of the patient's general status, through the understanding the physiotherapist had concerning his patient.

→ Trial 2: The second trial depended on what the patient could do and what the physiotherapist was expected such as: ambulation with two sticks then two canes,

Number of the columns	Contents of the columns
1	time code
2 to 9	SFx, ..., SCaLe
10	empty to make the file more readable
11	repeating time code
12 to 17	Fx, ..., Mz applying the whole set of six equations (equations 7.38, see section 7.9)
18 to 19	CaRi and CaLe applying the whole set of two equations 5.8 and 5.9 (see section 5.4.4)
20	empty
21 and 22	for each channel: maximum; minimum and median
23	empty
from 24	6 graphs, in N or N.m versus time in seconds, from top to bottom: Fx — A/P shear force Fy + two walking assistive devices — Axial loads Fz — M/L shear force Mx — M/L bending moment My — Transverse torque Mz — A/P bending moment

Table 8.4: The description of the template file named CALIMAT2.XLT (24 columns x 1000 rows = 15.6 seconds). The first page of such a template file is shown in figure VIII.1 (see appendix 11.VIII.2).

walking outside the physiotherapy room, and / or ramp ascent or descent. At the beginning of each new phase during the trial, an electronic label was added to the recorded file. They had a form such as M_1, M_2, M_3, ... when the stored file was processed on the computer screen. At the end of this trial, the patient had a new rest period on his wheel chair. To avoid any confusion, lack of information or forgetting, the operator had to note the gait events, which corresponded to the electronic labels M_1, M_2, M_3 and M_4 on the information chart shown in table 8.1.

→ Trial 3: A third trial was usually conducted to achieve and check the second one. The order of the tasks was inverted to minimise and control the subject's fatigue. If required a fourth, or even a fifth trial could be undertaken.

When the test was considered as finished, the recorded data were transferred into the computer (see section 5.3.2.3). Before any modification and dismantling of the prosthesis set up, a check of the raw data was performed to verify the validity of the test. The Myodata software MYOPRO.EXE was loaded on the computer and the eight raw traces of the conducted trials were displayed on the screen, as shown in figure 8.4.

If the performed checks were conclusive, i.e., no channels were missing, no noise, no artefacts. The prosthesis was doffed and:

• the prosthesis mass was measured by means of a subtraction of the weight of the therapist with and without the prosthesis through an accurate clinical weight – scale. This way of doing was chosen because a minimum mass of 10 kg was necessary to assume the mean accuracy given by the manufacturer (± 0.1 k);

• the stump length was measured as follows:

1. from the Anterior Tibial Tuberosity to the distal end of the Tibial bony shaft for a transtibial amputee;

2. from the top of the Greater Trochanter to the distal end of the residual Femur bone, with an accuracy of ± 5 mm for a transfemoral amputee, as stated by Boonstra *et al.*, (1994).

Table 8.5: The first rows of processed data file of the patient (TTR13). The frame is open at the bottom to show that the file is continuing (Units are N or N.m, MEDIANE, in French is MEDIAN in English).

time	Fx	Fy	Fz	Mx	My	Mz	Cane Right	Cane Left			
0.02	1.26	-1.0	-2.18	-0.53	-0.03	-0.15	125.5	130.8		MAX Fx	67.75
0.03	1.17	-3.8	-3.70	0.47	0.05	-0.04	120.2	126.1		MIN	-87.11
0.05	0.82	-4.2	-3.03	1.47	0.14	-0.15	114.5	120.9		MEDIANE	2.25
0.06	0.47	-6.2	-3.46	2.47	0.18	-0.16	108.8	115.1			
0.08	0.47	-5.4	-3.46	3.47	0.20	-0.16	103.8	109.8		MAX Fy	404.63
0.09	0.79	-5.8	-3.01	4.47	0.18	-0.15	98.8	104.6		MIN	-16.98
0.11	0.52	-6.3	-3.02	5.47	0.14	-0.16	94.2	99.8		MEDIANE	135.87
0.13	1.14	-4.8	-2.58	6.47	0.12	-0.15	89.4	94.6			
0.14	1.18	-4.0	-2.14	7.47	0.10	-0.15	85.0	90.4		MAX Fz	13.94
0.16	1.21	-3.9	-1.70	8.47	0.10	-0.15	81.2	85.6		MIN	-33.25
0.17	1.20	-5.6	-1.68	9.47	0.10	-0.15	76.6	81.4		MEDIANE	-4.56
0.19	1.22	-5.6	-1.24	10.47	0.10	-0.15	73.0	77.8			
0.20	1.22	-5.6	-1.24	11.47	0.10	-0.15	69.0	73.6		MAX Mx	997.47
0.22	2.56	-5.2	-1.30	12.47	0.10	-0.14	65.6	69.9		MIN	-0.53
0.23	2.28	-5.2	-1.96	13.47	0.10	-0.03	62.3	66.2		MEDIANE	498.47
0.25	2.58	-4.8	-1.96	14.47	0.10	-0.02	59.0	63.1			
0.27	2.31	-5.2	-1.52	15.47	0.10	-0.03	55.9	59.9		MAX My	1.10
0.28	3.35	-5.1	-1.58	16.47	0.10	-0.02	52.9	56.8		MIN	-2.45
0.30	3.33	-4.1	-3.13	17.47	0.07	0.10	50.2	54.1		MEDIANE	-0.12
0.31	3.35	-4.0	-2.69	18.47	0.07	0.10	47.2	51.0			
0.33	3.34	-4.4	-2.03	19.47	0.07	-0.02	44.9	48.3		MAX Mz	25.51
0.34	3.34	-4.4	-2.03	20.47	0.07	-0.02	42.2	45.7		MIN	-8.14
0.36	4.38	-2.4	-3.20	21.47	0.07	0.11	39.5	43.1		MEDIANE	-0.03
0.38	3.35	-4.0	-2.69	22.47	0.07	0.10	37.5	40.5			

8.2.3 Data treatment

The recorded file, having the name *.IMG had always the size of the memory card used, i.e., it usually was 4 Mb, whatever the duration of the test (see section 5.3.2.3). Therefore, some part of the file might be chosen for data treatment. An example of such a file is shown in figure 8.4. It represents the transtibial patient, shown in figure 8.1 and 8.3, walking with two sticks. From top to bottom, there are the 6 channels (Fx, Fy, Fz, Mx, My, Mz) then the right and left sticks. Therefore, the first step in such a data treatment was to recognise, within the recorded file, the different trials performed by the patient during the test, following the patient information chart (see table 8.1) filled in during the test.

Each trial had a mean duration of about 50 s. Considering the chosen sampling rate (64 Hz, see section 5.3.2), that gave 3200 rows which was a large file slow to run in a spreadsheet such as Excel® 4 and overall, not necessary for the requirements of the project. Some parts of the data had thus to be selected partially randomly: the operator moved two cursors on the screen to select a period of around 20 seconds, equivalent to 1280 rows. Random selection: because of the computer screen size used (14 inches) and the quantity of information shown on the screen, it was not useful for the operator to choose a particular sequence. Partial random selection: the first steps of each trial and those close to an about-turn were eliminated. The beginning and finishing times plus the duration of the selected sequence were noted on a test-information chart shown in table 8.2.

To evaluate the gait rate, the first cursor was placed at heel strike of one stride while the second was located at the same gait event ten or eleven strides further using axial load Fy trace. The programme provided automatically the time interval between the two cursors.

The next step was important because it had not been possible to automate it. The *.IMG files ran by MYOPRO.EXE have a special numerical framework, i.e., they cannot be read by any spreadsheet such as Excel®. They must be transformed in a conventional ASCII text configuration, having *.TXT as DOS extension. This had to be done channel by channel, one by one. The option export data was selected on the screen and the operator selected, manually, the channel, which had to be

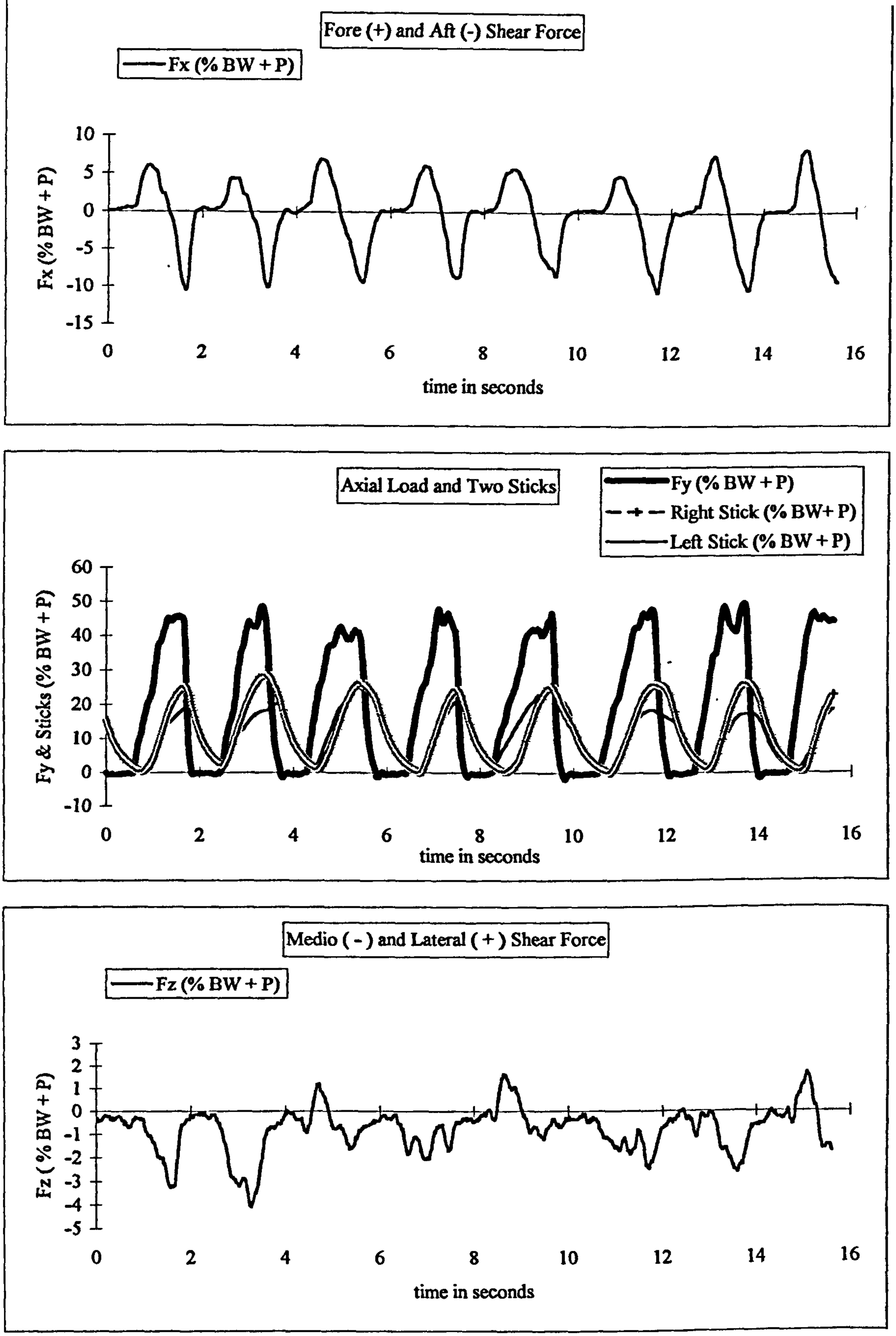

Figure 8.5: The three forces Fx (top), Fy with the two sticks (middle) and Fz (bottom), in % of BW, from a test of the patient TTR13 walking on a vinyl flat floor.

exported. To specify the end of each column, a tabulation mark was needed and the programme asked the operator to name the exported files. Because the Myodata programme did not provide any check procedure: if the operator mixed a channel and a file name, i.e., and as example, if the channel Fx was exported having FY.TXT as name, there was no alarm. All these exported files had the following imperative names, which were needed to achieve the macro commands described in the next section:

Channel 1	FX.TXT	Channel 4	MX.TXT	Channel 7	CARI.TXT
Channel 2	FY.TXT	Channel 5	MY.TXT	Channel 8	CALE.TXT
Channel 3	FZ.TXT	Channel 6	MZ.TXT		

CARI.TXT and CALE.TXT stood for respectively, the right and left sticks or canes.

8.2.3.1 DATA TREATMENT USING A SPREADSHEET

Raw data contents of the ASCII (*.TXT) files, exported by the Myodata programme, have the following model: unit is volt and for a sub-division such as millivolts, it is E-03 as shown in table 8.3. It shows the first seconds of a trial recorded from the same transtibial patient already shown in figures 8.1 to 8.4 (TTR13). These eight files (FX.TXT, FY.TXT, ..., CARI.TXT, CALE.TXT), having an average of 1280 rows, might be:

- converted into millivolts;
- mixed with a time code in 64th of second;
- calculated through the calibration matrix [C] determined in section 6.7;
- corrected applying the factors established in section 7.8.1;
- normalised in percentage of patient's body - weight (% of BW, for shear forces and axial load) or a fraction per unit mass ($N.kg^{-1}$ or $N\ m.kg^{-1}$, for bending moments);
- plotted into an appropriate form.

All of these tasks were fulfilled by two special macro-sheets using Microsoft Excel®, version 4.0. The first macro-sheet is named MYOGAIT2.XLM, having 575

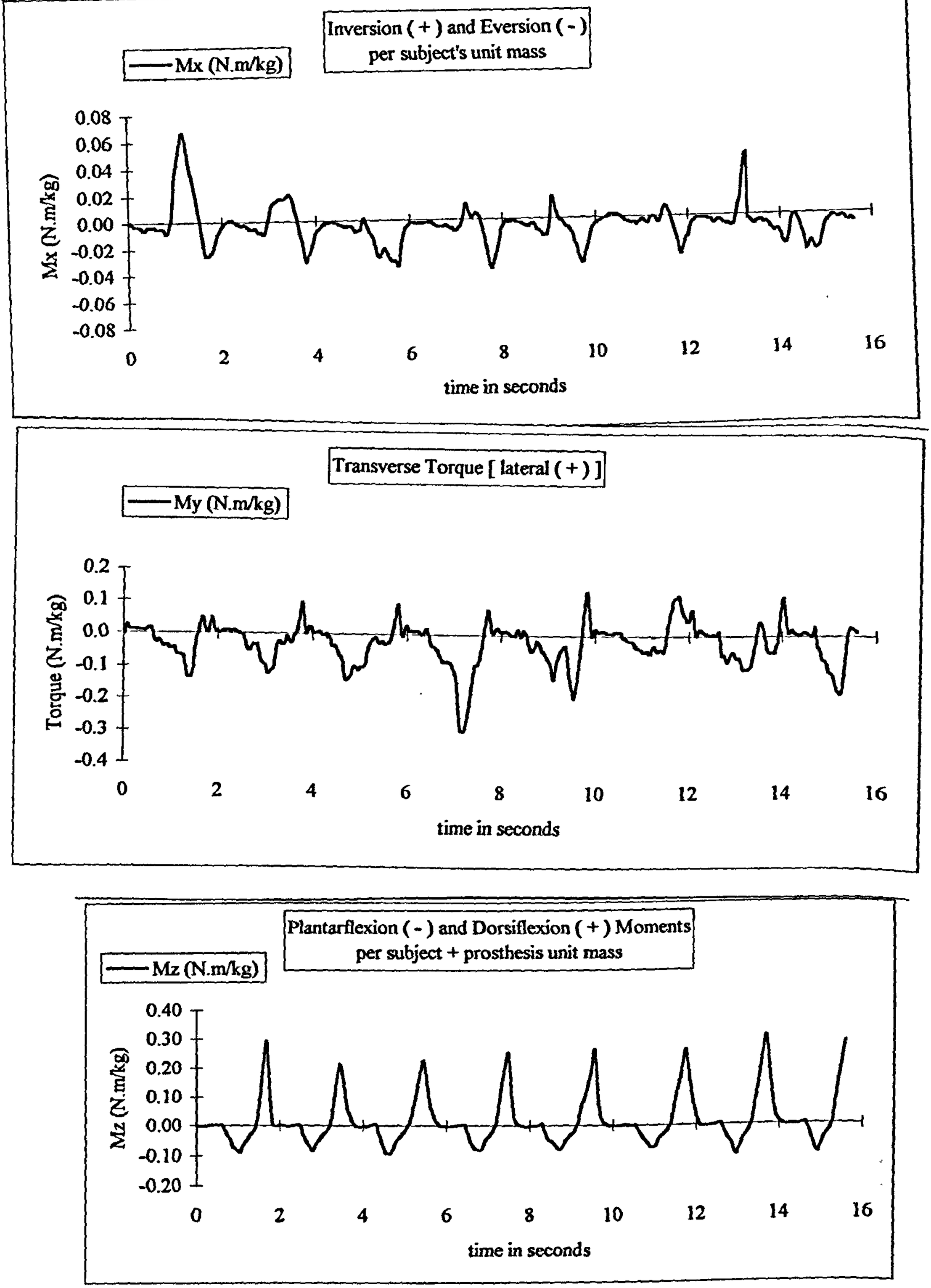

Figure 8.6: The M/L bending moment Mx (top), the torque My (middle) and the A/P bending moment Mz (bottom), in N.m/kg, from a test of the patient TTR13 walking on a vinyl flat floor.

rows, one for each instruction, when two assistive walking devices were used. It is shown in appendix 11.VIII.1. An equivalent macro-sheet named MYOGAIT1.XLM was utilised when only one walking aid was used. These two macro-sheets automated the different tasks, as follows:

The eight ASCII files (*.TXT) were successively opened, copied and pasted on an Excel® sheet under the form of eight side by side columns. They were converted in millivolts, with two decimal digits under the form of eight new columns, having as headings the following denomination: SFx, SFy, SFz, SMx, SMy, SMz, SCaRi, SCaLe. The prefix S stood for signal. These eight signal channels were then exported in a new spreadsheet file. A time code column, in tenth of second with two decimal digits, was added following the selected sampling rate (64 Hz, see section 5.3.2.3).

A graph, in millivolts versus time code of the eight raw data columns, was displayed to check the validity of the trial and if no channels were mixed when the export data task was undertaken (see section 8.2.3).

The last task performed by the macro-sheet was to open an Excel® file named CALIMAT2.XLT. The last letter of the extension « T » indicates that it was a template file used as a model. It was conceived conclusively having the arrangement shown in table 8.4.

As example, the first page (column 1 to 22) of the template file CALIMAT2.XLT is shown in appendix 11.VIII.2. The macro-sheet MYOGAIT2.XLM copied and pasted the eight raw data columns, having millivolts as unit, in the columns 2 to 9. These columns had an undetermined number of rows (commonly 1280 rows) whereas the columns 12 to 17 have been arbitrarily limited to 1000 rows, i.e., $\frac{1000}{64\ \text{Hz}} = 15.62$ s to limit the size of the file which although was 1.34 Mbytes. Following the gait rate usually recorded, this duration represented a mean number of 6 to 10 strides (see section 8.5.1 to 8.8.1 for results). However, it was always possible to extend the number of rows, the only limitation was provided by the spreadsheet programme (maximum of 6000 rows, duration = 93.75 s). It was also evident that such a file was very large (more than 6 Mbytes) and slow to run with a PC 486 DX 400 having only 8 Mb as RAM. Moreover, the discussion about the

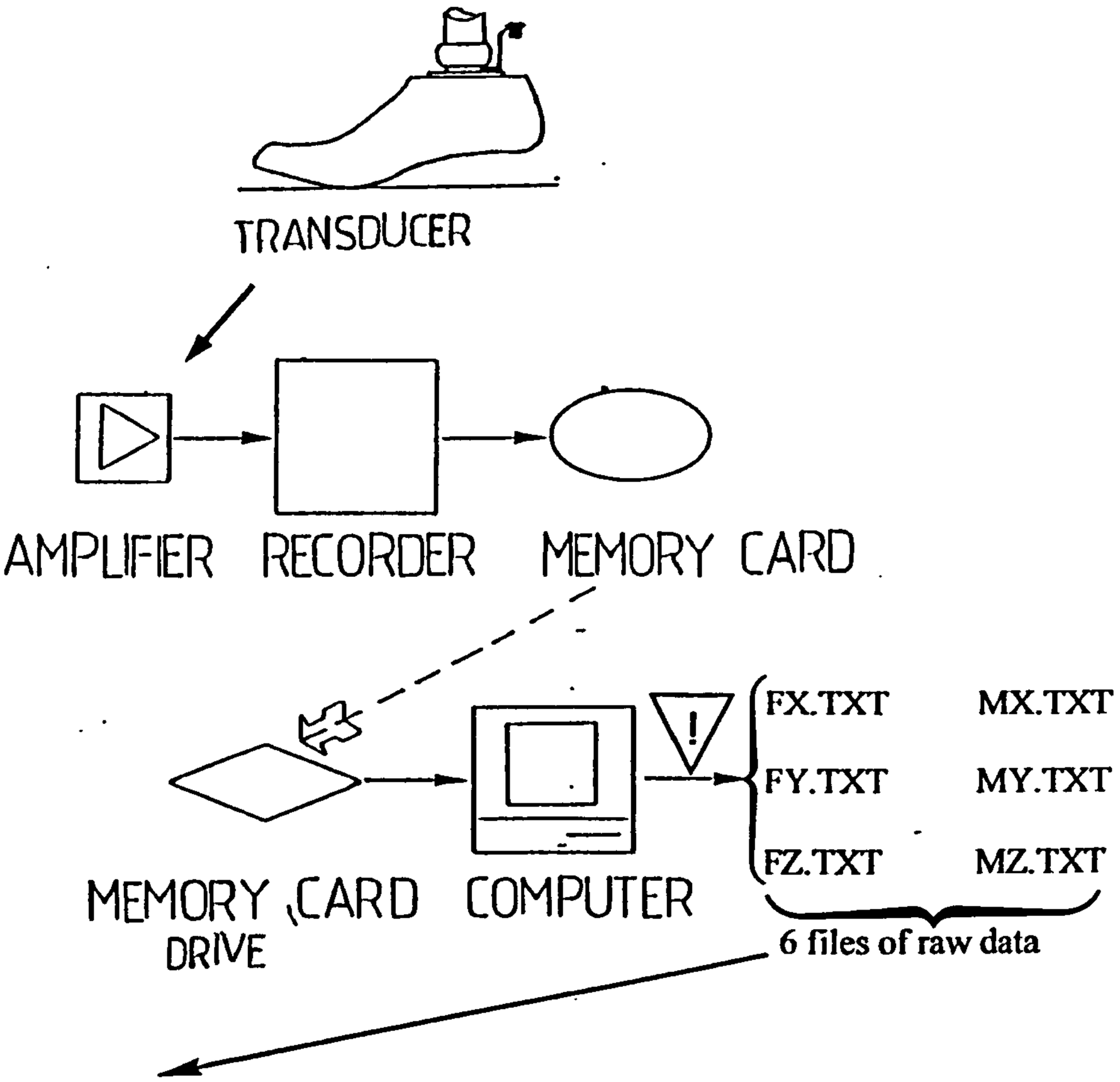

MYOGAIT2.XLM (Macro Sheet in Excel®)

applying

CALIMAT2.XLT (Template File in Excel®)

Processed Data in N or N.m showing 6 graphs

BODPERC2.XLM (Macro Sheet in Excel®)

applying

BODMASS.XLT and PERWEIG.XLT (Template Files in Excel®)

Processed Data in $N.kg^{-1}$ or $N.m.kg^{-1}$ showing 6 graphs

Processed Data in % of BW + P showing 6 graphs

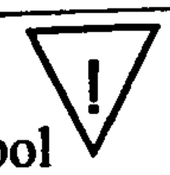

Table 8.6: The flow chart of data treatment (continuing the figure 5.3). The symbol shows the step in which the user must pay a high level of attention: the process is performed by hand.

results displayed in the following sections from 8.5 to 8.8 will reveal that 6 to 10 strides were sufficient for the aims expressed in chapter 1. Before any modification of the file, it was recorded. Its name having Excel® default extension .XLS was listed in the test-information chart shown in table 8.2.

Before the study of the results, an offset correction had to be performed. The way of doing was as follows:

1. For CaRi and CaLe, it was assumed that these two channels must not be negative. Thus, following the minimum provided by the programme in column 22, it was easy to find and apply the offset correcting factors of these two channels.

2. For Fx to Mz, the method, arbitrarily chosen, was the following: studying the channel 2, axial load Fy, the row corresponding to the first heel-strike was located. From it, five rows were counted towards the end of the file. This gap of five rows had been casually settled to minimise any error in the measurement of the heel strike event of the gait. This fifth row was chosen to be the basic level 0. It was noted in the test-information chart shown in table 8.2. It was now possible to register the offset correcting factors and to apply all of them in the 1000 rows.

All calculations were automated. Consequently, the six graphs, applying adequately corrected processed data, were provided automatically with units such as time in seconds for abscissa and N or N m, N % BW or N $m.kg^{-1}$, for ordinate.

Table 8.5 shows the first page (among usually 130, a smaller font reduced the size to 12 pages, see section 8.4.1) of the processed data (columns 12 to 17) of the same transtibial patient, TTR13 shown in figures 8.1 to 8.4 and tables 8.1 to 8.3. To print the six graphs, it was necessary to do a print preview to select the appropriate two pages (commonly 105-106 out of 130). Figure 8.5 shows the three graphs of forces (the two walking aids included and combined with the prosthetic axial load Fy, in the middle graph) while figure 8.6 shows the three graphs of bending moments and torque. Both figures represent the gait pattern of the same transtibial patient shown in figures 8.1 to 8.4 (TTR13).

Once these file manipulations were achieved, a new macro-sheet, named BODPERC2.XLM was opened and ran. The macro-sheet selected and copied all

AGE (years)	m = 64.83 range: 41 -88	
GENDER	26 males - 4 females PVD is a male illness (see chapter 2)	
DELAY FROM AMPUTATION (in months)	m = 4 range: 1.5 - 8	
SIDE	14 right side - 16 left side	
STUMP LENGTH (in mm)	141 range: 70 - 210	
TYPE OF SOCKETS	22 tests with gypsum socket (GS) 25 tests with acrylic resin socket (ARS)	The total is over 30 because some patients have been tested twice: with a gypsum socket then with an acrylic resin socket

Table 8.7: The main characteristics of the transtibial series (30 subjects)

AGE (years)	m = 59.9 range 40 - 76	
GENDER	9 males - 1 female PVD is a male illness (see chapter 2)	
DELAY FROM AMPUTATION (in months)	m = 3.9 range 1 - 9	
SIDE	4 right side - 6 left side	
STUMP LENGTH (in mm)	275 range: 118 - 378	
TYPE OF SOCKETS	2 patients wore gypsum socket (GS) 8 patients wore an acrylic resin quadrilateral socket (ARS-Q)	The total is equal to 10 but some patients have been tested twice: with a new socket having the same type
TYPE OF KNEE	2 GS tests with a Proteor® locked knee 4 ARS-Q tests with an Otto Bock® safety knee 4 ARS-Q tests with a Proteor® locked knee	

Table 8.8: The main characteristics of the transfemoral series (10 subjects)

values from the first cell of column 12 to the last (row 1000) of column 19. Then, they were pasted on a new Excel® template file named BODMASS.XLT in which the results were normalised to the subject's body mass unit, in kilogram. Once this done, the file was recorded and closed with the appropriate identification. The macro-sheet BODPERC2.XLM selected and copied the same cells to be pasted in a third template Excel® file named PERCWEIG.XLT in which the results were normalised in percentage of the subject's body weight in newtons for forces and N m per subject's body mass unit, for bending moments.

The two template files (BODMASS.XLT and PERCWEIG.XLT) ran above were programmed to a standard body mass of 70 kg. Therefore, the operator might indicate the exact body mass of the subject added with the mass of his artificial limb to have accurate results.

The flow chart of data treatment after one trial within a test is shown in table 8.6.

8.3 SUBJECTS' SELECTION AND DESCRIPTION

As stated in section 1.3, the series criteria to include patients were the following:

- PVD amputees (including acute arterial occlusion and Burger's disease) with a period since amputation less than 8 months without any discharge from the hospital or the rehabilitation centre;
- all of them had a large wound, never totally healed, stump pain and/or residual ache when tests were performed;
- they used at least one walking aid such as forearm sticks or simple canes.

Applying these criteria, the tested series was made up of 30 transtibial and 10 transfemoral amputees (40 patients). On the other hand, the age of the patient was considered not important. The complete description of these 40 subjects with all the tests performed is shown in appendix 11.VIII.3. However, the main characteristics of the subjects such as mean age, gender, average delay from amputation in months,

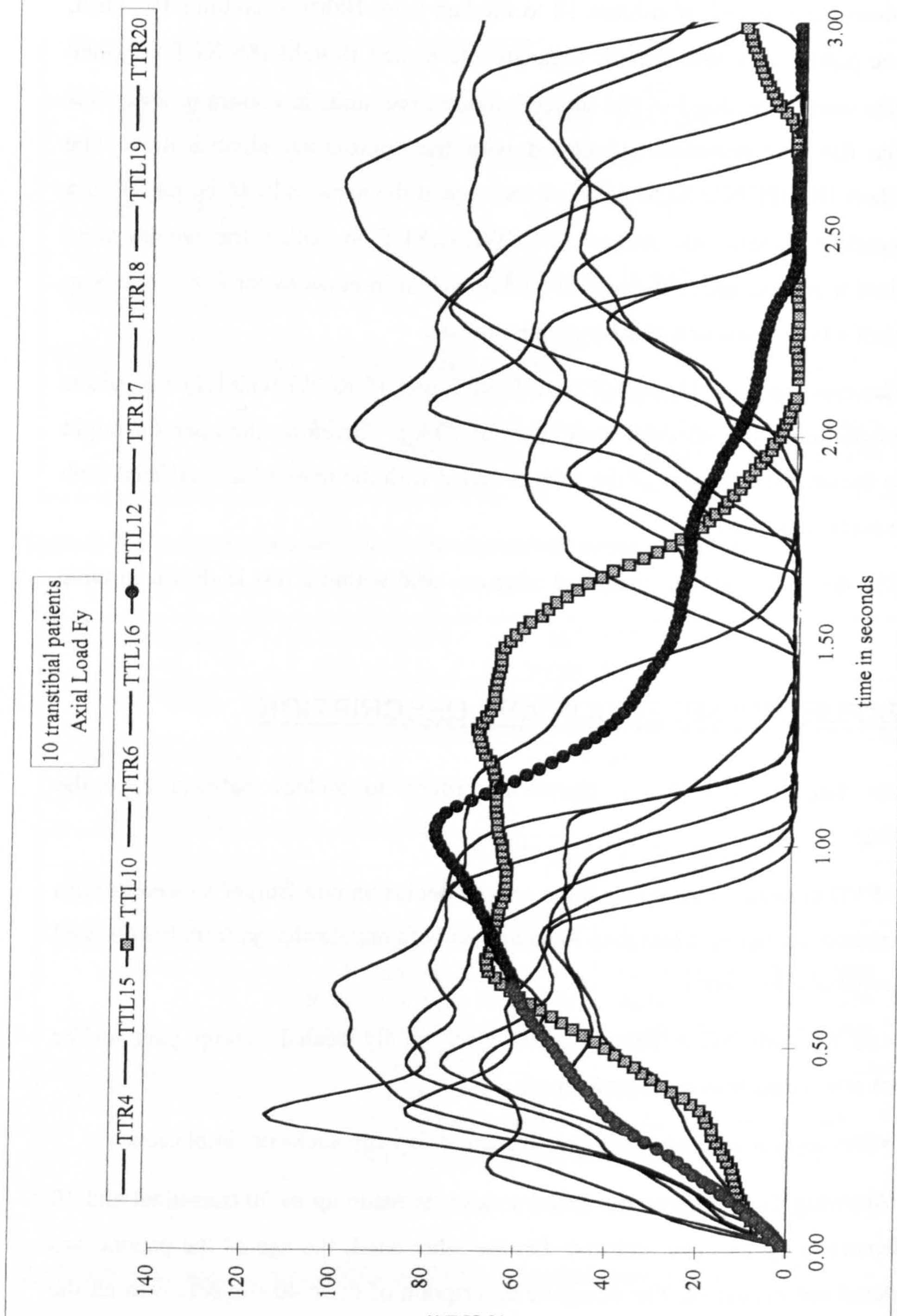

Figure 8.7: The prosthetic axial load Fy of ten TTP, two of them (TTL10 and TTL12) show a slow gait rate and thus, averaging the results was impossible.

stump length (in mm), amputated side and type of sockets, are shown in two tables: 8.7 for transtibial and 8.8 for transfemoral amputees.

As previously stated in section 8.2 (see also appendix 11.II.5), 8 out of 10 of the transfemoral tested patients wore an ARS-Q socket because usually the Plaster of Paris socket were fitted with a telescopic shank tube in which the distal part had not the standard dimension (26/30 mm). Therefore, the use of the VPT described in chapter 6 was impossible.

8.3.1 The 40 patients: kinetic study (30 transtibial, 10 transfemoral amputees: series 1a and 1b)

The 40 patients presented in tables 8.7 to 8.8 were studied under the following form:

1. Gait rate in $s.stride^{-1}$, from which the cadence ($strides.min^{-1}$) was extracted;

2. Maximum value of the axial load Fy designated as the prosthetic ground reaction force (PGRF);

3. Maximum value of A/P shear force Fx in both positive and negative directions;

4. Maximum value of A/P bending moment Mz in both positive (dorsiflexion) and negative (plantarflexion) directions;

5. Maximum value of the axial load applied on the right stick or the right cane;

6. Maximum value of the axial load applied on the left stick or the left cane;

7. Sum of these two maximum exhibiting the total axial load on both walking aids (WAGRF).

All of these results were expressed as a multiple of the body weight of the patient added with the prosthesis (% BW + P, for the shear forces and the axial load) or a fraction of the unit body mass of the subject (N m/kg, for the bending moments and the transverse torque), following the recommendation of Winter & Sienko (1988). This method is since usually followed by most of the researchers such as Pashalides (1989) or Hubbard & McElroy (1994). Practically, the results had usually the following form: 0.xx BW because the studied forces were usually lower than the

SUBJECT CODE	Age	Gender	Delay from Amput. in months	Stump Length in mm	B. Mass kg B. Height cm	Side	Type of Socket
TTR1	75	M	3.5	120	71 171	R	GS
TTL2	74	F	4	135	69 162	L	ARS
TTR3	41	M	1.5	140	54 173	R	ARS
TTR4	62	M	2	160	72 190	R	ARS
TTR5	47	M	2.5	160	74 188	R	GS
TTR6	65	M	4	65	59 176	R	ARS
TTL7	74	M	2.5	45	78 172	. L	ARS
TTL8	49	M	2	200	70 178	L	GS
TTL9	88	M	3	60	45 158	L	ARS
TTL10	75	F	6	80	42 155	L	ARS

Table 8.9: The characteristics of the ten TTP using 2 sticks then 2 canes during the same test (series 2)

The subjects' code was as follows, and for all the following tables, figures and sections:

TT = transtibial amputee
TF = transfemoral amputee

L = left side
R = right side

A number (having no signification) was added to these three letters.
As example, TTR1 was a right transtibial patient having the number 1.

body weight of the patient in the tested series.

However, a main drawback of such a series of recent vascular amputees (that is without any too severe selection, see chapter 1) was the discrepancy of the inter-patients' results that disallowed the possibility of performing accurate statistical analysis of the traces. As example, figure 8.7 shows the prosthetic axial load traces of ten patients, it is obvious that the patient named TTL10 had a very slow gait rate: approximately, he did one stride when some other patients did two. Moreover, none of the ten patients had a similar gait pattern.

Therefore, the average of the recorded values was not very accurate and besides means and standard deviation, the range of the results is shown in all cases.

Patients were carefully selected to have a consistent gait rate having a range of 1.7 to 1.9 $s.stride^{-1}$. This choice was made because, in this range, there was the greatest number of patients. Despite that, this reduced drastically the number of studied subjects in such or such aspect: 14 transtibial patients (series 4, section 8.3.4) and 4 transfemoral patients (series 6, section 8.3.6).

A statistical analysis of normalised maximum forces and bending moments is presented below in sections 8.5 and 8.7.

All these comments outline how disparate were the tested series and this might be one, among several, explanation concerning the lack of studies reported in the literature about recent vascular amputees in early stage of rehabilitation.

8. Four ratios were calculated as follows: 1) the ratio PGRF versus sticks or canes ground reaction forces; 2) ipsilateral stick or cane ground reaction force versus PGRF; 3) contralateral stick or cane ground reaction force versus PGRF; 4) the ratio ipsilateral versus contralateral stick or cane ground reaction force relatively to the amputated side of the patient.

To provide available comparison and accurate comments, the patients were listed by homogeneous groups such as: amputation level, amputated side, age, stump length and level of pain.

Because of their bad health condition, some patients could not be tested several

SUBJECT CODE	Age	Gender	Delay from Amput. in months	Stump Length in mm	B. Mass kg B. Height cm	Side	Type of Socket
TTL11	75	M	3	90	60 168	L	GS/ARS
TTL2	74	F	4	135	69 162	L	GS/ARS
TTR3	41	M	1.5	140	54 173	R	GS/ARS
TTR4	62	M	2	160	72 190	R	GS/ARS
TTL12	74	M	5	95	69 167	L	GS/ARS
TTR13	65	F	5	85	85 168	R	GS/ARS
TTL7	74	M	2.5	45	78 172	L	GS/ARS
TTL8	49	M	2	200	70 178	L	GS/ARS
TTL14	59	M	3	45	49 174	L	GS/ARS

Table 8.10: The characteristics of the 9 TTP using a gypsum socket at the beginning and an acrylic resin socket close to the end of the rehabilitation process (series 3).
Some patients are common in the two series shown in tables 8.8 and 8.9.
The body mass shown was checked at the beginning of the rehabilitation process when the patients wore a GS socket.

times and therefore the following test series had fewer subjects.

8.3.2 Comparison between different gait assistive devices (10 transtibial subjects: series 2)

The tests on 10 patients studied using two sticks then two canes, were made successively, during the same session. All things being equal, the patients walked a first trial by using two sticks (S) and then they immediately reversed their sticks and used them as if they were simple canes (C). Because the stick handle is not built for this purpose, the patient had to put the rod of the stick between his forefinger and his middle finger or, depending of the size of his hand, between the middle and the fourth finger as shown in figure 2.27 (see section 2.6.7.3). This was done to have the same loading set up as the one he could have with a standard cane (see figures 2.24 and 2.25). Each patient made several trials by changing the order of gait sequences to minimise, if possible, the stress, or any weakness phenomenon. The patients walked always in the same way: in a straight line, on a ceramic tiled floor, inside a corridor having the following dimensions: length 30 m, width 3 m. The list and main characteristics of the ten patients are shown in table 8.9. Once the tests were achieved, data were manipulated as stated above in section 8.2.3. All trials were examined and one was randomly chosen. However, the first trial was usually eliminated because the patient was insufficiently accustomed with the equipment. Once a trial was chosen, raw data were processed and transformed in processed data as shown above. The nine columns of digits (time, the six components of the gait plus the two walking aids) were then printed. The 1000 rows corresponding to a test of 15.62 seconds were in twelve pages. This hand data treatment is described in section 8.4.

8.3.3 Follow-up Rehabilitation (9 transtibial subjects: series 3)

The first test was undertaken when the patient was using his first distal provisional prosthesis with a Plaster of Paris (gypsum) socket (GS), during the initial gait training with two forearm counter-load sticks (S). The patients walked in a straight line, inside the physiotherapy room on a perfectly flat vinyl floor.

The second test was achieved with the same patients, wearing their last

SUBJECT CODE	Age	Gender	Delay from Amput. in months	Stump Length in cm	B. Mass kg B. Height cm	Side	Type of Socket
TFR1	68	M	4	29	60 165	R	ARS-Q LOCK
TFL2	52	M	4	37	48 162	L	ARS-Q OB SA K
TFL3	46	M	1.5	32	60 170	L	GS LOCK
TFL4	68	M	1	25	90 172	L	GS LOCK
TFL5	76	M	2	41	60 168	L	ARS-Q LOCK
TFR7	54	M	3	34	53 170	R	ARS-Q OB SA K
TFR6	67	M	4	36	79 175	R	ARS OB SA K
TFR8	66	M	3	37	69 177	R	ARS-Q LOCK
TFL9	40	F	4	38	42 170	L	ARS-Q OB SA K
TFL10	62	M	2.5	28	68 175	L	ARS-Q LOCK

Table 8.11: The characteristics of the ten transfemoral patients (series 1b).

The shaded cells show the four transfemoral amputees of series 6 (see section 8.8).

definitive prosthesis with an acrylic resin socket (ARS), before discharge from the Rehabilitation Centre. To allow a reliable comparison, the patients walked in the physiotherapy room on the same floor, with the same walking aids as in the first test although they were obviously able to do a lot better. They wore the same shoes. The difference between the two series of measures was on average 32.2 days (15 - 64, SD = 19). During this time interval, all patients had clearly improved their general status. The body mass had increased for eight subjects out of nine. For one patient, the body mass decrease was voluntary. Pain was reduced, muscular strength was developed. Between the two tests, variables were therefore numerous and these two series of measures had no other aim except to show an evaluation of the amputees' gait at two stages of their rehabilitation. The list of these 9 subjects is shown in table 8.10 with the same arrangement as table 8.9.

8.3.4 Main gait parameters and time events of recent vascular transtibial amputees (14 transtibial amputees: series 4)

Combining the two series 2 and 3 (see sections 8.3.2 and 8.3.3), it was possible to extract a series of 14 subjects (series 4). The number of subjects was less than the total of series 2 and 3 because some subjects were tested twice in each sample. Consequently, these 14 transtibial subjects, in which there were: 2 females versus 12 males and 8 left versus 6 right side amputees, had performed a total of 23 trials such as: GSocket or ARSocket with 2 sticks, GS and ARS with 2 canes. The complete characteristics of such a series are shown in appendix 11.VIII.3.

8.3.5 Ramp ascent and descent (4 transtibial patients: series 5) and presentation of the results

Among the selected patients, only four of them were fit enough to be tested outside They walked on a ramp ascent and descent on a tar ground floor. The results are shown following the way reported by Pashalides (1989): six figures of three diagrams, each of them showing the average values of the four patients of a particular channel when patients were walking on a flat tiled ceramic corridor then up and down the ramp. The four patients used sticks. All these results are shown in appendix 11.VIII.4. Concerning the three main channels in the A/P plane, shear force Fx, axial load Fy and bending moment Mz are presented on the same three graphs in

	Fx	Fy	Fz	Mx	My	Mz	Cane Right	Cane Left			
0.02	-0.3	-0.2	2.28	-0.11	-0.02	-0.01	11.20	22.96		MAX Fx	34.74
0.03	-0.3	-1.9	2.30	-0.11	-0.02	0.00	10.52	21.53		MIN	-146.90
0.05	-0.3	-1.9	2.30	-0.11	-0.02	0.00	10.06	20.09		MEDIANE	-33.15
0.06	0.7	-2.6	2.25	-0.11	0.00	0.01	RO 9.37	19.02			
0.08	0.7	-2.6	2.25	-0.11	0.00	0.01	8.92	17.22		MAX Fy	501.43
0.09	1.8	-2.5	2.18	-0.11	0.00	0.02	8.23	16.15		MIN	-6.27
0.11	2.6	-4.1	1.50	-0.06	0.00	0.13	7.77	15.07		MEDIANE	245.48
0.13	2.3	-4.4	1.50	-0.01	0.00	0.13	7.54	13.99	MSO		
0.14	4.3	-2.4	0.69	0.00	0.00	0.26	6.86	13.28		MAX Fz	9.91
0.16	5.4	-2.0	0.38	0.00	0.00	0.39	6.40	12.20		MIN	-34.42
0.17	7.2	-2.4	-1.01	0.05	0.01	0.63	6.17	10.41		MEDIANE	-1.65
0.19	9.4	-0.2	-0.86	0.05	0.01	0.76	5.72	10.05			
0.20	9.4	2.6	-1.13	0.05	-0.01	0.88	5.03	LO 8.97		MAX Mx	2.96
0.22	8.8	1.7	0.52	0.00	-0.03	0.75	4.80	7.90		MIN	-2.05
0.23	7.7	2.2	0.72	-0.01	-0.01	0.64	4.57	6.82		MEDIANE	-0.01
0.25	6.5	2.9	-0.10	0.00	0.02	0.62	4.12	6.10			
0.27	5.4	1.5	0.37	0.00	0.08	0.39	3.89	5.39		MAX My	2.98
0.28	11.9	18.7	-0.76	-0.25	0.22	-0.58	3.43	4.67		MIN	-1.68
0.30	15.7	44.2	0.56	-0.40	0.24	-1.69	3.20	3.59		MEDIANE	0.06
0.31	18.2	66.7	0.00	-0.48	0.24	-2.24	2.74	3.23			
0.33	20.6	81.8	0.78	-0.58	0.19	-3.02	2.52	2.52		MAX Mz	48.64
0.34	21.5	92.3	0.36	-0.58	0.13	-3.59	2.74	2.52		MIN	-8.08
0.36	22.2	101.1	0.64	-0.54	0.09	-4.04	3.43	3.23		MEDIANE	7.73
0.38	22.1	111.2	-0.23	-0.53	0.03	-4.39	3.20	3.23			
0.39	22.2	119.4	-1.75	-0.56	-0.01	-4.85	3.20	2.16		MAX CaRi	52.12
0.41	22.3	133.9	-2.46	-0.60	-0.04	-5.42	3.20	1.44		MIN	0.00
0.42	23.7	151.2	-2.20	-0.69	-0.10	-6.21	3.43	1.44		MEDIANE	19.43
0.44	MAX 26.3	174.5	-3.71	-0.77	-0.18	MAX -6.77	3.89	2.16			
0.45	FX + 26.6	194.1	-3.60	-0.82	-0.24	MZ - -7.11	4.12	3.23		MAX CaLe	117.65
0.47	23.4	216.6	-4.17	-0.77	-0.28	-6.82	4.57	4.31		MIN	0.00
0.48	19.6	229.5	-5.62	-0.76	-0.33	-6.07	4.80	5.74		MEDIANE	46.63
0.50	14.7	238.8	-6.96	-0.75	-0.36	-5.21	5.72	LSS 7.90			
0.52	10.0	244.6	-7.74	-0.74	-0.41	-4.24	6.40	10.05			
0.53	3.4	255.0	-8.75	-0.73	-0.47	-2.60	7.54	12.20	MSS		
0.55	-6.8	269.4	-10.14	-0.72	-0.56	0.02	8.23	14.71			
0.56	-16.7	289.3	-10.76	-0.72	-0.72	3.20	8.92	17.94			
0.58	-27.5	316.0	-9.13	-0.74	-0.92	6.57	RSS 9.83	20.45			
0.59	-38.6	345.5	-9.75	-0.65	-1.15	10.48	10.52	23.68			
0.61	-48.5	376.2	-8.60	-0.57	-1.36	14.55	11.43	26.91			
0.63	-58.1	407.1	-7.87	-0.54	-1.56	18.85	12.57	30.49			
0.64	-69.1	433.6	-6.59	-0.46	-1.64	23.07	13.49	34.08			
0.66	-76.7	460.1	-6.88	-0.46	-1.68	26.94	14.40	38.38			
0.67	-84.0	480.0	-6.74	-0.55	-1.64	29.96	15.77	42.69			
0.69	-90.4	493.9	-6.03	-0.72	-1.53	32.37	16.92	46.63			
0.70	-96.2	MAX FY + 501.0	-9.15	-0.91	-1.31	34.25	17.83	50.94			
0.72	-101.2	501.4	-10.78	-1.16	-1.03	35.68	18.97	55.24			
0.73	-105.5	496.6	-10.99	-1.32	-0.71	36.66	19.89	59.19			
0.75	-107.1	489.6	-12.14	-1.49	-0.42	37.42	20.57	63.13			
0.77	-108.0	478.1	-12.63	-1.56	-0.15	37.81	21.49	66.72			
0.78	-107.9	465.3	-13.24	-1.60	0.07	37.90	21.95	70.31			
0.80	-109.3	452.1	-16.11	-1.53	0.26	37.90	22.63	73.54			
0.81	-109.7	443.9	-16.79	-1.47	0.39	37.98	23.32	76.76			
0.83	-112.3	439.1	-17.34	-1.38	0.47	38.34	24.23	80.35			
0.84	-115.3	438.3	-17.85	-1.33	0.53	39.01	24.92	82.86			
0.86	-119.7	443.1	-16.04	-1.26	0.54	39.74	25.83	85.73			
0.88	-124.9	451.3	-16.42	-1.25	0.55	40.70	26.52	88.24			
0.89	-128.9	457.9	-13.84	-1.23	0.57	41.66	27.89	90.75			
0.91	-131.3	462.9	-14.36	-1.23	0.60	42.65	28.58	92.91			
0.92	-133.7	469.2	-13.39	-1.24	0.60	43.47	29.49	95.06			
0.94	-135.1	471.4	-13.26	-1.19	0.60	44.08	30.18	96.49			
0.95	-136.3	473.1	-13.96	-1.10	0.63	44.45	30.86	98.29			
0.97	-136.5	469.1	-11.64	-1.07	0.67	44.53	31.55	99.72			
0.98	-135.0	467.2	-11.75	-0.98	0.71	44.55	32.00	101.51			
1.00	-134.9	461.6	-11.75	-0.89	0.76	44.55	32.23	102.59			
1.02	-135.2	459.6	-13.24	-0.84	0.81	44.71	32.92	103.31			
1.03	-133.3	456.5	-11.05	-0.81	0.87	44.80	33.15	104.38			
1.05	-134.7	453.0	-12.48	-0.71	0.96	44.95	33.83	105.46			
1.06	-134.9	451.6	-12.43	-0.66	1.04	45.26	34.29	107.25			
1.08	-137.2	452.9	-13.78	-0.61	1.13	45.70	34.98	107.61			
1.09	-138.5	452.5	-13.64	-0.61	1.22	46.00	35.20	108.69			
1.11	-139.8	453.4	-15.07	-0.51	1.31	46.46	35.66	109.76			
1.13	-142.1	452.8	-15.66	-0.45	1.38	46.82	35.89	MAX LS 110.12			
1.14	-142.6	451.0	-15.61	-0.37	1.43	47.13	36.58	110.84			
1.16	-144.3	450.3	-16.28	-0.32	1.45	MAX 47.19	36.58	110.12			
1.17	MAX -144.5	448.4	-14.73	-0.29	1.47	MZ + 47.35	37.03	110.12			
1.19	FX - -145.5	445.7	-14.68	-0.24	1.44	47.34	37.26	110.12			
1.20	-145.5	440.1	-13.13	-0.25	1.43	47.18	37.72	109.76			
1.22	-145.5	436.8	-11.61	-0.27	1.39	47.03	37.72	108.69			

Table 8.12: The typical results of the patient (TTR6) from series 4 using an ARS with two sticks and showing the time parameters of the gait which allow to erect figures 8.8 and 8.9. (One page out of 12) ; (RO: Right Stick Off ; LO: Left Stick Off ; MSO: Mean Time Stick Off ; LSS: Left Stick Strike ; RSS: Right Stick Off ; MSS: Mean Time Stick Strike). The mean time was arithmetically calculated between left and right sticks.

section 8.6.

8.3.6 Comparison between different gait assistive devices (4 transfemoral subjects: series 6)

These subjects were extracted from the series 1b (complete description in table 8.11). The patients named TFL5, TFR7, TFL3 and TFL4, had the following particular characteristics: the two patients TFL4 and TFL3 had a very low activity level and they were not totally accustomed to their artificial limb; moreover, the patient TFL4 had a bad weight / height ratio (body mass: 90 kg, body height: 1.72 m). The patient TFR7 had, four weeks before the test, a new arterial by-pass on the « sound limb » and he was suffering pain. Hence, the series 6 was not totally typical as a randomly chosen series and thus the results will be precociously discussed in section 8.8.

8.4 HAND OR COMPUTER DATA TREATMENT AND PRESENTATION OF THE RESULTS

8.4.1 Hand data treatment

The data processing performed by hand concerns the following tests:

- 10 transtibial patients using 2 sticks then 2 canes (series 2, see above section 8.3.2);
- 9 transtibial patients using a gypsum socket then an acrylic resin socket (series 3, see above section 8.3.3);
- 4 transfemoral patients using also 2 sticks and 2 canes (series 6, see above section 8.3.6).

As previously stated (see section 8.2.3.1), each test was presented under the form of a file having 12 pages, 1000 rows and 9 columns (see table 8.12). The notation used in the following sections are shown in table VIII.6 in appendix 11.VIII.5. The scheduled task was as follows:

1. to make a guiding mark upon the nine columns corresponding to heel strike (HS) and toe off (TO). The event heel strike was considered as accomplished when

Table 8.13: The results processed by hand of patient TTR6 when he was using an acrylic resin socket and 2 sticks: 6 to 9 strides with mean values and standard deviation.

NAME : LEN Level : BK	WA : 2 S	Socket : ARS Side : Left	HS = Heel Strike SS = Sticks Strike TO = Toe Off SO = Sticks Off	MEAN	SD
Maximum Gait Rate from HS to the following HS			1.71, 1.83, 1.88, 1.75, 1.85, 1.79, 1.82, 1.93	1.82	0.07 s.stride^{-1}
Maximum Axial Load (Fy) in N			501.4, 459.6, 461.9, 479, 481.2, 476.6, 493.2, 482.4	479	14 N
% of Axial Load vs. Body Weight			Subject's Body Weight + Prosthesis in N : 59 + 1.7 = 60.7 kg = 595.5 N	80 %	
Maximum of Fx Shear negative			-145.5, -143.6, -135.8, -137.9, -131.6, -146.9, -135, -135.6	-139	5.6 N
Maximum of Fx Shear positive			26.6, 33.7, 34.1, 30.7, 34.7, 27.1, 33, 31.4, 31.5	31.4	2.91 N
Maximum Mz plantarflexion negative			-7.11, -5.93, -8.08, -6.52, -7.16, -7.22, -7.4, -7.06, -6.51	-6.99	0.61 N
Maximum Mz dorsiflexion positive			47.35, 46.82, 47.23, 46.65, 46.8, 47.02, 48.64, 47.02, 48.64, 47.23	47.24	0.6 N
Maxi Load on both sticks in N			148.79, 152.64, 155.07, 156.85, 153.36, 145.73, 141.76, 155.02	151.15	5.25 N
% of Sticks Load vs. Body Weight				25.38 %	
Maxi Load on Right Stick			37.95, 45.03, 52.12, 39.55, 45.03, 39.55, 32, 37.72	41.11	6.1 N
Maxi Load on Left Stick			110.84, 107.61, 102.95, 117.3, 108.33, 106.18, 109.76, 117.3	110.03	5.07 N
time between HS and TO = stance phase			1.21, 1.36, 1.32, 1.25, 1.32, 1.29, 1.32, 1.36	1.303	0.05 s
time between SS and SO = sticks stance phase			1.33, 1.41, 1.47, 1.39, 1.4, 1.34, 1.29, 1.44	1.38	0.05 s
time between HS and SS from HS to the following SS			0.26, 0.3, 0.27, 0.28, 0.32, 0.33, 0.39, 0.29, 0.25	0.34	0.13 s
time between SS and TO			0.95, 1.06, 1.05, 1.25, 1, 0.96, 0.93, 1.07	1.03	0.1 s
time between TO and SO			0.38, 0.35, 0.42, 0.39, 0.4, 0.38, 0.36, 0.37	0.38	0.02 s
time between Max Fy and Max Sticks = time - lag between axial load & sticks push-up			0.5, 0.47, 0.45, 0.55, 0.58, 0.45, 0.48, 0.58	0.5	0.05 s
time between Max Mz+, Fz- & Max Sticks			0.05, 0.03, 0.03, 0.11, 0.13, 0.11, 0.09, 0.04	0.07	0.04 s
SO to the following SS			0.4, 0.42, 0.39, 0.39, 0.44, 0.46, 0.51, 0.43, 0.37, 0.41	0.43	0.04 s

the axial load Fy exceeded 10 N (1.4 % of the average maximum value of this particular channel). Similarly, the event toe off was considered to occur when Fy was less than 10 N. These two events were used to count the number of strides, to calculate the gait rate in s.stride^{-1} (GR) and both prosthetic stance and swing phase (PSP and PSwP) in seconds;

2. to denote the different maximum values of axial load Fy in each stride;

3. to put a mark on each maximum and minimum of Fx and Mz corresponding of the 6 to 9 strides usually found in the time of a test (15.6 s).

4. to mark the maximum values of stick or cane axial loads in each stride

5. to mark the following events, for both sides, stick or cane strike (SS or CS) and stick or cane off (SO or CO) with the same threshold of 10 N. If the two sides of the subject were considered, the same gait events such as left and right SS (CS) or SO (CO) were usually not simultaneous. Averaging the results from series 4 (14 transtibial amputees), the time intervals between left and right sticks or canes were found equal to 0.12 s (SD = 0.04) and from series 6 (10 transfemoral amputees), 0.16 s (SD = 0.07). Hence, in order to have only one time value for SS or CS, the middle time between right SS or CS was taken in account; the same was done to have only one time value for SO and CO.

However, this introduced a lack of accuracy and therefore, these two time events were known with a level of uncertainty equal to the ratio of stick or cane stance phase divided by the time interval between right and left side. Once this was done, a chart for each trial was written as shown in table 8.13. Some results are shown in table 8.14, (same transtibial patient TTR6 as tables 8.12 and 8.13. All the tables of results from all the patients are shown in appendix 11.VIII.5.

6. the chronology of all these gait events was collected as shown in figure 8.8 with data from table 8.13.

2 STICKS VS. 2 CANES	Patient TTR6 ARS - RIGHT BK **2 sticks**				Patient TTR6 ARS - RIGHT BK **2 canes**			
	mean	SD	% of BW	N or N.m. kg^{-1}	mean	SD	% of BW	N or N.m. kg^{-1}
Maximum Gait Rate in $s.stride^{-1}$	1.82	0.07			1.67	0.07		
Maximum Axial Load (Fy) N	479	14		7.89	484	16.8		7.97
% of Axial Load vs. Body Weight	80 %				81 %			
Maximum Fx Shear negative N	-139	5.61	23	2.28	-126	8.57	21	2.08
Maximum Fx Shear positive N	31.4	2.97	5.3	0.51	37.7	7.34	6.3	0.621
Maximum Mz plantarflexion negative N.m	-6.99	0.61	1.17	0.11	-7.03	1.14	1.18	0.11
Maximum Mz dorsiflexion positive N.m	47.2	0.63	7.93	0.77	48.8	2.02	8.19	0.803
Maximum Load on both sticks or Canes N	151	5.24		2.49	135	14.12		2.22
% of Sticks or Canes Load vs. Body Weight	25 %				22 %			
Maximum Load on Right Stick or Cane N	41.1	6.12	6.91	0.67	48.5	10.93	8.13	0.79
Maximum Load on Left Stick or Cane N	110	5.07	18.5	1.81	86.4	17.96	14.5	1.42
time from HS to the following TO = prosthetic stance phase (PSP)	1.31		0.05		1.16		0.08	
time from SS (CS) to the following SO (CO) = sticks or canes stance phase (SSP or CSP)	1.39		0.05		1.26		0.07	
time from SO (CO) to the following SS (CS) = sticks or canes swing phase (SSwP or CSwP)	0.43		0.04		0.41		0.07	
time from SS to the following TO	1.03		0.1		0.88		0.08	
time from TO the following SO	0.38		0.02		0.37		0.05	
time-interval between HS and SS	0.34		0.13		0.27		0.03	
time between Max. Fy and Max. Sticks = time - interval between axial load & sticks or canes push-up	0.51		0.05		0.34		0.17	
time between Max. Mz +, Fx - and Max. Sticks or Canes = time - interval between dorsiflexion + posterior shear and sticks or canes push-up	0.07		0.04		0.06		0.03	

Table 8.14: The definitive results of patient TTR6 showing side by side the mean values when the patient wore a gypsum socket and then an acrylic resin socket.

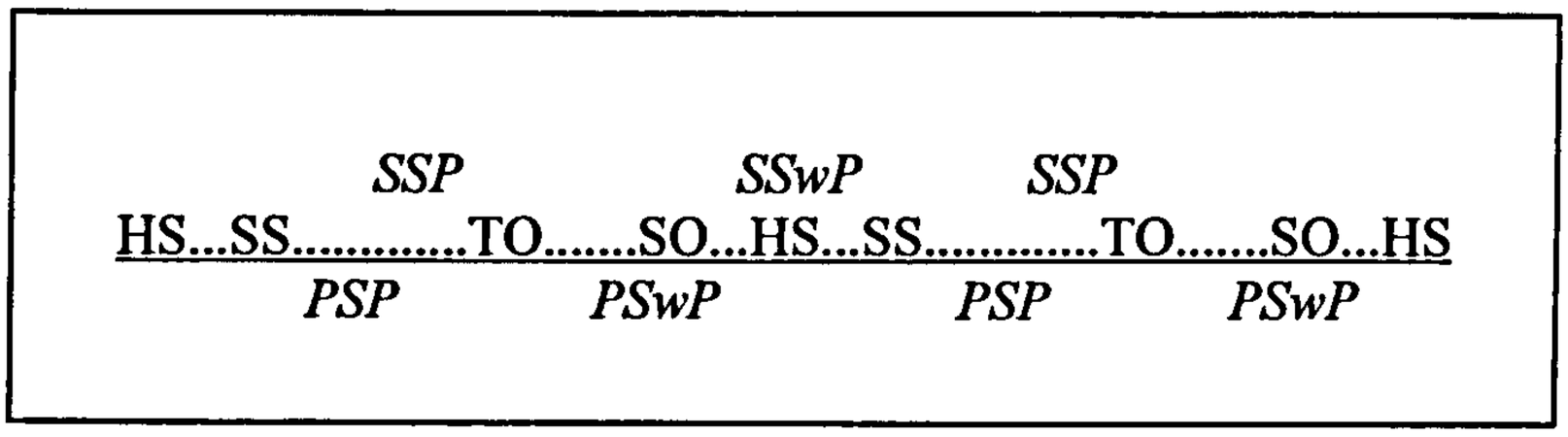

Figure 8.8: The gait pattern line (GPL) showing a typical chronology of the following gait events: Heel Strike, Stick Strike, Toe - off, Stick - Off.
The top line shows the stick time intervals such as: Stick Stance Phase (SSP) and Stick Swing Phase (SSwP).
The bottom line shows the prosthetic time intervals such as: Prosthetic Stance Phase (PSP) and Prosthetic Swing Phase (PSwP).
The distance between each event is proportional to the time interval.
(Patient TTR6 using an ARS and walking with 2 sticks)

Figure 8.8 displays the chronology of the main events of the gait but additional information is given in figure 8.9. The blank space (with a "?") refers to the sound limb about which nothing was known. The height of each column is proportional to the corresponding axial load Fy. This presentation was described by Opila (1985); it is known as the vertical impulse histogram (VIH):

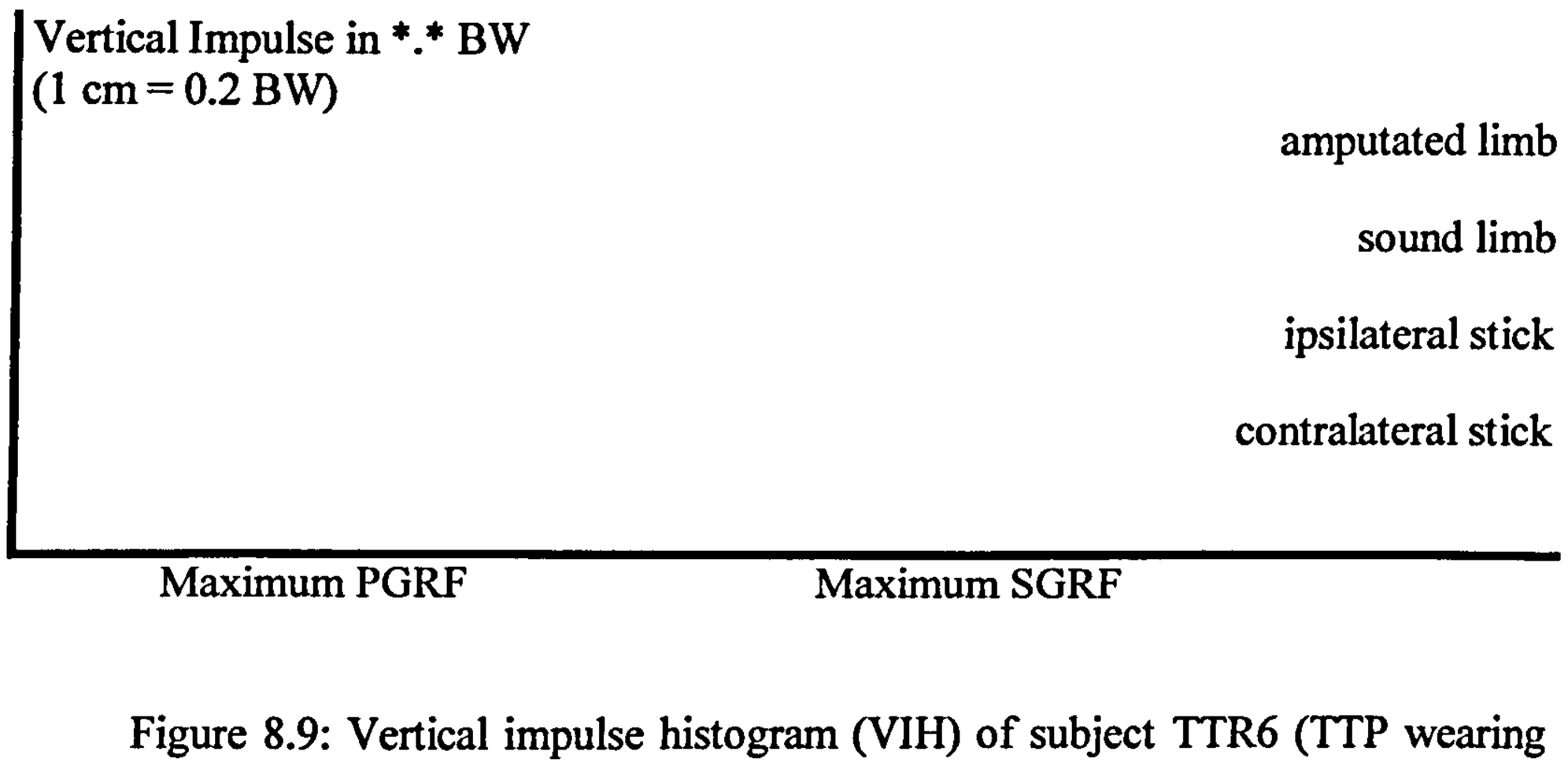

Figure 8.9: Vertical impulse histogram (VIH) of subject TTR6 (TTP wearing an ARS and using 2 sticks). Back view, right side of the subject on the right of the figure. Two gait events are shown with both the maximum prosthetic ground reaction force (PGRF) and the maximum stick ground reaction force (SGRF).

GAIT PHASE DURATIONS									
	Series Descriptions	Mean Gait Rate s.stride^{-1}		SD		p value	NS not significant S significant at $p \leq 0.05$	Range	
Series 1a	30 TTP	1.96		0.28				1.67 ; 2.78	
Series 2	10 TTP 2S vs. 2C	2S 1.87	2C 1.93	2S 0.36	2C 0.46	0.18	NS	2S 1.52 2.81	2C 1.47 3.05
Series 3	9 TTP GS vs. ARS	GS 2.23	ARS 1.83	GS 0.33	ARS 0.34	0.003	S	GS 1.81 2.87	ARS 1.66 1.68
Series 4	14 TTP	1.59		0.42				0.92 ; 2.81	

Table 8.15: The range of results of mean gait duration phases for the different series of transtibial subjects, expressed in s.stride^{-1}.

PROSTHETIC GROUND REACTION FORCE									
	Series Descriptions	Mean PGRF N.kg^{-1}		SD		p value	NS not significant S significant at $p \leq 0.05$	Range	
Series 1a	30 TTP	6.32		1.87				5.31 ; 7.88	
Series 2	10 TTP 2S vs. 2C	2S 6.94	2C 7.69	2S 2.03	2C 1.44	0.08	NS	2S 2.44 8.63	2C 4.51 9.12
Series 3	9 TTP GS vs. ARS	GS 5.62	ARS 7.32	GS 2.23	ARS 2.07	0.02	S	GS 3.21 8.81	ARS 4.96 11.7
Series 4	14 TTP	6.33		1.98				2.44 ; 11.7	

Table 8.16: The range of results of mean prosthetic ground reaction force for the different series of transtibial subjects, expressed in N.kg^{-1}

The results show large variations within individual subjects: usually a large standard deviation.

•All the tables such as table 8.14 are organised in the same way. For each subject, there are four vertical columns: 1) average values from 6 to 9 measures (usually one measure by stride) according to the subject's gait rate; 2) the corresponding standard deviation; 3) the forces normalised in percentage of body-weight; 4) the forces and moments per unit mass of the subject's body-weight expressed in kg ($N.kg^{-1}$ or $N\ m.kg^{-1}$).

Therefore, the results are focused on sagittal plane load actions, which have low variability as found by Winter & Sienko (1988) and Winter (1994c).

The last item in table 8.14 is interval between maximum dorsiflexion moment (Mz+) plus maximum negative anterior shear (Fx-) and the point where the subject is in maximum load on the walking devices.

8.4.2 Computer screen data treatment and presentation of the results

This relates to the series 1a and 1b (see section 8.3.1). The data processing was as follows: the absolute maximum values (among several maximums) of A/P shear forces Fx, axial load Fy and A/P bending moments Mz of each tests were considered on the screen under the form of tables as shown in table 8.12. The reported values are respectively the maximum of maximums of each test and not a mean from several strides; hence, the reported values should be upper limits.

8.4.3 Description of the common statistical analysis of the results

The treatment of the main results expressed below was a comparison between the mean of two samples. The hypothesis to be usually tested was: in axial load Fy, did a patient apply more load on his prosthesis when using two sticks than two canes. Therefore, two samples had to be compared and because they were extracted from two tests, they were independent, i.e., not paired samples.

The strategy for choosing the correct hypothesis-testing procedure for comparing two population means, shown by Weiss (1995), has been followed.

The flowchart, expressed by Weiss (1995) is helpful to observe. Before

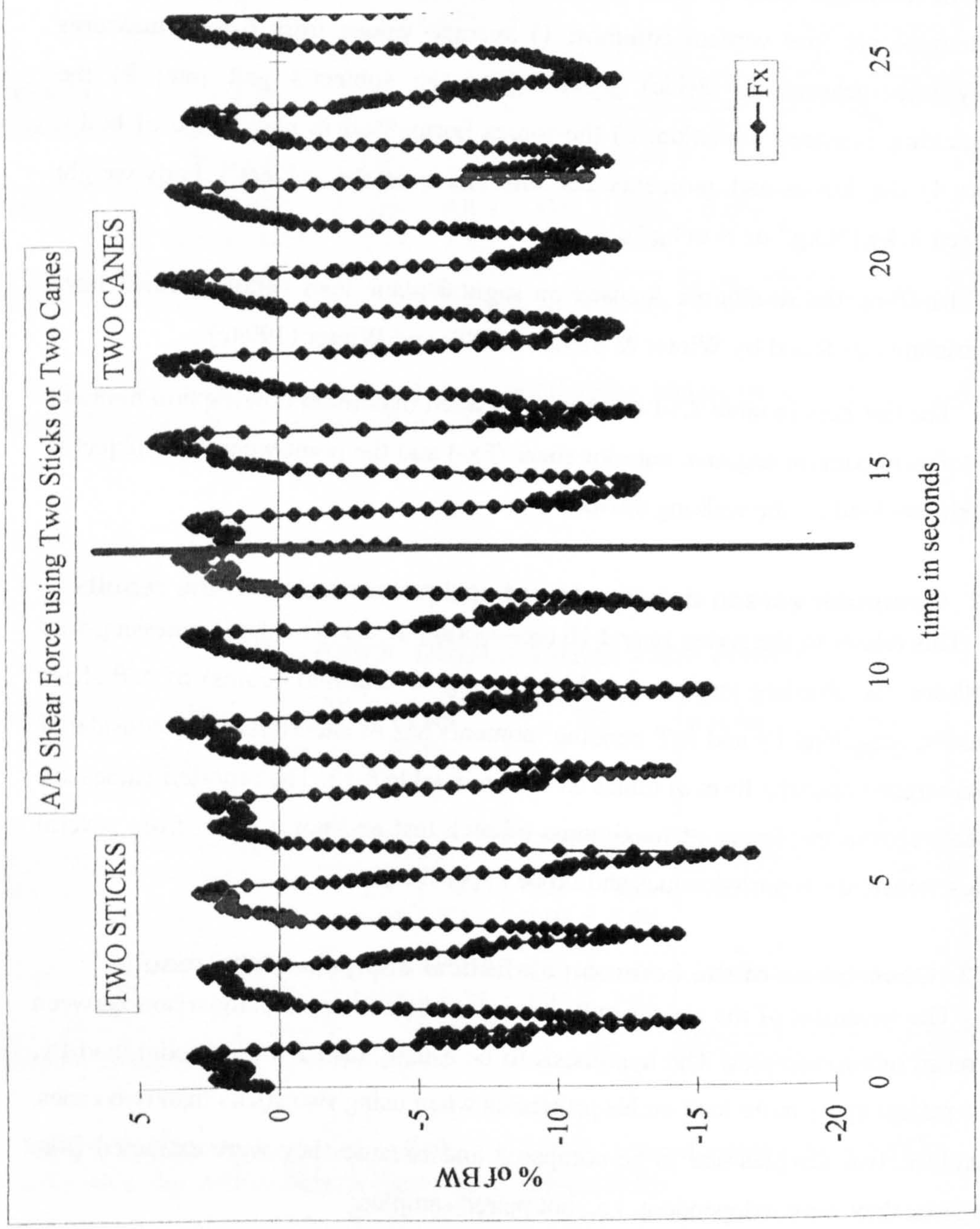

Figure 8.10: The A/P shear force Fx for the patient TTL9 is shown using two sticks (left part of the diagram, from 0 to 13 seconds) then two canes (right part of the diagram, from 13.1 to 26 seconds). It was the same trial, same day, same prosthesis, and same floor.

choosing the right procedure, it is only necessary to answer the three following questions:

1.Were the samples paired? The answer given above was NO.

2.Were the populations normal? The normal probability plots were established for each population. An example is shown in appendix 11.VIII.6 concerning the axial load Fy of one transtibial patient walking successively with two sticks then two canes. The traces were usually straight enough and thereby indicated that it was certainly reasonable to assume that forces and moments were approximately normally distributed. Therefore, the answer to the second question was YES.

3.Were the population standard deviations equal? A circumspect analysis of the results (see appendix 11.VIII.5) suggested that the population standard deviations were roughly equal. Thus, the answer of the third question was YES.

Consequently, samples were independent, populations were normal with equal standard deviations. The procedures to use should be two-sample z-test or pooled t-test (Weiss, 1995). The two procedures were tested with two different softwares (Minitab® 8.2 for the pooled t-test and Microsoft Excel® for the two-sample z-test); both gave similar results. Thus, because of its convenience, the two-sample z-test was used although it was more appropriate for large samples.

It was also important to note that all the hypothesis tests performed were right-tailed since a greater-than sign appeared in the alternative hypothesis or left-tailed since a lower-than sign appeared. In other words, the hypothesis tests performed were never two-tailed. The last task was now to employ the guidelines for using p-value to assess the evidence against the null hypothesis H_o with a significance level of $p < 0.05$ (Weiss, 1995):

p-value	Evidence against H_o
$p > 0.1$	weak or none
$0.05 < p \leq 0.10$	moderate
$0.01 < p \leq 0.05$	strong
$p \leq 0.01$	very strong

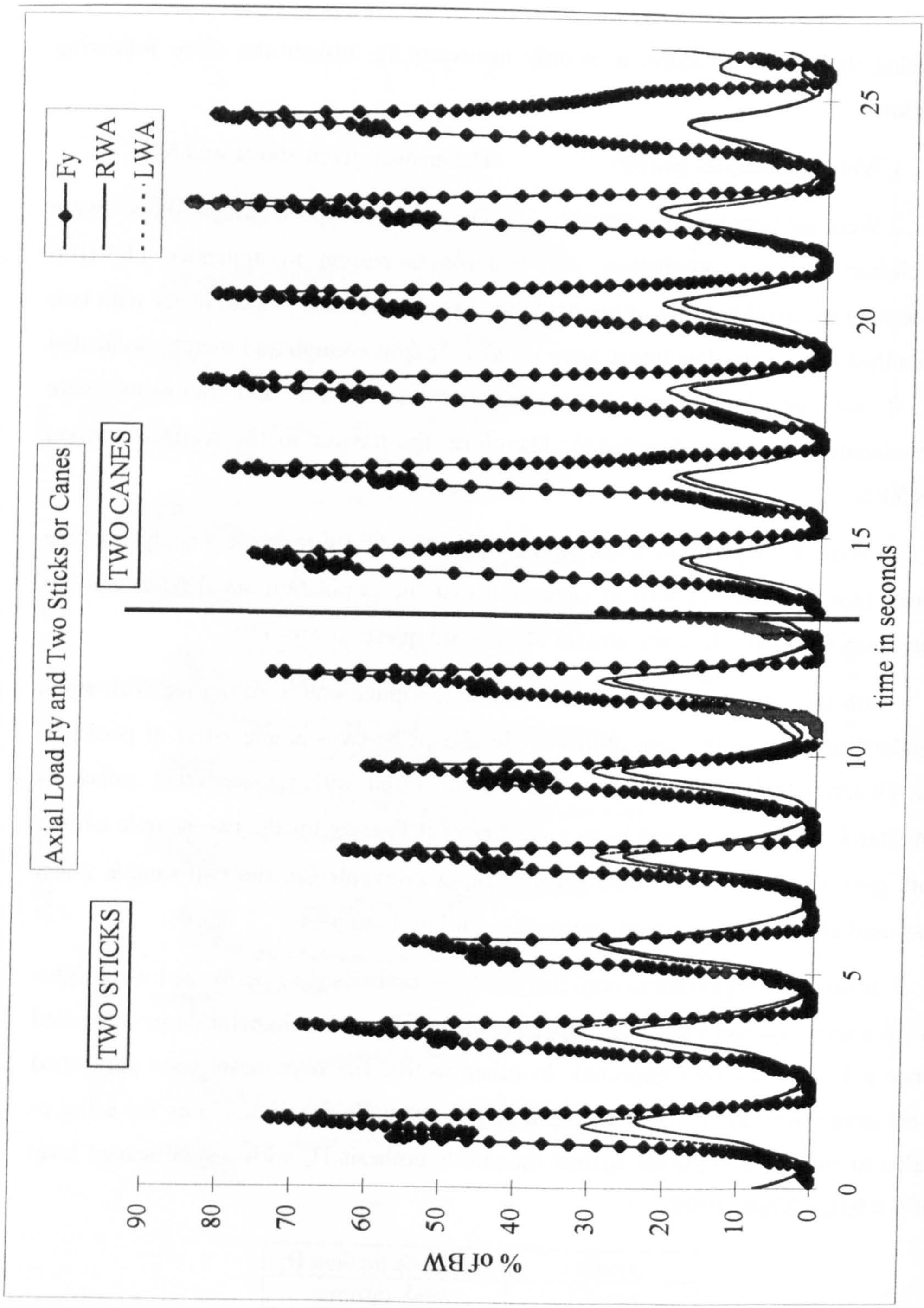

Figure 8.11: The prosthetic axial load Fy and the axial load on the two walking aids for the same patient TTL9 are shown using two sticks (left part of the diagram, from 0 to 13 seconds) then two canes (right part of the diagram, from 13.1 to 26 seconds). It was the same trial, same day, same prosthesis, and same floor.

8.5 RESULTS FOR TRANSTIBIAL PATIENTS

Because not all the patients were tested in the same manner, mainly because not all of them were able to accomplish the same task, the series described above could be separated in seven groups as stated in section 8.3.

8.5.1 Gait Phase Duration

Table 8.15 shows the results concerning the gait rate (s.stride^{-1}) or the prosthetic stride time (PST) of the different series, walking at a self selected pace.

The thirty transtibial amputees tested (series 1a) walked with an overall stride duration of 1.96 s (SD = 0.28) clearly greater than the values found in the literature: 1.3 s (Hubbard and McElroy, 1994) for elderly, vascular transtibial amputees but after rehabilitation and 1.23 s (Winter & Sienko, 1988) for traumatic transtibial amputees. As example, normal subjects, aged 70-79 years, had a mean cycle time of 1.04 s (Öberg *et al.* 1993) and 1.22 s for elderly inpatients walking with the aid of a stick (Hendry *et al.* 1990). It was thus possible to show that transtibial patients, at the beginning of their rehabilitation, had a gait rate divided of 1.45 than established TTP and 1.81 slower than elderly normal subjects.

The average cadence was 32 strides per minutes (SD = 12) compared to the average of 48 (SD = 5) found by Winter & Sienko (1988) assessing 5 traumatic below the knee amputees. These results obviously reflected the behaviour of the series that was globally in the beginning of the gait recovery with fragile and/or painful residual limbs: all amputees at early steps of their rehabilitation walked a minimum of 50 % slower than other populations of amputees.

If the 9 patients of series 3 using a GS then an ARS were examined, stride time was: 2.23 s (SD = 0.33) and 1.83 s (SD = 0.34) respectively. A statistical test shows a strong significant difference of p = 0.003 (see section 8.4.3). The decrease in percentage of the gait rate from GS to ARS was 22 %, which was far from the results reported by Baker & Hewison (1990). These researchers found a change in velocity from initial to discharge of 98 %, but some subjects admitted to the study were road trauma amputees. However, as stated in section 8.3.2, several factors could explain

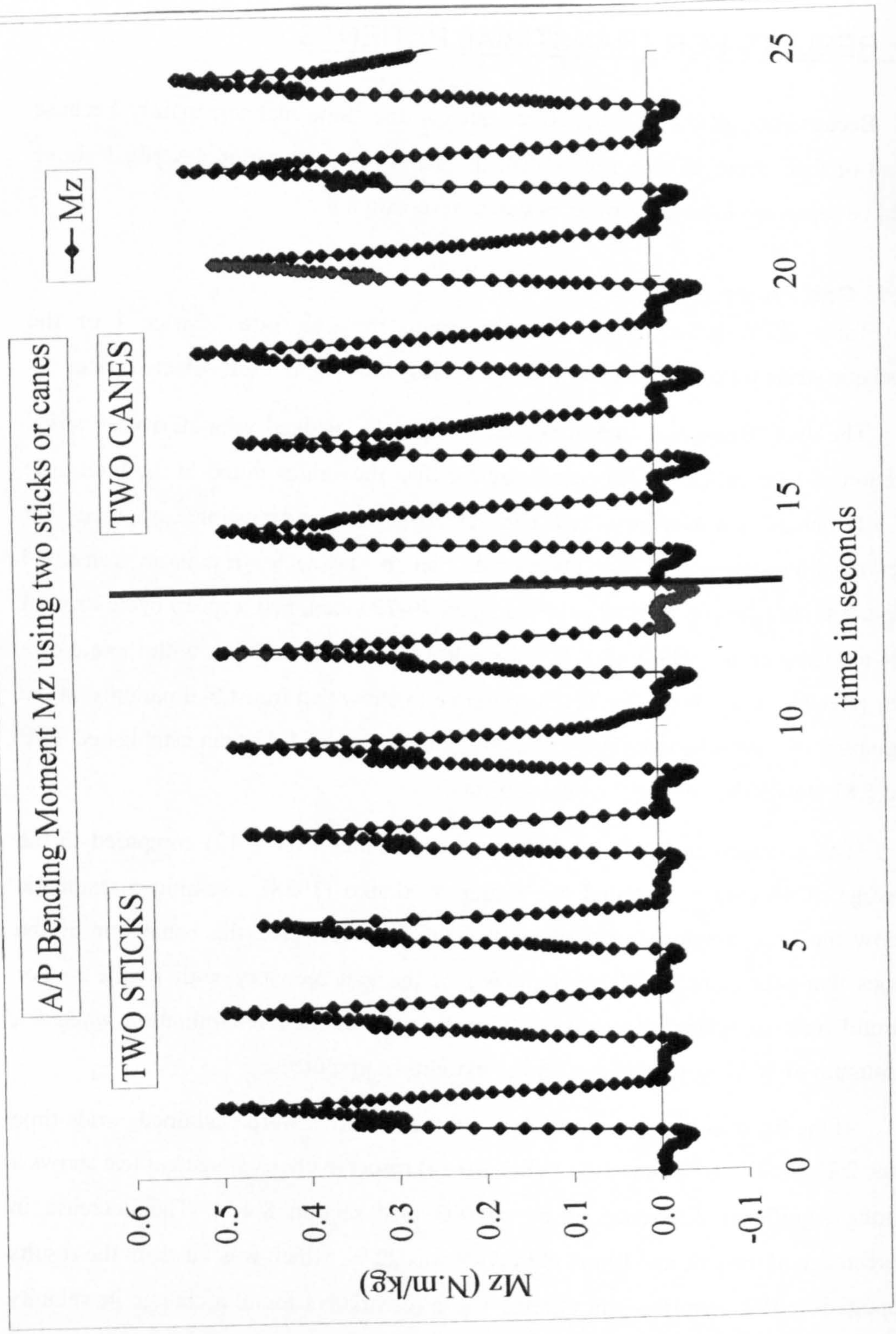

Figure 8.12: The A/P bending moment Mz for the same patient TTL9 is shown using two sticks (left part of the diagram, from 0 to 13 seconds) then two canes (right part of the diagram, from 13.1 to 26 seconds). It was the same trial, same day, same prosthesis, and same floor.

this improvement and therefore, firm conclusions could not be reached.

All the patients had the same pattern: the gait rate was increasing from GS to ARS except one patient (TTL12) who, for pain reasons on the end of the tibial crest had decreased his gait rate. Surprisingly, a patient with stump pain could walk slowly although the prosthetic stance phase was longer. This behaviour of amputees who reduce the gait velocity while lowering the axial load and thus increasing the load on their walking aids, is common (see below section 8.5.2).

If the PST of the ten patients (series 2) using successively two sticks then two canes was studied, the results were respectively: 1.87 s.stride^{-1} (SD = 0.36) and 1.93 s.stride^{-1} (SD = 0.46), which was not significant at the level of p = 0.18. Consequently, the changing of walking aids did not vary (only, + 3 %) the cadence which had a mean value of 31 strides per minute. Similarly, no significant correlation was found between the length of the stump and the gait rate (r = 0.17, p = 0.46). However, there was a large discrepancy in the results as follows:

- The subject TTR4: 1.52 s.stride^{-1} using 2 S and 1.47 s.stride^{-1} using 2 C.

This patient was the tallest of the series. His ratio $\frac{\text{stump length}}{\text{tibial length}}$ was 0.34[15], particularly favourable as reported by Gailey *et al.* (1994) who established that a ratio of 0.3 to 0.4 should be the best regarding both gait velocity and heart rate at self selected pace. The stump length was also within the range, commonly recommended by surgeons (Cormier, 1988): from 0.27 to 0.42 to have the best function. Moreover, this patient had no pain and his general health status was good.

- The subject TTL10: 2.81 s.stride^{-1} using 2 S and 3.05 s.stride^{-1} using 2 C.

This patient had a severe stump pain due to a lack of mobility of the skin around the wound facing the tibial crest and his ratio $\frac{\text{stump length}}{\text{tibial length}}$ was 0.2 that was not advantageous. However, this ratio must be interpreted with caution as, for example, subject TTL7 from the same series had a stump versus tibial length of only 0.1 and

---

[15] The tibial length equals 0.246 of body height, extracted from an anthropometric table, reported from Winter (1994).

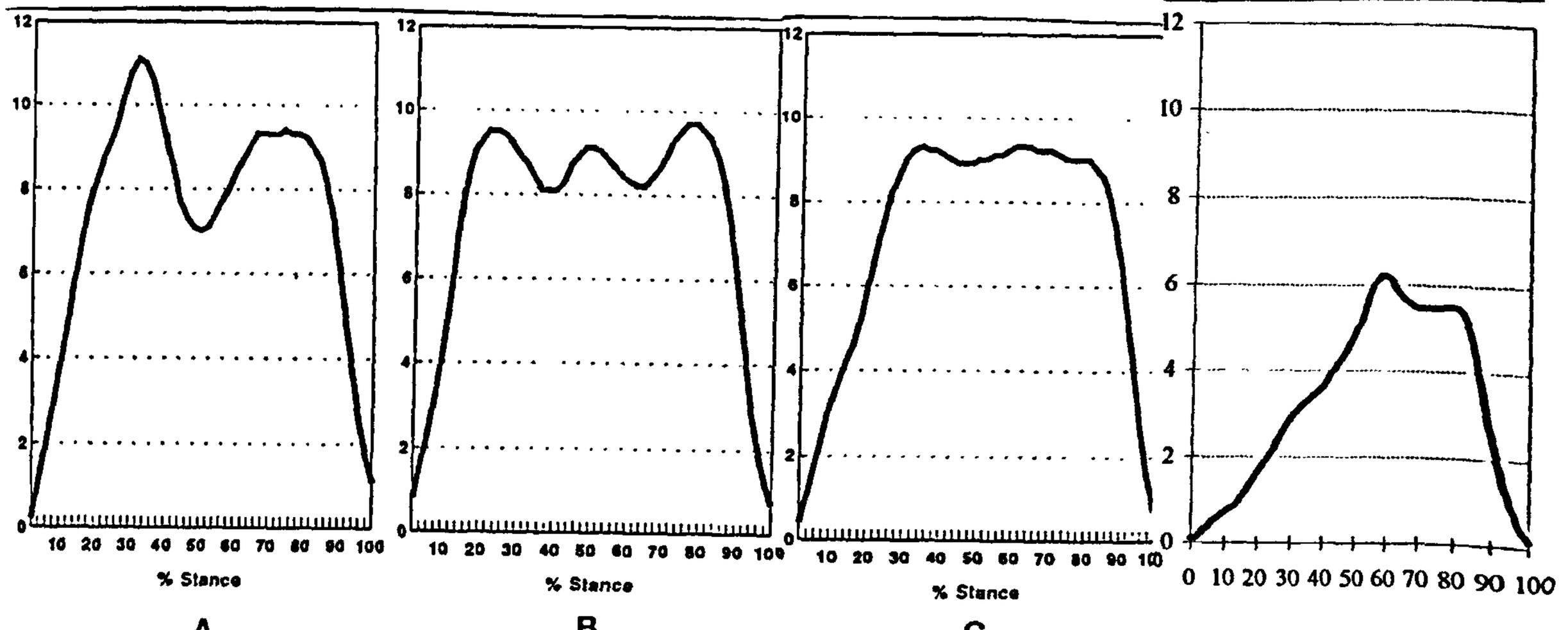

Figure 8.13: Four sample patterns of variation of maximum resultant prosthetic ground reaction force, in $N.kg^{-1}$ to a base of time.

two peak pattern	A	three peak pattern	B
flattened peak pattern	C	single peak pattern	D

(4 patients out of 10)

A, B, and C are derived from Hubbard & McElroy (1994), see also figure 2.1.

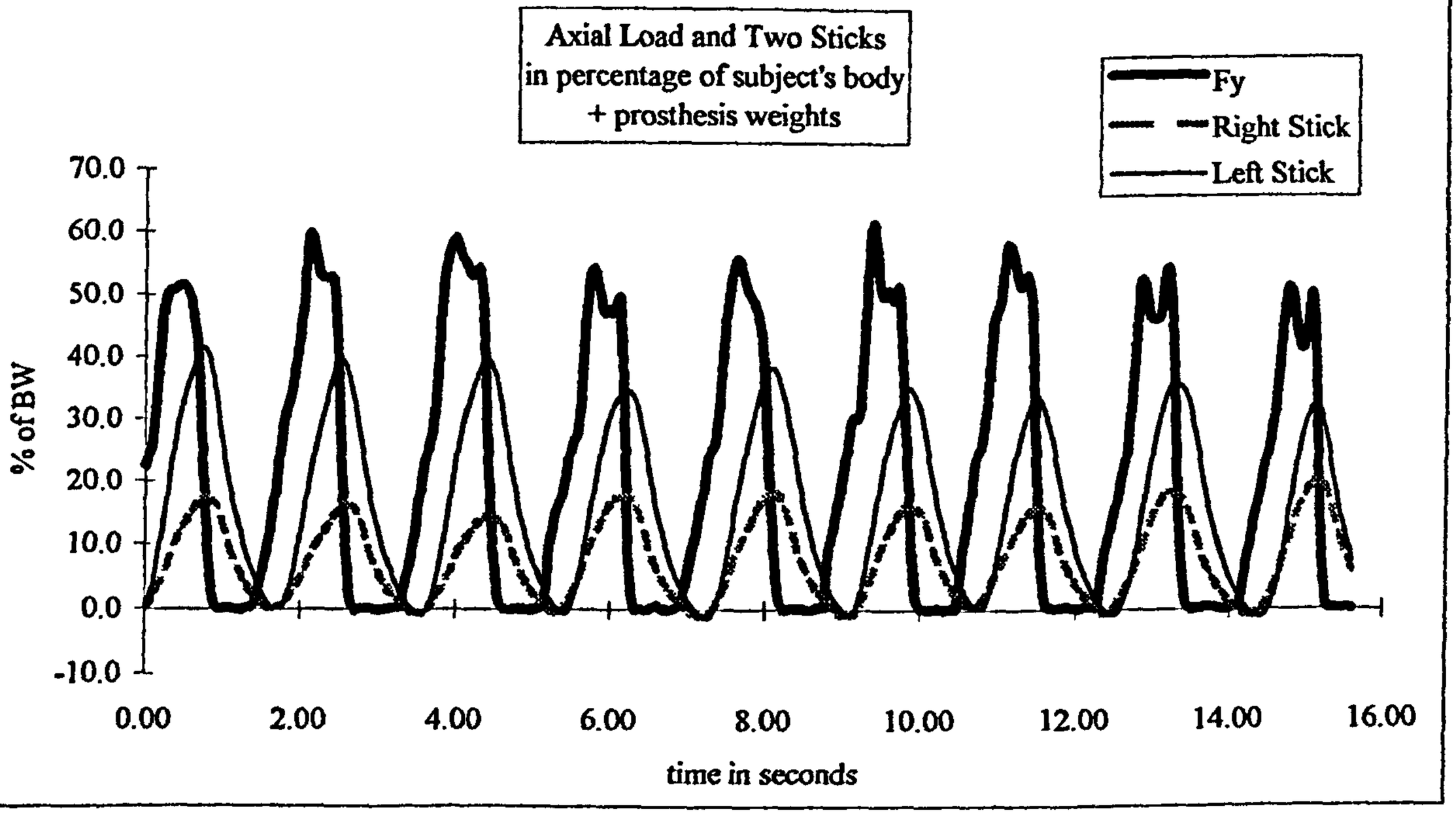

Figure 8.14: An example of a 9 strides of a patient (TTR13) showing traces from axial load Fy and two sticks: a mixing of single peak and two peak patterns.

his performances were in the middle of those of the considered series. Moreover, Gailey *et al.* (1994) showed a significant negative correlation between stump length and energy cost.

As example, the patient TTL9 (88 years old, just before the discharge from the Rehabilitation Unit and thus fitted with a definitive ARS) is shown in three graphs. In figure 8.10, the A/P shear force is shown when the patient was using two sticks (0 to 13 seconds) then two canes (13.1 to 26 seconds). In figure 8.11, the axial load Fy is shown with two sticks than two canes and figure 8.12 shows the A/P bending moment following the same sequence. Globally, figure 8.10 shows that Fx negative was decreased while Fx positive increased from two sticks to two canes. The prosthetic axial load Fy (figure 8.11) increased while axial loads on both walking aids decreased from two sticks to two canes. In both directions, the A/P bending moments (figure 8.12) were expanded from two sticks to two canes. These comments are only discussed as an example; it is impossible to infer any trend from only one patient.

8.5.2 The ground reaction forces

8.5.2.1 PROSTHETIC GROUND REACTION FORCE (PGRF)

Series 1a, 30 patients had a mean maximal prosthetic ground reaction force (PGRF) of 6.32 $N.kg^{-1}$ (SD = 1.87), equivalent to 0.63 BW. The results are shown in table 8.16. This single value had not any relevance and could not be compared to that found in the literature, since the load on the sticks or the canes was not taken into account. On the other hand, by adding the axial load on the prosthesis and the one acting on each walking assistive device, an average of 10.06 $N.kg^{-1}$ (SD = 1.8), equivalent as 1.06 BW was found. This was consistent with common mean values (10.6 $N.kg^{-1}$) as shown by Seliktar & Mizrahi (1986). Consequently, the sum of the forces on the aids and the prosthesis was just over one body weight, because of the low level of the gait rate. In other words, increasing the gait velocity should increase the level of whole axial loads on both prosthesis and walking aids. This indicates the presence of inertial forces in aided gait, already reported by Opila (1985). However, these inertial forces were never evaluated in the presented work.

In summary, this result shows that 35 % of the maximum vertical ground

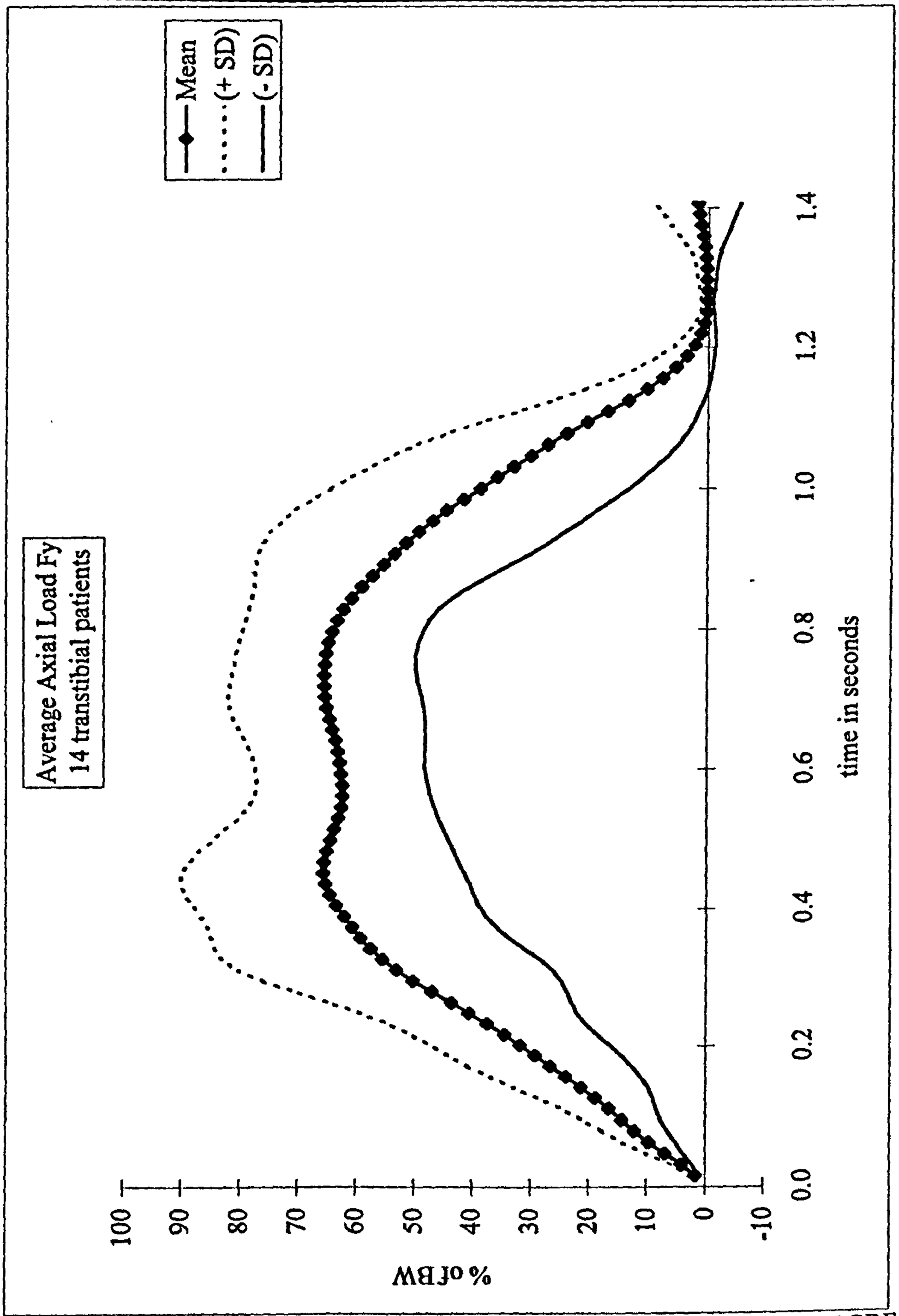

Figure 8.15: Mean results of 14 transtibial patients (series 4) showing the PGRF (± SD) to a base of time.

reaction force in prosthetic stance was transmitted by the walking aids. This result is consistent with Winter *et al.* (1993) who quoted that one cane carry about 25 % of the total reaction force, but one healthy subject carrying one aid was only studied. Moreover, Ely & Smidt (1977) quoted only 15 % as WAGRF, but it was the effect of one cane used at the contralateral side to the involved lower limb.

Similarly, the axial load on the prosthesis at two stages of rehabilitation (9 TTP, series 3), averaged 5.62 $N.kg^{-1}$ (SD = 2.23) and 7.32 $N.kg^{-1}$ (SD = 2.07) respectively. The difference was significant, at the level of p = 0.02, despite the behaviour of the patient TTL8 who had decreased his vertical load on his prosthesis on the advice of the physiotherapist after specific training.

If the same procedure was repeated for the sticks versus canes tests (10 TTP, series 2), the results were 6.94 N.kg-1 (SD= 2.03) and 7.65 N.kg-1 (SD= 1.44). The difference was moderately significant (p = 0.08). It was therefore shown what intuitively all patients indicated; namely that in the gait with two canes, they were forced to apply more load on the prosthesis, because the grip strength on the cane handle was reduced. The increase of the prosthetic ground reaction force was approximately 10 %.

Concerning the general shape of the curve reflecting the axial load during one stride, the literature shows that the maximum axial forces are below body weight. Moreover, the distinct double peak and trough found in normal healthy subjects were absent when a subject with a total hip replacement was walking slowly with two sticks (Opila *et al.* 1987). Hubbard and McElroy, (1994), in figure 8.13, see also figure 2.1), described three different basic patterns in the vertical PGRF of amputees:

1. a two peak pattern, typically recorded in normal gait pattern (3 patients out of 10, series

2. a pattern of three equal peaks: the middle peak corresponds to the shank tube being in the vertical position, (1 patient out of 10, series 2)

3. a flattened pattern all along the stance phase (2 patients out of 10, series 2).

Considering the presence of the sticks or canes, it was necessary to add a fourth pattern in the vertical PGRF:

WALKING AIDS GROUND REACTION FORCE									
	Series Descriptions	Mean WAGRF $N.kg^{-1}$		SD		p value	NS not significant S significant at $p \leq 0.05$	Range	
Series 1a	30 TTP	4.3		1.37				1.04 ; 4.83	
Series 2	10 TTP 2S vs. 2C	2S 3.87	2C 2.90	2S 0.08	2C 0.11	0.16	NS	2S 0.89 7.03	2C 1.92 4.53
Series 3	9 TTP GS vs. ARS	GS 4.72	ARS 3.80	GS 1.88	ARS 1.72	0.67	NS	GS 2.28 7.26	ARS 0.67 5.83
Series 4	14 TTP	3.73		1.69				0.74 ; 7.28	

Table 8.17: The range of results of mean walking aids (sticks or canes, 2S vs. 2C) ground reaction force for the different series of transtibial subjects, expressed in $N.kg^{-1}$

Amputation Level and Series Number	**Amputated Side** R = right L = left	**Ipsilateral Walking Aid**	**SD**	**Contralateral Walking Aid**	**SD**
30 TTP series 1a	14 R	2.11	0.5	2.68	0.8
	16 L	1.96	0.4	1.86	0.6
10 TTP series 2	R	2S 1.67	2C 1.39	2S 0.7	2C 0.5	2S 2.85	2C 1.72	2S 1.2	2C 0.7
	L	2S 1.64	2C 1.22	2S 0.9	2C 0.3	2S 1.59	2C 1.48	2S 0.5	2C 0.4
	5 R 2S + 2C	1.53		0.63		2.28		1.01	
	5 L 2S + 2C	1.43		0.68		1.53		0.43	
9 TTP series 3	6 L	GS 2.1	ARS 1.6	GS 0.1	AR S 0.9	GS 1.9	ARS 1.5	GS 0.7	AR S 0.6
	3 R	GS 2.2	ARS 1.9	GS 0.2	AR S 0.2	GS 3.8	ARS 3.3	GS 0.3	AR S 0.6
	6 L ARS + GS	1.84		0.1		1.72		0.7	
	3 R ARS + GS	3.53		0.5		2.06		0.2	
14 TTP series 4	6 R	1.86		0.57		2.24		0.92	
	8 L	1.95		1.04		1.78		0.65	

Table 8.18: The results concerning the axial load on the two walking aids separated from the amputated side of the different transtibial subjects ($N.kg^{-1}$)

4. a single important peak corresponding to the vertical and forward deceleration due to the contact of the heel with the ground and just after it when the subject starts his acceleration (from early to mid stance phase).

As example, figure 8.14 shows 9 strides of patient TTR13 with traces of axial load Fy and two sticks. However, nothing is always so simple, the gait pattern of the patient TTR13, shown in figure 8.14 had globally a one peak pattern but the steps number 8 and 9 were performed in a two peak pattern. The study of the gait pattern of such a patient must consequently be conducted with caution. The maximum magnitude of axial load occurs at 36 % of the stride or 50 % of the prosthetic stance phase (PSP).

For all the subjects and trials in this project taken together and averaged, this maximum of load on the prosthesis (PGRF) was commonly 60 to 80 % of the body weight of the subject. This was less than the usual PGRF reported in the literature concerning PVD amputees, due to the walking aids. From this maximum and at each stride, the value of the PGRF was regularly decreasing. To illustrate this comment, figure 8.15 shows the mean results of 14 transtibial patients (series 4). Globally, it is possible to see a large flattened shape corresponding to mid prosthetic stance phase. This flattened shape is longer (50 % of stride time) than those found in the literature (40 % of stride), (Winter & Sienko, 1988; Hubbard & McElroy, 1994). However, from the beginning of this flattened part, the level of axial load was slowly but regularly decreasing. Also there was an increase of the positive standard deviation at the maximum of the first « peak » (30 % of stride) of the flattened axial load trace. This highlights the large inter-patient pattern with a sharper first peak as shown in figures 8.13, 8.14 and 8.15.

In summary, the 14 dysvascular transtibial patients, in early stage of rehabilitation, applied less axial load on their prosthesis than dysvascular transtibial patients long after their rehabilitation treatment but the loading duration was longer.

8.5.2.2 WALKING AIDS GROUND REACTION FORCES (WAGRF)

The recording of the loads applied by the patients to the sticks or the canes during the gait cycle was one of the original features of this research. It was not possible to find any literature references about the use of the sticks by amputees,

NAME CODE	AMP. SIDE	RATIO STUMP LENGTH / SHANK LENGTH	RATIO IPSI / CONTRA STICK MEAN FROM DIFFERENT TESTS
TTL7	L	0.10	1.07
TTL14	L	0.10	1.30
TTL9	L	0.15	1.49
TTL10	L	0.20	0.96
TTL11	L	0.21	0.74
TTL12	L	0.23	1.21
TTL2	L	0.33	0.79
TTL8	L	0.45	0.79
TTR6	R	0.15	0.37
TTR13	R	0.20	0.50
TTR1	R	0.28	0.62
TTR3	R	0.32	0.57
TTR4	R	0.34	0.73
TTR5	R	0.40	0.46

Table 8.19: Different ratios from 14 transtibial patients (see text for comments)

except few words in Murray *et al.* (1969). Only, some papers about forces and impulses applied to walking devices by disabled people are available (Siereg *et al.* 1968, Ely & Smidt, 1977, Opila *et al.* 1987, Deathe *et al.*, 1993).

The results, mixing both walking aids and amputated sides are shown in table 8.17, while table 8.18 describes the results separately: 1) left and right amputees; 2) ipsilateral and contralateral walking stick or cane. An ipsilateral walking aid was defined as follows: the stick or the cane used on the same side of the amputation, i. e., a right amputee used his ipsilateral (ipsi) walking aid with his right upper limb. His contralateral (contra) was used by his left upper limb.

Averaging all tests, table 8.17 shows that the tested patients applied to both sticks or canes a total vertical force of 4.3 $N.kg^{-1}$ (SD = 1.37), a mean of 0.43 BW. By separating left and right walking aids relatively to the amputated side (see table 8.18):

- for the 16 left amputees, there was a difference opposite as expected, that was the main load was applied to the ipsilateral walking aid in relation to the amputated side;

- for the 14 right side amputees: they applied more load onto the opposite walking aid to their amputation, which was as expected.

In order to present a more accurate depiction of the WAGRF, the 14 subjects of the series 4 were analysed thoroughly: different ratios were calculated, such as:

1. WAGRF (2 sides) versus PGRF. In common amputee rehabilitation field, it is usual to consider that this ratio should be the lowest, to withdraw the walking aids when they are less and less necessary.

2. Ipsilateral WAGRF versus PGRF. Here also, the ratio should be the lowest having the aim to remove the ipsi walking aid.

3. Contralateral WAGRF versus PGRF. Following the results reported by Ely & Smidt (1977) concerning the use of a contralateral walking aid and the common sense found in rehabilitation (Engstrom & Van de Ven, 1993), it is expected that this ratio should be higher than the ipsilateral WAGRF versus PGRF.

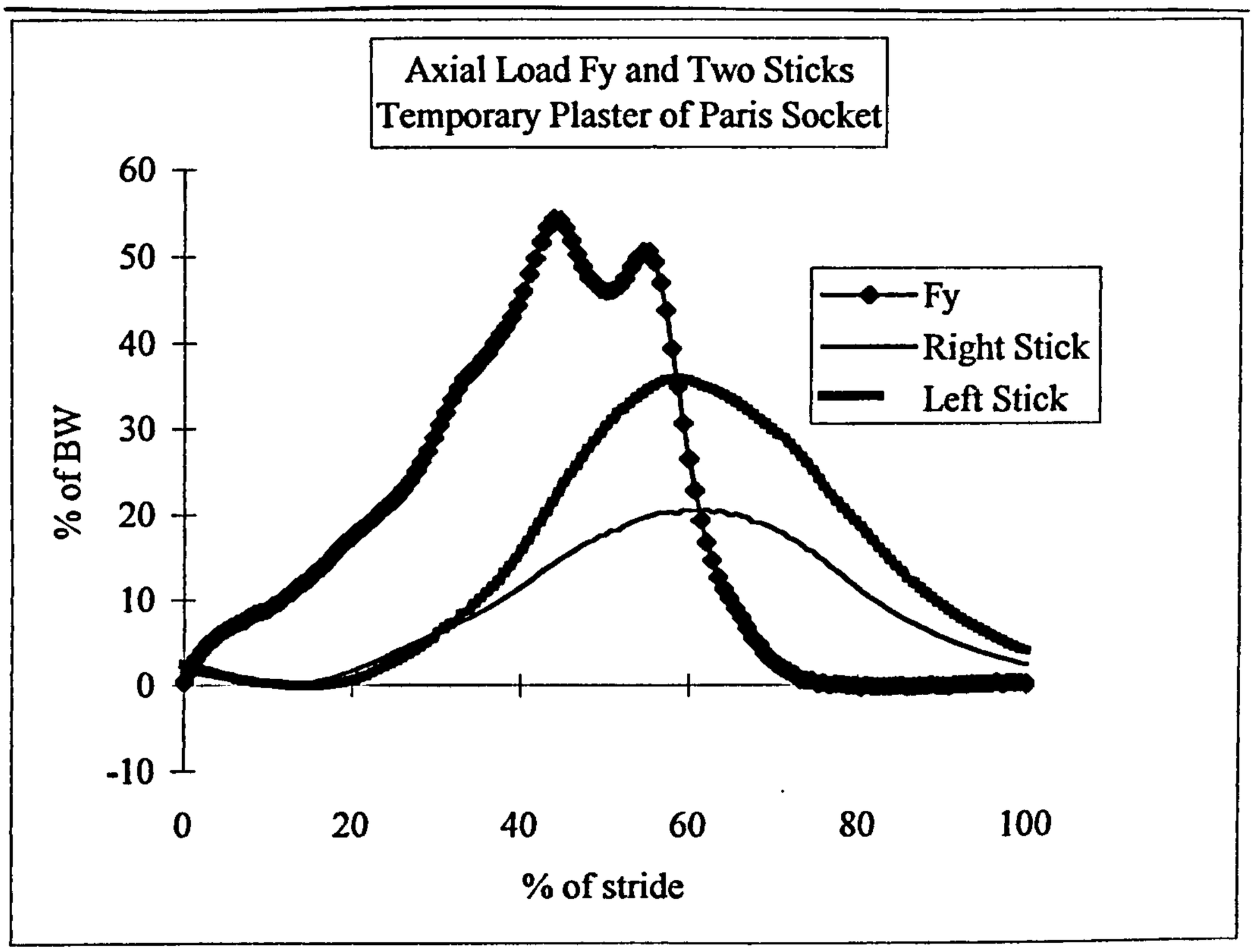

Figure 8.16: One stride of the right transtibial patient TTR13 using a plaster of Paris socket in early stage of rehabilitation: the axial load Fy and the two sticks.

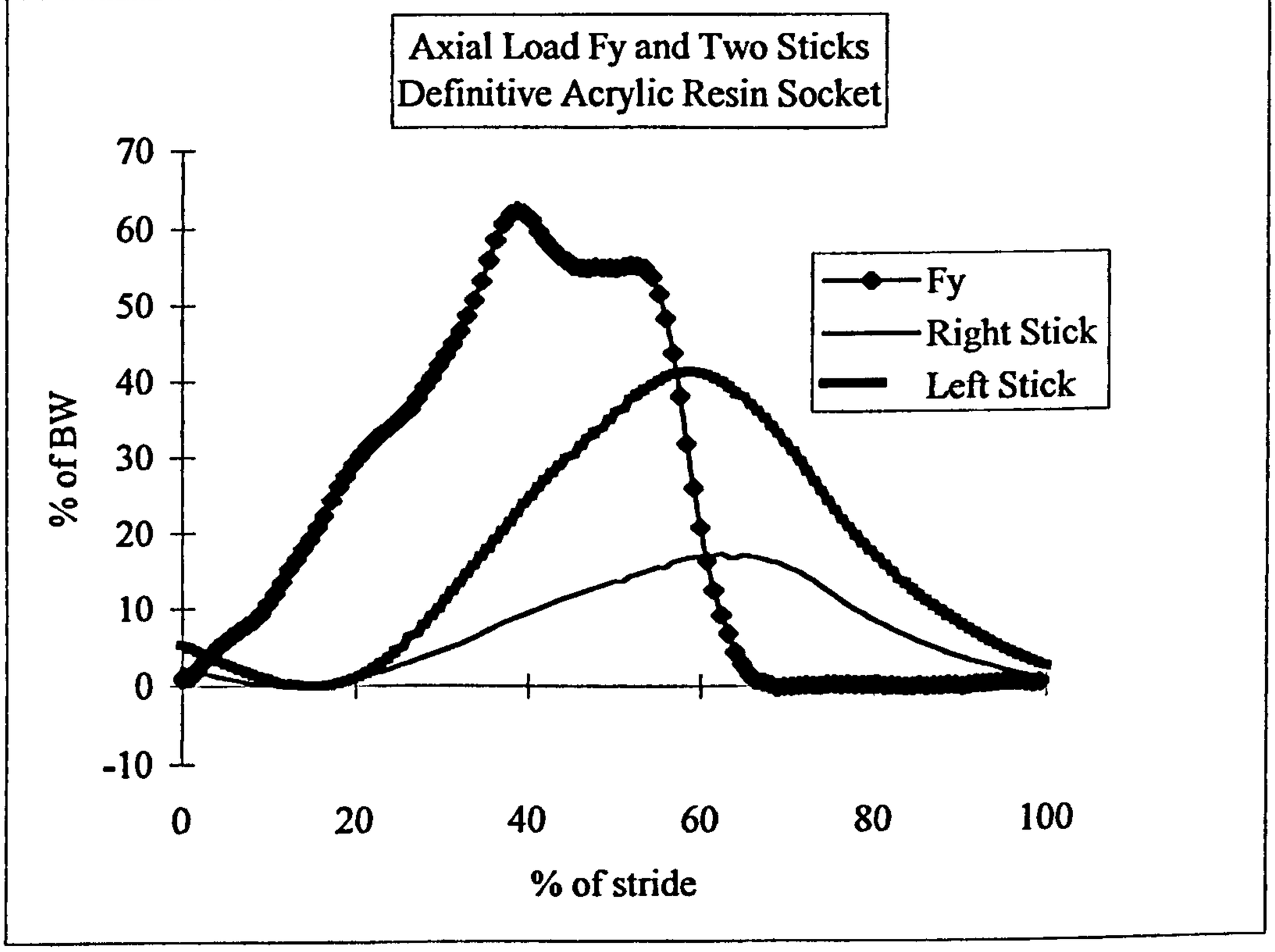

Figure 8.17: The same right amputee as above except using an acrylic resin socket close to the end of the rehabilitation process: the axial load Fy and the two sticks.

4. Ratio Ipsilateral to Contralateral. It should be constantly inferior to zero and the lower as possible to eliminate the ipsi walking aid.

The reported comments are the following:

The eight left transtibial patients loaded their two walking aids approximately equally (ratios ipsi WAGRF/PGRF and contra WAGRF/PGRF were respectively 0.37, 0.32). The six right amputees put a higher load on the contralateral walking aids (same ratios: 0.42, 0.74). These results were divergent, but having only 14 subjects and such a large standard deviation, no firm conclusion could be reached. By increasing the sample size, it could be possible to establish if the lower stability of the assisted gait requires the patients to improve the balance of the load on the walking aids between the two sides. It should also be interesting to take account of their handed-ness.

The ratio ipsi versus contralateral sticks was also totally different between left and right amputees: 1.02 for left amputees, the tested subjects put the same load on both sides and 0.57 for right amputees, the tested subjects put half load on the ipsi stick in comparison with the contra stick. Although, the sample was small, the difference was so large that it could be any explanation such as: upper limb asymmetry, amputation on the side of the neuro-physiological main lower limb but no references have been found concerning this problem.

Trying to descry an answer, another suggestion was made and is now discussed. Following the anthropometric method described by Winter (1994a), table 8.19, showing the ratio stump length/opposite shank length, is presented. The statistical analysis of this table shows that there was no statistical difference ($p = 0.07$) for the ratio between right and left side but obviously, a large statistical difference ($p < 0.000$) for the two ratios stump length/shank length. It was possible to identify a trend: when the ratio stump/shank length increased, the ratio ipsi/contra decreased (left side) and increased (right side). However, two patients out of 14 had a non-expected behaviour: the patients TTL12 and TTR5. Thus, there were no evident explanations but the sample was small and biased data could have been recorded.

Another suggestion should be born in mind that only axial load on the two

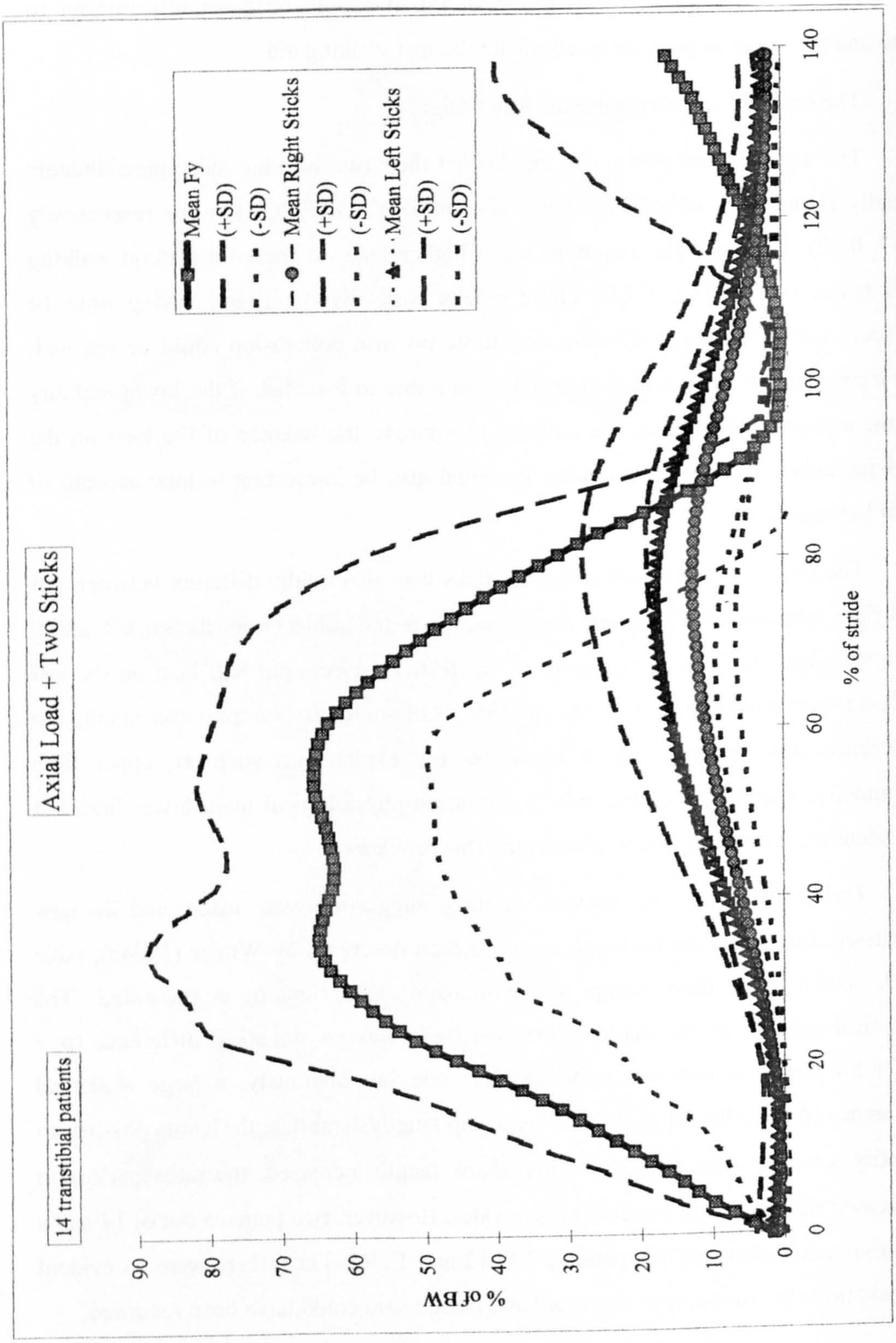

Figure 8.18: Mean results of 14 transtibial patients showing axial load Fy and two sticks (% of BW vs. % of stride, ± SD). See text for more details.

walking aids was recorded and researchers in this field assert that A/P bending moment exerted on the cane had a significant amount (Opila, 1985). Thus, instrumented walking aids with more than one recorded channel should exhibit more informative results.

Table 8.18 shows the two stages of rehabilitation (9 TTP, series 3), splitting the left amputees from the right one with a difference, at one stage of the rehabilitation, between left and right loads on the walking aids being not significant ($p = 0.16$).

However, the load decrease on the sticks when the patients wore an ARS instead of a GS was strongly significant ($p = 0.05$) but corresponded to both a different socket and stage of rehabilitation. For example, figures 8.16 and 8.17 show the ground reaction force values for the female patient TTR13 who was a right amputee (fig 8.16 = GS, fig 8.17 = ARS). She pushed more on her contralateral stick, which was expected. From GS to ARS, the PGRF was 55 to 65 % of BW, the axial load on the left stick was increased (38 to 42 % of BW) but decreased (21 to 17) on the right stick. The gait rate was also increased. However, the inter-patient behaviour was very changeable in this respect.

If the study of two sticks versus two canes is performed (10 TTP, series 2), the results are shown in table 8.18.

If the five right amputees were isolated by comparing the behaviour with two sticks with that of two canes, the results were divergent. The load on the right sticks was 1.67 (SD = 0.7) and 2.85 $N.kg^{-1}$ (SD = 1.2) on the left sticks. This difference was significant ($p = 0.03$). On the other hand, the load gap between a right cane (1.39 $N.kg^{-1}$; SD = 0.5) and a left one (1.72 $N.kg^{-1}$, SD = 0.7) was not significant ($p = 0.21$). If the same study was done for the five left amputees of the second series, the results were also divergent. The load on the left stick was 1.64 (SD = 0.9) and 1.59 $N.kg^{-1}$ (SD = 0.5) on the right stick. This difference was not significant at $p = 0.21$. The load on the left cane was 1.22 (SD = 0.3) and 1.48 $N.kg^{-1}$ (SD = 0.4) on the right cane. Here also, it was not significant at $p = 0.15$.

A first conclusion could be expressed from this study concerning both the PGRF and the WAGRF: all data showed a large inter-subject variability in the use of

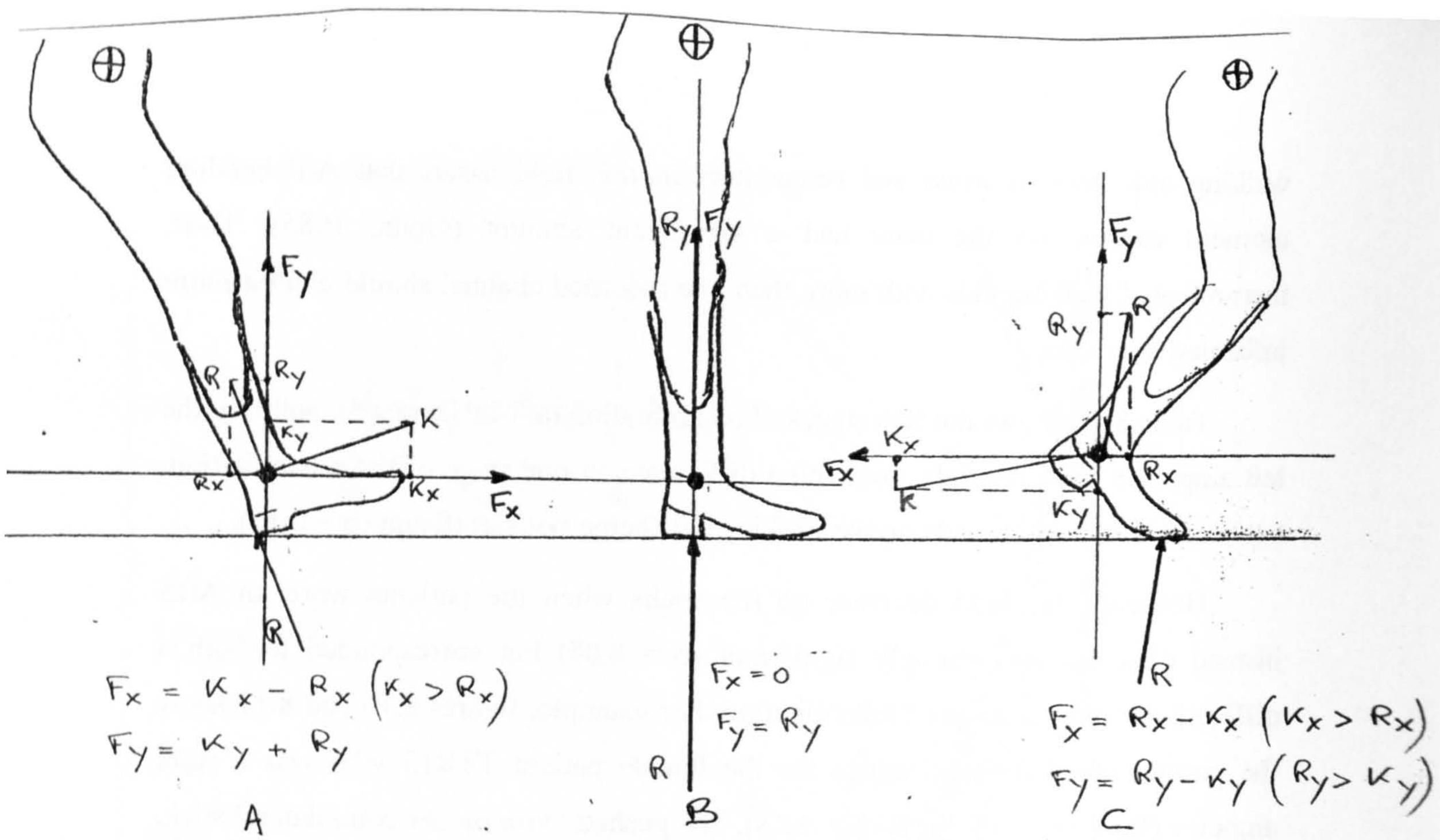

Figure 8.19: The diagram of the forces of a transtibial prosthesis and residual limb showing the A/P shear force and axial load acting from the ground R and the amputee K on the artificial ankle axis and recorded through the transducer by projection on the axes X and Y.
(A, heel strike; B, mid stance; C, push-off) extracted from Hughes & Taylor (1985).

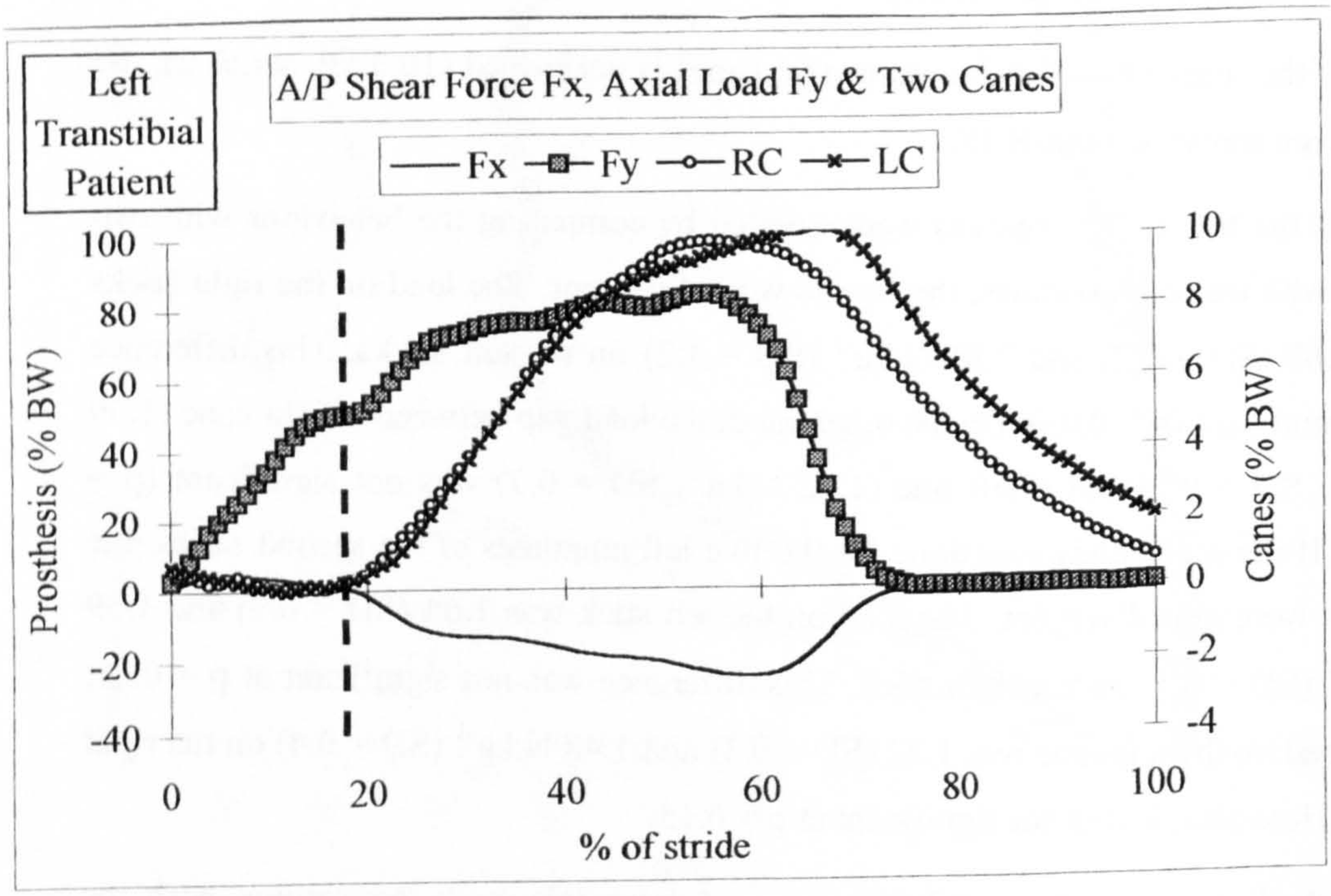

Figure 8.20: One stride of the transtibial patient TTL7 showing axial force Fy and A/P shear force Fx. *Dotted vertical line*: Fx = 0, inflection of Fy slope and beginning of load on the two canes: the prosthetic shank tube should be approximately vertical.

gait assistive units, as already noticed by Murray *et al.* (1969). It would seem that each subject had spontaneously adapted any strategy according to his handicap to minimise effort, to reduce pain and energy cost. However, it is only a feeling, nothing in the present research could prove what the reason was.

To illustrate these comments, figure 8.18 shows the mean results of 14 transtibial patients: axial load Fy and the two walking aids. Results are expressed in percentage of BW versus percentage of stride. Because there was a time interval between axial load and sticks' chronology, figure 8.18 shows more than one stride. This time interval will be discussed in the following section 8.5.7. The following comments could be made: mean maximum prosthetic axial load was 65 % of BW while the mean maximum axial load applied on the two sticks was about 12 to 15 % of BW for each sticks. Therefore, the stick axial loads were not equal on both sides (higher maximum value, right side than left side) but the series considered mixes right and left amputees. It could also be shown a relative high standard deviation (SD) for stick axial loads. Due to this large SD, any definitive conclusion is doubtful. As already stated, further research is needed with the following methods:

- to use improved instrumented walking sticks adding at least one channel such as A/P bending moment;

- to take account of heel strikes and toe offs of the sound limb;

- to expand the series of patients, however, due to the high level of inter-patient gait behaviour, to establish any trend or common gait pattern should be difficult.

8.5.3 The fore-aft shear force

The anterio-posterior shear force Fx begins to be positive at heel-strike and during early prosthetic stance then negative during the forward acceleration of the body at prosthetic late stance phase. According to the frame of reference adopted (see section 2.6.3.3), the direction of the recorded forces are only horizontal when the shank tube is vertical. An anterio-posterior force diagram is shown in figure 8.19: axial load Fy and Fx shear force, at early stance, mid and late prosthetic stance phase. What the Villiers Pylon Transducer records is the algebraic sum of these two forces projected on the two axes X and Y. Fx changed sign approximately when the

ANTERIO - POSTERIOR POSITIVE SHEAR FORCE (Fx+)									
	Series Descriptions	Mean Fx $N.kg^{-1}$		SD		p value	NS not significant S significant at $p \leq 0.05$	Range	
Series 1a	30 TTP	0.35		0.14				0.04 ; 1.46	
Series 2	10 TTP 2S vs. 2C	2S 0.37	2C 0.49	2S 0.18	2C 0.26	0.05	S	2S 0.21 0.83	2C 0.30 1.15
Series 3	9 TTP GS vs. ARS	GS 0.30	ARS 0.36	GS 0.23	ARS 0.15	0.13	NS	GS 0.04 0.82	ARS 0.20 0.66
Series 4	14 TTP	0.36		0.18				0.10 ; 0.83	

Table 8.20: The range of results of mean anterio-posterior transducer shear force positive (Fx-) for the different series of transtibial subjects, expressed in $N.kg^{-1}$

ANTERIO - POSTERIOR NEGATIVE SHEAR FORCE (Fx-)									
	Series Descriptions	Mean Fx- $N.kg^{-1}$		SD		p value	S significant at $p \leq 0.05$	Range	
Series 1a	30 TTP	1.63		0.41				0.79 ; 2.31	
Series 2	10 TTP 2S vs. 2C	2S 1.67	2C 1.79	2S 0.48	2C 0.38	0.13	S	2S 0.81 2.28	2C 1.61 2.31
Series 3	9 TTP GS vs. ARS	GS 1.22	ARS 1.62	GS 0.41	ARS 0.45	0.01	S	GS 0.83 0.99	ARS 2.18 2.21
Series 4	14 TTP	1.52		0.47				0.81 ; 2.28	

Table 8.21: The range of results of mean anterio-posterior transducer shear force negative (Fx-) for the different series of transtibial subjects, expressed in $N.kg^{-1}$

prosthetic shank tube was in the vertical position. This position of Fx zero was therefore coincident with the increase of the vertical PGRF and took place at the end of the early stance phase: 27 % of the stride, 39 % of the PSP. It is shown on the *dotted vertical line* in figure 8.20. The vertical position of the prosthetic shank tube corresponds to an inflection of the increasing slope of the axial load Fy (top of the *dotted vertical line* in figure 8.20). This figure represents one stride of the patient TTL7.

For all patients (30 patients, series 1a) in all recorded trials, the maximum positive shear force (Fx +) varied among 0.038 $N.kg^{-1}$ (patient TTL7, GS with two S) and 1.146 $N.kg^{-1}$ (patient TTL8, GS with two C). The average was 0.35 $N.kg^{-1}$ (SD = 0.14). This standard deviation indicated a high dispersion of values. The results are shown in table 8.20.

If a comparison of the maximum anterio-posterior shear force in positive direction was performed when the subjects were at two steps of the rehabilitation treatment, using a GS and an ARS (9 TTP, series 3, see table 8.20). The positive Fx difference became respectively 0.3 and 0.36 $N.kg^{-1}$. The difference was not statistically significant ($p = 0.13$).

The maximum anterio - positive shear force observed according to the different assistive walking devices used (10 TTP, series 2, see table 8.20) was about the average of 0.37 $N.kg^{-1}$ (SD = 0.18), with sticks and 0.49 $N.kg^{-1}$ (SD = 0.26), with canes. The difference was significant only at the level $p = 0.05$. If the oldest patient TTL9, who was the only patient to decrease Fx positive, was eliminated, the Fx gap became 0.406 $N.kg^{-1}$ (SD = 0.28) and 0.641 $N.kg^{-1}$ (SD = 0.36). The difference (35 %) was moderately significant ($p = 0.02$) and could be related to the reduced feeling of stability caused by the canes compared to sticks. For the nine patients of the series 3, the gait pattern was not homogenous: 4 patients out of 9 have increased the Fx value while 5 out of 9 have decreased. In both cases, the difference was of the range of 20 %.

However, for the 14 subjects of the series 4, the low value of the maximum anterior shear force was significant: 0.36 $N.kg^{-1}$, largely inferior to the mean values

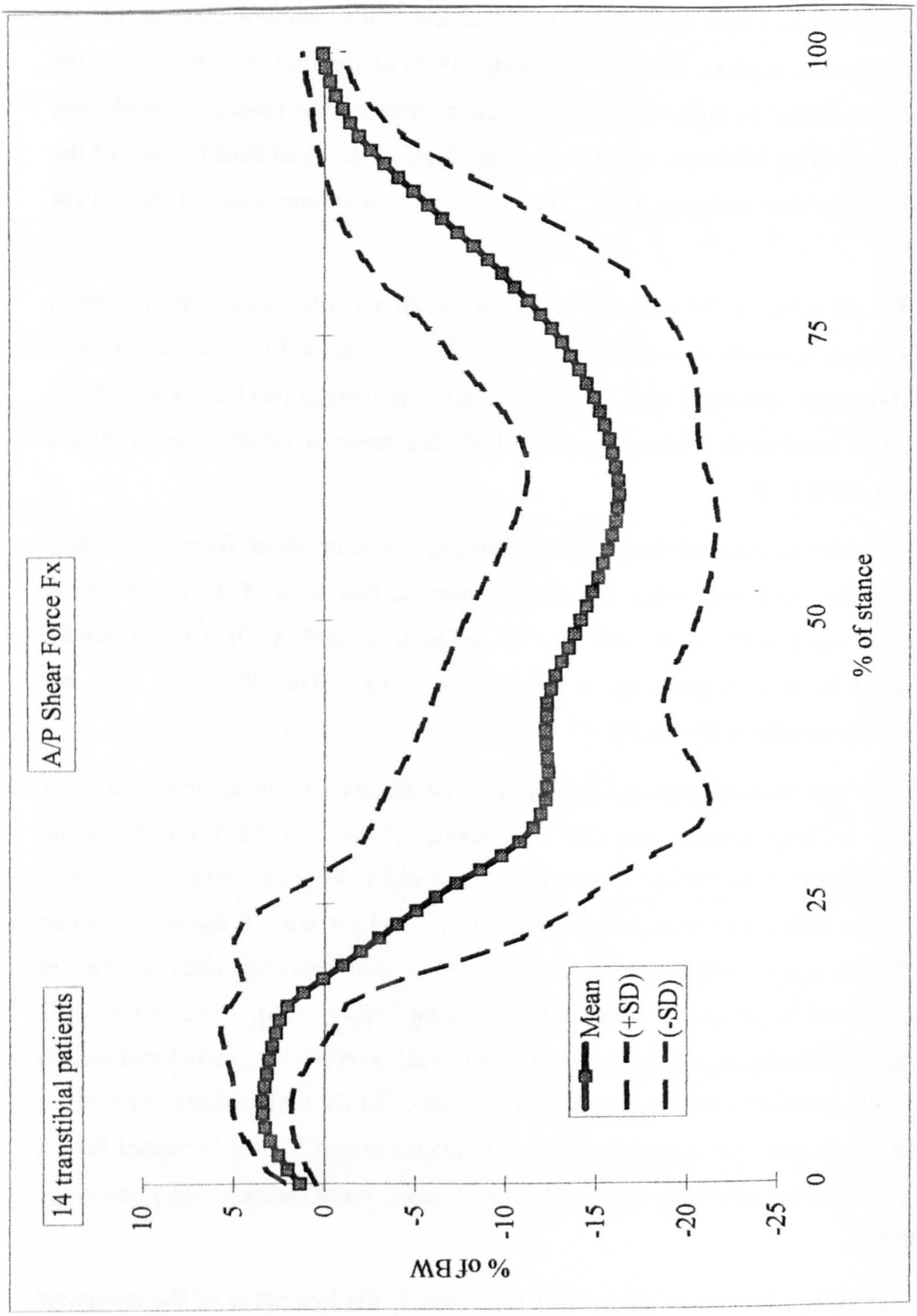

Figure 8.21: Mean results of 14 transtibial patients showing A/P shear force (% of BW vs. % of stance, ± SD), positive at early prosthetic stance phase and negative at late prosthetic stance phase (see text for comments).

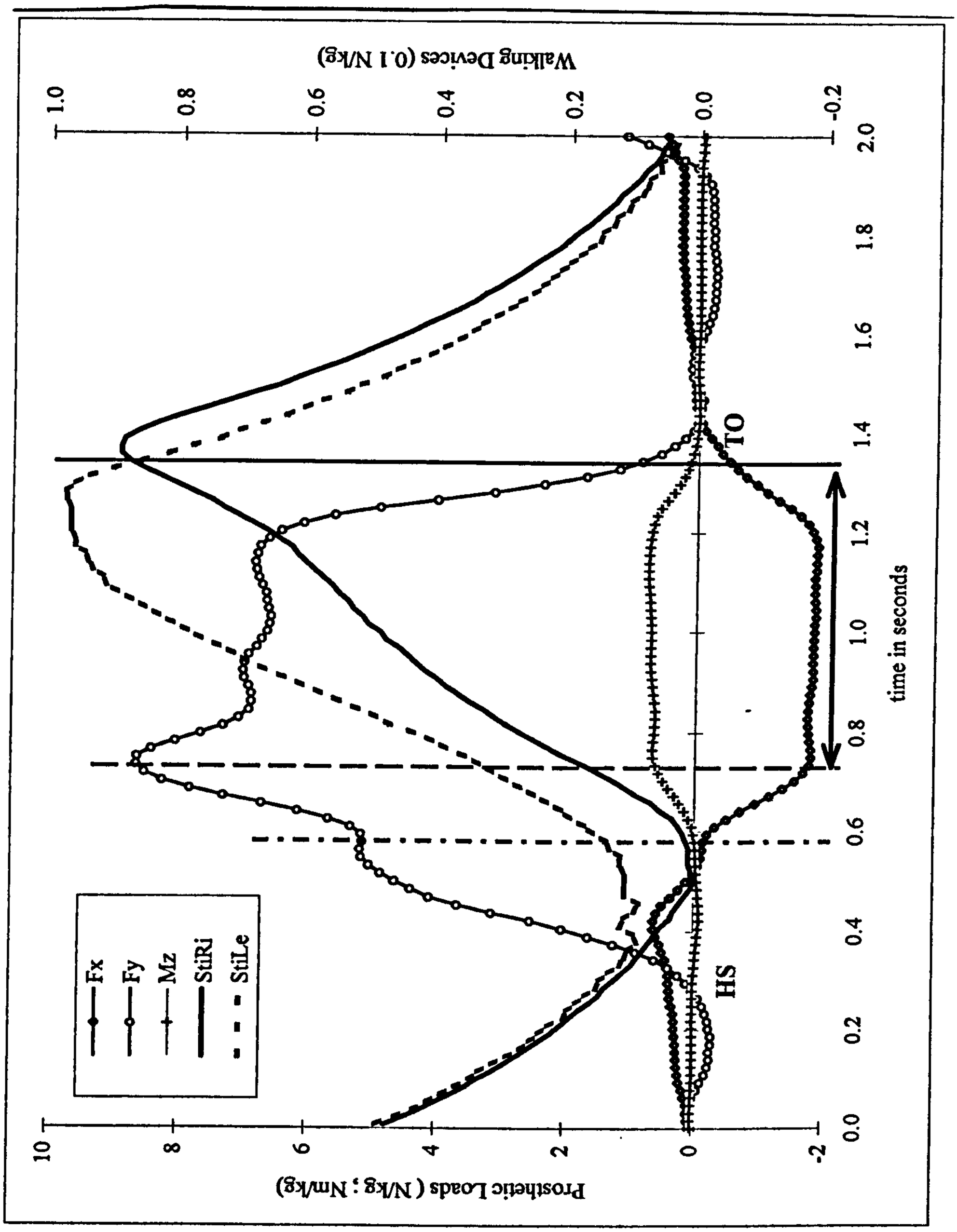

Figure 8.22: One stride of a right transtibial patient (TTR1) showing A/P shear force Fx, prosthetic ground reaction force Fy, A/P bending moment Mz and the forces transmitted by the walking aids in N or N.m per unit mass (N or $N.m.kg^{-1}$).
The heel strike (HS) and the toe-off (TO) instants are shown.
Dotted vertical line: Fx and Mz = 0, inflection of Fy and beginning of load on the two sticks, the prosthetic shank tube is approximately vertical (see figure 8.20).
Dashed vertical line: Fx and Mz = max., Fy = max., the subject starts to push-off.
Solid vertical line: Fx and Mz = decreasing, Fy = decreasing. The subject was in maximum load on the opposite stick to the amputated side. He was finishing his push-off on the prosthesis but he was still pushing on the two sticks.

instability created by the lower supportive devices changed the behaviour of the sound limb. It is also important to notice that the high value of the standard deviation exhibited a large inter-subject dispersion of the results. In other words, the patients had a full range of gait patterns. Faced with such a large discrepancy of results having the following range: 0.81 to 1.61 $N.kg^{-1}$ (from 2S to 2C, patient TTR5) and 2.17 to 2.31 $N.kg^{-1}$ (from 2S to 2C, patient TTL7), no conclusion was possible (see table WIII.5f, in appendix 11.VIII.5).

To illustrate these considerations, figure 8.21 shows the mean results in A/P shear force Fx, from 14 transtibial patients. Maximum Fx positive, at early prosthetic stance phase, was about 3 % of BW while Fx negative, at late prosthetic stance phase, was 17 % of BW.

8.5.4 The flexion - extension bending moments at the artificial ankle joint

In the sagittal plane, the behaviour of a prosthetic ankle during gait is equivalent to that of a normal ankle. A plantar flexion moment (Mz-) commences in early prosthetic stance. Then, at the end of the early prosthetic stance phase, when the shank tube is in the vertical position, A/P bending moment Mz becomes 0 (A/P shear force Fx also) while axial load Fy is in the middle of its rising grade with an inflexion of the slope. This is shown in figure 8.22. It is completed from figures 8.18 and 8.20. The *dotted vertical line* in figure 8.22 shows the vertical of the shank tube: Fx and Mz are zero. A dorsi flexion moment (Mz+) follows whose values are maximal from mid stance phase (*dashed vertical line* in figure 8.22) to the late stance phase when the foot is close to toe off (TO) at the push off event. Thus, the positive dorsiflexion moment has a flattened shape with a duration equivalent of negative shear force (22 % of a stride and 32 % of the PSP) and it stops at toe-off (*solid vertical line* in figure 8.22).

For the thirty patients and all trials, normalised to body mass, the average maximum bending moment was -0.06 N $m.kg^{-1}$ (Mz-, SD = 0.02, minimum 0.01, max. 0.17) and 0.62 N $m.kg^{-1}$ (Mz+, SD = 0.11, min. 0.18, max. 1.02), as shown in tables 8.22 and 8.23. Thus, plantar flexion bending moments were close to zero and there could therefore be many uncertainties. It was markedly less than the values

ANTERIO - POSTERIOR NEGATIVE BENDING MOMENT (Mz-)							
	Series Descriptions	Mean Mz- $N.m.kg^{-1}$		SD		p value	NS not significant S significant at $p \leq 0.05$	Range	
Series 1a	30 TTP	0.06		0.02				0.01 ; 0.17	
Series 2	10 TTP 2S vs. 2C	2S 0.07	2C 0.08	2S 0.04	2C 0.02	0.13	NS	2S 0.02 0.16	2C 0.04 0.14
Series 3	9 TTP GS vs. ARS	GS 0.05	ARS 0.07	GS 0.04	ARS 0.03	0.05	NS	GS 0.01 0.04	ARS 0.15 0.16
Series 4	14 TTP	0.06		0.02				0.01 ; 0.16	

Table 8.22: The range of results of mean negative anterio-posterior bending moment at the artificial ankle level for different series of transtibial subjects, expressed in $N.m.kg^{-1}$

ANTERIO - POSTERIOR POSITIVE BENDING MOMENT (Mz+)									
	Series Descriptions	Mean Mz $N.m.kg^{-1}$		SD		p value	NS not significant S significant at $p \leq 0.05$	Range	
Series 1a	30 TTP	0.62		0.11				0.18 ; 1.02	
Series 2	10 TTP 2S vs. 2C	2S 0.57	2C 0.64	2S 0.14	2C 0.09	0.11	NS	2S 0.29 0.77	2C 0.51 0.80
Series 3	9 TTP GS vs. ARS	GS 0.39	ARS 0.58	GS 0.17	ARS 0.17	0.005	S	GS 0.22 0.78	ARS 0.43 0.98
Series 4	14 TTP	0.59		0.14				0.22 ; 0.98	

Table 8.23: The range of results of mean positive anterio-posterior bending moment at the artificial ankle level for different series of transtibial subjects, expressed in $N.m.kg^{-1}$

found in the literature: -0.2 to 1 N m.kg^{-1} (Winter & Sienko, 1988). This may correspond to the fact that the studied subjects, at this stage of rehabilitation, were compelled to be cautious with their stump. They required using strongly two gait assistive aids to minimise any anterio-posterior loads on the residual limb.

In the follow up rehabilitation test (9 TTP, series 3, from GS to ARS, table 8.22), the change in the plantar flexion moment was -0.05 N m.kg^{-1} (SD = 0.04) to -0.07 N m.kg^{-1} (SD = 0.03). This difference was significant only at a level of p = 0.05. For the dorsi flexion moment, 0.39 N m.kg^{-1} (SD = 0.17) to 0.58 N m.kg^{-1} (SD = 0.17) was found (table 8.23). This difference was strongly significant (p = 0.005) and showed an increase of 48 %. Thus, from the beginning to the end of the early stage of the rehabilitation treatment, there was a significant improvement in the values of anterio-posterior ankle bending moments in the prosthetic stance phase. For the negative bending moment, all the patients except one had the same gait pattern: an increase of 43 %. The only subject (TTL12) who decreased his negative bending moment did it for a very small value as follows: from -0.06 to -0.05 N m.kg^{-1}. Concerning the positive bending flexion moment, all the patients expressed a higher moment from GS to ARS with the following values: from 0.22, 0.43 N m.kg^{-1} (not the same patient) to 0.78, 0.98 N m.kg^{-1} (patient TTL11).

For series 2 (10 TTP, 2S versus 2C, table 8.22), the difference for the plantar flexion moment was -0.07 N m.kg^{-1} (SD = 0.04) to -0.08 N m.kg^{-1} (SD = 0.02). This difference was not significant (p = 0.13, 14 %). For the dorsi flexion moment, 0.57 N m.kg^{-1} (SD = 0.14) to 0.64 N m.kg^{-1} (SD = 0.09) was found, equal to 12 % (table 8.23). This difference was not significant (p = 0.11). This statistically negative difference was logical, considering the decrease of the load on the canes, both plantar and dorsi flexion moments should increase. Probably, the unstable canes forced the patient to shorten the early stance phase. Concerning the plantar flexion moment, at early prosthetic stance phase, eight patients out of ten had increased the values, from 0.29, 0.51 N m.kg^{-1} (subject TTR5) to 0.77, 0.8 N m.kg^{-1} (subject TTR6) with a large range. The two patients who had decreased their plantar flexion moment (subjects TTL7 and TTL2). About the subject TTL7, it could only be noticed that he wore his acrylic resin socket for two days and the patient was not accustomed to his new

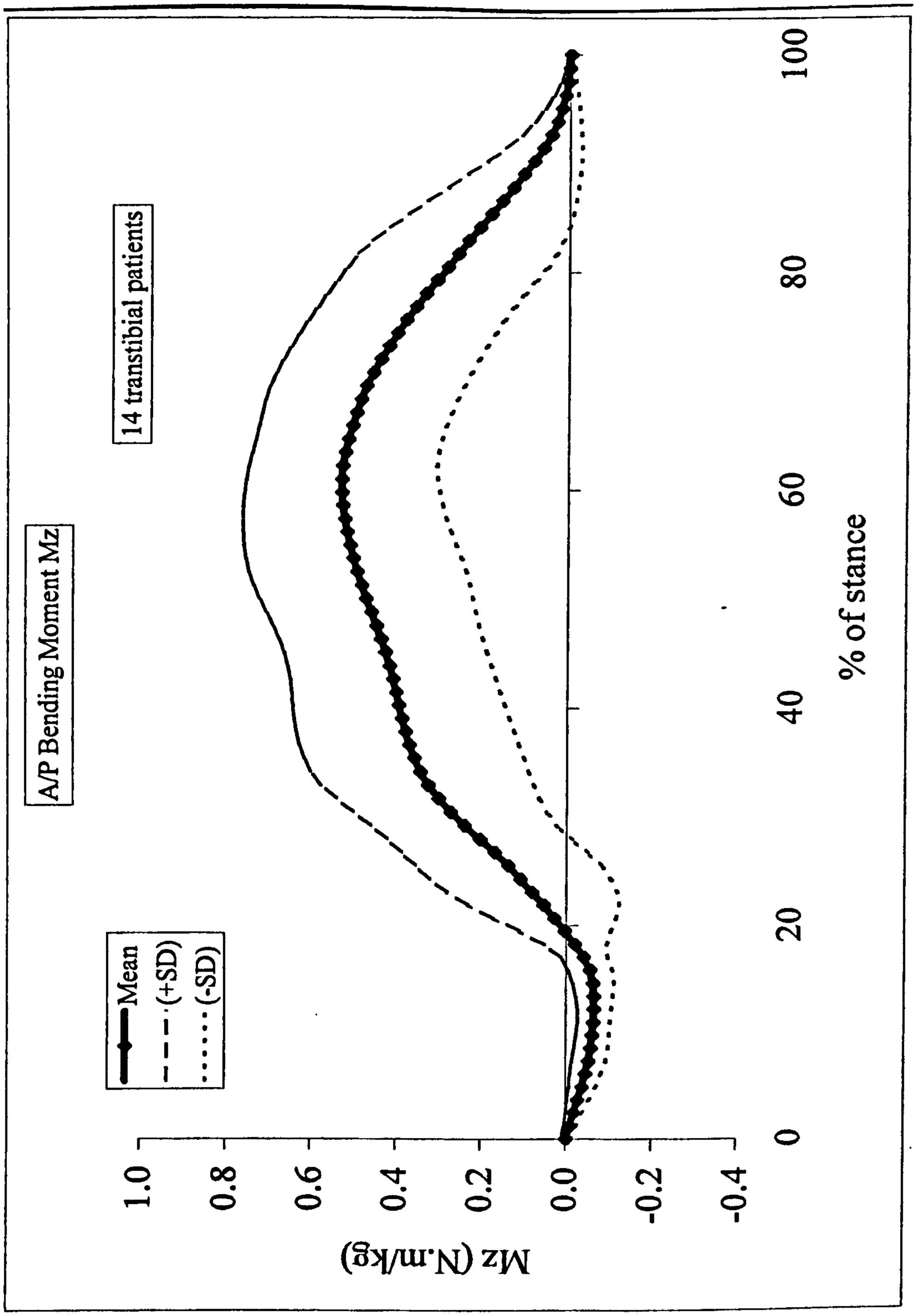

Figure 8.23: Mean results of 14 transtibial patients showing the A/P bending moment (N.m/kg vs. % of stance, ± SD), negative (plantarflexion) at early prosthetic stance phase and positive (dorsiflexion) at late prosthetic stance phase.

socket. Concerning the subject TTL2, she had pain into her stump due to reflex sympathetic dystrophy. Seven subjects out of 9 had increased their plantar flexion bending moment, one showed an equal value while 2 had decreased it (subjects TTL7 and TTL8). For the subject TTL8, it was consistent with the results in axial load (see section 8.5.2.1) on the advice of the physiotherapist after specific training to decrease all stresses applied on the residual limb.

However, *all the values of anterio-posterior bending moments were always lower than those found in the literature* whatever subjects were: young traumatic (Winter & Sienko, 1988) or traumatic or dysvascular elderly amputees (Lemaire *et al.* 1993; Hubbard & McElroy, 1994).

To illustrate these considerations, figure 8.23 shows the mean results in A/P bending moments from 14 transtibial patients. Mz negative, plantar flexion, at early prosthetic stance phase, is about 0.1 N m/kg while Mz positive, dorsiflexion, at late prosthetic stance phase, is approximately 0.5 N m/kg.

The three other components of the gait, namely M/L shear force Fz, M/L bending moment Mx and transverse torque My are shown, as example in appendix 11.VIII.7.

8.5.5 Temporal parameters: Chronology of gait events and loads during transtibial amputees ambulation

The prosthetic stance phase (PSP) is one of the main temporal parameters to study because it strongly reflects of the gait pattern and the way of using the artificial limb by the patient. Coupling the duration of this phase with the PGRF will be a strong assessment of the gait behaviour of a tested subject. For the 30 subjects (series 1a, table 8.24), the PSP duration, averaging all tests, was 1.42 s (SD = 0.31). If this value is compared with the mean duration of the gait rate yielded in section 8.5.1, namely 1.96 s.stride^{-1} (see table 8.15), one can conclude that the PSP occupies 72 % of the total duration of the prosthetic stride. This is more than for normal subjects, since classically, the stance phase occupies 60 % to 62 % to the stride (Hughes & Taylor, 1985; Lehmann *et al.* 1992) depending on walking speed. Most of the papers, shown as references, do not report any information about this ratio, the results being

	Prosthetic Stance Phase (PSP) duration
30 transtibial patients (series 1a)	1.42 s (SD 0.31)
10 transtibial patients (series 2)	1.32 s (SD 0.31)
9 transtibial patients (series 3)	1.61 s (SD 0.37)
14 transtibial patients (series 4)	1.35 s (SD 0.35)

Table 8.24: The average Prosthetic Stance Phase duration for different transtibial subjects, expressed in second, with the corresponding standard deviation

SUBJECT CODE			MEAN			MEAN			MEAN	MEAN
	2S	2C	2S + 2C	2S	2C	2S + 2C	2S	2C	2S + 2C	2C
	PSP / PST	PSP / PST	PSP / PST	SSP / PST	SSP / PST	SSP / PST	PSP / SSP	PSP / SSP	PSP / SSP	CSP / CST
TTL2	0.70	0.77	0.73	0.80	0.84	0.82	0.87	0.92	0.89	0.83
TTR1	0.86	0.71	0.79	0.83	0.80	0.82	1.04	0.88	0.96	0.80
TTL8	0.71	0.81	0.76	0.81	0.73	0.77	0.88	1.11	0.99	0.72
TTL9	0.70	0.70	0.70	0.79	0.80	0.79	0.88	0.88	0.88	0.79
TTR6	0.72	0.69	0.71	0.76	0.75	0.76	0.94	0.92	0.93	0.75
TTR5	0.61	0.64	0.62	0.85	0.88	0.87	0.71	0.72	0.72	0.88
TTR4	0.61	0.61	0.61	0.83	0.69	0.76	0.73	0.88	0.81	0.69
TTR3	0.68	0.68	0.68	0.83	0.80	0.81	0.82	0.85	0.84	0.80
TTL7	0.70	0.71	0.71	0.73	0.74	0.73	0.97	0.96	0.96	0.73
TTL10	0.76	0.79	0.77	0.75	0.77	0.78	0.96	1.02	0.99	0.77
MEAN	0.70	0.71	0.71	0.80	0.78	0.79	0.88	0.91	0.89	0.81
SD	0.07	0.06	0.04			0.03			0.09	
p			0.06						0.11	
Ideally from literature		0.60				unknown			unknown	0.63 or 0.58

Table 8.24a: Different ratios are shown, from left to right: PSP/PST, 2S then 2C and mean 2S + 2C; SSP/PST, 2S then 2C and mean 2S + 2C; PSP/SSP, 2S then 2C and mean 2S + 2C. The last column shows the time ratio between canes stance phase and canes stride (CSP/CST). For each column, the mean value is shown and for the mean of each row, the standard deviation and the p value. (see text for explanation)

PSP: prosthetic stance phase
PST: prosthetic stride time
SSP: stick stance phase

the most often standardised. Therefore, the patients had decreased the load on the prosthesis but had increased the duration of the prosthetic stance phase by comparison with the subjects gait pattern reported in the literature (Seliktar & Mizrahi, 1986; Winter & Sienko, 1988; Hubbard & McElroy, 1994).

The 10 patients of series 2 were found to show a PSP of 1.32 s (SD = 0.31) with 2 sticks and 1.38 s (SD = 0.19) with 2 canes (see table 8.24). The difference is not significant (p = 0.13). Among the ten patients, five increased their PSP, one did not change and 4 decreased it. Thus, it was not possible to conclude. However, asking the five patients who increased the PSP to express comments, the answers showed a lack of confidence on the equilibrium when using two canes versus two sticks. It also could be possible to refer to a lack of training about the use of this new set of walking aids.

The discrepancy of results was found large, from 0.92 s (2S), 0.90 s (2C, patient TTR4) to 2.13 s (2S), 2.41 s (2C, patient TTL10). The report of these values alone did not allow any conclusion, it seemed more interesting to study the prosthetic stance phase / prosthetic stride time ratio, as shown in table 8.24a. Using two sticks, the ratio was: 0.704 (SD = 0.07) and 0.709 (SD = 0.06) with two canes. This gap was not significant (p = 0.24). The patient TTR4 was found to show a PSP/PST ratio of 0.60 with two sticks and 0.61 with two canes. This is close to what it is found in the literature for amputees and healthy subjects gait (Hermodsson *et al.*, 1994b). The opposite patient TTL10 showed a PSP/PST ratio of 0.75 (2S) and 0.79 (2C). This was the maximum of the tested population but the patient information chart reported how much the patient suffered pain. Curiously, a patient who had stump pain wearing a socket did not minimise the PSP/PST ratio but he increased both prosthetic stance phase and stride time to reduce the dynamic and inertial effects of the gait. In other words, a patient with pain tended to minimise stresses of the stump onto the socket and vice versa, reducing his self-selected pace. The discussion concerning such a gait pattern is re-opened below when all the results will be summarised and discussed (see section 8.9).

The 9 patients of series 3 were found to show a PSP of 1.61 s (SD = 0.37) with a gypsum socket and 1.28 s (SD = 0.31) with an acrylic resin socket (see table 8.24).

SUBJECT CODE			MEAN			MEAN			MEAN	MEAN
	GS	ARS	GS + ARS	GS	ARS	GS + ARS	GS	ARS	GS + ARS	ARS
	PSP / PST	PSP / PST	PSP / PST	SSP / PST	SSP / PST	SSP / PST	PSP / SSP	PSP / SSP	PSP / SSP	SSP / SST
TTL11	0.81	0.72	0.78	0.85	0.71	0.79	0.95	1.01	0.98	0.71
TTL14	0.58	0.72	0.65	0.86	0.86	0.86	0.68	0.83	0.75	0.85
TTR3	0.70	0.68	0.69	0.80	0.83	0.81	0.87	0.82	0.85	0.82
TTR4		0.61	0.61	0.89	0.83	0.86	0.66	0.73	0.69	0.83
TTL2	0.83	0.70	0.77	0.83	0.80	0.82	1.00	0.87	0.94	0.80
TTL12	0.74	0.77	0.76	0.78	0.75	0.76	0.96	1.01	0.99	0.75
TTL8	0.72	0.68	0.70	0.76	0.86	0.81	0.95	0.79	0.87	0.88
TTR13	0.69	0.67	0.68	0.87	0.81	0.85	0.79	0.82	0.80	0.81
TTL7	0.77	0.70	0.74	0.90	0.73	0.84	0.85	0.97	0.89	0.73
MEAN	0.71	0.69	0.71	0.84	0.80	0.82	0.86	0.87	0.86	0.80
SD										
p										
Ideally from literature		0.60				unknown			unknown	0.63 or 0.58

Table 8.25: Different ratios are shown, from left to right: PSP/PST, GS then ARS and mean GS + ARS; SSP/PST, GS then ARS and mean GS + ARS; PSP/SSP, GS then ARS and mean GS + ARS. The last column shows the sticks stance phase versus sticks stride time ratio (SSP/SST). For each column, the mean values are shown (see text for explanation).

SUBJECT CODE	GS	ARS
	SSwP / SSP	SSwP / SSP
TTL11	0.18	0.41
TTL14	0.16	0.17
TTR3	0.26	0.21
TTR4	0.12	0.20
TTL2	0.21	0.24
TTL12	0.29	0.33
TTL8	0.32	0.13
TTR13	0.14	0.23
TTL7	0.10	0.37
mean	0.198	0.254

Table 8.26: The ratio between the sticks swing phase (SSwP) and the sticks stance phase (SSP), see text for comments.

This decrease had a strong statistical significance (p = 0.01). However, two patients had an opposite behaviour. They increased their PSP: the patient TTL4 (from 1.29 to 1.41 s = + 9 %, having a stump/opposite tibial length ratio of 0.1) and TTL12 (1.56 (GS), 2.06 (ARS) = + 31 %, stump/opposite tibial length ratio of 0.2). Both patients expressed the same reason: pain onto a short stump, especially at the end of the tibial crest.

As stated above, the PSP/PST ratio is interesting (see table 8.25): 0.71 with a GS at early rehabilitation treatment and 0.69 with an ARS just before the end of the stay-in hospital. Even prior to discharge from the Rehabilitation Centre, the PSP/PST ratio was more than that reported in the literature. Obviously, the rehabilitation treatment was not completed and performing other tests 6 months later, as Hubbard & McElroy (1994) did, should be important. The patient TTR4 was common in the two series 2 and 3. He was found to show the smallest PSP wearing a GS (1.11 s) or an ARS (0.92). He showed a PSP/PST ratio of respectively 0.59 and 0.60 (stump/opposite tibial length ratio = 0.35), close to the results reported in the literature. The patient TTL7 was the opposite, he showed a PSP/PST ratio of 0.76 (GS) and 0.70 (ARS, stump/opposite tibial length ratio = 0.1) which was over the mean PSP/PST ratio of the sample.

Combining the two series (14 TTP, series 4), the PSP/PST ratio, in percentage, is as follows:

14 TTP series 4	GS or ARS 2S	SD	GS or ARS 2C	SD
PSP s	1.3	0.3	1.4	0.4
PSP/PST %	70	7	71	6

The difference between two sticks and two canes was so small that it was impossible to conclude. However, the main comment it was possible to do was the following: ideally, the PSP/PST ratio should be 60 but it was at least 15 % more than other PVD amputees. Thus the PVD transtibial amputees, at early stage of the rehabilitation treatment, increased the prosthetic stance phase relative to the

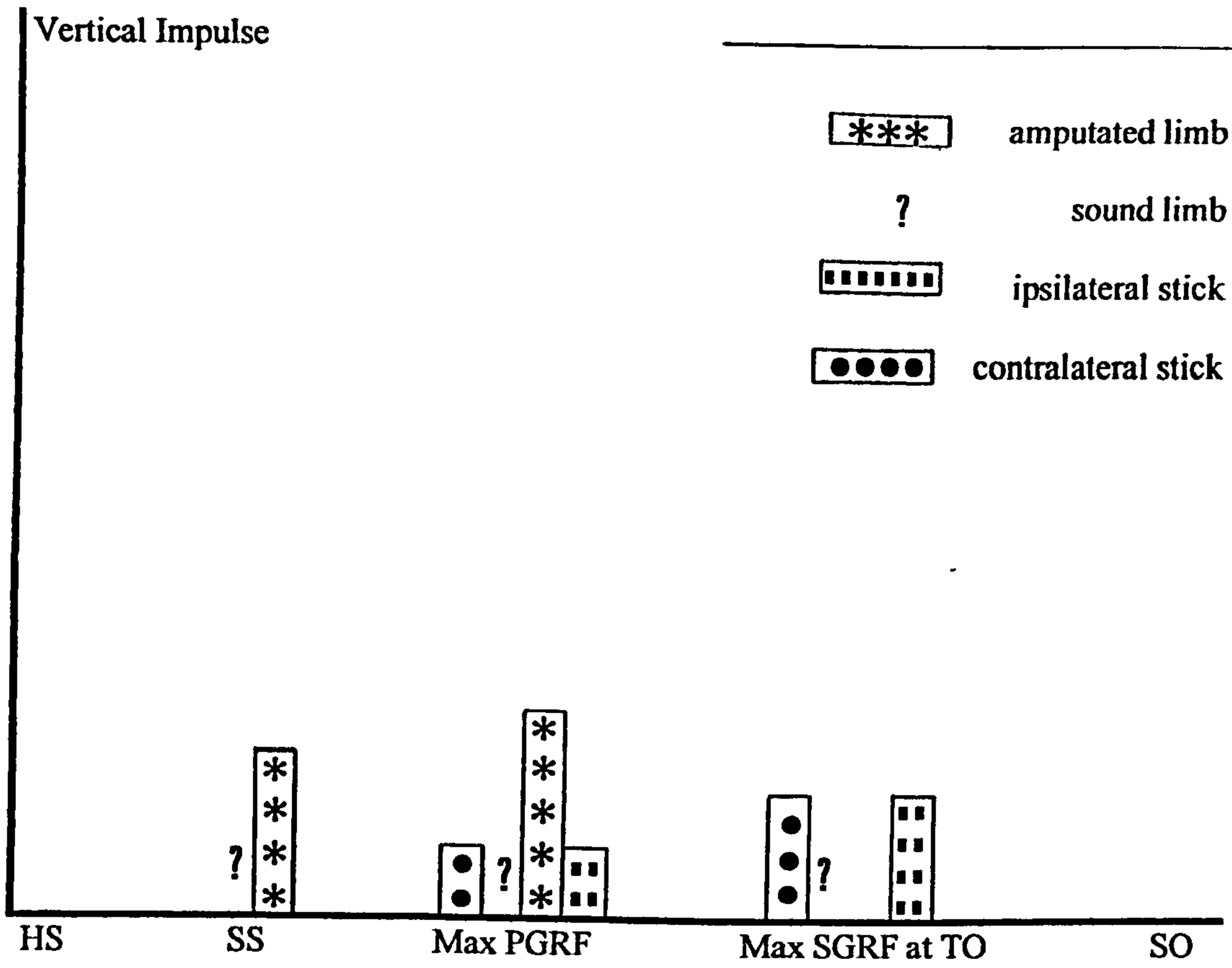

Figure 8.24: The vertical impulse histogram VIH (adapted from Opila, 1985) of the gait pattern 1 (see text for comments). The width of the columns is not significant. The height of the columns is only a mirror image of the axial loads and the gait pattern and does not show a particular value.
Figure 8.24 can be named VIH because it represents a force versus time, i.e., a stride.

prosthetic stride time, compared with PVD transtibial amputees tested more than 6 months after the date of the amputation (Hubbard & McElroy, 1994).

Averaging all tests (30 transtibial patients, series 1a), the duration of the sticks or cane stance phase was 1.54 s (SD = 0.38). The main factor to notice was that the duration of the SSP or CSP was 0.2 s greater than the PSP (a difference of 16 %). Obviously, the gait aids were used for something in addition to minimising the axial load on the prosthesis. The average time of stick-floor or cane-floor contact was 81 % of the total cane cycle. It exceeded published results: 63 % in Murray *et al.* (1969), 58 % in Winter *et al.* (1993) who reported that the longer duration positive A/P shear force reflects that the cane may be assisting in the forward propulsion of the body. Thus, the use of walking devices might subserve more than the obvious function of providing a prop for support but also provided forces to accelerate the body forward as stated by Murray *et al.* (1969).

The 10 patients of series 2 were found to show a SSP or CSP of respectively 1.5 s (SD = 0.2) and 1.51 s (SD = 0.4). Obviously, there was no difference, whatever the walking aids used. The patients had an equal aids floor contact duration. The discrepancy was large with a factor of 2: from 1.21 (2S), 1.02 (2C) to 2.21 (2S), 2.36 (2C). The study of different ratios was considered as interesting to compare results as shown in table 8.24. The results expressed in table 8.24 show an evident stability of these different ratios among the series of the 10 transtibial patients.

The 9 patients of series 3 were found to show a SSP of 1.88 s (SD = 0.36) with a GS and 1.46 s (SD = 0.26) with an ARS. This difference was strongly significant (p = 0.001). The diminution was 29 %. Therefore, the decrease of the walking aids stance phase was relevant to the improvement of the rehabilitation treatment. However, 2 patients out of 9 increased their stick stance phase: the SSP of the patient TTL12 rigorously followed the prosthetic stance phase which increased as stated above (ratio PSP/SSP = 1.01). The stick stance phase of the patient TTL8 increased after special rehabilitation training as explained in sections 8.5.2 and 8.5.3.

The different ratios were also studied as in series 2. They are shown in table 8.25. The main results are as follows:

BEST COPY

AVAILABLE

Variable print quality

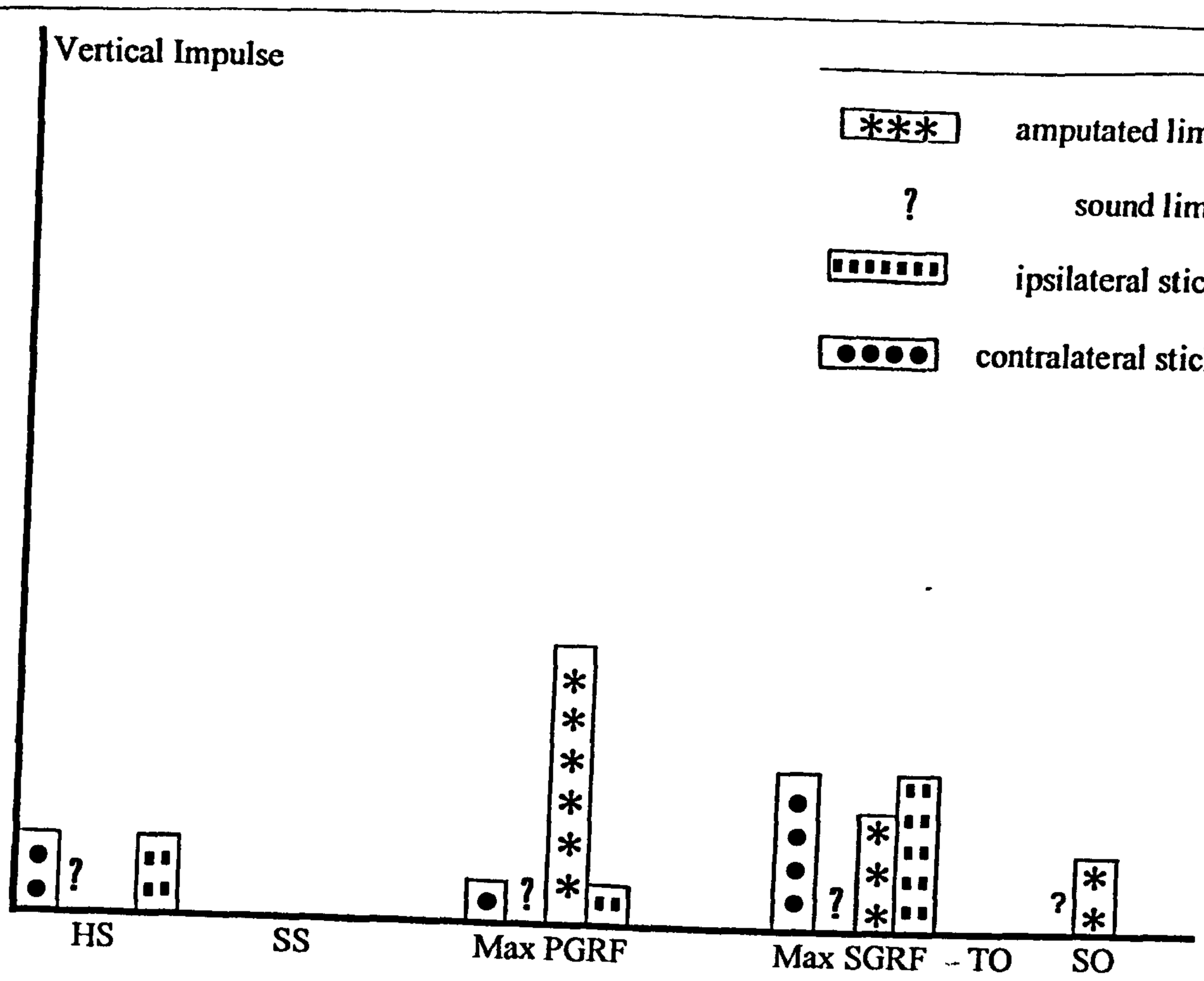

Figure 8.25: The vertical impulse histogram VIH (adapted from Opila, 1985) of the gait pattern 2 (see figure 8.24 for explanations and text for comments).

At SS: No PGRF, the sound limb ground reaction force is unknown

At TO: Prosthesis and sticks are in swing phase, the sound limb ground reaction force is also unknown

1) Even at the end of the rehabilitation treatment when the patients used a definitive acrylic resin socket, the ratio between the stick stance phase versus the stick stride time exceeded published results. In other words, the tested subjects applied axial load on the 2 walking aids during more time (+ 28 %) than traumatic amputees studied in the investigation conducted by Murray *et al.* (1969).

2) The ratio between the prosthetic and the stick stance phase was lower than 1 except for 2 patients out of 9. In other words, 7 patients out of 9 had a stick-floor contact duration longer than the prosthetic ground floor contact (+ 15 %). A thorough discussion concerning this statement will be conducted in section 8.9.4.

The sticks or canes swing phases were complementary to the stance phases. The results are as follows:

series 1a, 30 TTP:		0.39 s (SD = 0.13)	
series 2, 10 TTP:	2S	0.38 s (SD = 0.11)	
	2C	0.41 s (SD = 0.11)	p = 0.11, not significant
series 3, 9 TTP:	GS	0.35 s (SD = 0.08)	
	ARS	0.36 s (SD = 0.14)	p = 0.21, not significant.

However, these isolated values allow no definite conclusions. More important was the distribution of the walking aids cycle: the ratio between the swing and the stance sticks or canes phases. The results are shown in table 8.26. 7 patients out of 9 increased the part of the sticks swing phase in the walking aids cycle time. Two patients made the opposite: the patient TTL8 whose particular gait behaviour was known since section 8.5.2 and the patient TTR3 who was in a sudden rise of his Burger's disease. One patient (TTL14) did not change his walking aids behaviour. Thus, in a so small sample, finding any partial conclusion is difficult.

The most important results are presented now: the distribution of chronology between prosthesis and walking aids, showing the general gait pattern of the 30 transtibial patients tested.

The main question was to study the time intervals between, respectively, the beginning of the stance phase on walking aids (stick strike or cane strike) and

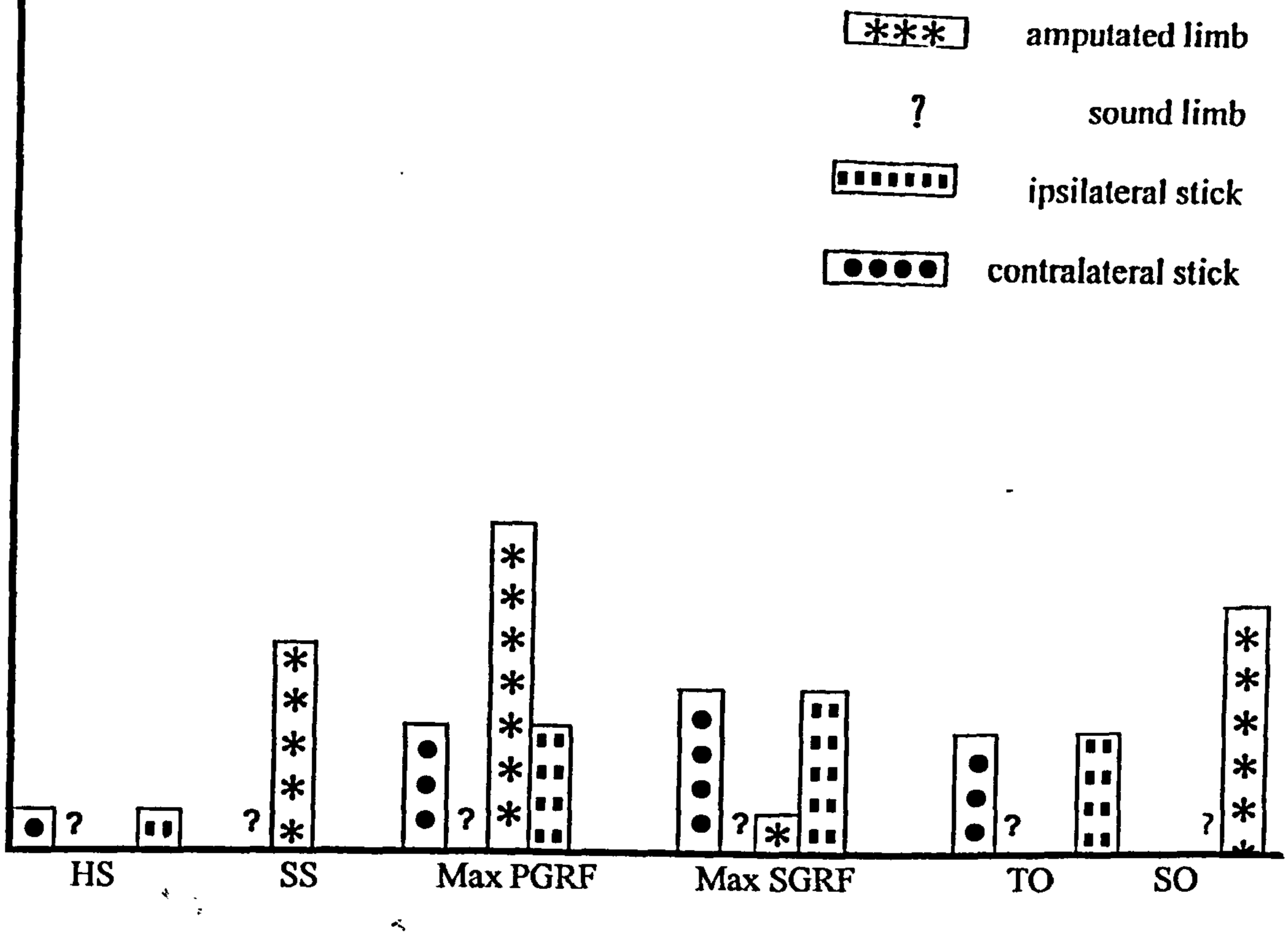

Figure 8.26: The vertical impulse histogram VIH (adapted from Opila, 1985) of the gait pattern 3 (see figure 8.24 for explanations and text for comments).

artificial limb (heel strike, HS), the end of the prosthetic stance phase (toe off, TO) and sticks or canes stance phase (sticks or canes off, SO and CO). It could therefore be possible to establish the different gait pattern lines (GPL shown in figure 8.8, section 8.4.1) and vertical impulse histograms (VIH, figure 8.9, section 8.4.1).

Among the 14 patients (23 trials) of the series 4 and thoroughly studied, it has been possible to established three main gait patterns:

1. HS close to SS or CS and TO close to SO or CO

The gait pattern line number 1 (GPL) concerned 6 patients out of 14 (42 %) performing 9 trials, (for scale, see caption in figure 8.9) and is as follows:

SSP	*SSwP*	*SSP*	
HS.SS.....TO..SO...HS.SS.....TO..SO...HS			
PSP	*PSwP*	*PSP*	*PSwP*

SSP and PSP had a steady chronology but SSP was shifted from PSP, overlapping TO and as previously stated, SSP was 1.25 PSP. From HS to SS (time interval between the beginning of the prosthetic and stick stance phases), there was 0.09 SSP. From TO to SO (time interval between the beginning of the prosthetic and stick swing phase), there was 0.22 SSP. The conclusion was that 90 % of the prosthetic stride time was performed applying axial load on walking aids.

The main remark concerning this gait pattern No 1 was to consider the overlap of the prosthetic and walking aids swing phases because, during this time interval, the subject had only one loading point: the contralateral sound limb. It was contained between SO and the following HS and the mean time for the six patients is 0.17 s (SD = 0.1), that was 0.07 prosthetic stride time.

During the time interval between HS and SS, the artificial limb was on load but not the walking aids. Nevertheless, it was not possible to establish with confidence if the opposite sound limb was floor-load contact. It was only a hypothesis. It was not possible to certify if this time interval was a one or a two loading points. This

comment identified one drawback of the conducted research: the lack of any knowledge concerning the sound limb.

The mean axial loads on the artificial limb and walking aids of the gait pattern 1 are shown under the form of a vertical impulse histogram (VIH, adapted from Opila, 1985) in figure 8.24.

2. SS before HS and close to TO, SO between HS and TO

The GPL number 2 concerns 5 patients out of 14 (36 %) performing 8 trials (same scale as above):

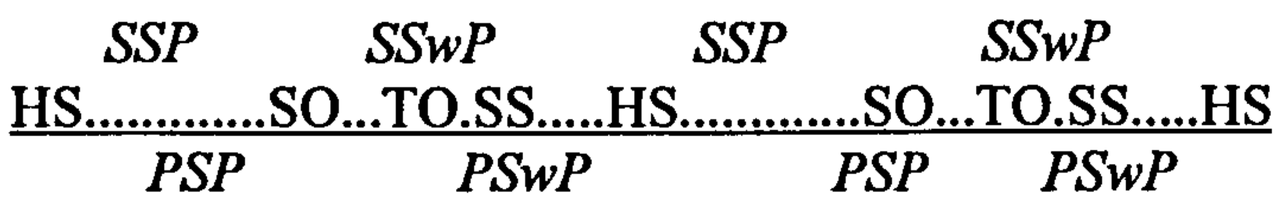

The stick and prosthetic stance phases had the same duration (PSP/SSP ratio = 0.99). SSP was more shifted from PSP than in pattern 1, overlapping the heel strike, that was a part of the SSwP occurred when the prosthesis was off floor contact. SS was close to TO (0.1 s after). In other words, walking aids had a floor contact during most of the PSwP. The heel strike occurred considerably before SO (time interval of 1.6 s) showing that SSwP happened when it was PSP. This gait pattern was self-selected by the patient to minimise the one point loading when both artificial limb and walking aids were off floor contact. The GPL of the gait pattern No 2 shows a one point loading only between TO and SS: 0.1 s = 0.04 prosthetic stride time. Here also, it is unfortunate to have not any information concerning the position of the sound limb.

The mean axial loads on the artificial limb and walking aids of the gait pattern 2 are shown under the form of a VIH in figure 8.25.

3. SO and the following SS (SSwP) between HS and TO (PSP)

The GPL number 3 concerns 3 patients out of 14 (22 %) performing 6 trials (same scale as above):

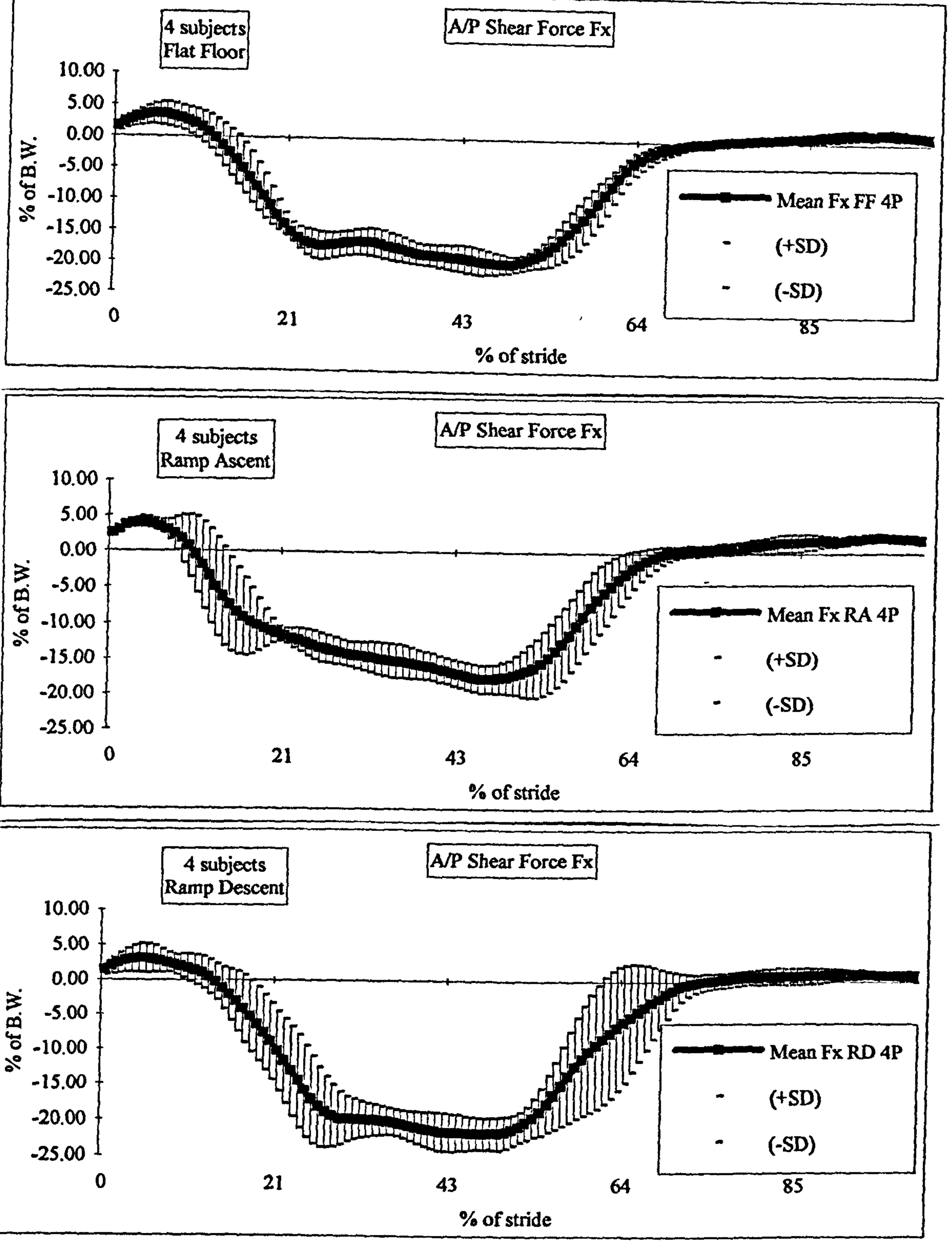

Figure 8.27: Mean A/P shear force of 4 patients, using two sticks, in percentage of BW versus percentage of stride: above, flat floor; middle, ramp ascent; bottom, ramp descent.

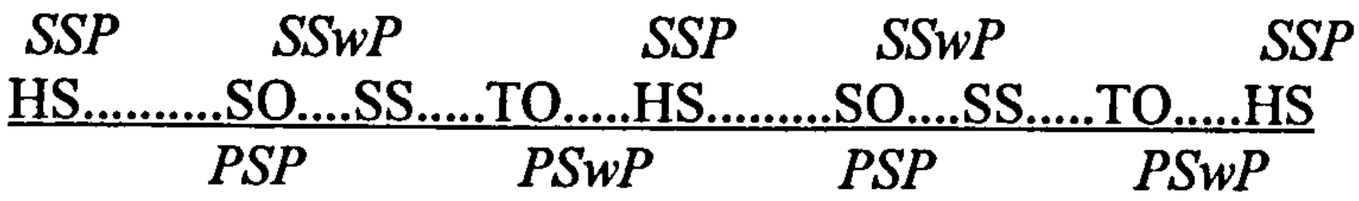

The stick and prosthetic stance phase had a regular chronology but SSP was completely shifted, overlapping both toe off and heel strike. SSP was 1.13 PSP. The mean time interval between HS and SO was 0.23 s and from SS to TO, there was 1.38 s.

This particular pattern provides one conclusion: the entire stick swing phase stood during the prosthetic stance phase. This is why there was no one point load shown on the GPL of the gait pattern 3.

This suggested the following explanation, but due to the lack of information concerning the sound limb, it was not possible to prove it:

- When it was PSwP, the 3 patients applied axial load on the two walking sticks plus the sound limb. It seemed impossible to imagine these patients having floor-contact only with two walking aids. Thus, during the prosthetic swing phase, the patient was on a three points loading.

- When it was SSwP, it was PSP and it might be, totally or partially, a sound limb floor-contact but it was only a probability and no proof could be provided.

The mean axial loads on the artificial limb and walking aids of the gait pattern 3 are shown under the form of a VIH (averaging 3 patients) in figure 8.26.

In summary, the three main gait patterns described above suggest the main following comments:

- *gait pattern 1: The patient applied axial load on the walking aids at late prosthetic stance phase when push-up on the artificial limb and forward acceleration occur. The patient minimised the stress on the residual limb when posterior shear force and dorsiflexion bending moment were maximum (42 % of the sample)*

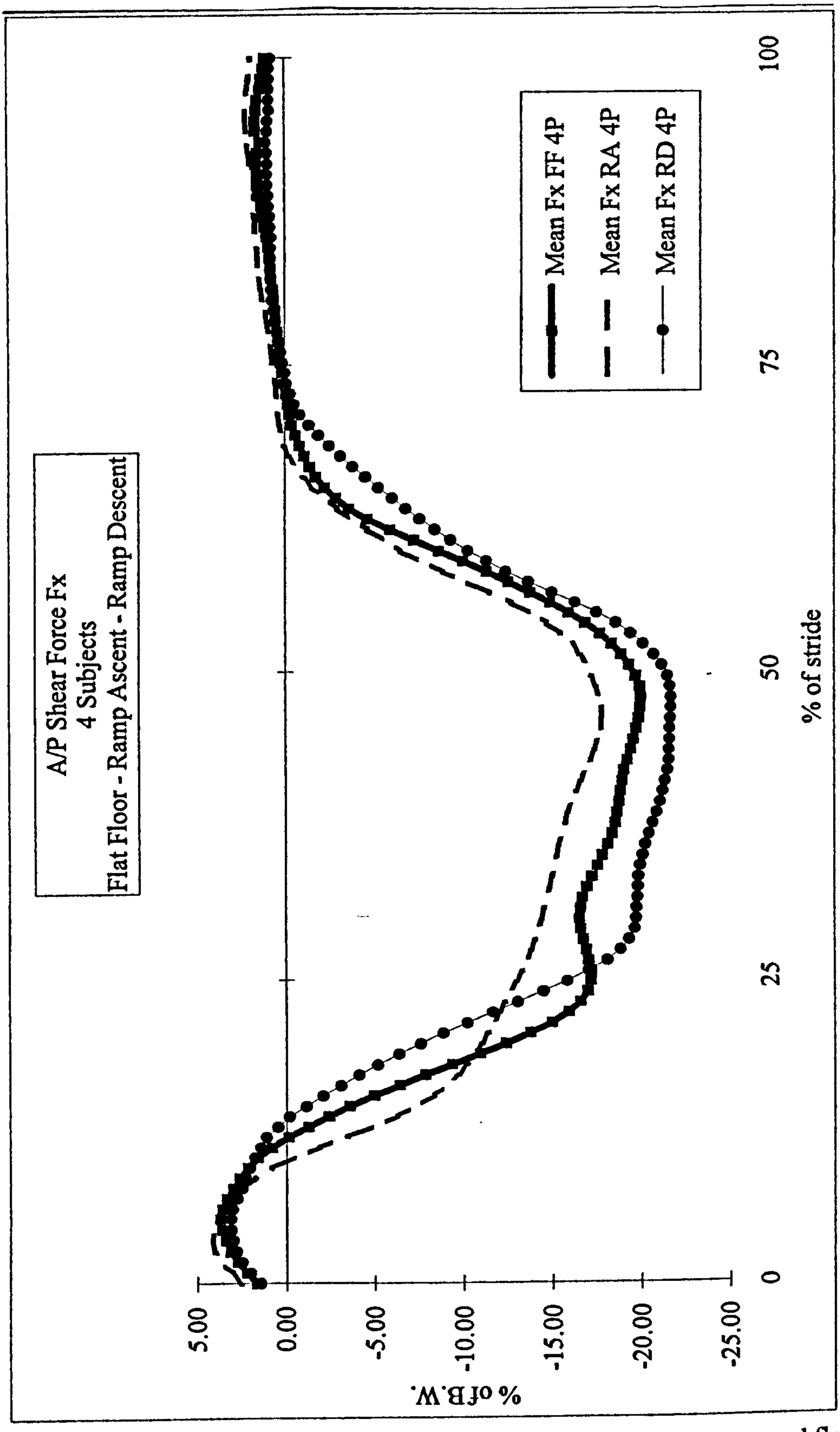

Figure 8.28: A/P shear force (% of BW versus % of stride) on three ground floors such as flat floor, ramp ascent and descent.

• *gait pattern 2: The patient did not apply axial load on the walking aids at late prosthetic stance phase. The patient minimised the stress on the residual limb at early stance phase when weight acceptance was occurred (36 % of the sample).*

• *gait pattern 3: The patient did not apply axial load on the walking aids at mid prosthetic stance phase. The patients protected the residual limb at early and late stance phase plus swing phase. In other words, he minimised the stress on the stump during the most dynamic phases of the gait cycle (22 % of the sample).*

Considering previous comments, evidently a patient could change his gait pattern according to the stump condition. As example, the patient TTL7, using a GS, had a gait pattern No 3 but No 2 when he used an ARS.

Considering the series 4 having 14 transtibial patients, if the time intervals between, respectively, the beginning of the stance phase on walking aids (SStrike or CStrike), the end of the prosthetic stance phase (TO) and sticks or cane stance phase (SO and CO) were studied, a mean difference of 1.04 s (SD = 0.41) between SS or CS and TO and 0.51 s (SD = 0.404) between TO and SO or CO was apparent. The instant TO was therefore located at approximately two-thirds of the SSP or the CSP. The prosthesis started its swing phase while canes were still under load for the final third of their loaded perusal. The canes had therefore a purpose other than the decreasing of the axial load on the prosthesis:

1. in the sagittal plane, the sticks or canes were used for the accelerating force
2. in the frontal plane, the sticks or canes were used to transfer load from side to side.

During the swing phase of walking aids, only the prosthetic and the contralateral leg had ground contact; it was thus important to know the ratio of the Stick-Swing-Phase or Cane-Swing-Phase relative to the prosthetic stride. For the fourteen subjects, walking devices swing phase was 0.36 s (SD = 0.08) while amputated leg stride was 1.89 s (SD = 0.36). Thus, the ratio was 19 %. In other words, during 81 % of the gait cycle, amputees had at least three ground contacts. This was all the more the real pattern because only one patient out of fourteen (TTL11) had a four-point alternating gait; the thirteen other patients had a non-

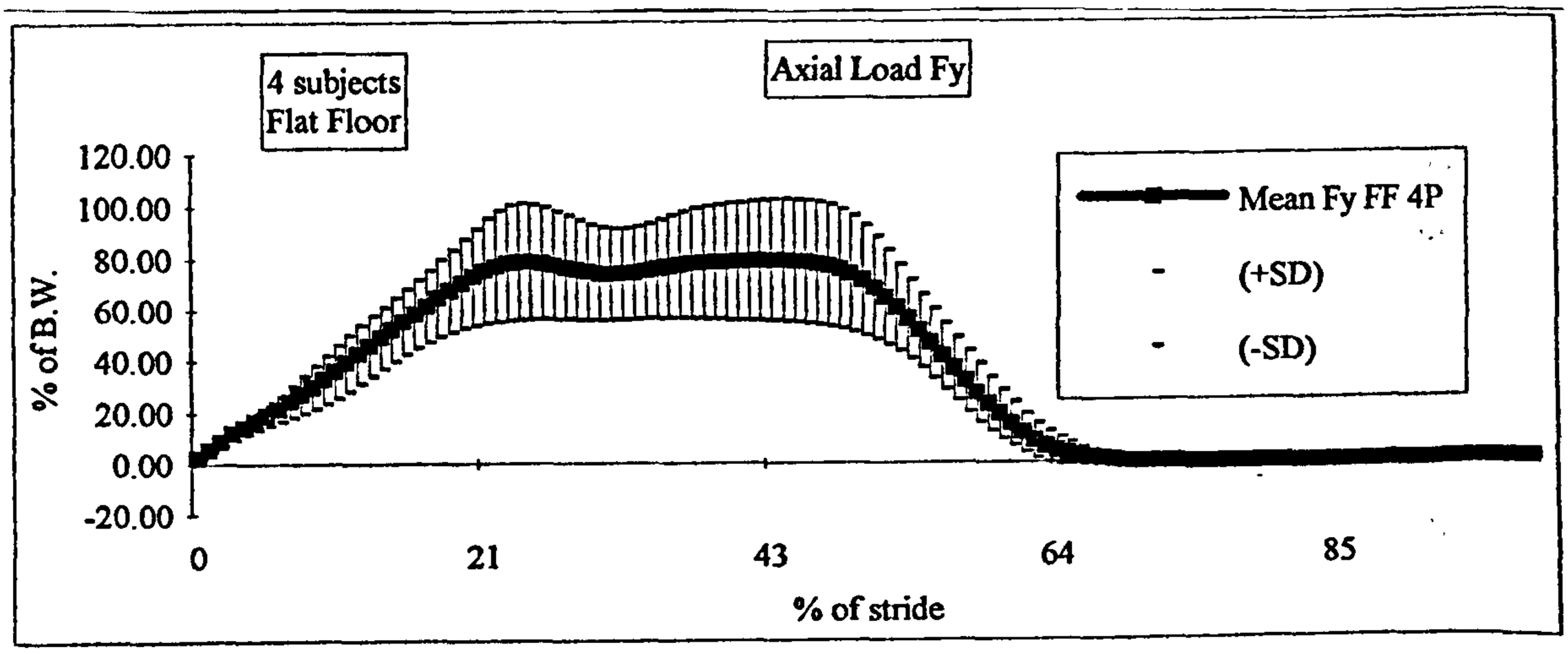

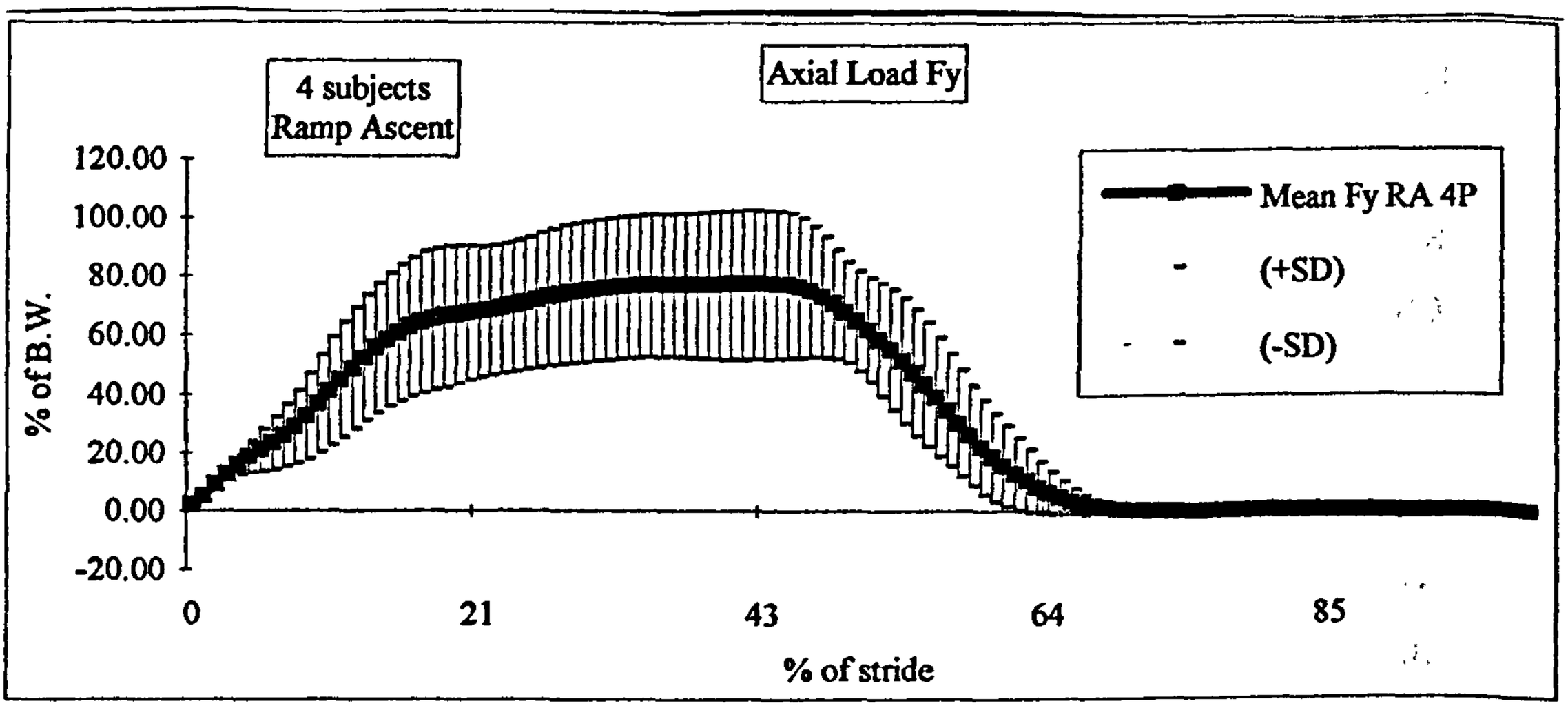

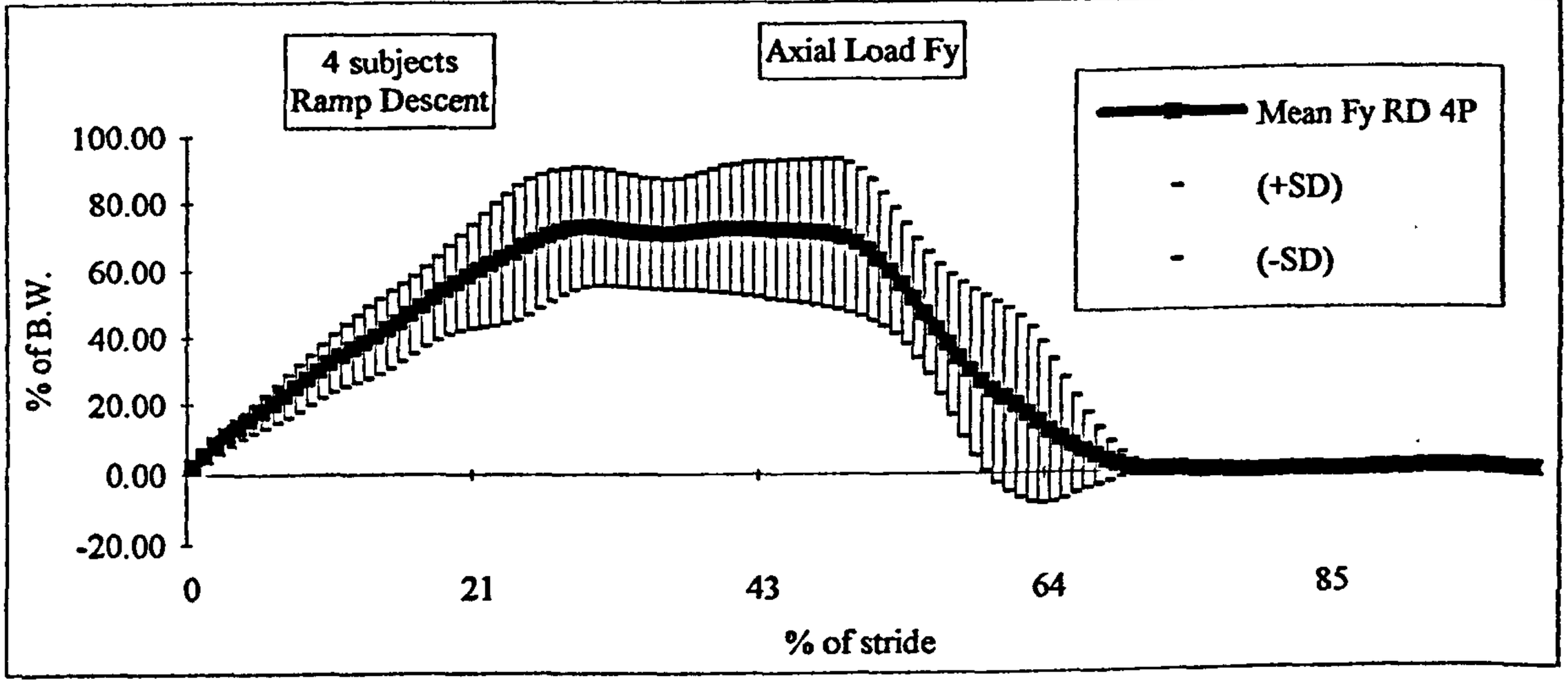

Figure 8.29: Mean axial load of 4 patients, using two sticks, in percentage of BW versus percentage of stride: above, flat floor; middle, ramp ascent; bottom, ramp descent.

weight-bearing « swing-to » gait pattern with the two canes used simultaneously.

This phenomenon was also found if the different series (2 and 3) were separately studied. The strategy of use of the sticks or the canes did not change by moving from one type of socket to another or by moving from one type of walking aid to another.

It had equally appeared interesting to study the time interval between the maximum axial load (Fy maximum) on the prosthesis, the maximum dorsiflexion bending moment of the artificial ankle (Mz+), the maximum posterior shear force (Fx-) and the maximum load applied on the sticks or canes.

Averaging all trials, the results were 0.27 s (SD = 0.17) for the time-interval between the maximum axial load on the prosthesis and the maximum load on the walking aids and 0.09 s (SD = 0.005) for the difference between the maximum dorsiflexion at the ankle plus posterior shear and the maximum load applied on the walking aids. These two intervals highlighted that the 14 patients used their sticks or canes like some « pushing off instruments » and not only for decreasing the load on the prosthesis as would have been expected. This difference seemed particular to recent vascular amputees because Murray *et al.* (1969) reported that for a traumatic above-knee patient these two maximum loads were simultaneous.

Figure 8.22 shows the maximum vertical axial load on the prosthesis (*dashed vertical line*) and the maximum load on the right and the left sticks (*solid vertical line*). The *solid vertical line* indicates the relative simultaneity of maximum of dorsiflexion (Mz+), posterior shear (Fx-) and maximum load on the walking aids by opposition to the time interval of the maximum vertical load on the prosthesis and maximum loads on the walking aids (*horizontal arrow* in figure 8.22).

8.6 RAMP ASCENT AND DESCENT (TRANSTIBIAL AMPUTEES)

Four transtibial patients, using two sticks, were able to walk outside the rehabilitation centre on a ramp used for ambulances to lead into the main entrance of the Vascular Unit which is at the first floor because of the slope of the park land.

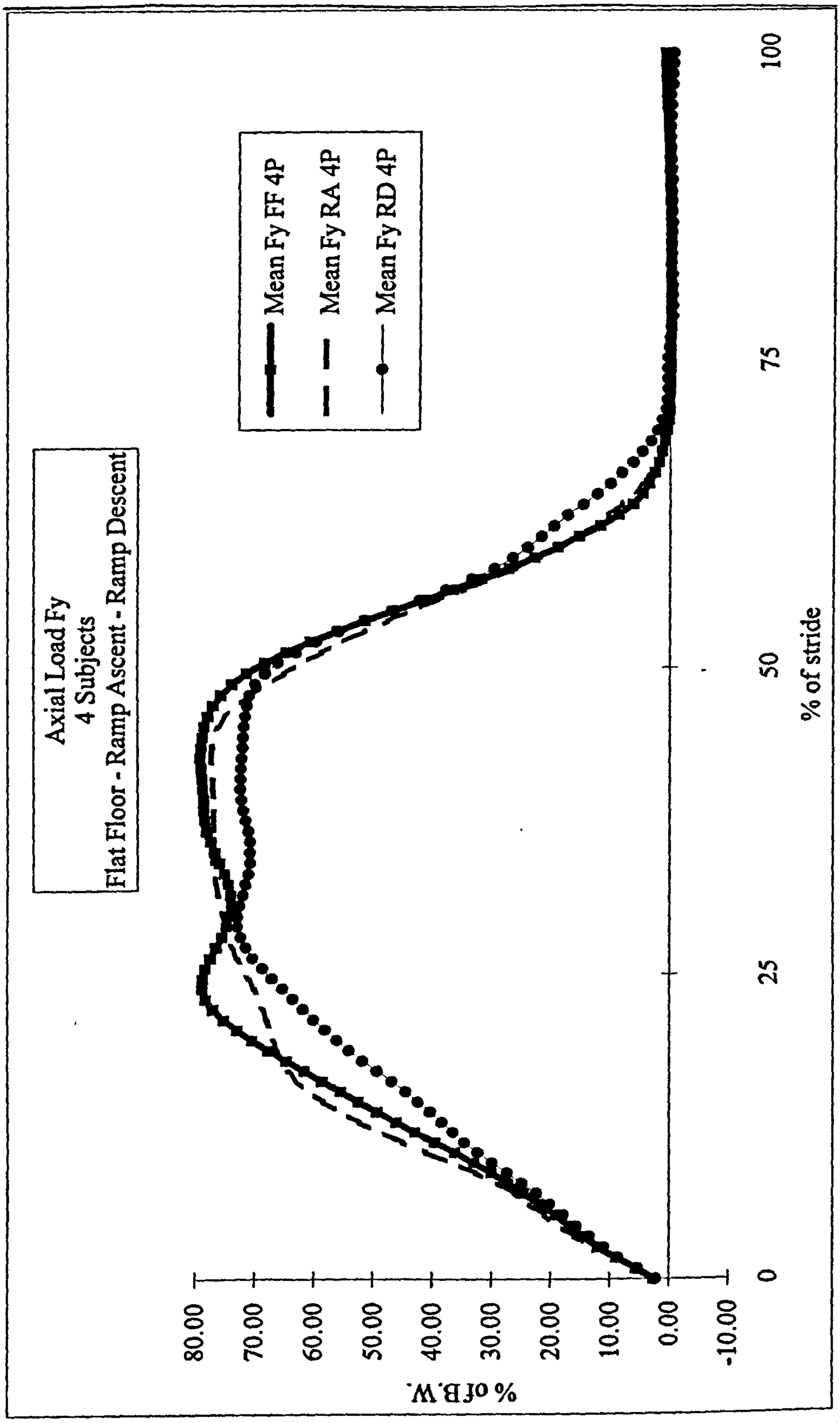

Figure 8.30: Axial load (% of BW versus % of stride) on three terrain such as flat floor, ramp ascent and descent.

This ramp is 22.7 metres long with a maximum height of 1.18 metres. Thus, the slope is 5.2 %. The floor is tar with small pebbles to avoid any slipping.

For each patient, all tests were performed with two parts having three steps: 1) a trial in the same flat ceramic tiled corridor as above, ramp descent then ascent; 2) the same trial but in a reverse order for ramp ascent and descent. Between the two trials, a sitting rest of 20 minutes was observed.

The results are shown in the following figures:

Figure 8.27 shows the mean A/P shear force from the two trials of the four subjects (in percentage of the body weight, ± SD) versus one stride (100 % from HS to the following HS). From top to bottom, one finds flat floor (FF), ramp ascent (RA) and ramp descent (RD). The first remark is to notice the low level of standard deviation when the patients walked on a flat floor opposed to ramp ascent and descent. When the patients were climbing the ramp, the main standard deviation occurred at early stance phase (before 21 % of stride). It was the opposite when the patients were in ramp descent: maximum SD at late stance phase (≈ 64 % of stride). Globally, the level of Fx positive at early stance phase was equivalent (3 to 4 % of BW) whatever the slope was. Fx negative was different: 15 % of BW in ramp ascent, 19 % of BW in flat floor and 22 % in ramp descent. These gaps are statistically significant: from FF to RD, $R = 0.96$, $p < 0.0001$; from FF to RA, $R = 0.97$, $p < 0.0001$ and from RA to RD, $R = 0.92$, $p < 0.0001$. The results are shown in figure 8.28 showing on the same graph the mean traces of the four patients extracted from each trial.

In axial load Fy, figures 8.29 and 8.30 have the same arrangement (see following pages).

As previously stated, the lowest standard deviations were found when the patients were walking in the ceramic tiled corridor but the differences were small. Figure 8.29 shows in flat floor an Fy trace having the usual pattern described in section 8.5.3, namely a first peak between 20 and 25 % of stride and from this peak a slow but consistent decrease until the late stance phase which started at 50 % of stride. The shapes of the Fy traces were not the same when the patients were 1)

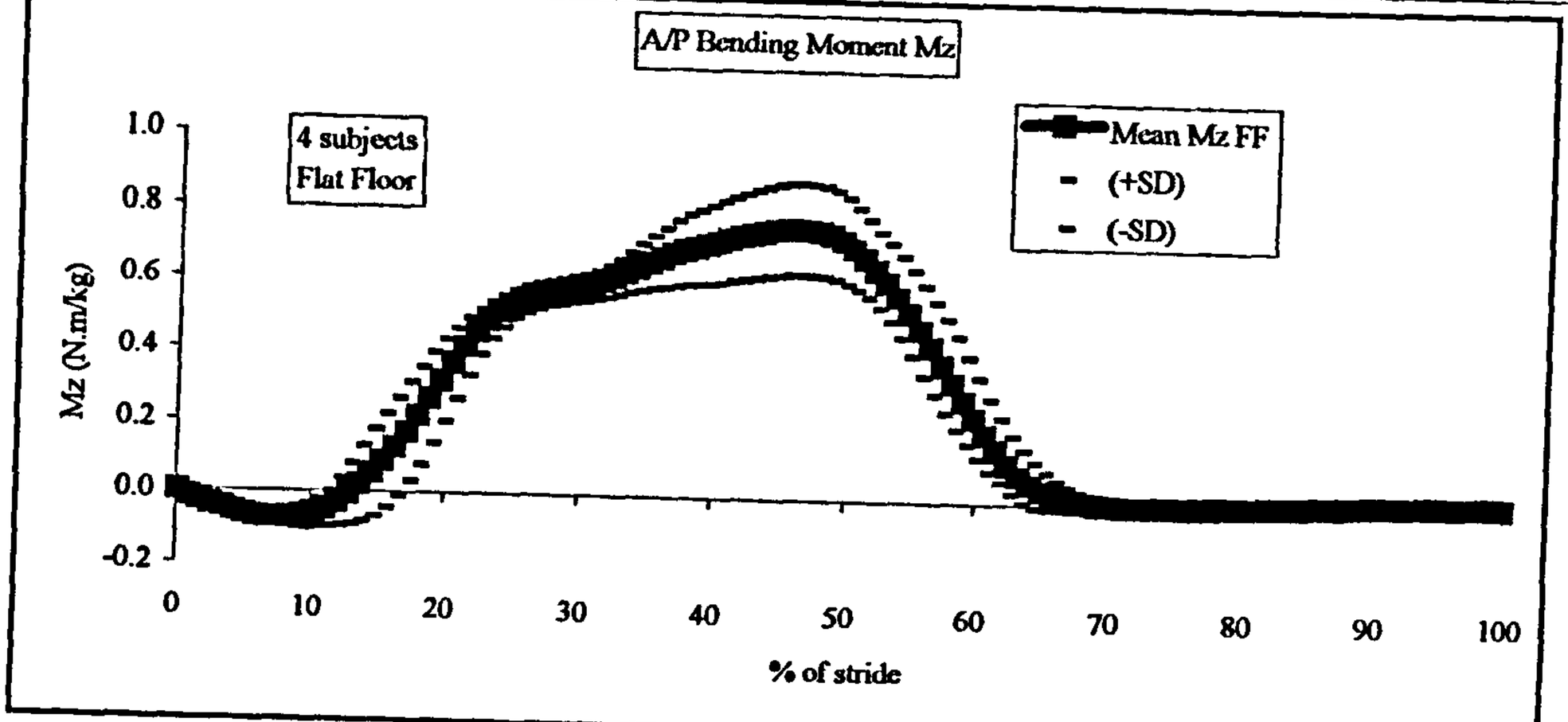

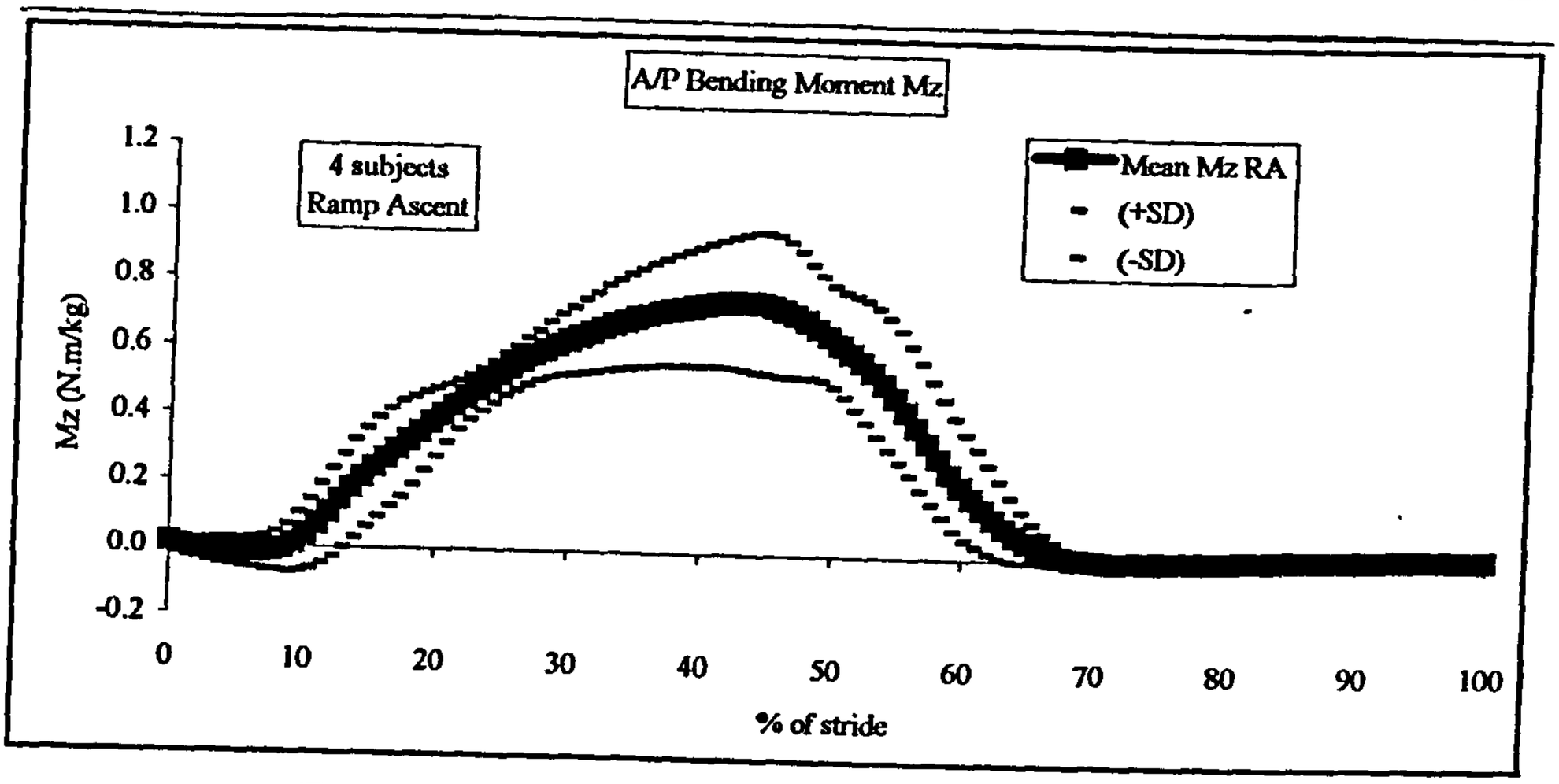

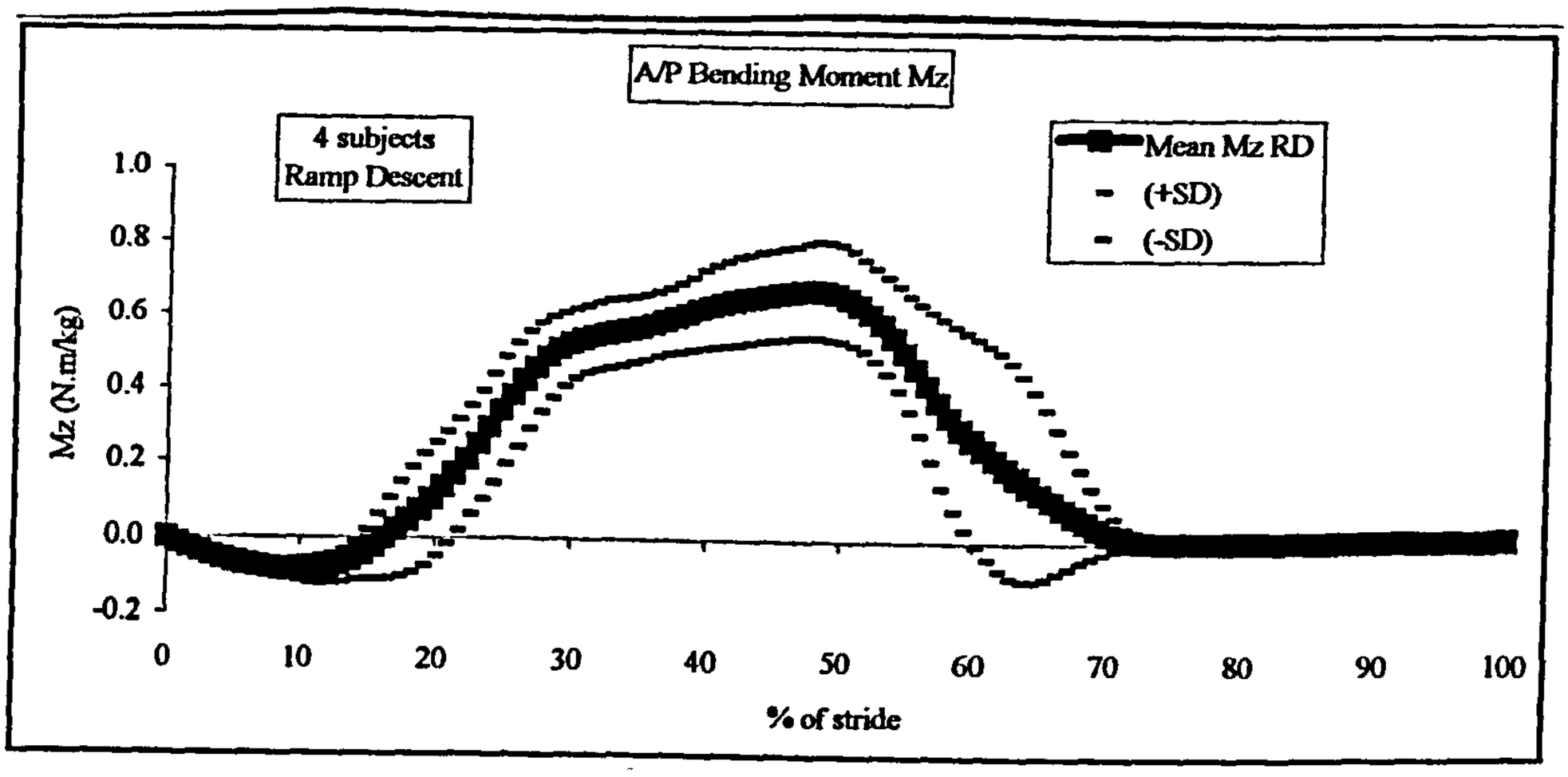

Figure 8.31: Mean A/P bending moments of 4 patients, using two sticks, in percentage of BW versus percentage of stride: above, flat floor; middle, ramp ascent; bottom, ramp descent.

climbing the ramp: a regular slope from 0 % (HS) to 10 % then a minor inflexion and a flattened shape until the beginning of the late stance phase; 2) descending the ramp: the shape was approximately the same but there was not any inflexion. A small peak at 25 % of stride could be notice. A statistical regression analysis of these traces showed a good correlation coefficient and the p values exhibited a very strong statistical significant (from FF to RD: $R = 0.98$, $p < 0.0001$; FF to RA: $R = 0.99$, $p < 0.0001$ and RA to RD: R 0.97, $p < 0.001$). The maximum of Fy axial load was as follows:

- flat floor: 81 % (first peak, 23 % of stride)
- ramp ascent: 77 % (end of mid stance phase, 47 % of stride)
- ramp descent: 73 % (beginning of mid stance phase, 30 % of stride)

The combined results concerning axial load Fy on the artificial limb when the four patients were walking on three terrains are shown in figure 8.30.

In A/P bending moments Mz, figures 8.31 and 8.32 have the same arrangement.

As previously, the lowest standard deviations were found when the patients were walking in the ceramic tiled corridor but the differences were small. However, the main difference was in plantarflexion moment, which was equal to zero when the patients were climbing the ramp. The ascending slope forced the patient to skip the heel strike. The floor contact was thus accomplished through the front part of the artificial foot and consequently the stride started by a dorsiflexion moment.

The statistical regression analysis showed the following results: from FF to RD: $R = 0.97$, $p < 0.0001$; FF to RA: $R = 0.93$, $p < 0.0001$ and RA to RD: $R = 0.89$, $p < 0.0001$. Because of the lack of plantarflexion and the difference in shape and maximum, the coefficient of correlation R exhibited a poor linearity. This was particularly evident showing simultaneously the Mz traces in flat floor, ramp ascent and descent. The main modification of this particular channel occurred in ramp ascent: lack of plantarflexion, premature dorsiflexion with a maximum value (0.7 N m/kg) close to maximum (0.78 N m/kg) expressed in flat floor.

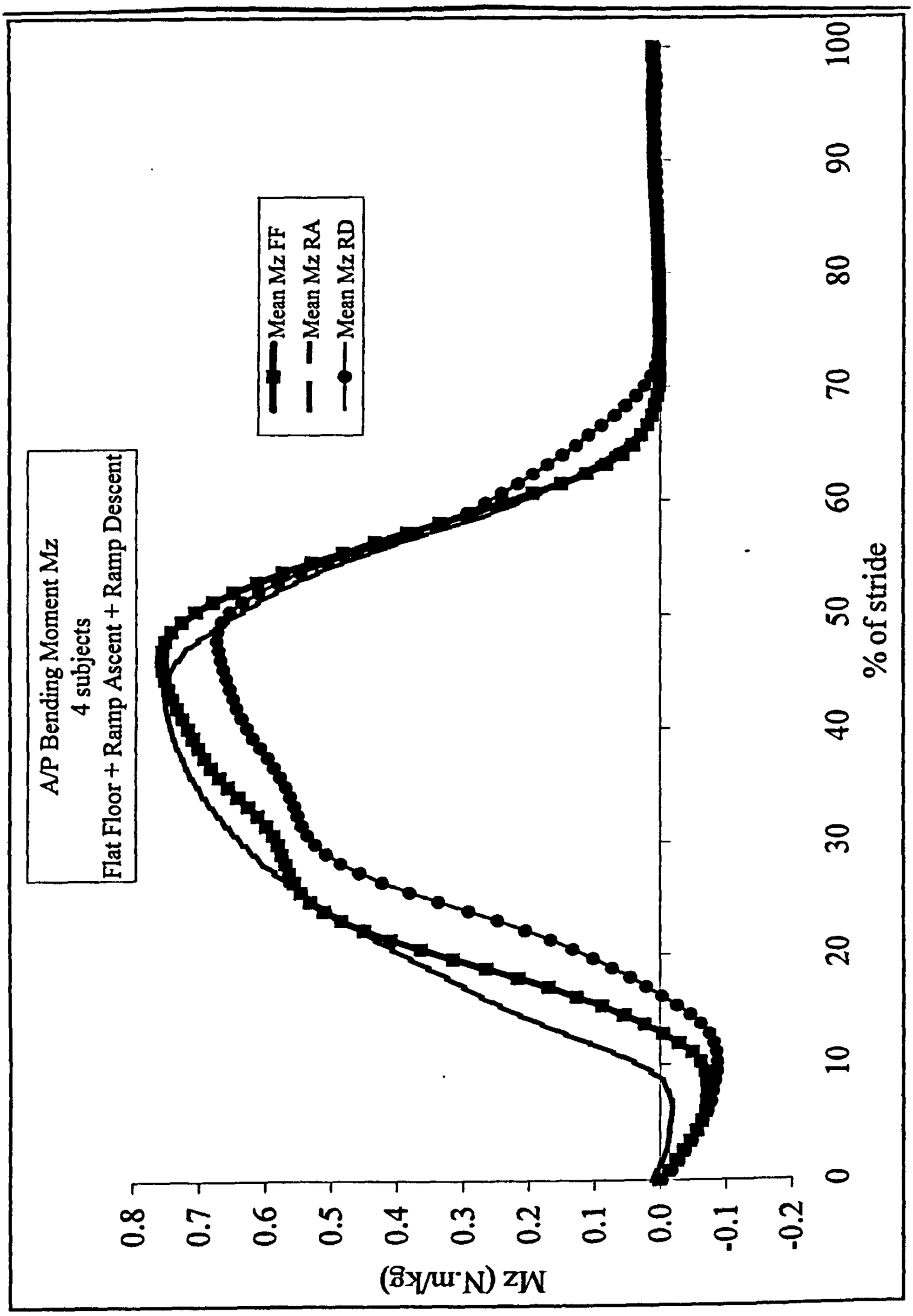

Figure 8.32: A/P bending moment Mz (% of BW versus % of stride) on three terrain such as flat floor, ramp ascent and descent.

As opposed, the maximum plantar flexion occurred in ramp descent, which is logic: to flatten the artificial foot on the ground required a bigger plantar range of motion of the artificial ankle. Thus, the increase in plantar flexion bending moment reflected this excessive range of motion. In ramp descent, the maximum of dorsiflexion bending moment was lower than it was in ramp ascent and flat floor: 0.6 N m/kg. In summarise, the results in positive bending moments (Mz+, dorsiflexion) were as follows:

- flat floor: 0.8 N m/kg (late stance phase, 49 % of stride)
- ramp ascent: 0.7 N m/kg (end of mid stance phase, 45 % of stride)
- ramp descent: 0.6 N m/kg (late stance phase, 52 % of stride).

8.7 RESULTS FOR TRANSFEMORAL AMPUTEES (10 PATIENTS)

Prior to discussing the results, a fundamental remark must be expressed: series 1b (10 TFP) had a computer screen data treatment and it was less accurate (see section 8.4.2) than hand data treatment. Screen data treatment only took into account one and only one absolute maximum value of each trial instead of the average maximum values recorded from six to ten strides. The values could therefore have been increased and over-estimated. The conclusions must therefore be carefully discussed.

8.7.1 Gait Phase Duration

Table 8.27 shows the results concerning the gait rate of the different series. It is expressed in second per stride ($s.stride^{-1}$). As previously stated, in all tests, it was a self selected pace. The 10 transfemoral amputees were studied in 22 trials in which they wore unlike types of sockets fitted with different artificial knee units. They continuously used two sticks. The ground was always a flat floor: vinyl carpet (physiotherapy room) or ceramic tiled corridor.

The mean stride duration was 2.4 $s.stride^{-1}$ (SD = 0.69; range 1.35 - 3.5). Studying this result, three main comments could be made:

GAIT PHASE DURATIONS						
	Series Descriptions	Mean Gait Rate s.stride^{-1}	SD	p value	NS not significant S significant at $p \leq 0.05$	Range
Series 1b	10 TFP	2.40	0.69			1.35 - 3.50

Table 8.27: The range of results of mean gait duration phases for the series 1b concerning 10 transfemoral amputees, expressed in s.stride^{-1}.

	TTP 30 subjects s.stride^{-1}	TFP 10 subjects s.stride^{-1}	Normal Subjects 70-79 years s.stride^{-1}	
early stage in rehabilitation	1.89	2.40		
well established amputees (TTP: Hubbard & McElroy, 1994) (TFP: Boonstra *et al.*, 1994)	1.30	1.38		
(Oberg *et al.*, 1993)			1.04	
Ratios	**1.45**	**1.73**	**TTP 1.81**	**TFP 2.30**

Table 8.28: The different stride times from transtibial, transfemoral amputees and normal subjects with the corresponding ratios.

PROSTHETIC GROUND REACTION FORCE						
	Series Descriptions	Mean PGRF N.kg^{-1}	SD	p value	NS not significant S significant at $p \leq 0.05$	Range
Series 1b	10 TFP	6.93	1.89			2.91 - 9.51

Table 8.29: The range of results of mean prosthetic ground reaction force for the transfemoral series 1b, expressed in N.kg^{-1}

1. The mean PST of the ten PVD transfemoral amputees at early stage of the rehabilitation treatment was obviously greater than the values (for traumatic amputees) found in the literature: 1.43 s (Zuniga *et al.* 1972); 1.37 s (James & Öberg, 1973); 1.38 s (Boonstra *et al.* 1994), 1.36 s (Jaegers *et al.* 1995) and 1.04 s for normal subjects being 70-79 years old (Öberg *et al.* 1993). However, in most papers found in the literature review, the PST could not be evaluated since only the speed of walking was known but not the number of steps or the distance walked (Goh *et al.* 1984)

2. The discrepancy was large (high level of standard deviation) because of the large range of our sample concerning the age of patients and their health status. The fastest walking cadence (1.35 $s.stride^{-1}$) was performed by the patient TFL9 who was 40 years old and amputated for acute ischaemia four months before. The lowest walking cadence (3.43 $s.stride^{-1}$) was achieved by the patient TFL4 who was not the oldest (68 y) but had an unfavourable weight / height ratio: 52 $kg.m^{-1}$, ideally 41 $kg.m^{-1}$, following the commonly metricated accepted formula[16] for ideal weight (Wirta *et al.* 1991). This patient had also the smallest time interval between amputation and test date (1 month).

3. However, even for the fastest patient, the PST performed by the tested amputees was slower than the gait velocity reported in the literature. It is thus possible to determine that transfemoral patients, at the beginning of their rehabilitation, had a gait rate 1.73 slower than established traumatic TFP and 2.30 slower than elderly normal subjects.

Table 8.28 shows the time interval of the gait rate between transtibial and transfemoral amputees: 1) in early stage of rehabilitation (amputees presented in this work), 2) when the rehabilitation is conducted for a long time (Hubbard & McElroy, 1994; Boonstra *et al.* 1994) and 3) normal elderly subjects (Öberg *et al.* 1993).

The different ratios for TTP and TFP exhibit:

---

[16] The formulas for ideal weight (W_i in kg) are the following: Males: $W_i = 51 + (H - 152)$; Females: $W_i = 48 + 0.83\ (H - 152)$ where H is the height in centimetres (Wirta *et al*, 1991). Another formula can be used: $20 < Mass/\ (Height\ in\ metre)^2 < 25$.

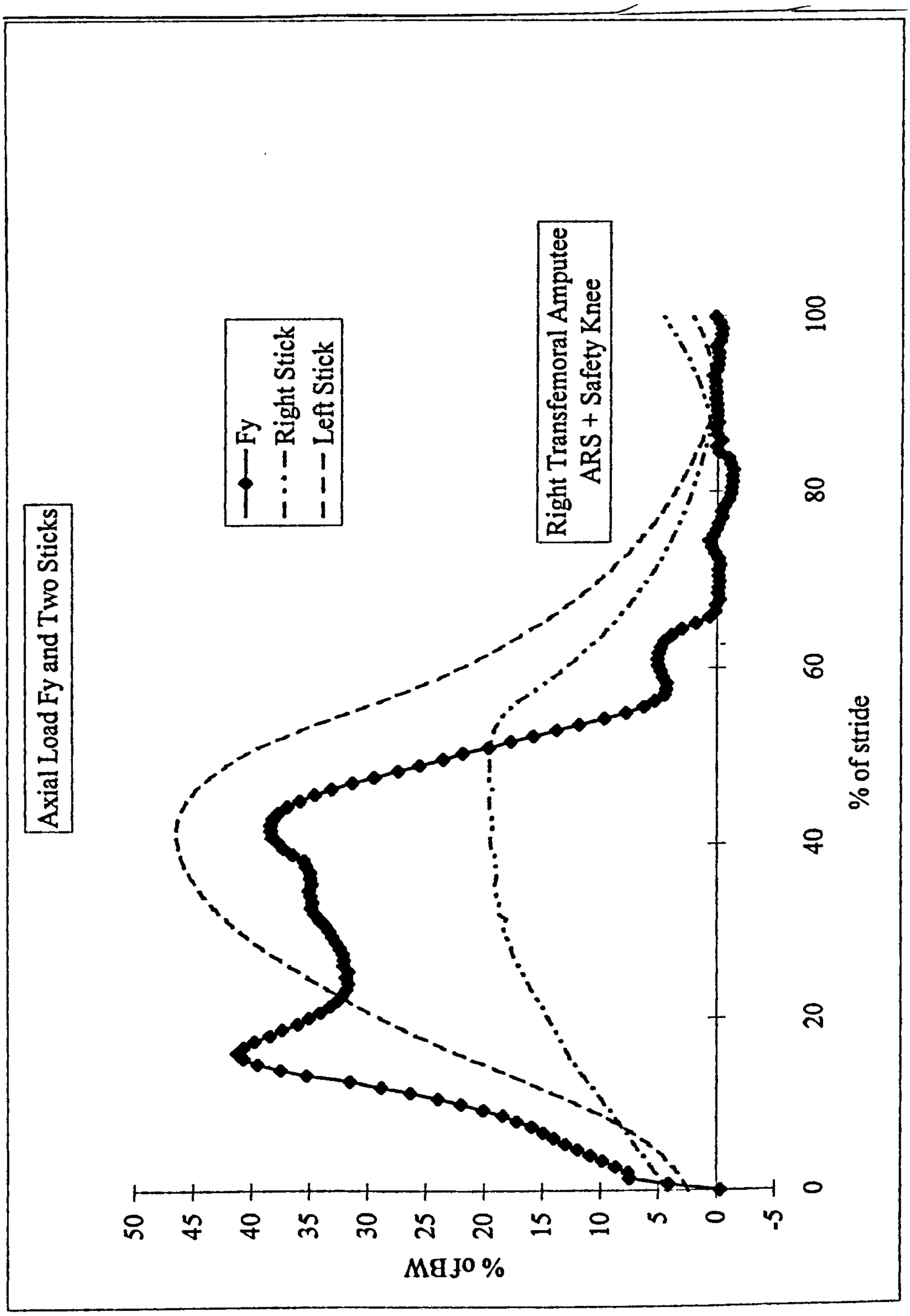

Figure 8.33: The prosthetic and the walking sticks axial load during one stride of the transfemoral patient TFR6 (in percentage of BW versus percentage of stride).

1. A small gap for TTP (1.45) than TFP (1.73) thus the rehabilitation treatment improved more (19 %) the gait rate of the ten transfemoral than transtibial amputees. It is far from what it is found in the literature. As an example, Baker & Hewison (1990) reported a change in velocity of 98 % between initial and discharge velocity (transtibial and transfemoral amputees using two sticks).

2. A smaller gap for TTP (1.81) than TFP (2.30) versus gait rate of normal subjects because of the loss of the knee joint, i.e., the pattern of the gait and thus its efficiency was more altered between respectively transfemoral amputees and transtibial amputees opposing normal subjects.

8.7.2 The ground reaction forces for transfemoral patients

8.7.2.1 PROSTHETIC GROUND REACTION FORCE (PGRF)

Series 1b, 10 transfemoral patients had a mean prosthetic ground reaction force (PGRF) of 6.93 $N.kg^{-1}$ (SD = 1.89, range 2.91, 9.51), equivalent to 0.69 BW. The results are shown in table 8.29 and saliently, they exhibited an equivalent range to those established with transtibial patients (7.3 $N.kg^{-1}$, SD = 2.07, see section 8.5.3.1). This value of 0.69 BW was consistent with what it was found in the literature: from 0.62 BW to 0.71 BW with patients who walked in parallel bars at free speed (Gravel *et al.* 1995). Because parallel bars were used, Gravel *et al.* (1995) did not report any information about the load applied on the walking aids.

As previously stated (see section 8.5.2.1), this separate value must be aggregated with the axial load on the two walking aids to be able to compare to that found in the literature. Therefore, by adding the axial load on the prosthesis and the one acting on each walking aid, an average of 11.17 $N.kg^{-1}$ (SD = 2.1) was found (see below section 8.7.2.2). Consequently, the sum of the forces on both aids and prosthesis was over one body weight, because of inertial forces in spite of the low level of the gait rate, in aided gait, as already reported by Opila (1985). In other words, if the cadence increased, the level of the axial loads on both prosthesis and walking aids should decrease. This phenomenon was also augmented by the necessity for the patient to control the medio-lateral stability, which is improved

WALKING AIDS GROUND REACTION FORCE						
	Series Descriptions	Mean WAGRF $N.kg^{-1}$	SD	p value	NS not significant S significant at $p \leq 0.05$	Range
Series 1b	10 TFP	4.24	1.24			2.34 - 8.18

Table 8.30: The range of results of mean walking aids (sticks) ground reaction force (WAGRF) for the transfemoral series 1b, expressed in $N.kg^{-1}$

Amputation Level and Series Number	Amputated Side R = right L = left	Ipsilateral Walking Aid		SD		Contralateral Walking Aid		SD	
10 TFP series 1b	4 R	2.07				3.62			
	6 L	1.64				2.35			
4 TFP series 6	1 R	2S 2.02	2C 1.31			2S 4.34	2C 2.55		
	3 L	2S 2.67	2C 1.61	2 S 0.9	2 C 0.3	2S 2.24	2C 2.03	2 S 0.6	2 C 0.4
	1 R 2 S + 2 C	1.66				3.45			
	3 L 2 S + 2 C	2.14		0.2		2.13		0.1	

Table 8.31: The results concerning the axial load applied on the two walking aids separated from the amputated side of the different transfemoral subjects ($N.kg^{-1}$)

when speed is increasing[17]. As example, the patient TFL9, having a gait rate of 3.23 s.stride^{-1} at the beginning of the prosthetic training, had axial loads on the prosthesis and the two sticks equal to 12.73 N.kg^{-1}. At the end of the stay-in the rehabilitation centre, the gait rate was 1.55 s.stride^{-1} and the full axial loads became equal as 11.63 N.kg^{-1}. This indicated the shifting of inertial forces. However, these inertial forces were never evaluated in the presented work.

In summary, this result showed that $\frac{4.24}{11.17} * 100 = 38\%$ of the total vertical ground reaction force was transmitted by the two walking devices, in agreement with Winter *et al.* (1993). Theses researchers quoted that one cane carried about 20 % of the total reaction force (hence, 40 % for two canes) but it was a study made through healthy subject. The comparison is thus not totally pertinent. As an example of the discrepancy of the results, Ely & Smidt (1977) quoted only 15 % of the BW as axial load on one cane (see section 8.5.2.2). To illustrate the subject, figure 8.33 shows the axial loads on the prosthesis and the two walking aids of one stride from the right transfemoral amputee TFR6 wearing a silicone liner inside a quadrangular acrylic resin socket fitted with a Otto Bock® safety knee. Figure 8.33 shows the typical gait pattern of a transfemoral patient in early stage of rehabilitation training: the second peak of prosthetic axial load was minimised by the axial load on the two walking aids which was maximum at late stance phase.

8.7.2.2 WALKING AIDS GROUND REACTION FORCES (WAGRF)

As previously stated in section 8.5.2.2, one of the novelties of this project was the recording of the axial loads applied on the two walking aids. There is a complete lack of research concerning this particular topic, except Murray *et al.* (1969) and Opila (1985). The results from both walking aids and amputated sides are shown in table 8.30 and separately in table 8.31: left and right amputated sides; ipsi and contralateral walking aids which are defined as above in section 8.5.2.2.

Averaging all tests performed with the ten TFP, the vertical force on the two walking aids was 4.24 N.kg^{-1} (0.42 BW). By separating left and right canes from the

---

[17]As a cyclist who tends to put his feet on the ground when speed is decreasing.

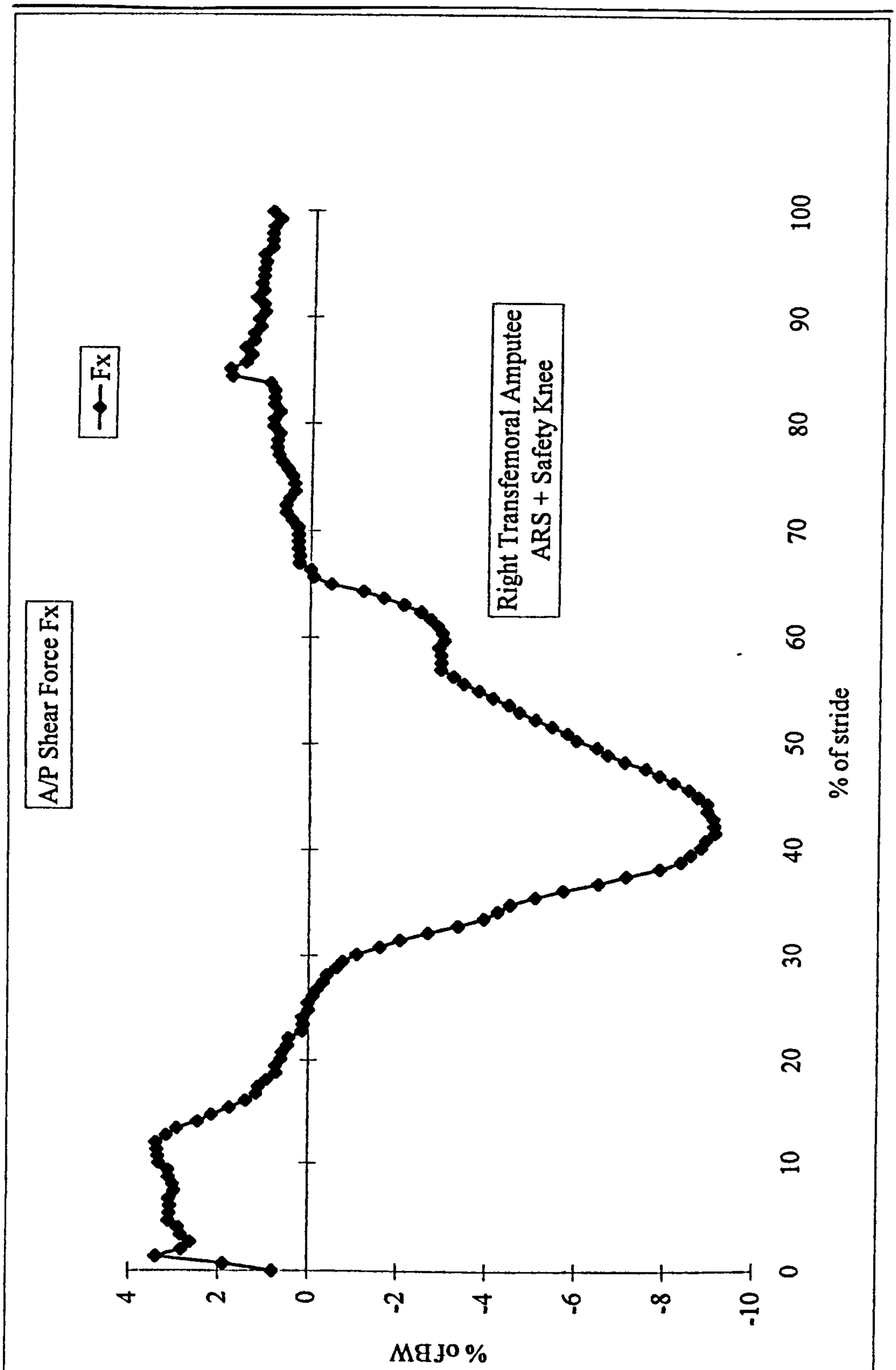

Figure 8.34: The anterio-posterior shear force during one stride of the transfemoral patient TFR6 (in percentage of BW versus percentage of stride).

amputated sides, the results (table 8.30) are:

- 4 right amputees: ipsi 2.07 (SD = 0.82); contra 3.62 $N.kg^{-1}$ (SD = 0.97)
- 6 left amputees: ipsi 1.64 (SD = 0.54); contra 2.35 $N.kg^{-1}$ (SD = 0.57)

In both cases, the difference was strongly significant (respectively p = 0.009 and 0.007), the transfemoral patients shown in the chosen sample applied different axial loads on the two walking aids they used. Moreover, the gap was as it was expected, the main load was always carried through the contralateral walking aids.

As for the transtibial amputees (see section 8.5.2.2), some ratios were calculated:

1. Ipsilateral and Contralateral Walking Aid GRF versus Prosthetic GRF: respectively 0.15 and 0.25. These ratios exhibited the same magnitude for both left and right amputees. Ideally, they should be the lowest, having the aim to deprive the patients of walking aids.

2. Ipsilateral versus Contralateral: 0.61; here also, equal magnitude for left and right amputated sides. There is not any ideal ratio, it depends of the gait behaviour of each subjects.

The results were as it was expected but the two samples were small and there were no references reported in the literature, it was therefore difficult to establish any conclusion. It was only possible to compare these values with the transtibial patients studied in the previous section 8.5.2.2. The ratio between the axial load on ipsilateral and contralateral walking sticks and the prosthesis was the following:

	Ipsi / PGRF	Contra / PGRF
transtibial amputees (averaging two sides)	0.40	0.53
transfemoral amputees	0.15	0.25

Hence, the transtibial group put more loads on the walking sticks than the transfemoral by a factor of 2.6 (ipsi) and 2.1 (contra). Studying the different test information charts, the explanation was clear: the transtibial patients, especially those, who were the nearest from the amputation date, suffered without exception

ANTERIO - POSTERIOR POSITIVE SHEAR FORCE (Fx+)									
	Series Descriptions	Mean Fx $N.kg^{-1}$		SD		p value	NS not significant S significant at $p \leq 0.05$	Range	
Series 1b	10 TFP	0.90		0.67				0.04 ; 1.97	
Series 6	4 TFP 2S vs. 2C	2S 0.80	2C 0.91	2S 0.76	2C 0.84	0.21	NS	2S 0.04 1.61	2C 0.11 1.79

Table 8.32: The range of results of mean anterio-posterior shear force positive (Fx-) for the different series of transfemoral amputees, expressed in $N.kg^{-1}$

ANTERIO - POSTERIOR NEGATIVE SHEAR FORCE (Fx-)									
	Series Descriptions	Mean Fx - $N.kg^{-1}$		SD		p value	NS not significant S significant at $p \leq 0.05$	Range	
Series 1b	10 TFP	- 0.93		- 0.55				-0.35; -2.28	
Series 6	4 TFP 2S vs. 2C	2S - 0.81	2C - 0.93	2S - 0.33	2C - 0.65	0.18	NS	2S -0.56 -0.35	2C -1.31 -1.86

Table 8.33: The range of results of mean anterio-posterior shear force negative (Fx-) for the different series of transfemoral amputees, expressed in $N.kg^{-1}$

more pain than transfemoral amputees. Thus, they put more loads on their walking sticks to ease stresses on their stump. This phenomenon is well reported in the literature (Davis, 1993; Van Dongen & Liem, 1995). This stump pain (especially at the caudal part of the tibial crest) when the residual limb is stressed must be explained to the patients because some of them ask for a higher level amputation to decrease the pain. However, the outcome is always so much better with transtibial amputation. It is therefore necessary to convince the patient of the importance of keeping the knee, see appendix 11.II about the physiotherapy against stump pain (Engstrom & Van de Ven, 1993, Rigal *et al.* 1997).

8.7.3 The fore-aft shear force

The anterio-posterior (A/P) shear force was studied following the same method as the one used for transtibial patients (see section 8.5.3). As example, figure 8.34 shows the A/P shear force of the same patient as figure 8.33 (TFR6). From heel strike, the A/P shear force was positive, then there was a decrease with a zero crossing and negative values arisen. These maximum A/P shear forces occurred when the patient made a push-off, at late stance phase. The same comments as those from section 8.5.4 could be expressed.

Tables 8.32 (A/P shear force positive) and 8.33 (A/P shear force negative) show the mean results from the ten transfemoral patients performing a total of sixteen trials. The mean results falsely look symmetrical (+ 0.90 and - 0.93 $N.kg^{-1}$) because the mean values did not reflect the gait pattern of typical patients. The main comments are thus the following:

1. There was a large discrepancy shown by the high levels of standard deviations. The ranges were 0.04 - 1.97 (+) and 0.35 - 2.28 (-) in $N.kg^{-1}$. The positive values were a little lower than those reported in the literature: 0.4 to 1.4 (Gravel *et al.*, 1995). In negative direction, the results were widely reduced in relation to those reported in the literature: 4.6 to 5.3 (Gravel *et al.*, 1995).

2. Three gait pattern of the tested transfemoral patients could be described:

- A large positive coupled with a small negative shear force (patients TFL5, TFL4). These patients had a more important early stance phase comparative to the late

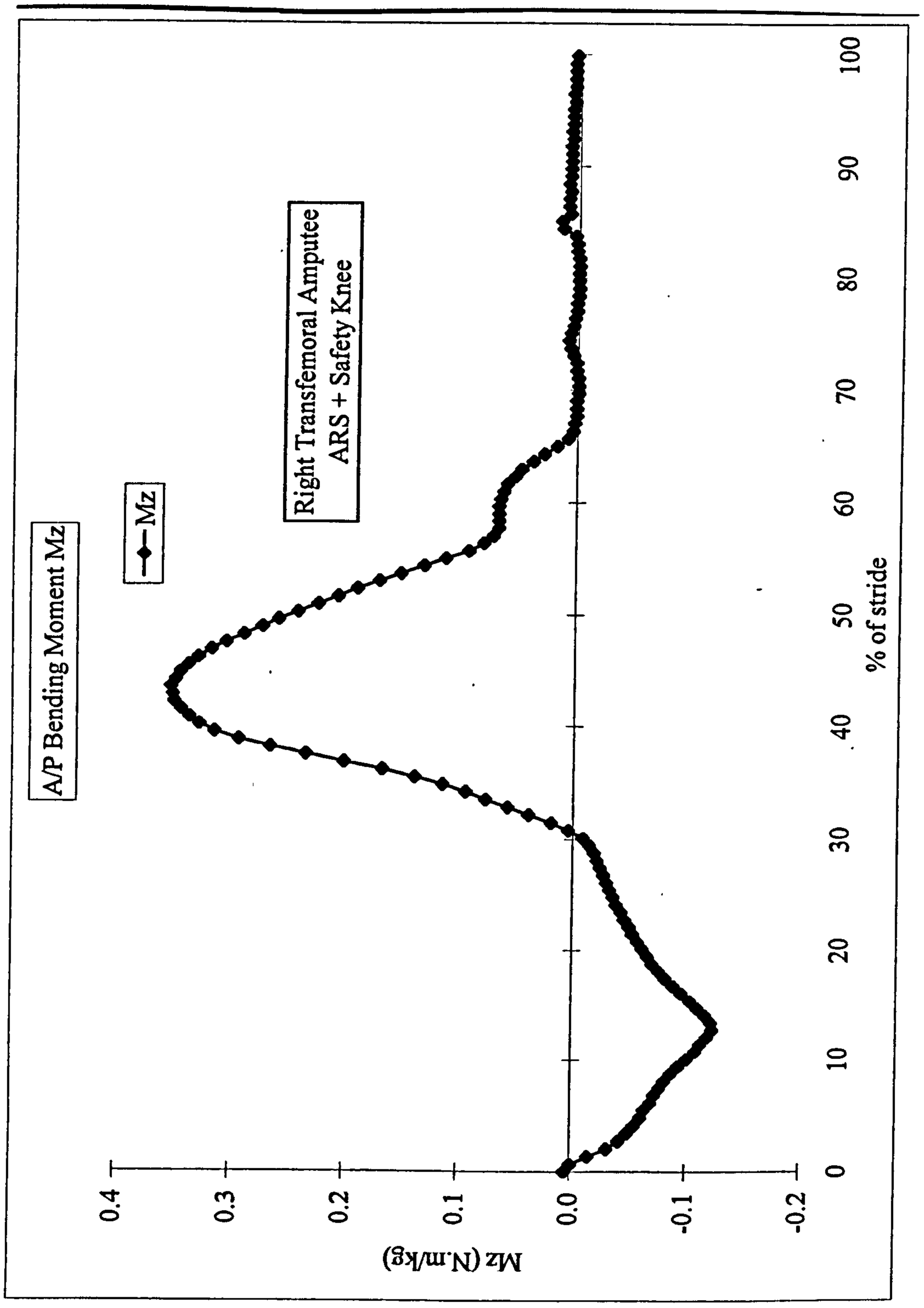

Figure 8.35: The anterio-posterior bending moment Mz during the same stride as figure 8.33 and 8.34 of the transfemoral patient TFR6 (in N.m/kg versus percentage of stride).

stance phase. However, the patient TFL4 had a more complex gait pattern and the discussion will be continued below in section 8.7.4;

- An equal A/P shear force in both directions (patients TFL10, TFR8 and TFL3);
- A small positive coupled with a large negative A/P shear force (patients TFR6 as shown in figure 8.34, TFR7, TFL9, TFR1 and TFL3).

Because of the relatively small sample, it was therefore difficult to form a conclusion. However, these three gait patterns could be related with the hip range of motion and / or the prosthesis alignment but these two parameters were not checked and controlled or measured in the present study.

8.7.4 The flexion - extension bending moments at the artificial ankle joint

In the sagittal plane, the same description, as the one made in section 8.5.4 for transtibial amputees, could be made. The cycle of the anterio-posterior (A/P) bending moments could be divided into three main phases:

1. From heel strike (HS), it began by a plantar flexion moment (Mz-) through early stance phase

2. From the end of early stance phase to the beginning of mid stance phase, a zero crossing could be described (vertical shank tube): Mz (and Fx) = 0.

3. From mid to late stance phase, there was a dorsi flexion bending moment Mz+, which was maximum when the patient was performing the forward acceleration of the body (push off), just before the toe off (TO).

These three phases are shown in figure 8.35 (same stride and patient (TFR6) as figures 8.33 and 8.34). The shape of the A/P bending moment trace was different from the one shown in figure 8.23 for transtibial amputees. The positive A/P bending moment was obviously a sharp peak having an approximately maximum value of 0.37 N m.kg^{-1}.

The mean A/P bending moment values from the ten transfemoral patients are shown in tables 8.34 (Mz-) and 8.35 (Mz+):

- negative plantar bending moment: - 0.16 N m.kg^{-1} (SD = 0.08, range -0.04, -0.31)

ANTERIO - POSTERIOR NEGATIVE BENDING MOMENT (Mz-)									
	Series Descriptions	Mean Mz - $N.m.kg^{-1}$		SD		p value	NS not significant S significant at $p \leq 0.05$	Range	
Series 1b	10 TFP	-0.16		-0.08				-0.08	-0.70
Series 6	4 TFP 2S vs. 2C	2S -0.13	2C -0.14	2S -0.10	2C -0.09	0.22	NS	2S -0.04 -0.26	2C -0.26 -0.28

Table 8.34: The range of results of mean negative anterio-posterior bending moment at the artificial ankle level for different series of transfemoral subjects, expressed in $N.m.kg^{-1}$

ANTERIO - POSTERIOR POSITIVE BENDING MOMENT (Mz+)									
	Series Descriptions	Mean Mz + $N.m.kg^{-1}$		SD		p value	NS not significant S significant at $p \leq 0.05$	Range	
Series 1b	10 TFP	0.25		0.16				0.04 - 0.31	
Series 6	4 TFP 2S vs. 2C	2S 0.22	2C 0.21	2S 0.08	2C 0.13	0.23	NS	2S 0.17 0.34	2C 0.08 0.38

Table 8.35: The range of results of mean positive anterio-posterior bending moment at the artificial ankle level for different series of transfemoral subjects, expressed in $N.m.kg^{-1}$

- positive dorsi bending moment: 0.25 N m.kg^{-1} (SD = 0.16, range 0.08, 0.7)

Compared with transtibial amputees, the plantar bending moment for transfemoral patients was higher while the dorsi bending moment was lower. In other words, the dorsi-plantar bending moment gap was not as substantial with transfemoral as with transtibial amputees. This showed that the early and late stance phases were shortened in the different gait patterns of the subjects tested. This could be related to a lesser equilibrium on a transfemoral than on a transtibial prosthesis, especially with a locked artificial knee unit.

Identically as for A/P shear force, the bending moment values had a large range. The exhibited mean results thus hide the particular behaviour of each patient, which must be now considered. The three main gait patterns described above for A/P shear force (see section 8.7.3) could be recognised:

➢ A large negative coupled with a small positive bending moment. Obviously, it should be the two patients (TFL4, TFL5) who had a large early stance phase (positive A/P shear force) comparatively with the late stance phase (negative A/P shear force). However, it was not exactly the same gait pattern for the two patients. Only one, the patient TFL5 had a gait pattern, as it was expected (higher value in negative bending moment than in positive). The patient TFL4 showed a large negative A/P bending moment (- 0.18 N m.kg^{-1}) coupled with a large positive A/P shear force (1.63 N.kg^{-1}) at early stance phase with the opposite (both were small) at late stance phase (0.16 N m.kg^{-1} and -0.66 N.kg^{-1}). In other words, this particular patient had a positive - negative symmetrical A/P bending moments, which was not usual in the observed series. To illustrate these comments, figure 8.36 shows one stride of this particular patient.

➢ All the other patients had A/P bending moments as normally expected: the positive values (at late stance phase) were higher than negative values (at early stride phase): + 0.24 N m.kg^{-1} (SD = 0.16), - 0.13 N m.kg^{-1} (SD = 0.06). The difference was strongly significant (p = 0.0004).

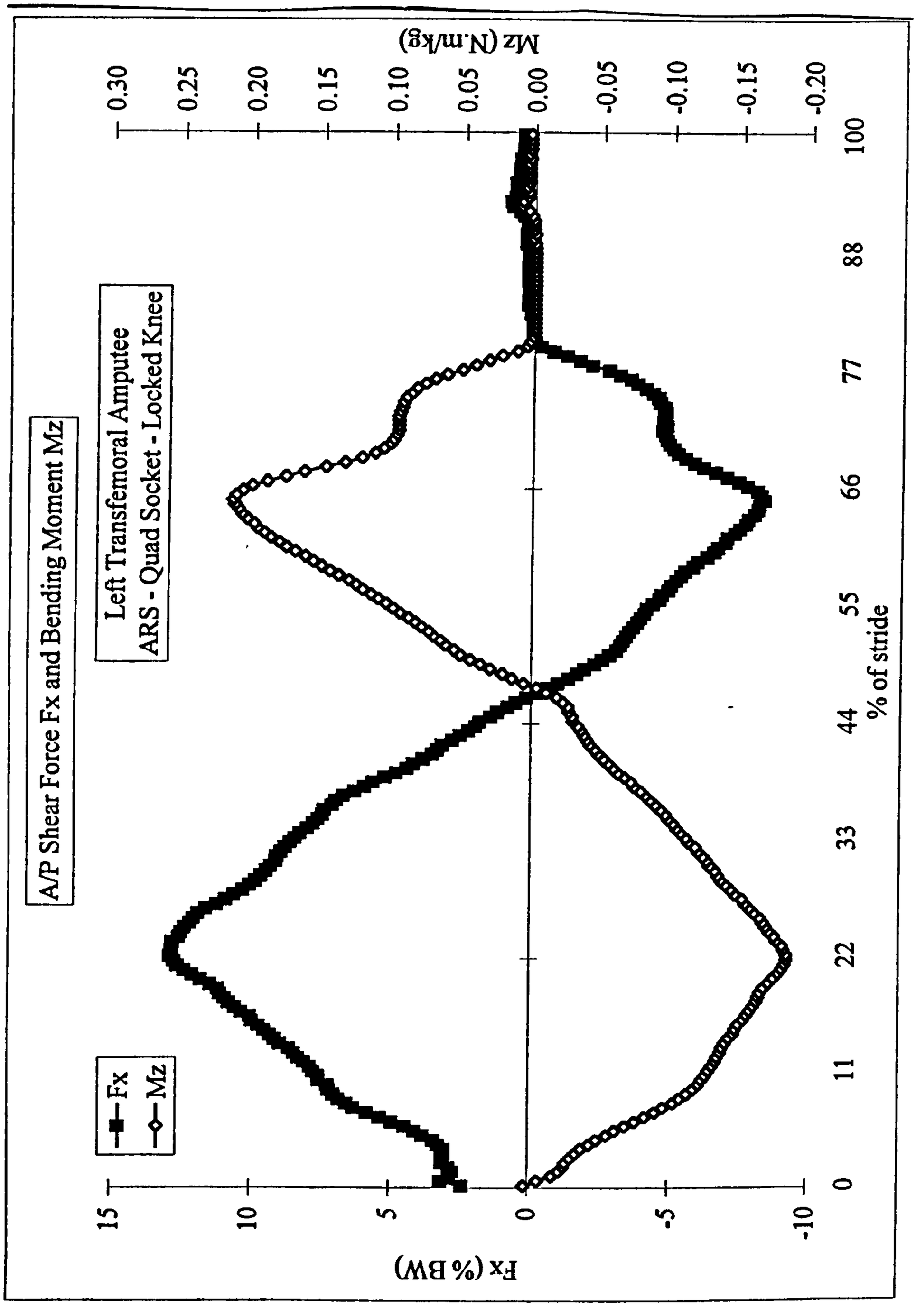

Figure 8.36: One stride of patient TFL4 showing simultaneously A/P shear force Fx (% of BW) and bending moment Mz (N.m/kg):

at early stance phase, large Fx positive (114 N) and Mz negative (18 N.m)

at late stance phase, small Fx negative (62 N) and Mz positive (21 N.m)

In both stance phases, the Mz values were equivalent.

The body mass of the patient TFL4 was 90 kg (see table 8.11).

8.8 RESULTS FOR TRANSFEMORAL AMPUTEES: 2 STICKS VS. 2 CANES (4 PATIENTS)

Four transfemoral amputees were tested more thoroughly, following the hand data treatment (see section 8.4.1). The tests were performed the same day, during the same session. The subjects were asked to walk straight on a ceramic tiled corridor. The patients wore the same socket and used successively two sticks then two canes, following the same protocol as described above for transtibial amputees (see section 8.3.2). All the patients were fitted with a definitive acrylic resin socket, having a quadrilateral shape and they used a locked artificial knee unit. The mean age of these four male amputees was 62 (SD = 12), ranging 55-76 years. Three of them were left amputees and one was right (see appendix 11.VIII.3, table X.4).

8.8.1 Gait Phase Duration

Table 8.36 shows the results concerning the gait rate (PST) in second per stride of the series 6. As for transtibial amputees, it always was a self-selected pace. The complete results are shown in appendix 11.VIII.8.

The four transfemoral patients walked with a prosthetic stride time of 2.83 $s.stride^{-1}$ (SD = 0.51) using two sticks and 2.96 $s.stride^{-1}$ (SD = 0.75) with two canes. The difference (4 %) was not significant (p = 0.19)

8.8.2 The ground reaction forces

8.8.2.1 PROSTHETIC GROUND REACTION FORCE (PGRF)

The mean maximal prosthetic ground reaction force was 5.53 $N.kg^{-1}$ (SD = 2.28) with two sticks and 6.73 $N.kg^{-1}$ (SD = 1.66) with two canes (see table 8.37, same as table 8.29). This difference was not significant at the level of p = 0.09. The discrepancy was important. The lowest values were respectively (2S; 2C): 2.91; 4.36 (patient TFL3) and 7.38; 8.11 (patient TFL5). There were two reasons about this large gap:

1) the patient TFL3 was using two canes since the day before the test and wore an acrylic resin socket for one week while patient TFL5 was accustomed to his canes for three weeks and to his socket for more than one month. Both were close to the

GAIT PHASE DURATIONS									
	Series Descriptions	Mean Gait Rate s.stride^{-1}		SD		p value	NS not significant S significant at $p \leq 0.05$	Range	
Series 6	4 TFP 2S vs. 2C	2S 2.83	2C 2.96	2S 0.51	2C 0.75	0.19	NS	2S 2.22 3.34	2C 2.16 3.31

Table 8.36: The range of results of mean gait duration phases for the series 6 concerning transfemoral amputees, expressed in s.stride^{-1}.

PROSTHETIC GROUND REACTION FORCE									
	Series Descriptions	Mean PGRF or WAGRF N.kg^{-1}		SD		p value	NS not significant S significant at $p \leq 0.05$	Range	
Series 6	4 TFP 2S vs. 2C	2S 5.53	2C 6.73	2S 2.28	2C 1.66	0.09	NS	2S 2.91 7.38	2C 4.36 8.11
WALKING AIDS GROUND REACTION FORCE									
Series 6	4 TFP 2S vs. 2C	2S 5.28	2C 3.70	2S 2.52	2C 1.65	0.07	NS	2S 2.38 8.18	2C 1.77 5.79

Table 8.37: The range of results of mean prosthetic and walking aids ground reaction force for the transfemoral series 6, expressed in N.kg^{-1}

	10 TFP series 1b N.kg^{-1}	4 TFP 2 sticks series 6 N.kg^{-1}	4 TFP 2 canes series 6 N.kg^{-1}
Prosthetic Axial Load PGRF	6.93	5.53	6.73
Walking Aids Axial Load WAGRF	4.24	5.28	3.70
Total GRF	**11.17**	**10.81**	**10.43**
Gait Rate	**2.40**	**2.83**	**2.96**

Table 8.38: Ground reaction forces on the artificial limb and walking aids in different series of transfemoral patients, the gait rate is also shown.

discharge from the rehabilitation centre but the patient TFL5 had to wait for social reasons.

2) the stump length/body height ratio of patient TFL3 (0.18) was less auspicious than the one of the patient TFL5 (0.24).

It seemed interesting to compare all these PGRF values with those of the ten transfemoral patients shown in section 8.7.2, the values are shown in table 8.38.

Studying these values, the following comment could be expressed: the 10 TFP of the series 1b included the four transfemoral amputees shown in column 2 and 3 plus six patients who were more established patients such as the patient TFL9 (relatively young and amputated for acute arterial occlusion without signs of chronic vascular disease, see section 8.3.6). It was therefore logical that the 10 patients of the series 1b had a PGRF higher, a WAGRF and a gait rate lower than the 4 patients of the series 6.

Hence, the same gait behaviour as the one found for transtibial amputees is shown, namely: when the gait rate was lower, the prosthetic axial load was higher. The stresses on the stump due to inertial forces and thus impacts between the residual limb bones (tibia or femur) and the rigid socket were minimised. However, these different ratios were not totally linear[18], a regression analysis showed a coefficient of correlation of $R = 0.91$ (ideally $R = 1$) with a p value of 0.005. The final consequence was a decreasing of pain and risk of skin breakdowns.

8.8.2.2 WALKING AIDS GROUND REACTION FORCES (WAGRF)

The values of the axial loads applied on the two walking aids are shown in table 8.38. The patients who used two sticks applied 5.28 $N.kg^{-1}$ (SD = 2.52) and 3.70 $N.kg^{-1}$ (SD = 1.65) with two canes; a mean of 0.45 BW. The decrease was 42 % but it is weakly significant ($p = 0.07$).

There was a large range of results: 2S = 2.38 to 8.18 $N.kg^{-1}$; 2 C = 1.77 to 5.79 $N.kg^{-1}$. These values were respectively recorded from two patients who wore the same type of prosthesis: quadrangular acrylic resin socket fitted with an artificial locked knee unit.

---

[18] But the question could be: should these ratios be linear?

Amputation Level and Series Number	Amputated Side R = right L = left	Ipsilateral Walking Aid		SD		Contralateral Walking Aid		SD	
4 TFP	1 R	2S 2.02	2C 1.31			2S 4.34	2C 2.55		
	3 L	2S 2.67	2C 1.61	2 S 0.9	2 C 0.3	2S 2.24	2C 2.03	2 S 0.6	2 C 0.4
	1 R 2 S+2 C	1.66				3.45			
	3 L 2 S+2 C	2.14		0.2		2.13		0.1	

Table 8.39: The results concerning the axial load applied on the two walking aids separated from the amputated side of the transfemoral subjects, series 6 ($N.kg^{-1}$)

AMPUTATED SIDE	RATIO IPSI / CONTRA STICK	
	2 S	2 C
L	1.2	0.8
R	0.46	0.51

Table 8.40: The ratio ipsi versus contralateral sticks from 4 transfemoral patients (see text for comments)

1. The patient TFL5 applied the lowest axial loads on the walking aids (0.24 BW with 2 S and 0.18 BW with 2 C), obviously he also was the subject who applied the highest axial load on its artificial limb (0.75 BW with 2S and 0.83 with 2C). The total axial loads on both prosthesis and walking aids was thus as follows: 0.99 BW with 2 S and 1.01 BW with 2 C. Studying the test information chart of the patient TFL5, it could be noticed that he had no pain, he was accustomed to the socket for one month and he used two sticks since more than three weeks (see section 8.8.2.1). The weight - height ratio of this particular patient was advantageous: 60 / 1.68 = 35 $kg.m^{-1}$ (Wirta *et al.* 1991, see section 8.7.1) and he also had a favourable stump length versus body height ratio: 0.41 / 1.68 = 0.24 (dimensionless number which should be the highest as reported by Jaegers *et al.* 1995);

2. The patient TFL3 applied the highest axial load on the walking aids (0.83 BW with 2 S and 0.59 BW with 2 C), that gave 0.3 BW (2S) and 0.45 BW (2C) on the prosthesis; the total axial load on both walking aids and prosthesis was 1.13 BW (2S) and 1.04 BW (2C) with a maximum gait rate of 2.61 (2S) and 2.55 $s.stride^{-1}$ (2C). The patient was fitted with a new acrylic resin socket for two days and he only had a short training period (less than one week) with two sticks and two canes. The weight / height ratio was equivalent as patient TFL5 (60 / 1.70 = 35 $kg.m^{-1}$) but the stump length versus body height was less favourable (0.32 / 1.70 = 0.18). Although, the patient TFL5 was older than the patient TFL3 and thus, it was possible to assert that there were several factors to sway the outcome of a patient beside the age.

It was interesting to notice that these four transfemoral patients applied more loads (0.45 BW) on the walking aids than the 14 transtibial patients (0.37 BW, series 4, see section 8.5.3.2.) and the 10 transfemoral amputees (0.42 BW, series 1b, see section 8.7.2.2). The small sample of series 6 with four transfemoral amputees was not totally characteristic of transfemoral amputees and thus results must be carefully discussed (see section 8.3.6).

Averaging the right walking aid in all performed tests, the value was 2.19 $N.kg^{-1}$ (SD = 0.91) with two sticks and 1.85 $N.kg^{-1}$ (SD = 0.8) with two canes. This 14 % difference was not significant (p = 0.14). The range was large and it was the same two patients as above: TFL5 (1.11; 1.04 $N.kg^{-1}$, respectively 2S, 2C) and TFL3

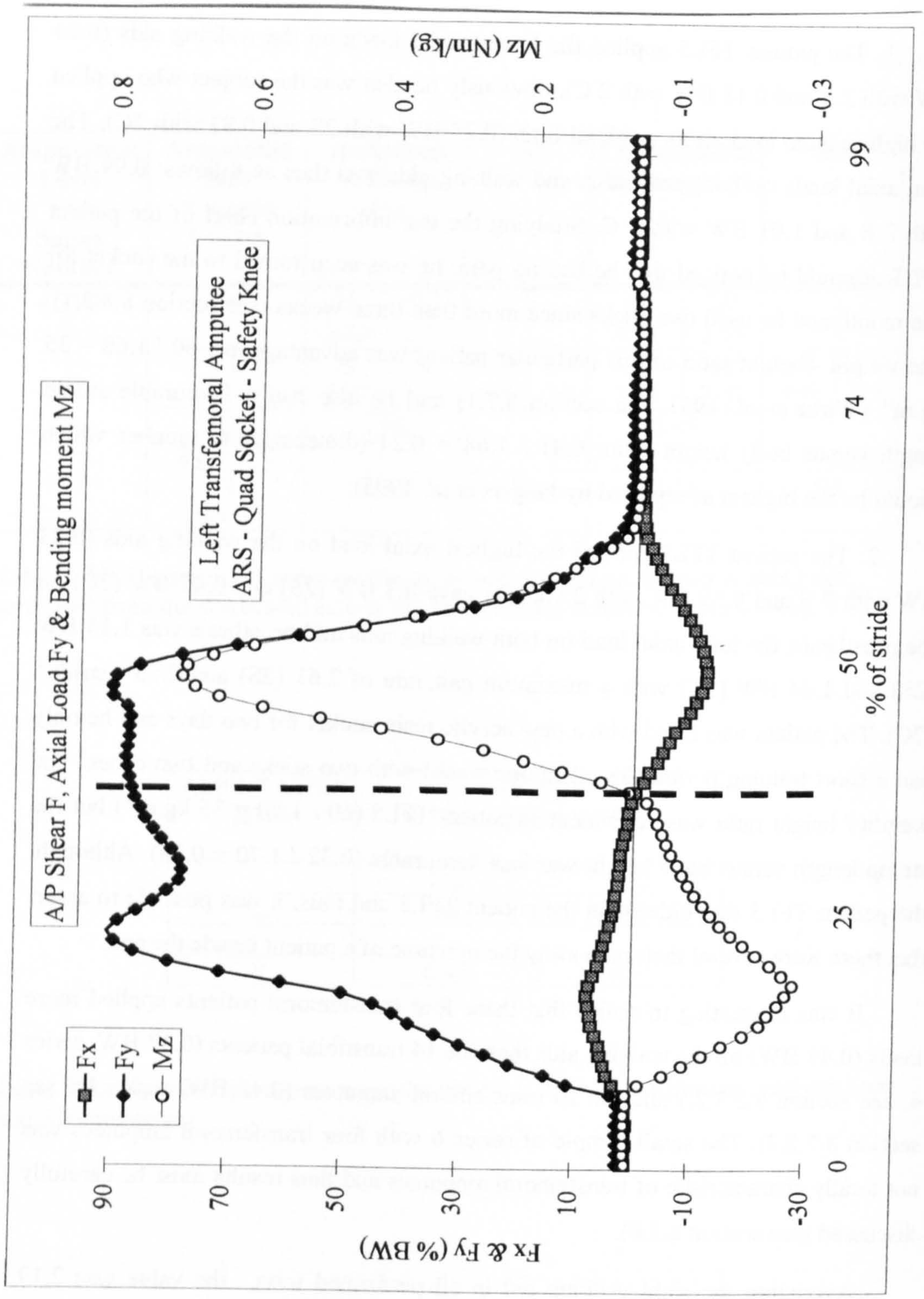

Figure 8.37: One stride of patient TFL9 showing A/P shear force Fx, axial load Fy and A/P bending moment Mz. The approximate instant of crossing the vertical by the shank tube of the prosthesis is shown by a dashed vertical line: Fx and Mz = 0, Fy is maximum. The two walking aids are not shown.

(3.34; 2.93 N.kg^{-1}, respectively 2S, 2C).

Averaging the left walking aid in all performed tests, the value was 3.09 N.kg^{-1} (SD = 1.6) with two sticks and 1.84 N.kg^{-1} (SD = 0.9) with two canes. This 63 % difference was weakly significant (p = 0.07). The range was large and it was again the same two patients as above: TFL5 (1.27 - 0.73 N.kg^{-1}, respectively 2S, 2C) and TFL3 (4.82 - 2.85 N.kg^{-1}, respectively 2S, 2C).

By separating left and right canes relatively to the amputated side, the results are shown in table 8.39:

- For the 3 left amputees: two sticks: right cane (contra) 2.24 N.kg^{-1} (SD = 0.6), left cane (ipsi) 2.67 (SD = 0.9); two canes: right cane (contra) 2.03 N.kg^{-1} (SD = 0.4), left cane (ipsi) 1.61 (SD = 0.3). Because of the small size of the sample, no statistics were calculated. However, the ipsi - contra gap showed opposite as it was expected, namely, the contralateral walking aid was more loaded than the ipsi with two canes and it was the opposite with two sticks. As previously stated for transtibial amputees, further research is necessary to assert any conclusion, including the recording of the predominant foot.

- For the unique right side amputee: two sticks: right cane (ipsi) 2.02 N.kg^{-1}, left cane (contra) 4.34 N.kg^{-1}; two canes: right cane (ipsi) 1.35 N.kg^{-1}, left cane (contra) 2.55 N.kg^{-1}; Because of the small size of the sample, neither statistics nor standard deviations were calculated. The right side amputee of the tested series applied more load on the opposite cane to his amputation, which was as expected.

Showing side by side the mean results, it comes:

	Left Side	Right Side
2 sticks N.kg^{-1}	3.50	2.02
2 canes N.kg^{-1}	2.08	1.67

This gap gave the impression that, whatever the amputation side was, the left walking aid was more loaded than the right.

It was thus possible to find again the same problem as previously stated for transtibial amputees: two out of three left amputees applied more load on the ipsi

ANTERIO - POSTERIOR NEGATIVE BENDING MOMENT (Mz-)									
	Series Descriptions	Mean Mz - $N.m.kg^{-1}$		SD		p value	NS not significant S significant at $p \leq 0.05$	Range	
Series 6	4 TFP 2S vs. 2C	2S 0.13	2C 0.14	2S 0.10	2C 0.09	0.22	NS	2S 0.04 0.26	2C 0.07 0.28

Table 8.41: The range of results of mean negative anterio-posterior bending moment at the artificial ankle level for series 6 of four transfemoral subjects, expressed in $N.m.kg^{-1}$

ANTERIO - POSTERIOR POSITIVE BENDING MOMENT (Mz+)									
	Series Descriptions	Mean Mz + $N.m.kg^{-1}$		SD		p value	NS not significant S significant at $p \leq 0.05$	Range	
Series 6	4 TFP 2S vs. 2C	2S 0.22	2C 0.21	2S 0.08	2C 0.13	0.23	NS	2S 0.17 0.34	2C 0.08 0.38

Table 8.42: The range of results of mean positive anterio-posterior bending moment at the artificial ankle level for series 6 of four transfemoral subjects, expressed in $N.m.kg^{-1}$

(left) lateral walking aid than the contra (right) lateral walking aid. This gait pattern was the opposite to that expected. The right amputees had a gait pattern as usually described in the literature (Engstrom & Van de Ven, 1993; Deathe *et al.* 1993). A discussion about this question, found in transtibial as well as transfemoral series, is conducted in chapter 9.

As for transtibial amputees (see 8.5.5), some ratios could be calculated. The noteworthy comments are the following:

- WAGRF (2 sides) versus PGRF (10 subjects, series 1b) = 0.61; thus, in early stage of rehabilitation, the transfemoral patients applied 60 % of the body weight on the prosthesis and 40 % on the two walking aids.

- Ipsilateral and contralateral WAGRF versus PGRF:

	Amputated Left Side		Amputated Right Side	
	2 S	2 C	2 S	2 C
ipsi vs. PGRF	0.48	0.23	0.36	0.19
contra vs. PGRF	0.40	0.30	0.78	0.37

As stated in section 8.5.3.2, the ratio contra vs. PGRF should exceed the ratio ipsi vs. PGRF: this was true for the right amputee whatever the walking aid used. For left amputees, it was as expected when the patients used two canes but not with two sticks. Therefore, it was difficult to establish some accurate conclusion.

The ratio of forces ipsilateral versus contralateral walking aid is shown in table 8.40. It should be always less than 1 and as low as possible to eliminate the use of the ipsi walking aid. As above, the same comment could be made: the three left transfemoral amputees applied more load on the ipsilateral relatively to the contralateral stick and there was no evident explanation.

8.8.3 The fore-aft shear force

The gait pattern in that particular channel was the same as it was for transtibial amputees: the anterio-posterior shear force Fx begun to be positive at heel-strike and during early prosthetic stance then negative during the backward acceleration at prosthetic late stance phase. The results were the followings:

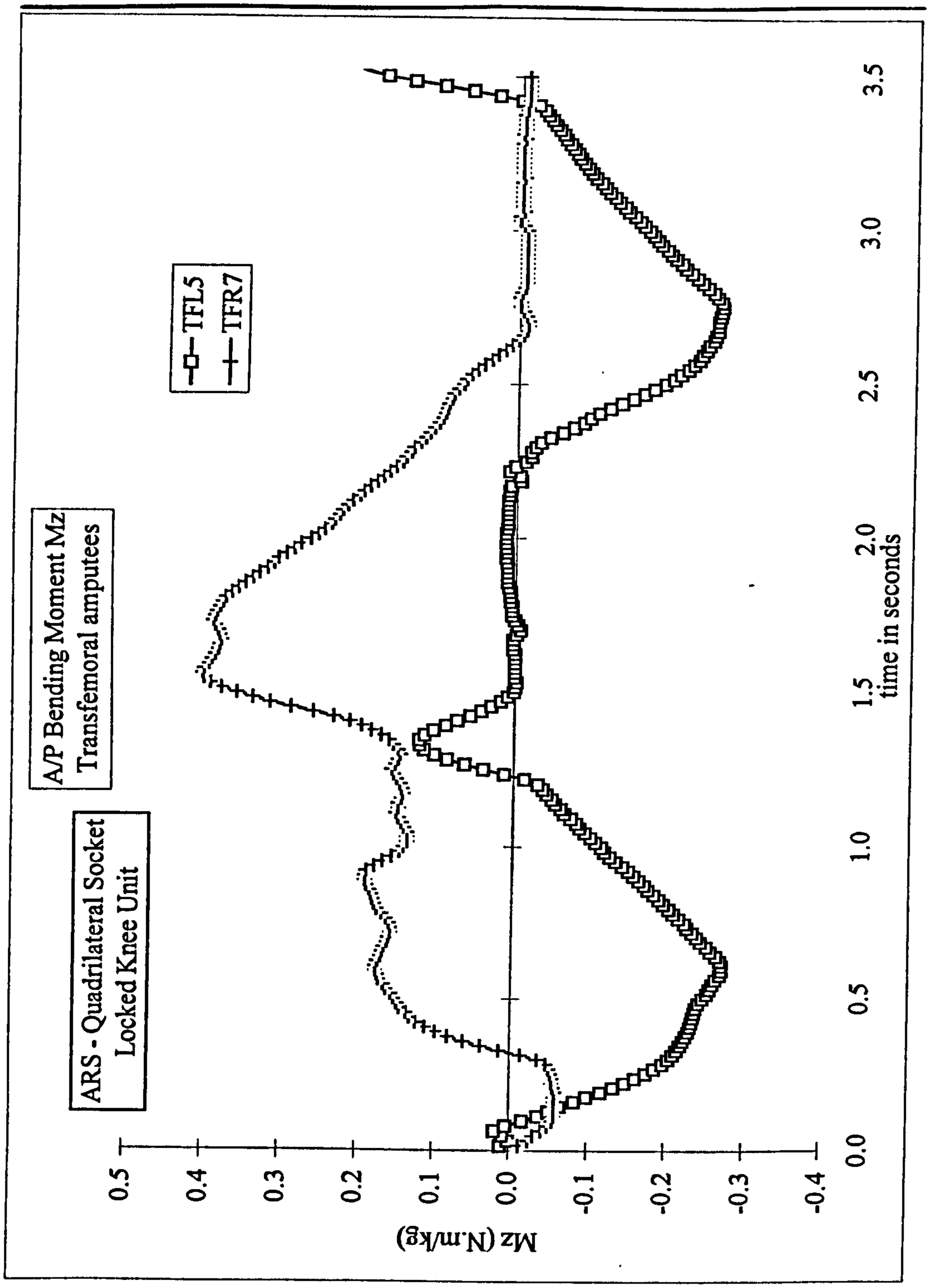

Figure 8.38: One stride (patient TFR7) and one stride and half (patient TFL5) of two transfemoral amputees (the gait rate was not the same) showing the A/P bending moment Mz: from – 0.3 (TFL5) to 0.04 (TFR7) N.m/kg.

2 sticks	- 0.81N.kg^{-1} (SD = 0.33)	
	+ 0.80 N.kg^{-1} (SD = 0.76)	(8 % BW)
2 canes	- 0.93 N.kg^{-1} (SD = 0.65)	
	+ 0.90 N.kg^{-1} (SD = 0.84)	(9 % BW)

In both negative and positive directions, the gap was approximately 14 % and it was not significant (p = 0.18 and 0.21, respectively). It was interesting to remark that the negative and positive values were symmetrical. Three out of four patients wore a locked artificial knee unit. These values were slightly lower in both directions than those found in the literature: -6 to -12 % BW and 10 to 12 % BW (Yang *et al.* 1991). It is however interesting to note that these researchers found a non symmetrical negative positive A/P shear force (-6 to +11 % BW) with patients fitted with a uniaxial knee with extension bias and symmetrical (-12 to + 11 % BW) with patients fitted with a uniaxial knee joint and pneumatic swing phase control. It is thus obvious that the knee unit and globally the fitting of the patient have a major importance in the gait pattern.

Some comments could be expressed. Two patients out of four decreased the Fx negative value when they moved from two sticks to two canes which was not as expected because with more unstable walking aids, all forces should increase. There was also a large discrepancy of the results: -0.56 to -1.31 N.kg^{-1} with 2S and -0.35 to -1.86 N.kg^{-1} with 2C. The results exhibited thus a large uncertainty. These extreme values were recorded from two patients: patient TFL5 (-0.56, -0.35) and patient TFR7 (-1.31, -1.86). The characteristics of the left side amputee TFL5 were given above in section 8.8.2.2. The patient TFR7 was a right side amputee, relatively young (53). He was fitted with a silicone soft socket with a quadrilateral acrylic resin socket fitted with a safety artificial knee unit. However, he had an arterial by-pass surgery four weeks before and he was suffering pain in his sound limb (see section 8.3.6).

Three patients out of four showed decreased Fx positive values with large unfocused results: 0.04 to 1.61 (2S) and 0.11 to 1.79 N.kg^{-1} (2C). Here also, the extreme values were recorded from the two same patients TFL5 (1.61 to 1.79) and

Subject Code	Trend of PSP from 2S to 2C	Trend of GR from 2S to 2C	Ratio PSP vs. GR		Ratio Axial Load (2S) vs. Axial Load (2C)
			2S	2C	
TFL4	↓	↓	0.80	0.80	0.98
TFR7	↑	↑	0.72	0.81	0.63
TFL5	↓	↓	0.68	0.66	0.91
TFL3	↑	↓	0.63	0.70	0.66

Table 8.43: The trends of prosthetic stance phase (PSP) and gait rate (GR) from 2S to 2C for the four transfemoral amputees of the series 6. The ratios PSP / GR and axial load 2S / axial load 2C are shown (see text for comments)

TFR7 (0.04 to 0.11). The patient TFL5 was incapable of improving his gait pattern although he had a special and long gait training (four weeks, full stay-in, see section 8.8.2.1). As previously stated, both hip joint disorder and / or prosthetic alignment problem could be blamed of such a problem.

8.8.4 The anterio-posterior bending moments at the artificial ankle joint

In the sagittal plane, the behaviour of a prosthetic ankle during gait, is equivalent to that of a normal and a transtibial amputee ankle: a plantar flexion moment (Mz-) during early prosthetic stance phase, crossing the followed by a dorsiflexion (Mz+) at late stance phase. The crossing of the zero line is the instant at which the fore-aft component of the ground reaction force changes from negative to positive. The shank tube is approximately vertical. As example, figure 8.37 shows one stride of patient TFL9 with the traces from A/P shear force (Fx), axial load (Fy) and A/P bending moment (Mz). The dashed vertical line shows approximately the vertical position of the prosthetic shank tube. In this position and at the ankle level:

1. there was only compression: axial load Fy was close to the maximum
2. there were no fore–aft shear forces: A/P shear force was zero
3. there were no fore–aft bending moments: A/P bending moment was zero

The results display a large discrepancy in both directions and they are shown in tables 8.41 and 8.42.

From two sticks to two canes, 3 patients out of 4 increased the value of Mz negative (plantarflexion). The range of the values was as follows: 0.04, 0.26 N m.kg^{-1} (2S) and 0.07, 0.28 N m.kg^{-1} (2C). These values were recorded from two tests performed by the two same patients described above when A/P shear forces were discussed: TFR7 and TFL5.

From two sticks to two canes, 2 patients out of 4 decreased the level of Mz positive (dorsiflexion) at late stance phase. The range of values was the following: 0.17, 0.34 N m.kg^{-1} (2S) and 0.08, 0.38 N m.kg^{-1} (2C). These extreme values were coming from the two same patients. They were fitted with opposite knee devices

Subject Code	Trend of PSP from 2S to 2C	Trend of GR from 2S to 2C	Trend of SSP or CSP	Ratio SSP or CSP vs. GR	
				2S	2C
TFL4	↓	↓	=	0.92	0.94
TFR7	↑	↑	↑	0.86	0.91
TFL5	↓	↓	=	0.73	0.76
TFL3	↑	↓	=	0.85	0.88
			Mean	**0.84**	**0.87**

Table 8.44: The same trends as table 8.42 in relation with the trend of the stick stance phase (SSP) or cane stance phase (CSP). The ratio between the stick or cane stance versus the gait rate is shown.

Subject Code	Ratio SSP or CSP vs. SST or CST		Ratio PSP vs. SSP or CSP	
	2S	2C	2S	2C
TFL4	0.92	0.94	0.87	0.84
TFR7	0.86	0.91	0.84	0.89
TFL5	0.74	0.76	0.92	0.86
TFL3	0.85	0.88	0.73	0.80
mean	**0.84**	**0.87**	**0.84**	**0.84**

Table 8.45: Side by side, two important ratios: the stick or cane stance phase (SSP or CSP) versus the stick or cane stride time (SST or CST); the prosthetic stance phase (PSP) versus the stick or cane stance phase (see text for comments).

Subject Code	Ratio SSwP or CSwP vs. GR	
	2S	2C
TFL4	0.08	0.06
TFR7	0.14	0.09
TFL5	0.27	0.24
TFL3	0.15	0.12
mean	**0.16**	**0.13**

Table 8.46: The ratios between the stick swing phase (SSwP) and the cane swing phase (CSwP) versus the gait rate (GR).

such as:

- TFR7: silicon soft socket + quadrilateral ARS + safety knee unit
- TFL5: quadrilateral ARS + locked knee

The results were thus consistent. These two patients walked with an exactly opposite gait pattern. However, it should be hazardous to draw conclusions with such a small sample. By way of illustration, figure 8.38 shows simultaneously the A/P bending moment of one stride, chosen among ten strides and recorded from the patients TFL5 and TFR7. The A/P bending moment was approximately within the range of 0.3 N m/kg (negative) and 0.4 N m/kg (positive). These mean values were lower the those found in the literature with transfemoral amputees due to trauma: -0.4 N m/kg (negative) and 0.8 N m/kg (Yang *et al.* 1991). These researchers pointed out that the magnitude of the dorsiflexion moment about the prosthetic ankle joint was limited by the length of the artificial foot. However, the instant at which the plantar flexion moment changed into dorsiflexion moment (Mz = 0) was sensitive to the orientation angle of the foot relative to the ground (Yang *et al.* 1991)[19]. This comment is discussed again when the temporal parameters of the gait are shown (see the following section 8.8.5). The other channels such as M/L shear force Fz, M/L bending moment Mx and transverse torque are shown in appendix 11.VIII.9.

8.8.5 Temporal parameters: Chronology of gait events and loads during transfemoral amputees ambulation

As stated when the results from transtibial amputees were discussed, the duration of the prosthetic stance phase (PSP) is one of the main temporal parameters to study. It is a strong reflection of the gait pattern and the way of using the artificial limb by the patient. For the four subjects (see table 8.43), the mean PSP was 2.03 s (SD = 0.55) with two sticks and 2.25 s (SD = 0.77) with two canes. This time interval of 10 % was not significant (p = 0.16). As previously stated for transtibial amputees, the duration performed by these four transtibial amputees in early stage of rehabilitation, was larger than those found in the literature: 0.83 s (Zuniga *et* al, 1972); 0.77 s (James & Öberg, 1973); 0.74 s (Boonstra *et al.*, 1994). The ratio was

---

[19] The toe-out angle changes the length of the artificial foot.

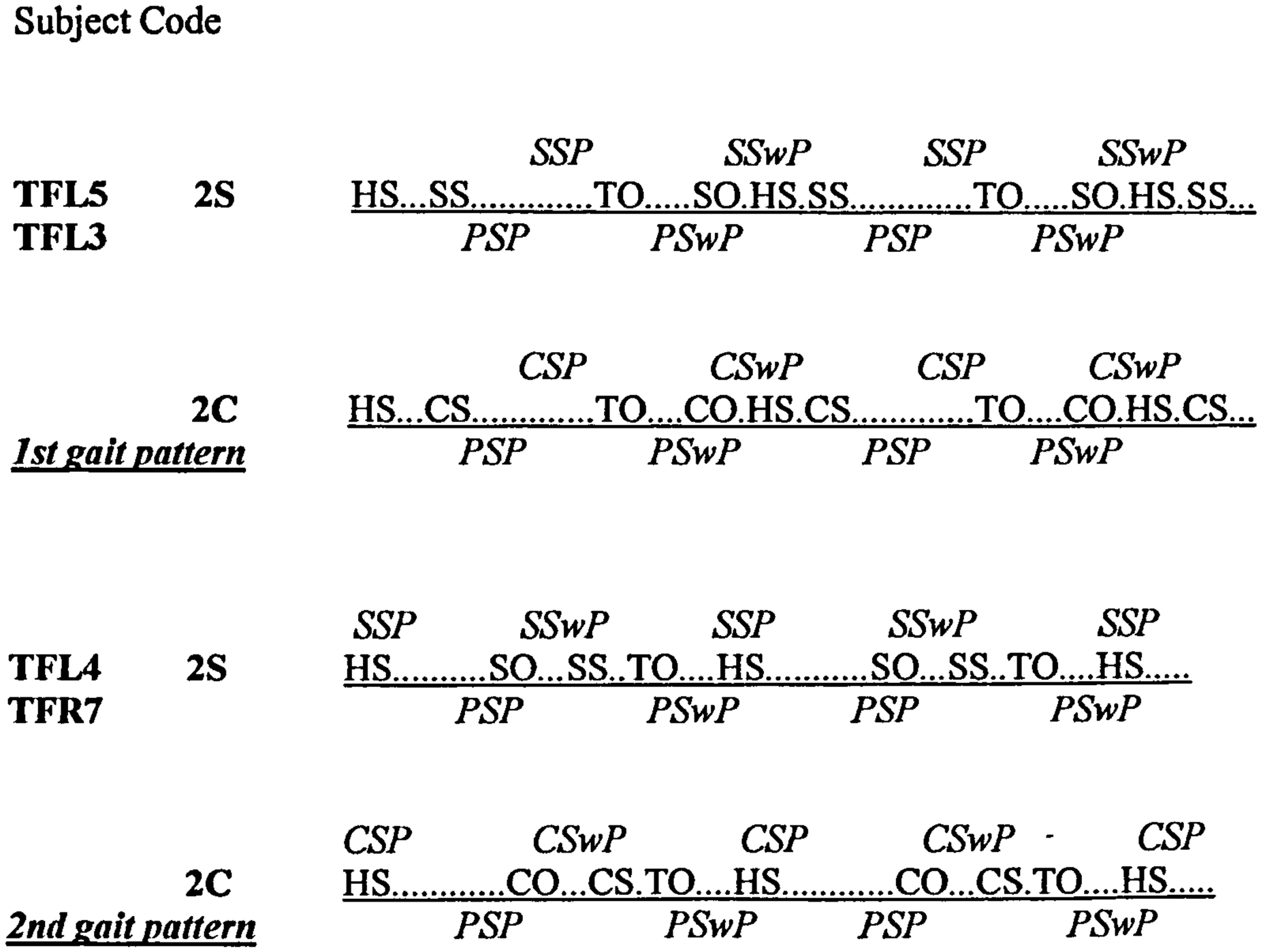

Figure 8.39: The average Gait Pattern Line (GPL) extracted from six to eight strides of four vascular transfemoral amputees.

The two top lines averaged the similar gait pattern of the subjects TFL5 and TFL3 when they used two sticks (2S) then two canes (2C): **GAIT PATTERN 1**

The two bottom lines averaged the similar gait pattern of the subjects TFL4 and TFR7 when they used two sticks (2S) then two canes (2C): **GAIT PATTERN 2**

All the lines begin at heel strike (HS) and the gradation respects the scale of sizes of the different intervals (see explanations in figure 8.8)

about one to three.

Two patients out of four had decreased their PSP when they changed from two sticks to two canes (see table 8.43). It was thus impossible to conceive any opinion. The discrepancy was large: 1.51 s to 2.31 s (2S) and 1.43 s to 3.12 s (2C). As in fore-aft shear force and bending moments, it was the same two patients who performed these extreme values, the patient TFL5: 1.51 s (2S), 1.43 s (2C) and the patient TFR7: 2.31 s (2S) and 3.12 s (2C). The patient TFR7 had a gait pattern opposite to that of the three others. He increased his gait rate and his PSP from two sticks to two canes. The ratio PSP versus GR (equivalent as prosthetic stride time PST) was 0.72 (2S) and 0.81 (2C). Therefore, from two sticks to two canes, the patient TFR7 walked more slowly with a longer duration of the prosthetic stance phase. This gait pattern was usually linked with an increase of prosthetic ground reaction force and thus a decrease of the load applied on the walking devices. The gait pattern described for transtibial patients was thus found again (see section 8.5.5): velocity and prosthetic axial load were inversely related. This was explained by the two patients TFR7 and TFL3: they increased their prosthetic stance phase from two sticks to two canes and the corresponding axial load ratio was about 0.65. The two other patients decreased their gait rate and the corresponding ratio was about 0.94. However, this should be confirmed by increasing the size of the sample.

Globally, from 2S to 2C, the stick or cane stance phase lasted longer. In other words, the subjects applied less load on the walking aids but longer. The results are summarised and shown in table 8.44. The values were as follows: two sticks 2.42 s (SD = 0.62), two canes 2.62 s (SD = 0.84). However, this 8 % time interval was not statistically significant (p = 0.17). Here also, there was a large discrepancy of the results: 1.64 to 3.08 s (2S) and 1.65 to 3.49 (2C). The patient TFL5 was still the patient who had the shorter stick or cane floor contact: 1.64 s (2S) to 1.65 s (2C). On the other hand, the two longest SSP or CSP did not come from the same subject.

Thus, approximately, the ratio SSP or CSP versus gait rate (GR) was practically identical (the gap was only + 3.5 %) from two sticks to two canes. In the mean time, the load on the walking devices decreased by about 42 % (see chapter 8.7.2.2). In other words, as opposed to the two sticks, the canes, which are more

	Subject Code		SS (CS) to TO	TO to SO (CO)
Gait Pattern 1	TFL5	2S	1.16	0.48
		2C	1.18	0.47
	TFL3	2S	1.53	0.71
		2C	1.57	0.68
Gait Pattern 2	TFL4	2S	0.38	2.70
		2C	0.22	2.90
	TFR7	2S	0.11	2.62
		2C	0.18	3.31

Table 8.47: The time intervals in the two gait patterns described in the text:
1. from the gait event stick (SS) or cane strike (CS) to prosthetic toe off (TO)
2. from prosthetic toe off to stick (SO) or cane off (CO)

unstable, are used to maintain the medio-lateral equilibrium of the patient (long cane stance phase) rather than to accelerate forward the body or to minimise the axial load on the artificial limb (low axial load on the canes).

As previously stated in section 8.5.5, the study of another ratio is necessary to describe more thoroughly the gait pattern of transfemoral amputees in the early stage of rehabilitation. The ratios walking aids stance phase (SSP or CSP) versus sticks or cane stride time (SST) and prosthetic stance phase (PSP) versus stick or cane stance phase (SSP or CSP), are shown in table 8.45.

These two ratios were similar, they expressed a gait pattern in which the walking aids were widely used: a long duration of floor contact during the walking aid cycle and the gait cycle itself. It was interesting to compare these two ratios with those found in gait of transtibial amputees: 0.81 to 0.89. Therefore, the ratio between aid stance versus aid cycle was found equal. However, between prosthetic and aid stance, it was found lower from transfemoral than transtibial patients. In other words, the walking aids cycle was the same whatever the amputation level was; but transfemoral amputees seemed to use walking aids during less time than transtibial amputees. The explanation looked evident if the item « stump pain » was taken into account: the information charts showed that more transtibial patients expressed the idea of pain, especially during ambulation, than the transfemoral group. The ratio walking aid versus prosthetic stance for transfemoral amputees in early stage of rehabilitation was also above the one reported in the literature: 0.63 in Murray *et al.* (1969) but as previously stated in chapter 1, it was an investigation on traumatic amputees.

By mirror image of the stance phase with the walking devices, from two sticks to two canes, the swing phase of the walking aids was decreasing: 0.41 s (SD = 0.13) to 0.33 s (SD = 0.13). This 24 % decrease was all the same not significant ($p = 0.102$).

Besides the ratio aid stance phase versus gait rate shown above, the complementary ratio stick or cane swing phase versus gait rate could be summarised as shown in table 8.46.

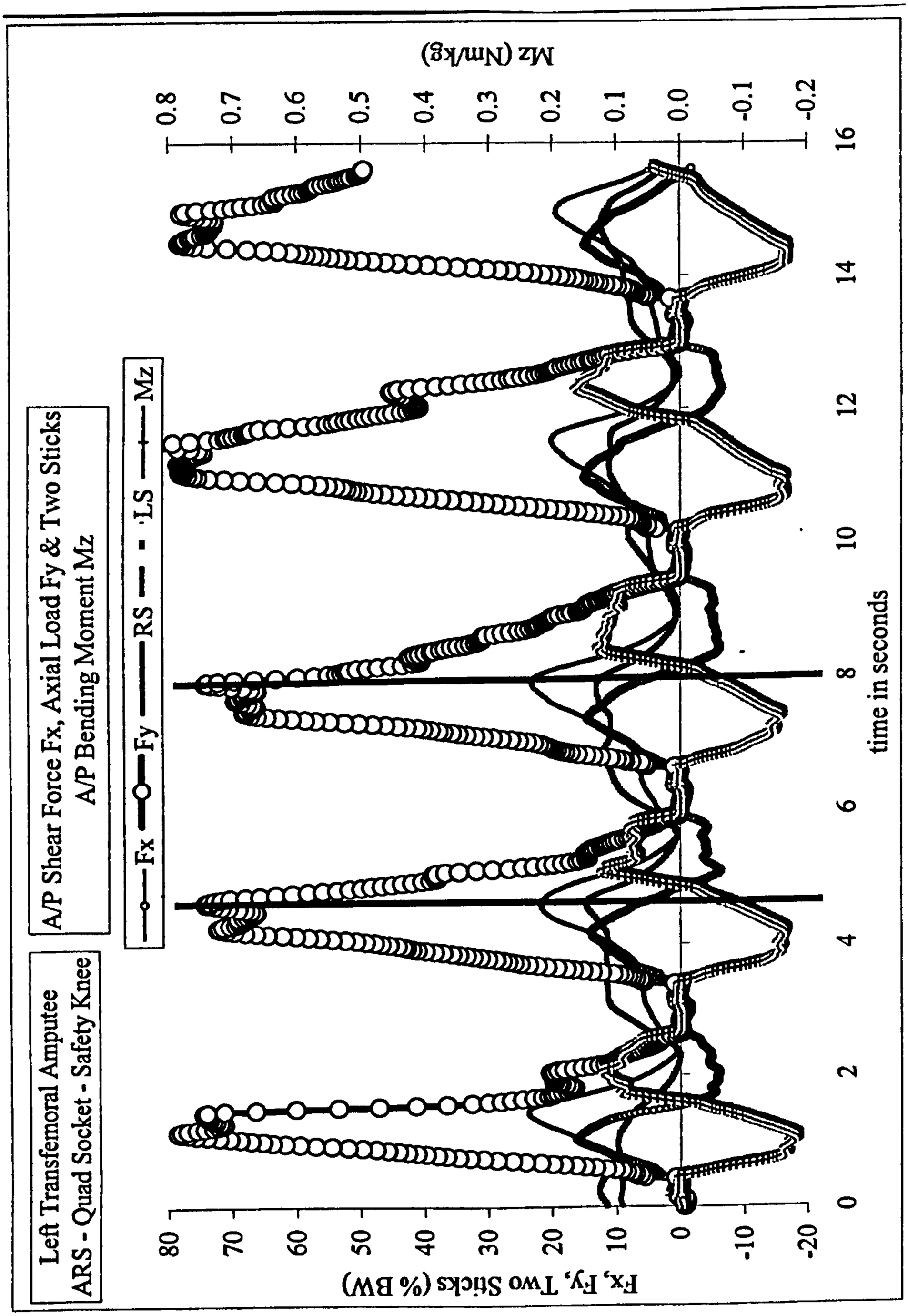

Figure 8.40: Four strides of the left transfemoral amputee TFL4 showing simultaneously: the A/P shear force (Fx); axial load (Fy); A/P bending moment (Mz) and the loads applied on the right stick (RS) and the left stick (LS). The results are in percentage of BW for the forces and N.m/kg for the bending moment versus time in seconds. Concerning the vertical solid lines, see text for explanations and comments.

The main comments are the following:

1) the ratio between stick stance phase versus stick stride time exceeded published results. The four vascular transfemoral amputees tested in this work had a floor contact of the walking devices during more time (+ 28 %) than the two transfemoral traumatic amputees studied in the investigation conducted by Murray *et al.* (1969).

2) the ratio between the prosthetic and the stick stance phase was lower than 1 for all patients. In other words, the four transfemoral amputees had a stick or cane floor contact duration longer than the prosthetic ground floor contact (+ 15 %). It could be also noticed that this ratio was nearly constant for each patient. An amputee selects his own gait pattern following several reasons such as: stump length, joint range of motion, muscle strength, health status of the sound limb and previous gait pattern.

This adaptation of the gait behaviour was made to 1) decrease the pain, the energy expenditure; 2) increase the comfort of ambulation, the efficiency of gait and the equilibrium (see shaded cells in table 8.45).

As for transtibial amputees, the question was likewise to study the different time intervals between the main events of the gate cycle of the artificial limb such as heel strike (HS) and toe off (TO) with the walking aid cycle, namely, stick or cane strike (SS or CS) and stick or cane off (SO or CO), as shown in section 8.5.5. The main aims are:

1) To describe the different gait pattern lines from the four tested subjects (GPL shown in figure 8.8, section 8.4.1)

2) To compare transfemoral patients with each other

3) To establish (if possible with a so small size sample) one or several common trends about the aided gait of vascular transfemoral amputees in early stage of rehabilitation

4) To relate these results with those found in the literature (but there are very few papers on this topic) and with aided gait of recent vascular transtibial amputees

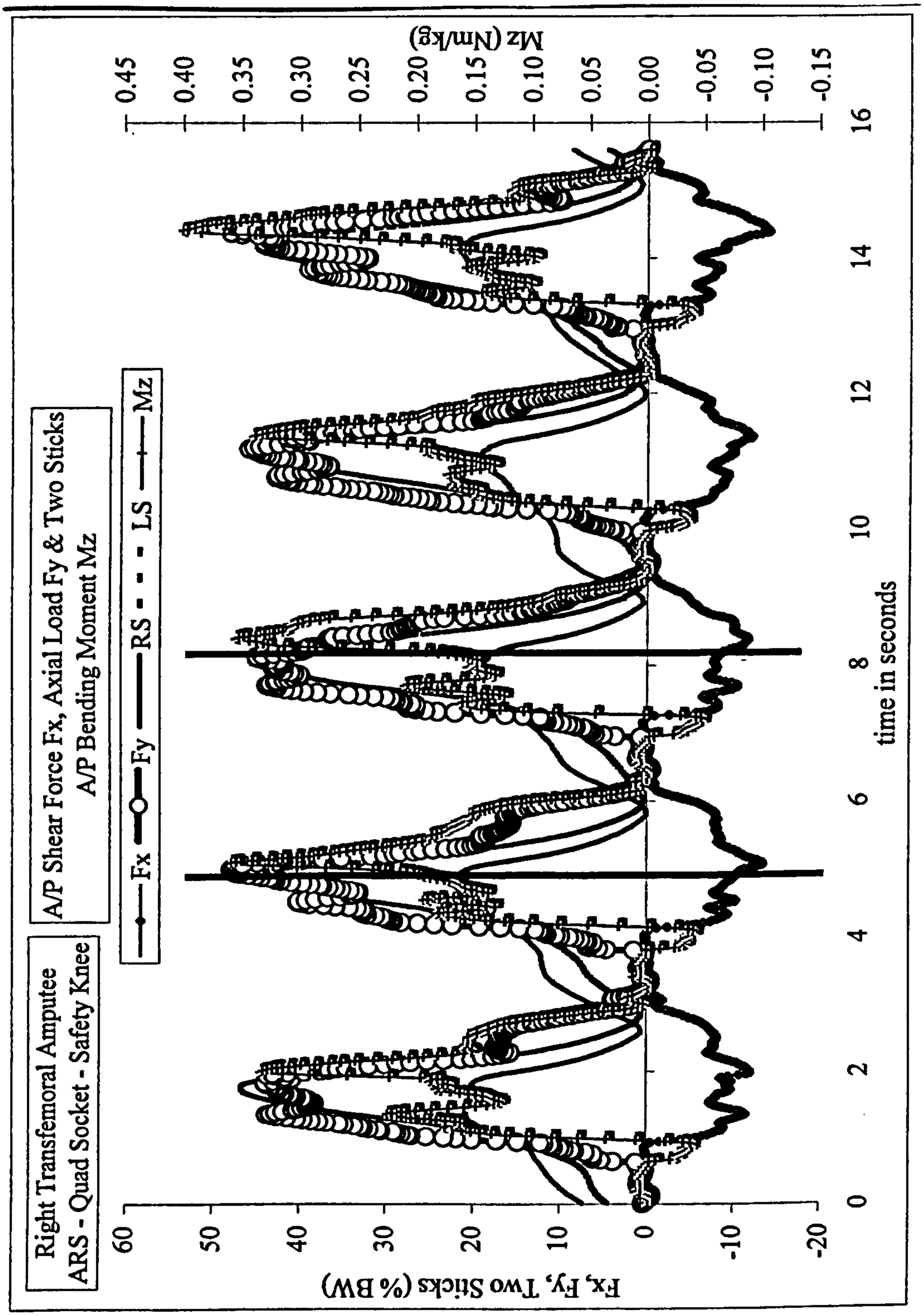

Figure 8.41: Five strides of the right transfemoral amputee TFR7 showing simultaneously: the A/P shear force (Fx); axial load (Fy); A/P bending moment (Mz) and the loads applied on the right stick (RS) and the left stick (LS). The results are in percentage of BW for the forces and N.m/kg for the bending moment versus time in seconds. Concerning the vertical solid lines, see text for explanations and comments.

(if such a comparison makes sense).

The four GPLines are shown in figure 8.39. Studying the different time intervals expressed by the four patients, two main gait patterns are shown as follows:

GAIT PATTERN 1: The Stick or Cane Strike was started just after Heel Strike (0.2 s); the Stick or Cane Off was after Toe Off (0.6 s) and just before the next Heel Strike (subjects TFL5 and TFL3). In other words, the prosthetic stance phase (PSP) was totally included in the stick or cane stance phase, except the time interval between HS and SS or CS, which had a mean duration of 0.2 seconds. There was an overlap of the aid stance phase on the prosthetic swing phase. Therefore, the two walking aids were used 1) to minimise the stress at stump - socket interface during prosthetic stance phase and 2) to accelerate the body forward during the early prosthetic swing phase. In this particular gait pattern, during late prosthetic swing phase, the subject was off loaded with both aids and prosthesis. He applied load only on his sound limb: one point load during sound limb stance phase and three points load during sound limb swing phase. However, as previously stated in section 8.5.5, there was a main drawback in the set up used which did not allow to record and check the position of the sound limb or the acceleration of the trunk.

GAIT PATTERN 2: The Stick or Cane Strike was started just before the prosthetic Toe Off (0.2 s); the Stick or Cane Off was after and far from Toe Off (2.91 s). In other words, the stick stance phase started when the prosthetic swing phase begun and the SSP finished before the end of the prosthetic stance phase; thus a part of the PSP was accomplished with the walking aids off load. It is thus possible to say that these two subjects needed two props during prosthetic swing phase, it could be for equilibrium reasons, but nothing, in the present work, can prove it.

It is important to express the place of the TO event inside the stick or cane stance phase as shown in table 8.47. The main differences between the two gait patterns can be summarised as follows:

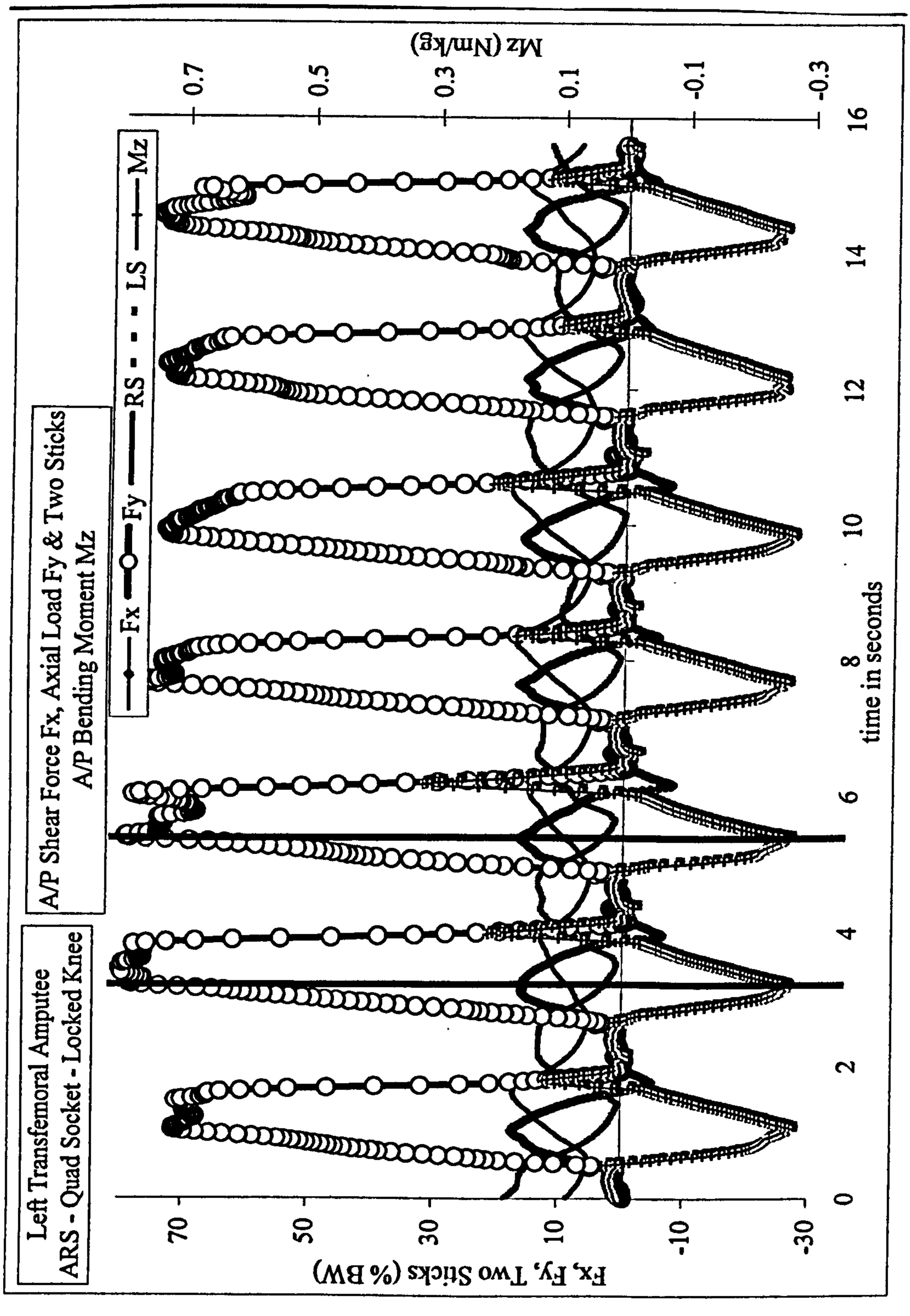

Figure 8.42: Seven strides of the left transfemoral amputee TFL5 showing simultaneously: the A/P shear force (Fx); axial load (Fy); A/P bending moment (Mz) and the loads applied on the right stick (RS) and the left stick (LS). The results are in percentage of BW for the forces and N.m/kg for the bending moment versus time in seconds. Concerning the vertical solid lines, see text for explanations and comments.

	1st Gait Pattern (TFL5 & TFL3)	2nd Gait Pattern (TFL4 & TFR7)
PSP	3 points load (P + 2 WA) except 15 % from HS to SS	3 points load (P + 2 WA) except 11 % from SO to SS (ratio SSwP vs. PSP) or 1 point load ? (P)
PSwP	1 point load (SL) from SO to HS	3 points load (2 WA + SL)
SSwP or CSwP	1 point load (SL) from SO to HS 1 point load (P) or 2 points load ? (SL +P) from HS to SS	2 points load (P + SL) or 1 point load (P) ?

P, SL and WA stand respectively for prosthesis, sound limb and walking aids. The interrogative point expresses a hypothetical conclusion because of the uncertainties concerning 1) the position of the sound limb and 2) the gait event of the contralateral foot relative to the amputated side.

Therefore, the main difference between the two gait patterns was the place of the stick or cane swing phase inside the prosthetic gait cycle:

1st gait pattern: the aid swing phase overlapped the prosthetic heel strike and thus the time during which there was <u>one point load was widened</u> and moving towards the prosthetic swing phase.

2nd gait pattern: the aid swing phase was completely included during the prosthetic stance phase and thus the time during which there was <u>one point load was shortened</u> and moving toward the prosthetic stance phase.

However,

These conclusions are vitiated by the lack of knowledge concerning the position of the sound limb.

These considerations are only an average of a small sample of transfemoral patients.

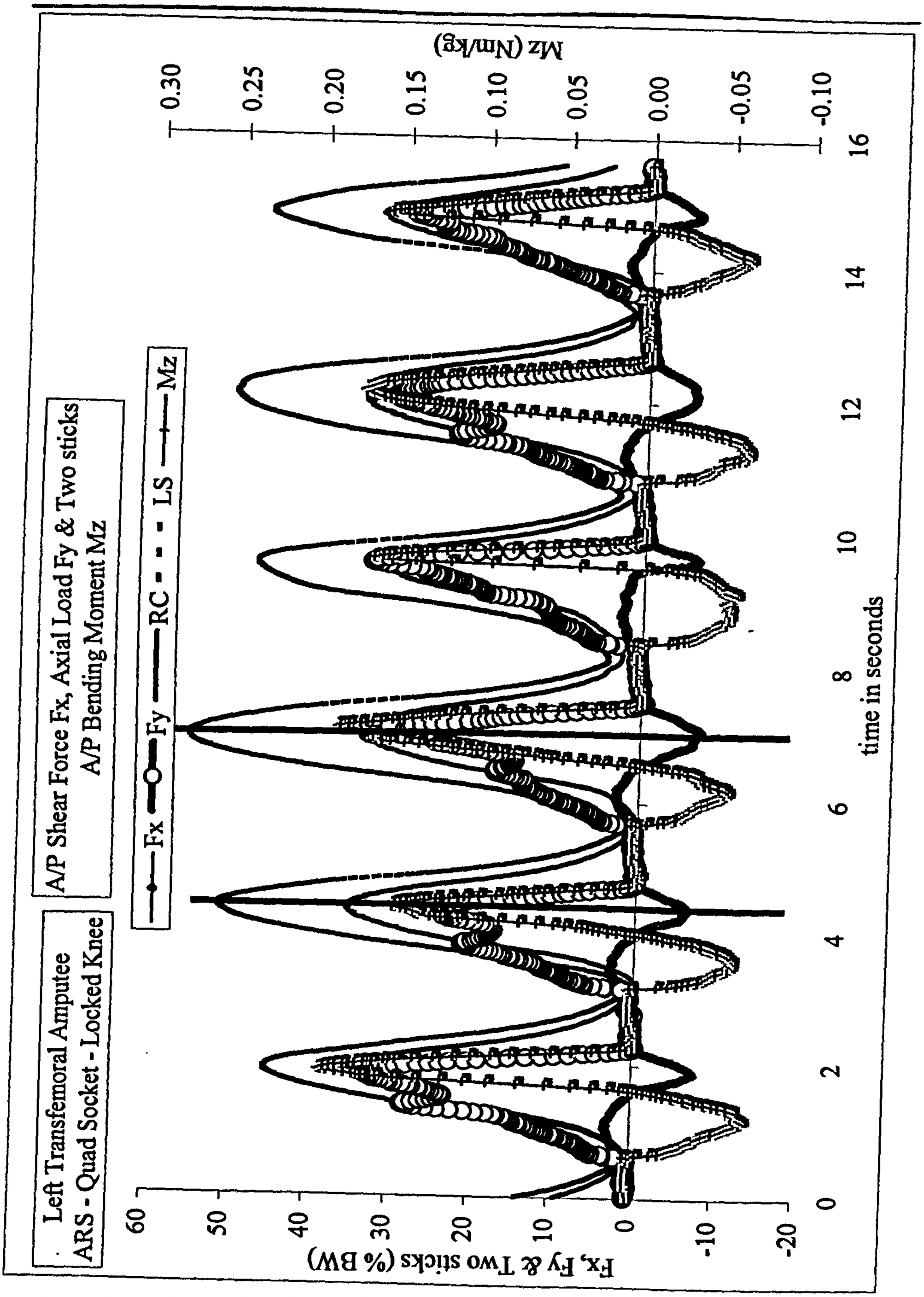

Figure 8.43: Six strides of the left transfemoral amputee TFL3 showing simultaneously: the A/P shear force (Fx); axial load (Fy); A/P bending moment (Mz) and the loads applied on the right stick (RS) and the left stick (LS). The results are in percentage of BW for the forces and N.m/kg for the bending moment versus time in seconds. Concerning the vertical solid lines, see text for explanations and comments.

It will seen below that the gait pattern of such amputees in the early stage of rehabilitation is more complex and the description of two mean gait patterns is simplistic (see section 8.9).

It has equally appeared interesting to study the time interval between the maximum axial load (Fy maximum) on the prosthesis, the maximum dorsiflexion bending moment of the artificial ankle (Mz+), the maximum posterior shear force (Fx-) and the maximum load applied on the sticks or the canes.

Globally, transfemoral patients applied the maximum axial load on the walking aids closer to the maximum prosthetic axial load than transtibial patients. Therefore, for transfemoral patients, the sticks or the canes were less used for forward body propulsion and the weight transfer from one side to the other could occur earlier in the gait cycle than for transtibial patients.

However, there was a large discrepancy of the results. Thus, rather consider a mixing of the four subjects (which could introduce some erroneous conclusion), each subject can be separately studied. The results are shown in four figures 8.40 to 8.43 having the following characteristics: 5 to 7 strides showing simultaneously, the A/P shear forces, the axial load on the prosthesis and the walking aids and the A/P bending moments. The forces are in percentage of the BW while the moments are in N m/kg.

The comments are as follows:

- Subject TFL4 (figure 8.40): the two solid vertical lines show the simultaneousness of the maximum axial loads (prosthesis and walking aids) and the zero crossing of the A/P shear force and bending moment (particularly at 8 seconds).

- Subject TFR7 (figure 8.41): the two solid vertical lines equally show the simultaneousness of the maximum loads (prosthesis and walking aids), plus the maximum of A/P shear force negative (-13 % BW) and maximum A/P bending moment Mz (0.35 to 0.40 N m/kg). As previously stated, the patient TFR7 was fitted with a safety knee, the three others subjects used a locked knee unit.

- Subject TFL5 (figure 8.42): the solid vertical lines are perfectly laid out

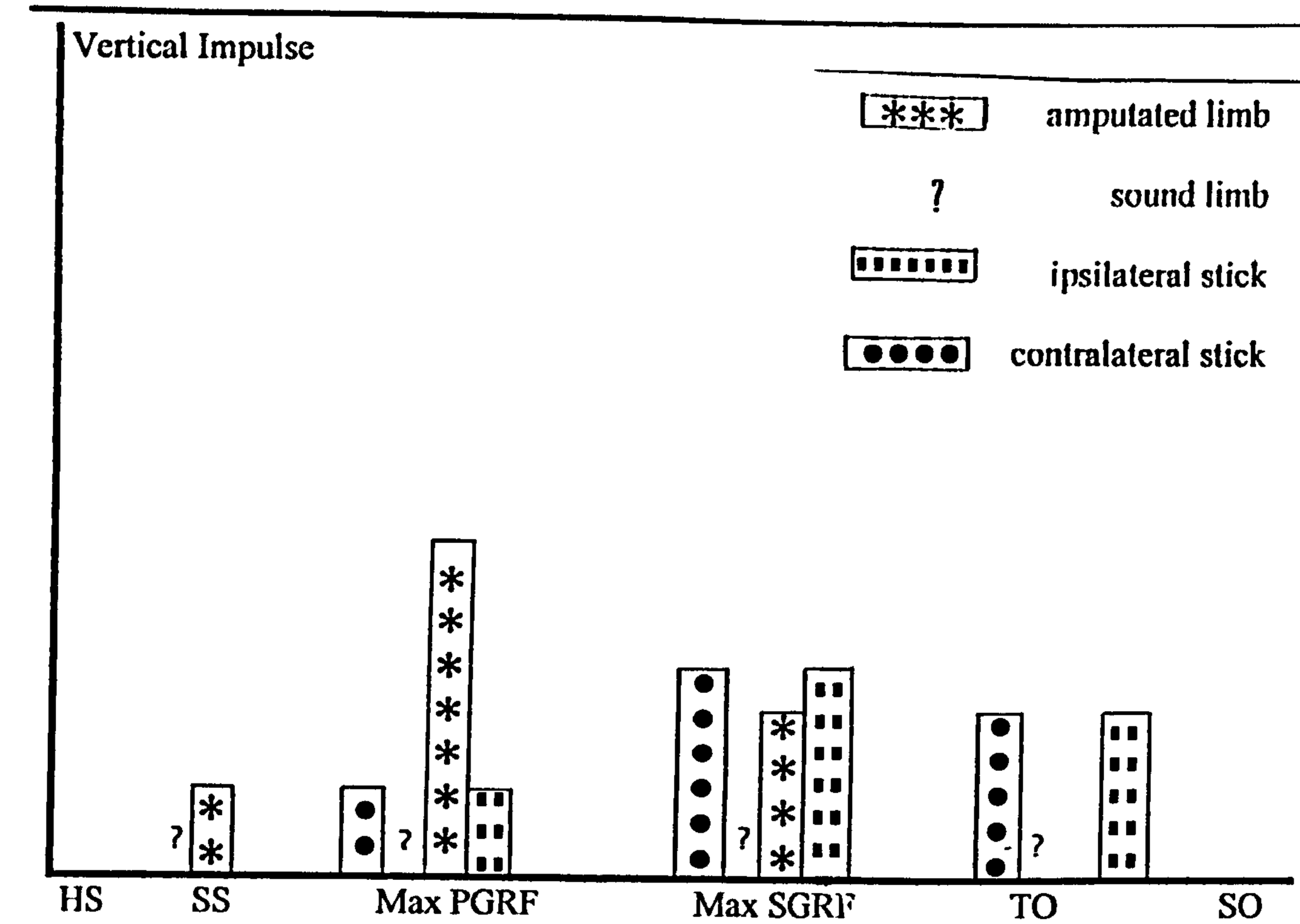

Figure 8.44: Vertical Impulse Histogram (VIH) of the mean gait pattern 1 concerning two transfemoral patients (TFL5 and TFL3), (see explanations in figures 8.9 and 8.24).

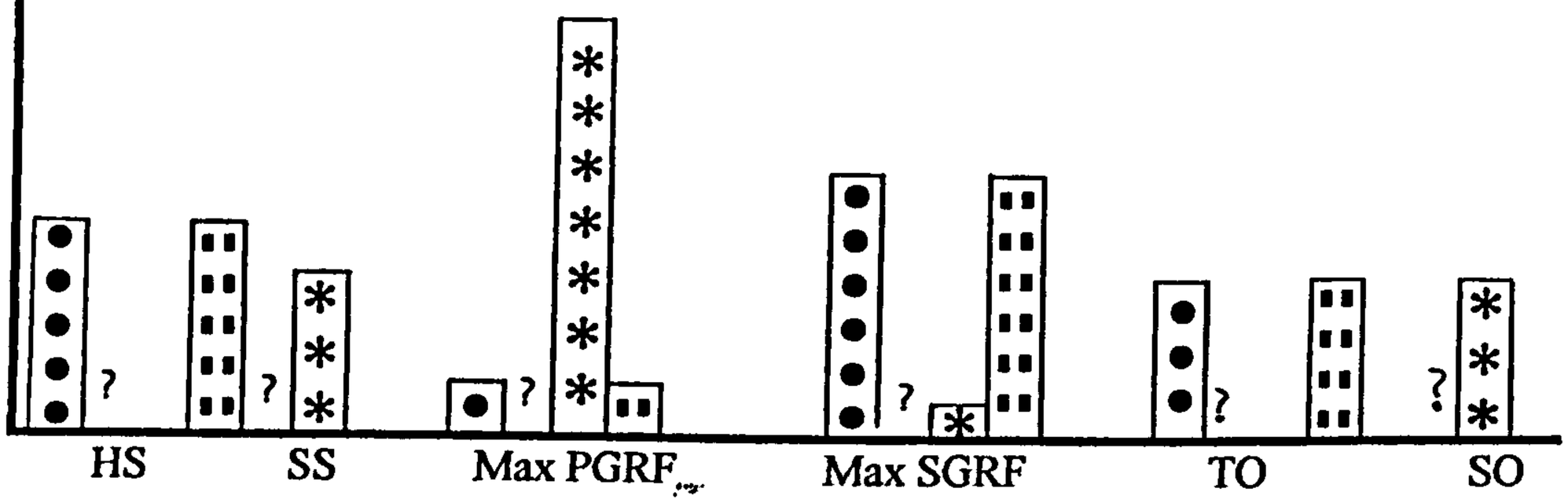

Figure 8.45: VIH of the mean gait pattern 2 of two transfemoral patients (TFL4 and TFR7) (see explanations in figure 8.9 and 8.24).

between the maximum of prosthetic axial load, A/P shear force positive and negative A/P bending moment Mz. However, the maximum load applied on the contralateral stick happened at late stance phase (there was a small shifting of the maximal load applied on the ipsilateral stick). This load difference between the two walking aids seemed particular to recent vascular amputees because Murray *et al.* (1969) reported that for a traumatic above-knee patient these two maximum loads are simultaneous. The stick was thus used like some « pushing off instruments » and not only for decreasing the load on the prosthesis as it would have been expected. The subject TFL5 was the one to walk with a "Cross Strolling" gait pattern (see section 2.6.7).

• Subject TFL3 (figure 8.43): the two solid vertical lines are perfectly laid out between the maximum of prosthetic and stick axial loads, A/P shear force Fx and bending moment Mz. Thus, the gait pattern of such a patient was as it would have been expected just as well in the literature concerning the rehabilitation of amputees (Engstrom & Van de Ven, 1993) than a targeted investigation such as Murray *et al.* (1969).

The main conclusion was evident: *four patients and four distributions of the loads into the prosthetic and walking aids gait cycle*. With a so small sample, it was therefore difficult to demonstrate any predominant gait pattern. In other words, it has been possible to describe some gait patterns concerning the temporal parameters of the gait cycle, as shown in sections 8.7 for 10 (series 1b), 8.8 for 4 (series 6) transfemoral amputees and 8.5 for transtibial amputees (series 4). However, it was not possible to describe such gait patterns concerning the kinetic aspect of the gait.

Nevertheless, to have a rough idea concerning the load gait patterns of such transfemoral patients, the two following VIH figures (vertical impulse histogram, modified from Opila, 1985) show the mean axial loads on the artificial limb and walking aids of the gait pattern 1 (patients TFL5 and TFL3, figure 8.44) and gait pattern 2 (patients TFL4 and TFR7, figure 8.45).

8.9 SUMMARY AND CONCLUSIONS

This study was a gait study of recent vascular lower limb amputees in early

stages of rehabilitation. The discussion concerning the recorded results was conducted throughout the previous sections. However, some certainties could be expressed and presented as a conclusion: the main one was the difference between load patterns and temporal parameters of the gait cycle. In other words, it was possible to establish:

1. Load patterns were specific for each patient and thus they cannot be summarised;

2. Temporal parameters were common to some groups of subjects and thus they could be summarised in two (transfemoral patients) or three (transtibial patients) gait patterns.

These two considerations showed how dissimilar were the tested subjects. Not only, they walked with a self selected pace but each of them chose also a typical gait pattern according to factors such as: amputation level, stump length, pain and muscle strength (open list, see appendix 11.II.7.1).

8.9.1 Axial Loads

Globally, all the patients had a prosthetic ground reaction force of 0.63 BW (transtibial patients) and 0.69 BW (transfemoral patients). Therefore, the walking aid ground reaction forces were about 0.3 to 0.4 BW. These results were found relevant with those reported in the literature. The transtibial patients applied less load on the prosthesis but more on the walking aids than transfemoral amputees (see section 8.5.2, 8.7.2 and 8.8.2). This could be related to the stump pain which was more severe in below the knee amputation level (especially, at the distal part of the tibial crest) than in above the knee amputation level, in early stage of rehabilitation, a short time after the amputation surgery.

Separating both sides of the walking devices relative to the amputated side, a non - expected result was found:

⇒ Left amputees put the same maximum axial load on both sides;

⇒ Right amputees put half load on the ipsilateral stick or cane in comparison with the contralateral side.

This was found in both levels of amputation and no evident explanation could be expressed.

The prosthetic ground reaction force, the anterio-posterior shear forces and dorsiflexion bending moments at the artificial ankle level were inversely related to the gait rate, in both ambulation of transtibial and transfemoral amputees (see sections 8.5.2 and 8.7.2). These changes in gait pattern were found in all the trials where the subject tried to minimise the stresses due to inertial forces at stump-socket interface.

This was particularly true if there was some stump pain, because a patient (whether transfemoral or transtibial) who had such a stump suffering did not minimise the ratio prosthetic stance phase versus prosthetic stride time but increased both the prosthetic stance phase and stride time to reduce the dynamic and inertial effects of the gait. In other words, a painful patient tended to minimise stresses on the stump from the socket and vice versa, reducing his self-selected pace.

Thus the vascular amputees, in early stage of rehabilitation, increased the prosthetic stance phase relatively to the prosthetic stride time, in comparison with vascular transtibial amputees tested more than 6 months after the date of the amputation (Hubbard & McElroy, 1994).

In other words, the tested subjects applied axial load during more time (+ 28 %) than traumatic amputees as those in the investigation conducted by Murray *et al.* (1969).

8.9.2 Anterio-posterior shear forces and bending moments

Compared with transtibial amputees, the plantar bending moment for transfemoral patients had a higher value while the dorsi bending moment had a lower one. Thus, the dorsi - plantar bending moment gap was not as substantial with transfemoral as with transtibial amputees. This showed that the early and late stance phases were shortened in the different gait patterns of the tested subjects. This could be related to a lesser equilibrium on transfemoral than on transtibial prosthesis, especially with a locked artificial knee unit.

8.9.3 Temporal parameters

The gait rates or prosthetic stride durations of the tested subjects were found equal as 1.96 s (transtibial amputees) and 2.4 s (transfemoral amputees). These two values were greater than those found in the literature, but there were no published papers concerning such a population. In other words, any comparison was thus quite impossible.

It was possible to group the studied subjects in three temporal gait patterns (see sections 8.5.5 and 8.8.5) named gait pattern lines (GPL).

- *Gait pattern 1: The patients applied axial load on the walking aids at late prosthetic stance phase when push-up on the artificial limb and forward acceleration occurred. The patients minimised the stress on the residual limb when posterior shear force and dorsiflexion bending moment were maximum. During approximately half of the prosthetic swing phase, the subjects were in walking aids swing phase, thus the patients were in one loading point onto the sound limb. (6 out of 14 transtibial and 2 out of 4 transfemoral patients).*

- *Gait pattern 2: The patients did not apply axial load on the walking aids at late prosthetic stance phase. The patients minimised the stress on the residual limb at early stance phase when weight acceptance occurred. The one loading time was approximately equivalent as the one of the gait pattern 1 but it was shifted from late to early stance phase (5 out of 14 transtibial patients, none transfemoral amputees).*

- *Gait pattern 3: The patients did not apply axial load on the walking aids at mid prosthetic stance phase. The patients protected the residual limb at early and late stance phase plus swing phase. In other words, they minimised the stress on the stump during the most dynamic phases of the gait cycle. Probably, there was not any one loading time: when it was walking aids swing phases, the subjects applied loads on both prosthesis and sound limb. (3 out of 14 transtibial and 2 out of 4 transfemoral patients).*

In other words, 5 patients out of 18 (27 %, about a quarter of the population) have spontaneously selected a gait pattern so that they had always at least two floor contacts. Consequently, they had not a special rehabilitation training to do so.

8.9.4 Strategy of using the walking aids

The main conclusion concerning the use of walking sticks could be expressed into words as follows:

The walking aids of transtibial patients were overall used for the push off. Any transtibial patient, wearing a monoaxial foot, needed some devices such as sticks or canes to progress in walking while the residual limb remained fragile and painful. The walking aids were also used to transfer the body weight from the prosthetic to the opposite side. The maximum of load on walking aids occurred simultaneously with the dorsiflexion of the artificial ankle and the patient's posterior push on the prosthesis. It was not coincident with the maximum value of the vertical ground reaction force.

The walking aids of transfemoral patients were differently used. The maximum value of the load on walking aids was shifted towards the maximum value of the prosthetic vertical ground reaction force. It was thus possible to establish that the walking aids were similarly used to push off and to transfer the body weight from one side to the other. However, transfemoral patients fitted with a locked knee, needed more prop from walking aids than transtibial patients. In other words, the walking aids cycle was the same whatever the amputation level; but transfemoral amputees seemed to use walking aids during a shorter time than transtibial amputees, due to the higher level of pain in transtibial amputations.

By contrast to sticks, the unstable canes, were used to maintain the M/L equilibrium of the patient (long cane stance phase) rather than to accelerate forward the body or to minimise the axial load on the artificial limb (low axial load on the canes).

9 CONCLUSION

At the end of this work, the conclusions can be expressed following two directions:

1) Are the requirements expressed in chapter 1 satisfied?

2) Is further work required?

The thesis objectives, shown in section 1.3.1, were

1) to develop a procedure for monitoring the gait of vascular amputees under realistic conditions and daily rehabilitation with special attention to the cost, the simplicity of use, the time taken to obtain the results and their presentation;

2) to recognise and to understand the gait patterns of amputees while using different walking aids with the major objective to achieve the following point 3;

3) to improve the rehabilitation process of patients providing objective indications and contraindications;

4) to attempt to acquire a knowledge of why VSD patients have commonly a less favourable outcome than those trained in other Rehabilitation Centre.

Globally, the first target has been fulfilled. Chapters 4, 5, 6 and 7 present the description and the use of the equipment employed. These were:

- a new removable pylon load transducer which allows to multiple tests to be performed without dismantling the prosthesis (see sections 4.8 and 4.9 with its calibration in chapter 6);
- a portable data acquisition system totally carried by the patient which allows the recording of data under realistic condition (see section 5.3);
- the instrumented assistive walking devices with their calibration (see section 5.4);
- the validation tests performed to assess all the equipment used (see chapter 7).

The details of the tests performed have been described in section 8.2. In this section, it has been demonstrated that the time required for test subject preparation and data analysis was short enough (90 minutes, see section 8.2.1) to expect an extensive utilisation in the clinical scene.

Concerning the above points 2 and 3, three gait patterns have been recognised and thus, the new acquired knowledge allowed the VSD physiotherapists to improve the rehabilitation process. This is especially true for the guidance the physiotherapist gives to the patient about the position, in space and on ground during swing and stance phases of the gait, of both prosthetic and sound feet.

The most important result found was the distribution of the axial loads between the prosthesis and the two walking devices. The determination of this distribution is essential particularly since there is a total lack of information concerning this problem in the literature (see chapter 2). Here also, following this procedure, the way of doing the VSD rehabilitation process has been modified. The patient is now asked to appreciate how the walking aids are used to push the body forward instead of decreasing the axial load on the prosthesis. Therefore, the physiotherapist teaches the patient to strongly push on the walking aids, from mid to late stance phase, when they are behind his feet to increase the forward thrust.

Incidentally, the author of this thesis is also a teacher in three Parisian rehabilitation schools and his lecture material has been changed to include the new gait patterns of VSD amputees.

Concerning the point number 4, no obvious and fundamental explanations have been found. This is the main shortcoming of the presented work. A combination of multiple factors must probably be involved, such as: surgical background, bad general health status of the patients and short stay-in hospital. It has been stated that the VSD patients have a lower gait rate (see sections 8.5.1, 8.7.1 and 8.8.1) than the patients described in the literature. Moreover, the results presented in sections 8.5.5 and 8.8.5 show an inverse proportionality between gait speed and ground reaction forces of prosthesis plus walking aids. Following this investigation and the results found, the VSD physiotherapists started to ask the patients to walk faster than

previously to minimise the use of the walking aids. The final target remains to throw away the walking aids, but only few patients would be capable of doing so. However, in all the papers consulted, the populations studied are never equivalent to the VSD weak patients; no pertinent and reliable comparisons can thus be established.

However, despite these successful points, some problems remain.

It has been difficult to convince the physiotherapy team of the Villiers-Saint-Denis Rehabilitation Centre to use the system as widely as it could be. Several reasons can be provided to explain this fact, mostly:

→ the difficulty of demonstration a strong and evident relation between the results of a test — which provide information of the gait of the patient at a certain time — and the advice the physiotherapist can provide to the patient;

→ the lack of information concerning the sound limb has been also an obstacle to the adoption of the method.

→ the duration of a test (1 h 30) also made it difficult to perform multiple tests on the same patient (see chapter 8).

Concerning these three points, it is suggested that the use of a pylon load transducer being capable of measuring the six signals corresponding to the components of forces and moments developed during gait was too sophisticated a piece of equipment. A more simple pylon load transducer (capable of measuring only the axial load Fy and the A/P forces and moments) could be sufficient for a day to day use. However, the duration of a test would be more or less the same and thus, the gain of time and simplification would be negligible. In section 2.3.4, a discussion has been introduced concerning the use of a wearable multisensor system able to minimise the duration of a test. However, it has been proved, by reviewing the literature, that these components have a low accuracy, insufficient to provide any accurate conclusion.

Also, to save time and to improve the quality of the presentation of the results, more convenient software should be developed providing the choice of the stride to

be interpreted with an automatic calculation of the results in percentage of the body mass.

Finally, the choice of a complete pylon load transducer appeared to be pertinent. Being the chief of a team of physiotherapists, the author of this thesis will have to try harder to convince his colleagues to use the equipment described in this thesis more widely.

Concerning the novel pylon load transducer, further researches could be undertaken in two directions:

1. to perform a new complete calibration of the Villiers Pylon Transducer, having in mind to solve some problems such as: the interaction between axial load and torque and uncertainties in both M/L shear force and transverse torque channels (see chapters 6 and 7):

   - Special attention should be focused at the pylon/bell interface, which cannot be guaranteed to transmit axial load uniformly.
   - Are bending moments transmitted accurately without application of axial load? and is axial load transmitted without bending moment?
   - Could the special ring designed to grip the prosthetic shank tube on the bell, introduce some modifications into M/L and A/P bending moments?
   - Concerning the dimensions of the transducer: is 5 mm at the top and the bottom of the sensor section between the strain gauges and the end of the transducer enough to avoid any end effects?
   - The raw traces of the M/L shear force, Fz, were similar in shape to the A/P bending moment, Mz, raw traces (see chapter7): are these loads related?

2. The instrumented assistive walking devices were fitted with only an axial load channel and no bending channels. Is this enough to satisfy the proposed aims? A lack of research concerning the biomechanical use of forearm crutches and canes has been noted.

Concerning the will of the author of the presented work to increase benchmark data for elderly vascular amputees and to be a "communication interface" between

the biomechanical scientific and the physiotherapy world, it can be said that two papers have been already published (Pillu *et al.*, 1998b, 1999a) and some oral communications have also been voiced (Pillu *et al.*, 1998a, 1998c, 1999). These two aims have thus been achieved.

The new Villiers Pylon Transducer designed and described in this work (see chapter 4) has the main advantage of being easily fitted and removed from the prosthesis. It is light and small enough to be used with recent dysvascular amputees with sufficiently minor modifications to the gait pattern to display reliable results. It was found reliable, accurate and linear enough for the purpose for which it was built. The data acquisition system, designed and described in chapter 5, is easy to use, light enough for the patient to carry, accurate and reliable for the therapist. It gives interesting results for the patients who have always been curious about their performance and wish to be more involved in their rehabilitation improvement. The processed data (see chapter 8) are sufficiently significant to be inserted in the medical follow up file of the patient, showing the progression of his gait pattern, interesting for both medical doctor and Social Security controller. Moreover, the data acquisition system is sufficiently multi purpose to offer the possibility of performing further research, such as, kinetics in the fore – aft plane coupled with surface electromyography and / or electrogoniometry at the knee joint level; kinetics in fore – aft plane coupled with multi channel instrumented assistive walking devices (A/P bending moments with A/P and M/L shear forces).

However and because or despite all the above points, the main aim of the presented work has been achieved, namely, the use with a sufficient accuracy and reliability of a rehabilitation tool allowing the gait monitoring of vascular lower limb amputees at an early stage of their rehabilitation.

10 REFERENCES

ABU-FARAJ ZO, HARRIS GF, ABLER JH, WERTSCH JJ. A Holter-type, microprocessor-based, rehabilitation instrument for acquisition and storage of plantar pressure data. J Rehabil Res Develop. **1997** ; 34 N°2 : 187-194

ADER P, GRUMLER B, POURPRIX C, DULIEU V, CASILLAS JM. Apport des emboîtures contentives à la cicatrisation guidée après ambulation majeure de membre inférieur. Ann Kinésithér. **1997** ; 24 N°6 : 300-303

ALEXANDER IJ, CHAO EYS, JOHNSON KA. The assessment of Dynamic Foot-to-Ground Forces and Plantar Pressure Distribution : A review of the Evolution of Current Techniques and Clinical Application. Foot & Ankle. **1990** ; 11 N°3 : 152-167

ANDERSON CP. Disvascular amputees: What can we expect? J Prosthet Orthot. **1995** ; 7 N°2 : 43-50

ANTONSSON EK, MANN RW. The frequency content of gait. J Biomech. **1985** ; 18 N°1 : 39-47

ARUIN AS, NICHOLAS JJ, LATASH ML. Anticipatory postural adjustements during standing in below-the-knee amputees. Clin Biomech. **1997** ; 12 N°1 : 52-59

AYYAPPA E. Normal Human Locomotion, Part 1: Basic concepts and Terminology. J Prosthet & Orthot. **1997** ; 9 N°1 : 10-17

AYYAPPA E. Normal Human Locomotion, Part 2: Motion, ground-reaction force and muscle activity. J Prosthet & Orthot. **1997** ; 9 N°2 : 49-57

BAGLEY AM, FOERSTER SA, MOTE CD, SKINNER HB. Optimisation of above-knee prosthesis weight and weight distribution. Orthopaedic Research Society. 366-367

BAILEY MJ, MacWHANNELL C. Clinical Monitoring of Dysvascular Lower Limb Amputees during Initial Gait Training. Physiotherapy, **1997** ; 83 : 278-283

BAKER JS. An evaluation of the effectiveness of a variety of data smoothing techniques compared to criterion force platform generated data. J of Human Movement Studies. **1994** ; 26 : 75-86

BAKER PA, HEWISON SR. Gait recovery pattern of unilateral lower limb amputees during rehabilitation. Prosth Ortho Inter. **1990** ; 14 : 80-84

BALMELLE G. Handicap et Travail de Deuil. In Izard MH, Nespoulous R eds. Expériences en Ergothérapie, Rencontres en Rééducation N°2. Masson. Paris. **1988** ; pp 116-121

BARBATO G, BRAY A, GERMAK R, LEVI R. Calibration and verification of multicomponent dynamometers in the meganewton range. **1986**. Amsterdam. Proceedings of the XIth International Conference on Measurement of Force and Mass.

BARBATO G, BRAY A, LEVI R. Multicomponent dynamometers for control of parasitic components on force standard machines. **1985**. Beijing. China. Science Press. Proceedings of the International Conference on Experimental Mechanics. p.784

BARDOT P, ROUX C, ANRIGO-PEYRON C, COSTES O, DELARQUE A, BARDOT A. Proposition pour une échelle d'évaluation de la prothétisation des amputés de cuisse artéritiques. Ann Réadaptation Méd Phys **1992 ; 35 : 105-111**

BARRAUT JJ, NABITZ C, VIDAL F, de GODEBOUT J, STER F. Place et technique de la rééducation chez l'amputé du membre inférieur. In Bonnel F ed. Appareillage des Membres Inférieurs. Springer Verlag. Paris. **1989 ;** pp. 104-111

BARTH DG, SCHUMACHER L, SIENKO-THOMAS S. Gait analysis and energy cost of below-knee amputees wearing six different feet. J. Prosthet Orthot. **1992 ; 4 N°2 : 63-75**

BAUMANN JU. Requirements of clinical gait analysis. Hum Mov Science. **1991 ; 10 : 535-542**

BECQUET G, LAVIE C, MARIOTJP, BARBEDETTE B, DESLANDES J, PAUVERT D, HAON G, NADEAU G. Problèmes posés par la mesure en isocinétisme, des couples musculaires développés au niveau du genou chez l'amputé de jambe. In Codine, Brun, André ed. Amputation du Membre Inférieur - Appareillage et Rééducation. Masson. Paris. **1996.** pp. 359-366

BEGG RK, WYTCH R, HUTCHISON JMS, WARDLAW D. Microcomputer-based system for clinical gait studies. Clin Biomech. **1991 ; 6 : 168-172**

BENEZET P, MESURE S, CINCERA M, DELARQUE A. Analyse par plateforme de forces de la marche de l'amputé. In Codine, Brun, André ed. Amputation du Membre Inférieur - Appareillage et Rééducation. Masson. Paris. **1996.** pp. 329-337

BENHAM PP, CRAWFORD RJ. Mechanics of engineering materials. **1988.** Longman Scientific Technical. London

BERME N, LAWES P, SOLOMONIDIS SE, PAUL JP. A shorter pylon transducer for measurement of prosthetic forces and moments during amputee gait. Engineering in Medicine. **1975 ; 4 N°4 : 6-8**

BERME N, PURDEY, SOLOMONIDIS SE. Measurement of prosthetic alignment. Orthotics International. **1978 ; 2 N°2 : 73-76**

BERME N. Load transducers. In Biomech of human movement: applications in rehabilitation sports and ergonomics (Eds N Berme and A. Cappozzo). **1990** (Bertec Corporation, Worthington, Ohio)

BERTHE A, DOTTE P. Les ambulations et les aides de marche en traumatologie. Masson. Paris. **1987.** pp. 31-47

BERTHOLUS P, BRAULT JF, LEGRAND C, BURLOT PM, VERHAEGHE M, CHARPENTIER P. Appareillage temporaire. Encycl Med Chir (Paris-France), Kinésithérapie-Rééducation fonctionnelle, 26-160-A-10, **1990,** 24p.

BESSER MP, KOWALK DL, VAUGHAN CL. Mounting and calibration of stairs on piezoelectric force platforms. Gait & Posture. **1993 ; 1 : 231-235**

BIEFANG S, POTTHOF P. Assessment methods for rehabilitation. Int. J. Rehabil Res. **1995 ; 18 N°3 : 201-213**

BILESIMO M, CASILLAS JM, JAVELAS S, et coll. Reflexe veino-articulaire : Modifications en fonction de l'âge. Ann Réadap Méd Phys. **1988 ; 31 : 279-288**

BILISKO C. L'amputé artéritique et sa rééducation. Ann Kinésithér. **1986 ; 13 N°4 : 155-162**

Biomech of Above-Knee Prostheses. Prosthetics and Orthotics. Post Graduate Medical School. New York University. **1968**

Biomech of Below-Knee Prostheses. Prosthetics and Orthotics. Post Graduate Medical School. New York University. **1968**

BOENICK U, STEFFENS HP, ZEUK E, ENGELKE E. Amputee performance measurement outside the laboratory. In Proceedings of a Seminar on Rehabilitation of the Disabled. Disability, RM Kenedi, JP Paul, J Hughes ed. MacMillan Press. London. **1979**. pp 145-153

BOHANNON RW, ANDREWS AW, THOMAS MW. Walking Speed: Reference Values and Correlates for Older Adults. J Scie & Phy Ther (JOSPT). **1996** ; 24 N°2 : 86-90

BOONSTRA AM, FIDLER V, EISMA WH. Walking speed of normal subjects and amputees: aspects of validity of gait analysis. Prostet & Orthot Int. **1993** ; 17 : 78-62

BOONSTRA AM, SCHRAMA J, EISMA WH, et al. Aspects of the validity of gait analysis. J Rehab Scie. **1994** ; 7 N°3 : 35-37

BOONSTRA AM, SCHRAMA J, FIDLER V, et al. The gait of unilateral transfemoral amputees. Scand J Rehab Med. **1994** ; 26 : 217-223

BOONSTRA AM, SCHRAMA JM, EISMA WH, HOF AL, FIDLER V. Gait analysis of transfemoral amputee patients using prostheses with two different knee joints. Arch Phys Med Rehabil. **1996** ; 77 : 515-520

BOUTEN CVC, KOEKKOEK KTM, VERDUIN M, KODDE R, JANSSEN JD. A triaxial accelerometer and portable data processing unit for the assessment of daily physical activity. . IEEE Trans Biomed Engineering. **1997** ; 44 : 136-147

BRANDSMA JW, HEERKENS YF, VAN RAVENSBERG CD. The international classification of impairments, disabilities, and handicaps (ICIDH) : a manual of classification relating to the consequences of disease? J Rehab Scie. **1995** ; 8N°1 : 2-7

BRAY A, BARBATO G, LEVI R. Theory and Practice of force measurement. **1990.** Academic Press Harcourt Brace Jovanovich Publishers. London

BREAKEY JW. Body Image : The inner mirror. J Prosthet & Orthot. **1997** ; 9 (3) : 107-111

BREAKEY JW. Body Image : The lower limb amputee. J Prosthet & Orthot. **1997** ; 9 (3) : 58-66

BREAKEY JW. Gait of unilateral below knee amputees. Orthot & Prosthet. **1976** ; 30 N°3 : 17-24

BRENIERE Y, DO MC, SANCHEZ J. A biomechanical study of the gait initiation process. J. Biophys. et Méd. Nucl. **1981** ; 5 N°4 : 197-205

BRODZKA WK, THORNILL HL, ZARAPKAR SE, MALLOY JA, WEISS L. Long term function of persons with atherosclerotic bilateral below-knee amputation living in the inner city. Arch Phys Med Rehabil. **1990** ; 71 : 895-900

BRUCKNER L. A standardised trans-tibial amputation method following chronic occlusive arterial disease. Prosthet & Orthot Inter. **1992** ; 16 : 157-162

BRUNT D, WILLIAMS J, RICE R. Analysis of EMG activity and temporal components of gait during recovery from perturbation. Arch Phys Med Rehabil. **1990** ; 71 : 473-477

BUCKLEY JG, SPENCE WD, SOLOMONIDIS SE. Energy cost of walking: Comparison of « Intelligent Prosthesis » with Conventional Mechanism. Arch Phys Med Rehabil. **1997** ; 78 : 330-333

BUHOT G, THUILLIER P. Cours de Mécanique, Tome 2, Résistance des Matériaux. Masson. Paris. **1986.**

BURGESS EM. Clinical and laboratory study of amputation surgery and rehabilitation. J Rehabil Res Develop. **1994** ; 31 N°4 : 355-356

CAPPOZZO A. Three-dimensional analysis of human walking: Experimental methods and associated artefacts. Hum Mov Science. **1991** ; 10 : 589-602

CARLET G. Sur la locomotion humaine. Ann Sci Naturelles. **1872** ; 5 : 1-92

CASILLAS JM, AURELLE B, COGET P, BECKER F, MARCER I, DIDIER JP. Mesure transcutanée de la pression partielle en oxygène : aide à la définition de l'appareillage après amputation de jambe pour artérite. Ann Réadaptation Méd Phys. **1990** ; 33 : 553-561

CASILLAS JM, DULIEU V, BECKER F, COHEN M, BRENOT R, DIDIER JP. Réadaptation dans l'artériopathie des membres inférieurs. Editions Techniques. Encycl. Méd Chir. (Paris-France), Kinésithérapie-Rééducation Fonctionnelle, 26-560-A-05, **1994**, 10p.

CASILLAS JM, DULIEU V, COHEN M, COTTIN Y. Physiologie musculaire et coût énergétique de la marche normale. In Pelissier, Brun ed. La Marche Humaine et sa Pathologie : Explorations et Rééducation. Masson. Paris. **1994**. pp. 20-41

CASILLAS JM, DULIEU V, COHEN M, MARCER I, DIDIER JP. Bioenergetic comparison of a new energy-storing foot and SACH foot in traumatic below-knee vascular amputations. Arch Phys Med Rehabil. **1995** ; 76 : 39-44

CASILLAS JM, KOTZKI N, HERMANN-SERREAU I, DIDIER JP. Critères du prognostic de marche après amputation pour artériopathie oblitérante des membres inférieurs. Ann Réadaptation Méd Phys. **1987** ; 30 : 169-174

CAURET D. Evolution du flexum du genou chez l'amputé tibial artéritique en fonction de la durée d'hospitalisation. Mémoire en vue de l'obtention du Certificat National de Moniteur Cadre en Masso-Kinésithérapie. Ecole de Cadres de Kinésithérapie « Bois-Larris ». **1986-1987**

CHANU B, ROUFFY J. Facteurs de risques. In Natali J ed. Artériopathies Athéromateuses des Membres Inférieurs. Masson. Paris. **1988** ; pp 110-119

CHARPENTIER P, ABOIRON H, BERNOT R. Amputations des membres inférieurs. Editions Techniques. Encycl Méd Chir. Paris - France. Kinesithérapie - Rééducation Fonctionnelle. 26270 A^{10}, **1992.** 22p

CHARPENTIER P, TOURNEUX A. Matériaux utilisés en appareillage. Encycl Med Chir (Paris-France), Kinésithérapie-Rééducation fonctionnelle, 26-272-A-10, **1994**, 10p.

CHATAIN M, COURTADE D, DUPUI P, MONTOYA R, DARMANA R, PAGES B, ROQUES CF. Evaluation de la marche par locomètre, baro-podomètre et plateau de forces chez trois amputés tibiaux appareillés de différents pieds. In Codine, Brun, André ed. Amputation du Membre Inférieur - Appareillage et Rééducation. Masson. Paris. **1996**. pp. 324-328

CHATFIELD Ch. Statistics for technology. **1981**; Chapman and Hall. London

CHEUNG C, WALL JC, ZELIN S. A microcomputer-based system for measuring temporal asymmetry in amputee gait. Prosthet Orthet Int. **1983** ; 7 : 131-140

CHRISTANSEN H, SØGAARD K, JENSEN BR, et al. Intramuscular and surface EMG power spectrum from dynamic and static contractions. J Electromyogr Kinesiol. **1995** ; 5 N°1 : 27-36

CHRISTENSEN B, ELLEGAARD B, BRETLER U, et al. The effect of prosthetic rehabilitation in lower limb amputees. Prosthet & Orthoto Int. **1995** ; 19 : 46-52

COLLIN C, WADE DT, COCHRANE GM. Functional outcome of lower limb amputees with peripheral vascular disease. Clin Rehabil. **1992** ; 6 : 13-21

COMMEAN PK, SMITH KE, CHEVERUD JM, VANNIER MW. Precision of surface measurements for below-knee residua. Arch Phys Med Rehabil. **1996** ; 77 : 477-486

COMMEAN PK, SMITH KE, VANNIER MW. Lower extremity residual limb slippage within the prosthesis. Arch Phys Med Rehabil. **1997** ; 78 : 476-485

CONDIE E, TREWEEK S, JONES D, SCOTT H. A one - year national survey of patients having a lower limb amputation. Physiotherapy. **1996** ; 82 N°1 : 14-20

CORMIER JM. Amputations d'indications vasculaires. **Encycl Méd Chir** (Paris, France). Techniques Chirurgicales Chirurgie Vasculaire. 4.2.11, 43320. **1982** ; 18p

CORMIER JM. Traitement chirurgical de l'artériopathie oblitérante chronique. In Natali J ed. Artériopathies athéromateuses des membres inférieurs. Masson. Paris. **1988** ; pp. 393-397

CORNU JY, GRANDPERRET S, GHARBI T, GUYOT J, PENFORNIS D, AITOUARES Y, MASSOL J, NARBONI G. Intérêt et pratique de la baropodométrie électronique comme exploration fonctionnelle biomécanique à usage clinique chez le diabétique. Med Chir Pied. **1997** ; 13 N°1 : 54-66

CRAIK RL, OATIS CA. Gait Analysis, Theory and Application. Mosby. St Louis. **1995.**

CRISPILS C., KERDILES Y, TURPIN J, BRISSOT, VERSINI C, OLLIVIER A. Réadaptation des amputés de membre inférieur pour athérosclérose. **Encycl Méd Chir** (Paris, France). Kinésithérapie, Appareillage des Amputés des Membres Inférieurs. 26270 A^{10}. **1984** ; 4p

CUNNINGHAM DM, BROWN GW. Two devices for measuring the force acting on the human body during walking. Society of Experimental Stress Analysis. **1952** ; IX (2) , pp 75

CUTSON TM, BONGIORNI D, MICHAEL JW, et al. Early management of elderly dysvascular below-knee amputees. J of Prosthet & Orthot. **1994** ; 6 N°3 : 62-66

CZERNIECKI JM, GITTER A, MUNRO C. Joint moments and muscle power output characteristics of below-knee amputees during running: the influence of energy storing prosthetic feet. J Biomech. **1991** ; 24 N°1 : 63-75

CZERNIECKI JM, GITTER A, WEAVER K. Effect of alterations in prosthetic shank mass on the metabolic costs of ambulation in above-knee amputees. Am J Phys Med Rehabil. **1994** ; 73 N° : 348-352

CZERNIECKI JM, GITTER A. Gait analysis in the amputee: has it helped the amputee or contributed to the development of improved prosthetic components? Gait & Posture. **1996** ; 4 N°3 : 258-268

CZERNIECKI JM, GITTER A. Insights into amputee running. A muscle work analysis. Am J Phys Med Rehabil. **1992** ; 71 : 209-218

CZERNIECKI JM, GITTER AJ, BECK JC. Energy transfer mechanisms as a compensatory strategy in below knee amputee runners. J. Biomech. **1996** ; 29 N°6 : 717-722

CZERNIECKI JM, HARRINGTON RM, WYSS CR, SANGEOZAN BJ, MATSEN FA. The effects of age and peripheral vascular disease on the circulatory and mechanical response of skin to loading. Am J Phys Med Rehabil **1990** ; 69 N°6 : 302-307

CZERNIECKI JM. Rehabilitation in limb deficiency. 1. Gait and Motion Analysis. Arch Phys Med Rehabil. **1996** ; 77 : S3-S8

D'ANGELI-CHEVASSUT M, GAVIRIA M. La marche humaine : Description et repères sémantiques. In Pelissier, Brun ed. La Marche Humaine et sa Pathologie : Explorations et Rééducation. Masson. Paris. **1994**. pp. 9-20

DATTA D, ARIYARATMAN R, HILTON S. Timed walking test - an all-embracing outcome measure for lower - limb amputees. Clin Rehabil. **1996** ; 10 : 227-232

DAVIDOFF GN, LAMPMAN RM, WESTBURY L, et al. Exercise testing and training of persons with dysvascular amputation: Safety and Efficacy of arm ergometry. Arch Phys Med Rehabil. **1992** ; 73 : 334-338

DAVIS RB, ÕUNPUU S, TYBURSKI D, GAGE JR. A gait analysis data collection and reduction technique. Hum Mov Scie. **1991** ; 10 : 575-587

DAVIS RW. Phantom Sensation, Phantom Pain, and Stump Pain. Arch Phys Med Rehabil. **1993** ; 74 : 79-91

DAY HJB. The assessment and description of amputee activity. Prosthet Orthot Int. **1981** ; 5 : 23-28

DE FRANG RD, TAYLOR Jr LM, PORTER JM. Données de base concernant les amputations. Ann Chir Vasc **1991** ; 5 : 202-207

DE FRETES A, BOONSTRA AM, VOS LDW. Functional outcome of rehabilitated bilateral lower limb amputees. Prosthet Orthot Int. **1994** ; 18 : 18-24

DE LUCA CJ. The use of surface electromyography in biomechanics. J App Biomech. **1997** ; 13 : 135-163

DEATHE AB, HAYES KC, WINTER DA. The biomechanics of canes, crutches and walkers. Crit Rev Phys & Rehabil Med. **1993** ; 5 : 15-29

DECHAMPS E, PILLU M. La Rééducation et l'Appareillage des amputés du membre inférieur d'origine vasculaire. Encycl Pratique Masso-Kinésithérapie, Kiné Scien. **1994** (C XII) ; 335 et suiv

DECHAMPS E. Appareillage et rééducation des amputés artéritiques. Mémoire. Univ d'Amiens. Ecole de Cadre de Bois - Larris. **1982**.

DEVITA P. The selection of a standard convention for analyzing gait data based on the analysis of relevant biomechanical factors. J. Biomech. **1994** ; 27 : 501-508

DEWAR ME, JUDGE G. Temporal asymmetry as a gait quality indicator. Med. & Biol. Eng. & Comput. **1980** ; 18 : 689-693

DIDIER JP, CASILLAS JM. Bioénergétique de la marche. Ann Réadaptation Méd Phys. **1986** ; 29 : 169-187

DIDIER JP, ROUX J, GRUMLER B, CASILLAS JM, RAUPP JC. La prise en charge par la rééducation fonctionnelle de l'artéritique amputé. Cah. Kinésithér **1982** ; 96 (n°4) : 37-45

DIDIER JP. BECKER F. JAVELAS S. CASILLAS JM. Place des explorations fonctionnelles vasculaires dans la prise en charge en rééducation des arteriopathes. Ann de Réadap et Méd Physique. **1988** ; 31 : 513-531

DILLINGHAM TR, LEHMANN JF, PRICE R. Effect of lower limb on body propulsion. Arch Phys Med Rehabil. **1992** ; 73 : 647-651

DILLINGHAM TR. The biomechanics of normal gait as derived from a link segment model. Physical Med Rehabil Clinics of North America. **1992** ; 3 N°1 : 111-123

DINGWELL JB, DAVIS BL, FRAZIER DM. Use of an instrumented treadmill for real - time gait symmetry evaluation and feedback in normal and trans - tibial amputee subjects. Prosthet & Orthot Int. **1996** ; 20 : 101-110

DONN JM, PORTER D, ROBERTS VC. The effect of footwear mass on the gait patterns of unilateral below-knee amputees. Prosthet & Orthotot Int. **1989** ; 13 : 140-144

DONN JM, ROBERTS C. A review of the energy expenditure of disabled locomotion with special reference to lower limb amputees. Phys Theory & Practice. **1992** ; 8 : 97-108

DOUTRELLOT PL, DURLENT V, LAGERSIE M, CHAVET P, GAVIRIA M, PERUCHON E, RABISCHONG P, LAUDE M. Mesure de la force verticale d'appui au cours de la marche : étude comparative entre plate-forme dynamométrique et système portable à multicapteurs plantaires. Ann Réadaptation Méd Phys. **1997** ; 40 : 37-42

DREYFUS F. Le bandage des moignons du membre inférieur. Revue Suisse des Infirmières. **1971** ; 6 : 2-8

DULIEU V, CASILLAS JM, COTTIN Y, MOUALLEM J, MARCER I, DIDIER JP, BRENOR R. Coût énergétique de la marche chez l'amputé de membre inférieur. In Pelissier, Brun ed. La Marche Humaine et sa Pathologie : Explorations et Rééducation. Masson. Paris. **1994**. pp. 274-281

DUPONT C, CAILLET F, MATHIEU Y, MOREL C, CHERPIN J, EYSSETTE M, BOSSON D. Etude comparative de la marche de l'amputé tibial pied Sach *versus* pied Multiflex. In Codine, Brun, André ed. Amputation du Membre Inférieur - Appareillage et Rééducation. Masson. Paris. **1996**. pp. 337-343

DUPONT C, CAILLET F, MOREL C, CHERPIN J, EYSSETTE M, BOISSON D. Etude de la marche appareillée de sujets amputés tibiaux par un système d'analyse tridimensionnelle du mouvement. Ann Réadapt Méd Phys. **1994** ; 37 : 33-40

DUPONT C, CAILLET F, MOREL. Analyse kinésigraphique et électromyographique de la marche appareillée de sujets amputés tibiaux. Rev Réadapt Fonct Prof Soc. **1994** ; 21 : 13-18

DUPONT C. Etude électromyographique et kinésigraphique par système Vicon de la marche appareillée de l'amputé tibial. Mémoire. Diplôme d'Université d'Appareillage des Handicapés Moteurs. **1992.**

DUPRE JC, EVENO D, PILLU M, DECHAMPS E. Les Amputés de Cuisse d'Indication Vasculaire : Notre expérience sur l'année 1984. **1985** ; Congrès de l'Association Française pour l'Appareillage. Vallauris. France.

DURANCE JP, WARREN WK, KERBEL DB, STROUD TWF. Rehabilitation of below-knee amputees : factors influencing outcome and costs in three programmes. Int Disabil Studies. **1989** ; 11 : 127-132

EAKIN CL, QUESADA PM, SKINNER H. Lower-Limb Proprioception in above-knee amputees Clin Orthopaedics and Related Res. **1992** ; 241 : 239-246

EAMES RA, LANGE LS. Clinical and pathological study of ischaemic neuropathy. J Neurol Neurosurg Psychiat **1967** ; 30 : 215-226

EBERHART HD, INMAN VT, SAUNDERS JB, LEVENS AS, BRESLER B, McCOWAN TD. Fundamental studies on human locomotion and other information relating to design of artificial limbs. **1947** A report to the National Research Council. Committee on Artificial Limbs. Berkeley, University of California.

EBSKOV LB. Level of lower limb amputation in relation to aetiology : an epidemiological study. Prosthet & Orthot Inter. **1992** ; 16 : 163-167

EBSKOV LB. Lower limb amputations for vascular insufficiency. Int J of Rehabil Research. **1991** ; 14 : 59-64

Effects of Force Actions. University of Strathclyde. Bioengineering Unit. Post Graduate Diploma in Biomechanics

EGHIAYAN P. Aspects psychologiques d'une prise en charge groupale des personnes amputées. J Ergothér. **1993** ; 15 N° : 94-95

ELLITSGAARD N, BORNEFELDT B, PHILIPSEN A, ELLISGAARD V. Is the number of lower extremity amputations still decreasing ? Acta Orthop Scand. **1997** ; 68 (Suppl 227) : 39-40

ELY DD, SMIDT GL. Effect of canes on variables of gait for patients with disorders. Phys Ther. **1977** ; 57 : 507-512

ENEROTH M, PERSSON BM. Amputation for occlusive arterial disease. A prospective multicentre study of 177 amputees. Int Orthopaedics. **1992** ; 16 : 383-387

ENEROTH M, PERSSON BM. Risk factors for failed healing in amputation for vascular disease: a prospective, consecutive study of 177 cases. Acta Orthop Scand. **1993** ; 64 N°3 : 369-372

ENGLISH RD, HUBBARD WA, McELROY GK. Establishment of consistent gait after fitting of new components. J. of Rehabil Res & Dev. **1994** ; 32 N°1 : 32-35

ENGSBERG JR, LEE AG, TEDFORD KG, HARDER JA. Normative ground reaction force data for able-bodied and trans-tibial amputee children during running. Prosthet & Orthotot Int. **1993** ; 17 : 83-89

ENGSBERG JR, SPRINGER MJN, HARDER JA. Quantifying interface pressures in below-knee amputee sockets. J Ass Child Prosth-Orthot Clin. **1992** ; 27 N°3 : 81-88

ENGSBERG JR, TEDFORD KG, SPRINGER MJN, HARDER JA. Weight distribution of below-knee amputee and able-bodied children during standing. Prosthet & Orthotot Int. **1992** ; 16 : 200-202

ENGSBERG JR, TETFORD KG, HARDER JA. Center of mass location and Segment angular orientation of below-knee amputee and able-bodied children during walking. Arch Phys Med Rehabil. **1992** ; 73 : 1163-1168

ENGSTROM B, VAN de VEN C. Physiotherapy for amputees The Roehampton Approach. **1993** Second Edition Churchill - Livingstone. Edinburgh

ENJALBERT M, LUIGI A, MICALEFF JP, PERUCHON E. Cinématique et cinétique de la marche chez l'amputé des membres inférieurs. In Pelissier, Brun ed. La Marche Humaine et sa Pathologie : Explorations et Rééducation. Masson. Paris. **1994**. pp. 269-273

ESQUENAZI A. Analysis of prosthetic gait. Phys Med & Rehabil. **1994** ; 8 N°1 : 201-220

FARBER BS, MOREINIS ISH. Biomechanical basis of choosing the rational mass and its distribution throughout the lower limb prosthesis segments. J Rehabil Res Develop. **1995** ; 32 N°4 : 325-336

FAUVET MH, DECHAMPS E, PILLU M. Relation d'aide et amputation : Surveillance de l'appareillage. Soins Cardiologie. **1985** ; 32 : 37-42

FELEZ A, COURTADE D. Evaluation de l'équilibre du patient amputé de membre inférieur. In Codine, Brun, André ed. Amputation du Membre Inférieur - Appareillage et Rééducation. Masson. Paris. **1996**. pp. 318-324

FERRAND T. Conception et réalisation d'un enregistreur autonome multivoies d'activité électromyographique et electrocardiographique. **1990**. Thèse Université Joseph Fourier - Grenoble 1. France

FIORETTI S, TOMMASO L, PISANI E, CORRADINI ML. A computer-added movement analysis system. IEEE Transactions on Biomedical Engineering. **1990** ; 37 N°8 : 812-819

FRANCO A, LEGRAND E, GUIDICELLI Ch, QUESADA C, SARRAZIN R. Résultats de la rééducation des arthériopathes par entraînement programmé à l'effort. J Mal Vascul. **1980** ; 5 : 185-189

FREUND JE. Mathematical Statistics. Fifth Edition. **1992** ; Prentice Hall. Oxford

GAILEY RS, WENGER MA, KIRK RN, et al. Energy expenditure of transtibial amputees during ambulation at self-selected pace. Prostet Orthot Int. **1994** ; 18 : 84-91

Gait Analysis of the Above-Knee Amputee. Prosthetics and Orthotics. Post Graduate Medical School. New York University. **1968**

Gait and Activities Training. Prosthetics and Orthotics. Post Graduate Medical School. New York University. **1968**

GARIBALLA S, ARDRON M. Low Frequency Transcutaneous Nerve Stimulation (LFTNS) increases skin blood flow in young and elederly subjects. J. of Tissue Viability. **1995** ; 5 N°2 : 67-71

GELLER S. Abrégé de Statistique. Troisième Edition. **1979** ; Masson Paris

GERMANAUD J. Etude épidémiologique des amputations majeures du membre inférieur dans le régime général en France (sur 3 130 cas). Rev Med Assurance Maladie. **1996** ; 2 : 1-13

GERST P, BACCIALONE V, GROSS M, SENGLER J. Evaluation de l'appareillage précoce d'amputation de jambe sur plateforme de marche. Ann Kinésithér. **1996** ; 23 N°2 : 54-57

GEURTS ACH, MUDER TW. Reorganisation of postural control following lower limb amputation : Theoretical considerations and implications for rehabilitation. Physiotherapy Theory and Practice. **1992** ; 8 : 145-157

GILBERT N. Statistiques. **1988** ; Editions HRW Ltée. Montréal

GITTER A, CZERNIECKI J, MEINDERS M. Effect of prosthetic mass on swing phase work during above-knee amputee ambulation. Am J Phys Med & Rehabil. **1997** ; 76 N°2 : 114-121

GITTER A, CZERNIECKI JM, DeGROOT DM. Biomechanical analysis of the influence of prothetic feet on below-knee amputee walking. Am J Phys Med Rehab. **1991** ; 70 : 142-148

GITTER A, CZERNIIECKI J, WEAVER K. A reassessment of center-of-mass dynamics as a determinate of the metabolic inefficiency of above-knee amputee ambulation. Am J Phys Med Rehabil. **1995** ; 74 N°5 : 332-338

GOH JC, SOLOMONIDIS SE, SPENCE WD, et al. Biomechanical evaluation of SACH and uniaxial feet. Prosthet Orthot Int. **1984** ; 8 : 147-154

GOTTSCHALK FA, STILLS M. The biomechanics of transfemoral amputation. Prostet Orthot Int. **1994** ; 18 : 12-17

GRANAT MH, MAXWELL DJ, BOSCH CJ, FERGUSON ACB, LEES KR, BARBENEL JC. A body-worn gait analysis system for evaluating hemiplegic gait. Med. Eng. Phys. **1995** ; 17 N°5 : 390-394

GRANT-THOMSON JC. Amputee gait analysis techniques using pylon data. **1977** MSc thesis, University of Strathclyde, Glasgow

GRAVEL D, GAUTHIER-GAGNON C, MURIE C, et al. Changes in ground reaction forces during rehabilitation of the above knee amputee. Gait & Posture. **1995** ; 3 N°2 : 96

GRISE MCL, GAUTHIER-GAGNON C, MARTINEAU G. Prosthetic Profile of People with Lower Extremity Amputation: Conception and Design of a Follow-up Questionnaire. Arch Phys Med Rehabil. **1993** ; 74 : 862-870

GUILMOT JL, LASFARGUES G, DARDAINE V. Sémiologie clinique. In Natali J ed. Artériopathies athéromateuses des membres inférieurs. Masson. Paris. **1988** ; pp. 175-187

GWYER J, Measurement characteristics and sources of measurement error. J. Prosthet & Orthot. **1995** ; 7 N°3 : 100-104

HAGBERG E, BERLIN OK, RENSTROM P. Function after through-knee compared with below-knee and above-knee amputation. Prosthet & Orthot Int **1992** ; 16 : 168-173

HALE SA. Analysis of the swing phase dynamics and muscular effort of the above-knee amputee for varying prosthetic shank loads. Prosthet & Orthot Inter. **1990** ; 14 : 125-135

HAM R, de TRAFFORD J, VAN de VEN C. Patterns of recovery for lower limb amputation. Clin Rehabil. **1994** ; 8 : 320-328

HARLAAR J. The clinical use of biomechanics in gait analysis. J of Rehabil Sci. **1991** ; 4 N°2 : 35-40

HARRIS GF, WERTSCH JJ. Procedures for Gait Analysis. Arch Phys Med Rehabil. **1994** ; 75 : 216-225

HAUSDORFF JM, LADIN Z, WEI JY. Footswitch system for measurement of the temporal parameters of gait. J. Biomech. **1995** ; 28 N°3 : 347-351

HAYS RD, LEIMKUEHLER JP, MIKNEVICH MA, et al. An Alternative bent-knee prosthesis. Arch Phys Med Rehabil. **1992** ; 73 : 1118-1121

HE P, XUE K, MURKA P. 3-D imaging of residual limbs using ultrasound. J Rehabil Res & Develop. **1997 ; 34 : 269-278**

HENDRY A, GILCHRIST W, DUNCAN G, EVANS AL, SMITH DC. Measurement of walking speed in elderly inpatients. Med & Bio Eng & Comput. **1990 ; 28 : 602-604**

HERMODSSON Y, EKDAHL C, PERSSON BM, et al. Standing balance in trans-tibial amputees following vascular disease or trauma: a comparative study with healthy subjects. Prosthet Orthot Int. **1994a ; 18 : 150-158**

HERMODSSON Y, EKDAHL C, PERSSON BM, et al. Gait in male transtibial amputees: a comparative study with healthy subjects in relation to walking speed. Prosthet & Orthot Int. **1994b ; 18 : 68-77**

HOFFMAN MD, SHEDAHL LM, BULEY KJ, SANDFORD PR. Physiological comparison of walking among bilateral above-knee amputee and able-bodied subjects, and a model to account for the difference in metabolic cost. Arch Phys Med Rehabil. **1997 ; 78 : 385-392**

HUBBARD WA, McELROY GK. Benchmark data for elderly, vascular trans-tibial amputees after rehabilitation. Prosthet & Orthot Int. **1994 ; 18 : 142-149**

HUGHES J, JACOBS N. Normal human locomotion. Prosthet & Orthot Int. **1979 ; 3 : 4-12**

HUGHES J, TAYLOR JS. Biomechanics and prosthetic practice. In Murdoch, and Donovan ed. Amputation surgery and lower limbs prosthetics. Blackwell. Oxford. **1985.** pp. 41-51

HURLEY GRB, McKENNEY R, ROBINSON M, ZADRAVEC M, PIERRYNOWSKI MR. The role of the contralateral limb in below-knee amputee gait. Prosthet & Orthot Inter. **1990 ; 14 : 33-42**

HUSKISSON EC. Measurement of Pain. Lancet. **1974 ; 9 : 1127-1131**

Instructions for checkout of Above-Knee Prosthesis. Prosthetics and Orthotics. Post Graduate Medical School. New York University. **1968**

Instructions for checkout of Below-Knee Prosthesis. Prosthetics and Orthotics. Post Graduate Medical School. New York University. **1968**

International Organisation for Standardisation (ISO). Prosthetics – Structural testing of Lower Limb Prostheses. ISO 10328. **1993** ; Parts 1 to 4

INTERNATIONAL SOCIETY of BIOMECHANICS (ISB). Quantities and Units of Measurement in Biomechanics. **1987** ; Revision 1

Introductory Mechanics. University of Strathclyde. Bioengineering Unit. Post Graduate Diploma in Biomechanics

ISAKOV E, BURGER H, GREGORIC M, MARINCEK C. Isokinetic and isometric strength of the thigh muscles in below - knee amputees. Clin Biomech. **1996 ; 11 N°4 : 233-235**

ISAKOV E, BURGER H, KRAJNIK J, GREGORIC M, MARINCEK C. Double-limb support and step-length asymetry in below-knee amputees. Scand J Rehab Med. **1997 ; 19 : 75-79**

ISAKOV E, MIZRAHI J, RING H, SUSAK Z, HAKIM N. Standing sway and weight-bearing distribution in people with below-knee amputations. Arch Phys Med Rehabil. **1992 ; 73 : 174-178**

JACOBS NA. Biomechanics of above-knee prostheses. In Murdoch, and Donovan ed. Amputation surgery and lower limbs prosthetics. Blackwell. Oxford. **1985.** pp. 130-139

JACOBSON WC, GABEL RH, BRAND RA. Surface vs. fine-wire electrode ensemble-averaged signals during gait. J. Electromyo Kinesiol. **1995** ; 5 N°1 : 37-44

JAEGER RJ, VANITCHATCHAVAN P. Ground reaction forces during termination of gait. J Biomech. **1992** ; 25 N°10 : 1233-1236

JAEGERS SMJ, ARENDZEN JH, de JONGH HJ. An electromyographic study of the hip muscles of transferral amputees in walking. Clin Orthot & Relat Res. **1996** ; 328 : 119-128

JAEGERS SMJ, ARENDZEN JH, de JONGH HJ. Prosthetic gait of unilateral transfemoral amputees: a kinematic study. Arch Phys Med Rehabil. **1995** ; 76 : 736-743

JAMES U, OBERG K. Prosthetic gait pattern in unilateral above-knee amputees. Scand J Rehabil Med. **1973** ; 5 : 35-50

JENDRZEJCZYK DJ. Flexible Socket Systems. Clin. Prosthet & Orthot. **1985** ; 11 N°3 : 27-31

JIED A, DEJOUR D, CHEZE L, DIMNET J. Système et méthode d'analyse de la cinématique du membre inférieur lors de la marche en vue d'applications cliniques. Innov Techn Biol Med. **1996** ; 17 N°4 : 325-336

JOUBLIN C, JOUBLIN B. Les amputés des membres inférieurs en centre de rééducation fonctionnelle et d'appareillage : Catamnèse sur 232 cas. Ann Kinésithér. **1986** ; 13 N°6 : 267-275

JOYCE BM, KIRBY RL. Canes, Crutches and Walkers. J Am Fed Phys Therapy (AFP). **1991** ; 43 : 535-542

KABADA MP, RAMAKRISHMAN HK, WOOTTEN ME. Measurement of lower extremity kinematics during level walking. J of Orthop Res. **1990** ; 8 : 383-392

KAY J. Domiciliary rehabilitation of elderly patients. Physiotherapy **1991** ; 77 N°1 : 60-61

KEGEL B, BURGESS EM, STARR TW, DALY WK. Effects of isometric muscle training on residual limb volume, strength and gait of below-knee amputees. Phys Ther. **1981** ; 61 (10) : 1419-1426

KHOURY SA. Evaluation of amputees. Int J. Rehab. Research. **1983** ; 6 N°4 : 449-454

KIRKER S, KEYMER S, TALBOT J, LACHMANN S. An assessment of the intelligent prosthesis. Clin Rehabil. **1996** ; 10 : 267-273

KIURU A, KUUSELA T, VANHARANTA H. Early detection of muscle lesion induced by immobilisation of an extremity : an experimental study on rabbits. J. Biophysic and Biomechanic. **1987** ; 11 N°2 : 79-81

KLEIN PJ, BENNETT SE, GOLFEN DM, WALKER CL, ZAMIELA KE. Feasibility of computer-assisted motion analysis in physical therapy. Physical Therapy. **1992** ; 72 N°6 (Suppl) : 11-12

KOTZKI N, BRUNON A, PELISSIER J. Amputation et Schéma Corporel. in Appareillage et Rééducation du Membre Inférieur. Masson, Paris. **1996** ; pp 450-455

KOTZKI N, BRUNON A, PELISSIER J. Amputation et Schéma Corporel. Kiné Scien. **1997** ; 371 : 47-50

KOTZKI N, MAITRE M, ENJALBERT M, PELISSIER J. Rééducation à la marche de l'amputé artéritique. In Pelissier, Brun ed. La Marche Humaine et sa Pathologie : Explorations et Rééducation. Masson. Paris. **1994**. pp. 281-287

KREBS DA. Interpretation Standards in Locomotion Studies. In Craik and Oatis ed. Gait Analysis, Theory and Application. Mosby. St Louis. **1995**. pp. 336-337.

KULKARNI JR, KEARSLEY M. Relevance of social class and smoking in lower limb amputees. Clinic Rehabil. **1993** ; 7 : 201-203

KUSTER M, SAKURAI S, WOOD GA. Kinematic and kinetic comparison of downhill and level walking. Clinical Biomech. **1995** ; 10 N°2 : 79-84

LAASSEL EM, LOSLEVER P, VOISIN PH, HERLANT M. Analyse multidimensionnelle des forces de réaction du pied au cours de la marche normale. Acta Orthopaedica Belgica. **1992** ; 58 N°3 :272-279

LABOISSE JJ. Les capteurs à jauges d'extensométrie: Bases expérimentales. **1991** ; Laboratoire de Mécanique du Solide. Ecole Nationale Supérieure des Arts et Métiers - Centre de Châlons-sur-Marne. France

LACHMANN SM. Stump care and skin problems. The Limb Service and Related Matters. **1994** ; 2 : 33-34

LAMBERT A, JOHNSON J. Stump Shrinkers: A survey of their use. Physiotherapy. **1995** ; 81 N°4 : 234-236

LATOUR G, LAUREILLARD C, MARGOTIN M. Le moignon de l'amputé. In Rabourdin JP ed. Rééducation en Gériatrie. Masson. Paris. **1989** ; pp 357-369

LAURIAN C, GIGOU F, BRISSET D, ANGEL F. Indications du fixateur externe dans les troubles trophiques du pied. Cah. Kinésithér. **1995** ; 176 N°6 : 27-32

LAWES P. Alignment kinetics in patient-prosthesis matching. **1982** PhD thesis, Bioengineering Unit, University of Strathclyde, Glasgow

LE ROUX P. Techniques de rééducation pour amputés artéritiques. Kinésithér Scie. **1986** ; 252 : 26-30

LEE VSP, SOLOMONIDIS SE, SPENCE WD. Stump-socket interface pressure as an aid to socket design in prostheses for trans-femoral amputees — a preliminary study. Proc Instn Mech Engrs. **1997** ; 211 Part H : 167-180

LEHMANN JF, de LATEUR BJ, PRICE R. Biomech of normal gait. Physical Med Rehabil Clinics of North America. **1992** ; 3 N°1 : 95-109

LEHNEIS HR. Beyond the quadrilateral. Prosthet and Orthot Int. **1985** ; 9 N°4 : 6-8

LEMAIRE ED, FISHER FR, ROBERTSON DGE. Gait patterns of elderly men with trans-tibial amputations. Prosthet & Orthot Int. **1993** ; 17 : 27-37

LEMAIRE R. L'écoulement du sang dans les artères athéromateuses Essai de Biomécanique Médicale. **1988** Laboratoire L. Lafon. B.P. 22. 94701 Maisons-Alfort Cedex France

LEUNG CCE, RUSH PJ, DEVLIN M. Predicting prosthetic rehabilitation outcome in lower limb amputee patients with the functional independance measure. Arch Phys Med Rehabil. **1996** ; 77 : 605-608

LEVY P. Technique du plateau de force double de grande longueur : Système Ceraval. Mémoire Certificat de Moniteur Cadre de Masso-Kinésithérapie. **1985**. INK Paris.

LI N. Biomechanical determination of load actions transmitted by nex generation lower limb prostheses. **1996** PhD Thesis, Bioengineering Unit, University of Strathclyde, Glasgow, Scotland

LIJA M, JOHANSSON T. Adherent cicatrix after below-knee amputation. J of Prosthet & Orthot. **1993** ; 5 N°2 : 65-66

LILJA M, ÖBERG T. Proper time for definitive transtibial prosthetic fitting. **1997** ; 9 (2) : 90-94

LITTLE CE, KIRBY RL, CONNORS M. Spandex shorts to assist stump shrinkage of lower-limb amputees : a pilot study. Physiotherapy Canada. **1997** ;

LITTLE EG. Strain Gauge Measurement. In Miles, Tanner ed. Strain Measurement in Biomechanics. Chapman & Hall. London. **1990**. pp. 39-57

LO CONTE LR, MERLETTI R. Advances in processing of surface myoelectric signals: Part 2. Medical & Biological Engineering & Computing. **1995** ; 33 : 373-384

LO CONTE LR, MERLETTI R. Advances in processing of surface myoelectric signals: Part 1. Medical & Biological Engineering & Computing. **1995** ; 33 : 362-372

LOCQUENEUX G, BONJEAN M, TREBERN F, BAUDIN P, BOUSSARD D, RIGAL F. Electrostimulation antalgique et douleur fantôme de l'amputé. Etude clinique réalisée sur 19 patients. Ann Kinésithér. **1993** ; 20 N°3 : 141-144

LOGIEZ M, BIBRE P, VOISIN P. Mesure des périmètres du moignon chez l'amputé. Kiné Scien. **1994** ; 344 : 27-29

LOSLEVER P, LAASSEL EM, ANGUE JC. Combined statistical study of joint angles and ground reactions forces using component and multiple correspondence analysis. IEEE Transactions on Biomedical Engineering. **1994** ; 41 N°12 : 1160-1167

LOVELY DF. Portable tape recorder system for prosthetic load data acquisition. **1981** PhD thesis, Bioengineering Unit, University of Strathclyde, Glasgow

LOWE PJ. Knee mechanism performance during amputee activity. **1969** PhD thesis, Bioengineering Unit, University of Strathclyde, Glasgow

LUIGI A. Les troubles de l'équilibre chez l'adulte amputé : Apport de l'analyse de la posture et de la marche à la rééducation.. Mémoire - Ecole de Cadres de Masso-Kinésithérapie de Montpellier. **1992** pp. 15

LUNSFORD BR, Screening and Data Summary. J Prosthet & Orthot. **1993** ; 5 N°4 : 125-130

LUNSFORD TR, LUNSFORD BR. The research sample, Part 1: Sampling. J. of Prosthetics and Orthotics. **1995** ; 7 N°3 : 105-112

LUNSFORD TR, LUNSFORD BR. The research sample, Part 2: Sampling Size. J. of Prosthetics and Orthotics. **1995** ; 7 N°4 : 137-141

MACFARLANE PA, NIELSEN DH, SHURR DG, MEIER K. Gait comparisons for below-knee amutees using a Flex-Foot™ versus a conventional prosthetic foot. J Prosthet & Orthot. **1991** ; 3 N°4 : 150-161

MacGREGOR J. Rehabilitation Ambulatory Monitoring. In RM Kenedi, JP Paul, J Hughes ed. MacMillan Press. London. **1979**. pp 159-172

MAGNISSALIS EA. Studies of prosthetic loading by means of pylon transducers. **1992** PhD thesis, Bioengineering Unit, University of Strathclyde, Glasgow

MAK AFT, LIU GHW, LEE SY. Biomechanical assessment of below-knee residual limb tissue. J. of Rehabil Res & Dev. **1994** ; 31 N°3 : 188-198

MANOLI A. A long posterior flap in below-knee amputations for peripheral vascular disease: Rationale and Technique. Foot & Ankle Int. **1998** ; 19 N°2 : 110-112

MAREY EJ. De la locomotion terrestre chez les bipèdes et les quadrupèdes. J Anat et Physiol. **1873** ; 9 : 42-49

MARTINET N, PAYSANT J, MAUPAS E, ANDRE JM. Analyse ambulatoire de la marche de l'amputé. In Codine, Brun, André ed. Amputation du Membre Inférieur - Appareillage et Rééducation. Masson. Paris. **1996**. pp. 344-350

McDONOUGH AL, RAZZA-DOHERTY M. Some biomechanical aspects of crutch and cane walking: The relationship between forward rate of progression, symmetry and efficiency — A case report. Clin Pod Med & Sur. **1988** ; 5 : 677-693

MELCHIORRE PJ, FINDLEY T, BODA W. Functional outcome and comorbidity indexes in the rehabilitation of the traumatic versus the vascular unilateral lower limb amputee. Am J Phys Med Rehabil. **1996** ; 75 : 9-14

MENAGER D, CHIESA G. L'appareillage des amputés du membre inférieur. J. Réadapt Med. **1995** ; 15 N°3 : 95-105

MIAULT D. BRUN JP, DUPRE JC, PILLU M, et coll. L'appareillage du pied des artéritiques diabétiques. Cah. Kinésithér. **1995** ; 176 N°6 : 20-26

MICHAEL JW, BOWKER JH. Prosthetics/Orthotics Research for the twenty-first century: Summary of 1992 conference proceedings. J Prosthet & Orthot. **1994** ; 6 N°4 : 100-107

MICHAUT E, PELISSE F, MAZAS Y. Chaîne de mesure destinée à l'analyse mécanique de la marche. Acta Orthopedica Belgica. **1975** ; Supp I : 69-77

MILES AW, TANNER KE. Strain Measurement in Biomechanics. Chapman & Hall. London. **1990.**

MINNS RJ, HOGARTH S, BAINBRIDGE A, PEMBROKE S. The design of a functional assessment and gait analysis facility for rehabilitation studies. Clin Rehabil. **1991** ; 5 : 293-300

MORIMOTO S, TSUCHIYA K. Evaluation of amputee prosthesis system of lower limb using pylon study method. Bulletin JSPE. **1984** ; 18 : 57-58

MOSS SE, KLEIN R, KLEIN BEK. Long term incidence of lower-extremity amputations in a diabetic population. Arch Fam Med. **1996** ; 5 : 391-398

MUECKE L, SHEKAR S, DWYER D, ISRAEL E, FLYNN JPG. Functionnal screening of lower-limb amputees : a role in predicting rehabilitation outcome ? Arch Phys Med Rehabil. **1992** ; 73 : 851-858

MUELLER MJ, ALLEN BT, SINACORE DR. Incidence of skin breakdown and higher amputation after transmetatarsal amputations: Implications for rehabilitation. Arch Phys Med Rehabil. **1995** ; 76 : 50-54

MUELLER MJ, SINACORE DR. Rehabilitation factors following transmetatarsal amputation. Phys Ther. **1994** ; 74 N°11 : 1027-1033

MULLER EA. Influence of training and inactivity on muscle strength. Arch Phys Med & Rehabil. **1970** ; 51 : 449-462

MURDOCH G. Levels of amputation and limiting factors. Annals Royal College Surgeons of England. **1967** ; 40 : 204-216

MURRAY MP, SEIREG AH, SCHOLTZ RC. A survey of the time, magnitude and orientation of forces applied to walking sticks. Am J Phys Med. **1969** ; 48 N°1 : 1-13

MURRAY WM, STEIN PK. Strain Gage Techniques - Lectures and Laboratories Exercices. Massachusetts Institute of Technology. **1957** ; Cambridge, Massachusetts, USA. Part I

MURRAY WM, STEIN PK. Strain Gage Techniques. Fundamentals Applications. Lectures and Laboratory Exercises. Massachusetts Institute of Technology. **1957** ; Cambridge, Massachusetts, USA. Part II. pp. 360-367

NAGASHIMA H, INOUE H, TAKECHI H. Incidence and prognosis of dysvascular amputations in Okayama Prefecture (Japan). Prosthet & Orthot Int. **1993** ; 17 : 9-13

NG EK, BERBRAYER D, HUNTER GA. Transtibial amputation: Preoperative vascular assessment and functional outcome. J of Prosthet & Orthot. **1996**; 8 N°4 : 123-129

NIELSEN DH, SHURR DG, MACFARLANE PA, MARCO LM, et al. Physiological gait analysis of type IIIC tibial limb salvage patients versus traumatic transtibial amputees. J. of Prosthet & Orthot. **1995** ; 7 N°3 : 80-86

NIETERT M, BRENDEL T, GOTTWALS K, KREIL P. Ein portables Meßsystem zur Erfarssung von Belastungs-werten in Beinprothesen als Altenative zu stationären Ganganalysesystem. Othopädie-Technik. **1998** ; 1 : 13-32

NIKOLAJSEN L, ILKJAER S, KRONER K, CHRISTENSSEN JH, JENSEN TS. The influence of pre amputation pain on post amputation stump and phantom pain. Pain. **1997** ; 72 : 393-405

NING L, SOLOMONIDIS SE, SPENCE WD, et al. The influence of new generation prosthetic lower-limbs on the gait of trans-femoral amputees. Gait & Posture. **1995** ; 3 N°2 : 97

NISHIARA K, KAWAMURA J, KANDA A. A much shorter pylon load cell and its wide range of applications in prosthetics. VI World Congress of ISPO. **1989**. Kobe, Japan

NISSAN M. The initiation of gait in lower limb amputees: Some related data. J Rehabil Res Develop. **1991** ; 28 N°2 : 1-12

NITZ JC. Rehabilitation outcomes after bilateral lower limb amputation for vascular disease. Physiotherapy Theory & Practice. **1993** ; 9 : 165-170

O'TOOLE DM, RICHARD T, RYAN B. Functional changes in vascular amputee patients: Evaluation by Barthel index, Pulses profile and Escrow scale. Arch Phys Med Rehabil **1985** ; 66 : 508-511

ÖBERG T, KARSZNIA A, ÖBERG K. Basic gait parameters: Reference data for normal subjects, 10-79 years of age. J Rehabil Res Develop. **1993** ; 30 N°2 : 210-223

OPILA KA, NICOL AC, PAUL JP. Forces and impulse during aided gait. Arch Phys Med Rehabil. **1987** ; 68 : 715-722

OPILA KA. Impulse characteristics and upper limb loadings of aided gait. **1985** PhD Thesis. Bioengineering Unit. University of Strathclyde. Glasgow

OPILA-CORREIA KA. Kinematics of high-heeled gait with consideration for age and experience of wearers. Arch Phys Med Rehabil. **1990** ; 71 : 905-909

OTTENBACHER KJ. Why rehabilitation research does not work (As well as we think it should). Arch Phys Med Rehabil. **1995 ; 76 : 123-129**

OZIALCIN H, SESLI E. Temporary prosthetic fitting for below-knee amputation. Prosthet & Orthotot Int. **1989 ; 13 : 86-89**

PAQUIN JM, ANDRE JM, BENEZT P, MARTINET N, TESSIER A. L'appareillage et les principes de la rééducation de l'amputé fémoral âgé. In Rabourin JP ed. Rééducation en Gériatrie. Masson. Paris. **1989 ;** pp. 370-378

PAQUIN JM, ANDRE JM, MARTINET N, ORHAN B. Les anomalies de la marche des amputés fémoraux et tibiaux. In Codine, Brun, André ed. Amputation du Membre Inférieur - Appareillage et Rééducation. Masson. Paris. **1996.** pp. 350-359

PARK E, MEEK SG. Adaptive filtering of electromyographic signal for prosthetic control and force estimation. IEEE Transactions on Biomedical Engineering. **1995 ;** 42 N°10 : 1048-1052

PASHALIDES S. Design of a portable recording system for the measurement of prosthetic loading. **1989** PhD thesis, Bioengineering Unit, University of Strathclyde, Glasgow

PAUL JP. Gait analysis in lower limb amputees. J Rehabil Scie. **1994 ;** 7 N°3 : 38-42

PAUL JP. Gait analysis. Annals of the Rheumatic Diseases. **1989 ; 48 : 178-181**

PAUL JP. Letter to the editor: Visual guidance to forceplates does not influence ground reaction force reliability and Author's Response. J Biomech. **1996 ;** 29 N°6 : 833

PEDERSEN NW, PEDERSEN D. Nutrition as a prognostic indicator in amputations : A prospective study of 47 cases. Acta Orthop Scand. **1992 ;** 63 N°6 : 675-678

PEERAER L, AEYELS B, VAN der PERRE G. Development of EMG-based mode and intent recognition algorithms for a computer-controlled above-knee prosthesis. J. Biomed. Eng. **1990 ; 12 : 178-182**

PELISSE F. Single and Double Long Forces Plate. Dundee Congress. Workshop on the Clinical Application of Gait Analysis. **1981**

PELISSIER J, BOISSON D. Les paramètres de la marche humaine : Techniques actuelles d'Exploration. In Pelissier, Brun ed. La Marche Humaine et sa Pathologie : Explorations et Rééducation. Masson. Paris. **1994.** pp. 41-55

PELLAS F, BENEZT P, RAGAVAN R, DELARQUE A. Evaluation quantifiée de la marche chez deux patients appareillés pour désarticulation de la hanche : apport d'un programme spécifique d'analyse de la locomotion. Ann Rédaptation Méd Phys. **1994 ;** 37 : 105-121

PERNOT HFM, DE WITTE LP, LINDERMAN E, CLUITMANS J. Daily functioning of the lower extremity amputee: an overview of the literature. Clin Rehabil. **1997 ; 11 : 93-106**

PERRY J, BOYD LA, RAO SS, MULROY SJ. Prosthetic weight acceptance mechanics in transtibial amputees wearing the Single Axis, Seatlle Lite and Flex Foot. IEEE Trans Rehabil Engineering. **1997 ; 5 : 283-289**

PERRY J. Gait analysis systems in gait analysis : normal and pathological function. Thorofare NJ : Slack, **1992 : 353-411**

PHILLIPS G. Acquire version 1.8. Internal Report, Bioengineering Unit, University of Strathclyde. **1990.** Glasgow. Scotland

PILLU M, DESPEYROUX L, MELONI J, DECHAMPS E, DUPRE JC, MATHIEU JF. Réadaptation des amputés vasculaires. Encycl Med Chir (Paris-France), Kinésithérapie-Rééducation fonctionnelle, 26-270-A-10, 1995, 9p.

PILLU M, SOLOMONIDIS SE, LABOISSE JJ, PAUL JP. A removable six-component pylon load transducer for prosthetic gait assessment. ISPO'98 IXth World Congress, 1998a. Amsterdam. The Netherlands

PILLU M, SOLOMONIDIS SE, LABOISSE JJ, PAUL JP. Description d'une chaîne de mesure pour l'étude de la marche des amputés du membre inférieur. OASIS European Congress. 1999. Paris. France

PILLU M, SOLOMONIDIS SE, LABOISSE JJ, PAUL JP. La marche des amputés vasculaires étudiée en situation réelle au moyen d'un nouveau capteur. Ann Kinésithér. 1998b ; 25 N°4 : 149-160

PILLU M, SOLOMONIDIS SE, LABOISSE JJ, PAUL JP. Practice of walking assistive devices during locomotion of recent vascular transtibial amputees. Arch Physiol & Biochemistry. 1999a ; 107 : 13-15

PILLU M, SOLOMONIDIS SE, LABOISSE JJ, PAUL JP. Strategy of using walking assistive devices during locomotion of recent vascular transtibial and transfemoral amputees. ISPO'98 IXth World Congress, 1998. Amsterdam. The Netherlands

PILLU M. Arthrocame et flessum de genou chez l'amputé tibial vasculaire. Communication orale au XXIème Journées de l'Institut National de la Kinésithérapie. Paris. 1989

PINZUR MS, COX W, KAISER J, MORRIS T. The effect of Prosthetic Alignment on Relative Limb Loading in persons with trans-tibial Amputation : a preliminary report. J Rehabil Res Develop. 1995 ; 32 N°4 : 373-378

PINZUR MS, GOTTSCHALK F, SMITH D. Functional outcome of below-knee amputation in peripheral vascular insuffisency. Clin Ortho and Relat Research 1993 ; 286 : 247-249

PINZUR MS, LEVINE PD, TRIMBLE J, HAAG K, SHERMAN R. Qualitative and Quantitative Gait Phase Analysis by Continuous Monotiring of Inter - Ankle Distance. J Rehabil Res Develop. 1984 ; 21 N°2 : 50-53

PINZUR MS, PERONA P, PATWARDHAN A, HAVEY R. Loading of the contralateral foot in peripheral vascular insufficiency below-knee amputees. Foot & Ankle 1991 ; 11 N°6 : 368-371

PINZUR MS, REDDY N, CHARUK G, OSTERMAN H, VRBOS L. Control of the residual tibia in transtibial amputation. Foot & Ankle International. 1996 ; 17 N°9 : 538-539

PINZUR MS. Gait analysis in peripheral vascular insufficiency through-knee amputation. Jour of Rehabil Research Develop. 1993 ; 30 N°4 : 388-392

PITKIN MR. Effects of design variants in lower-limb prostheses on gait synergy. J Prosthet Orthot. 1997 ; 9 N°3 : 113-122

PITKIN MR. Mechanical outcomes of a rolling-joint prosthetic foot and its performance in the dorsiflexion phase of transtibial amputee gait. J Prosthet Orthot. 1995 ; 7 N°4 : 114-122

PLAS F, VIEL E, BLANC Y. La marche humaine. Masson. Paris. 1979. pp.35-39

PORTER D, ROBERTS VC. A review of gait assessment in the lower limb amputee Part 1 : Temporal and kinematic analysis. Clin Rehabil. 1989 ; 3 : 65-74

POWERS CM, BOYD LA, FONTAINE CA, PERRY J. The influence of lower - extremity muscle force on gait characteristics in individuals with below - knee amputations secondary to vascular disease. Physical Therapy. **1996** ; 76 : 369-3777

POWERS CM, BOYD LA, TORBURN L, PERRY J. Stair ambulation in persons with transtibial amputation : an analysis of the Seattle LightFoot™. J Rehabil Res & Dev. **1997** ; 34 N°1 : 9-18

POWERS CM, BOYD LA, TORBURN L, PERRY J. Stair ambulation in persons with transtibial amputation : an analysis of the Seattle LightFoot™. J Rehabil Res & Develop. **1997** ; 34 : 9-18

PRINCE F, ALLARD P, THERRIEN RG, McFADYEN BJ. Running gait impulse asymmetries in below-knee amputees. Prosthet & Orthot Int. **1992** ; 16 : 19-24.

PRINCE F, CORRIVEAU H, HEBERT R, WINTER DA. Gait in the elderly. Gait and Posture. **1997** ; 5 : 128-135

PRINCE F, WINTER DA, SJONNENSEN G, et al. A New Technique for the Calculation of the Energy Stored, Dissipated, and Recovered in Different Ankle-Foot Prostheses. IEEE Transactions on Rehabilitation Engineering. **1994** ; 2 N°4 : 247-255

PURDEY CR. Socket axis determination in lower limb prosthetic alignment. **1977** MSc thesis, Bioengineering Unit, University of Strathclyde, Glasgow

QUESADA P, SKINNER HB. Analysis of a below-knee patellar tendon-bearing prosthesis: a finite element study. J Rehabil Res Dev. **1991** ; 28 n°3 : 1-12

RAMIRO J, VERA P, HOYOS JV, GARCIA-RAIMUNDO M. Aspectos biomecánicos de la marcha del amputado de miembro inferior. Fisioterapia. **1986** ; 31 : 13-20

RAUPP JC, GRUMLER B, LARDRY JM. La rééducation et l'appareillage des amputés. Dossiers de Kinésithérapie. Masson. Paris. **1991**

REIBER GE. Who is at risk of limb loss and what to do about it? J Rehabil Res Dev. **1994** ; 31 N°4 : 357-362

RENZI RM. Lower extremity amputations of US elderly population. On the rise. J Am Pod Med Ass. **1996** ; 86 N°4 : 176-179

RIGAL F, REYMOND E, PAVAN M. Le moignon douloureux. J Réadapt Méd. **1997** ; 17 N3 : 120-124

ROARK RJ. Formulas for stress and strain. **1954**. McGraw-Hill Book Company. New-York

ROBINSON JL, SMIDT GL, ARORA JS. Accelerographic, temporal and distance gait factors in below-knee amputees. Phys Ther. **1977** ; 57 (8) : 898-904

ROSA SERRA G. La sophrologie dans le traitement de l'amputé. Ann. Kinésithér. **1995** ; 22 N°3 : 135-137

ROSE GK. Clinical gait assessment : a personal view. J Med Eng & Tech. **1983** ; 7 N°6 : 273-279

ROSSI SA, DOYLE W, SKINNER HS. Gait initiation of persons with below-knee amputation: The characterization and comparison of force profiles. J. of Rehabil Res and Development. **1995** ; 32 N°2 : 120-127

ROTH EJ, MERBITZ CT, GRIP JC, BOGOLUB M, MROCZEK K, DUGAN S, DONADIO K. The time-logger-communicator gait monitor: recording temporal gait parameters using a portable computerised device. Int Disabil Studies. **1990** ; 12 : 10-16

ROTH EJ, PARK KL, SULLIVAN WJ. Cardiovascular didease in Patients with dysvascular amputation. Arch Phys Med Rehabil. **1998** ; 79 : 205-215

ROZENDAL RH. Clinical gait analysis: Problems and solutions? Hum Mov Science. **1991** ; 10 : 555-564

RUNCINAM RJ, NICOL AC. Strain gauged six-component load transducer for use in upper limb biomechanics. Proc Instn Mech Engrs. **1993** ; 207 : 231-237

SABOLICH J. Contoured Adducted Trochanteric-Controlled Alignment Method (CAT-CAM) : Introduction and Basic principles. Clin. Prosthet & Orthot. **1985** ; 11 N° 4: 15-26

SABOLICH JA, ORTEGA GM. Sense of feel for lower-limb amputees : a phase one study. J Prosthet Orthot. **1994** ; 6 N°2 : 36-41

SALVI FJ, HOFFMAN MD, SABHARWAL S, CLIFFORD PS. Physiologic comparison of forward and reverse wheelchair propulsion. Arch Phys Med Rehabil. **1998** ; 79 : 36-40

SANDERS JE, DALY CH, BURGESS EM. Clinical measurement of normal and shear stresses on a trans-tibial stump: characteristics of wave-form shapes during walking. Prosthet & Orthot Int. **1993** ; 17 : 38-48

SANDERS JE, DALY CH. Normal and shear stresses on a residual limb in a prosthetic socket during ambulation: Comparison of finite element results with experimental measurements. J. Rehabil Res Develop. **1993** ; 30 N°2 : 191-204

SANDERS JE, MILLER RA, BERGLUND DN, ZACHARIAH SG. A modular six-directional force sensor for prosthetic assessment : a technical note. J Rehabil Res Develop. **1997** ; 34 N°2 : 195-202

SANDERS JE, SMITH LM, SPELMAN FA, WARREN DJ. A portable measurement system for prosthetic triaxial force transducers. IEEE Transactions on Rehabilitation Engineering. **1995** ; 3 N°4 : 366-372

SANDERS JE, SMITH LM, SPELMAN FA. A small and lightweight three-channel signal-conditioning unit for strain-gage transducers: A technical note. J. Rehabil Res Develop. **1995** ; 32 N°3 : 210-213

SANDERSON DJ, MARTIN PE. Joint kinetics in unilateral below-knee amputee patients during running. Arch Phys Med Rehabil. **1996** ; 77 : 1279-1285

SANDERSON DJ, MARTIN PE. Lower extremity kinematic and kinetic adaptations in unilateral below-knee amputees during walking. Gait & Posture. **1997** ; 6 : 126-136

SCHUCH CM, PRITHAM CH. International Standards Organisation Terminology: Application to Prosthetics and Orthotics. J Prosth Orth. **1994** ; 6 N°1 : 29-33

SCHUCH CM. Report from: International workshop on above-knee fitting and alignment techniques. Clin. Prosthet & Orthot. **1988** ; 12 N°2 : 81-98

SCHWARTZ SJ, STURR M, GOLDBERG G. Statistical methods in rehabilitation literature : a survey of recent publications. Arch Phys Med Rehabil. **1996** ; 77 : 497-500

SCREMIN AME, TAPIA JI, VICHICK DA, et al. Effect of age on progression through temporary prostheses after below-knee amputation. Am J Phys Med Rehabil. **1993** ; 72 : 350-354

SEIREG AH, MURRAY MP, SCHOLZ RC. Method for recording the time, magnitude and orientation of forces applied to walking sticks. Am J Phys Med. **1968** ; 47 N°6 : 307-314

SELIKTAR R, MIZRAHI J. Some gait characteristics of below-knee amputees and their reflexion on the ground reaction force. Eng Med. **1986** ; 15 : 27-33

SELIKTAR R. Biomechanics of prosthetic gait. Phys Med & Rehabil. **1994** ; 8 N°1 : 89-107

SEROUSSI RE, GITTER A, CZERNIECKI JM, WEAVER K. Mechanical work adaptations of above-knee amputee ambulation. Arch Phys Med Rehabil. **1996** ; 77 : 1209-1214

SILVER-THORN MB, CHILDRESS DS. Generic, geometric finite element analysis of the transtibial residual limb and prosthetic socket. J Rehabil Res & Develop. **1997** ; 34 : 171-186

SIRIWARDENA GJA, BERTRAND PV. Factors influencing rehabilitation of arteriosclerotic lower limb amputees. Jour of Rehabil Res Dev. **1991** ; 28 n°3 : 35-44

SMITH CR, SMITH CA. Patient Education Information: Readability of prosthetic publications. J Prosthet & Orthot. **1994** ; 6 N°4 : 113-118

SNYDER RD, POWERS CM, FONTAINE C, PERRY J. The effect of five prosthetic feet on the gait and loading of the sound limb in dysvascular below-knee amputees. J Rehabil Res Develop. **1995** ; 32 N°4 : 309-315

SOLOMONIDIS SE. Personnal communication **1989**

STALLARD J, SANKARANKUTTY M, ROSE GK. Lower-limb vertical ground reaction forces during crutch walking. J Med Eng & Tech. **1978** ; 2 : 201-202

STAM HJ, EIJSKOOT F, BUSSMANN JBJ. A device for long term ambulatory monitoring in trans-tibial amputees. Prosthet & Orthoto Int. **1995** ; 19 : 53-55

STANHOPE SJ, KEPPLE TM, McGUIRE DA, ROMAN NL. Kinematic-based technique for event time determination during gait. Med & Biol Eng & Comput. **1990** ; 28 : 355-360

STAROS A. Problèmes d'appareillage chez l'amputé âgé. Prosth Int. **1967** ; 2 N°4-5 : 15-28

STEFANYSHYN DJ, ENGSBERG JR, TEDFORD KG, et al. A pilot study to test the influence of specific prosthetic features in preventing trans-tibial amputees from walking like able-bodied subjects. Prosthet & Orthot Int. **1994** ; 18 : 180-190

STEWART CPU, JAIN AS, OGSTON SA. Lower limb amputee survival. Prosthet & Orthot Int. **1992** ; 16 : 11-18

STEWART CPU, JAIN AS. Cause of death of lower limb amputees. Prosthet & Orthotot Int. **1992** ; 16 : 129-132

STEWART CPU, JAIN AS. Dundee revisited — 25 years of a total amputee service. Prosthet & Orthotot Int. **1993** ; 17 : 14-20

SUBBARAO KV, BAJORIA S. The effect of stump length on the rehabilitation outcome in unilateral below-knee amputees for vascular disease. Clin Rehabil. **1995** ; 9 : 327-330

SZULC J. Telescopic limbs for above-knee amputees. **1984** PhD Thesis, Bioengineering Unit, University of Strathclyde, Glasgow, Scotland

TABARY JC, TABARY C, TARDIEU C, TARDIEU G, GOLDSPINK G. Physiological and structural changes in the cat's soleus due to immobilisation at different lengths by plaster casts. J of Physiology (London). **1972** ; 224 : 231-244

TABARY JC, TARDIEU C,. Experimental rapid sarcomere loss with concomitant hypoextensibility. Muscle and Nerve. **1981** ; 4 : 198-203

TANAKA S, YAMAKOSHI K, ROLFE P. New portable instrument for long-term ambulatory monitoring of posture change using miniature electro-magnetic inclinometers. Med & Biolog Eng & Comput. **1994** ; 32 : 357-360

TARDIEU C, BLANCHARD O, LE LOUIS K. Tendon adaptation to bone shortening. Connect. Tissue Res. **1984** ; 11 : 35-44

TARDIEU C, TARDIEU G, TABARY C. Adaptation of connective tissue length to immobilisation in the lengthened and shortened position in cat soleus muscle. J of Physiology (Paris). **1982** ; 78 : 214-220

THEVENON A, LAHAYE F, LEDUQUE J, LEVET B. Contact Sol / Semelles au cours de la marche et glissade : Bases Théoriques et Revue de la Littérature. Ann Réadap Méd Physique. **1989** ; 32 : 727-735

THEYS S, SCHOEVAERDTS JC, CLERIN M, DIEDERICH Ch, Influence différentielle d'une contraction isotonique du quadriceps sur la vélocité artérielle distale des membres inférieurs selon la topographie et la répercussion fonctionnelle des lésions. Cah Kinésithér. **1982** ; 96 N°4 : 25-32

TORBURN L, PERRY J, AYYAPPA E, SHANFIELD SL. Below-knee amputee gait with dynamic elastic response. J Rehabil Res Dev. **1990** ; 27 N°4 : 369-384

TORBURN L, POWERS CM, GUITERREZ R, PERRY J. Energy expenditure during ambulation in dysvascular and traumatic below-knee amputees: a comparison of five prosthetic feet. J. of Rehabil Res and Development. **1995** ; 32 N°2 : 111-119

TUCKER CA, LIN HY. Assessment of gait symmetry of an individual with bilateral below knee amputees using the force measuring treadmill. Gait and Posture. **1996** ; 4 : 205

UYGUR F, SENER G. Application of ultrasound in neuromas: Experience with seven below-knee stumps. Physiotherapy. **1995** ; 81 N°12 : 758-762

VAN DONGEN VCPC, LIEM AL. Phantom limb and stump pain and its treatment with spinal cord stimulation. J. of Rehabil Science. **1995** ; 8 N°4 : 110-114

VANJAARSVELD HWL, GROOTENBOER HJ, DE VRIES J. Acceleration due to impact at heel strike using below-knee prosthesis. Prosthet & Orthotot Int. **1990** ; 14 : 63-66

VANNIER MW, COMMEAN PK, SMITH KE. Three-dimensional lower extremity residua measurement systems error analysis. . J Prosthet & Orthot. **1997** ; 9 N°2 : 67-76

VAUCHER J. Etude statistique sur l'évolution de 101 cas d'amputation des membres inférieurs pour insuffisance artérielle. Thèse de Médecine. **1976**. Genève. Suisse

WAGNER J, SIENKO S, SUPAN T, BARTH D. Motion analysis of Sach vs. Flex-Foot™ in moderately active below-knee amputees. Clin Prosthet Orthot. **1987** ; 11 N°1 : 55-62

WARD KH, MEYERS MC. Exercise performance of lower-extremity amputees. Sports Med. **1995** ; 20 N°4 : 207-214

WATERS RL, PERRY J, ANTONELLI D, HISLOP H. Energy cost of walking of amputees : the influence of level of amputation. J Bone Jnt Surg (Am). **1976** ; 58 (1) : 42-46

WEIL D. Traitement des états dépressifs succédant aux amputations des membres. Nervure **1991** ; N° spécial mai 1991 : 34-38

WEIR RF, CHILDRESS DS. A portable, real-time, clinical gait velocity analysis system. IEEE Trans Rehabil Engineering. **1997** ; 5 : 310-320

WEISS NA. Introductory Statistics. **1995** Fourth Edition Addison-Wesley Publishing Company, Inc. Reading, Mass.

WEISSLAND T, MASSE P, FOURMAUX P, VOISIN P, VANDELCENAHER J, VANHEE J-L. Amputation de membre inférieur et course à pied. Ann. Kinésithér. **1996** ; 23 N°3 : 125-134

WERTSCH JJ, WEBSTER JG, TOMPKINS WJ. A portable insole plantar pressure measurement system. J Rehabil Res and Devel. **1992** : 29 N°1 : 13-18

WHITTLE MW. Clinical gait analysis : A review. Human Movement Science. **1996** ; 15 : 369-387

WIKOFF EK. Preprosthetic management. Phys Med & Rehabil. **1994.** ; 8 N°1 : 61-72

WILLIAMS PE, GOLDSPINK G. Changes in sarcomere length and physiological properties in immobilised muscle. J Anat. **1984** ; 138 N°2 : 337-341

WILLIAMS PE, GOLDSPINK G. Connective tissue changes in immobilised muscle. J Anat. **1984** ; 138 N°2 : 343-350

WILLIAMS RB, PORTER D, ROBERTS VC, REGAN JF. Triaxial force transducer for investigating stresses at the stump / socket interface. Med & Bio Eng & Comput. **1992** ; 30 : 89-96

WILSON AL. Enquête sur les amputés du membre inférieur âgés. Prosth Int. **1967** ; 2 N°4-5 : 37-40

WINTER DA Kinematic and kinetic patterns in human gait : variability and compensating effects. Hum Mov Scie. **1984** ; 3 : 51-76

WINTER DA, DEATHE AB, HALLIDAY S, ISHAC M, OLIN M. A technique to analyse the kinetics and energetics of cane-assisted gait. Clin Biomech. **1993** ; 8 : 37-43

WINTER DA, SIENKO S. Biomechanics of below-knee amputee gait. J. Biomech. **1988** ; 21 N°5 : 361-367

WINTER DA. Anthropometry. In Biomechanics and Motor Control of Human Movement. John Wiley & Sons Inc. New York. **1994a.** pp. 51-73

WINTER DA. Force transducers and force plates. In Biomechanics and Motor Control of Human Movement. John Wiley & Sons Inc. New York. **1994b.** pp. 84-96

WINTER DA. Kinetics : Forces and Moments of Force. In Biomechanics and Motor Control of Human Movement. John Wiley & Sons Inc. New York. **1994c.** pp. 75-84

WINTER DA. Processing of Raw Kinematic Data. In Biomechanics and Motor Control of Human Movement. John Wiley & Sons Inc. New York. **1994d.** pp. 27-45

WIRTA RW, GOLBRANSON FL, MASON R. Analysis of below-knee suspension systems: Effect on gait. J Rehabil Res Develop. **1990** ; 27 n°4 : 385-396

WIRTA RW, MASON R, CALVO K, GOLBRANSON FL. Effect on gait using various prosthetic ankle-foot devices. J Rehabil Res Develop. **1991** ; 28 N°2 : 13-24

WU G, CAVANAGH PR, ISB recommendations for standardisation in the reporting of kinematic data. J Biomech. **1995** ; 28 N°10 : 1257-1261

WU Y, KRICK H. Post-Surgical and early management of Lower Limb Amputations. Proceedings, Seventh World Congress of ISPO. **1992** ; Chicago Illinois USA

WU Y. Postoperative and preprosthetic management for lower extremity amputations. Capabilities. **1996** ; 5 N°2 : 1-11

YABLON SA, NOVICK ES, JAIN SS, INHOFFER M, et al. Postoperative transcutaneous oxygen measurement in the prediction of delayed wound healing and prosthetic fitting among amputees during rehabilitation. Am J Phys Med Rehabil. **1995** ; 74 N°3 : 193- 198

YANG L, SOLOMONIDIS SE, SPENCE WD, et al. The influence of limb alignment on the gait of above-knee amputees. J Biomech. **1991** ; 24 N°11 : 981-997

ZAHEDI MS, SPENCE WD, SOLOMONIDIS SE, et al. Alignment of lower-limb prostheses. J Rehabil Res Develop. **1986** ; 23 N°2 : 2-19

ZAHEDI MS, SPENCE WD, SOLOMONIDIS SE. The influence of alignment on prosthetic gait. In Murdoch and Donovan ed. Amputation surgery and lower limbs prosthetics. Blackwell. Oxford. **1985**. pp. 367-377

ZHANG L, DRURY CG, WOOLEY SM. Constrained standing: Evaluating the foot/floor interface. Ergonomics. **1991** ; 34 N°2 : 175-192

ZUNIGA EN, LEAVITT LA, CALVERT JC, CANZONERI J, PETERSEN CR. Gait Pattern in above-knee amputees. Arch Phys Med Rehabil. **1972** ; 53 : 373-382

11 APPENDICES (VOLUME 2)